Evolution of Colistin Resistance in *Acinetobacter baumannii* and Disrupting the Colistin Resistance Mechanisms

Brunel University London, Department of Life Science College of Health and Life Sciences

RES Biosciences PhD

Academic Year 2021 - 2024

Kavita Gadar

This thesis is submitted in fulfilment of the requirements for the degree of Doctor of Philosophy

Abstract

The emergence of antibiotic resistance is a global threat, rendering our reservoir of antibiotics ineffective against many bacterial pathogens. In 2019, 4.95 million people died with an antibiotic-resistant associated infection. One major contributor to this crisis is *Acinetobacter baumannii*, a Gram-negative multi-drug resistant (MDR) pathogen listed by the World Health Organisations (WHO) as a priority for novel therapeutic interventions.

This thesis explores innovative approaches against MDR *A. baumannii,* focusing on the therapeutic properties of phytochemicals and plant extracts, more specifically kaempferol and tormentil. Kaempferol, a phytochemical derived from capers and strawberries, in combination with colistin, reduces the growth of *A. baumannii* and inhibits biofilm formation when used on its own. Additionally, kaempferol disrupts iron homeostasis, resulting in increased reactive oxygen species under colistin stress, leading to bacterial death. Similarly, tormentil, a plant used in traditional Irish folklore medicine for treating burn wounds, and its constituents exhibit significant antimicrobial and antibiofilm activity against *A. baumannii.* Our mechanistic studies reveal that these extracts also impact bacterial iron homeostasis. These findings demonstrate the potential of iron-chelating compounds as colistin potentiators or standalone antimicrobials against MDR *A. baumannii.*

Additionally, we investigate the fitness and virulence costs associated with colistin resistance. Our laboratory evolved colistin-resistant mutants (CRMs) show varied growth rates in the presence of colistin and slow growth rates in the absence. The CRMs also show an increased biofilm formation and reduced virulence, illustrating the trade-offs of evolved colistin resistance. *In vivo* analysis of known and novel mutations in PmrB revealed structural changes that may enhance kinase activity and mediate colistin resistance.

These findings uncover metabolic vulnerabilities in *A. baumannii,* suggesting new strategies to enhance colistin efficacy through phytochemicals and plant extracts and further our knowledge in understanding the trade-offs of evolved resistance in *A. baumannii.* Together, these insights can contribute to the design and development of more effective treatments against MDR *A. baumannii.*

Acknowledgements

Throughout my PhD I faced many challenges that I could not have possibly overcome without the help of the truly inspiring people around me. Firstly, I would like to thank my supervisor Professor Ronan McCarthy for his invaluable help and mentorship throughout my undergraduate and postgraduate years. I am extremely grateful for the impact that you have made on my academic career. Thank you so much for all your encouragement and excitement about my achievements.

I would like to thank all the members of the RMC lab, with whom I have had the absolute pleasure of working with over the years. To Post-docs Dr Rubén de Dios, Dr Sophie Howard and Dr Chris Proctor, thank you for your advice and for enduring my endless amounts of questions with so much patience. Your insights and experiences continue to inspire me to strive for greatness. To lab members Evgenia Maslova, Lyuboslava Harkova, Jie Han and Dominika Krawiel, thank you for your support and friendship throughout the years, especially for the camaraderie during our lab shenanigans. You made long lab days and tedious lab tasks less daunting and tremendously enjoyable. A huge thank you to Amal Tayamoi and Sophie Preston for all the laughs we shared in Loco's, and for making attending uni everyday a pleasure.

I would like to acknowledge and thank our collaborators at Trinity College Dublin for their work and insights on Bogland species' therapeutic properties. I would also like to thank Dr Despoina Mavridou and Dr Nikol Kaderábková for their valued contributions to our research into Kaempferol.

A special thank you goes to my family, whose unwavering support and encouragement fueled my perseverance to complete my PhD. Especially to my mum, who served as my pillar of strength. Lastly, to my partner Christopher D'Souza, thank you so much for all of your support, for facing the highs and lows with me as if they were your own and for being my constant throughout this journey.

Declaration of originality and collaborative work

I declare that the work presented in this thesis is my own. The contributions are appropriately referenced throughout the text and also acknowledged below:

- '1.10 Next-generation antibiotics' section in chapter 1 is adapted from our review paper published in *npj Antimicrobials and Resistance* (Gadar and McCarthy., 2023).

- Chapter 2 is adapted from our paper published in *Communications Biology* (Gadar *et al.*, 2023).

    - Membrane permeability analysis and assessment of the combination treatment against clinical strains was conducted by Dr Despoina Mavridou and Dr Nikol Kaderábková, our collaborators at the University of Texas.

    - *A. baumannii* derivative strains listed in Appendix A.4 were constructed by Dr Rubén De Dios, a post-doctoral researcher in our lab.

- HPLC on the tormentil derivatives in chapter 3 was conducted by our collaborators at Trinity College Dublin.

Contents

List of Figures

List of Tables

Chapter 1
Introduction

1.1 The Rise of Antibiotics

Up until the early 1900s, infectious diseases were the leading cause of death in England, accounting for 25% of all mortalities (ONS., 2021, Smith and Coast, 2013, Shaw-Taylore., 2020, Armstrong *et al*., 1999). During the mid-1900s, England's infectious disease mortality rate decreased to less than 1% due to Sir Alexander Fleming's discovery of the first true antibiotic in 1928, commonly known as penicillin (Smith and Coast, 2013). The term 'antibiotic' was first described in 1941, by Selman Waksman, as a small molecule produced by a microbe that possesses antagonistic properties against the growth of other microbes (Clardy, Fischbach and Currie, 2009).

The discovery of antibiotics such as streptomycin, tetracycline, and chloramphenicol soon followed. This era, spanning from 1950 to 1960, marked the Antibiotic Golden Age, a period when scientific progress and innovation reshaped the landscape of healthcare (Clardy, Fischbach and Currie, 2009). As a result of this era, millions of lives were saved, and the medical and surgical fields saw remarkable advancements (Gould and Bal, 2013). Beyond the lab, antibiotics became the frontline defence, effectively treating and preventing bacterial infections that had once posed grave threats to World War II soldiers, surgical patients, chemotherapy recipients, and individuals managing chronic conditions like diabetes (Peleg, Seifert and Paterson, 2008; Rossolini *et al*., 2014).

In the 1900s the average life expectancy in the UK was a modest 46.81 years. With the aid of antimicrobial therapy, this figure increased dramatically, reaching 81.80 years in the modern era (Price, 2016). This extension of life was not limited to the UK but had a global impact, reshaping the future of healthcare and longevity worldwide (Rossolini *et al*., 2014).

1.2 The Fall of Antibiotics

Antibiotics work by inhibiting the growth of bacteria (bacteriostatic) or by killing the bacteria (bactericidal) (Baquero and Levin, 2021). Their mechanisms of action vary but they typically target essential bacterial functions such as transcription, translation, cell wall synthesis and DNA replication. Targeting such essential processes imposes a strong negative selection pressure upon bacteria, driving the evolution of antibiotic resistance (MacLean and San Millan, 2019). This has meant that the efficacy of frontline antibiotics is being eroded continually by the spread of transmissible resistance-conferring genetic elements and the evolution of multidrug-resistant (MDR) pathogens. This has led to the antibiotic resistance crisis, a major threat to our global healthcare infrastructure and modern medicine.

The emergence of antibiotic resistance is attributed to the misuse and/or overuse of antibiotics (Ventola., 2015). The reduced efficacy of antibiotics has allowed bacterial infections to endanger millions of lives once again. A recent study suggests that 41% of oncologists have seen a rise in antibiotic-resistant infections within the past 12 months, with 5% of their surgical patients already developing antibiotic-resistant infections. When extrapolated globally, 65,000 surgical cancer patients could develop life-threatening antibiotic-resistant bacterial infections within the next decade (Longitude Prize, 2020). Statistics show that deaths in the UK due to antibiotic-resistant pathogens have increased from 2110 to 2202 from the years 2021 to 2022 (Mahase, 2023).

On a global scale, the death toll is expected to rise from an annual 700,000 deaths to a staggering 10 million deaths by the year 2050 (Price, 2016, O'Neill, 2014). The scale of mortality in this underreported crisis is akin to other major threats facing humanity such as the climate emergency, with 4.95 million deaths associated with bacterial antimicrobial resistant (AMR) infections in 2019, compared to 5.08 million deaths due to climate change (Zhao *et al*., 2021; Murray *et al*., 2022). Worryingly, there is an emerging body of compelling evidence that climate change is exacerbating the AMR crisis, with an increased regional ambient temperature being associated with a higher prevalence of antibiotic resistance (MacFadden *et al*., 2018; Li *et al*., 2023).

The options for effective treatment against MDR bacteria are limited as first- and second-line antibiotics have been rendered less effective. This predicament compels healthcare professionals to resort to antibiotics that not only possess greater toxicity but also pose heightened risks to patients, and often carry a more substantial financial burden (Lushniak, 2014). Studies have shown that patients afflicted by these MDR infections experience prolonged hospital stays, enduring an additional 6.4 to 12.7 days of treatment (Golkar, Bagasra and Pace, 2014).

Our current systems and infrastructure for the clinical development of antibiotics and their transition from the bench to the bedside are failing with an exponential decline in the number of newly developed and approved antibiotics over the last three decades (Ventola, 2015). The significant costs and time associated with bringing a new class of antibiotics to the market and their lack of financial return have disincentivised the pharmaceutical industry. As a result, most multinational pharmaceutical companies have shelved their antibiotic development pipelines over the last two decades and many start-ups folding under these significant pressures. This maelstrom of exits has created a major vulnerability in our healthcare infrastructure driving alarming increases in the number of deaths associated with antibiotic-resistant infections (Murray *et al*., 2022).

The financial burdens associated with treating antibiotic-resistant infections are also a major consideration with the estimated medical cost of one patient with an antibiotic-resistant infection in the US ranging from 18,588 to 29,069 (Golkar, Bagasra and Pace, 2014). Collectively, this financial liability, placed on the US economy, adds 20 billion a year to healthcare costs (Golkar, Bagasra and Pace, 2014). With the increasing rates of AMR, it is predicted that the annual cost of AMR could rise to 100 trillion by 2050 (Dadgostar, 2019). This is forcing a global rethink of how we bring new antibiotics to market and driving more research into the exploration of alternatives to traditional antibiotics such as phage, vaccines and virulence targeting next-generation antimicrobials (NGAs). Additionally, the repurposing of existing drugs as anti-virulence treatments has gained momentum, providing rapid development with a lower cost, and expanding the range of potential combination therapy options.

1.3 Clinical Significance of *Acinetobacter baumannii*

Acinetobacter baumannii is a Gram-negative opportunistic pathogen that has demonstrated a significant role in the prevalence of multidrug-resistant (MDR) infections. It is recognised as the number one critical bacterium under WHOs priority pathogen list for research and development of novel antibiotics (World Health Organisation., 2024). *A. baumannii* is also the top priority on the list of most threatening ESKAPE organisms, consisting of *Enterococcus faecium, Staphylococcus aureus, Klebsiella pneumoniae*, *A. baumannii*, *Pseudomonas aeruginosa*, and *Enterobacter species*. An ESKAPE organism can develop resistance to antibiotics by using resistance mechanisms (Boucher *et al*., 2009; Mulani *et al*., 2019).

A. baumannii is associated with a spectrum of infections, both within hospital settings and the wider community. Predominantly, it is recognised for its role in wound infections, bloodstream infections (BSI) and pneumonia affecting individuals in hospitals and the community (Dexter *et al*., 2015). Common clinical manifestations of *A. baumannii* BSIs include fever, severe sepsis, skin rash, or alterations in mental states (Park *et al*., 2017). These symptoms serve as critical indicators for identifying and addressing *A. baumannii* infections. *A. baumannii* BSIs within an ICU setting have been associated with a mortality rate ranging from 34% to 43.4%. In contrast, outside the ICU, the mortality rate is notably lower at 16.3% (Wisplinghoff *et al*., 2004).

Hospital-acquired pneumonia (HAP) and ventilator-associated pneumonia (VAP) stand out as significant clinical manifestations caused by *A. baumannii*. This respiratory condition manifests with distressing symptoms such as dyspnoea, fever, and a productive cough (Brotfain *et al*., 2017). The mortality rate attributed to HAP is reported to range from 35% to 70%, with earlier studies showing a mortality rate varying from 23% to 68% (Leung *et al*., 2006; Maragakis and Perl, 2008; Freire *et al*., 2010). Concurrently, the mortality rate for VAP is 30% to 70% (Chouhdari *et al*., 2018). However, attributing a specific cause of death in cases of comorbidities still remains challenging.

1.4 Epidemiology

Historically, *A. baumannii* is known as the ‘Iraqibacter’ due to its prevalence in US military

hospitals based in Iraq, Kuwait and Afghanistan during the Iraq War (Scott *et al*., 2007, CDC., 2004). The prevalence of MDR *A. baumannii* among clinical isolates in the Middle East is 4.6% (Lob *et al*., 2016). The origins of these outbreaks may be linked to the bacterium's natural presence in the soil of these temperate climates (Eveillard *et al*., 2013; Erdönmez, Rad and Aksöz, 2017). The MDR strains of *A. baumannii* that originated within these military settings were then found to spread beyond the army to civilian healthcare settings. The emergence of MDR *A. baumannii* strains is believed to be linked to the return of wounded soldiers from war zones seeking treatment in hospitals (Villegas and Hartstein, 2003; Peleg, Seifert and Paterson, 2008, Scott *et al*., 2007).

Research findings highlight a concerning trend regarding *A. baumannii*, particularly in military and civilian contexts. In a military burn centre, a study spanning from 2003 to 2008 revealed a notable increase in the prevalence of *A. baumannii*, reaching 22% (Keen *et al*., 2010). Moreover, a retrospective analysis of military personnel infected with *A. baumannii* during the Iraq War emphasised a significant prevalence of antimicrobial resistance in this pathogen (CDC, 2004). Focusing on Europe, the WHO and the European Centre for Disease Prevention and Control (ECDC) provided insights into the status of carbapenem-resistant *Acinetobacter spp*. in 2020. Across 38 countries and areas, substantial variations were observed. Three nations reported low occurrence rates below 1% and 35 countries reported alarming rates of 50% or higher, particularly in Southern and Eastern Europe (European Centre for Disease Prevention and Control., 2022).

The emergence of these infections likely stems from *A. baumannii*'s rapid evolution of antibiotic resistance mechanisms. These mechanisms act as shields against the efficacy of antimicrobial agents, fostering the emergence and persistence of resistant *A. baumannii* strains (Bernards *et al*., 2004; Handel, Regoes and Antia, 2006; Asif, Alvi and Rehman, 2018). Several studies have documented the devastating consequences of these antibiotic-resistant strains on vulnerable patients in intensive care units (ICUs). This increase can be attributed to the utilisation of increasingly invasive diagnostic and treatment procedures (Bergogne-Bérézin and Towner, 1996; Zhou *et al*., 2019).

Community-acquired infections, on the other hand, tend to be prevalent in regions with hot and humid climates and among immunocompromised individuals such as patients

undergoing chemotherapy, neonates, patients haemological disorders or chronic lung diseases such as chronic obstructive pulmonary disease (COPD) and cystic fibrosis. Additionally, those who engage in excessive alcohol consumption and smoking are also at risk of *A. baumannii* infections (Dexter *et al*., 2015; Cavallazzi and Ramirez., 2022; Cavallo *et al*., 2023). Notably, community-acquired *A. baumannii* infections have been associated with a high mortality rate of 68%, possibly due to inappropriate antimicrobial therapy (Patamatamkul *et al*., 2017). These challenges underscore the urgent imperative to develop novel antibiotics that can effectively combat *A. baumannii* infections.

1.5 *A. baumannii* Resistance Mechanism

Our antibiotic armamentarium against *A. baumannii* infections initially included carbapenems, such as imipenem (Nguyen and Joshi., 2021, Shafiee *et al*., 2021, Penwell *et al*., 2015, Turner and Greenhalgh, 2003). Although these drugs remained effective against carbapenem-susceptible *A. baumannii* isolates, multiple studies have revealed their ineffectiveness against multidrug-resistant (MDR) *A. baumannii* strains (Kuo *et al*., 2012; Su *et al*., 2012). The spectrum of resistance increased following further exposure to other antibiotics to combat the resistance, ultimately leading to strains that exhibited susceptibility solely to polymyxins and tigecycline antibiotics (Gordon and Wareham, 2009). Further complicating matters, the emergence of pandrug-resistant *A. baumannii* isolates, demonstrating resistance to all known antibiotics, was later observed (Hameed *et al*., 2019; Rangel *et al*., 2020). The evolution of resistance mechanisms underscores the growing imperative for research into antibiotic-resistant *A. baumannii* and the development of effective strategies to counteract it.

Of particular concern is the emergence of colistin-resistant *A. baumannii*, as colistin represents the last-resort antibiotic in our arsenal. To address this pressing challenge, it is essential to delve into the mechanisms employed by *A. baumannii* in evolving antibiotic resistance, as outlined below.

1.5.1 Inactivation of β-lactams

β-lactams, a class of antibiotics characterised by the presence of a beta-lactam ring in their

molecular structure, are proficient in their ability to hinder susceptible *A. baumannii* from synthesising a stable cell wall. This bacteriostatic effect is accomplished by inhibiting key enzymes known as Penicillin-Binding Proteins (PBPs), including carboxypeptidase, which plays a crucial role in peptidoglycan synthesis. The *β*-lactam antibiotics covalently bind to these PBPs, strategically situated on the cytoplasmic membrane of bacterial cells, thus preventing these enzymes from crosslinking with peptidoglycan chains. This cross-linking is essential for the construction of the cell wall, cell growth, and cell division. When these critical processes are disrupted, the autolytic system is activated, ultimately leading to the lysis of the bacterial cell (Zeng and Lin., 2013). However, *A. baumannii* in response acquired *β*-lactamase enzymes that hydrolyse the beta-lactam ring, rendering the antibiotic agent ineffective (Smith *et al*., 2018; De Rosa *et al*., 2021).

The analysis of sequence homology has facilitated the identification of four classes of *β*-lactamases. In Table 1, the different classes of *β*-lactamases in *A. baumannii* and their corresponding proteins are presented. A diverse array of class A *β*-lactamases have been found within *A. baumannii*; however, these enzymes have limited impact on the bacterium's resistance to the antimicrobial effects of *β*-lactams due to their narrow substrate spectrum and can be inhibited by substances like clavulanic acid. Class B *β*-lactamases, also detailed in Table 1, require heavy metal catalysis, particularly zinc, to hydrolyse *β*-lactams. These metallo-*β*-lactamases (MBLs), identified in *A. baumannii*, possess a wide substrate spectrum and exhibit potent carbapenemase activity, thereby conferring resistance to all *β*-lactam antibiotics, except monobactams (Jeon *et al*., 2015). Class C *β*-lactamases encompass naturally occurring AmpC enzymes, which exhibit resistance to penicillin, cephamycins, cephalosporins, and combination therapies involving *β*-lactamase inhibitors. This resistance is particularly notable when these enzymes are overexpressed (Jeon *et al*., 2015). Class D *β*-lactamases are referred to as OXA enzymes, as they are able to hydrolyse isoxazolylpenicillin oxacillin more rapidly than benzylpenicillin (Jeon *et al*., 2015). They also possess the capability to hydrolyse extended-spectrum cephalosporins and render carbapenems inactive (Perez *et al*., 2007). Sub-groups of OXA carbapenemases, identified in *A. baumannii*, are outlined in Table 1.

1.5.2 Modification of Aminoglycosides

Aminoglycosides, recognised for their broad-spectrum antibiotic properties, exert their action by disrupting bacterial protein synthesis, ultimately leading to cell death (Krause *et al*., 2016). Aminoglycoside resistance is more complex than resistance to most other antibiotics. Resistance arises from the exchange of coding genes among diverse pathogenic bacteria through various mechanisms, including plasmid exchange, integrons, transposons, transformation, and transduction. These genes encode aminoglycoside-modifying enzymes (AMEs), encompassing phosphotransferases, acetyltransferases, and adenyltransferases, which possess the ability to chemically alter aminoglycosides, rendering them ineffective (Lin and Lan, 2014). For resistance to arise there must be double mutations in these AME encoding genes, for example in aminoglycoside 2"-O-phosphotransferase (*aph2''*), mutations such as N196D/D268N and R92H/D268N can lead to aminoglycoside resistance (Toth *et al*., 2011).

In a previous investigation, PCR and PCR multiplex were used to detect the presence of AME genes in 100 clinical isolates. This study found a correlation between high aminoglycoside MIC levels and the presence of AME genes (Jouybari *et al*., 2021). Similarly, a study by Saleh *et al*. 2023, found the presence of six AME genes in aminoglycoside-resistant clinical isolates of *A. baumannii*. This underscores the pressing need for innovative strategies in the battle against aminoglycoside resistance.

1.5.3 Alteration of Target Sites

Modifications in antibiotic target sites have been proven to drive antibiotic resistance in *A. baumannii*. When alterations occur in penicillin-binding proteins (PBPs), their affinity for imipenem can diminish, potentially leading to imipenem resistance. Moreover, when these modified PBPs are overexpressed, they can reduce imipenem's efficacy, as the antibiotic's entry into bacterial cells becomes compromised (Montaner *et al*., 2023). Similarly, the insertion of a sequence within the gene responsible for encoding PBP6b's target site has been acknowledged as a contributor to carbapenem resistance, although further analysis is required to elucidate the underlying mechanisms (Cayô *et al*., 2011). Furthermore, in the context of quinolone-resistant *A. baumannii* isolates, studies have uncovered mutated *gyrA* and *parC* gyrase genes. Alterations at Ser-83 within *gyrA* encoding genes have been pinpointed as the source of

resistance (Liu *et al*., 2012, Roy *et al*., 2021).

1.5.4 Efflux Pumps

Efflux pumps have emerged as mediators of antimicrobial resistance in *A. baumannii*, mounting effective defences against a spectrum of antibiotics, including tigecycline and imipenem (Wang *et al*., 2019, Amiri *et al*., 2019). Comprising of three integral components - the outer membrane channel, the periplasmic lipoprotein, and the inner membrane transporter - these efflux pumps play a pivotal role in the microorganism's ability to modulate its internal environment.

The mechanism of efflux pumps can involve the upregulation of a single component or multiple components, all strategically designed to enable the microorganism to maintain its internal equilibrium by expelling substances from the cell, including antibiotics (Sharma *et al*., 2023). This expulsion mechanism culminates in the release of antibiotics from the cell, ultimately leading to a reduced accumulation of the drug within the bacterial cell. Consequently, this raises the minimum inhibitory concentration of the antibiotic required to inhibit bacterial growth.

Studies have classified four principal categories of efflux pumps within *A. baumannii*, each contributing to resistance mechanisms. These categories encompass the resistance-nodulation-division (RND) superfamily, the small multidrug resistance (SMR) family transporters, the major facilitator superfamily (MFS), and the multidrug and toxic compound extrusion (MATE) family (Siasat and Blair., 2023). These multifaceted efflux systems collectively underscore the intricacies of *A. baumannii*'s defence mechanisms against antibiotics. Among the array of efflux pumps, the MFS (Major Facilitator Superfamily) and RND (Resistance-Nodulation-Division) transporters have drawn the focus of numerous relevant studies. The MFS efflux pumps, with their encoded genes carried by genetic elements, have become pivotal players in gaining resistance. Notably, genes such as *tetA* and *cmlA* have been identified as key players in conferring resistance to tetracycline and chloramphenicol (Beheshti *et al*., 2020, Coyne *et al*., 2011).

Resistance to fluoroquinolones or imipenem in *A. baumannii* isolates is associated with the MATE family of efflux pumps; specifically, an H-coupled pump designated AbeM (Hou *et al*., 2012, Darby *et al*., 2023). Mutated AbeS SMR pumps, on the other hand, have been

shown to confer resistance against chloramphenicol and erythromycin in *A. baumannii* clinical isolates (Almasaudi *et al*., 2018). The RND efflux pump, AdeABC, consists of a three-component structure with implications for antibiotic susceptibility, including tigecycline and aminoglycoside resistance (Almasaudi *et al*., 2018, Nowak *et al*., 2015). Although toxic when overexpressed, AdeIJK plays a role in inducing natural resistance making its impact on acquired resistance relatively minimal. Meanwhile, AdeFGH emerges as another contributor to multidrug resistance (MDR) when its expression is increased (Coyne, Courvalin and Périchon, 2011, Sun *et al*., 2014, Darby *et al*., 2023).

1.6 Colistin mechanisms of action

Polymyxin B and colistin (Polymyxin E) belong to a group of 5 polycationic peptide antibiotics. These two differ from their relatives as they are the only two that display bactericidal effects against *A. baumannii* and are therefore used clinically. Furthermore, they differ from each other with disparate efficacies against the bacteria due to a single amino acid discrepancy (Liu *et al*., 2014). In comparison to colistin, polymyxin B is able to reach its target faster as it is not reliant on the conversion to an active drug form from a prodrug (Sandri *et al*., 2013). On the other hand, the concentration of polymyxin B that is safe to use in combination therapy is restricted in order to prevent nephrotoxicity, despite its favourable pharmacokinetics (Dubrovskaya *et al*., 2015).

Colistin has also been reported to cause nephrotoxicity and neurotoxicity in the past; however, upon re-evaluation, the incidence rate of toxicity caused by colistin has become less frequent and severe in comparison to prior reports. This reduction in toxicity may be due to the avoidance of concurrent administration of colistin and other nephrotoxic and/or neurotoxic drugs, monitored and careful dosing and/or an improved formulation of colistimethate sodium (Falagas *et al*., 2006).

Colistin is proposed to exert rapid bactericidal effects on *A. baumannii* via a two-step mechanism, shown in Figure 1.1. This commences with the initial fusion of colistin to lipid A, the innermost region of the outer membrane (OM) component, lipooligosaccharide (LOS). This occurs due to the electrostatic interactions between the anionic phosphate groups on lipid A and

the cationic diaminobutyric acid (Dab) residues of colistin. During this interaction, the divalent cations, Mg^{2+} and Ca^{2+}, on the negatively charged phosphate groups of membrane lipids, are competitively displaced by colistin. In turn, this destabilises the LOS molecules, causing permeability changes and thus, be able to permit the uptake of colistin. Once colistin has entered the OM, it can then destabilise the cell's cytoplasmic membrane causing leakage of cell contents and cell lysis (Falagas and Kasiakou, 2005; Li *et al*., 2005; Kaye *et al*., 2016; Andrade *et al*., 2020; Gogry *et al*., 2021).

Colistin has also been found to exhibit antibacterial activity through vesicle-to-vesicle contact. This mechanism is similar to the aforementioned two-step mechanism; however, the cationic colistin molecules bind to the anionic phospholipid vesicles after entering through the OM. Thus, resulting in the fusion of the inner leaflet of the OM with the outer leaflet of the cytoplasmic membrane. Upon fusion, phospholipid exchange occurs, which in turn promotes the loss of phospholipids. This eventually results in an osmotic imbalance and lytic cell death, as shown in Figure 1.1. (Gurjar, 2015; Kaye *et al*., 2016; Andrade *et al*., 2020; Gogry *et al*., 2021).

Another mechanism of colistin is the hydroxyl radical death pathway, which involves the disruption of respiration enzymes causing multiple downstream effects. As colistin transits through the outer membrane (OM) and crosses the inner membrane (IM), it interacts with key components of the electron transport chain. This interaction may disrupt ATP production, induce redox imbalance, and lead to oxidative stress. One potential consequence is the generation of superoxide (O_2^-), which can be converted into hydrogen peroxide (H_2O_2) by superoxide dismutase (SOD). The H_2O_2 is then available to oxidase ferrous iron (Fe^{2+}) into ferric iron (Fe^{3+}). This reaction is designated Fenton's reaction and induces oxidative damage to the bacteria's proteins, lipids and DNA via the production of reactive oxygen species (ROS), resulting in cell death. This mechanism was shown to occur in polymyxin-sensitive MDR *A. baumannii* isolates, as illustrated in Figure 1.1 (Yu *et al*., 2015; Andrade *et al*., 2020; Gogry *et al*., 2021).

However, the effects of colistin on respiration enzymes extend beyond ROS production; they may also lead to the accumulation of toxic metabolites through alternative metabolic pathways, such as fermentation (El-Sayed Ahmed *et al*., 2020).

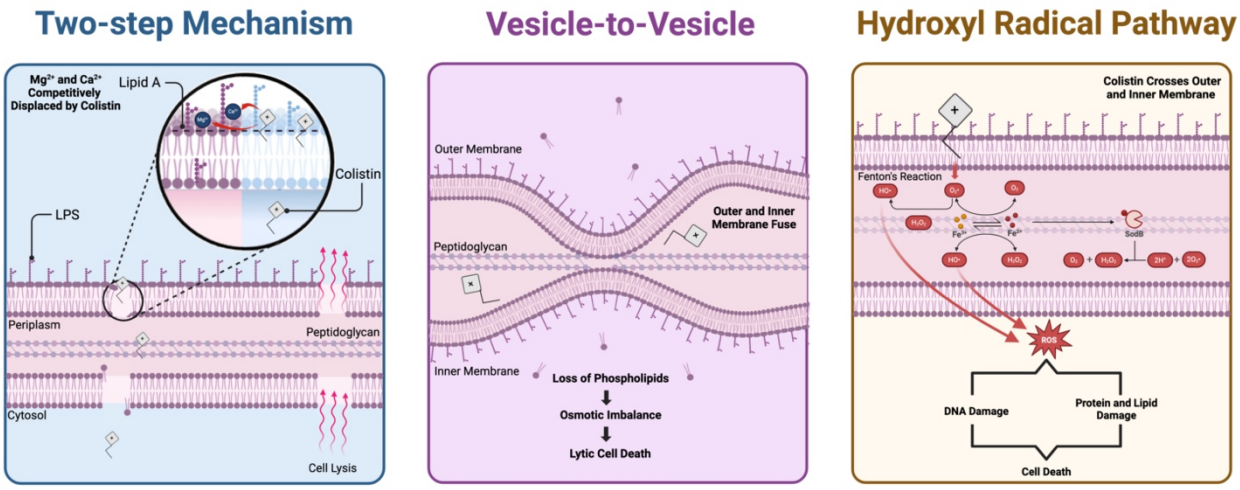

Figure 1.1: Mode of action of colistin in gram-negative bacteria. A) In the two-step mechanism of colistin the Dab residue of colistin displaces the Mg^{2+} and Ca^{2+} on the outer membrane and disrupts the outer and inner membrane leading to cell lysis. B) The colistin molecules bind to the anionic phospholipid vesicles leading to outer and inner membrane fusion. This results in a loss of phospholipids an osmotic imbalance and lytic cell death. C) In the hydroxyl radical pathway colistin acts via the production of ROS in Fenton's reaction causing DNA, protein and lipid damage, resulting in cell death.

The inhibition of the respiratory enzyme's pathway is considered a secondary mechanism of colistin. In *A. baumannii*, the respiratory chain consists of three complexes with quinones and reduced nicotinamide adenine dinucleotide (NADH). These complexes transport both electrons and protons between larger protein complexes. Colistin has been found to inhibit quinone oxidoreductase, an alternative NADH-dehydrogenase, activity within this chain within *A. baumannii* (Deris *et al*., 2014; Andrade *et al*., 2020; Gogry *et al*., 2021).

1.7 Emerging colistin resistance mechanisms in *A. baumannii*

A. baumannii has developed a wide range of resistance mechanisms to combat the antibacterial activity of colistin. These mechanisms include the use of efflux pumps, a complete loss of lipooligosaccharides (LOS) and modifications to lipid A, which is present in the LOS of the bacteria's outer membrane. The outer membrane of *A. baumannii* is an asymmetric barrier that

consists of an inner leaflet composed of glycerophospholipids and an outer leaflet composed of LOS. LOS has a tripartite structure comprising of lipid A, that anchors LOS to the outer leaflet of the OM; the core oligosaccharide (herein core), that in unison with lipid A, aids in maintaining the integrity of the OM; and lastly, O antigen polysaccharides, which connects with the herein core and has repeating oligosaccharide units that are in contact with the external environment of the cell (Whitfield and Trent, 2014).

In addition to maintaining the integrity of the cell, LOS increases the rigidity of the cell and decreases its permeability. The lipid A of LOS is the endotoxin that is recognised at picomolar levels by toll-like receptor 4 (TLR4) and enables cationic antimicrobial peptides (CAMPs) to adhere to them and initiate cell lysis. The mechanisms that mediate resistance to colistin are described in greater detail below. The evolution of colistin-susceptible to -resistant strains, under the exposure of antibiotics, is increasingly reported within clinical settings, as well as in laboratory settings (Rolain *et al*., 2011; López-Rojas, Smani and Pachón, 2013; Hraiech *et al*., 2014; Sun *et al*., 2020). This intensifies the importance of investigating the evolutionary pathways that determine the rate and extent of gained resistance, and what the mediating mutations are.

1.7.1 LOS

Lipid A is produced in a nine-step process designated the Raetz pathway. The first step in the pathway is the acytalation of UDP-GlcNAc to UPD-3-O-[(R)-3-OH-C12]-GlcNAc by the enzyme LpxA (Raetz and Whitfield, 2002). The next step is the deacetylation of UDP- 3-O-[(R)-3-OH-C12]-GlcNAc to form UDP-3- O-[(R)-3-OH-C12]-GlcN, catalysed by LpxC (Jackman, Raetz and Fierke, 1999). The third step consists of the addition of a second β-hydroxyacyl chain from acyl-ACP to generate UDP-2,3-diacyl-GlcN. This step is catalysed by LpxD (Bartling and Raetz, 2008) UDP-2,3-diacyl-GlcN is then hydrolysed by LpxH, a membrane-associated phosphodiesterase, to form lipid X. LpxB catalyses the condensation of lipid X and UDP-2,3-diacyl-GlcN to generate tetracylated disaccharide 1-monophosphate (DSMP) (Babinski, Kanjilal and Raetz, 2002) LpxK, the integral membrane kinase, then phosphorylates the DSMP, at the 4’ position to form lipid IVA (Garrett, Que and Raetz, 1998). Secondary acyl chains and 3-deoxy-D-manno-oct-2-ulosonic acid (Kdo) sugars are then

added to the lipid IVA at positions 2' and 3' to produce lipid A. This reaction is catalysed by the enzymes LpxL and LpxM, respectively (Whitfield and Trent, 2014).

Colistin resistance can occur due to the complete loss of LOS in *A. baumannii*. Studies conducted by Moffatt *et al*. (2010) and Henry *et al*. (2012) show that the inactivation of any of the first three enzymes involved in the Raetz pathway, LpxA, LpxC or LpxD, results in the complete loss of LPS production in *A. baumannii*. The consequential complete loss of LOS triggers a cascade effect, influencing the expression of transport and biosynthesis systems. This, in turn, modifies the structure of the outer membrane (OM), causing a reduction in affinity for colistin. Notably, the downregulation of *lpxACD* expression has been identified in certain colistin-resistant *A. baumannii* isolates resulting in a decrease in LOS expression (Kabic *et al*., 2022, Ušjak *et al*., 2022, Kamoshida *et al*., 2022).

1.7.2 Target Modification

Lipid A is thought to be the key target of colistin; however, this therapeutic mechanism has been shown to be ineffective when a modification of lipid A occurs in *A. baumannii*. One modification is thought to be mediated by the two-component system (TCS), PmrABC. PmrAB consists of a response-regulator (PmrA), a sensor-kinase (PmrB) and also a phospho-ethanolamine (PetN) transferase (PmrC). When overexpressed, pmrC contributes to colistin resistance by the addition of PetN to lipid A at the 4' phosphate position (Pelletier *et al*., 2013).

In turn, this reduces the negative net charge of the OM and thus decreases the ability of colistin to bind (Beceiro *et al*., 2011). The expression of pmrC is regulated by the PmrAB components of this TCS and has been shown to occur when there is either an up-regulation in the expression of *pmrA* and/or *pmrB* (Adams *et al*., 2009; Boll *et al*., 2015; Anandan *et al*., 2017; Lopalco *et al*., 2017). A study by Sun *et al*. (2020) identified the main cause of colistin resistance to be mediated by mutations *pmrA*P102R, *pmrB*P233S, *pmrB*T235N, *pmrA*I13M and *pmrB*Q270P. In their study, the colistin resistant mutants were evolved in a laboratory from *A. baumannii* strain ATCC 19606 and were predicted to have the novel *pmrA*I13M and *pmrB*Q270P mutants. They also discovered that a second mutation alongside the *pmrA*P102R mutation, designated *miaA*I221V, led to a 4-fold increase in the bacteria's MIC for colistin.

However, the occurrence of the *miaA*I221V mutation alone had little effect on the colistin MIC (Sun *et al*., 2020).

Another study used whole genome sequencing on clinical colistin resistant *A. baumannii* isolates collected from Vietnam designated BAL505, BAL543 and BAL719. They found that isolate BAL505 harboured a H266Y mutation located in the histidine kinase domain of the pmrB gene, which may result in a gain of resistance to colistin. They also found isolates BAL543 and BAL719 to have harboured amino acid mutations L94W and P170L in the *pmrB* gene (Boinett *et al*., 2019). Additionally, the P170L mutation has previously been reported for conferring colistin resistance in clinical *A. baumannii* isolates by Arroyo *et al*. (2011); however, the other two mutations are novel and may also mediate resistance to colistin.

The MRC proteins (MRC 1-10), encoded by the *mrc-1-10* genes, also belong to the phosphoethanolamine transferase enzyme family. In a similar manner to PmrC, MRC proteins have the ability to attach phosphoethanolamine to the 1 and 4' headgroup positions on lipid A, resulting in the mediation of colistin resistance. Hameed *et al*. (2019) reported the emergence of an *mcr-1* encoded colistin-resistant *A. baumannii* strain collected from Pakistan. The occurrence of this strain suggests that this is another mechanism for the evolution of colistin resistance mediated by lipid A modifications. Additionally, the increased expression of *mcr-1* in *E. coli* has been shown to reduce virulence in *G. mellonella* and result in acute toxicity to the bacteria when overexpressed. This study highlights the cost of acquiring colistin resistance (Yang *et al*., 2017). Additionally, *mcr-2, mcr-3, mcr-4* and *mcr-4.3* genes have been reported in *A. baumannii,* contributing to colistin resistance (Lowe *et al*., 2020).

Reports highlight the genetic integration of insertion sequence elements, specifically ISAba1, upstream of the *pmrC* homolog *eptA* (ethanolamine phosphotransferase A) in international clone 2. In some instances, a single isolate of this clone harboured more than three copies of EptA. It's important to note that the mere presence of the *eptA* gene does not inherently confer resistance to colistin. However, the integration of ISAba1 may lead to the overexpression of *eptA*, consequently conferring resistance to colistin (Trebosc *et al*., 2019). Interestingly, a prior study demonstrated that the disruption of the gene encoding the global regulator H-NS by ISAba125 resulted in high colistin resistance in *A. baumannii*. This resistance was attributed to increased expression of the *eptA* gene in the mutant strain affected by ISAba125 (Deveson *et*

al., 2018). Conversely, the presence of ISAba1 upstream of the *eptA* gene occurred in both colistin-susceptible and colistin-resistant counterparts and overexpression of EptA was only detected in isolates with specific mutations, namely R127L in the *eptA* gene and A→T in position 1091 of ISAba1 (Gerson *et al*., 2019).

1.7.3 Other Resistance Mechanisms

Colistin resistance may also be attributed to mutations in genes other than *pmrAB* and *lpxACD* operon. A study conducted by Lee *et al*. (2011) reported that a decrease or loss of porin OmpW was the reason for displayed resistance in an *A. baumannii* OmpW mutant. However, the mechanism by which this may occur has not been characterised, and further research is required. Thi Khanh Nhu *et al* (2016) identified mutations in both *vacJ* and *pldA* genes that may play a role in mediating colistin resistance in clinically isolated *A. baumannii* strains, as these genes are involved in the maintenance of the outer-membrane asymmetry. Asymmetric distribution of lipids is essential for the OM to be able to maintain the integrity of the cell and to function as a barrier. The organisation of the LOS can be disrupted by the accumulation of phospholipids in the OM, resulting in increased permeability to small toxic molecules in the cell. Phospholipids in the OM inner leaflet and LOS in the OM outer leaflet are maintained by a transporter system, Vps-VacJ (Malinverni and Silhavy, 2009). PldA is a phospholipase, which also maintains OM asymmetry. Its mechanism of action consists of removing phospholipids from the OM. In clinically isolated colistin resistant mutants this enzyme was found to be increased, resulting in destabilisation in the OM (Mikheyeva *et al*., 2023). Thus, mutations in these genes may result in a decreased affinity for colistin due to the disruption of asymmetry at the OM, which is the target of colistin (Thi Khanh Nhu *et al*., 2016).

Colistin resistance in *A. baumannii* facilitated by efflux pumps, still awaits comprehensive characterisation. However, a study investigating genes *A1S_1772* (*emrB*) and *A1S_1773* (*emrA*) has unveiled an intriguing connection. These genes are co-transcribed as a single operon, orchestrating the efflux pump EmrAB, which has been linked to colistin resistance, however, the mechanism remains unknown (Lin, Lin and Lan, 2017). Boinett *et al* (2019) identified disruption mutations in genes (*baeR*) that are involved in the *baeSR* TCS in

clinical colistin resistant *A. baumannii* isolates collected from Vietnam. These mutations may result in the over-expression of efflux pumps, AdeIJK and MacAB, that have been shown to mediate colistin resistance in *A. baumannii* (Lin, Lin and Lan, 2017). Another noteworthy study delved into the influence of NaCl on *A. baumannii* strain ATCC 17978, uncovering a response where eighteen genes experienced upregulation. This cluster of genes includes those encoding efflux transporters, which appear to orchestrate a defence against various antibiotics, colistin included (Hood *et al*., 2010). Furthermore, a study led by Ni *et al*. (2016) observed that the utilisation of efflux inhibitors, such as cyanide 3-chlorophenylhydrazone (CCCP), led to a reduction in the MIC of colistin in *A. baumannii*. These collective findings strongly imply a role for efflux pumps in colistin resistance in *A. baumannii.*

Table 1.1: Antimicrobial resistant mechanisms in *A. baumannii* and their associated proteins.

Resistance Mechanisms	Class or Family	*A. baumannii* Protein	References
β-lactamases	Class A	CARB-4	Ramirez *et al*., 2009
		CRAB-10	Potron *et al*., 2009
		CTX-M-2	Nagano *et al*., 2004
		CTX-M-15	Potron *et al*., 2011
		GES-1, GES-5	Al-Agamy *et al*., 2017
		GES-11,GES-12,GES-14	Bogaerts *et al*., 2010
		KPC-2	Martinez *et al*., 2016
		KPC-10	Robledo *et al*., 2009
		PER-1	Aly *et al*., 2016
		PER-2	Pasteran *et al*., 2006
		PER-7	Bonnin *et al*., 2011
		SCO-1	Poirel *et al*., 2007
		SHV-5	Naas *et al*., 2007
		TEM-1	Krizova *et al*., 2013
		TEM-92	Endimiani *et al*., 2007
		VEB-1	Poirel *et al*., 2009
	Class B	IMP-1	Tognim *et al*., 2006
		IMP-2	Riccio *et al*., 2000
		IMP-4	Chu *et al*., 2001
		IMP-5	Koh *et al*., 2007
		IMP-6	Gales *et al*., 2003
		IMP-8, IMP-24, VIM-2, VIM-3, VIM-11	Lee *et al*., 2008
		IMP-11, IMP-19	Yamamoto *et al*., 2011
		NDM-1	Voulgari *et al*., 2016
		NDM-2	Espinal *et al*., 2011
		SIM-1	Lee *et al*., 2005

		VIM-1, VIM-4	Papa *et al*., 2009
	Class C	AmpC	Liu *et al*., 2015
	Class D	Listed in OXA subgroups below	
	OXA-2 Subgroup	OXA-21	Vila *et al*., 1997
	OXA-10 Subgroup	OXA-128	Giannouli *et al*., 2009
	OXA-20 Subgroup	OXA-37	Navia *et al*., 2002
	OXA-23 Subgroup	OXA-23 OXA-133 OXA-239	Li *et al*., 2015 Mendes *et al*., 2009 Gonzalez-Villoria *et al*., 2016
	OXA-24 Subgroup	OXA-24 OXA-25, OXA-26, OXA-27 OXA-40 OXA-72 OXA-143 OXA-182	Acosta *et al*., 2011 Afzal-Shah *et al*., 2001 Quinteira *et al*., 2007 Kuo *et al*., 2016 Higgins *et al*., 2009 Kim *et al*., 2010
	OXA-48 Subgroup	OXA-48, OXA-48b, OXA-162, OXA-163, OXA-181, OXA-199, OXA-204, OXA-232, OXA-244, OXA-245, OXA-247	Poirel *et al*., 2004 Holden *et al*., 2021
	OXA-51 Subgroup	OXA-51 OXA-64, OXA-65, OXA-66, OXA-68, OXA-70, OXA-71 OXA-69, OXA-75, OXA-76 OXA-77, OXA-79, OXA-80, OXA-104, OXA-106, OXA-112, OXA-82, OXA-83, OXA-84 OXA-86, OXA-87	Fang *et al*., 2016 Biglari *et al*., 2017 Heritier *et al*., 2005 Evans *et al*., 2007 Vahaboglu *et al*., 2006

		OXA-88, OXA-91, OXA-93, OXA-94, OXA-95, OXA-96 OXA-92 OXA-113	Koh *et al*., 2007 Tsakris *et al*., 2007 Naas *et al*., 2007
	OXA-58 Subgroup	OXA-58	Hou et al., 2015
		OXA-96	Koh et al., 2007
		OXA-97	Poirel et al., 2008
	OXA-143 Subgroup	OXA-253	de Sá Cavalcanti et al., 2016
	OXA-235 Subgroup	OXA-235	Higgins et al., 2013
Efflux Pumps	RND Superfamily	AdeABC AdeFGH AdeIJK	Sun *et al*., 2016 He *et al*., 2015 Damier-Piolle *et al*., 2008
	MFS	TetA TetB CmlA CraA AmvA AbaF	Ribera *et al*., 2003 Vilacoba *et al*., 2012 Coyne *et al*., 2011 Roca *et al*., 2009 Rajamohan *et al*., 2010 Sharma *et al*., 2017
	MATE Family	AbeM	Su *et al*., 2005
	SMR Family	AbeS	Srinivasan *et al*., 2009
Aminoglycoside-modifying enzymes	-Aminoglycoside-acetyltransferases	AAC3 (aaC1, aaC2) AAC(6')(aacA4) ANT(2") (aadB) ANT(3") (aadA1)	Nemec *et al*., 2004 Bakour *et al*., 2014 Nemec *et al*., 2004; Lin *et al*., 2013 Nemec *et al*., 2004; Lin *et al*., 2013
	Aminoglycoside-phosphotransferases	APH(3')(aphA1) APH(3")	Gallego *et al*., 2001; Cho *et al*., 2009 Gallego *et al*., 2001; Cho *et al*., 2009

Permeability Defects	Porin	OmpA CarO Omp22-23 Omp33-36 Omp37, Omp44, Omp47 Omp43	Wu *et al*., 2016 Jin *et al*., 2011 Bou *et al*., 2000 Tomas *et al*., 2005 Quale *et al*., 2003 Dupont *et al*., 2005
Modification of Target Sites	PBP Alteration	PBP2	Gehrlein *et al*., 1991
	16S rRNA Methylation	ArmA	Bakour *et al*., 2014
	Ribosomal protection	TetM	Ribera *et al*., 2003
	DNA Gyrase	GyrA/ParC	Higgins *et al*., 2004
	Dihydrofolate Reductase	DHFR, FolA	Lin *et al*., 2013; Mak *et al*., 2009
	Lipooligosaccahrides	PmrC, LpxA, LpxC, LpxD	Arroyo *et al*., 2011

1.8 Tolerance, Persistence and Hetero-resistance

The terms ‘tolerance’ and ‘persistence’ are described as modes of survival for bacteria that were able to survive antimicrobial treatment but do not possess resistance mutations (Huemer ., 2020). Unlike resistance, tolerance and persistence allow the bacteria to survive in high concentrations of the antimicrobial without changing the MIC. Instead, the minimum duration for killing 99% of the bacteria is increased (MDK99). Survival of tolerant bacteria is achieved by the essential bacterial processes being slowed down; for example, the process of assembling the cell wall is slowed down in the presence of *β*-lactams. In turn, this prevents the bacteria from dying as the *β*-lactams only affect active cell wall assembly (Geisinger *et al*., 2020). This mechanism causing intrinsic colistin tolerance has been associated with over 30 different genes in *A. baumannii* (Hood *et al*., 2013).

Persistence also increases the MDK but differs from tolerance and resistance as it occurs when the majority of the population is killed. A small subpopulation of the persistent bacteria remains, resulting in a biphasic time-kill curve (Balaban *et al*., 2004). A similar phenotype has been previously described by Li *et al* (2006) as hetero-resistance. This poorly understood phenomenon may be caused by the emergence of a subpopulation of resistant bacteria derived from its susceptible population (MIC 2 mg/L). This phenotype has since been reported in *A. baumannii* in a number of studies; however, the mechanism by which this occurs has not yet been explained (Cai *et al*., 2012; Falagas *et al*., 2010; Yau *et al*., 2009; Sherman *et al*., 2019).

1.9 Pathogenesis/Virulence

The pathogenesis and virulence of *A. baumannii* have been extensively researched, however, despite the progress made, there is still a major lack of knowledge surrounding *A. baumannii*’s repertoire. The mechanisms that contribute to the success of *A. baumannii* are of great interest to researchers/clinicians, due to the limited number of traditional virulence factors, of which most are not conserved across all strains (Morris *et al*., 2019). However, phenotypic and genomic analyses of the pathogen have identified new potential virulence factors responsible for the bacteria’s pathogenicity. These proposed factors are described below.

1.9.1 Outer membrane proteins

Outer membrane proteins (OMPs) are integral membrane proteins that are anchored within the outer membrane of the bacteria. They consist of β barrel structures formed by 8 to 26 strands; between the strands on the extracellular side, there are large extended loop structures and short loops on the periplasmic side. These loops provide the OMPs with high stability within the membrane even in harsh environments (Rollauer *et al*., 2015). Outer membrane protein A (OmpA) is an outer membrane protein in *A. baumannii* that contributes significantly to the virulence of the bacterium. It has been shown to form an eight-stranded β barrel, consisting of a 2 nm pore diameter and a C-terminal periplasmic globular extension and can accommodate molecules that are up to 500 Da (Choi *et al*., 2008). OmpA is also an abundant and highly conserved *A. baumannii* virulence factor. The protein was found to be abundant in 103 clinical isolates, with 83 showing a 99% sequence identity and the most diverse isolate showing an 85% sequence identity (Ahmad *et al*., 2016; Jahangiri *et al*., 2017). OmpA is thought to contribute to a reduction in outer membrane permeability in *A. baumannii* (Sugawara and Nikaido, 2012). OmpA can be present on the surface of the bacterial cell or concentrated in the outer membrane vesicles. Here it can interact and bind with the host epithelial cells and thus adhere to cell surface death receptors. Binding to the surface death receptors thus induces cell cytotoxicity (Ahmad *et al*., 2016). Following internalisation, OmpA is translocated to the nucleus or the mitochondria. OmpA can translocate to the nucleus depending on its nucleus localisation signal (KTKEGRAMNRR) located between residues 320 and 330. In the nucleus of host cells, OmpA can cause DNA degradation in a similar manner to DNase I (Choi *et al*., 2007, 2008). On the other hand, OmpA can induce mitochondrial dysfunction when translocated into the mitochondria. Mitochondrial dysfunction is achieved through the activation of Bcl-2 family proteins, the release of cytochrome C and the stimulation of apoptosis-inducing factors. This then results in the formation of an apoptosome, leading to apoptosis of the host cell (Choi *et al*., 2005).

As an abundant factor present on the surface of *A. baumannii*, OmpA also demonstrates involvement in resistance to complement-mediated killing, as it aids in the binding of an alternative complement pathway inhibitor, factor H (Kim *et al*., 2009). OmpA has further been identified to contribute to the formation of biofilms, which in turn aids in the development of

antibiotic resistance (Richards, Abu Kwaik and Lamont, 2015).

Omp34 is a fourteen-stranded β barrel, thought to contribute to the pathogenesis of *A. baumannii* (Jahangiri *et al*., 2018). It is a highly conserved virulence factor that is present in over 1,600 strains, all consisting of a 98% sequence identity. Omp34s function is similar to that of OmpA, as it has the ability to induce apoptosis in epithelial cells. However, this is mediated through caspase-dependant mechanisms and promotes bacterial persistence in the autophagosome by inhibition of autophagy (Rumbo *et al*., 2014).

1.9.2 Phospholipase

A. baumannii harbours a pair of phospholipase C enzymes and a trio of phospholipase D enzymes, each distinguished by their distinctive cleavage sites. Phospholipase C operates by cleaving before the phosphate, yielding a head group containing phosphate Conversely, phospholipase D cleaves after the phosphate, yielding both a separate phosphate-containing head group and phosphatidic acid (Djordjevic, 2010; Cocco *et al*., 2015). These phospholipases, both C and D, are firmly established as significant virulence factors within *A. baumannii* and are under the transcriptional regulation of Fur, an iron-sulfur cluster assembly system (Isc). Both enzymes play pivotal roles in the acquisition of iron and are capable of exerting haemolytic activity on human erythrocytes (Fiester *et al*., 2016). Furthermore, the three phospholipase D genes are associated with epithelial cell invasion and resistance to serum (Stahl *et al*., 2015).

1.9.3 Siderophore-mediated iron-acquisition system

Iron is an essential nutrient requirement for *A. baumannii* as it is involved in critical processes such as DNA repair and replication and gene expression functions (Cook-Libin *et al*., 2022). It is also a crucial cofactor for enzymes such as superoxide dismutase's, cytochromes and catalases (Caza and Kronstad *et al*., 2013, Jakubovics and Jenkinson., 2001, Heindorf., 2014). Within human hosts, the abundance of iron is sequestered by iron-binding chelators, such as haemoglobin, with a high affinity for the metal (Crichton, 2009). This is to prevent cytotoxicity caused by free iron and to also control microbial infection mechanisms that iron is a requisite

for (Weinberg, 2009). However, *A. baumannii* has demonstrated iron acquisition systems that overcome this host infection prevention system (Gaddy *et al*., 2012). *A. baumannii* uses a variety of iron acquisition systems to meet its iron requirements including systems that assist in the long-term survival of *A. baumannii* in iron-deficient conditions.

A. baumannii strains can encode various siderophores that are all transcriptionally regulated by the ferric uptake regulator, Fur, which is responsible for the regulation of iron metabolism and uptake in *A. baumannii* (Ajiboye *et al*., 2018). Siderophores, released during iron acquisition, play a pivotal role in scavenging extracellular iron (Khasheii *et al*., 2012). Once bound with an iron molecule, these siderophores bind to specific receptors and are allowed entry into the cell (Page., 2019).

Within *A. baumannii*, there are three classes of siderophore iron chelators: acinetobactins, fimsbactins, and baumannoferrins (Conde-Pérez *et al*., 2021). Notably, the acinetobactin class is highly conserved in clinical isolates and serves as a versatile metal chelator with two distinct isomers. One isomer exhibits optimal activity at neutral and basic pH, while the other is more active in acidic conditions (Kim *et al*., 2021; Shapiro *et al*., 2016). Compared to baumannoferrin and fimsbactins, acinetobactin is indispensable for both growth and pathogenesis when utilising host iron sources (Sheldon and Skaar., 2020).

1.9.4 Motility

Historically, *A. baumannii* was regarded as a non-motile microorganism, primarily due to the absence of swarming motility. This lack of swarming motility can be directly attributed to the absence of flagellar genes within *A. baumannii*'s genome sequence (Clemmer, Bonomo and Rather, 2011). However, studies have shed new light on this matter. They revealed that *A. baumannii*'s genome contains the necessary genes for the assembly of type IV pili, which are integral to twitching motility. This discovery implies that *A. baumannii* is not entirely non-motile, as it can exhibit twitching motility, allowing it to rapidly spread on abiotic surfaces. This twitching ability is believed to be mediated by the action of extending and retracting type IV pili (McQueary *et al*., 2012; Vijayakumar *et al*., 2016). Furthermore, a study utilising clinical isolates has demonstrated a positive correlation between the degree of twitching motility and the sequence homology of pilin filament, emphasising the importance of these

motility components (Eijkelkamp *et al*., 2011). Type four fimbriae (TFF) also plays a significant role in *A. baumannii*'s motility and virulence. These large protein complexes, found on the bacterium's surface, are involved in its ability to move and adhere to surfaces in both abiotic and biotic environments. This adherence facilitates biofilm production, ultimately increasing the bacterium's virulence potential (Eijkelkamp *et al*., 2011; Pakharukova *et al*., 2018; Shadan *et al.,* 2023).

1.9.5 Biofilm Formation

Biofilms are communities of bacterial cells that adhere to each other or a surface and are encased in a matrix made up of structural components such as polysaccharides, proteins, and extracellular DNA (Limoli, Jones and Wozniak, 2015). Bacteria utilise biofilm as a growth mechanism, both inside and outside the host, due to the benefits it provides in terms of increased protection from antibiotics, disinfectants and the host's immune system. In comparison to cells in a planktonic state, bacteria embedded in biofilms display increased tolerance to antibiotics by over 1000-fold due to poor penetration of antibiotics, heterogeneous transcription and the presence of persister cells (Pisithkul *et al*., 2019; Uruén *et al*., 2020; Dar *et al*., 2021). These factors are all exacerbated in a poly-species biofilm where additional behaviours such as cooperation between sensitive and resistant strains or species can occur (Frost *et al*., 2018; Amanatidou *et al*., 2019). Studies have found that approximately 80% of recurrent or chronic infections are attributed to the formation of bacterial biofilms highlighting their importance in infection (Sharma, Misba and Khan, 2019). The formation of biofilms is a multi-step process that starts with the attachment of bacteria to a biotic or abiotic surface or their aggregation to each other. These microcolonies then grow and expand with the recruitment of surrounding cells or aggregates and develop into larger three-dimensional community structures with complex nutrient transportation networks. As the biofilm grows, it enters the final stage of its lifecycle, where cells detach from the biofilm and may spread as planktonic cells or aggregates, as shown in Figure 1.2 (Sauer *et al*., 2022).

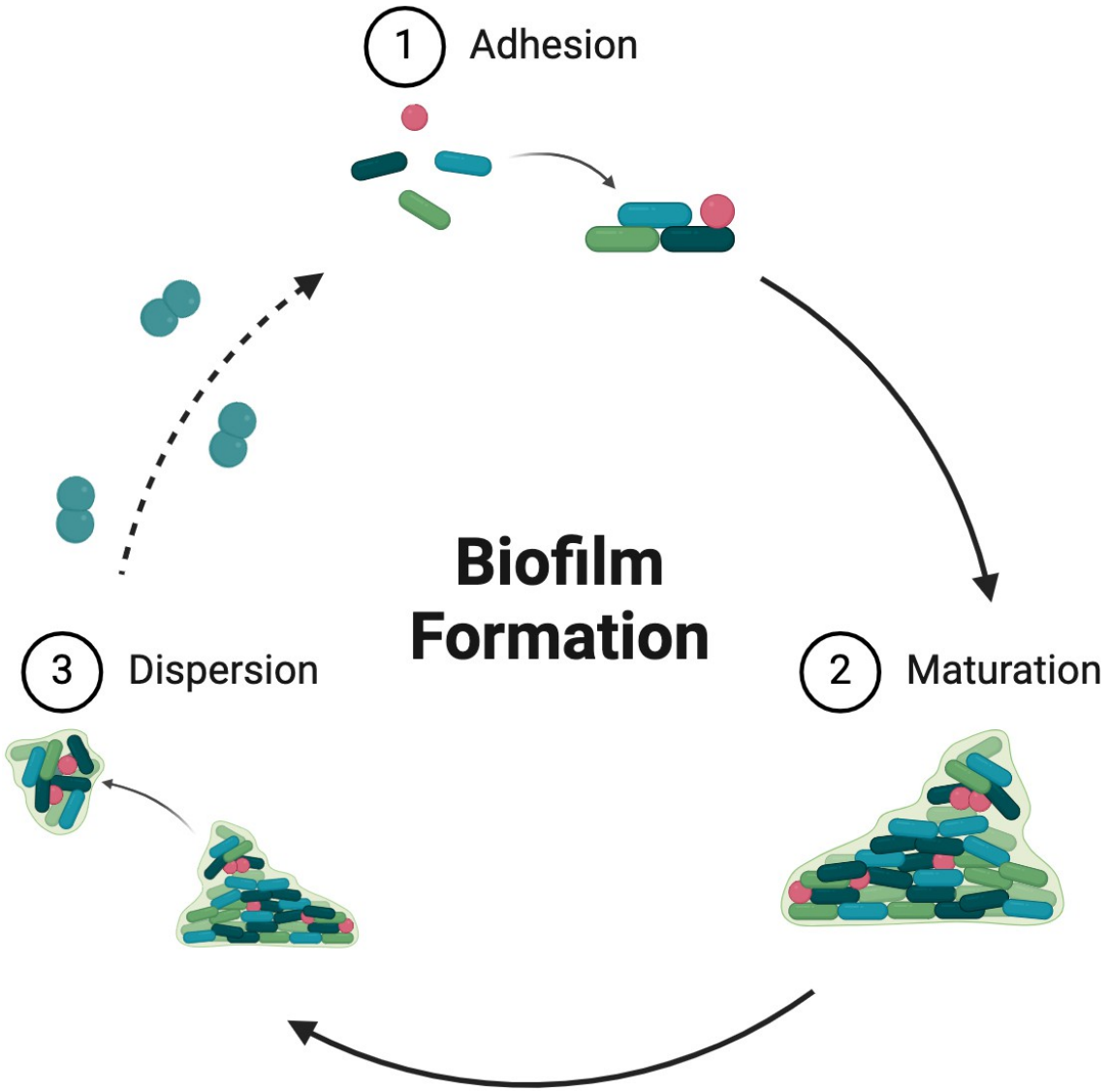

Figure 1.2: Cycle of biofilm formation. The characteristics of biofilm formation include 1. Adhesion, where motile cells aggregate together or attach to abiotic and biotic surfaces; 2. Maturation, where the microcolonies grow into a community and 3. Dispersion, where cells detach and spread as aggregates or planktonic cells. This figure was created using biorender.

Biofilm formation relies on a number of factors, among which OmpA plays a pivotal role. OmpA contributes significantly to the development of biofilms on non-living surfaces, such as plastic (Gaddy and Actis, 2009; Richards, Abu Kwaik and Lamont, 2015). This is supported by a study conducted by Schweppe *et al*. (2015), in which the use of anti-OmpA serum and antibodies effectively impeded the adherence and subsequent invasion of host cells by *A. baumannii*. Furthermore, *A. baumannii* utilises a surface protein known as biofilm-associated protein (BAP) to facilitate binding to both biotic and abiotic surfaces.

BAP also orchestrates the initiation of microcolony formation and the development of biofilm structures. Comprising of four modules labelled A, B, C, and D, along with multiple internal repeats, BAP assumes a pivotal role in stabilising mature biofilms when bound to both biotic and abiotic surfaces. This, in turn, aids in biofilm formation and fosters cell-to-cell adhesion (Gaddy and Actis, 2009; Brossard and Campagnari, 2012; Morris *et al*., 2019). A study by Loehfelm *et al*. (2008) discovered that disruptions in the bap gene resulted in diminished biofilm thickness and volume, reduced interbacterial cell adhesion, and a decreased ability to form intricate structures on non-living surfaces.

The Csu Type 1 chaperone-usher pili also plays a significant role in initiating biofilm formation and mediating cell-to-cell attachment on non-living surfaces, but not on host surfaces (Mihara *et al*., 2004; de Breij *et al*., 2009; Brossard and Campagnari, 2012). The chaperone-usher secretion system primarily falls under the regulation of the two-component system (TCS) known as BfmRS. Additionally, the GacAS TCS has been shown to have a modulatory effect on its expression (Cerqueira *et al*., 2014). The chaperone-usher secretion system is encoded in many *A. baumannii* strains within a highly conserved single six-gene operon, which includes csuA/B, A, B, C, D, and E (Pakharukova *et al*., 2018). CsuA/B polymerises in the presence of the CsuC Chaperone to form the major pilus subunit, with Csu A and B serving as minor pilin subunits. CsuD and E have been demonstrated to function as the usher and adhesive tip, respectively (Moon, Weber and Feldman, 2017).

The regulation of biofilm formation is mediated by the TCS BfmRS, as elucidated by a study conducted by Liou *et al*. (2014), showcasing that *A. baumannii* mutants lacking *bfmS* exhibited reduced biofilm production, resulting in decreased adhesion to eukaryotic cells and serum resistance when compared to the wild-type strain. Similarly, the TCS AdeRS has also been demonstrated to modulate biofilm formation where *A. baumannii* mutants lacking adeS showed a decrease in biofilm formation (Richmond *et al*., 2016).

Furthermore, environmental signals in the form of metal cations have been identified by Gaddy and Actis (2009) as aiding *A. baumannii* in surface adherence. Greene *et al*. (2016) have depicted biofilm formation as an adaptive survival response to dry and adverse conditions, with strains producing higher levels of biofilm displaying enhanced resistance to desiccation compared to those producing lower levels. This adaptation allows the bacterium to persist on

medical devices in hospital settings, potentially leading to the contact of susceptible patients in intensive care units (ICUs) that rely on these devices (Ryu, Baek and Kim, 2017).

1.9.6 Quorum Sensing

Quorum sensing (QS) systems serve as a pivotal means of communication among bacteria, playing a vital role in the regulation of various virulence factors, including motility, biofilm formation, and resistance. Within these systems, bacteria detect and respond to cell-cell signalling molecules known as acyl homoserine lactones (AHL), which, in turn, govern the activation of these virulence factors (Clemmer, Bonomo and Rather, 2011; Bhargava *et al*., 2015; Subhadra *et al*., 2018).

A. baumannii has its own QS system, referred to as AbaRI, which bears homology to the LuxRI QS system found in *Vibrio fisheri* (Bhargava *et al*., 2010). The *A. baumannii* QS system encompasses an AbaI autoinducer synthase responsible for AHL molecule production, such as N-(3-hydroxydodecanoyl)-L-HSL (Niu *et al*., 2008). When a substantial density of AHL molecules interacts with the second component of *A. baumannii*'s QS system, the AbaR AHL receptor, it triggers downstream transcriptional responses (Bhargava *et al*., 2010). In 2015, He *et al*. identified that the efflux pump AdeFGH facilitates the synthesis and transport of AHLs during biofilm formation, and this process is under the regulation of the AbaRI QS system. This finding suggests a direct association between the secretion of AHLs and multidrug efflux pumps.

1.9.7 Capsule

The capsule is a polysaccharide-rich outer layer that plays a pivotal role in virulence, biofilm formation and antimicrobial resistance within *A. baumannii*. The capsule is able to limit drug penetration against outer membrane targeting antibiotics, such as colisitin, by limiting access to the target sites on the outer membrane. It acts as a protective barrier, limiting the penetration of outer membrane-targeting antibiotics, such as colistin, by restricting access to key target sites. Studies have shown that thicker capsules are associated with more virulent *A. baumannii* strains, increased resistance to host-derived antimicrobials, and enhanced biofilm formation. Within

biofilms, bacteria exhibit high resistance to antibiotics and immune responses, and a thicker capsule further increases biofilm formation, contributing to greater antibiotic tolerance (Chin *et al*., 2018).

1.9.8 Intracellular evasion

Although *A. baumannii* is traditionally considered an extracellular pathogen, it has previously demonstrated the capacity to develop an intracellular lifestyle to persist within host cells and evade antibiotics. This intracellular lifestyle allows for the invasion of various host cell types such as macrophages, where the bacteria can resist phagocytosis and survive killing via oxidative stress, epithelial cells, which contribute to VAP infections and endothelial cells, which facilitate vascular invasion and bloodstream infections. Within these host cells, *A. baumannii* becomes shielded from antibiotics that cannot penetrate host cells effectively, these include aminoglycosides, polymyxins and beta-lactams. This intracellular persistence further enhances its resistance to antibiotics, posing a significant clinical challenge leading to chronic infections (Maure *et al.*, 2023).

1.10 Next-Generation Antibiotics

NGAs are compounds that have antivirulence properties at concentrations that do not impact bacterial viability, therefore minimising the selective pressure they apply and the probability of resistance evolution. The primary function of virulence factors in an infection context is to allow the pathogen to colonise the host (Sharma *et al*., 2017). Thus, targeting virulence factors disrupts the pathogenic potential of these bacteria making it more difficult for them to colonise the host, making them more vulnerable to clearance by the immune system and potentially rendering them more susceptible to traditional antibiotics (Figure 1.3).

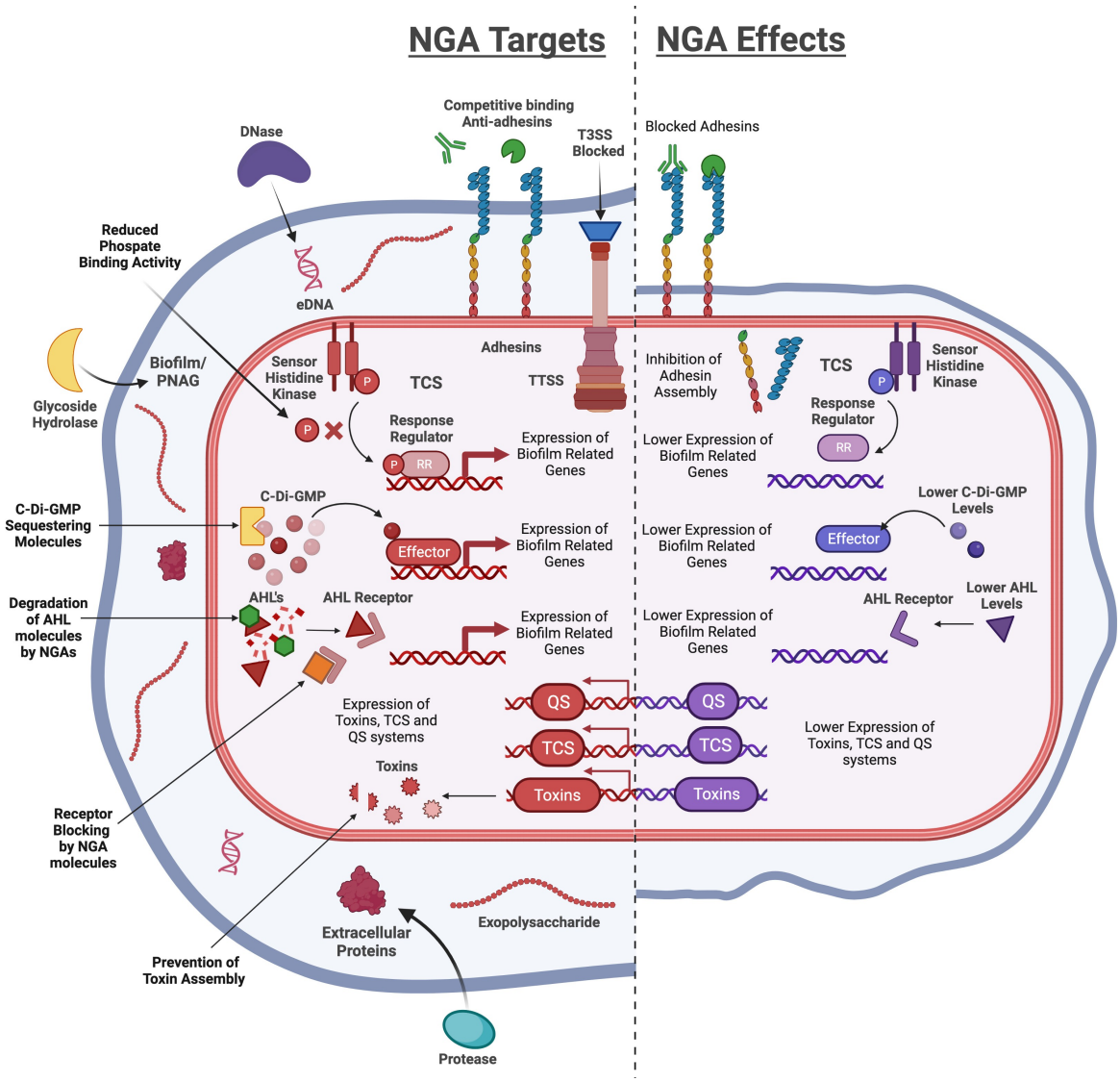

Figure 1.3: NGA targets and their impact. A summary of the different cellular and extracellular targets of NGA (left) and the impact on different virulent phenotypes (Right).

The discovery and development of next-generation antibiotics that possess pharmacological activity are heavily based on nature. Natural products played an imperative role in yielding antibiotics such as penicillin in the 1940s and tetracyclines in 1948 (Cushnie and Lamb, 2005). Over the last 4 decades, 75% of novel antibacterial compounds introduced to clinical practice have been derived from natural products, specifically in the small molecule category of approved novel chemical entities from 1981 to 2021, where more than 50% of 1,073 molecules were sourced from natural products, such as phytochemicals (Newman and Cragg, 2020).

Phytochemicals occupy a chemical space with far greater structural diversity and complexity than synthetic compound libraries that consist of simpler molecules. Natural

molecules tend to be more 'drug-like', with superior ADME/T (absorption, distribution, metabolism, excretion and toxicity) properties and more favourable toxicity profiles (Atanasov *et al*., 2015). This is in accordance with the molecular properties of Lipinski's rule of five, whereby the chemical compound has a molecular weight of less than 500 Da, less than 5 hydrogen bond donors with less than 10 hydrogen bond acceptors and a calculated Log P of less than 5 (Lipinski *et al*., 2000; Lipinski *et al*., 2001). This is due to the evolutionary pressures faced by plants, which have endured millennia of intensive selective pressure to develop small molecules that target specific pathways in bacteria to prevent colonisation. However, the toxicity and efficacy of natural antimicrobials can vary, and some may be too toxic for therapeutic use despite their potency.

Phytochemicals have also been shown to exist in a chemical space that is compatible with the basic machinery of eukaryotic cells and can interact with conserved protein domains. This allows for a high rate of novel beneficial molecules to be discovered (Li and Vederas, 2009). For example, artemisinin and quinine are used for the treatment of malaria (Saito *et al*., 2019). This is all indicative of phytochemicals representing a promising source of novel antibacterial compounds that could aid in combating the antimicrobial resistance crisis and fill the drug discovery pipeline.

1.10.1 NGA Targets and Advancements

The remarkable impact of antibiotics on human health is being eroded at an alarming rate by the emergence of multidrug-resistant pathogens. There is a recognised consensus that new strategies to tackle infection are urgently needed to limit the devasting impact of antibiotic resistance on our global healthcare infrastructure. Next-generation antimicrobials (NGAs) are compounds that target bacterial virulence factors to disrupt pathogenic potential without impacting bacterial viability. By disabling the key virulence factors required for infection, NGAs make pathogens more vulnerable to clearance by the immune system and can potentially render them more susceptible to traditional antibiotics. This section explores, the developing field of NGAs and how advancements in this area could offer a viable standalone alternative to traditional antibiotics or an effective means to prolong antibiotic efficacy when used in combination.

1.10.2 Colonisation – Disrupting the structural integrity of a biofilm

The use of extracellular enzymes that can disrupt biofilms by degrading the structural components of the biofilm matrix is one of the primary strategies for biofilm dispersal (Table 2). By focusing on the structural integrity of the biofilm, enzymes such as DNase I, PodA and NucB can induce forced dispersal of cells from the biofilm colony and release them into the environment in a more antibiotic susceptible planktonic form (Nemoto *et al*., 2003; Rice *et al*., 2007; Thomas *et al*., 2008; Nijland, Hall and Burgess, 2010; Tetz and Tetz, 2010; Sahu *et al*., 2012; Shakir *et al*., 2012; Shields *et al*., 2013; Costa *et al*., 2017; Waryah *et al*., 2017; Rumbaugh and Sauer, 2020).

Targeting Extracellular DNA

Extracellular DNA (eDNA) in biofilm functions as structural scaffolding within the matrix and can also modulate aggregation and adhesion to host cells and tissues (Okshevsky and Meyer, 2015). Many studies have shown that the addition of exogenous deoxyribonuclease (DNase) can inhibit biofilm formation in both Gram-negative and Gram-positive bacteria, without impacting bacterial growth (Sharma and Singh, 2018). DNase I cleaves biofilm-associated eDNA resulting in decreased biofilm biomass and an increased antibiotic penetration. This effect has been shown *in vitro* and *in vivo* in rat models against *A. baumannii* and a wide range of other pathogens including *P. aeruginosa, E. coli, S. aureus* and *E. faecalis* highlighting the broad-spectrum versatility of this approach (Nemoto *et al*., 2003; Rice *et al*., 2007; Thomas *et al*., 2008; Tetz, Artemenko and Tetz, 2009; Tetz and Tetz, 2010; Sahu *et al*., 2012; Waryah *et al*., 2017). Indeed, recombinant DNAse I has been used therapeutically for cystic fibrosis (CF) patients for over 20 years as a means to decrease the viscoelasticity of sputum slowing the rate of lung function decline. It is likely, based on *in vitro* data, that the DNAse is also limiting pathogen biofilm formation within the CF lung (Kaplan *et al*., 2012). DNases to treat wound biofilms are relatively underexplored in comparison but they have been shown to disrupt established biofilms and promote healing when administered in combination with silver nanoparticles *in vivo* (Patel *et al*., 2019). This disruption of mature biofilms is attributed to the cleavage of extracellular DNA by DNAse, compromising the structural integrity of the biofilm, which in turn greater penetration of DNAase enzymes (Tetz, Artemenko and Tetz, 2009). The

application of DNases to chronic diabetic wounds has also been shown to promote healing, but this is thought to occur through the breakdown of neutrophils extracellular traps (NETs). However, this suggests that a DNase-based chronic wound treatment has the potential to target both host and pathogen factors that are impediments to wound healing (Wong *et al*., 2015; Fadini *et al*., 2016).

Rather than targeting the eDNA after it has been integrated into the biofilm matrix, an alternative approach is to inhibit eDNA release. Purified pyocyanin demethylase (PodA) has been shown to inhibit the pyocyanin-dependent release of eDNA into the biofilm matrix, disrupting *P. aeruginosa* biofilm formation and limiting biofilm aggregate populations (Costa *et al*., 2017). This approach, however, will not overcome the eDNA that is available through both host and pathogen cell lysis, suggesting that the efficacy of these more targeted approaches may be limited in comparison to exogenous DNAse application (Whitchurch *et al*., 2002). Another factor to consider is that eDNA has been shown to be protected from DNase degradation by cationic exopolysaccharides such as the *P. aeruginosa* polysaccharide Pel, potentially limiting therapeutic efficacy (Jennings *et al*., 2021). The multifaceted approaches related to eDNA manipulation hold great potential in tackling *A. baumannii* infections, with the balance between disruption and protection of eDNA playing a pivotal role in their effectiveness.

Targeting Extracellular Proteins

Extracellular proteins are major constituents of the biofilm matrix (Jiao *et al*., 2010). Proteins such as biofilm-associated proteins and DNA-binding proteins play a crucial role in the adhesion, scaffolding and stability of the biofilm matrix (Hobley *et al*., 2015). The integral role of these proteins within the biofilm matrix makes them promising candidates for the development of biofilm dispersal agents. The stable yet highly reactive protease, Proteinase K, has been shown to exhibit biofilm dispersal activity *in vitro* against a wide range of bacteria (Chaignon *et al*., 2007; Fredheim *et al*., 2009; Shukla and Rao, 2013; Nguyen and Burrows, 2014; Cui, Ma and Lin, 2016). Trypsin, a pancreatic serine protease, was found to have a non-cytotoxic biofilm-degrading effect on *P. aeruginosa* (Banar *et al*., 2016). Similarly, the exogenous application of staphylococcal cysteine proteases Staphopain A (ScpA) and Staphopain B (SspB) have been shown to demonstrate biofilm dispersal abilities against

established *S. aureus* biofilms (Mootz *et al*., 2013; Loughran *et al*., 2014).

Targeting the immune system towards biofilm-associated proteins has been shown to significantly disrupt the structural lattice of eDNA and the overall biofilm. Antisera directed towards the DNABII family of proteins such as integration host factor A, IhfA, has been shown to disrupt biofilms formed by *A. baumannii* and other high-priority ESKAPE pathogens (*Enterococcus faecium, S. aureus, Klebsiella pneumoniae, P. aeruginosa, Enterobacter spp*.,) as well as numerous other clinically relevant pathogens (Goodman *et al*., 2011; Novotny *et al*., 2013). This approach has also been shown to potentiate DNase-induced biofilm damage, antibiotic killing and to increase the capacity of macrophages to kill bacteria (Goodman *et al*., 2011; Novotny *et al*., 2013). When purified *E. coli* IHF was used as an immunogen in a chinchilla animal model, with an established biofilm-associated infection, the resultant targeted immune response led to rapid resolution of the infection (Goodman *et al*., 2011). This strategy has also been shown to be effective when targeting polymicrobial biofilms within CF sputum solids (Gustave *et al*., 2013). Humanised monoclonal antibodies directed against the DNABII family of proteins have also shown remarkable efficacy in disrupting single and multispecies biofilms and potentiating antibiotic activity (Novotny *et al*., 2016; Jurcisek *et al*., 2022; Kurbatfinski, Goodman and Bakaletz, 2022). In this context, the ability to target extracellular proteins within biofilms proves to be a promising avenue for the treatment of *A. baumannii* infections, as it offers both direct disruption of the biofilm structure and enhanced immune responses against this pathogen.

Targeting Extracellular Polysaccharides

Secreted extracellular polysaccharides are key components of the biofilm matrix that contribute to the initial establishment and persistence of biofilms (Bales *et al*., 2013; Watters *et al*., 2016). Many studies have demonstrated the efficacy of dispersin B, a glycoside hydrolase produced by *Actinobacillus actinomycetemcomitans*, against established biofilm of *A. baumannii* and other pathogens such as *S. aureus, S. epidermidis, K. pneumoniae, Yersinia pestis* and *Pseudomonas fluorescens*. This glycoside hydrolase degrades the polysaccharide poly(1,6)-N- acetyl-d-glucosamine (PNAG) by hydrolysing the β(1,6) glycosidic linkages (Gawande *et al*., 2014; Waryah *et al*., 2017). Dispersin B has been used in combination with DNase 1 to limit *S. aureus*

skin colonisation and increase biocide sensitivity in an *in vivo* porcine model (Kaplan *et al*., 2018). Similarly, caspofungin, an antifungal natural product, has been shown to weaken PNAG polymerisation by inhibiting N-acetylglucosamine transferase in *S. aureus*, resulting in the structure of the biofilm matrix becoming more susceptible to fluoroquinolones *in vitro* and *in vivo* in rat models (Siala *et al*., 2016). These findings all suggest that the manipulation of extracellular polysaccharides offers a promising strategy to weaken the biofilm structure and enhance the susceptibility of *A. baumannii* biofilms to antimicrobial agents A key consideration with NGAs that are developed to target and disperse biofilms is their potential capacity to send the aggregates and/or planktonic cells into the local microenvironment, potentially facilitating the dissemination of the bacteria to different possible infection sites or triggering bacteraemia (Rumbaugh and Sauer, 2020). Therefore, their application must be carefully considered with respect to the type and location of the infection.

Reducing adhesion

The physicochemical properties of the bacterial cell surface and the receptors that decorate it, play a key role in infection, with pili binding to host cell glycoproteins for example often initiating colonisation. Disrupting surface receptor biogenesis has been shown to lead to a decrease in bacterial adhesion to host cells and tissues (Krachler and Orth, 2013). These changes have been shown to occur due to misfolding or abnormal production of chaperone-usher pili in the outer membrane, which is responsible for the assembly and secretion of fimbrial adhesins. The resultant inhibition of host receptor interactions and alteration in surface charge effectively limits bacterial adhesion (Breines and Burnham, 1994; Dal *et al*., 2002; Wojnicz and Jankowski, 2007). This suggests that targeting the assembly of pili, such as Type 1 and P pili found in *Escherichia, Salmonella, Yersinia, Pseudomonas, Klebsiella* and *Haemophilus*, may be a promising strategy for preventing bacterial infections via adhesion inhibition (Chen *et al*., 2006; Nuccio and Bäumler, 2007).

Small molecules called pilicides have been found to prevent pilus assembly and disrupt the formation of the chaperon-pilin-usher complex by binding to the active site of the periplasmic chaperones PapD and PapG that are required for the assembly of Type 1 and P pili, and thus preventing bacterial adhesion (Benz and Schmidt, 1992; Svensson *et al*., 2001; Berne

et al., 2015). Sub-inhibitory concentrations of antibiotics like ciprofloxacin and amikacin can also alter the bacterial surface, impairing adhesion to host cells (Wojnicz and Jankowski, 2007). Bicyclic 2-pyridones, such as FN075 and BibC6, have demonstrated inhibitory effects on the assembly of curli by preventing polymerisation of the major curli subunit protein CsgA (Connell *et al*., 1997; Sherlock *et al*., 2004; Sherlock, Vejborg and Klemm, 2005; Roos, Nielsen and Klemm, 2006; Nuccio and Bäumler, 2007; Cegelski *et al*., 2009). Curli, which are thinner amyloid polymers compared to fimbriae, play a role in adhesion and the formation of biofilms (Trebino *et al*., 2021).

Exploiting carbohydrates that mimic host cell surfaces is a competition-based strategy to prevent bacterial infection, with initially pioneering work by Duguid and Gillis demonstrating the anti-adhesive properties of mannose when applied to *E. coli* (Duguid and Gillies, 1957). This paved the way for the development of a vast array of sugar-based inhibitors and glycomimetic compounds that act as anti-adhesives by competitively inhibiting the binding of pathogens to host cells (Duguid and Gillies, 1957; Krachler and Orth, 2013). Multivalent compounds with increased binding avidity and monovalent inhibitors with novel aglucan moieties have been shown to inhibit uropathogenic *E. coli* (UPEC) infections by targeting the adhesive subunit FimH (Almant *et al*., 2011; Schierholt, Hartmann and Lindhorst, 2011). 3′-chloro-4′-(-d-mannopyranosyloxy) biphenyl-4-carbonitriler, a FimH inhibitor has shown promising therapeutic potential in the mouse urinary tract infection model, reducing bacterial load in the bladder by almost 1000-fold 3 h after infection while also displaying favourable pharmacokinetics, such as low toxicity and renal excretion (Kleeb *et al*., 2015).

Anti-adhesion antibodies and vaccines are also being explored as strategies to combat bacterial infections. This approach requires targeting surface-exposed antigens in order to elicit an effective immune response as the antigens must be accessible to the antibodies to enable them to bind and activate the complement system and cell lysis. These antibodies also should facilitate phagocytosis by immune cells to enhance bacterial clearance. Previous studies have demonstrated the role of monoclonal antibodies in mediating clearance of and protection against *A. baumannii* infection, which emphasizes the potential of antibody-mediated immunity in protection against *A. baumannii* (Nielson *et al*., 2017; Islam *et al*., 2023). Various approaches have been demonstrated, including immunisation with bacterial adhesins or

subunits, immunogenic peptide fragments, or DNA vaccines encoding adhesins (Krachler and Orth, 2013). Studies have targeted the *Salmonella enterica serovar Typhi* adhesin T2544 using a T2544 antiserum that enhances the uptake and clearance of bacteria by host macrophages and complement-mediated lysis in mice (Ghosh *et al*., 2011). Although antigenic variability may pose challenges, many adhesins are conserved and could serve as promising vaccine candidates for *A. baumannii* infections. By focusing on reducing bacterial adhesion through various methods, we can improve our strategies for treating and preventing infections caused *A. baumannii*.

Table 1.2: NGAs that target and disrupt the structural integrity of biofilm

Active Molecule	Organism	Mode of Action	Molecular Target	*in vivo*/*in vitro*	Reference
Extracellular DNA					
DNase I	*P. aeruginosa, E. coli, Acinetobacter baumannii, S. aureus, Enterococcus faecalis*	Cleaves the eDNA of established biofilms, decreasing biomass by altering biofilm structure	eDNA	*in vitro*, *in vivo*	Nemoto *et al*., 2003; Rice *et al*., 2007; Thomas *et al*., 2008; Tetz and Tetz, 2010; Sahu *et al*., 2012; Waryah *et al*., 2017
PodA	*P. aeruginosa*	Prevents release of extracellular DNA in the matrix of biofilm	methyl group present in pyocyanin	*in vitro*	Costa *et al*., 2017

NucB	*B. licheniformis, S. aureus, S. epidermidis, Staphylococcus salivarius, Staphylococcus constellatus, S. Staphylococcus lugdunesis, Staphylococcus anginosus, E. coli, Streptococcus intermedius, Micrococcus luteus, Bacillus subtilis*	Bacterial DNase that degrades established biofilms	eDNA	*in vitro*, *in vivo*	Nijland, Hall and Burgess, 2010; Shakir *et al*., 2012; Shields *et al*., 2013
Extracellular Proteins					
Proteinase K	*E. coli, S. aureus, Listeria monocytogenes, Staphylococcus lugdunensis and Staphylococcus heamolyticus*	Degradation of proteins in the biofilm to aid in biofilm dispersal	Biofilm-associated proteins and DNA binding proteins	*in vitro*	Fredheim *et al*., 2009; Shukla and Rao, 2013; Nguyen and Burrows, 2014; Cui, Ma and Lin, 2016
Trypsin	*P. aeruginosa*	Cleaves peptides in the biofilm	Biofilm peptides	*in vitro*	Banar *et al*., 2016

Staphopain A ScpA and Staphopain B ScpB	*S. aureus*	Staphylococcal cysteine proteases that degrade biofilm-associated proteins	Biofilm-associated proteins	*in vitro*	Mootz *et al.*, 2013; Loughran *et al.*, 2014
Antisera	*Enterococcus faecium, S. aureus, Klebsiella pneumoniae, A. baumannii, P. aeruginosa, Enterobacter spp.*, and *E. coli*	Potentiate DNase induced biofilm damage, antibiotic killing and to increase the capacity of macrophage to kill bacteria	DNABII family of proteins	*in vitro*	Goodman *et al.*, 2011; Novotny *et al.*, 2013
E. coli IHF	*E. coli*	Potentiate DNase induced biofilm damage	DNABII family of proteins	*in vitro*, *in vivo*	Goodman *et al.*, 2011
Humanized monoclonal antibody	*P. aeruginosa, S. aureus, Burkholderia cenocepcia, and M. catarrhalis*	Potentiate DNase induced biofilm damage	DNABII family of proteins	*in vitro*, *in vivo*	Novotny *et al.*, 2016; Jurcisek *et al.*, 2022; Kurbatfinski, Goodman and Bakaletz, 2022
Extracellular Polysaccharides					

Dispersin B	*S. aureus, A. actinomycetemcomitans, Staphylococcus epidermidis, A. baumannii, Klebsiella pneumoniae, Yersinia pestis and Pseudomonas fluorescens*	Degradation of PNAG by hydrolysing the β1,6 glycosidic linkages	PNAG	*in vitro*	Gawande *et al*., 2014; Waryah *et al*., 2017
Caspofungin	*S. aureus*	Weaken PNAG polymerization by inhibiting N-acetylglucosamine transferase	PNAG	*in vitro*, *in vivo*	Siala *et al*., 2016
Hydroxamic acid	*P. aeruginosa*	Reduces eDNA in biofiflm matrix	Targets the zinc ion active site in elastase enzyme, LasB	*in vitro*	Kany *et al*., 2018
Adhesions					
Pilicides	*Escherichia, Salmonella, Yersinia, Pseudomonas, Klebsiella, and Haemophilus*	Prevent pilus assembly and disrupt formation of the chaperon-pilin-usher complex	PapD and PapG	*in vitro*	Svensson *et al*., 2001

FN075	*Escherichia coli*	Prevents polymerisation of CsgA	CsgA	*in vitro*	Cegelski *et al.*, 2009; Chapman *et al.*, 2002
BibC6	*Escherichia coli*	Prevents polymerisation of CsgA	CsgA	*in vitro*	Chapman *et al.*, 2002; Cegelski *et al.*, 2009
LPRDA	*S. aureus*	Inhibits sortase A	Sortase A	*in vitro*	Bozhkova *et al.*, 2022
Fucosides	*Aspergillus fumigatus*	Aggregate and inhibit targeted lectins	FleA	*in vitro*	Duca *et al.*, 2022
T2544 Antiserum	*Salmonella enterica serovar Typhi*	Enhances the uptake and clearance of bacteria	T2544	*in vitro*, *in vivo*	Ghosh *et al.*, 2011

1.10.3 Targeting Global Virulence Regulatory Pathways

The process of colonisation and pathogenesis is governed by the ability of bacteria to perceive their external environment and the population density. This is regulated by the interconnected systems designated quorum sensing (QS), cyclic di-GMP (CdiGMP) signalling and two-component signalling (TCS) systems. As these pathways play diverse roles in controlling bacterial behaviour, disrupting them represents a promising strategy to combat multiple virulence factors at once while typically not impacting bacterial growth directly (Table 3).

Disrupting QS

In the context of treating *A. baumannii* infections, the disruption of quorum sensing (QS) systems, which play a pivotal role in the virulence of various pathogens, has emerged as a promising avenue. There are three main QS systems. Gram-positive bacteria use specific signalling peptides such as autoinducing peptides (AIPs), and Gram-negative bacteria use N-acylhomoserine lactones (AHLs). Autoinducer-2 (AI-2), is a furanosyl borate diester and is a non-pathogen-specific QS molecule. It can facilitate interspecies communication as it is utilised by both Gram-positive and Gram-negative species (Kaur, Capalash and Sharma, 2018). Given the prevalence of QS systems among pathogens and the key role they play in virulence, targeting QS has become one of the most well-studied strategies for the development of NGAs.

The entire QS regulatory system has been shown to be vulnerable to targeted disruption resulting in virulence attenuation. QS inhibitors can inhibit the expression of components of the QS system or disrupt the interaction between the autoinducer and their cognate receptor proteins. By doing so, these inhibitors can block cell-to-cell communication, biofilm formation and virulence factor production (Soukarieh *et al*., 2018; Proctor, McCarron and Ternan, 2020). Salicylic acid and trans-cinnamaldehyde have both been shown to effectively down-regulate the las (LasRI) and rhl (RhlIR) QS systems in *P. aeruginosa*, *in vitro* (Rajkumari *et al*., 2018; Ahmed *et al*., 2019). The specificity of these effects however varies from species to species with salicylic acid having been shown to stabilise *S. aureus* biofilms, preventing dispersal (Dotto *et al*., 2021). Several classes of coumarins have also been identified as potent inhibitors of AHL-based QS systems, with the simple coumarin molecule being shown to reduce expression of the las, rhl and pqs QS systems in *P. aeruginosa* and as a result decrease biofilm formation, motility, Type III Secretion System (T3SS) and phenazine production (Gutiérrez-Barranquero *et al*., 2015; Zhang *et al*., 2018). This activity has been shown to extend to several clinically relevant Gram-positive and Gram-negative bacteria, although the precise mechanism of QS inhibition remains to be uncovered. However, it is worth noting that molecular docking suggests direct interactions with autoinducer synthases (Reen *et al*., 2018; Qais *et al*., 2021). A small-molecule virulence inhibitor, savarin, has been shown to inhibit the Agr QS system in *S. aureus* by binding to AgrA, preventing its ability to bind to target promoters and ultimately blocking Agr-regulated gene expression, critically at concentrations that do not impact growth (Sully *et al.,*

2014). This molecule has demonstrated efficacy in animal models of biofilm-related *S. aureus* skin, subcutaneous and prosthetic joint infections by rendering the bacteria more susceptible to clearance by skin host defence mechanisms (Sully *et al*., 2014; Pant *et al*., 2022).

Bacteria often compete with other species for the same ecological niche in the natural environment, one strategy that has evolved to increase fitness in this scenario is to disrupt communication between members of the competitor species. The extracellular hydrolysis of autoinducer molecules lowers their local concentration in a process known as quorum quenching (QQ), triggering biofilm dispersal and reducing virulence factor production. QQ enzymes include lactonases, acylases and oxidoreductases and predominantly target AHLs (Rémy *et al*., 2018). Intriguingly, some eukaryotes have been shown to encode QQ enzymes with the capacity to disrupt virulence, in either an example of chance functional promiscuity or perhaps an evolved antivirulence strategy (Teiber *et al*., 2008). Several QQ enzymes have been purified and shown to exhibit potent antivirulence potential against *P. aeruginosa* in a range of *in vivo* infection models such as a rat pneumonia model, mouse burn wound model, and mouse pulmonary infection model. The diversity of formulation and delivery of these enzymes also demonstrates their clinical potential with aerosolisation, direct application and incorporation into hydrogels and coatings all proving effective delivery mechanisms (Hraiech *et al*., 2014; Gupta, Chhibber and Harjai, 2015; Utari *et al*., 2018; Sakr *et al*., 2021).

In the early 21st century, there was considerable excitement about the clinical potential of strategies to target QS, with several pilot clinical trials taking place (Smyth *et al*., 2010; Walz *et al*., 2010; van Delden *et al*., 2012). However, despite the results of these trials being largely positive, the clinical momentum has slowed. This may be impacted due to the emerging evidence that one of the most well-studied and targeted QS pathways, the LasRI QS system in *P. aeruginosa*, is prone to mutations causing loss of function. This indicates that targeting specific QS systems in infection scenarios may not be as effective as originally hoped or as observed in lab-adapted strains (Smith *et al*., 2006; Feltner *et al*., 2016; O'Connor *et al*., 2022). There has also been some evidence that resistance can evolve to certain classes of QS inhibitors such as furanones (Bove´ *et al*., 2021a). However, despite these clear limitations, there is still considerable therapeutic promise in targeting QS as a means to tackle the rise in MDR infections. In the case of *A. baumannii* infections, reducing adhesion through QS disruption presents a

valuable strategy in preventing and treating these challenging infections.

Blocking CdiGMP Signalling

CdiGMP is a secondary messenger molecule produced by diguanylate cyclases (DGCs) and utilised by bacteria to control a wide range of cellular processes, such as biofilm formation, adhesion, motility and virulence (Jenal, Reinders and Lori, 2017; Andersen *et al*., 2021). When CdiGMP binds to effector proteins, it has the potential to influence activity, stability, subcellular location, and the proteins' ability to interact with other proteins (Jenal, Reinders and Lori, 2017). High levels of CdiGMP are a known trigger of biofilm formation within numerous bacterial species, making approaches to disrupt the regulatory influence of CdiGMP an attractive target for the development of NGAs (Valentini and Filloux, 2016). Approaches to disrupt CdiGMP signalling include the use of synthetic CdiGMP analogues to jam the signalling cascade (Zhou *et al*., 2013; Fernicola *et al*., 2016), disrupting intracellular nucleotide pools (Antoni- ani *et al*., 2013) and the use of DGC active site inhibitors (Sambanthamoorthy *et al*., 2012; Fernicola *et al*., 2016; Trebino *et al*., 2021).

One of the most developed strategies, however, is the use of nitric oxide to modulate the activity of phosphodiesterases, the enzymes that break down intracellular CdiGMP. Exposure to NO has been shown to breakdown and reduce CdiGMP levels by activating CdiGMP-specific phosphodiesterases in bacteria (Barraud *et al*., 2015; Cutruzzola` and Frankenberg-Dinkel, 2015; Williams and Boon, 2019; Rumbaugh and Sauer, 2020). Low-dose nitric oxide was also found to cause a significant reduction in *P. aeruginosa* biofilm aggregates, in CF patients, highlighting the clinical potential of this approach (Howlin *et al*., 2017). Cahuitamycins were observed to exert minimal influence on the growth of *A. baumannii*. However, they demonstrated a substantial ability to impede biofilm formation. This noteworthy effect can be attributed to the terminal 2-hydroxybenzoyl-oxazoline group, which serves as a crucial pharmacophore within the cahuitamycins. This group effectively obstructs CdiGMP signaling in *A. baumannii*. Collectively these studies suggest that blocking CdiGMP signaling in Gram-negative bacteria such as *A. baumannii*, holds promise as a means to disrupt crucial bacterial processes, potentially reducing virulence and enhancing the effectiveness of treatment strategies.

Inhibiting Two-Component Systems (TCS)

Two-component systems (TCS) are utilised by *A. baumannii* and other bacteria to sense and respond to changes in the surrounding environment. These systems are critical for bacteria to quickly recognise and adapt to different environmental conditions or threats such as changes in temperature, pH, or nutrient availability (Sultan, Arya and Kim, 2021). TCS are typically comprised of two proteins, a sensor kinase, and a cognate response regulator (Brannon and Hadjifrangiskou, 2016). The sensor kinase contains a sensor domain that is sensitive to specific environmental signals and undergoes a conformational change that activates the kinase domain of the protein. This change then results in the phosphorylation of the histidine residue within the protein. This phosphorylated sensor kinase can then go on to transfer its phosphate group to the response regulator, which contains a DNA-binding domain. Phosphorylation of the response regulator results in a conformational change, which allows for the binding of specific promoter DNA sequences that can then result in the activation or repression of the transcriptional targets (Marina, Waldburger and Hendrickson, 2005; Stewart, 2010).

Maprotiline, an FDA-approved tetracyclic antidepressant drug, reduces *Francisella novicida* biofilm formation through a predicted interaction with the periplasmic sensor domain of histadine kinase, QseC. Treatment of mice infected with *F. novicida* was shown to improve survival and delay disease onset (Dean and van Hoek, 2015). Another QseC inhibitor, the small molecule LED209, was shown to inhibit QseC ligand binding and the resulting autophosphorylation without impacting bacterial viability but critically disabling several virulence mechanisms. It has demonstrated promising efficacy against *S. typhimurium* and *F. tularensis* in mouse infection models (Rasko *et al*., 2008; Curtis *et al*., 2014). Xanthoangelol B, a prenylated chalcone from the plant *Angelica keiskei*, along with structural derivatives have been shown to directly bind to SaeS, the sensor component of the TCS SaeRS, a major regulator of virulence factor expression in *S. aureus* (Mizar *et al*., 2018).

Mucin glycans have also recently been demonstrated to directly inhibit the TCS GacS-GacA in *P. aeruginosa* by binding to the antagonistic RetS sensor kinase. This then causes the downregulation of the type 6 secretion system (T6SS) which is associated with bacterial killing (Wang *et al*., 2021). Despite their role in responding to stimuli, TCS remain a comparatively

understudied area for the development of NGAs perhaps due to the essentiality of certain two-component sensors or the potential for host toxicity due to the similarity between kinase domains among bacteria and eukaryotes (Tiwari *et al*., 2017; Chen *et al*., 2022). Nonetheless, targeting TCS presents a promising strategy for addressing *A. baumannii* infections and other bacterial pathogens.

Table 1.3: NGAs that target the virulence regulatory pathways in bacteria.

Active Molecule	Organism	Mode of Action	Molecular Target	*in vivo*/*in vitro*	Reference
Quorum Sensing Gene Expression					
Salicylic acid	*P. aeruginosa*	Down-regulate QS systems las LasRI and rhl RhlIR	las LasRI and rhl RhlIR	*in vitro*	Ahmed *et al*., 2019
Trans-cinnamaldehyde	*P. aeruginosa*	Down-regulate QS systems las LasRI and rhl RhlIR	las LasRI and rhl RhlIR	*in vitro*, *in vivo*	Rajkumari *et al*., 2018; Ahmed *et al*., 2019

Coumarins	*P. aeruginosa*	Reduce expression of rhl and pqs	rhl and pqs	*in vitro*	Zhang *et al*., 2018; Gutiérrez-Barranquero, Cazorla and de Vicente, 2019
Savarin	*S. aureus*	Blocks Agr-regulated gene expression preventing biofilm formation	Agr QS system	*in vitro*, *in vivo*	Sully *et al*., 2014; Pant *et al*., 2022
Quorum Sensing Communication					
Zingerone	*P. aeruginosa*	Binds and blocks receptor proteins LasR, RhlR and MvfR	las, rhl and pqs QS systems	*in vitro*	Kumar *et al*., 2015
Acylhomoserine lactonase	Erwinia carotovora, Gram-negative species	Degrades the lactone ring present in AHL molecules	AHL molecules	*in vitro*	Dong *et al*., 2000, 2001

Lactonase	*P. aeruginosa*	Quorum quenching	Signal molecules N-3-oxododecanoyl-Lhomoserine lactone 3-oxo-C12 HSL and butyryl-homoserine lactone C4 HSL	*in vitro*, *in vivo*	Hraiech *et al*., 2014; Rémy *et al*., 2020
Acylases	*P. aeruginosa*	Quorum quenching	AHL molecules	*in vitro*, *in vivo*	Utari *et al*., 2018; Sakr *et al*., 2021
Oxidoreductases	*P. aeruginosa*	Quorum quenching	AHL molecules	*in vitro*, *in vivo*	Weiland-Bräuer *et al*., 2016
Garlic	*P. aeruginosa*	Blocks Quorum sensing	LasRI QS system	*in vitro*, *in vivo*	Smyth *et al*., 2010
Azithromycin	*P. aeruginosa*	Down-regulation of QS genes	Las, Rhl and Pqs QS systems	*in vitro*, *in vivo*	Nalca *et al*., 2006; van Delden *et al*., 2012
5-fluorouracil	*S. aureus*	Quorum quenching, inhibits AI-2 production	LuxS/AI-2	*in vitro*, *in vivo*	Walz *et al*., 2010; Sedl-mayer *et al*., 2021

Furanone C-30	*P. aeruginosa*	Potentiator of tobramycin	LasRI QS system, mexT	*in vitro*, *in vivo*	Bove´ *et al*., 2021b
Cyclic di-GMP					
Nitric oxide	*P. aeruginosa*, *Vibrio cholerae*, *E. coli*, Fusobacterium nucleatum, Serratia marcescens, Shewanella woodyi, Pseudoalteromonas, Vibrio fischeri, *S. aureus*, Legionella pneumophila, Nitrosomonas europaea, Psudemondas putida, Candida albicans and *Ulva linza*	Creates oxidative stress in the bacterial biofilm inducing dispersal and motility	NO sensors, NosP or H-NOX	*in vitro*, *in vivo*	Barraud *et al*., 2009, 2015; Howlin *et al*., 2017; Williams and Boon, 2019; Cai and Webb, 2020; Soren *et al*., 2020

Cahuitamycins	*A. baumannii*	Reduces cyclic di-GMP levels	CahJ protein	*in vitro*, *in vivo*	Tripathi *et al*., 2018
cis-DA, diffusible signal factor DSF	*Xanthomonas campestris, P. aeruginosa, E. coli, K. pneumoniae, S. aureus* and *C. albicans*	Modulation of cyclic-di-GMP levels and dispersal of biofilms	rpf gene cluster	*in vitro*	Dow *et al*., 2003; Davies and Marques, 2009
BdcA	*E. coli, P. aeruginosa, Pseudomonas fluorescens*, and *Rhizobium meliloti*	Sequesters unbound cyclic di-GMP, reducing the available concentration of cyclic di-GMP	Cyclic di-GMP	*in vitro*	Ma *et al*., 2011; Ma, Zhang and Wood, 2011; Lord *et al*., 2014; Yang *et al*., 2018
Analogs of cyclic di-nucleotidic acid	*Synechocystis sp*	Inhibits Slr1143	Slr1143	*in vitro*	Ching *et al*., 2010
Triazole-Linked Analogues	*P. aeruginosa, E. coli*	Binds allosteric inhibitory site I-site	Diguanylate cyclases DGCs	*in vitro*	Fernicola *et al*., 2015

Azathioprine	*P. aeruginosa, E. coli*	Inhibits biosynthesis of cyclic- di-GMP	WspR protien a diguanylate cyclases DGCs	*in vitro*	Antoniani *et al*., 2013
Catechol-Containing Sulfono-hydrazide Compounds	*P. aeruginosa, A. baumannii*	Inhibitors of the Diguanylate Cyclase PleD	PleD protien a diguanylate cyclases DGCs	*in vitro*	Fernicola *et al*., 2016
Sulfasalazine and eprosartan	*P. aeruginosa, E. coli*	Bind to the GTP active site of WspRN and YdeH	*P. aeruginosa* WspR and *E. coli* YdeH	*in vitro*	Wiggers *et al*., 2017
ABC-1 and2-[4-chlorobenzylthio 5-methoxy-1H-benzimidazole ABC-2	*Vibrio cholerae* -	Reduce the intracellular concentration of c- di-GMP	VC1673-lux	*in vitro*	Sambantha-moorthy *et al*., 2012
ABC-1	*Pseudomonas aeruginosa, K. pneu-moniae, E. amylovora, S. boydii*, and *S. aureus*	Reduce the intracellular concentration of c- di-GMP	*P. aeruginosa* WspR and *E. coli* YdeH	*in vitro*	Sambantha-moorthy *et al*., 2012

2'-F-c-di-GMP	*Pseudomonas aeruginosa*	I-site allosteric inhibition of diguanylate cyclases	I-site of DGC	*in vitro*	Zhou *et al.*, 2013
Two Component Systems					
Radicicol	*Salmonella*	Down-regulates expression of lasI/lasR and rhlI/rhlR QS systems	PhoQ	*in vitro*	Guarnieri *et al.*, 2008
Mucin glycans	*P. aeruginosa*	Binds to TCS GacS-GacA, downregulating the T6SS	GacS-GacA	*in vitro*	Wang *et al.*, 2021
Maprotiline	*F. novicida*	Interaction with the periplasmic sensor domain of QseC	QseC	*in vitro*, *in vivo*	Dean and Van Hoek, 2015
LED209	*S. typhimurium and F. tularensis*	QseC inhibitor	QseC	*in vitro*, *in vivo*	Rasko *et al.*, 2008, Curtis *et al.*, 2014
Xanthoangelol B	*S. aureus*	Bind to SaeS Sensor component of TCS	SaeS	*in vitro*, *in vivo*	Mizar *et al.*, 2018

1.10.4 Targeting Toxins

Targeting bacterial toxin functionality as a means to limit disease has a long and established history. This approach traces back to the late 19th century when von Behring and Kitasato developed antibody-based antitoxins for Corynebacterium diphtheriae toxin and Clostridium tetani toxin. Their ground-breaking work earned the Nobel Prize for Medicine in 1901 (Kantha, 1991). Over the years, antibody-based antitoxins, such as engineered antibodies, obiltoxaximab and raxibacumab, have made significant progress and have since made their way to the clinic. Notably, human monoclonal antibodies targeting *Clostridium difficile* toxins A and B (actoxumab and bezlotoxumab respectively) have been shown to significantly reduce C. difficile recurrence in several animal models at non-toxic concentrations (Hernandez *et al*., 2015; Yang *et al*., 2015) and in human clinical trials (Lowy *et al*., 2010; Wilcox *et al*., 2017). However, in phase III clinical trials, only bezlotoxumab alone was shown to reduce C difficile recurrence and as a result was given FDA approval in 2016 (Alonso and Mahoney, 2018). Toxin-targeting antibodies have also shown considerable therapeutic promise against other pathogens such as *P. aeruginosa, S. aureus* and *Salmonella spp* (Neely *et al*., 2005; DiGiandomenico *et al*., 2014; Tkaczyk *et al*., 2016; Surewaard *et al*., 2018; Nguyen *et al*., 2021).

Consequently, secretion systems can be targeted with NGAs at the level of component expression, apparatus assembly, toxin localisation or toxin activity (Table 4). In V. cholera, the transcription of cholera toxin and the toxin coregulated pilus are both regulated by the transcriptional activator ToxT. Through high-throughput screening, the compound 4-[N- (1,8-naphthalimide)]-nbutyric acid (virstatin) was found to prevent ToxT dimerisation which is required for promoter binding. In turn, this inhibition blocks the production of the cholera toxin without affecting the growth of the bacteria (Hung *et al*., 2005; Shakhnovich, Sturtevant and Mekalanos, 2007). The plant phenolic compounds TS027 and TS103 have been shown to affect the regulation of the GacSA-RsmYZ-RsmA-ExsA regulatory pathway in *P. aeruginosa* which mediates the expression of the toxins of the T3SS (Kauppi *et al*., 2003). Salicylidene acylhydrazides have been shown to interfere with T3SS genetic regulation by altering iron availability in bacteria such as *Yersinia pseudotuberculosis* and *Chlamydia trachomatis* (Uusitalo *et al*., 2017). Since this initial discovery, the salicylidene acylhydrazide INP0341 has

gone on to show considerable therapeutic promise in corneal, burn and vaginal *in vivo* models of *C. difficile, P. aeruginosa, S. typhimurium, Shigella, C. trachomatis, E. coli* infections (Muschiol *et al*., 2006; Bailey *et al*., 2007; Hudson *et al*., 2007; Tree *et al*., 2009; Veenendaal, Sundin and Blocker, 2009; Yang *et al*., 2015; Anantharajah *et al*., 2017; Uusitalo *et al*., 2017; Feng *et al*., 2019).

Tanshinones, herbal compounds commonly used in traditional Chinese medicine, have been shown to bind directly to components of the *P. aeruginosa* T3SS needle, preventing needle biogenesis (Feng *et al*., 2019). Several tanshinones have now been shown to prevent the secretion of T3SS-associated toxins to macrophages *in vitro* and demonstrated efficacy in a murine model of acute pneumonia (Aiello *et al*., 2010). Phenoxyacetamide MBX 1641 was found to bind to the PscF component of the T3SS needle protein in *Yersinia pestis* and *P. aeruginosa*, preventing assembly. This inhibitor was found to decrease T3SS-mediated cytotoxicity against eukaryotic cells (Bowlin *et al*., 2014; Williams *et al*., 2015; Foulkes *et al*., 2021). Several small molecule inhibitors of toxin function have been identified and characterised with promising clinical potential. Pseudolipasin A was shown to be an inhibitor of the *P. aeruginosa* T3SS toxin, ExoU. This inhibitory activity is predicted to occur through the direct binding of this compound to the ExoU catalytic domain (Tam *et al*., 2015).

An alternative strategy to overcome toxin-mediated virulence is to disrupt the eukaryotic intracellular trafficking of the toxin to its target. Endosome-lysosome acidification is required for the delivery of the *C. difficile* toxin, TcdB, across the endosomal membrane. This can be effectively inhibited by the general v-ATPase inhibitor bafilomycin A1 as well as several other compounds with lysosomotropic features including the antimalarial drug quinacrine. Preventing the transition of TcdB across the endosomal membrane was sufficient to inhibit TcdB-induced cell rounding (Zhang *et al*., 2014; Azarnia Tehran *et al*., 2015). The intracellular trafficking of several botulinum neurotoxins has been shown to be inhibited by 4-bromobenzaldehyde N-(2,6-dimethylphenyl) semicarbazone (EGA) effectively reducing neurotoxicity in mouse models (Azarnia Tehran *et al*., 2015). The cellular toxicity of Shigatoxins STx, STx1, and STx2 is dependent on their retrograde trafficking to their cytosolic target, ribosomes. Several promising compounds have been identified that can disrupt this trafficking and limit toxin activity, including the FDA-approved breast cancer chemotherapeutic tamoxifen, which was

shown to be a potent inhibitor of STx2 trafficking. Mouse toxicity studies demonstrated that human-approved doses of 10 M of tamoxifen could significantly improve survival after exposure to a lethal amount of STx1 or STx2 (Selyunin *et al*., 2019; Li, Selyunin and Mukhopadhyay, 2020; Savinova *et al*., 2022).

In the case of *A. baumannii* a novel toxin-antitoxin system, known as mazEF, has been identified as being conserved within 85 clinical isolates, revealing its ubiquity within *A. baumannii*. Additionally, this research has shed light on the prevalence of toxin-antitoxin genes residing on the bacterial chromosomes and actively transcribed within *A. baumannii*. These findings suggest that further investigation into the modulation of the toxin proteins within the mazEF toxin-antitoxin system may offer a potential target for developing antibacterial strategies against *A. baumannii* (Ghafourian *et al*., 2014). While targeting toxin production may be an effective mechanism to limit acute infection, there is evidence that as a chronic infection develops, toxin production declines, with examples of T3SS inactivation mutations in *P. aeruginosa* chronic CF and wound isolates (Jain *et al*., 2004; McCarthy *et al*., 2017; Karash *et al*., 2021).

Table 1.4: NGAs that target toxin production and secretion in bacteria.

Active Molecule	Organism	Mode of Action	Molecular Target	*in vivo*/*in vitro*	Reference
Toxins					
Daio-kanzo-to	*Vibrio cholerae*	Inhibit the function of cholerae toxin	Cholerae toxin	*in vitro*, *in vivo*	Oi *et al*., 2002
Apple polyphenol extract APE	*Vibrio cholerae*	Inhibit the ADP-ribosylation activity	Cholera toxin A1 fragment	*in vitro*, *in vivo*	Saito *et al*., 2002

4-[N- 1,8-naphthalimide]-n-butyric acid virstatin	*Vibrio cholerae*	Post-transcriptionally inhibits ToxT, blocking the production of the cholerae toxin	ToxT	*in vitro*, *in vivo*	Hung *et al*., 2005; Shakhnovi-ch *et al*., 2007
MDT 3-methylthio-1,4-diphenyl-1H-1,2,4-triazolium bromide	*E. coli*	Formation of a complex that prevents the assemble of the toxin	Entry point of a single B pentamer	*in vitro*, *in vivo*	Hovey *et al*., 1999; Hardy *et al*., 1988; Yang *et al*., 2014
TS027 and TS103	*P. aeruginosa*	Interfere with the regulation of the GacSA-RsmYZ-RsmA-ExsA regulatory pathway reducing expression of the exoS toxin	GacSA-RsmYZ-RsmA-ExsA	*in vitro*, *in vivo*	Yamazaki *et al*., 2011

Salicylidene acylhydrazides	*Yersinia pseudotuber-culosis* and *Chlamydia trachomatis*	Interferes with TTSS genetic regulation by altering cellular metabolism	Reporter gene signal expressed from the yopE promoter	*in vitro*	Uusitalo *et al*., 2017; Kauppi *et al*., 2003; Hudson *et al*., 2007; Veenen-daal *et al*., 2009; Muschiol *et al*., 2006; Bailey *et al*., 2007; Tree *et al*., 2009; Anan-tharajah *et al*., 2017; Yang *et al*., 2015
Resveratrol tetramer-hopeaphenol	*Yersinia pseudotuber-culosis*	Inhibits the secretion of *Yersinia* outer proteins by binding to the TTSS	Not identified	*in vitro*	Zetterstrom *et al*., 2013

Bezlotoxumab	*Clostridium difficille*	Neutralising antibody against toxin A and B	Toxin A and B	*in vitro*, *in vivo*	Alonso and Mahony., 2019; Granata *et al*., 2022
Fluorothiazinon	*Chlamydia spp., Pseudomonas aeruginosa*, and *Salmonella*	Not identified	T3SS	*in vitro*, *in vivo*	Zigangirova *et al*., 2021, Sheremet *et al*., 2018
Anethole	*V. cholera*	Downregulation of cholera toxin expression	cAMP receptor protein	*in vitro*, *in vivo*	Zahid *et al*., 2015
Pseudolipasin A	*P. aeruginosa*	Inhibits T3SS toxin ExoU cellular toxicity	T3SS toxin ExoU	*in vitro*	Foulkes *et al*., 2021
Bafilomycin A1	*C. difficile*	v-ATPase inhibitor	TcdB	*in vitro*	Tam *et al*., 2015, Zhang *et al*., 2014
4-bromobenzaldehyde N-2,6-dimethylphenyl semicarbazone EGA	*Clostridium botulinum*	Inhibits several botulinum neurotoxins	Neurotoxins	*in vitro*, *in vivo*	Tehran *et al*., 2015

Tamoxifen	*E. coli*	Inhibitor of STx2 trafficking	Ribosomes	*in vitro*, *in vivo*	Li *et al*., 2020, Selyunin *et al*., 2019
Tanshinones	*P. aeruginosa*	Prevents needle biogenesis	T3SS needle	*in vitro*	Feng *et al*., 2019
Phenoxyacetamide MBX 1641	*Yersinia pestis* and *P. aeruginosa*	Binds to PscF component of TTSS needle, preventing assembly	PscF	*in vitro*	Aiello *et al*., 2010; Williams *et al*., 2015; Bowlin *et al*., 2014
Endogenous antibodies eAbs	*C. difficile*	Binds and neutralises Clostridium difficile toxin B	Clostridium difficiletoxin B	*in vitro*, *in vivo*	Kelly *et al*., 2020
Suvratoxumab	*S. aureus*	Binds and neutralises α toxin	α toxin	*in vitro*, *in vivo*	Françios *et al*., 2021
Raxibacumab	*Bacillus anthracis*	Binds to PA, blocking its binding to host cell receptors	Protective antigen PA in anthrax	*in vitro*, *in vivo*	Tsia and Morris., 2017; Xu *et al*., 2017

Anthrax immune globulin AIG	*Bacillus anthracis*	Binds to PA, blocking its binding to host cell receptors	Protective antigen PA in anthrax	*in vitro*, *in vivo*	Xu *et al*., 2017
ETI-204	*Bacillus anthracis*	Binds to PA, blocking its binding to host cell receptors	Protective antigen PA in anthrax	*in vitro*, *in vivo*	Xu *et al*., 2017
Obiltoxaximab	*Bacillus anthracis*	Binds to PA, blocking its binding to host cell receptors	Protective antigen PA in anthrax	*in vitro*, *in vivo*	Greig, 2016

1.10.5 Challenges and Future Perspectives

The urgent need for novel therapeutic strategies to tackle MDR infection is clear and NGAs represent a promising therapeutic strategy that could overcome key issues like the propensity for resistance evolution associated with traditional antibiotics. The proposed weaker selection pressure while widely accepted does not necessarily mean that NGAs are resistance proof and the capacity for bacteria to develop mechanisms to overcome their activity is an aspect that needs to be explored in greater detail. NGA's are also expected to typically constitute less interference with mammalian signalling pathways and therefore reduce toxicity as they are designed to target virulence pathways that are only found in pathogens, although this obviously is not the case for all NGAs and candidates that target TCSs or host intracellular trafficking in particular need to be robustly screened for off-target effects on the host. There is also the potential that although targeted towards specific pathogens, NGAs could disrupt the behaviour of commensals within our microbiome, with for example disrupting cyclic di-GMP potentially impacting interspecies competition and the biofilm-forming capacity of commensals within the gut microbiome (McCarthy *et al*., 2017).

Plant extracts are considered a rich reservoir of bioactive chemicals with high therapeutic potential and have proven to be a rich source of NGA leads. Phytochemicals occupy a chemical space with far greater structural diversity than synthetic compound libraries and tend to be more 'drug-like', with superior ADME/T (absorption, distribution, metabolism, excretion and toxicity) properties. This is due to the evolutionary pressures faced by plants which have endured millennia of intensive selective pressure to develop small molecules that target specific pathways in bacteria to prevent colonisation (Borges *et al*., 2016). However, a key limitation to the potential of phytochemicals as NGAs is the inherent difficulty in identifying the active molecule within a bioactive plant extract and understanding the specific cellular targets and underlying mechanisms of action, information often necessary for the pre-clinical development of NGAs.

In contrast, semi-synthetic antimicrobials are designed to harbor the beneficial properties of natural compounds but with improved stability and potency. This overcomes the limitations of natural compounds by enhancing pharmacokinetic properties and maintaining antibacterial activities. Comparatively, fully synthetic drugs are designed and robustly tested for maximum antibacterial activity and minimal host toxicity, to allow for improved efficacy and safety. Therefore, although natural products have evolved to target specific bacterial pathways, they may not be as viable for clinical application compared to semi- or fully synthetic drugs that overcome the challenges faced by natural products. This highlights the potential of repurposing FDA-approved drugs as NGAs, with numerous examples having already been described of drugs having off-target antivirulence effects on bacteria (Dean and van Hoek, 2015; Selyunin *et al*., 2019; Savinova *et al*., 2022). Similar potential has been seen with dietary compounds, with artificial sweeteners for example having been recently shown to limit the pathogenicity of several MDR pathogens when used at sub-inhibitory concentrations (de Dios *et al*., 2023).

To effectively stem the tide of MDR pathogens, such as *A. baumannii*, sweeping through our hospitals it is essential we continue to develop multiple different approaches to tackle these pathogens. Targeting virulence rather than viability is an alternative approach that holds significant therapeutic potential and is likely to have increased clinical importance in the coming years.

1.11 Aims and Objectives

Aim One

Aim one is to identify phytochemicals that demonstrate potential therapeutic properties against *A. baumannii* and may also be able to increase the efficacy of colistin. This will uncover novel approaches to combat *A. baumannii* infections by harnessing the therapeutic properties of phytochemicals. This will be achieved by the following objectives:

1. Screen various phytochemical libraries in both the presence and absence of colistin. This will allow for the identification of antimicrobials and colistin potentiators, respectively.
2. Determine the mechanisms of action of the phytochemicals against *A. baumannii* utilising RNA-Seq analysis.

Aim Two

Aim two is to understand the evolutionary trajectories and mechanisms that *A. baumannii* follows when evolving resistance to colistin, and to determine the fitness and virulence costs of resistance. Evaluating fitness and virulence costs associated with resistance will identify weaknesses that can be exploited through the development of more targeted and effective treatments. Understanding evolutionary trajectories will also aid in predicting resistance patterns. This will be achieved by the following objectives:

1. Profile the virulence and fitness of 50 colistin resistant mutants (CRM). Profiling these mutants will allow us to gain knowledge of the rates of resistance and to determine if the level of resistance is directly proportional to fitness and virulence.
2. Sequence and compare the genomes of the chosen CRMs against the wild-type *A. baumannii* genome, to identify any novel mutations that mediate colistin resistance.

Chapter 2

Kaempferol Potentiates Colistin by Disrupting Iron Homeostasis

2.1 Introduction

Colistin is a polycationic peptide that acts on Gram-negative bacteria by binding to the anionic lipid A component of the lipooligosaccharide (LOS) in the outer membrane, as well as the lipid A found in the inner membrane (Sabnis *et al*., 2021, Andrade *et al*., 2020). Colistin was first introduced in the clinic in the 1950s, however severe side effects, such as nephrotoxicity and neurotoxicity, led to its removal from therapeutic use in the 1970s. Nonetheless, the increased prevalence of MDR pathogens over the last three decades, and in particular the continuous emergence of resistance against β-lactam antibiotics like carbapenems, has forced clinicians to re-introduce colistin for the treatment of challenging infections (Rolain *et al*., 2011; Rhouma *et al*., 2016; Snyman *et al*., 2020; Yoon *et al*., 2021). Despite needing to resort to treating patients with colistin, its efficacy in the clinic remains limited primarily due to strict dose restrictions. Indeed, only 50% of patients with normal renal function are able to maintain concentrations of colistin in their serum at levels that are sufficient to eliminate bacteria (Satlin *et al*., 2020; Tran *et al*., 2016). Moreover, colistin is less effective when applied *in vivo*, since its efficacy often does not match results obtained by *in vitro* studies, with up to 70% of patients failing to respond to colistin treatment (Paul *et al*., 2018).

In addition to the constraints encountered in the clinical application of colistin, the emergence of multiple resistance mechanisms against this antibiotic further limits its efficacy during the treatment of recalcitrant infections (Boll *et al*., 2015; Furniss *et al*., 2020; Moffatt *et al*., 2010; Sun *et al*., 2020, Beceiro *et al*., 2011, Arroyo *et al*., 2011). The interaction between colistin and lipid A has been shown to induce membrane permeabilisation and cell leakage (Manioglu *et al*., 2022). This process is accompanied by an increase in the production of reactive oxygen species (ROS) within the bacterial cell, which ultimately leads to cellular death

(Sampson *et al*., 2012).

The limited treatment options against carbapenem-resistant *A. baumannii* stem from the various colistin resistance mechanisms found in this organism. Additionally, the challenges faced in the clinical use of polymyxin antibiotics highlight an urgent need for innovative strategies that can enhance the effectiveness of colistin or render colistin resistant strains more susceptible. To this aim, colistin potentiators have emerged as promising agents in enhancing colistin-mediated cell death. These combination potentiator therapies increase the efficacy of colistin and also mitigate its potential nephrotoxicity and neurotoxicity, which are common concerns during colistin monotherapy. By reducing the required dosage of colistin in the combination treatment, these therapies offer a safer alternative (MacNair and Brown, 2020). Additionally, potentiators have shown the capability to tackle resistance issues by augmenting the activity of existing antibiotics against Gram-negative multidrug-resistant (MDR) bacteria (Klobucar and Brown, 2022).

Various other antimicrobials have been identified as potentiators of colistin. For example, colistin-rifampin combinations have demonstrated effectiveness against MDR infections in murine *A. baumannii* thigh-infection models (Fan *et al*., 2016). Similarly, combinations such as colistin-meropenem, colistin-rifampicin, and colistin-minocycline have shown promise in reducing mortality rates associated with XDR *A. baumannii* strains, outperforming colistin monotherapy (Liang *et al*., 2011). Furthermore, colistin-tigecycline has emerged as an effective treatment for XDR *A. baumannii* pneumonia, as evidenced by studies conducted in rat lung models (Mutlu Yilmaz *et al*., 2012).

Innovative approaches beyond traditional antibiotic combinations have also been explored. Nano-formulations, such as the self-assembled guanidinium and ionic silver nanoparticles [AD-L@Ag(0)], have exhibited significant efficacy in inhibiting the growth and viability of colistin-resistant Gram-negative bacteria (Kumar *et al*., 2022). Additionally, the short linear antibacterial peptide-S25 has been found to enhance the activity of colistin, as well as other antibiotics against *A. baumannii*, such as rifampicin and vancomycin, which is notable for its specificity against Gram-positive bacteria (Song *et al*., 2020).

Plants have a rich reservoir of phytochemicals which offer a promising source of antimicrobial agents with therapeutic potential, serving as potentiators of antibiotics. The

catechol-type flavonoids, 7,8- dihydroxyflavone, myricetin, and luteolin were, found to greatly potentiate the efficacy of colistin against gram-negative bacteria (Zhong *et al*., 2023). These diverse strategies highlight the variety of sources available to enhance the efficacy of colistin, offering valuable resources to tackle this pressing global health crisis.

2.2 Aim of the study

The aim of this study is to identify phytochemicals that increase the efficacy of colistin against *A. baumannii*. These findings will uncover novel approaches for combating *A. baumannii* infections by leveraging the potentiation effects of phytochemicals on colistin, offering new avenues for antimicrobial therapy against multidrug-resistant pathogens.

- We will choose a phytochemical for further testing based on the level of activity of the phytochemical.
- Next, the efficacy of the phytochemical in combination with sub-MIC concentrations of colistin against *A. baumannii* will be investigated.
- Finally, we will elucidate the mechanism of action of the phytochemical-colistin combination against *A. baumannii*.

2.3 Results

2.3.1 Screening of Phytochemical Libraries for Antimicrobials and Potentiators

We began by screening compounds sourced from both Kew Gardens and the Caithness phytochemical library in combination with the sub-inhibitory concentration of colistin (1.22 µg/mL) against *A. baumannii* (Figure 2.1A). This approach sought to determine if any of the compounds could enhance colistin's efficacy, given that, when used alone at this sub-MIC concentration, colistin does not affect bacterial growth (Figure 2.1A). A parallel screen was conducted without colistin in order to determine if any potentiating effects were a result of the potentiator having antimicrobial activities. All compounds were tested at a concentration of 0.05 mM against a DMSO vehicle control (Appendix A.1). Following the growth screening assay, both screens, with and without colistin, were subjected to a biofilm assay to assess the impact of the compounds on *A. baumannii* biofilm formation (Appendix A.2). Subsequent analysis focused on the top-hit compounds, incorporating insights from existing literature to identify potential novel antimicrobials, antibiofilm agents or potentiators (Table 2.1). This selection was then refined to accommodate the availability of standards of the compounds and associated costs (Figure 2.1B and Table 2.1). Furthermore, a more in-depth analysis was conducted to explore the effects of kaempferol as a colistin potentiator against *A. baumannii*, considering its potential significance in enhancing antibacterial efficacy, its fit into the budget and availability for the time of the project. During the two years of working on elucidating the mechanism of action of kaempferol, another group published an alternative mechanism and the similarities between their paper and our study are discussed in detail throughout this chapter.

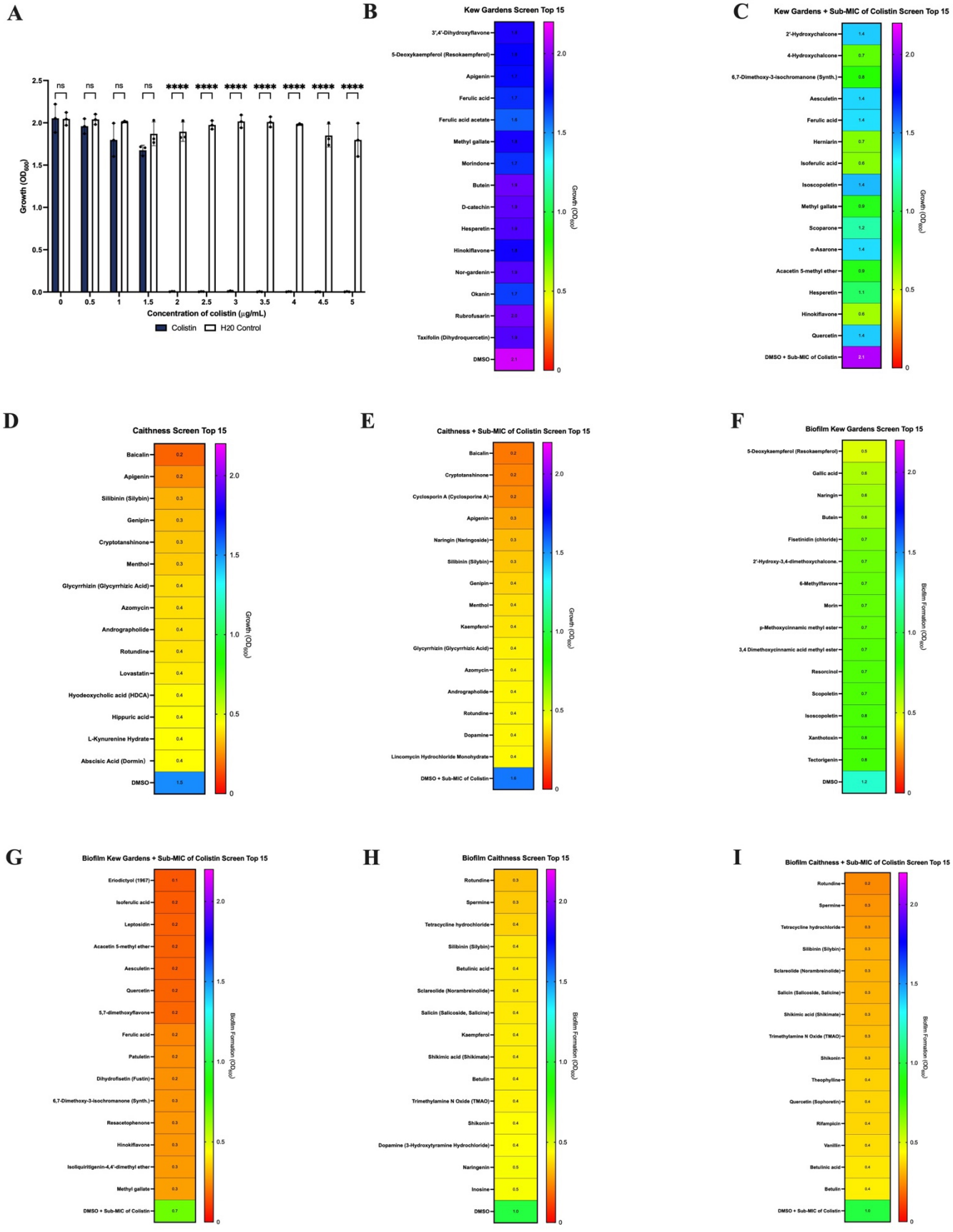
A
ns
****
Growth (OD600)
Concentration of colistin (μg/mL)
Colistin
H20 Control
B
Kew Gardens Screen Top 15
3',4'-Dihydroxyflavone
5-Deoxykaempferol (Resokaempferol)
Apigenin
Ferulic acid
Ferulic acid acetate
Methyl gallate
Morindone
Butein
D-catechin
Hesperetin
Hinokiflavone
Nor-gardenin
Okanin
Rubrofusarin
Taxifolin (Dihydroquercetin)
DMSO
Growth (OD600)
C
Kew Gardens + Sub-MIC of Colistin Screen Top 15
2'-Hydroxychalcone
4-Hydroxychalcone
6,7-Dimethoxy-3-isochromanone (Synth.)
Aesculetin
Ferulic acid
Herniarin
Isoferulic acid
Isoscopoletin
Methyl gallate
Scoparone
α-Asarone
Acacetin 5-methyl ether
Hesperetin
Hinokiflavone
Quercetin
DMSO + Sub-MIC of Colistin
Growth (OD600)
D
Caithness Screen Top 15
Baicalin
Apigenin
Silibinin (Silybin)
Genipin
Cryptotanshinone
Menthol
Glycyrrhizin (Glycyrrhizic Acid)
Azomycin
Andrographolide
Rotundine
Lovastatin
Hyodeoxycholic acid (HDCA)
Hippuric acid
L-Kynurenine Hydrate
Abscisic Acid (Dormin)
DMSO
Growth (OD600)
E
Caithness + Sub-MIC of Colistin Screen Top 15
Baicalin
Cryptotanshinone
Cyclosporin A (Cyclosporine A)
Apigenin
Naringin (Naringoside)
Silibinin (Silybin)
Genipin
Menthol
Kaempferol
Glycyrrhizin (Glycyrrhizic Acid)
Azomycin
Andrographolide
Rotundine
Dopamine
Lincomycin Hydrochloride Monohydrate
DMSO + Sub-MIC of Colistin
Growth (OD600)
F
Biofilm Kew Gardens Screen Top 15
5-Deoxykaempferol (Resokaempferol)
Gallic acid
Naringin
Butein
Fisetinidin (chloride)
2'-Hydroxy-3,4-dimethoxychalcone
6-Methylflavone
Morin
p-Methoxycinnamic methyl ester
3,4 Dimethoxycinnamic acid methyl ester
Resorcinol
Scopoletin
Isoscopoletin
Xanthotoxin
Tectorigenin
DMSO
Biofilm Formation (OD600)
G
Biofilm Kew Gardens + Sub-MIC of Colistin Screen Top 15
Eriodictyol (1967)
Isoferulic acid
Leptosidin
Acacetin 5-methyl ether
Aesculetin
Quercetin
5,7-dimethoxyflavone
Ferulic acid
Patuletin
Dihydrofisetin (Fustin)
6,7-Dimethoxy-3-isochromanone (Synth.)
Resacetophenone
Hinokiflavone
Isoliquiritigenin-4,4'-dimethyl ether
Methyl gallate
DMSO + Sub-MIC of Colistin
Biofilm Formation (OD600)
H
Biofilm Caithness Screen Top 15
Rotundine
Spermine
Tetracycline hydrochloride
Silibinin (Silybin)
Betulinic acid
Sclareolide (Norambreinolide)
Salicin (Salicoside, Salicine)
Kaempferol
Shikimic acid (Shikimate)
Betulin
Trimethylamine N Oxide (TMAO)
Shikonin
Dopamine (3-Hydroxytyramine Hydrochloride)
Naringenin
Inosine
DMSO
Biofilm Formation (OD600)
I
Biofilm Caithness + Sub-MIC of Colistin Screen Top 15
Rotundine
Spermine
Tetracycline hydrochloride
Silibinin (Silybin)
Sclareolide (Norambreinolide)
Salicin (Salicoside, Salicine)
Shikimic acid (Shikimate)
Trimethylamine N Oxide (TMAO)
Shikonin
Theophylline
Quercetin (Sophoretin)
Rifampicin
Vanillin
Betulinic acid
Betulin
DMSO + Sub-MIC of Colistin
Biofilm Formation (OD600)

Figure 2.1: Initial screening of Kew Gardens and Caithness library. Top 15 hits from the Initial Screening of Kew Gardens and Caithness Library. **(A)** Minimum Inhibitory Concentration of Colistin against AB5075. Complete inhibition of visible growth of *A. baumannii* was observed with 2 μg/mL of colistin. Assays were carried out in biological triplicate (n=3), with three technical repeats. **(B – E)** Inhibition of growth of *A. baumannii* with 0.05 mM of the compounds. **(F – I)** Inhibition of biofilm formation of *A. baumannii* with 0.05 mM of the compounds. Assays were carried out in biological triplicate (n=3). Statistical analysis of panel **(A)** consisted of two-way ANOVA between the treated samples and the H_2O growth control, each comparison includes controls with increasing amounts of H_2O as the second variable factor. Error bars represent average values ± S. D. Significance is indicated as * = $p < 0.05$, ** = $p < 0.01$, *** = $p < 0.001$, and **** = $p < 0.0001$. Graphpad Prism statistical software package was used to create and analyse these figures.

Table 2.1: Top hit compounds and their existing literature.

Compound	Library	Activity	Previous Literature	References
Morindone	Kew Gardens	Antibiotic	Antimicrobial activity against *Candida lipolytica* and oxacillin-resistant *Staphylococcus aureus*	Borroto *et al*., 2010; Ismail, M *et al*., 2000
Okanin	Kew Gardens	Antibiotic	Quorum sensing inhibitor against Chromobacterium violaceus. Antimicrobial activity against *Micrococcus luteus,* *E. coli, S. aureus, Raoultella planticola* and *Acinetobacter*	Mu *et al*., 2020; Behera *et al*., 2013
Hinokiflavone	Kew Gardens	Antibiotic	Attenuates the virulence of MRSA	Kong *et al*., 2022

Cryptotanshin-one	Caithness	Antibiotic	Antibacterial activity against Gram positive and negative pathogens – not including *A. baumannii*	Chen *et al*., 2021

Cyclosporin A	Caithness	Colistin Potentiator	Immunosuppressant	Tedesco *et al*., 2012
Kaempferol	Caithness	Colistin Potentiator	Antimicrobial and antioxidant activity of kaempferol rhamnoside derivatives from Bryophyllum pinnatum	Tatsimo *et al*., 2012
Isoliquiritigen-in-4methyl ether	Kew Gardens	Colistin Potentiator	Antimicrobial activity against *Ralstonia solanacearum*. Drug resistance reversal against MRSA.	Zhoa *et al*., 2011; Gaur *et al*., 2016
Biochainin A	Kew Gardens	Colistin Potentiator	Antimicrobial against *Xan-thomonas axonopodis* pv. glycines (Xag). Potentiates ciprofloxacin against clinical isolates of *S. aureus*.	Hu *et al*., 2021; Liu *et al*., 2011
2-hydroxychalc-one	Kew Gardens	Colistin Potentiator	Antibiofilm activity against *A. baumannii*.	Usˇjak *et al*., 2023
3,4 Dimethoxycin-namic acid methyl ester	Kew Gardens	Antibiofilm	Antioxidant, Anti-Inflammatory and Hypolipidemic Functionality	Theodosis-Nobelos *et al*., 2023
Naringin	Kew Gardens	Antibiofilm	Antimicrobial against b-lactam resistant *A. baumannii*.	Duda-Madej *et al*., 2020

Kaempferitrin	Kew Gardens	Antibiofilm	Antimicrobial and antibiofilm effects against Methicillin-resistant *Staphylococcus aureus* when functionalised with Metal nanoparticles	Shamprasad *et al*., 2022
Inosine	Caithness	Antibiofilm	Prevents *Alicyclobacillus acidoterrestris* contamination	Liu *et al*., 2023
Artesunate	Caithness	Antibiotic	Enhancement on antibacterial activity of B-lactams (inhibition of efflux pumps NorB and NorC), no antibacterial effect on its own	Jiang *et al*., 2013
Ethyl ferulate	Caithness	Antibiotic	Anti-inflammatory properties – no studies on *A. baumannii*.	Nazare´ *et al*., 2014
Indole-3-carbinol	Caithness	Colistin Potentiator	Antioxidant properties, synergistic activity in combination with ampicillin against drug- resistant isolates – not shown against *A. baumannii*	Sung *et al*., 2008

2.3.2 Kaempferol is a potentiator of the antimicrobial activity of colistin

From the initial screen, we found that kaempferol, a natural flavanol flavonoid that can be isolated from many plant-derived foods like strawberries and capers (Alam *et al*., 2020), had one of the most potent and consistent antimicrobial effects when combined with sub-MIC amounts of colistin *in vitro*. Titration assays revealed that this effect is dose-dependent and that a concentration of 0.375 mM of kaempferol combined with 1.22 µg/mL of colistin leads to complete inhibition of visible bacterial growth (Figure 2.2A). We further confirmed that this concentration of kaempferol had no impact on *A. baumannii* growth when administered as a

monotherapy (Figure 2.2B), suggesting that kaempferol potentiates the activity of colistin without affecting bacterial growth.

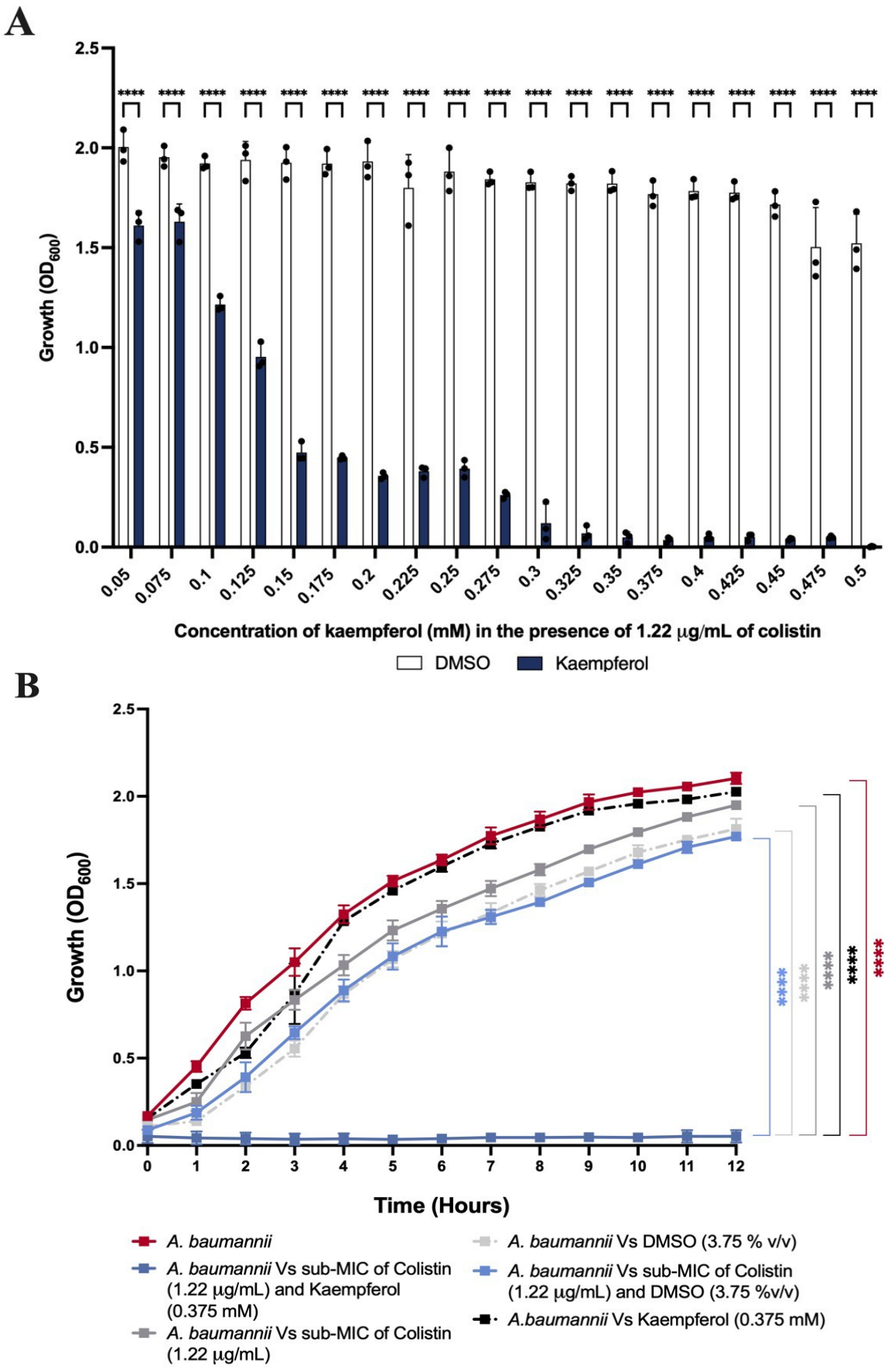

Figure 2.2: Kaempferol potentiates the activity of colistin. (A) Minimum Inhibitory Concentration (MIC) of the kaempferol-colistin combination treatment. Complete inhibition of visible growth of *A. baumannii* was observed when 0.375 mM of kaempferol was combined with sub-MIC amounts of colistin (1.22 μg/mL). Inhibition was shown to be dose-dependent. **(B)** Inhibition of *A. baumannii* growth by kaempferol in combination with sub-MIC amounts of colistin. Monotherapy with 1.22 μg/mL of colistin or 0.375 mM of kaempferol did not inhibit growth. For both panels, assay results were carried out in biological triplicate (n=3), each performed in technical triplicate. Statistical analysis consisted of two-way ANOVA for panel **(A)** and two-way repeated measures ANOVA for panel **(B)** between the treated samples and the respective DMSO growth controls, each comparison includes controls with increasing amounts of DMSO as the second variable factor.. Error bars represent average values ± S. D. Significance is indicated as * = $p < 0.05$, ** = $p < 0.01$, *** = $p < 0.001$, and **** = $p < 0.0001$.

2.3.3 Kaempferol is a better potentiator than its derivatives

To explore the relationship between the chemical structure of kaempferol and its promise as a colistin potentiator, we tested a panel of kaempferol derivatives (Figure 2.3A). The native kaempferol structure was found to be the most efficacious at reducing the growth of *A. baumannii* when combined with sub-MIC amounts of colistin (Figure 2.3B). In particular, we found that there was an inverse relationship between the extent of chemical modifications applied to these compounds and their bactericidal activity in combination with colistin. For example, heavily modified derivatives such as kaempferol 3-glucoside 4',7-dirhamnoside were unable to potentiate colistin activity, while compounds with minor modifications (5-Deoxykaempferol a.k.a Resokaempferol) acted as colistin potentiators.

A

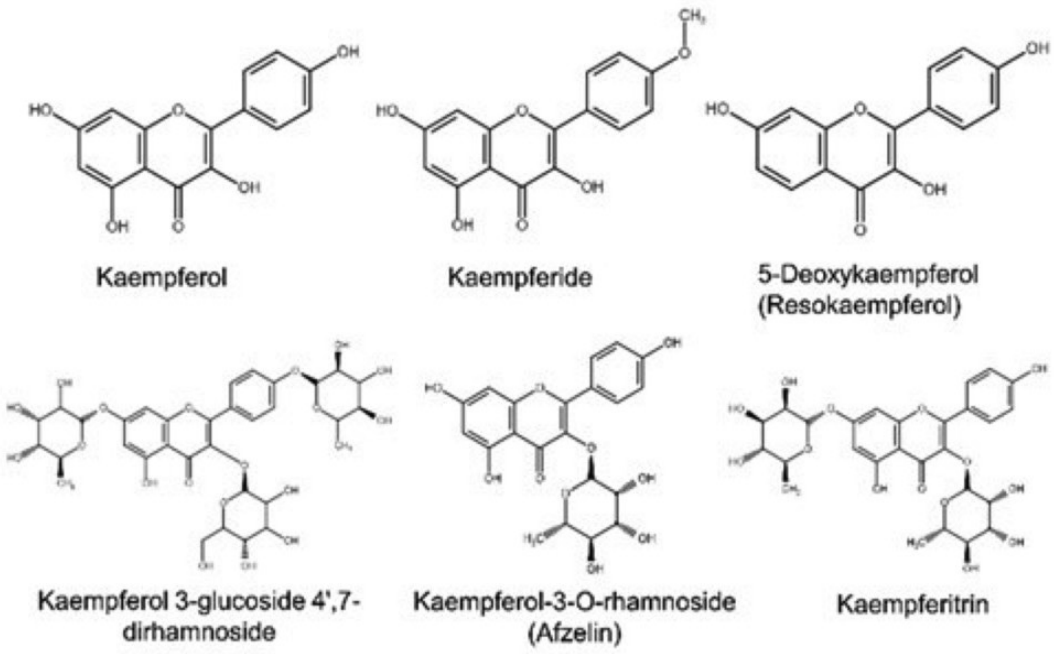
Kaempferol
Kaempferide
5-Deoxykaempferol
(Resokaempferol)
Kaempferol 3-glucoside 4',7-
dirhamnoside
Kaempferol-3-O-rhamnoside
(Afzelin)
Kaempferitrin

B

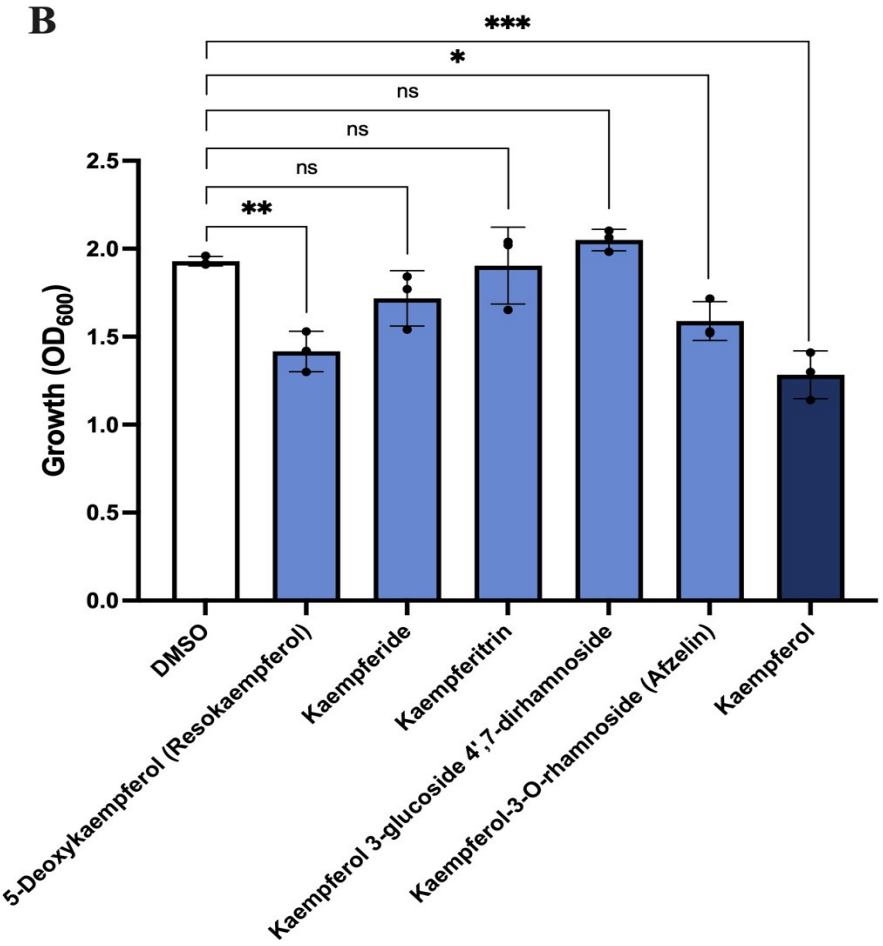
***
*
ns
ns
ns
**
Growth (OD600)
2.5
2.0
1.5
1.0
0.5
0.0
DMSO
5-Deoxykaempferol (Resokaempferol)
Kaempferide
Kaempferitrin
Kaempferol 3-glucoside 4',7-dirhamnoside
Kaempferol-3-O-rhamnoside (Afzelin)
Kaempferol

Figure 2.3: Kaempferol and structurally related compounds potentiate the antimicrobial activity of colistin. (A) Chemical structures of kaempferol and kaempferol-like molecules. **(B)** Impact of kaempferol derivatives at a concentration of 0.05 mM on the growth of *A. baumannii*. The native structure of kaempferol has the highest potentiating activity against *A. baumannii* when combined with sub-MIC amounts of colistin (1.22 μg/mL). For panel **(B)**, assays were carried out in biological triplicate (n=3), with three technical repeats. Statistical analysis consisted of one-way ANOVA between the treated sample and the DMSO carrier control. Error bars represent average values ± S. D. Significance is indicated as * = $p < 0.05$, ** = $p < 0.01$, *** = $p < 0.001$, and **** = $p < 0.0001$.

2.3.4 Kaempferol has antibiofilm activity when applied as a monotherapy

Flavonoids have been previously reported to have activity against biofilm formation (Raorane *et al*., 2019) and, more specifically, kaempferol has been shown to inhibit *Staphylococcus aureus* biofilms (Ming *et al*., 2017). Given the well-established link between bacterial antibiotic tolerance and biofilm formation (Bowler *et al*., 2020), we wanted to explore whether kaempferol or its derivatives have antibiofilm potential. We found that the native structure of kaempferol is active against the formation of *A. baumannii* biofilms, and some heavily modified structures such as kaempferol 3-glucoside 4',7-dirhamnoside had even higher antibiofilm activities (Figure 2.4A). Considering heavily modified derivatives, such as kaempferol 3-glucoside 4',7- dirhamnoside, showed almost no colistin potentiation (Figure 2.3B), these results suggest that the mechanism through which biofilm formation is inhibited is independent of mediating colistin potentiation.

We further explored the antibiofilm formation capacity of the native structure of kaempferol by performing a minimum biofilm inhibitory concentration (MBIC) assay. We found that kaempferol has a dose-dependent impact on biofilm formation, where lower concentrations (<0.05 mM) have minimal effects on biofilm formation, as previously reported by Zhou *et al*. (2022) and higher concentrations (0.3 mM) reduce biofilm by >90%, compared to the carrier control, without impacting bacterial growth (Figure 2.4B). These findings suggest that kaempferol and some of its derivatives can be classified as next-generation antimicrobials i.e., compounds that do not inhibit growth on their own, but can inhibit processes associated with virulence and infection progression.

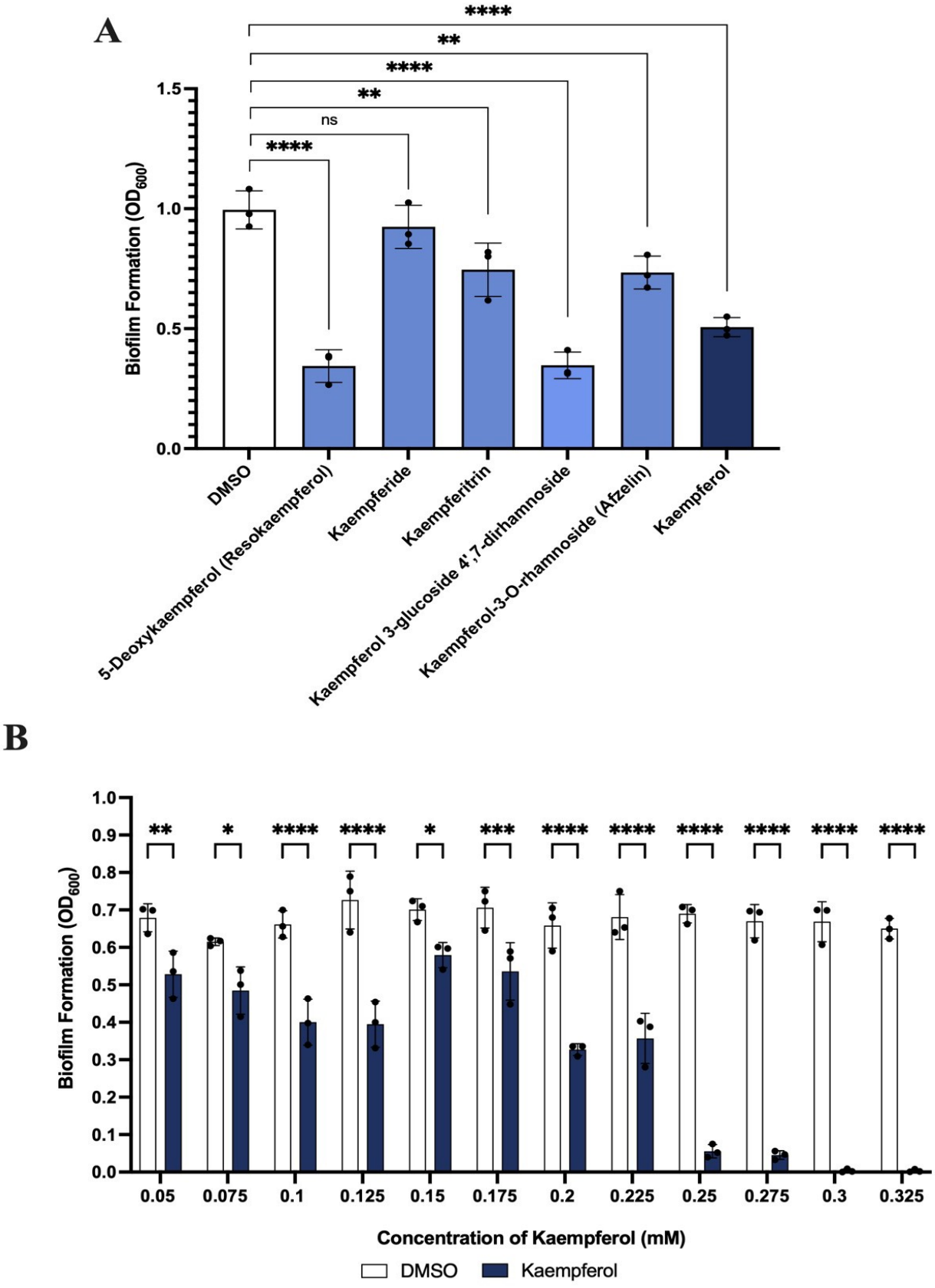

Figure 2.4: Kaempferol and structurally related compounds inhibit biofilm formation. (A) Impact of kaempferol-like compounds at a concentration of 0.05 mM on *A. baumannii* biofilm formation. The native structure of kaempferol, along with some of its derivatives, have activity against *A. baumannii* biofilms when applied as a monotherapy. **(B)** Minimum Biofilm

Inhibitory Concentration (MBIC) of kaempferol on *A. baumannii*. Complete biofilm inhibition was observed at a concentration of 0.3 mM, and inhibition is shown to be dose-dependent. For all panels, assays were carried out in biological triplicate (n=3), with three technical repeats. Analysis consists of one-way ANOVA for panel 2.4A and two-way ANOVA for panel 2.4B, between the treated samples and the DMSO carrier control, each comparison includes controls with increasing amounts of DMSO as the second variable factor. Significance is indicated as * = $p < 0.05$, ** = $p < 0.01$, *** = $p < 0.001$, and **** = $p < 0.0001$.

2.3.5 Kaempferol affects iron homeostasis in *A. baumannii* AB5075

Subsequently, we delved into investigating the mechanism through which kaempferol enhances colistin efficacy in *A. baumannii* by performing a differential RNA sequencing (dRNA-seq) experiment. We treated cells with kaempferol at a concentration where it is most effective when combined with colistin (0.375 mM) and compared the gene expression profile to cells only exposed to the DMSO carrier control. We found that 117 genes were differentially expressed at significant levels (log fold change, with 99 being upregulated and 18 downregulated (Figure 2.5A). We further analysed our dRNA-seq data by using the current *A. baumannii* AB5075-UW annotated genome (Gallagher *et al*. 2015) as a reference and performing Gene Set Enrichment Analysis with FUNAGE-Pro (de Jong *et al*., 2022) to obtain more information about the

functionality of the differentially regulated genes (Table Appendix A.7). Numerous genes related to siderophore biosynthesis and transport in *A. baumannii* AB5075 were upregulated, including the acinetobactin (*bar-bas-bau* cluster, ABUW 1168-1188) and bauminoferrin (*bfn* gene cluster, ABUW 2178-2189) biosynthetic pathways. In addition, two bacterioferritin orthologues (*bfr*, ABUW 0306 and *bfrA*, ABUW 3125) that likely function as iron storage proteins, were found to be downregulated. Together these data suggest that kaempferol is affecting the iron homeostasis in AB5075, and more specifically indicate that cells are suffering from low iron levels in the presence of this compound. Our dRNA-seq data suggests that kaempferol acts as an iron chelator. We confirmed this by measuring the shift in the spectroscopic absorption peak of kaempferol in the presence and absence of iron (Figure 2.5B and Appendix A.8), which agrees with previous work (Marković *et al*., 2014). The data generation for this assay was supported by Dr Ruben De Dios.

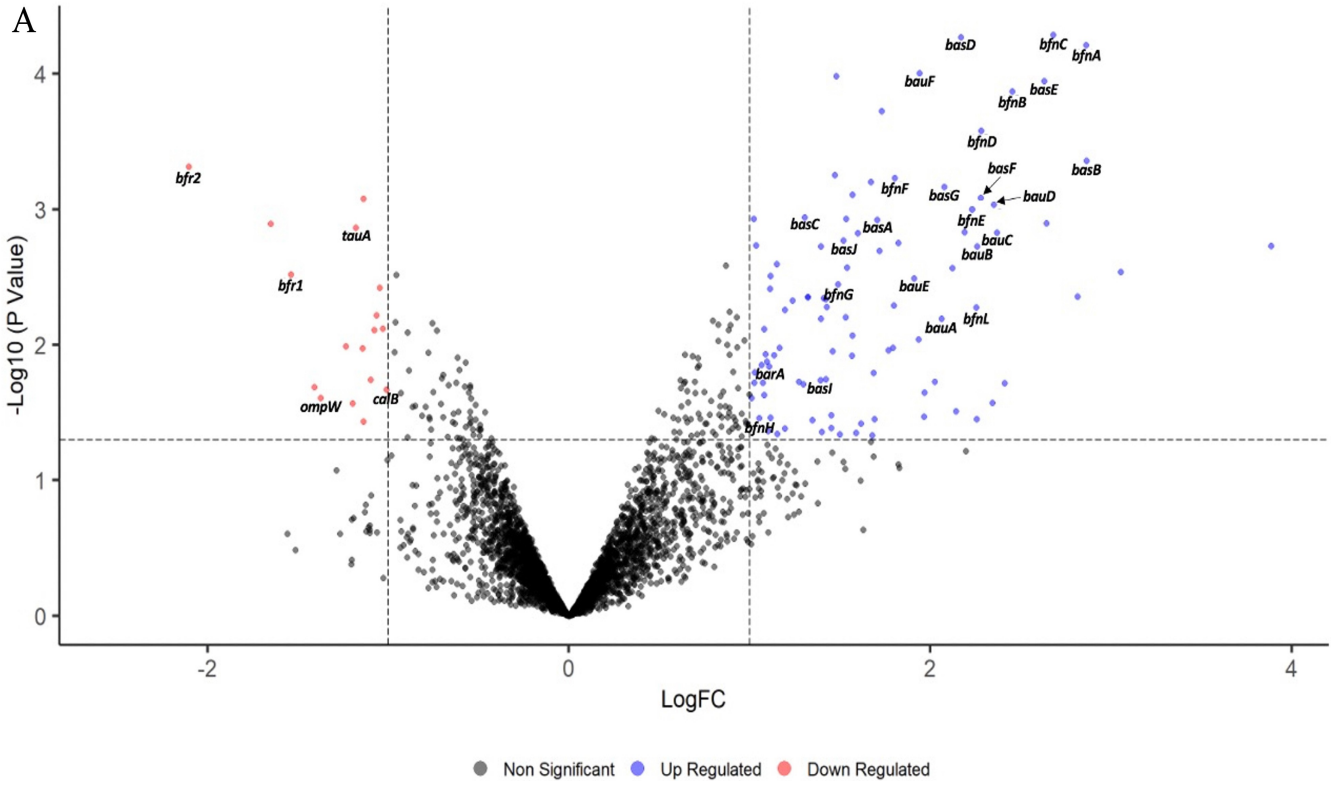

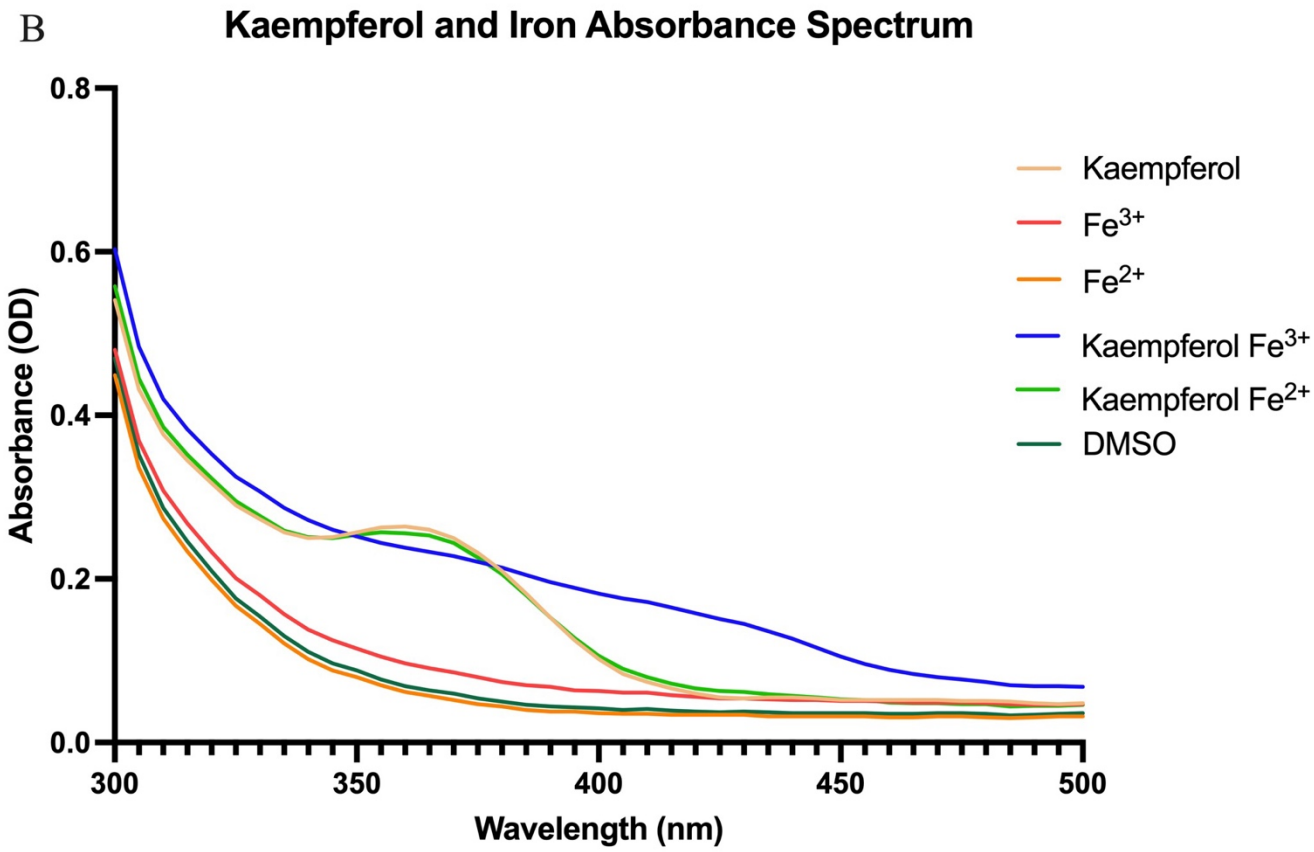

Figure 2.5: Kaempferol affects iron homeostasis in *A. baumannii* AB5075. (A) Volcano plot representing the results of the dRNA-seq analysis performed on cells exposed to kaempferol or the DMSO carrier control. Genes with no change in their expression levels are shown in black, whereas significantly downregulated and upregulated genes are labelled in red and blue, respectively. A total of 117 genes were found to have significantly altered expression levels (99 upregulated and 18 downregulated). Representative cases are indicated, for example, upregulated genes related to siderophore biosynthesis and transport pathways, such as acinetobactin (*bar-bas-bau* cluster) and bauminoferrin (*bfn* gene cluster), as well as downregulated genes related to iron storage (bacterioferritin orthologues *bfr1* and *bfr2*) or encoding iron-dependent proteins (*calB, tauA*, and *ompW*). **(B)** Kaempferol binds to Fe^{3+}, absorption spectra in the 300- 500 nm range of kaempferol (peak at 360 nm), compared to the DMSO control (kaempferol carrier) and mixtures of kaempferol with either Fe^{2+} or Fe^{3+}. The kaempferol absorbance remained unaffected upon the addition of Fe^{2+}, in the mixtures with the 1:1 -> 0.05:0.05 mM kaempferol:Fe^{2+} ratio. However, after the addition of Fe^{3+}, in the mixtures with the 1:1 -> 0.05:0.05 mM kaempferol:Fe^{3+} ratio, the kaempferol absorbance increases, indicating that kaempferol specifically interacts with Fe^{3+}, suggesting complex formation.

2.3.6 Kaempferol-induced iron dysregulation drives colistin potentiation

According to the transcriptomic data (Figure 2.5A), the presence of kaempferol affects iron homeostasis in treated *A. baumannii* cells. To investigate whether this kaempferol-induced dysregulation of cellular iron content underpins colistin potentiation, we supplemented cells grown in the presence of colistin and kaempferol with Fe^{3+} or Fe^{2+}. The increase in bioavailability of Fe^{3+} reversed the previously observed growth defect (Figure 2.6A). In agreement with the spectroscopic assays, the addition of Fe^{2+} did not rescue growth (Figure 2.6B). These data suggest that Fe^{3+} homeostasis is critical during exposure of bacteria to colistin, even at sub-inhibitory concentrations. To further demonstrate the importance of iron homeostasis during colistin treatment, we exposed cells to a non-specific iron chelator, EDTA, in the presence of a sub-inhibitory concentration of colistin (George and Brady, 2023). Similar to kaempferol, EDTA potentiated the activity of colistin (Figure 2.6C), thus highlighting the key role of iron homeostasis for bacteria that are trying to overcome colistin exposure. In addition, we used specific iron chelators, ExJade and 8-Hydroxyquinoline (Pierre *et al*., 2003; Cappellini, 2007), and found that they could also potentiate the activity of colistin, supporting our hypothesis that it is iron chelation by kaempferol that mediates killing of *A. baumannii* in sub-inhibitory amounts of colistin (Figure 2.6D). Finally, we measured the levels of intracellular Fe^{3+} and Fe^{2+} in the presence of kaempferol and observed a significant decrease compared to the carrier control (Figure 2.6E), further confirming the impact of kaempferol on iron availability within the cell.

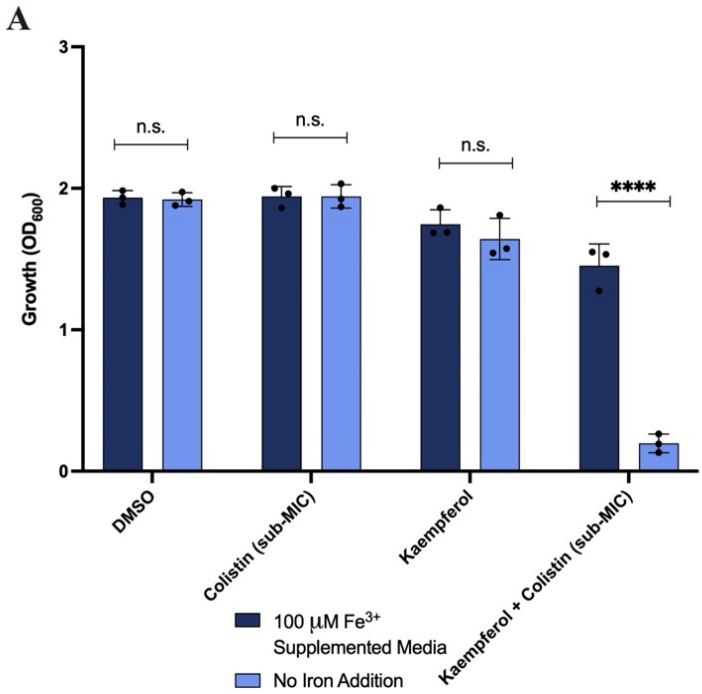
A
Growth (OD_{600})
n.s.
n.s.
n.s.
****
DMSO
Colistin (sub-MIC)
Kaempferol
Kaempferol + Colistin (sub-MIC)
100 μM Fe^{3+} Supplemented Media
No Iron Addition

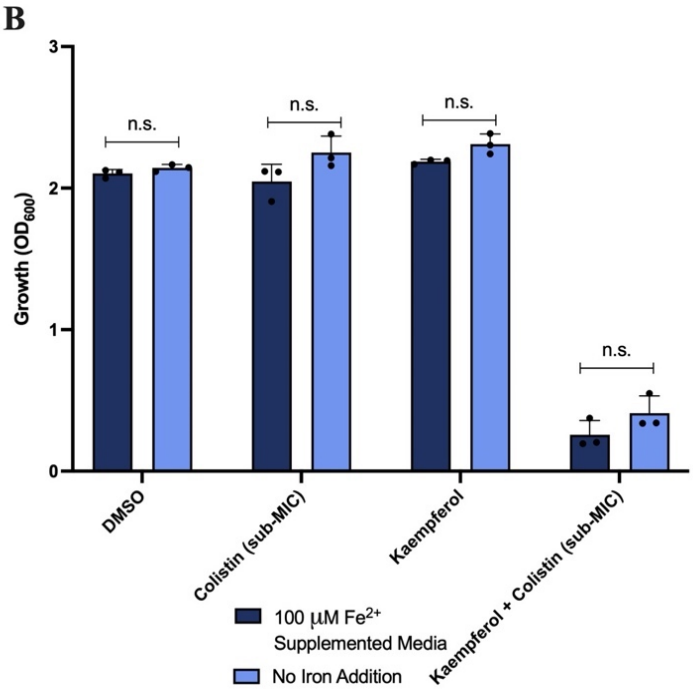
B
Growth (OD_{600})
n.s.
n.s.
n.s.
n.s.
DMSO
Colistin (sub-MIC)
Kaempferol
Kaempferol + Colistin (sub-MIC)
100 μM Fe^{2+} Supplemented Media
No Iron Addition

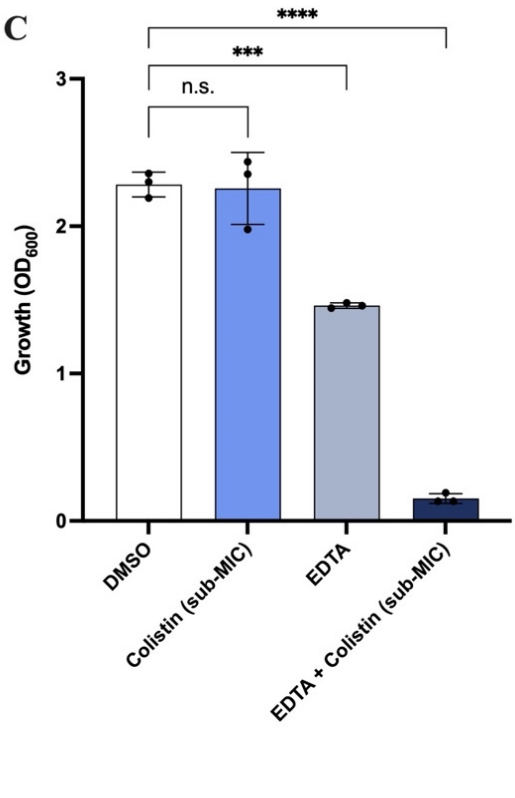
C
Growth (OD_{600})
****
***
n.s.
DMSO
Colistin (sub-MIC)
EDTA
EDTA + Colistin (sub-MIC)

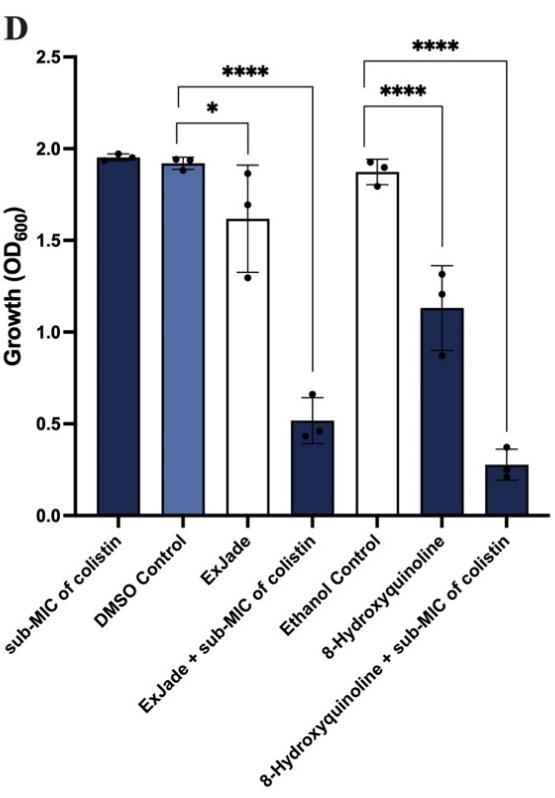
D
Growth (OD_{600})
****
*
****
****
sub-MIC of colistin
DMSO Control
ExJade
ExJade + sub-MIC of colistin
Ethanol Control
8-Hydroxyquinoline
8-Hydroxyquinoline + sub-MIC of colistin

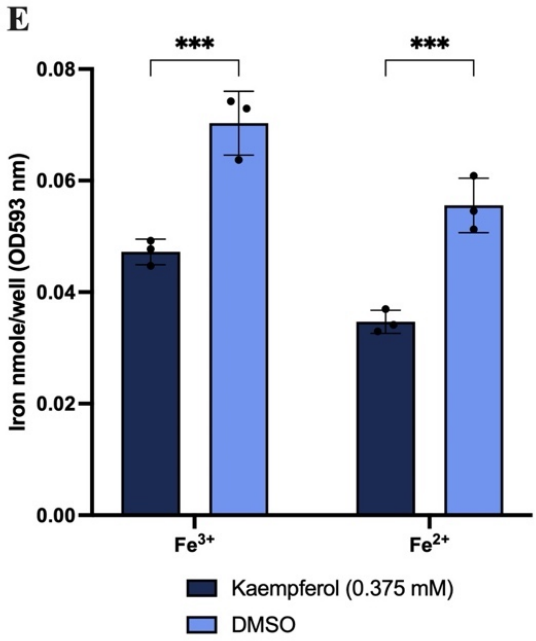

Figure 2.6: Dysregulation of iron homeostasis underpins colistin potentiation by kaempferol. (A-B) Growth inhibition of *A. baumannii* in the presence of 0.375 mM kaempferol concentration in combination with sub-MIC amounts of colistin (1.22 µg/mL) is rescued by Fe^{3+} **(A)**, but not Fe^{2+} **(B)** supplementation. **(C)** EDTA at 100 µM potentiates the activity of colistin; colistin was used at sub-MIC amounts (1.22 µg/mL). **(D)** ExJade and 8-Hydroxyquinoline at 25 µM potentiate the activity of colistin. Colistin was used at sub-MIC amounts (1.22 µg/mL). **(E)** The concentration of available intracellular Fe^{3+} and Fe^{2+} was decreased in the presence of the kaempferol, compared to the DMSO control. For all panels, assays were carried out in biological triplicate (n=3), with three technical repeats. Analysis consists of independent t-test for panels **(A)**, **(B)** and **(E)**, one-way ANOVA for panel **(C)** and two-way ANOVA for panel **(D)**, between the treated samples and the DMSO carrier control, marked using asterisks (* = $p < 0.05$, ** = $p < 0.01$, ns = non-significant) with standard deviation error bars. Each comparison includes controls with increasing amounts of DMSO as the second variable factor. Error bars represent average values ± S. D. Significance is indicated as * = $p < 0.05$, ** = $p < 0.01$, *** = $p < 0.001$, and **** = $p < 0.0001$.

2.3.7 Kaempferol does not increase membrane permeability

In a contemporaneous report, Zhou *et al*., 2022 also reported the potentiation of colistin by kaempferol and proposed that the potentiation of colistin by kaempferol against *A. baumannii* relies on increased membrane permeability. To explore this hypothesis, we investigated the

effect of the kaempferol-colistin combination on the integrity of the outer and inner membranes of *A. baumannii*. Our collaborators Dr Despoina Mavridou and Dr Nikol Kaderábková carried out a membrane permeability assay, using 1-N-phenylnapthylamine (NPN) and propidium iodide (PI), and found that there was no effect on the integrity of the outer membrane when cells were treated with the combination, kaempferol or colistin alone at the experimental concentrations that we have used throughout this study. By contrast, in the positive control, significant NPN uptake was observed when treated with a high concentration of colistin (16 μg/mL) (Figure 2.7A). Notably, the presence of kaempferol, either alone or in combination with colistin, is protective (first two bars) for the outer membrane, resulting in significantly decreased permeability. Similarly, we did not record any inner membrane permeabilisation when treated with either the combination, kaempferol or colistin alone at the same concentrations, whereas PI uptake was observed when treated with a high concentration of colistin (16 μg/mL) (Figure 2.7B). Together, these results suggest that neither of the two components of our combination treatment (colistin or kaempferol) applied at the concentrations used in this study compromise the integrity of the cell envelope and that there is an alternative primary mechanism of action for colistin potentiation by kaempferol.

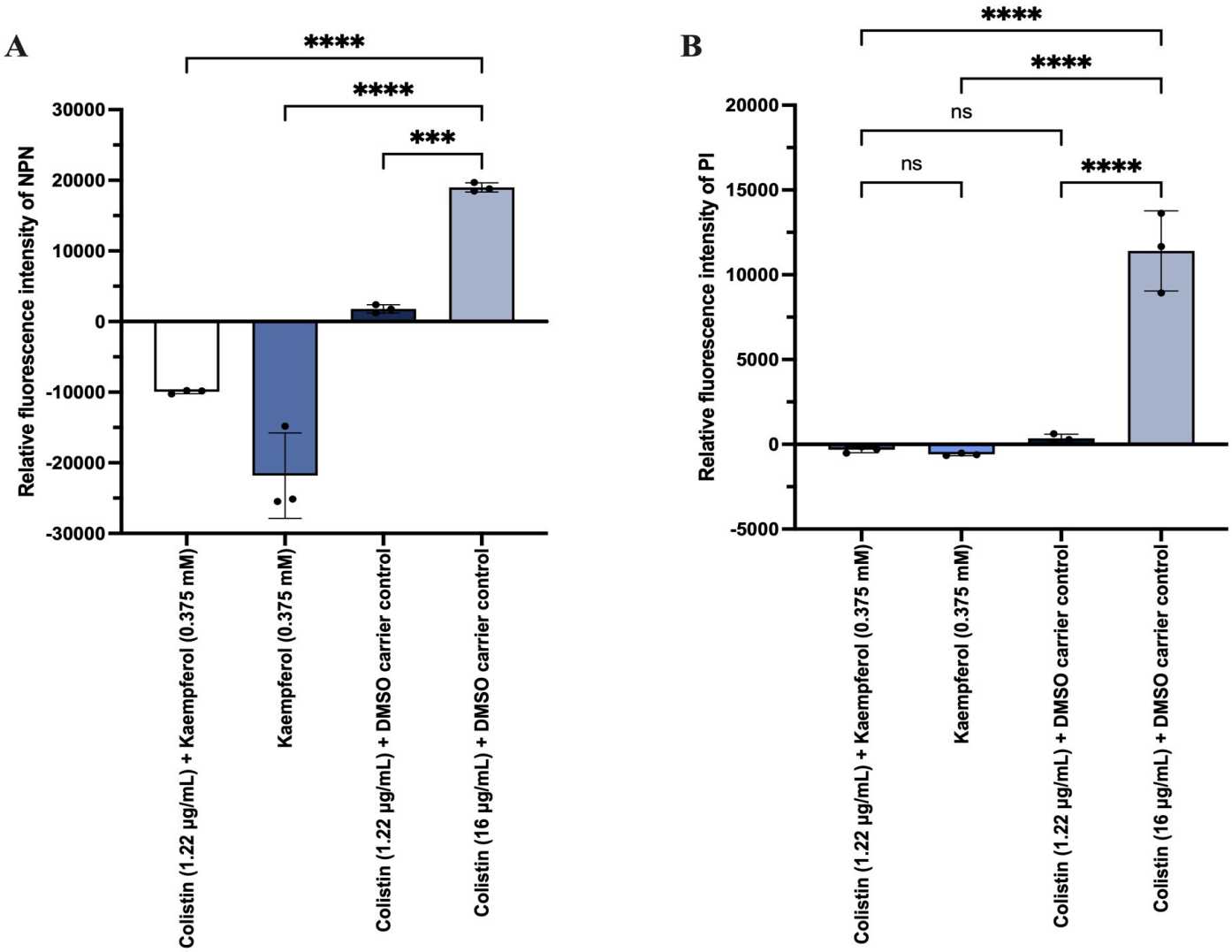

Figure 2.7: Kaempferol-colistin combination treatment or its individual components do not increase membrane permeability in *A. baumannii*. **(A)** Combination of sub-MIC amounts of colistin (1.22 µg/ml) and kaempferol (0.375 mM), or kaempferol (0.375 mM) or colistin (1.22 µg/ml) alone, do not increase NPN uptake in *A. baumannii* cells, and thus do not increase the permeability of the outer membrane. High amounts of colistin (16 µg/mL) permeabilise the outer membrane. **(B)** A combination of sub-MIC amounts of colistin (1.22 µg/ml) and kaempferol (0.375 mM), or kaempferol (0.375 mM) or colistin (1.22 µg/ml) alone, do not increase PI uptake in *A. baumannii* cells, and thus do not increase the permeability of the inner membrane. High amounts of colistin (16 µg/mL) permeabilise the inner membrane. All assays were carried out in biological triplicate (n=3), with three technical repeats. For both panels, DMSO (the kaempferol carrier) was added to all experiments where cells were treated with colistin only. For both panels, DMSO (the kaempferol carrier) was added to all experiments where cells were treated with colistin only. Analysis consisted of one-way ANOVA between the treated samples and the colistin (16 µg/mL) control. Error bars represent

average values ± S. D. Significance is indicated as * = p <0.05, ** = p <0.01, *** = p <0.001, and **** = p <0.0001.

2.3.8 Kaempferol in combination with colistin causes lethal accumulation of ROS

Given that the cell envelope integrity of *A. baumannii* is not affected by combination treatment with kaempferol and colistin, we explored other potential mechanisms through which potentiation might be occurring. One of the known mechanisms of action of colistin against *A. baumannii* is the hydroxyl radical death pathway, whereby superoxide (O_2-) is generated after colistin transits through the outer membrane and crosses the inner membrane (Sampson *et al*., 2012). Superoxide is then detoxified into hydrogen peroxide (H_2O_2) by superoxide dismutase (SOD) enzymes in the cytoplasm, and the generated H_2O_2 subsequently oxidises Fe^{2+} into Fe^{3+} (Yu *et al*., 2015; Gogry *et al*., 2021). This conversion is designated Fenton's reaction and, together with the Haber-Weiss reaction, is a main source of reactive oxygen species (ROS) in the cell (Das *et al*., 2015; Salgado *et al*., 2013).

Considering that kaempferol impacts iron homeostasis (Figures 2.5 and 2.6), we posited that its combination with colistin might affect the downstream production of ROS. We started investigating this hypothesis by measuring total ROS production in cells exposed to kaempferol, colistin or both. We found that sub-inhibitory concentrations of colistin induced ROS production, while kaempferol alone did not (Figure 2.8A). In agreement with our hypothesis, the combination treatment induced levels of ROS that significantly exceeded those induced by colistin alone. Further supporting this, the amount of ROS produced by colistin alone was not sufficient to affect growth (Figure 2.8A), suggesting that the ROS detoxification systems that would normally rescue the cells from exposure to colistin at sub-MIC amounts, may be impaired in the presence of kaempferol, in turn leading to the accumulation of ROS at levels that are lethal for the cell. These assays were conducted in the presence of a 10% H_2O_2 control as using a ROS species allowed for the evaluation of the effectiveness of various ROS-generating agents (Figure 2.8B). In *A. baumannii*, the only annotated SOD coding genes are *sodB* (*ABUW 1216)* and *sodC* (*ABUW 0339*). Intriguingly, these enzymes require metal

cofactors for activity, with SodB binding iron, and SodC depending on copper or zinc. To investigate whether either of these enzymes are essential for the detoxification of ROS produced as a result of colistin exposure, we treated transposon mutants in the respective coding genes obtained, and validated using qPCR, from the Manoil *A. baumannii* transposon mutant library (Gallagher *et al*., 2015) with colistin at sub-MIC amounts. Both mutants grew comparatively to the wild-type strain when exposed to the carrier control or to kaempferol alone (Figure 2.8C), highlighting that dysregulation of iron homeostasis under normal growth conditions i.e., conditions where excess ROS is not generated, is not detrimental to the cell. Nonetheless, when colistin was used at sub-MIC levels, the growth of the *sodB* mutant was completely impaired, while the *sodC* mutant growth was only marginally affected (Figure 2.8C).

With SodB requiring iron as a cofactor for activity, it is possible that the potential decrease of available iron in the presence of kaempferol, in addition to affecting Fenton's reaction, also affects SodB function. This would further decrease the ability of the cell to detoxify the excess ROS produced in the presence of colistin, even at sub-MIC amounts (Figure 2.8A) (Heindorf *et al*., 2014). In order to investigate whether the iron-dependency of SodB contributes to the potentiation of colistin by kaempferol, another member of the lab Dr Rubén De Dios constructed two wild-type derivative strains overexpressing either *sodB* or *sodC* under a chromosomally integrated IPTG-inducible promoter and we then challenged them with our kaempferol and colistin combination treatment. We hypothesised here that if iron was essential for SodB activity, then overexpressing *sodB* in the presence of the combination treatment would not rescue the cells, however, overexpression of *sodC*, which does not bind iron, should be beneficial. Indeed, this assay confirmed that this is the case, with only *sodC* overexpression partially rescuing the lethal phenotype of the kaempferol and colistin combination treatment (Figure 2.8D). This suggests that colistin potentiation in the presence of kaempferol is affected by the abundance and enzymatic activity of the different SOD enzymes.

To further explore this, Dr Rubén De Dios generated mutants with gfpmut3 transcriptional fusions to the *sodB* and *sodC* promoter regions. We then used these mutants to measure the expression of these genes in the presence and absence of the combination treatment. As shown in Figure 2.8E, the levels of expression of both genes remained invariant across the combination

treated samples and DMSO controls, highlighting that the effects of kaempferol are not occurring at the transcriptional level, but at the enzyme activity level of SOD proteins.

The results in Figure 2.8E also confirm the dRNA-Seq data, where greater levels of *sodB* expression were measured compared to those of *sodC*. These observations, together with the fact that overexpression of *sodC* only partially rescued the lethal phenotype of the combination treatment (Figure 2.8D), further highlight the importance of SodB in ROS detoxification. To assess whether other metal cofactors or cations can overcome the influence of kaempferol, we supplemented the media with Cu^{2+}, Mg^{2+}, Zn^{2+} or Ca^{2+} and found that they could not rescue growth inhibition from the combination treatment (Figure 2.8F). Altogether, these results indicate that the iron sequestration by kaempferol disables the ROS protection mechanisms of *A. baumannii*, which cannot be overcome by iron-independent mechanisms, leading to greater colistin susceptibility.

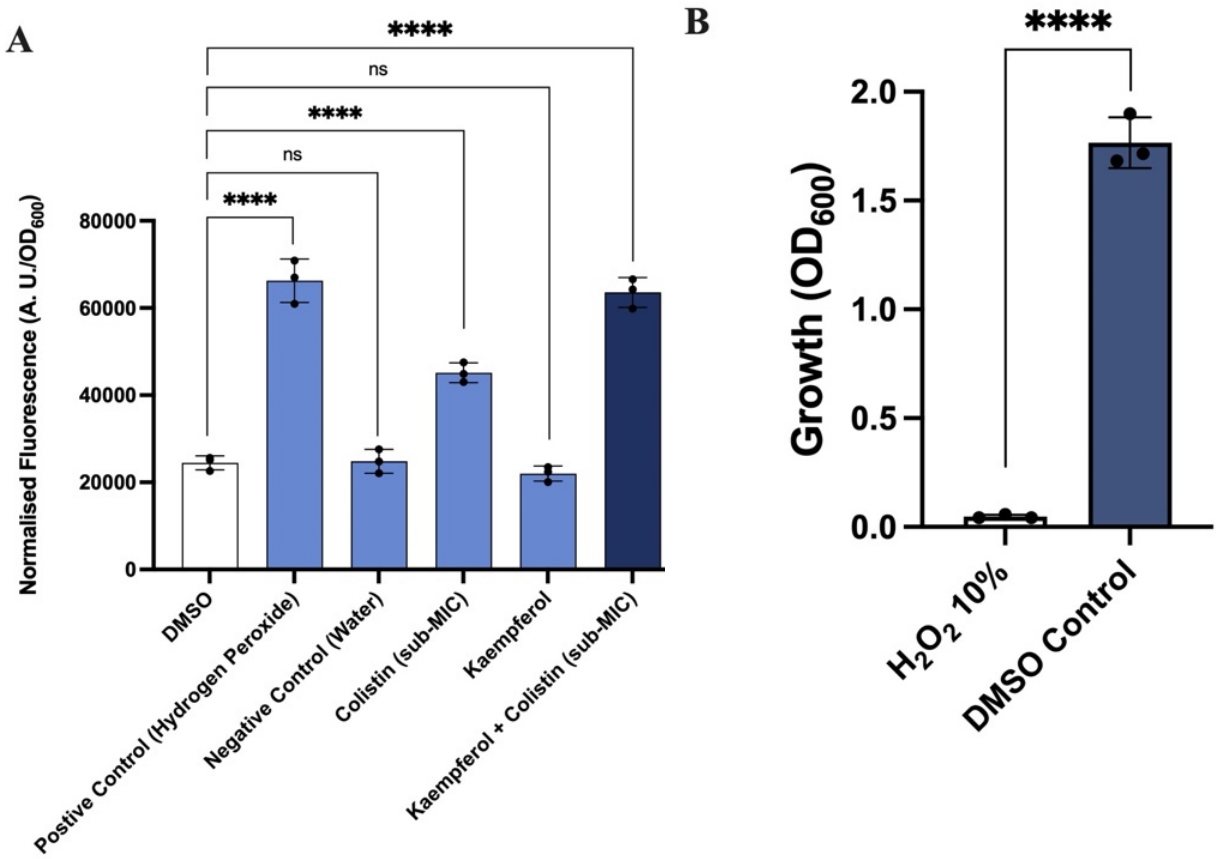

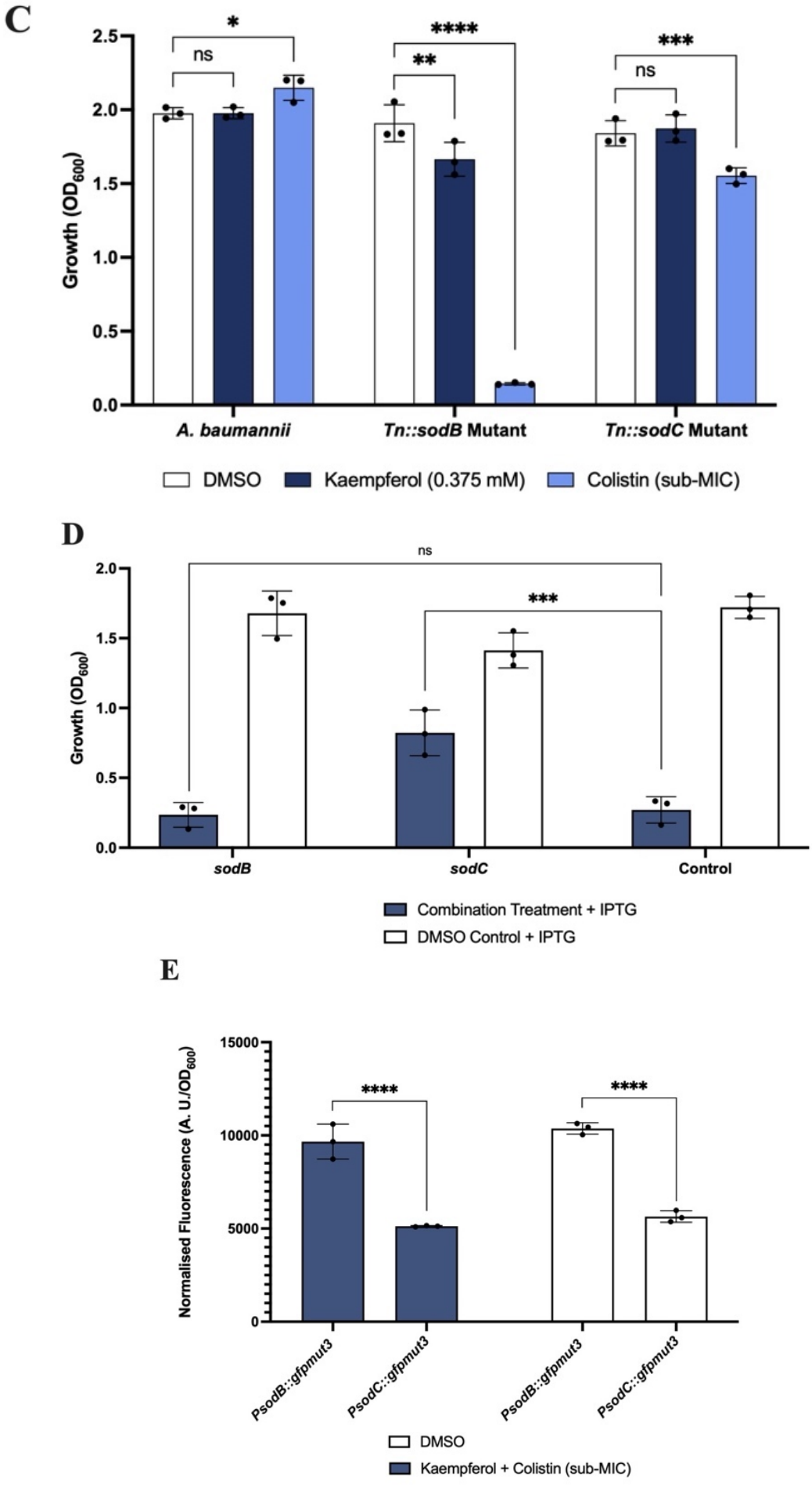
C
Growth (OD600)
2.5
2.0
1.5
1.0
0.5
0.0
*
ns
****
**
***
ns
A. baumannii
Tn::sodB Mutant
Tn::sodC Mutant
DMSO
Kaempferol (0.375 mM)
Colistin (sub-MIC)
D
Growth (OD600)
2.0
1.5
1.0
0.5
0.0
ns
***
sodB
sodC
Control
Combination Treatment + IPTG
DMSO Control + IPTG
E
Normalised Fluorescence (A. U./OD600)
15000
10000
5000
0
****
****
PsodB::gfpmut3
PsodC::gfpmut3
PsodB::gfpmut3
PsodC::gfpmut3
DMSO
Kaempferol + Colistin (sub-MIC)

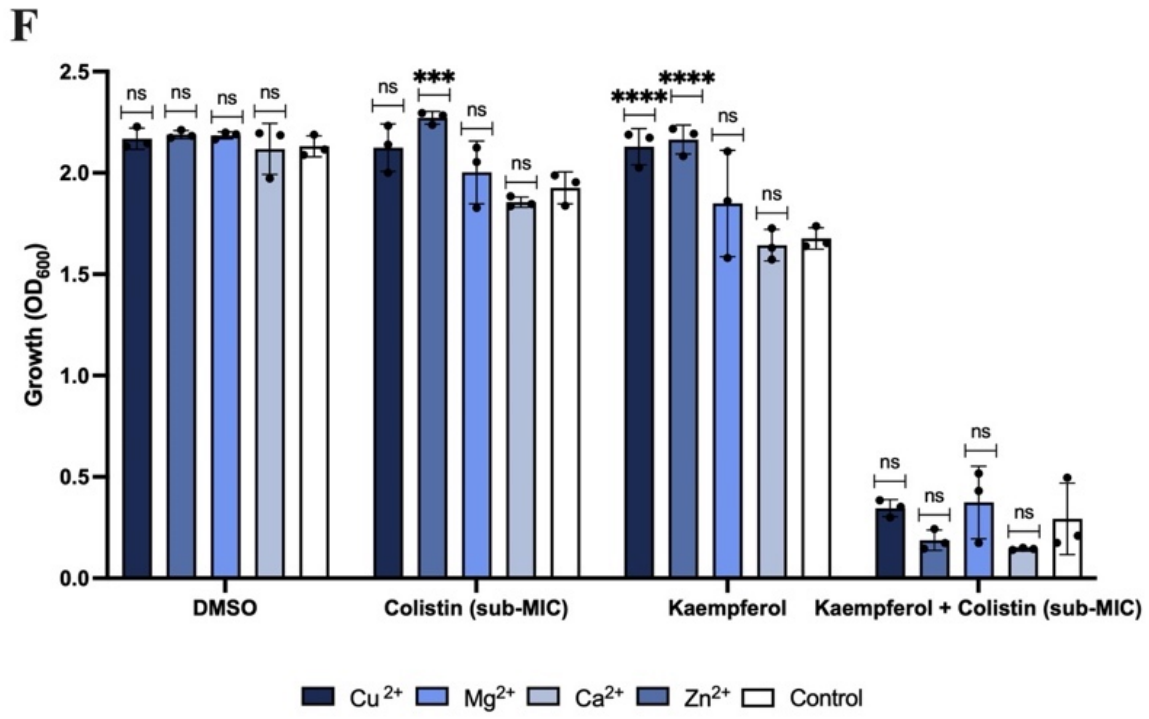

Figure 2.8: Kaempferol inhibits ROS detoxification during colistin treatment. **(A)** Sub-MIC amounts of colistin (1.22 µg/ml) induce ROS production, while kaempferol alone (at 0.375 mM) does not. The kaempferol and colistin combination treatment (colistin at 1.22 µg/ml and kaempferol at 0.375 mM) induces levels of ROS that significantly exceed those induced by colistin alone. **(B)** The positive control consisted of hydrogen peroxide at a concentration lethal to *A. baumannii* (10% v/v). **(C)** Growth of *sodB* and *sodC* transposon mutants in the presence of DMSO, kaempferol, colistin and the combination of kaempferol and colistin (colistin was used at 1.22 µg/ml and kaempferol at 0.375 mM). The *sodB* mutant is more susceptible to sub-MIC amounts of colistin compared to wild-type *A. baumannii* or the *sodC* mutant. **(D)** Growth of AB5075 derivative strains overexpressing either *sodB* or *sodC* from a miniTn7- based IPTG-inducible system compared to an empty vector control. The overexpression of *sodB* could not restore the growth after treatment with kaempferol and colistin (colistin was used at 1.22 µg/ml and kaempferol at 0.375 mM). However, the overexpression of *sodC* could significantly alleviate growth inhibition. Statistical comparisons were performed between the overexpression strains and the empty-vector control. **(E)** Fluorescence measurements from a transcriptional *gfp* fusion to the *sodB* and *sodC* promoter regions (*PsodB* and *PsodC,* respectively) after growth for 2 h in the presence of DMSO or the combination of kaempferol and colistin (colistin was used at 1.22 µg/ml and kaempferol at 0.375 mM). For both conditions (carrier control or combination treatment) *sodB* is expressed at higher levels than *sodC.* **(F)**

Growth inhibition of *A. baumannii* in the presence of 0.375 mM kaempferol concentration in combination with sub-MIC amounts of colistin (1.22 μg/mL) is not rescued by Cu^{2+}, Mg^{2+}, Zn^{2+} or Ca^{2+} supplementation. All assays were carried out in biological triplicate (n=3), with three technical repeats. Analysis consisted of one-way ANOVA for panel **(A)**, independent t-test for panel **(B)**, and two-way ANOVA for panel **(C)**, comparing the treated samples with the DMSO carrier control. Two-way ANOVA analysis was carried out for panels **(D)** and **(F)** comparing the treated samples and the DMSO control. Two-way ANOVA analysis was carried out for panel **(E)** between *PsodB::gfpmut3* and *PsodC::gfpmut3*. Each comparison includes controls with increasing amounts of DMSO as the second variable factor. Error bars represent average values ± S. D. Significance is indicated as * = $p < 0.05$, ** = $p < 0.01$, *** = $p < 0.001$, and **** = $p < 0.0001$.

2.1.1 Kaempferol sensitises colistin-resistant clinical strains

Colistin potentiation is critical for safeguarding this last resort antibiotic as it is often our only treatment option against highly resistant Gram-negative pathogens. We have shown that in *A. baumannii* kaempferol chelates iron (Figures 2.5 and 2.6), increases cytoplasmic ROS production and prevents ROS detoxification during colistin treatment (Figure 2.8). To assess whether these effects would be sufficient to increase the efficacy of colistin against strains that are resistant to this antibiotic, our collaborators Dr Despoina Mavridou and Dr Nikol Kadérábková first tested the potentiation approach on laboratory model strains. Since iron homeostasis and ROS detoxification are important for most bacteria (Runci *et al*., 2019, Vaishampayan *et al*., 2022) we started our investigation using *Escherichia coli* K-12; we selected the W3110 strain, along with its colistin-resistant counterparts, strain WD101, a *pmrA* mutant with 4-amino-4-deoxy- L-arabinose (L-Ara4N)-modified lipid A (Trent *et al*., 2001), and strain W3110, carrying the *mcr-1* gene on a medium copy-number plasmid that bears PEtN-modifications on its lipid A (Dortet *et al*., 2018).

The use of these strains allowed us to assess our approach on a well-controlled system with defined lipid A modifications, devoid of confounding effects that might arise had we only tested non-isogenic clinical isolates. We then compared the colistin MIC values for these strains recorded under EUCAST specifications in the presence of 50 μM kaempferol to ones obtained only in the presence of the DMSO carrier control. We found that for colistin-susceptible strain

backgrounds (W3110 and W3110 carrying an empty-vector control (pDM1)), the addition of kaempferol did not have any major effects on their colistin MIC values (Figure 2.9A and 2.9B). However, for strains with chromosomal (WD101) and plasmid-encoded (W3110+*mcr*-1) resistance, the use of kaempferol resulted in colistin MIC drops of 8 and 4 μg/mL, respectively (Figure 2.9A and 2.9B). This demonstrates that colistin potentiation due to kaempferol exposure might be a useful avenue to reverse colistin resistance, irrespective of the mechanism of lipid A modification.

Encouraged by these results, we tested our approach on *E. coli* clinical isolates; we selected a colistin-susceptible *E. coli* (ATCC25922, standardly used as a EUCAST MIC assay control), a colistin-resistant *mcr*-1-carrying strain (1073944), and two colistin-resistant isolates harbouring chromosomal mutations (1252394 and CNR1728). For all three colistin-resistant isolates, the addition of kaempferol resulted in complete sensitisation to colistin, while the sensitive strain remained unaffected (Figure 2.9C). We then proceeded to investigate whether similar results could be obtained in *A. baumannii* clinical strains (Figure 2.9D and Table Appendix.1). We exposed highly resistant *A. baumannii* isolates (colistin MIC values of 256 μg/mL) to the combination treatment and observed a 64-fold drop in MIC values (colistin MIC values of 4 μg/mL; we note that the EUCAST breakpoint for colistin is 2 μg/mL). Although sensitization was not achieved for *A. baumannii* isolates, these drastic drops in colistin MIC values demonstrate the potential of kaempferol as a colistin potentiator, particularly in light of colistin's high toxicity and low bioavailability during treatment (Satlin *et al*., 2020).

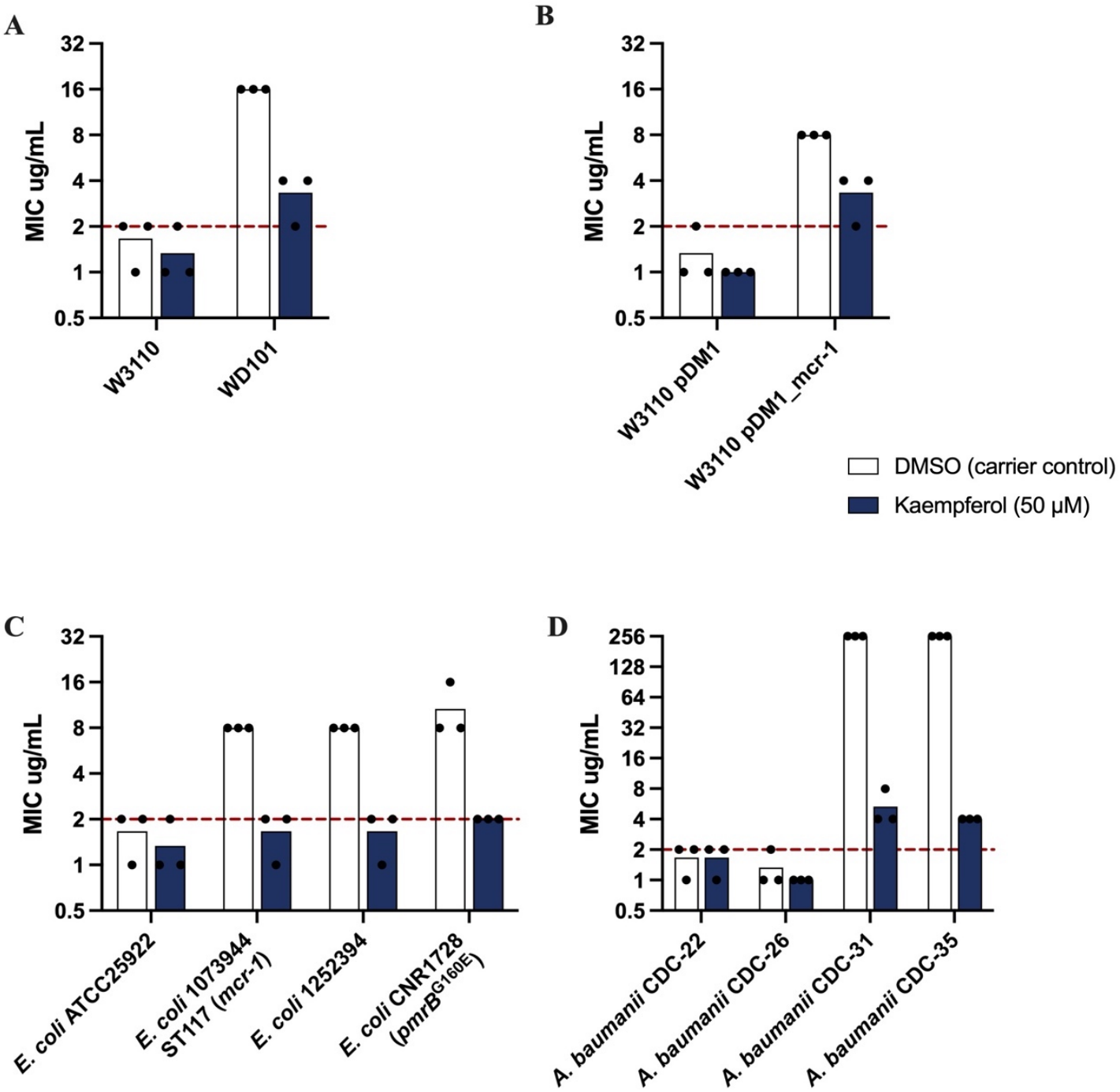
A
B
C
D
MIC ug/mL
32
16
8
4
2
1
0.5
W3110
WD101
W3110 pDM1
W3110 pDM1_mcr-1
DMSO (carrier control)
Kaempferol (50 µM)
E. coli ATCC25922
E. coli 1073944 ST117 (mcr-1)
E. coli 1252394
E. coli CNR1728 (pmrB G160E)
256
128
64
A. baumanii CDC-22
A. baumanii CDC-26
A. baumanii CDC-31
A. baumanii CDC-35

Figure 2.9: Kaempferol addition results in colistin potentiation when applied to clinical strains of *E. coli* and *A. baumannii.* (A-B) Combination of colistin with kaempferol, results in a decrease of colistin MIC values for colistin-resistant *E. coli* K-12 strains, independent of the mechanism of colistin resistance; sensitive strains remain unaffected. WD101 is a *pmrA* mutant with 4-amino-4-deoxy-L-arabinose (L-Ara4N)-modified lipid A derived from strain W3110, and W3110 pDM1 *mcr*-1 expresses the mobile colistin resistance protein MCR-1 and, therefore bears PEtN-modifications on its lipid A. **(C)** Combination of colistin with kaempferol sensitises colistin-resistant *E. coli* clinical isolates. **(D)** The combination of colistin with kaempferol results in a 64-fold drop of the colistin MIC values of colistin-resistant *A. baumannii* clinical isolates. All assays were carried out in biological triplicate (n=3), with four technical repeats; red dotted lines indicate the EUCAST clinical breakpoint for colistin.

2.1.2 Kaempferol promotes clearance of *A. baumannii in vivo*

To further assess kaempferol's potential as a colistin potentiator we tested our combination approach *in vivo* by using the *Galleria mellonella* wax moth model of infection (Ménard *et al*., 2021, McCarthy *et al*., 2017). Since the efficacy of antibiotics *in vivo* is often different from the MIC values reported *in vitro* (Mouton *et al*., 2018), we first performed a titration of different concentrations of colistin in our infection model. We found that the lowest concentration of colistin allowing larval survival after lethal infection with *A. baumannii* is 0.1 µg/*G. mellonella*. Therefore, we chose to use the sub-MIC concentration, consisting of 0.08 µg of colistin/*G. mellonella*, this concentration when used alone does not allow the survival of the larvae (Figure 2.10A) in our subsequent experiments with kaempferol. We then assessed whether any of the compounds we intended to use had underlying toxicity in this model.

Cytotoxicity assays (Figure 2.10B, 2.10C and 2.10D) showed that the DMSO carrier control (1-5 µL), kaempferol (0.5 mM/*G. mellonella*), colistin (0.08 µg/*G. mellonella*) and the combination of kaempferol and colistin at the amounts used were not toxic to the larvae, which have a probability of survival of >90% if exposed to any of these molecules at these concentrations. Finally, we tested the efficacy of our combination therapy approach in this infection model. We infected *G. mellonella* larvae with a lethal dose of *A. baumannii* and treated this infection with the carrier control (untreated), colistin at 0.08 µg/*G. mellonella* (monotherapy), kaempferol at 0.5 mM/*G. mellonella* (monotherapy), or with colistin at 0.08

μg/*G. mellonella* and kaempferol at 0.5 mM/*G. mellonella* (combination therapy). We found that if the infection remained untreated (carrier control) or was treated only with colistin, all the larvae died (Figure 2.10E). Kaempferol monotherapy also resulted in less than 10% survival of the larvae. By contrast, combination therapy led to the survival of 60% of the larvae, demonstrating that targeting iron bioavailability in an infection setting potentiates colistin activity. Amount per *G. mellonella* was used rather than amount per milligram of *G. mellonella* body weight in order to account for potential variability in pharmacokinetics (pK) and pharmacodynamics (pD) across individual *G. mellonella*. This allowed for a more consistent and comparative analysis of the effects of the treatment *in vivo* by preventing the influence of individual variability in body weight.

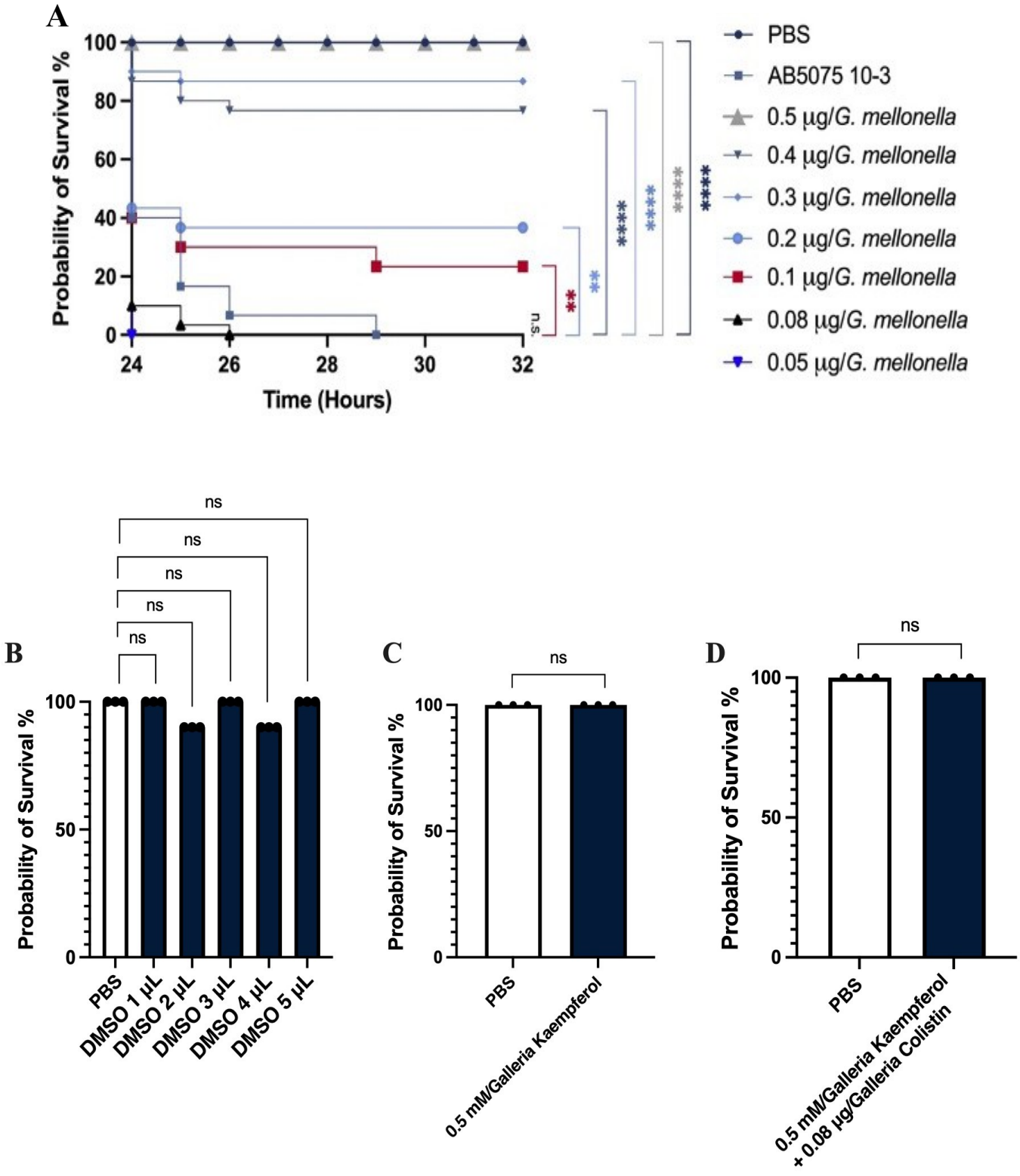
A
Probability of Survival %
100
80
60
40
20
0
24
26
28
30
32
Time (Hours)
n.s.
**
**
****
****
****
****
PBS
AB5075 10-3
0.5 µg/G. mellonella
0.4 µg/G. mellonella
0.3 µg/G. mellonella
0.2 µg/G. mellonella
0.1 µg/G. mellonella
0.08 µg/G. mellonella
0.05 µg/G. mellonella
B
ns
ns
ns
ns
ns
Probability of Survival %
100
50
0
PBS
DMSO 1 µL
DMSO 2 µL
DMSO 3 µL
DMSO 4 µL
DMSO 5 µL
C
ns
Probability of Survival %
100
50
0
PBS
0.5 mM/Galleria Kaempferol
D
ns
Probability of Survival %
100
50
0
PBS
0.5 mM/Galleria Kaempferol
+ 0.08 µg/Galleria Colistin

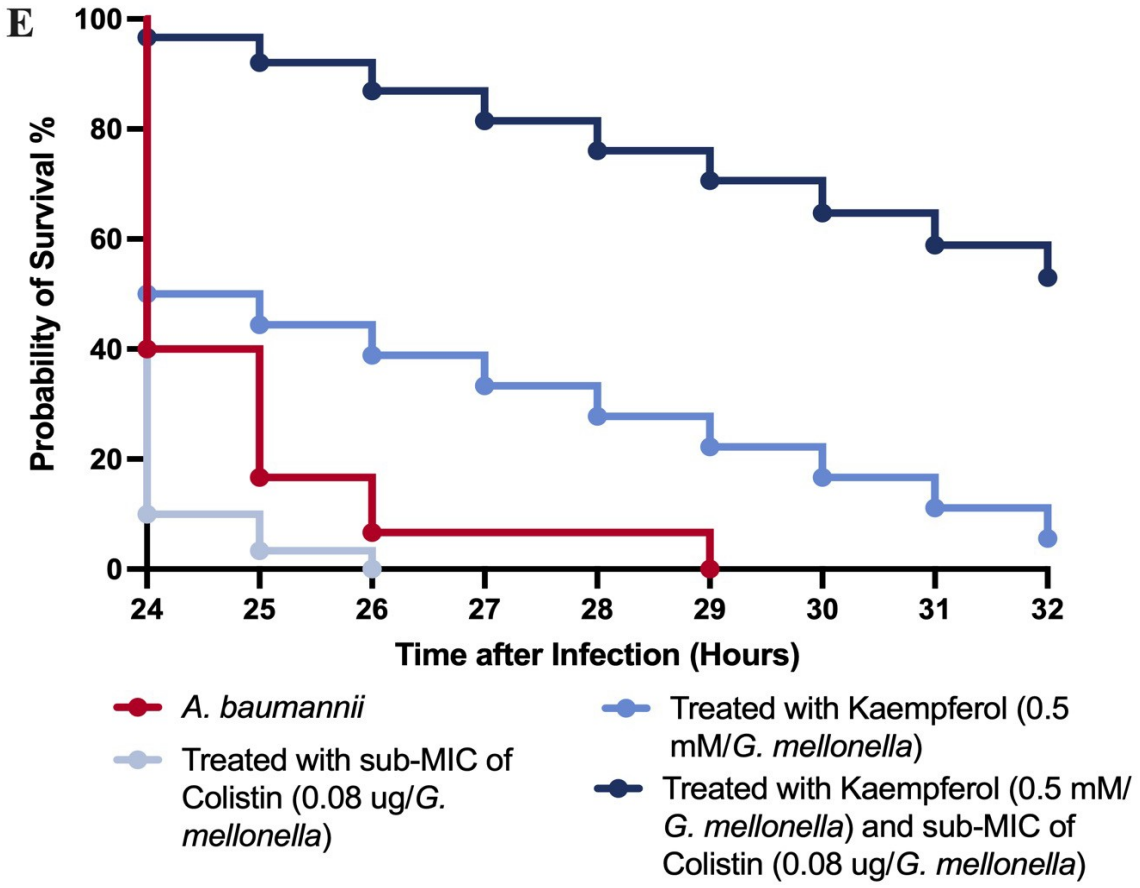

Figure 2.10: Kaempferol potentiates colistin activity in the *Galleria mellonella* infection model. (A) Cytotoxicity assays in the *Galleria mellonella* 32-hour infection model with varying amounts of colistin combined with the DMSO carrier control, **(B)** varying amounts of DMSO **(C)** kaempferol alone and **(D)** sub-MIC of colistin with kaempferol. All tested conditions were demonstrated to not be cytotoxic to the larvae. **(E)** 60% of larvae survived *A. baumannii* infection when *G. mellonella* was treated with colistin at 0.08 µg /*G. mellonella* and kaempferol at 0.5 mM/*G. mellonella*. Lack of treatment (carrier control) and colistin monotherapy results in larval death, while kaempferol monotherapy allows less than 10% survival of the larvae. The control and treatment with the sub-MIC of colistin data was reused for panels A and E. Assays were carried out in biological triplicate per treatment group, with 30 *G. mellonella* used per group (n = 30). Statistical analysis for all panels consisted of Log-rank (Mantel-Cox) test, where no significant difference was seen between the samples and PBS control in panels **(A-D)**, and where *A. baumannii* Vs *A. baumannii* + colistin was not significant, *A. baumannii* Vs *A. baumannii* + kaempferol was not significant and *A. baumannii* Vs *A. baumannii* + colistin + kaempferol had a Log Rank p <0.001 in panel **(E)**.

2.2 Discussion

During the screening of compounds from the Caithness library and Kew Gardens library, kaempferol emerged as a potential inhibitor of *A. baumannii* growth when combined with the sub-MIC concentration of colistin. At the time of this finding, this effect had not been previously documented in previous literature, prompting an investigation into the efficacy of this combination and its mechanism of action against *A. baumannii*. Kaempferol has been used in clinical trials for the treatment of diseases like acute and chronic inflammation, cancer, obesity, diabetes, and liver injury (Alam *et al*., 2020). Studies have also shown that it has antimicrobial and antibiofilm activity against the Gram-positive bacteria *S. aureus* and *E. faecalis* (del Valle *et al*., 2016; Huang *et al*., 2015; Ming *et al*., 2017). Here, we go on to demonstrate that the native form of kaempferol combined with sub-MIC amounts of colistin, is the most efficacious at reducing the growth of *A. baumannii* compared to its modified larger derivates (Figure 2.3B). We also demonstrate that the native form of kaempferol has antibiofilm activity (Figure 2.4) against the Gram-negative opportunistic pathogen *A. baumannii* and can potentiate the activity of colistin, bypassing resistance in *A. baumannii* and *E. coli* clinical strains. We found that the latter effect is, overall, due to the ability of kaempferol to disrupt intracellular iron homeostasis. Interestingly, a report conducted concurrently with this study, published as we were submitting ours, suggested that the combination treatment of kaempferol and colistin resulted in increased membrane permeability of the outer membrane as measured through alkaline phosphatase release after 6 hours (Zhou *et al*., 2022). This posed a challenge as Zhou *et al*. (2022) presented conflicting results to our study, creating inconsistencies between the two studies. However, the data in this study did not support this hypothesis; by using membrane-specific dyes we observed no increased inner membrane or outer membrane permeability caused by the concentrations of kaempferol or colistin used in this study (Figure 2.7A and 2.7B).

Another study conducted concurrently with ours, published by Zhong *et al*. (2023), also explores the mechanism of action of compounds that potentiate colistin. They investigated three catechol-type flavonoids: 7,8-dihydroxyflavone, myricetin, and luteolin, in the Gram-negative bacteria *Salmonella*. Zhong *et al*. (2023) proposed that these flavonoids enhance colistin's

activity by targeting iron homeostasis, inducing the reduction of ferric ions to the ferrous form. This alteration inactivates the *pmrA/pmrB* two-component system, leading to changes in membrane charge that facilitate colistin binding. Interestingly, our study also indicates an increase in ferrous iron levels. However, our transcriptomic analysis did not reveal downregulation of *pmrA/pmrB* at the gene level, as observed in the study by Zhong *et al*. (2023). This disparity suggests that while both studies implicate dysregulation of iron homeostasis in colistin potentiation, they may operate through distinct mechanisms.

While iron is an invaluable micronutrient that is critical for a wide array of metabolic functions in bacteria (Bradley *et al*., 2020), free iron is toxic, and for this reason, its concentration is tightly regulated (Recalcati *et al*., 2017). The dRNA-Seq analysis (Figure 2.5A) showed that kaempferol exposure resulted in the upregulation of genes responsible for the biosynthesis and transport of the siderophores acinetobactin (*bar-bas-bau* cluster) and bauminoferrin (*bfn* gene cluster). At the same time, we observed the downregulation of two bacterioferritin orthologues (*bfr*) that promote iron storage, as well as genes encoding proteins that need iron as a cofactor (*calB* and *tauA*). Moreover, we recorded the downregulation of the *ompW* gene, a key component of the iron regulon that controls iron homeostasis (Catel-Ferreira *et al*., 2016). Together the transcriptomics data suggests that kaempferol disturbs the intracellular iron homeostasis in *A. baumannii* and in particular drives the cell to acquire additional extracellular iron via increased siderophore production and decreased iron storage and usage. While disturbing iron homeostasis is stressful for the cell, it is clear from our iron rescue data that in rich media it can be overcome through these diverse responses. Nonetheless, during stress conditions, for example under colistin treatment, kaempferol-induced iron depletion becomes lethal, potentiating the activity of colistin (Figure 2.2A).

In agreement with our dRNA-Seq and absorbance spectra (Figure 2.5A), as well as previous reports (Markovic´ *et al*., 2014, Ferrali *et al*., 1997) kaempferol binds to Fe^{3+}. The role of kaempferol in iron chelation, and ultimately depletion, is further supported by the decrease of available intracellular iron in the presence of kaempferol (Figure 2.6E), and the fact that supplementation of the growth media with Fe^{3+} rescues the cells from the lethal effects of the kaempferol and colistin combination treatment (Figure 6A and 6B). The importance of iron homeostasis for overcoming colistin treatment, which explains the lethal effects of the

kaempferol/colistin combination, is demonstrated by the fact that non-specific and specific iron chelators (EDTA, ExJade and 8-Hydroxyquinoline) also potentiate the activity of colistin (Figure 2.6C and Figure 2.6D).

We delved deeper into the mechanism of colistin potentiation by investigating whether kaempferol-induced iron imbalance in combination with colistin treatment led to the enhancement of the hydroxyl radical death pathway, a known mechanism of colistin against *A. baumannii*. In this pathway, O_2- generated due to colistin traversing through the outer and inner membrane is converted into H_2O_2 by SOD enzymes. H_2O_2 can then participate in the Fenton reaction to oxidise Fe^{2+}into Fe^{3+}, concomitantly producing •OH (R2, below). Considering the data in this study and the previous literature (Marković *et al*., 2014) that implicate kaempferol in chelating ferric iron thus making it unavailable, its presence could imbalance Fenton's reaction 1 and 2 (R1 and R2 below). Since kaempferol on its own does not have a growth inhibitory effect nor increases ROS production or damage the membrane (Figure 2.2B, Figure 2.8A and Figure 2.7, respectively), the cell can compensate for this imbalance when kaempferol is applied as a monotherapy. However, this imbalance is exacerbated by the toxic superoxide (O_2-) generated in the presence of colistin (Chen *et al*., 2009; Sampson *et al*., 2012), as shown by the increased ROS production during combination treatment (Figure 2.8A). Since iron is a cofactor for SodB, a protein that is key for the detoxification of ROS during colistin treatment (Figure 2.8C), chelation of iron by kaempferol further reduces the ability of the cell to detoxify the superoxide produced by colistin in the hydroxyl radical pathway. Overall, the synergy between colistin-induced ROS production and kaempferol-mediated disruption of the Fenton reaction results in a dramatic increase of ROS species, while rendering the cell unable to detoxify them with lethal consequences (Figure 2.11).

R1 (Fenton's Reaction) $Fe^{3+} + O_2^{\bullet} \longleftrightarrow Fe^{2+} + O_2$

R2 (Fenton's Reaction) $Fe^{2+} + H_2O_2 \longleftrightarrow Fe^{3+} + {}^{\bullet}OH + H^+$

R3 (Haber-Weiss Reaction) $O_2^{\bullet} + H_2O_2 \longleftrightarrow {}^{\bullet}OH + H^+ + O_2$

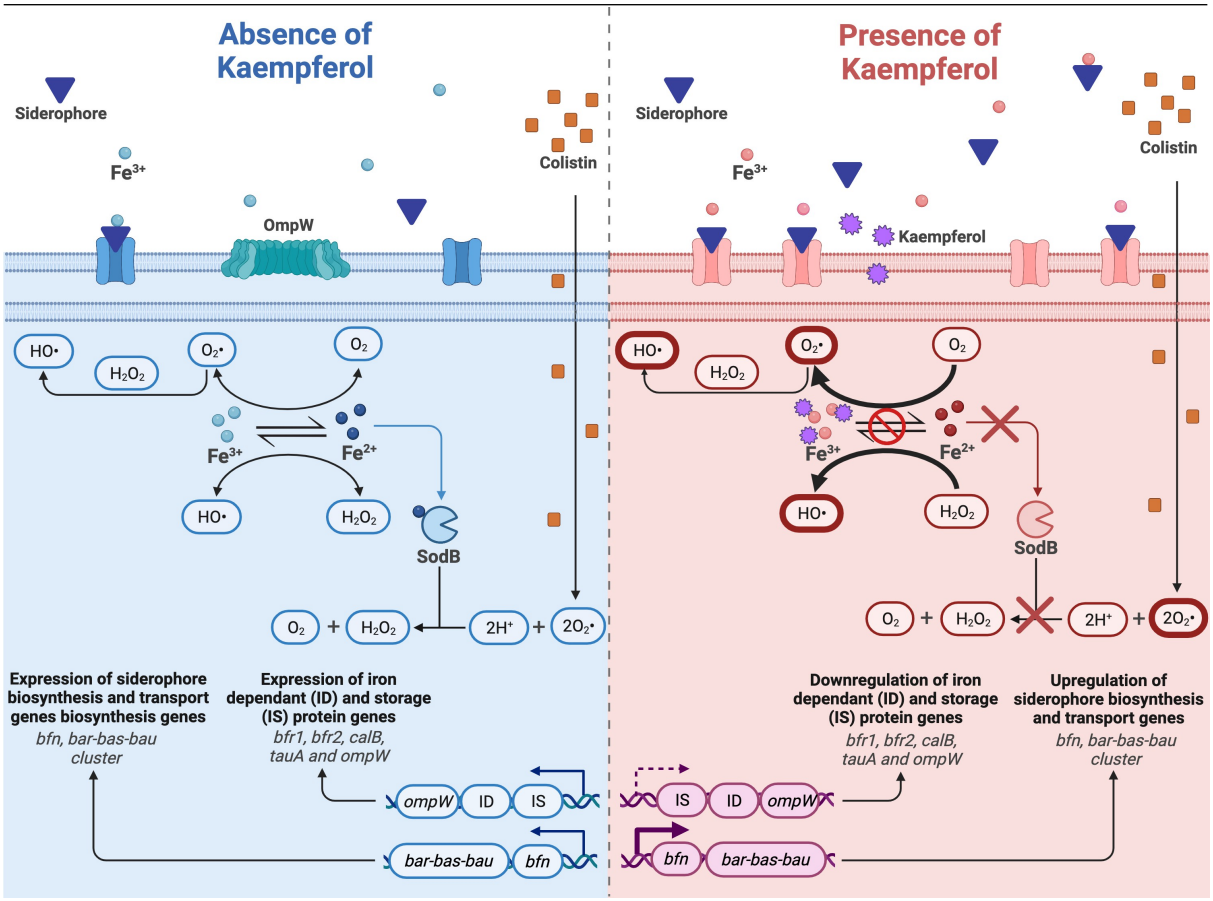

Figure 2.11: Model for the mechanism of synergy between kaempferol and colistin. The blue section of the diagram (left) describes cellular processes when bacteria are exposed only to sub-MIC amounts of colistin. In this case, ROS production can be reversed as Fenton's reaction can take place, while the superoxide generated from the action of colistin can be converted to less toxic products by SodB. A normal expression of iron-dependent and iron-storage proteins, as well as siderophore biosynthesis and transport genes are depicted. The red section of the diagram (right) describes the dysregulation of iron homeostasis caused by the action of kaempferol that chelates Fe^{3+}, including downregulation of genes encoding iron-dependent and iron-storage proteins and upregulation of siderophore biosynthesis and transport genes. Dysregulation of iron homeostasis, in turn, results in the accumulation of ROS due to the action of colistin and inhibition of the Fenton reaction (thick red borders). In addition, an imbalance in the intracellular iron content makes less iron available for SodB and therefore inhibits the superoxide detoxification process. Eventually, this accumulation of ROS leads to extensive damage to lipids, proteins, nucleic acids and, ultimately, cell death. The figure was created using BioRender.com.

In addition to elucidating the mechanism of the synergy between kaempferol and colistin, Myself and our collaborators (Despoina Mavridou and Nikol Kadeřábková) demonstrate that the colistin potentiation activity of iron-chelating compounds can be exploited to reverse intrinsic and acquired resistance mechanisms (Figure 2.9A, 2.9B and 2.9C). This approach can be used for highly colistin-resistant *A. baumannii* clinical strains (Figure 2.9D), whereby a 64-fold drop in colistin MIC was observed. Moreover, in agreement with Zhou *et al* (2022), the combination of kaempferol with colistin at amounts of the latter that would normally not rescue the *G. mellonella* larvae from a lethal dose of *A. baumannii*, results in 60% survival of the animals (Figure 2.10E). This shows that kaempferol can in principle also be used to reduce the therapeutic dose of colistin, something that, considering the toxicity of colistin and the co-morbidities of patients that usually need to be treated with it, would improve patient outcomes. In addition, colistin in combination with kaempferol is effective against colistin-resistant *E. coli* clinical strains. Isolates expressing MCR-1, as well as strains with chromosomal mutations causing colistin resistance, were sensitized against colistin in the presence of kaempferol, highlighting the promise of this next-generation antimicrobial.

Overall, this study unveils a previously underappreciated metabolic vulnerability of bacterial pathogens i.e., their reliance on iron homeostasis for overcoming the action of colistin. Kaempferol disrupts the delicate balance of ROS production and detoxification that takes place during colistin treatment with detrimental effects on the cell. Beyond the promise that this compound holds as a colistin potentiator, this work opens new avenues towards the potentiation of colistin via molecules that broadly target processes and pathways whose role is to keep the ROS levels in the cell balanced.

Future investigations could focus on the exploration of the mechanistic details surrounding kaempferol's interaction with Fe^{3+} and its disruptive role in iron homeostasis could benefit from more targeted biochemical assays. Potential approaches include developing *A. baumannii* constructs with Fe^{2+} and Fe^{3+} sensitive reporters, such as GFP under an iron-regulated promoter (Guan *et al*., 2013). This innovative strategy would enable the real-time monitoring of changes in iron levels in response to kaempferol, allowing for direct and quantitative analysis of iron homeostasis.

Future work could be formulation development of the kaempferol and colistin combination

treatment. Kaempferols therapeutic use is limited due to its low solubility in aqueous solutions. Studies have been conducted in order to improve the dissolution of kaempferol in water by synthesizing derivatives such as kaempferol-SO_3-Gallium. The solubility of kaempferol-SO_3-Gallium in water was found to be 300-fold higher than kaempferol-Gallium alone (Deng *et al*., 2019). This suggests that a more soluble form of kaempferol can be derived, providing an alternative that can be used in clinical testing. In turn, this water-soluble formulation would reduce cytotoxic effects, increase ease of dosing and bioavailability.

Safety and toxicity evaluations of the combination treatment would then be conducted to determine the potential adverse effects that may occur in clinical settings. Following formulation development and safety evaluations, *in vivo* studies on animal models, such as mice, could be conducted to evaluate the cytotoxicity of the treatment and to determine if the treatment is effective *in vivo* against *A. baumannii* infections. Subsequently, a clinical trial could then be designed and conducted in order to evaluate the efficacy and safety of the treatment for therapeutic use in humans.

Key Findings

1. Efficacy of Native Kaempferol Form and Antibiofilm Activity:
    - The native form of kaempferol, in combination with colistin, exhibits the highest efficacy in reducing *A. baumannii* growth compared to its modified larger derivatives.
    - Kaempferol also demonstrates antibiofilm activity against *A. baumannii*.
2. Disruption of Intracellular Iron Homeostasis by Kaempferol:
    - Kaempferol disrupts intracellular iron homeostasis in *A. baumannii*, leading to the upregulation of siderophore biosynthesis and transport genes while downregulating genes involved in iron storage and usage.
    - This disruption drives the cell to acquire additional extracellular iron, which becomes lethal under stress conditions such as colistin treatment.
    - The synergy between colistin-induced ROS production and kaempferol-mediated disruption of the Fenton reaction results in a dramatic increase of ROS species, rendering the cell unable to detoxify them with lethal consequences.

3. Exploiting Iron-Chelating Compounds to Treat Colistin Resistant *A. baumannii*:
    - The colistin potentiation activity of iron-chelating compounds, including kaempferol, can be exploited to treat intrinsic and acquired mediated resistance in *A. baumannii*.
    - This approach shows promise in combating highly colistin-resistant *A. baumannii* and *E. coli* clinical strains.
4. Contributions:
    - Kaempferol can potentially reduce the therapeutic dose of colistin, improving patient outcomes.
    - The study unveils a metabolic vulnerability of bacterial pathogens, highlighting new avenues for the potentiation of colistin via iron-chelating molecules.

2.3 Materials and Methods

2.5.1 Bacterial Strains

A. baumannii (virulent colony variant) (Tipton *et al*., 2015) and *E. coli* strains were routinely grown in LB media (Miller), either solid or liquid, static or shaking (180 rpm), respectively, at 37°C. *A. baumannii* strain AB5075 used throughout this study was sourced from the Manoil Lab (University of Washington, Seattle, USA), with a colistin MIC of 2 μg/ml (Figure 2.1A). *A. baumannii* and *E. coli* strains, plasmids and oligonucleotides used in this study are listed in the appendix, in Table Appendix.2, Table Appendix.3 and Table Appendix.4, respectively.

2.5.2 Plasmid and Strain Construction

In order to overexpress *sodB* and *sodC*, AB5075 miniTn7T-Tc derivative strains carrying those genes under the lacIq-Ptac expression system were generated. The plasmid pUC18T-miniTn7T-Tc-lacIq-Ptac was used as the backbone for cloning into miniTn7T-Tc (de Dios *et al*., 2022). A DNA fragment containing the *sodB* coding region was PCR amplified from AB5075 genomic DNA using oligonucleotides *sodB* forward RBS PtsI and *sodB* reverse KpnI. The *sodB* fragment was digested with PstI and KpnI and cloned into pUC18T-miniTn7T-Tc-lacIq-Ptac cut with the same enzymes. Similarly, a fragment containing sodC was amplified using primers *sodC* forward RBS PstI and *sodC* reverse HindIII, digested with PstI and HindIII and cloned into pUC18T- miniTn7T-Tc-lacIq-Ptac cut with the same enzymes. These resulted in pUC18T-miniTn7T-Tc-lacIq-Ptac::*sodB* and pUC18T-miniTn7T-Tc-lacIq-Ptac::*sodC,* respectively.

To construct the AB5075 derivatives bearing P*sodB* and P*sodC* promoter fusions to *gfp-mut3*, a pUC18T-miniTn7T-zeo-*gfpmut3* vector was used as the backbone for cloning (Choi and Schweizer, 2006). A 1 kb DNA fragment including the P*sodB* promoter region was PCR amplified using primers *sodB* trx forward EcoRI and *sodB* trx reverse BamHI, digested with EcoRI and BamHI and cloned into pUC18T-miniTn7T-zeo-*gfpmut3* cut with the same enzymes. Similarly, A 1 kb DNA fragment including the P*sodC* promoter region was PCR amplified using primers *sodC* trx forward EcoRI and *sodC* trx reverse BamHI, digested with EcoRI and BamHI and ligated into pUC18T-miniTn7T-zeo-*gfpmut3* cut with the same enzymes. These resulted

in plasmids pUC18T-miniTn7T-zeo-P*sodB::gfpmut3* and pUC18T-miniTn7T-zeo-P*sodC::gfpmut3,* respectively.

To integrate miniTn7-based constructions in the attTn7 neutral chromosomal site, a previously established four-parental mating strategy was followed (Kumar *et al*., 2010), using pRK2013 and pTNS2 as helper plasmids (Figurski and Helinski, 1979; Choi and Schweizer, 2006). Selection was performed on LB agar supplemented with gentamicin (50 mg/L) and either tetracycline (2.5 mg/L) or zeocin (300 mg/L), depending on the selection marker carried in the miniTn7T backbone. Insertions were validated by PCR using oligonucleotides AB5075-glmS forward and Tn7R (de Dios *et al*., 2023).

2.5.3 Phytochemical Potentiator Screen

A. baumannii overnight cultures were diluted in cation-adjusted Mueller-Hinton broth (pH 7.4, CAMHB) to OD_{600} 0.1. A sub-MIC of colistin (1.22 µg/ml) was added to the bacterial suspension. 199 µl of the suspension was added to each well on a 96-well plate followed by the addition of 1 µl (0.05 mM) of each phytochemical from a stock concentration of 10 mM (Caithness Library). 1 µl of DMSO was added as a vehicle control. In parallel, these assays were conducted in the presence of a sub-MIC of colistin (1.22 µg/ml). In this case, a growth control of the bacterial suspension supplemented with the sub-MIC of colistin was included. OD_{600} readings were taken every 10 min over 12 h with a Clariostar Plus plate reader (BMG LabTech), at 37°C, 200 rpm. All hits (compounds that produced a significant reduction in growth in the presence of a sub-MIC of colistin compared to the absence of colistin) were validated by repeating this assay with just those phytochemicals for a further three biological repeats. The results represent the average of three biological replicates ± S.D.

2.5.4 Biofilm Assay

For screening antibiofilm activity, we used the same experimental setup as for the antibiotic/potentiator screening, using LB media instead of CAMBH. The plates were then incubated at 37°C, 200 rpm, for 16 hours. Once grown, the biofilm was stained using the crystal violet method (O'Toole *et al*., 2011), with mild modifications (washes were performed by

pipetting and the staining was performed with 1% crystal violet). The absorbance of ethanol solubilised crystal violet was then read at 600 nm using a Clariostar Plus plate reader (BMG LabTech). All hits (compounds that produced a significant reduction in biofilm formation with respect to the vehicle control) were validated by repeating this assay with just those phytochemicals for a further three biological repeats. The results represent the average of three biological replicates ± S.D.

2.5.5 Minimum Inhibitory Concentration (MIC) and Minimum Biofilm Inhibitory Concentration (MBIC) Assays

A. baumannii overnight cultures were diluted in CAMHB (pH 7.4) to OD_{600} 0.1. A 2-fold sub-MIC of colistin was added to the initial suspension. 200 µl of the bacterial suspension were added to a 96-well plate. To the first well 1 µl (0.05 mM) of kaempferol, from a 10 mM stock, was added. The following wells had an increased volume of kaempferol added by 0.5 µl each time. As a control, 200 µl of the bacterial solution and 200 µl of sterile CAMBH was plated in separate wells and tested. A control assay was performed in parallel using equivalent volumes of DMSO as a vehicle control. The 96-well plate was then incubated at 37°C, 200 rpm. Endpoint OD_{600} was measured after 16 hours using a Clariostar Plus plate reader (BMG LabTech). MIC was defined as the lowest kaempferol concentration that completely inhibited bacterial growth. The results represent the average of three biological replicates ± S.D. For MBIC testing, the same experimental setup as for MIC assessment was followed in the absence of colistin. Plates were incubated for 16 hours at 37 °C, 200 rpm. Subsequently, biofilms were stained using the crystal violet protocol as explained above. MBIC was determined as the lowest kaempferol concentration that completely inhibited biofilm formation. The results represent the average of three biological replicates ± S.D.

When evaluating colistin MICs for colistin resistant *E.coli* and *A. baumannii* strains, the assays were carried out in accordance with the EUCAST recommendations using broth microdilution. A series of the following colistin (MP Biomedicals) concentrations was prepared individually: 256 µg/mL, 128 µg/mL, 64 µg/mL, 32 µg/mL, 16 µg/mL, 8 µg/mL, 4 µg/mL, 2 µg/mL, 1 µg/mL, 0.5 µg/mL, 0.25 µg/mL in $CaCl_2$ (0.223 mM) supplemented

MH broth and transferred to a clear-bottomed 96-well microtiter plate. Either DMSO (carrier control) or kaempferol (final concentration of 50 μM [0.05 mM]) were added to the medium, as required. This change in kaempferol concentration compared to previous assays is attributed to the limited availability of kaempferol. IPTG (0.5mM) was added to induce *mcr* expression for the *E. coli* K-12 strain carrying pDM1-*mcr*-1. Overnight cultures of each strain were standardised and added to the wells at approximately 1×10^5 colony-forming units (CFU) per well and the plates were incubated for 18–24 hours at 37°C. The MIC was defined as the lowest antibiotic concentration with no visible bacterial growth in the wells. The results represent the average of three biological replicates ± S.D.

2.5.6 Growth Assays

Overnight *A. baumannii* AB5075 cultures were diluted in CAMHB (pH 7.4) to get an OD_{600} of 0.1. Treatments consisted of kaempferol only (0.375 mM), the sub-MIC of colistin (1.22 μg/ml) and the combination treatment of kaempferol and the sub-MIC of colistin, using the respective DMSO vehicle controls. The plate was then incubated at 37 °C, 200 rpm in a Clariostar Plus plate reader (BMG LabTech), where OD_{600} readings were taken every 10 minutes for 12 hours. When testing if the overexpression of *sodB* or *sodC* affected the efficacy of the combination treatment the same experimental design was followed. The respective AB5075 derivative strains bearing the overexpression insertions (AB5075/miniTn7T-Tc-lacIq-Ptac::*sodB* and AB5075/miniTn7T-Tc-lacIq-Ptac::*sodC*) or the empty control (AB5075/miniTn7T-Tc-lacIq- Ptac) were used. When indicated, CAMHB was supplemented with IPTG 1 mM to induce expression from the Ptac promoter. The results represent the average of three technical replicates and three biological replicates ± S.D.

2.5.7 RNA-seq and Gene Set Enrichment Analysis (GSEA)

AB5075 cells were grown in 20 ml CAMHB (pH 7.4) to mid-exponential phase (OD_{600} 0.6) in either the presence of kaempferol or DMSO. To preserve RNA integrity, the bacterial cells were then centrifuged and washed in RNAlater. The RNA was then isolated using the RNAeasy Kit with in-column DNAase digestion (Qiagen). The RNA integrity of each sample was determined

using a Bioanalyzer (Agilent 2100 Bioanalyzer and Agilent RNA 6000 Nano Kit), according to the amplitude and sharpness of the peaks corresponding to the 23S and 16S rRNAs. Sequencing and downstream analyses were performed at the Microbial Genome Sequencing Centre (Pittsburgh, Pennsylvania, U.S.A), using an Illumina MiSeq, with 12 million reads per sample. Quality control and adapter trimming was performed with bclfastq. Read mapping was performed with HISAT. Differential expression analysis was performed using edgeR's exact test for differences between two groups of negative-binomial counts with an estimated dispersion value of 0.1, using the *A. baumannii* AB5075-UW genome annotation as a reference (Gallagher *et al*., 2015). The volcano plot was generated using R, by plotting the log fold change on the x-axis and p-value on the y-axis. 117 genes were differentially expressed based on a log fold change $x \geq 5$ 1 and p value <0.05 (adjusted p-value). Peak profiles were used in order to determine RNA integrity. A Gene Set Enrichment Analysis (GSEA) was performed using FUNAGE-Pro with the default parameters (de Jong *et al*., 2022).

2.5.8 Iron Complex Formation Assay

When flavonoids, such as kaempferol, form a complex with a metal, they exhibit a shift in their absorbance peak to higher wavelengths. To explore whether kaempferol forms a complex with iron and if this complex formation is specific for either Fe^{2+} or Fe^{3+}, we measured the absorption spectra in the 300-500 nm range of kaempferol mixed with either form of iron in different proportions, similarly to Catapano *et al*., 2017. Briefly, we mixed kaempferol with either Fe^{2+} or Fe^{3+} in different molecular proportions while keeping a total concentration of both complexes of 0.1 mM in a total volume of 100 µl. Mixes were incubated at room temperature for 10 minutes. After that, the absorbance was measured in a Clariostar Plus plate reader (BMG LabTech). As a baseline control, mixtures with DMSO and water volumes equivalent to those of kaempferol and iron, respectively, were used. For measuring the kaempferol spectra, iron volumes were replaced by equivalent volumes of water. Three independent experiments were performed.

2.5.9 Rescue Assay

A. baumannii AB5075 overnight cultures were diluted in LB to an OD_{600} of 0.1. Treatments were set up in a 96-well plate and consisted of kaempferol (0.375 mM), the sub-MIC of colistin (1.22 μg/ml) and the combination treatment of kaempferol and the sub-MIC of colistin, with the respective DMSO vehicle controls. The media was supplemented with 100 μM $FeCl_3$, $FeCl_2$, $CuCl_2$, $MgCl_2$, $ZnCl_2$ or $CaCl_2$. This assay was adapted from Nwugo *et al.*(2011) to stimulate iron rescue. The plate was then incubated at 37°C, 200 rpm, in a Clariostar Plus plate reader (BMG LabTech), where an OD_{600} reading was taken every 10 minutes for 12 hours. The results represent the average of three technical replicates and three biological replicates ± S.D.

2.5.10 Chelation Assay

A. baumannii AB5075 overnight cultures were diluted in LB to an OD_{600} of 0.1. Treatments were set up in a 96-well plate and consisted of kaempferol (0.375 mM), EDTA (100 μM), ExJade 25 μM or 8-Hydroxyquinoline 25 μM, the sub-MIC of colistin (1.22 μg/ml) and the combination treatment of kaempferol, EDTA, ExJade or 8-Hydroxyquinoline and the sub-MIC of colistin, with the respective DMSO vehicle controls. The plate was then incubated at 37°C, 200 rpm, in a Clariostar Plus plate reader (BMG LabTech), where an OD_{600} reading was taken every 10 minutes for 12 hours. The results represent the average of three technical replicates and three biological replicates ± S.D.

2.5.11 Quantifying Intracellular Iron

AB5075 overnight cultures were diluted in LB to an OD_{600} of 0.1. Samples were then treated and incubated for 2 hours at 37ºC, under aerobic conditions. Treatments consisted of kaempferol (0.375 mM), colistin (1.22 μg/mL), combination of colistin and kaempferol and DMSO carrier control. Following the incubation period, the samples were centrifuged and re-suspended in 200 μL of PBS. The samples were then sonicated on ice. 100 μL of each sample was put into a well on a 96-well plate. For the Fe^{2+} assay, 5 μL of the assay buffer was added to each sample, for the Fe^{3+} assay, 5 μL of the iron reducer was added. The plate was then

incubated at 37°C for 30 minutes. 100 µL of the iron probe was then added and incubated under those same conditions for 1 hour. The plate was then measured on a colorimetric plate reader (OD 593 nm), Clariostar Plus (BMG LabTech). Standards were carried out according to the iron kit (Abcam, iron kit) protocol.

2.5.12 NPN Uptake Assay

Mid-log phase cultures of *A. baumannii* were diluted to OD_{600} 0.5 in 5 mM HEPES (pH 7.2) and 100 µL was transferred to clear-bottomed 96-well microtiter plates (Corning). Kaempferol was added to the final concentration of 0.375 mM and colistin sulphate (in 5 mM HEPES, Thermo Scientific) was added to a final concentration of 1.22 µg/mL (for experimental conditions) or 16 µg/mL (for positive control). Equal volumes of the kaempferol carrier (DMSO) were included in colistin only wells as required. 1-N-phenylnaphthylamine (NPN) (Acros Organics) was then added to a final concentration of 10 µM. Immediately after the addition of NPN, fluorescence was measured at 1-minute intervals for 20 minutes using a Synergy H1 microplate reader (BioTek); the excitation wavelength was set to 355 nm and emission was recorded at 405 nm (Helander and Mattila-Sandholm, 2000).

2.5.13 PI Uptake Assay

Mid-log phase cultures of *A. baumannii* were centrifuged, resuspended in phosphate buffered saline (PBS, pH 7.4), diluted to a final OD_{600} of 0.4 and 100 µL was transferred to clear-bottomed 96-well microtiter plates (Corning). Kaempferol was added to the final concentration of 0.375 mM and colistin sulphate (in PBS, Thermo Scientific) was added to a final concentration of 1.22 µg/mL (for experimental conditions) or 16 µg/mL (for positive control). Equal volumes of the kaempferol carrier (DMSO) were also included in the colistin only wells as required. Propidium iodide (PI, Acros Organics) was then added at a final concentration of 3 µM and the plate was incubated at room temperature for 10 minutes. The PI fluorescence was measured at 1-minute intervals for 20 minutes using a Synergy H1 microplate reader (BioTek); the excitation wavelength was set to 493 nm and emission was recorded at 636 nm.

2.5.14 ROS Production

A. baumannii AB5075 overnight cultures were diluted in LB 1/100 (v/v) and grown to an OD_{600} of 0.5 at 37°C, 200 rpm. Cells were then washed three times with PBS and resuspended in PBS. Cells were then treated with 20 µM 2',7'-dichlorofluorescin diacetate (DCFDA) and incubated at 37°C for 2 h in the dark. Following this incubation period, samples were placed in a 96-well plate. Fluorescence intensity (excitation: 488 nm; emission: 530 nm) was measured in a Clariostar Plus plate reader (BMG LabTech). The fluorescence readings were then normalised against the OD_{600} readings of the samples. The results represent the average of three technical replicates and three biological replicates ± S.D.

2.5.15 Hydrogen Peroxide Growth Assays

Overnight *A. baumannii* AB5075 cultures were diluted in CAMHB (pH 7.4) to get an OD_{600} of 0.1. Treatment consisted of hydrogen peroxide at 10% concentration, using the respective DMSO vehicle controls. The plate was then incubated at 37°C, 200 rpm in a Clariostar Plus plate reader (BMG LabTech), where OD_{600} readings were taken every 10 minutes for 12 hours. The results represent the average of three technical replicates and three biological replicates ± S.D.

2.5.16 GFP-based expression assay

The expression from the P*sodB* and P*sodC* promoters was measured using miniTn7T insertions carrying either a P*sodB::gfpmut3* or a P*sodC::gfpmut3* transcriptional fusion (strains AB5075/miniTn7T-zeo-P*sodB::gfpmut3* and AB5075/miniTn7T-zeo-P*sodC::gfpmut3*, respectively). An AB5075/miniTn7T-zeo-*gfpmut3* strain (carrying and empty control), was used as a baseline control. Saturated overnight cultures of the different strains were diluted 1:100 (v/v) in fresh LB broth supplemented with the kaempferol and colistin combination treatment or a DMSO mock treatment. Cultures were incubated for 2 h at 37°C, 180 rpm. Afterwards, 1 mL samples were washed with PBS and eventually resuspended in PBS. Then, samples were placed in a 96-well plate and their OD_{600} and GFP fluorescence (excitation: 485 nm; emission: 535 nm) were measured in a Clariostar Plus plate reader (BMG LabTech). The

fluorescence readings were normalised by their respective OD_{600} and the baseline fluorescence obtained from the empty transposon control was subtracted from those obtained with the strains bearing either the P*sodB::gfpmut3* or the P*sodC::gfpmut3* the promoter fusions. Three biological replicates (two technical replicates each) were performed for each experimental condition.

2.5.17 Cytotoxicity and *in vivo* Efficacy

All *in vivo* experiments were conducted using *G. mellonella* (Live Foods Ltd) of 0.278 g average weight. *A. baumannii* AB5075 overnight cultures were diluted in PBS to an OD_{600} of 1.0 and then further diluted 1/1000 (v/v) in PBS, to get a concentration of approximately 2.56 x 10^5 CFU/ml. 10 µl of each diluted bacterial solution was then injected into the *G. mellonella* larvae. Following a 15-minute incubation period at room temperature, the *G. mellonella* were then injected with 10 µl of kaempferol (0.5 mM), an *in vivo* sub-MIC of colistin (0.8 µg/Galleria) and the combination treatment of kaempferol and the *in vivo* sub-MIC of colistin, compared to the respective DMSO vehicle controls. Larvae survival was assessed over 32 hours and complete melanisation with no response to mechanical stimulation was recorded as a death. A total of 30 larvae were tested per condition, performing 10-larvae repeats on different days. Prior to these assays, the same method was followed to assess the *in vivo* sub-MIC of colistin in *G. mellonella*. Cytotoxicity controls were carried out using the same methodology but injecting the larvae with PBS instead of *A. baumannii* AB5075.

2.5.18 Statistics and Reproducibility

All assays were carried out in biological triplicate (n=3), with three technical repeats, individual data points are included in each graph. Analysis consisted of ANOVA tests comparing the treated samples with the respective carrier control. Average values ± S. D. are represented. Significance is indicated as ns = non-significant, * = $p \leq 0.05$, ** = $p \leq 0.01$, *** = $p \leq 0.001$, **** = $p \leq 0.0001$. Statistical analyses were performed using GraphPad Prism v10.0.3. For normally distributed data, parametric tests (one-way and two-way ANOVA) were applied. Post-hoc analyses included Šídák's multiple comparisons test and Tukey's multiple comparisons test to adjust for multiple comparisons. For survival analyses in *G. mellonella* assays, the Log-rank (Mantel-Cox) test and Gehan-Breslow-Wilcoxon test were used.

Chapter 3

Irish Bogland Phytochemicals Inhibit Growth and Potentiates Colistin Through Iron Sequestration

3.1 Introduction

A. baumannii is at the top of the World Health Organisation's priority pathogen list and is an opportunistic pathogen that displays a remarkable capacity to overcome antibiotic therapy through a wide array of acquired and intrinsic antibiotic resistance mechanisms (Asokan *et al*., 2019). As part of our study to identify novel plant compounds that could inhibit pathogen growth, we screened the library of plant extracts from Irish boglands generated as part of the 'Unlocking Nature's Pharmacy from Bogland Species' (UNPBS) Project (grant number DOJProject209825) held at NatPro, Trinity College Dublin, against carbapenem-resistant *Acinetobacter baumannii.* Through our screening, we identified that extracts of *Potentilla erecta* L. have antimicrobial effects against a multidrug-resistant strain of *A. baumannii*.

Potentilla erecta L., commonly known as tormentil, is an acid peat-loving member of the Rosacea family native to Europe and Western Asia. It is a small clump forming plant with bright yellow 4-petalled flowers blooming from May to September and the leaves are sessile and trifoliate. The rhizomatous root is thick turning a dark red colour when cut. The *Potentilla* genus has been used in herbal medicine since ancient times by the Greek physician Dioscorides and *Potentilla* species are prominent plants in European herbal texts through the centuries (Tomczyk and Latté, 2009). The use of *Potentilla erecta* to treat diarrhoea and dysentery and as an antiseptic for the mouth and throat is consistently reported. In Ireland, reports of ethnomedical uses of tormentil as a cure for diarrhoea in humans or animals can be found in the Schools' Collection of the National Folklore Collection compiled by pupils between 1937 and 1939 with the objective of preserving Irish oral heritage including entries on local cures and herbs. (Dúchas National Folklore Collection, a; Dúchas National Folklore Collection, b).

In Europe today, the scientific conclusion of the Committee on Herbal Medicinal Products (HMPC) of the European Medicines Agency (EMA) is that traditional herbal medicinal products of *Potentilla erecta* (L.) Raeusch., rhizoma (tormentil rhizome) can be used for symptomatic treatment of mild diarrhoea or minor inflammations of the oral mucosa exclusively based upon long-standing use (EMA, 2021). According to the European Pharmacopoeia monograph, the rhizome contains not less than 7% of tannins, expressed as pyrogallol ($C_6H_6O_3$, Mr126.1) with reference to the dried herbal substance and the high tannin content makes medicinal use in the proposed indications plausible (EMA, 2018). Tannins are astringent polyphenols with probable roles in protection against animals, pathogens and abiotic stresses such as temperature extremes and UV light in the plants that produce them (Constabel *et al*., 2014, Dehghanian *et al*., 2022). In addition to conferring antioxidant activity, tannin hydroxyl groups can interact with moieties on proteins and polysaccharides to tighten mucous membranes serving to increase barrier function and reduce permeability. Due to this astringency effect, preparations of tormentil were also traditionally used externally for haemostasis, prosthetic pressure points, frostbite, burns, haemorrhoids and poorly healing wounds (EMA HMPC, 2011).

3.2 Aim of the study

The aim of this study is to identify the antimicrobial and antibiofilm effects of Irish bogland species against *A. baumannii*.

- We will conduct an in-depth exploration of extracts that demonstrate potential novel therapeutic properties against ESKAPE pathogens.
- Next, our collaborators at Trinity College Dublin will explore the chosen extracts pharmacological properties, including their HPLC profile, to determine the bioactive components within the extracts.
- Through RNA-Seq analysis and validation, we will then elucidate the mechanisms underlying the antimicrobial activity of the extracts and it constituents.
- Finally, we will evaluate the potential of the extract and its constituents as lead compounds for the development of antimicrobials that can increase the efficacy of currently used antibiotics, such as colistin.

3.3 Results

3.3.1 Screening Irish bogland species to assess their antimicrobial and antibiofilm activity

To identify phytochemicals that inhibit the growth of *A. baumannii*, we screened a library of 201 plant extracts from Irish bogland species against the MDR *A. baumannii* strain, AB5075. These plant specimens were collected from various locations in Ireland, dried and subjected to Soxhlet extractions method. Methanol extraction yielded all MeOH extracts, while sequential hot-water and cold-water extractions produced Hot-Water Soluble Polysaccharides and Cold-Water Soluble Polysaccharide, respectively. MeOH extracts were resolubilised in DMSO due to the hydrophobicity of the organic solvents extracted using this method. Alternatively, polysaccharide extracts are more polar and hydrophilic therefore, more soluble in aqueous solutions like PBS. Subsequently, the extracts were then evaluated for their antibiofilm activity against *A. baumannii*.

In the initial screening, extracts 99, 152, 154-156, 168–170, 182–184, 191, and 193 demonstrated antimicrobial effects against *A. baumannii*, when compared to the respective PBS or DMSO vehicle control (Figure 3.1A - F). All extracts were tested at a concentration of 0.05 mg/mL against a vehicle control, consisting of an equal volume of DMSO or PBS. Furthermore, the antibiofilm screening revealed 46 plants exhibiting antibiofilm effects against *A. baumannii*, in comparison to the respective DMSO or PBS vehicle control (Figure 3.1G - L). Extracts that displayed a significantly different result, compared to the control, were considered to possess antibiofilm effects. Extracts 101-106, 108, 125 and 132 are removed from the initial screening results as they are derivatives of extract 99 and are later reported in this study.

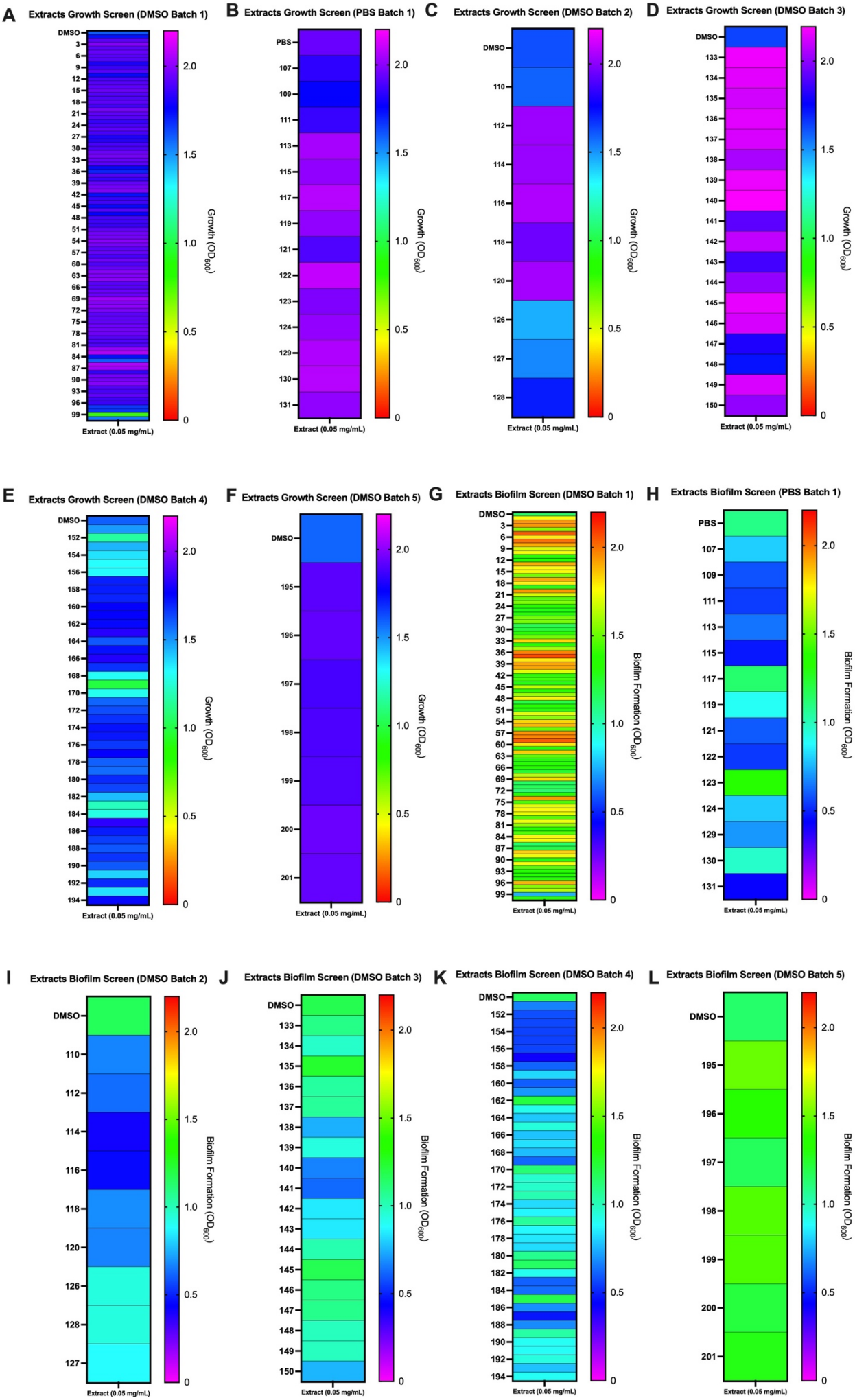
A
Extracts Growth Screen (DMSO Batch 1)
B
Extracts Growth Screen (PBS Batch 1)
C
Extracts Growth Screen (DMSO Batch 2)
D
Extracts Growth Screen (DMSO Batch 3)
E
Extracts Growth Screen (DMSO Batch 4)
F
Extracts Growth Screen (DMSO Batch 5)
G
Extracts Biofilm Screen (DMSO Batch 1)
H
Extracts Biofilm Screen (PBS Batch 1)
I
Extracts Biofilm Screen (DMSO Batch 2)
J
Extracts Biofilm Screen (DMSO Batch 3)
K
Extracts Biofilm Screen (DMSO Batch 4)
L
Extracts Biofilm Screen (DMSO Batch 5)
Extract (0.05 mg/mL)
Growth (OD600)
Biofilm Formation (OD600)

Figure 3.1: Initial screening of Irish bogland species. (A - F) Impact of plant extracts at a concentration of 0.05 mg/mL on the growth of *A. baumannii*. **(G-L)** Impact of plant extracts at a concentration of 0.05 mg/mL on *A. baumannii* biofilm formation. Screenings were carried out in CAMHB and the results above display the average of three biological assays (n=3) that were read at 12 hours. Screenings were taken place in batches depending on the harvesting and extraction of extracts taken place by Trinity Collage Dublin, thus each batch has an individual DMSO/PBS control and this accounts for the variation in sample numbers between panels.

3.3.2 Assessing aerial and roots segments of tormentil for their antimicrobial and antibiofilm activity against *A. baumannii*

Of the tested extracts, extract 99 stood out due to its dual efficacy in both antimicrobial and antibiofilm activities. It is worth noting that the antibiofilm effect displayed by extract 99 could be attributed to the reduction in viable bacterial cells caused by the antimicrobial effect of the extract. In addition to its effectiveness, the choice of extract 99 was also influenced by its abundant availability and prevalence within Irish boglands. Upon unblinding the initial screening results, it was revealed that extract 99 corresponds to the aerial segment of the *P. erecta* L. plant. This specific segment was sourced from a bogland situated in the Wicklow area. Motivated by these findings, we conducted a more in-depth exploration into the antimicrobial and antibiofilm attributes of the *P. erecta* L. plant. This involved investigating the correlation between different plant segments and their respective levels of antimicrobial and antibiofilm activity. Furthermore, to assess the conservation of these effects across diverse boglands, we screened a panel of aerial and root plant segments obtained from tormentil plants harvested in various bogland areas in Ireland (Figure 3.2A). The results of this analysis are presented in Figure 3.2B - K.

Plant specimens of *P. erecta* (L.) samples were selected to determine if levels of antibacterial or antibiofilm activity differed between the same species growing at different sites. Wicklow tormentil root extract, Tipperary tormentil aerial extract, Tipperary tormentil root extract and Kerry tormentil aerial extract were all found to significantly reduce the growth of *A. baumannii* (Figure 3.2B and Table 3.1). Titration assays revealed that six extracts

displayed a dose dependent antibacterial effect. From the tested concentrations, 0.95 mg/mL was shown to have the highest inhibition of growth for each of the six extracts (Figure 3.2D, E, F, G, H and I), demonstrating a conservation in antimicrobial activity across sites. Concentrations above 0.95 mg/mL were excluded from the MIC testing as the difference between the DMSO effects on the growth of *A. baumannii* and some of the extracts were no longer significant.

In the case of antibiofilm activity, Wicklow tormentil root (H_2O) and Tipperary tormentil root (H_2O) polysaccharides both demonstrated a significant reduction in biofilm formation, without reducing the growth of the bacteria (Figure 3.2C), suggesting a true antibiofilm effect (Gadar and McCarthy, 2023). This demonstrates a conservation in antibiofilm activity across sites. Titration assays revealed that the antibiofilm effect exerted by Wicklow tormentil root (H_2O) polysaccharide and Tipperary tormentil root (H_2O) polysaccharide were not dose dependent, with 0.05 mg/mL of both extracts shown to have the highest inhibition of biofilm formation (Figure 3.2J and K). As Wicklow tormentil root extract displayed one of the most potent antibacterial effects and due to its abundance, it was used for further testing.

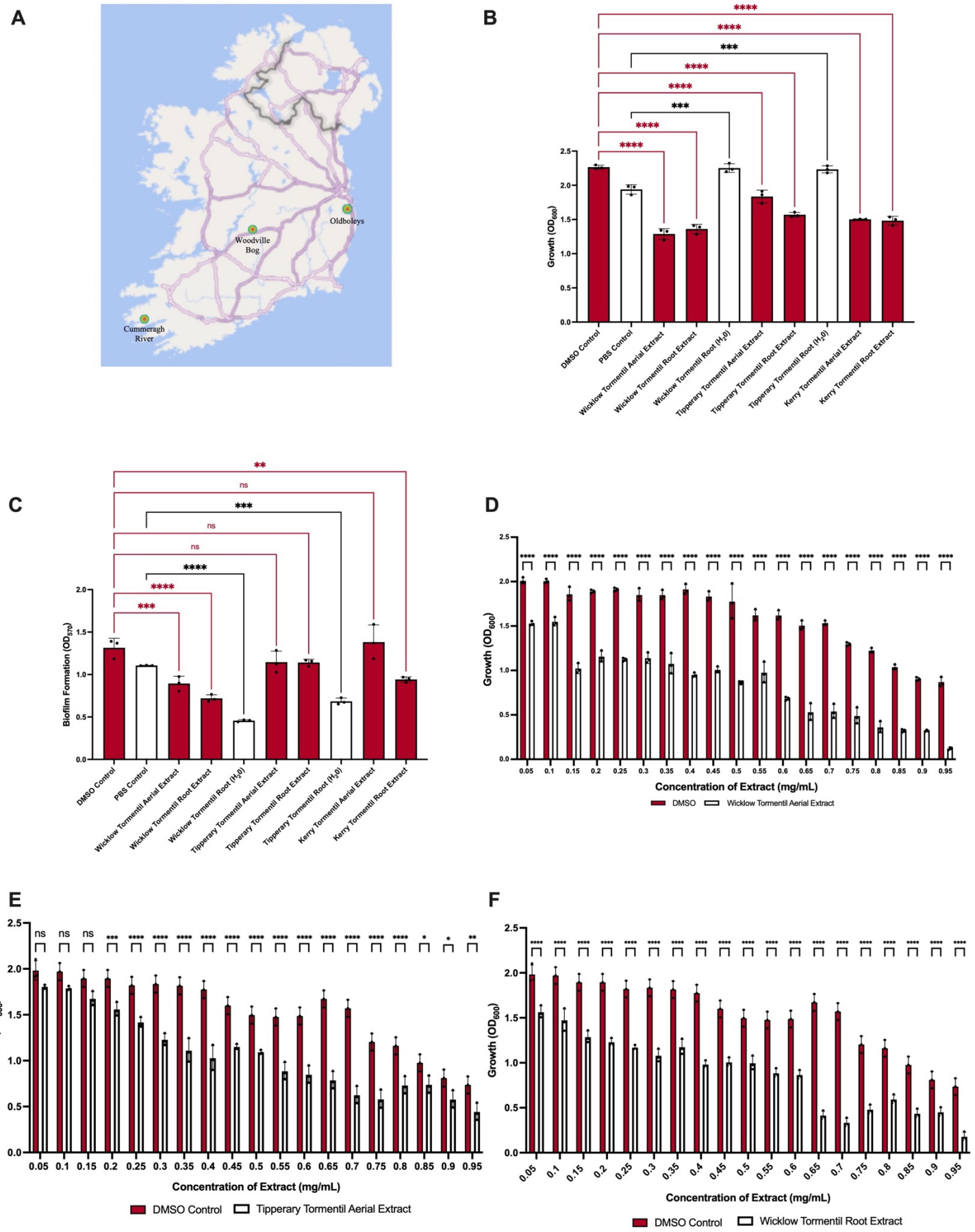
A
Oldboleys
Woodville Bog
Cummeragh River
B
Growth (OD_{600})
DMSO Control
PBS Control
Wicklow Tormentil Aerial Extract
Wicklow Tormentil Root Extract
Wicklow Tormentil Root (H_2O)
Tipperary Tormentil Aerial Extract
Tipperary Tormentil Root Extract
Tipperary Tormentil Root (H_2O)
Kerry Tormentil Aerial Extract
Kerry Tormentil Root Extract
C
Biofilm Formation (OD_{570})
D
Growth (OD_{600})
Concentration of Extract (mg/mL)
DMSO
Wicklow Tormentil Aerial Extract
E
Growth (OD_{600})
Concentration of Extract (mg/mL)
DMSO Control
Tipperary Tormentil Aerial Extract
F
Growth (OD_{600})
Concentration of Extract (mg/mL)
DMSO Control
Wicklow Tormentil Root Extract

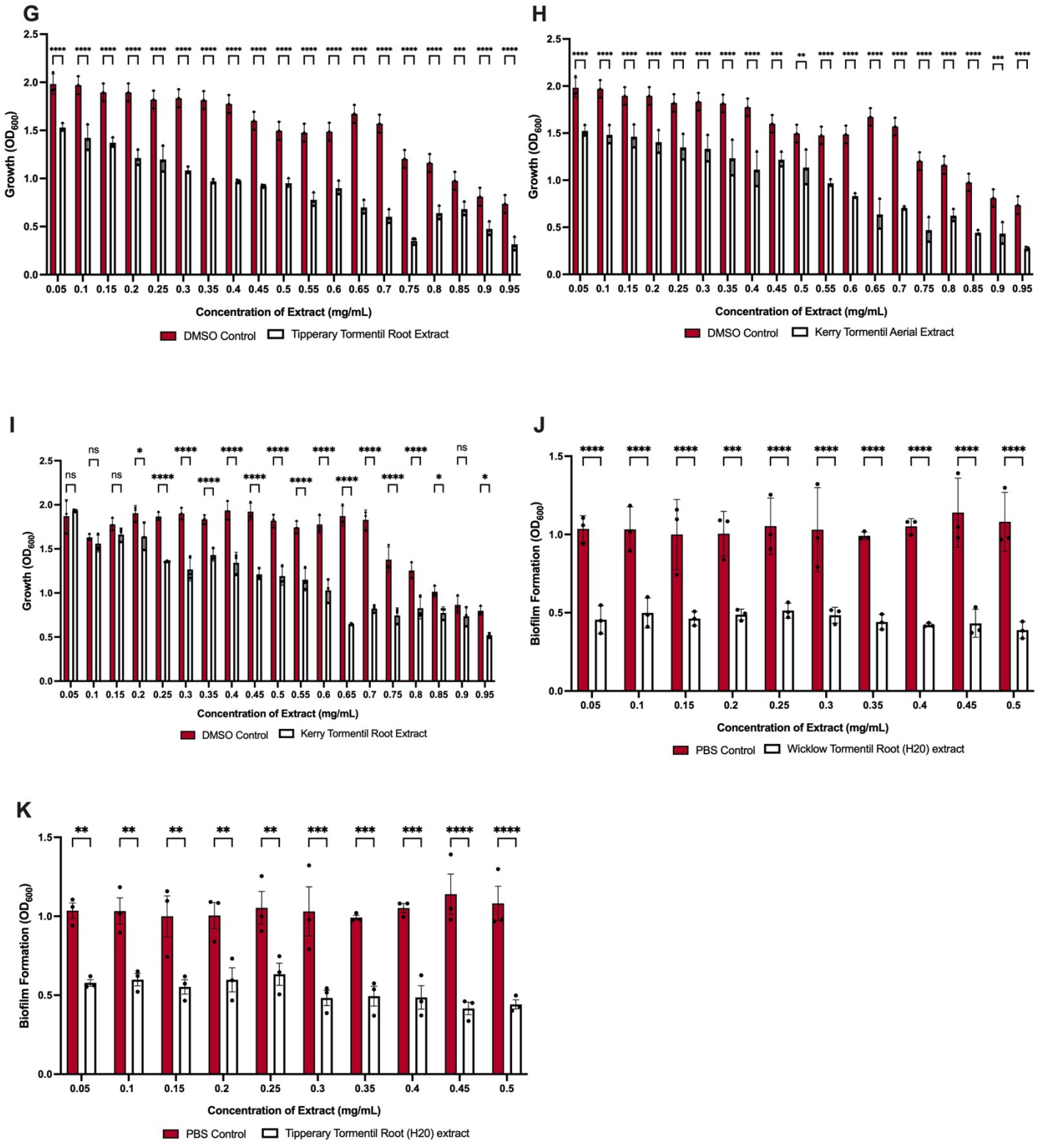

Figure 3.2: Tormentil extracts exhibit antibacterial properties against *A. baumannii.* (A) Map of Ireland indicating the tormentil collection sites: Oldboleys, Co. Wicklow; Woodville Bog, Co. Tipperary; Cummeragh River Bog, Co. Kerry **(B)** Impact of tormentil derivatives at a concentration of 0.05 mg/mL on the growth of *A. baumannii*. **(C)** Impact of tormentil derivatives at a concentration of 0.05 mg/mL on biofilm formation of *A. baumannii*. **(D-I)**

Minimum Inhibitory Concentration (MIC) of aerial and root segments of tormentil. Inhibition was shown to be dose dependent with 0.95 mg/mL of tormentil inhibiting visible growth of *A. baumannii* by >90%. **(J - K)** Minimum Biofilm Inhibitory Concentration (MBIC) of tormentil derivatives. Inhibition was shown to not be dose dependent for Wicklow tormentil root (H_2O) and Tipperary tormentil root (H_2O) polysaccharides. Assays were carried out in biological triplicate, each performed in technical triplicate. Statistical analysis consisted of one-way ANOVA for panels **(B-C)**, between the treated samples and the respective vehicle control and two-way ANOVA for panels **(D-K)**, between the treated samples and the respective vehicle control, each comparison includes controls with increasing amounts of DMSO or PBS as the second variable factor. Average values ± SD are represented as error bars. Significance is indicated as * = $p < 0.05$, ** = $p < 0.01$, *** = $p < 0.001$, and **** = $p < 0.0001$.

Table 3.1: *P. erecta* collections, growing locations, plant parts and corresponding MeOH extracts prepared by Soxhlet extraction. % yield compares the amount of product obtained to the theoretical maximum amount possible (based on initial material mass) and is a measure of the Soxhlet extraction process.

Plant material collection ID	Growing location	Plant parts	% yield MeOH extract (Soxhlet)	MeOH extract ID
NTP127	Mountain bog, Oldboleys, Co. Wicklow, Ireland East	Aerial (leaf, stem and flower)	22.6%	Wicklow aerial
NTP127	Mountain bog, Oldboleys, Co. Wicklow, Ireland East	Underground (rhizome and root)	35.3%	Wicklow root
NTP218	Cummeragh River Bog, Co. Kerry, Ireland Southwest	Aerial (leaf, stem and flower)	18.5%	Kerry aerial
NTP218	Cummeragh River Bog, Co. Kerry, Ireland Southwest	Underground (rhizome and root)	22.7%	Kerry root
NTP236	Woodville Bog, Co. Tipperary, Ireland midlands	Aerial (leaf, stem and flower)	25.9%	Tipperary aerial
NTP236	Woodville Bog Co. Tipperary, Ireland midlands	Underground (rhizome and root)	36.7%	Tipperary root

3.3.3 Tormentil derivatives exhibit antibacterial properties against ESKAPE pathogens

As the MeOH extracts exhibited antimicrobial effects against *A. baumannii*, we hypothesised whether the derivatives could yield similar effects on the growth of the remaining ESKAPE pathogens; *Enterococcus faecium, Staphylococcus aureus, Klebsiella pneumoniae, Pseudomonas aeruginosa*, and *Enterobacter cloacae*. To explore this further, we conducted tests on each tormentil derivative at a concentration of 0.05 mg/mL against the growth of each ESKAPE pathogen (Figure 3.3).

The results revealed that Wicklow tormentil aerial extract effectively reduces the growth of *E. faecium* at the tested concentration (Figure 3.3A). Interestingly, this extract increased the growth of *S. aureus*. This suggests that a component, specifically within the aerial segment of the Wicklow tormentil extract may be influencing the growth of *S. aureus*. This could be through increasing biofilm formation which would in turn increase nutrient availability or interact with signaling pathways such as quorum sensing, ultimately resulting in increased growth. Additionally, Wicklow tormentil root extract demonstrated growth inhibition against *E. faecium, K. pneumoniae and E. cloacae* (Figure 3.3B). Moreover, Tipperary tormentil aerial extract exhibited growth reduction against *E. cloacae* (Figure 3.3D), while Tipperary tormentil root extract had an inhibitory effect on *E. faecium, K. pneumoniae* and *E. cloacae* (Figure 3.3E). Together, this suggests that the Wicklow and Tipperary tormentil root extracts have a broader application against inhibiting the growth of Gram-negative and Gram-positive bacteria compared to the aerial extracts. Kerry tormentil aerial extract showed growth reduction against *E. cloacae* (Figure 3.3G), whilst Kerry tormentil root extract did not demonstrate growth inhibition against any of the tested pathogens in this assay (Figure 3.3H). However, both Kerry tormentil aerial and root extracts were shown to increase the growth of *K. pneumoniae,* this suggests that components within these segments may be influencing the growth of *K. pneumoniae,* possibly through the aforementioned reasons above. Wicklow tormentil root polysaccharide and Tipperary tormentil root polysaccharide did not exhibit any effects on the growth of either ESKAPE pathogen (Figure 3.3C and F). This may be due to the extraction process for these polysaccharides not obtaining the bioactive components that are present within the MeOH extracts, therefore the same growth inhibition effects as the MeOH extracts are not observed.

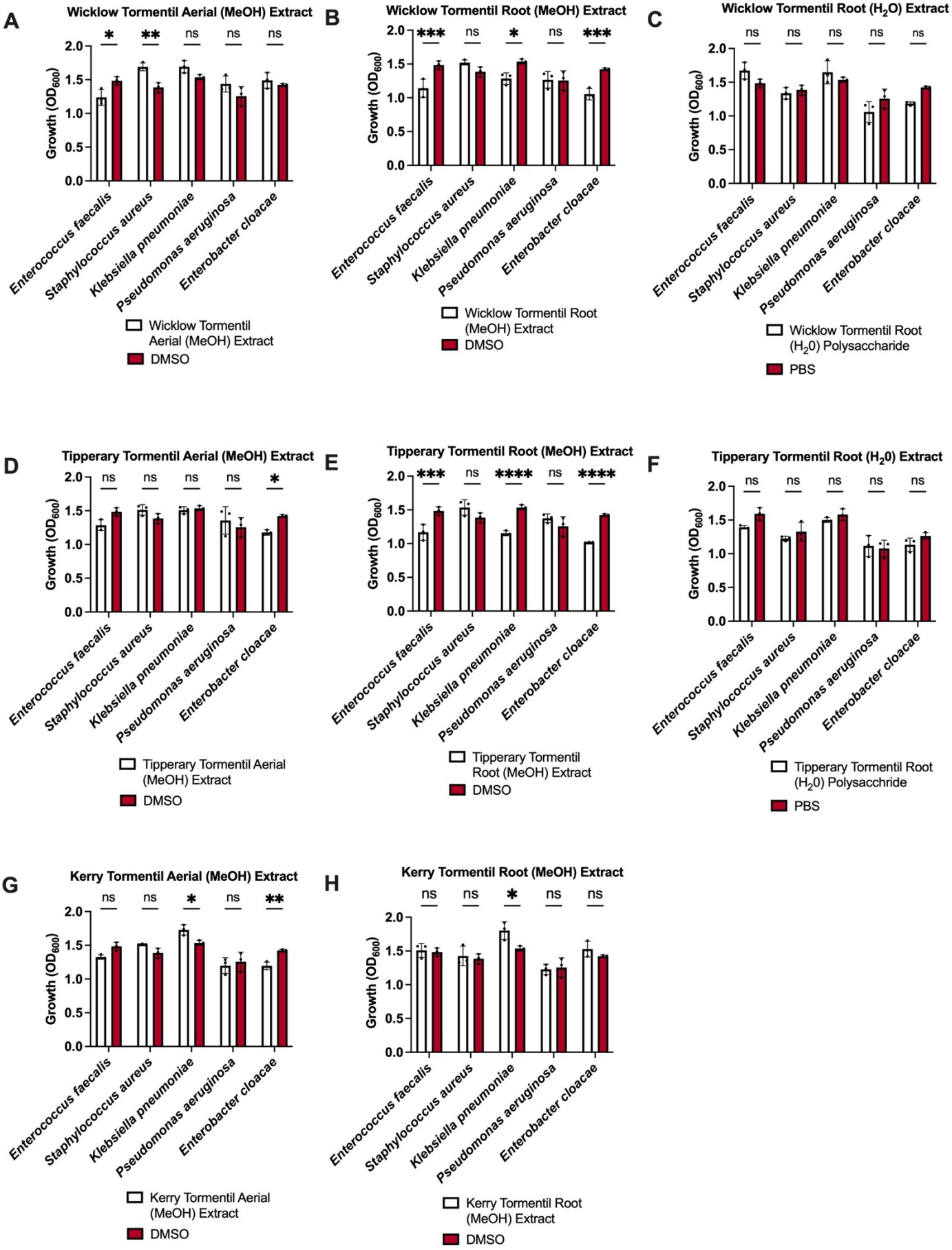
A
Wicklow Tormentil Aerial (MeOH) Extract
B
Wicklow Tormentil Root (MeOH) Extract
C
Wicklow Tormentil Root (H2O) Extract
D
Tipperary Tormentil Aerial (MeOH) Extract
E
Tipperary Tormentil Root (MeOH) Extract
F
Tipperary Tormentil Root (H20) Extract
G
Kerry Tormentil Aerial (MeOH) Extract
H
Kerry Tormentil Root (MeOH) Extract
Growth (OD600)
Enterococcus faecalis
Staphylococcus aureus
Klebsiella pneumoniae
Pseudomonas aeruginosa
Enterobacter cloacae
Wicklow Tormentil Aerial (MeOH) Extract
Wicklow Tormentil Root (MeOH) Extract
Wicklow Tormentil Root (H2O) Polysaccharide
Tipperary Tormentil Aerial (MeOH) Extract
Tipperary Tormentil Root (MeOH) Extract
Tipperary Tormentil Root (H20) Polysacchride
Kerry Tormentil Aerial (MeOH) Extract
Kerry Tormentil Root (MeOH) Extract
DMSO
PBS

Figure 3.3: Tormentil derivatives demonstrate antimicrobial effects against various ESKAPE pathogens. (A-H) Impact of tormentil derivatives at a concentration of 0.05 mg/mL on the growth of ESKAPE pathogens in CAMHB, at 24 hours. Assays were carried out in biological triplicate, each performed in technical triplicate. Statistical analysis consisted of two-way ANOVA for all panels, between the treated samples and the respective vehicle control, each comparison includes controls with increasing amounts of vehicle as the second variable factor. Average values ± SD are represented as error bars. Significance is indicated as * = $p < 0.05$, ** = $p < 0.01$, *** = $p < 0.001$, and **** = $p < 0.0001$.

3.3.4 Agrimoniin and ellagic acid are the main active components in tormentil

Potentilla spp. contain high concentrations of tannins and tannins have recognised antimicrobial action regardless of plant source (Constabel *et al*., 2014). *Potentilla erecta* contains condensed tannins and hydrolysable tannins and while more associated with the rhizome, they are also found in the aerial parts (Tomczyk and Latté, 2009). Tormentil's condensed tannins consist of dimeric and trimeric type B proanthocyanidins together with biosynthetic precursors. The main hydrolysable tannin is agrimoniin, a dimeric ellagitannin. The presence of agrimoniin and its hydrolysis product ellagic acid was confirmed and quantified in the six tormentil extracts by HPLC in comparison to commercial standards by our collaborators at Trinity College Dublin (Figure 3.4).

A

MeOH extract	Agrimoniin content (%)	Ellagic acid content (%)
Wicklow aerial	4.15	1.15
Wicklow root	6.81	0.74
Tipperary aerial	1.66	1.12
Tipperary root	10.09	0.58
Kerry aerial	2.33	1.04
Kerry root	3.37	0.37

B

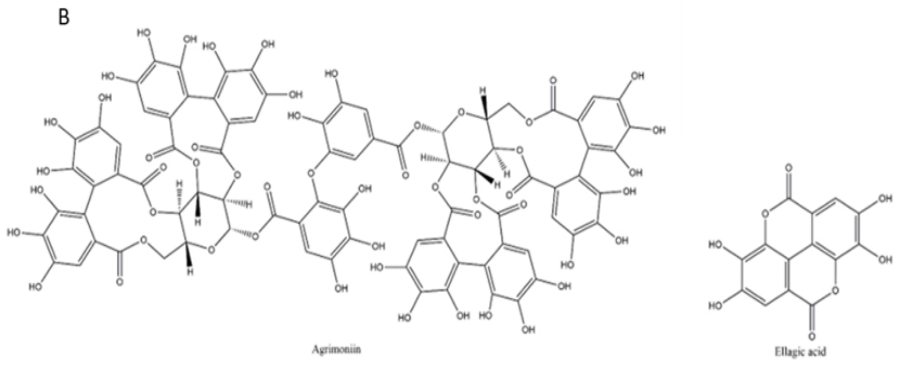

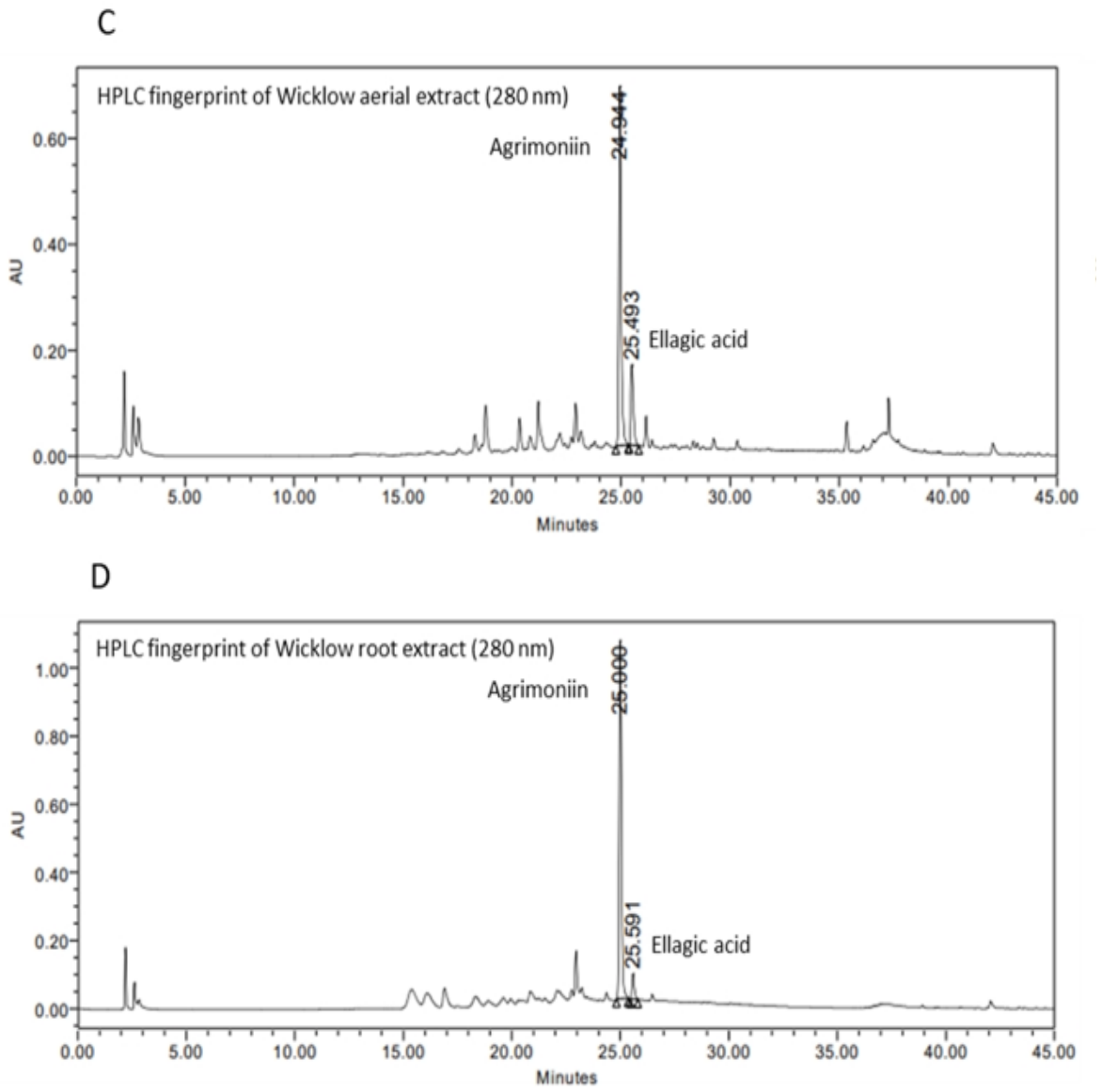

Figure 3.4: Tormentil methanol extracts contain agrimoniin and ellagic acid. (A) Percentage content of agrimoniin and ellagic acid in the tormentil methanol extracts **(B)** Structures of agrimoniin and ellagic acid **(C-D)** Representative HPLC chromatograms **(C)** HPLC fingerprint of the Wicklow aerial extract at 280 nm **(D)** HPLC fingerprint of the Wicklow root extract at 280 nm.

3.3.5 Select constituents of *P. erecta* extract, agrimoniin and ellagic acid, exhibit antibacterial effects against *A. baumannii*

Agrimoniin and ellagic acid have previously demonstrated antimicrobial activity against the gastric pathogen *Helicobacter pylori*. Agrimoniin displays a minimum inhibitory concentration (MIC) in the range of 12.5-50 μg/mL (Funatogawa *et al.* 2004) and ellagic acid in the range of 5-30 μg/mL (De *et al*., 2018). Given that both agrimoniin and ellagic acid have shown antimicrobial effects against Gram-negative bacteria and are both present in all the tormentil extracts, we explored the possibility that these compounds could inhibit MDR *A. baumannii* growth. Titration assays revealed that both compounds could inhibit the growth of *A. baumannii.* However, only the impact of ellagic acid was seen to be dose dependent over the concentration ranges tested (Figure 3.5A and 3.5B).

Biofilm formation, a method of growth where bacterial cells attach to each other or a surface and encase themselves in polysaccharide matrix, is a key defence mechanism adopted by *A. baumannii* to overcome treatments and the rigors of the host immune system (Lee *et al.*, 2017; Gedefie *et al*., 2021). Given the challenges posed by biofilm-associated *A. baumannii* infections, we wanted to investigate whether agrimoniin and ellagic acid also harbour antibiofilm properties along with their antimicrobial potential. We found that agrimoniin and ellagic acid both display dose dependent effects against *A. baumannii* biofilm formation (Figure 3.5C-D). In the context of agrimoniin, particularly at the concentration of 500 μM, a much greater impact on biofilm formation was seen compared to bacterial viability (Figure 3A and 3C). This suggests that agrimoniin displays next generation antimicrobial (NGA) activity, possessing antivirulence properties at a concentration that does not compromise bacterial viability further (Gadar and McCarthy, 2023). However, it is likely that the antibiofilm effects caused by ellagic acid are at least in part mediated through its antimicrobial activity.

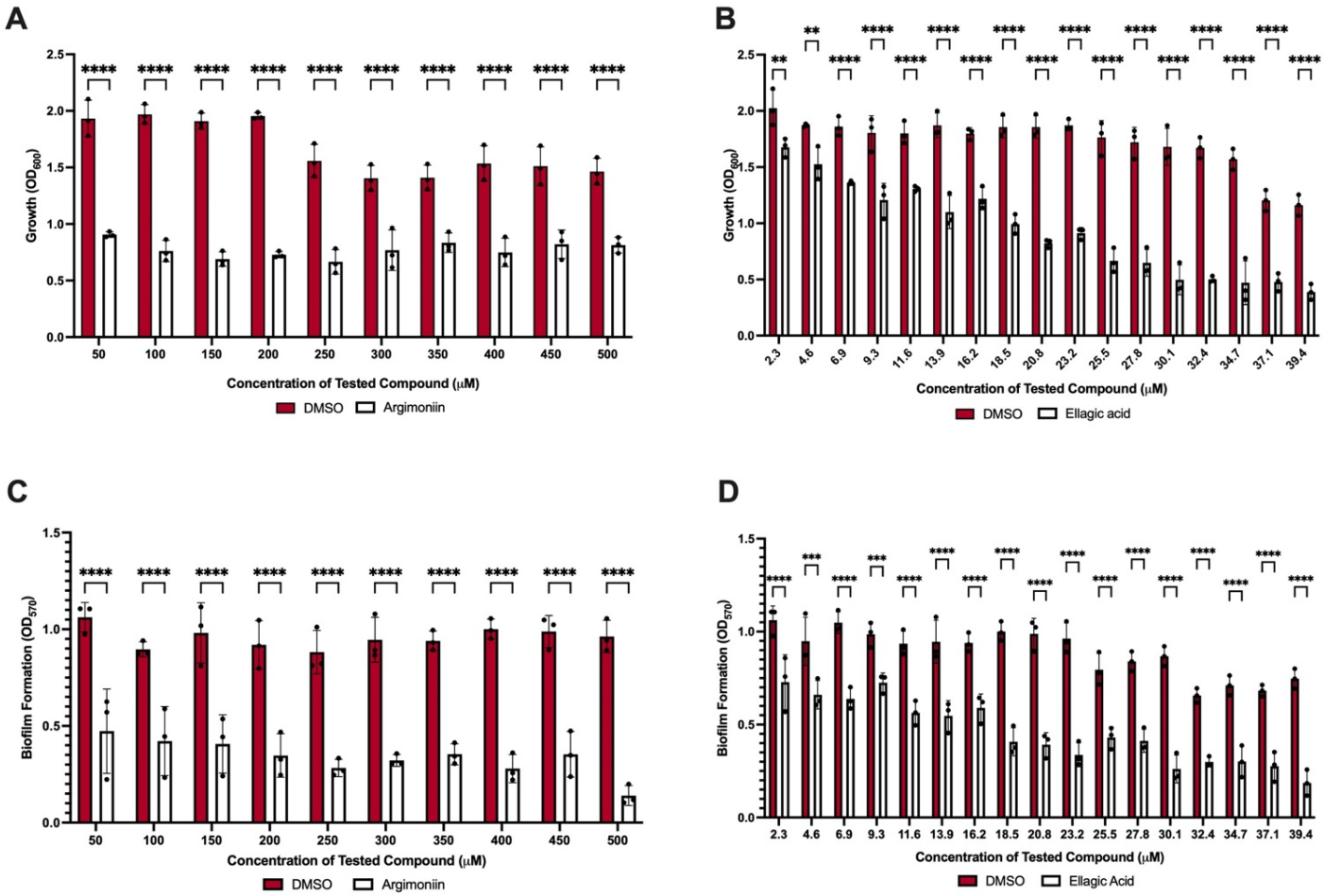

Figure 3.5: Agrimoniin and ellagic acid impact the growth and biofilm formation of *A. baumannii*. (A) Inhibition of *A. baumannii* growth by agrimoniin, tested in LB media and data read at 16 hours. Inhibition effects were not dose dependent in the tested concentration range. **(B)** Inhibition of *A. baumannii* growth by ellagic acid, tested in LB media and data read at 16 hours. Inhibition effects are shown to be dose dependent. **(C-D)** Inhibition of *A. baumannii* biofilm formation by agrimoniin **(C)** and ellagic acid **(D)**, tested in LB media and data read at 16 hours**.** The effect was dose dependent for both agrimoniin and ellagic acid within the tested concentration ranges. Assays for all panels were carried out in biological triplicate, each performed in technical triplicate. Statistical analysis consisted of two-way ANOVA for panels 3.5A, 3.5B, 3.5C and 3.5D between the treated samples and DMSO vehicle control. Each comparison includes controls with increasing amounts of DMSO as the second variable factor. Average values ± SD are represented as error bars. Significance is indicated as * = $p \leq 0.05$, ** = $p \leq 0.01$, *** = $p \leq 0.001$, **** = $p \leq 0.0001$.

3.3.6 Agrimoniin, ellagic acid and Wicklow tormentil root extract alter global gene expression in *A. baumannii* with iron associated pathways primarily impacted

To understand the mechanism underlying the growth and biofilm inhibitory effects of agrimoniin and ellagic acid on *A. baumannii* growth and biofilm formation, we performed a differential RNA sequencing (dRNA-seq) experiment. Wicklow tormentil root extract was also selected for testing based on its availability and high levels of antimicrobial activity (Figure 3.2B), which could be attributed to the presence of both agrimoniin and ellagic acid resulting in a combined effect against *A. baumannii* (Table 3.2 and Figure 3.5C). Wicklow tormentil root extract was chosen for further testing over the other tormentil derivatives due to its availability.

We treated the cells separately at inoculation with agrimoniin, ellagic acid and Wicklow tormentil root extract. The cells were treated with the lowest concentrations displaying a significant reduction in growth from the previously tested ranges, 50 μM, 2.3 μM and 0.05 mg/mL respectively. This was done to capture the antimicrobial effects of the treatments, without completely killing all the cells. Therefore, using a lower concentration of the compounds allowed for more accurate and reliable RNA-Seq data. The cells were then grown in LB to mid-exponential phase (OD_{600} 0.6) and harvested for RNA extraction. The RNA was then isolated using the RNAeasy Kit with in-column DNAase digestion (Qiagen) and sent for sequencing. Here, the samples underwent cDNA synthesis, library preparation and then were sequenced using Illumina MiSeq. The profiles were then compared to bacterial cells exposed to the DMSO vehicle control only. Our dRNA-Seq analysis revealed significant changes in gene expression, of which 236 are conserved amongst all three data sets (Figure 3.6A). Agrimoniin elicited a response that led to significant differential expression in 414 genes, with 216 showing upregulation and 198 showing downregulation (Figure 3.6B). Ellagic acid exerted an even more pronounced effect, with 636 genes exhibiting significant differential expression; among these, 455 were upregulated and 181 were down-regulated (Figure 3.6C). Similarly, Wicklow tormentil root extract impacted gene expression resulting in significant differential expression in 517 genes, wherein 378 were upregulated, and 139 were downregulated (Figure 3.6D). To gain further insights into the functional implications of the differentially regulated

genes, we performed Gene Set Enrichment Analysis (GSEA) with FUNAGE-Pro (de Jong *et al*., 2022) using the annotated genome of *A. baumannii* AB5075-UW (Gallagher *et al.,* 2015) as a reference (Appendix Table B.1).

Based on the functional GSEA clustering, the dRNA-seq analysis unveiled dysregulation in distinct gene clusters that significantly impact *A. baumannii's* iron homeostasis across all three conditions under investigation. Notably, there was consistent upregulation observed in bacterioferritin orthologues, *bfr* (ABUW_0306) and *bfrA* (ABUW_3125), which are pivotal for intracellular iron storage. Conversely, the gene clusters involved in the biosynthesis of siderophore proteins exhibited a downregulation in response to exposure to all three conditions. Specifically, a notable downregulation was observed in the expression of the *bar-bas-bau* gene cluster. This cluster is responsible for overseeing the export, biosynthesis and transport pathways of the iron-scavenging siderophore acinetobactin (ABUW_1168-1180). Consequently, the downregulation of this cluster impairs the bacterium's ability to scavenge iron from its environment (Figure 3.6 and Table B.1).

This aligns with the observed downregulation in genes associated with various functional groups linked to iron uptake including the *feoB* Fe^{2+} transporter encoding gene (ABUW_3632) which has decreased expression in the agrimoniin and ellagic acid datasets (Figure 3.6A). It is likely that this downregulation was not observed within the Wicklow tormentil root extract data set as the amounts of agrimoniin and ellagic acid may not be high enough to induce this effect. Furthermore, a consistent downregulation was observed in the expression of *foxA* ferrioxamine receptor genes (ABUW_1800) across all three conditions (Figure 3.6). A downregulation of *foxA* expression is likely aimed at preserving intracellular iron levels by mitigating its encoded protein's high-affinity interaction with iron ions. This strategic downregulation serves to maintain iron homeostasis within the bacterial cell (Miller and Morgan, 2014).

The global transcriptional response suggests that when exposed to tormentil extracts or its constituents, *A. baumannii* faces substantial iron stress. Specifically, the decrease in iron acquisition and increase in iron storage may lead to a restriction in intracellular iron concentration, thereby limiting essential cellular functions that are reliant on iron

(Cook-Libin *et al.*, 2022). Interestingly, genes associated with the biofilm formation pathway, specifically the *csu* cluster (ABUW_1487-1488) were solely downregulation within the agrimoniin dataset (Figure 3.6A and B). Additionally, in the ellagic acid dataset, there is notable downregulation of the *bfmR* gene (ABUW_3181), which is associated with the two-component system (TCS) BfmRS (Figure 4A and 4C). This TCS is known to regulate virulence in *A. baumannii* and is the target of drug discovery efforts (Russo *et al*., 2016; Tomaras *et al.* 2008). Notably, no downregulation of biofilm-related genes were observed in the Wicklow tormentil root extract dataset (Figure 3.6C and D). However, it is well established that biofilm formation is impacted by iron availability, suggesting that the antibiofilm effect displayed by agrimoniin and ellagic acid (Figure 3.5C-D) can be attributed at least in part to their capacity to induce iron stress within the bacterium (Cook-Libin *et al.*, 2022).

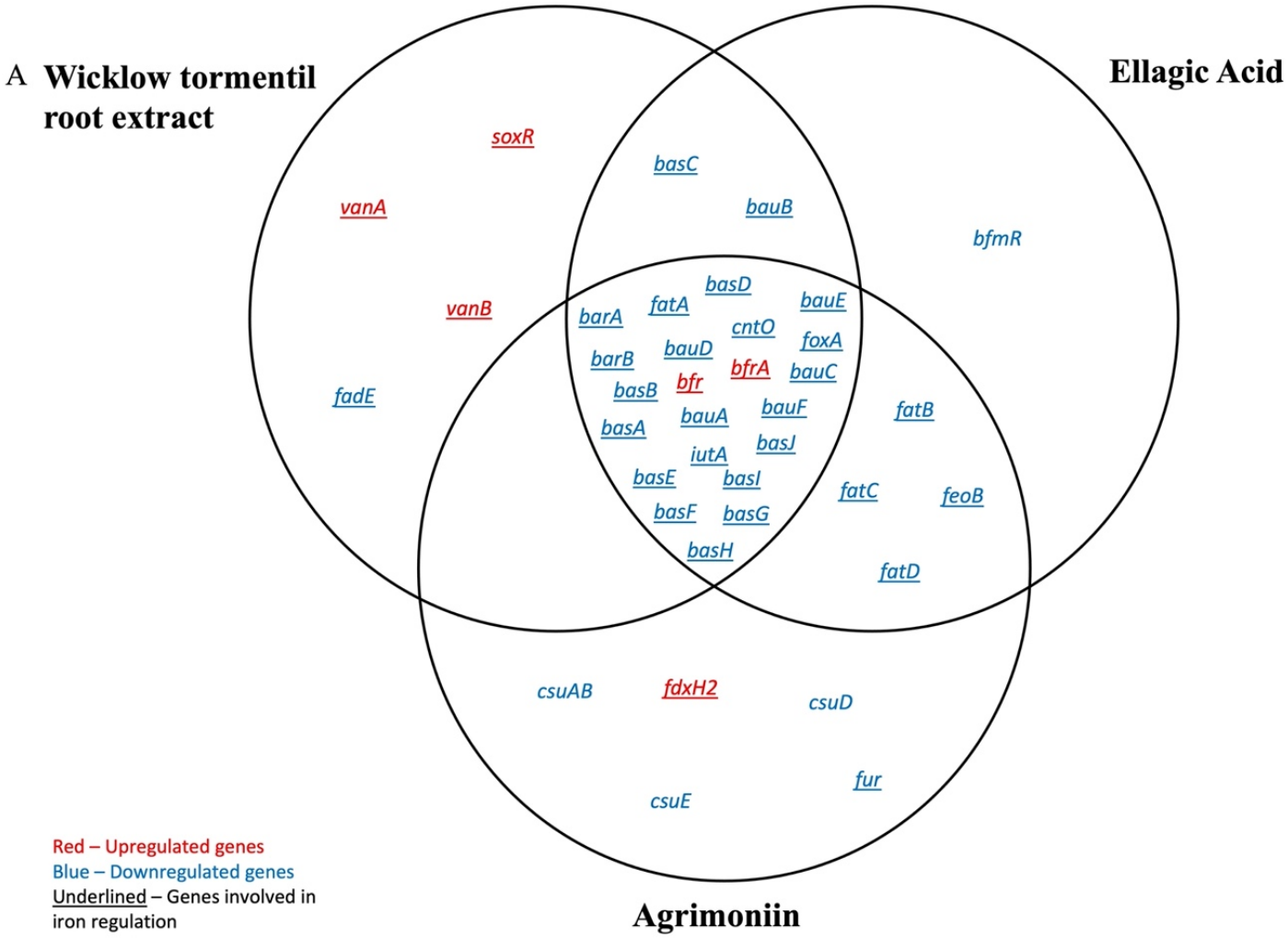

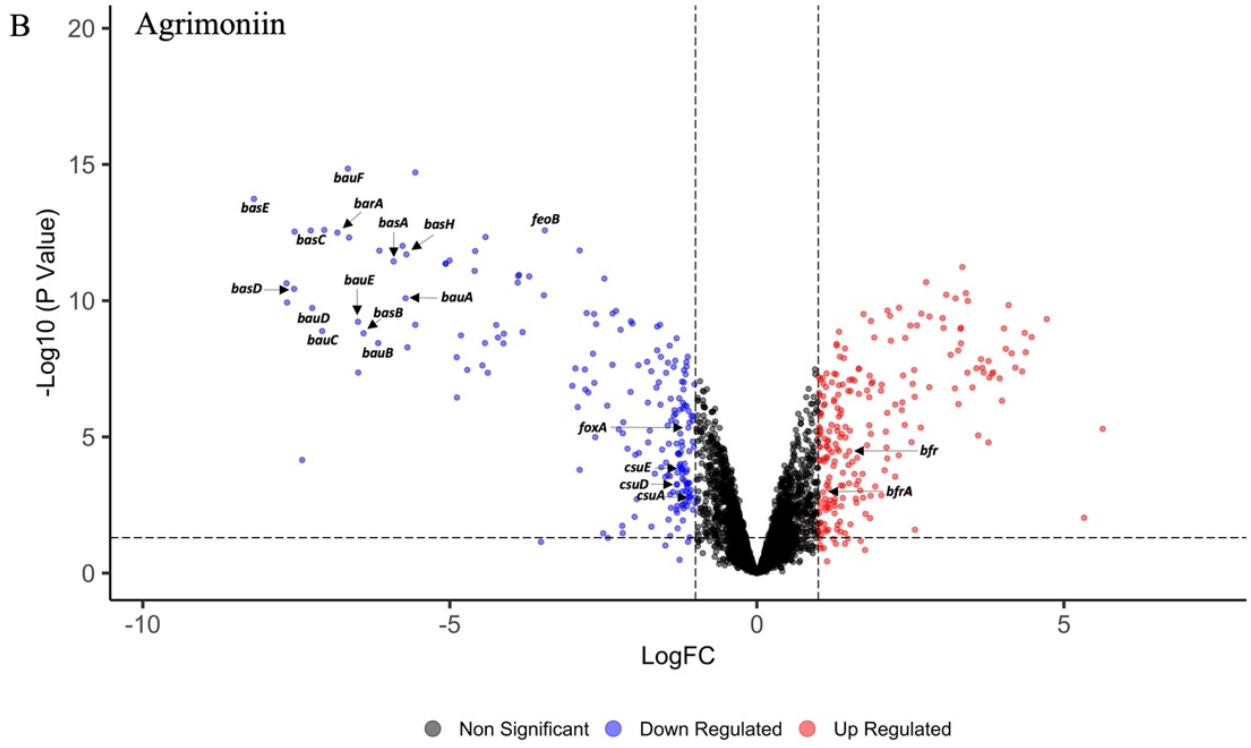
B
Agrimoniin
-Log10 (P Value)
LogFC
bauF
basE
barA
basA
basH
feoB
basC
basD
bauE
bauA
bauD
basB
bauC
bauB
foxA
csuE
csuD
csuA
bfr
bfrA
Non Significant
Down Regulated
Up Regulated

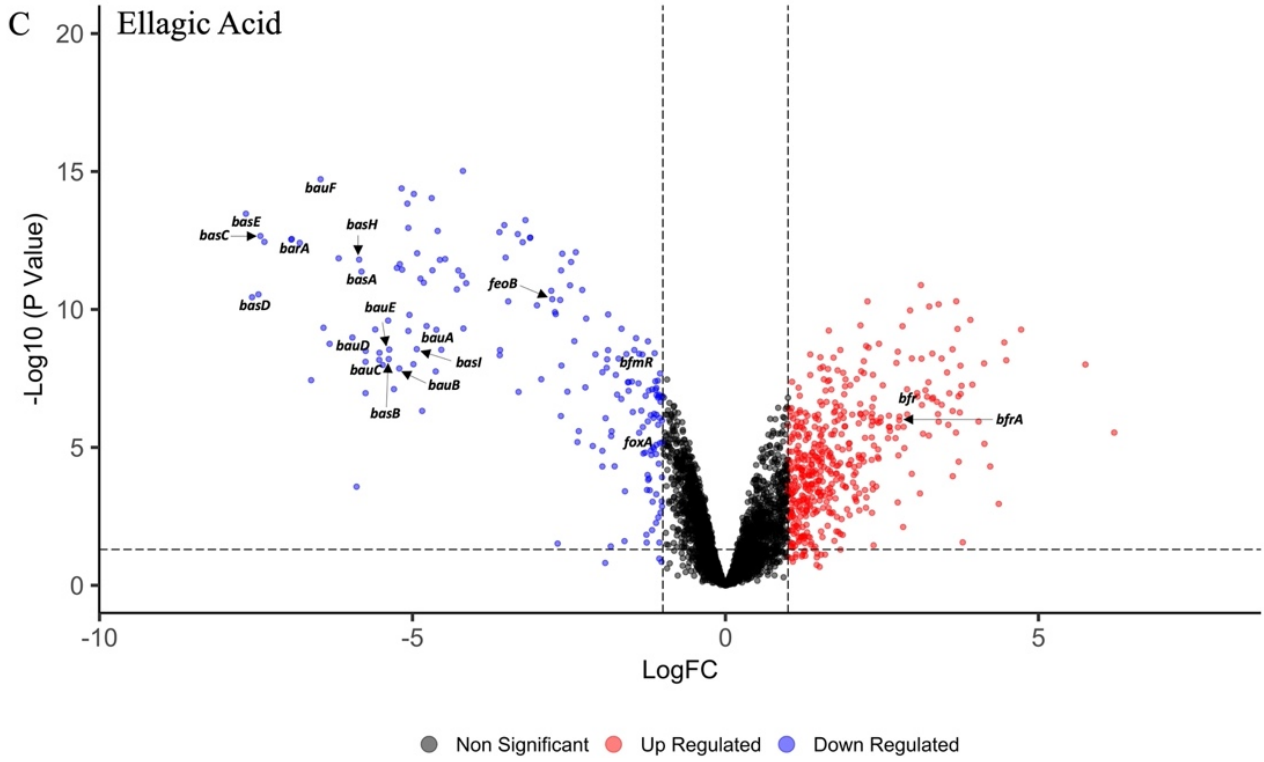
C
Ellagic Acid
-Log10 (P Value)
LogFC
bauF
basE
basC
barA
basH
basA
basD
feoB
bauE
bauA
bauD
basI
bauC
bauB
basB
bfmR
foxA
bfr
bfrA
Non Significant
Up Regulated
Down Regulated

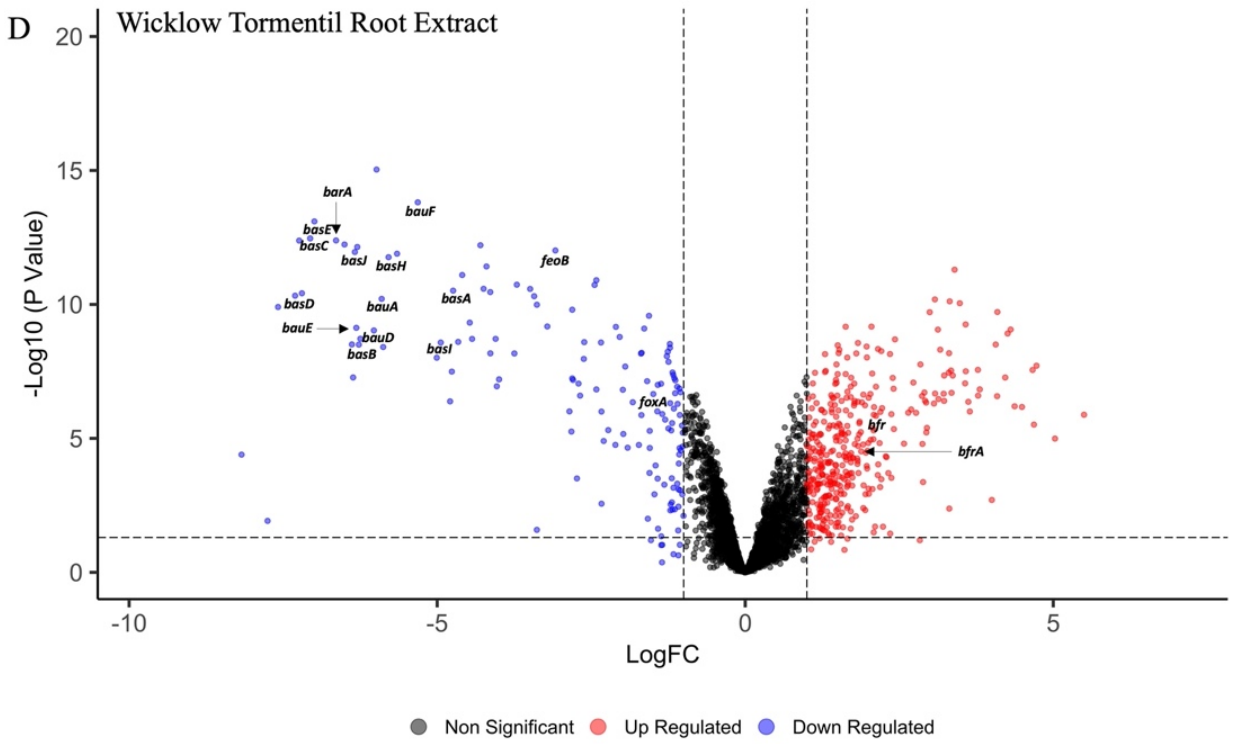

Figure 3.6: Alteration of the iron signature in *A. baumannii* by agrimoniin, ellagic acid and Wicklow tormentil root extract. **(A)** Venn diagram depicting the commonalities and differences in differentially expressed genes related to iron and biofilm, between the three data sets agrimoniin, ellagic acid and Wicklow tormentil root extract. Downregulated genes are represented in blue, and upregulated genes are represented in red. Genes that are involved in iron processes are underlined and genes that are involved in biofilm processes are not. **(B, C and D)** Volcano plots representing the results of the dRNA-seq analysis performed on cells exposed to **(B)** agrimoniin, **(C)** ellagic acid and **(D)** Wicklow tormentil root extract compared to cells exposed to DMSO vehicle control. Genes with no change in their expression levels are shown in black, whereas significantly downregulated and upregulated genes are shown in blue and red, respectively. Representative genes related to iron in panels 4B, 4C and 4D are labelled, for example upregulated genes related to iron storage, such as bacterioferritin (*bfr*, ABUW_0306) and *bfrA* (ABUW_3125), downregulated genes related to siderophore biosynthesis, transport, and export, such as the acinetobactin (*bar-bas-bau* cluster, ABUW_1168-1188) biosynthetic pathway and the biofilm formation pathway (*csu* cluster, ABUW_1487-1488).

3.3.7 Iron supplementation can reverse the antimicrobial effects of agrimoniin and ellagic acid and Wicklow tormentil root extract

Given that previous studies have demonstrated the iron-chelating capabilities of agrimoniin and ellagic acid (Shendge *et al*., 2018; Fedotcheva *et al*., 2021) and that our transcriptomic data (Figures 3.6 and Table B.1) highlights that agrimoniin, ellagic acid and Wicklow tormentil root extract have significant impact on iron homeostasis in *A. baumannii*, we were then incited to investigate whether this property underpins their antimicrobial and antibiofilm activities. To determine if this dysbiosis was responsible for the antimicrobial and antibiofilm effects of tormentil, ellagic acid and agrimoniin, we supplemented the treated bacteria cells each with Fe^{2+} or Fe^{3+}. Strikingly, supplementing with either Fe^{2+} or Fe^{3+} led to the complete rescue of both bacterial cell growth and biofilm-forming capabilities (Figure 3.7). This finding shed light on the pivotal role of iron chelation in the observed antimicrobial and antibiofilm effects of agrimoniin, ellagic acid and Wicklow tormentil root extract.

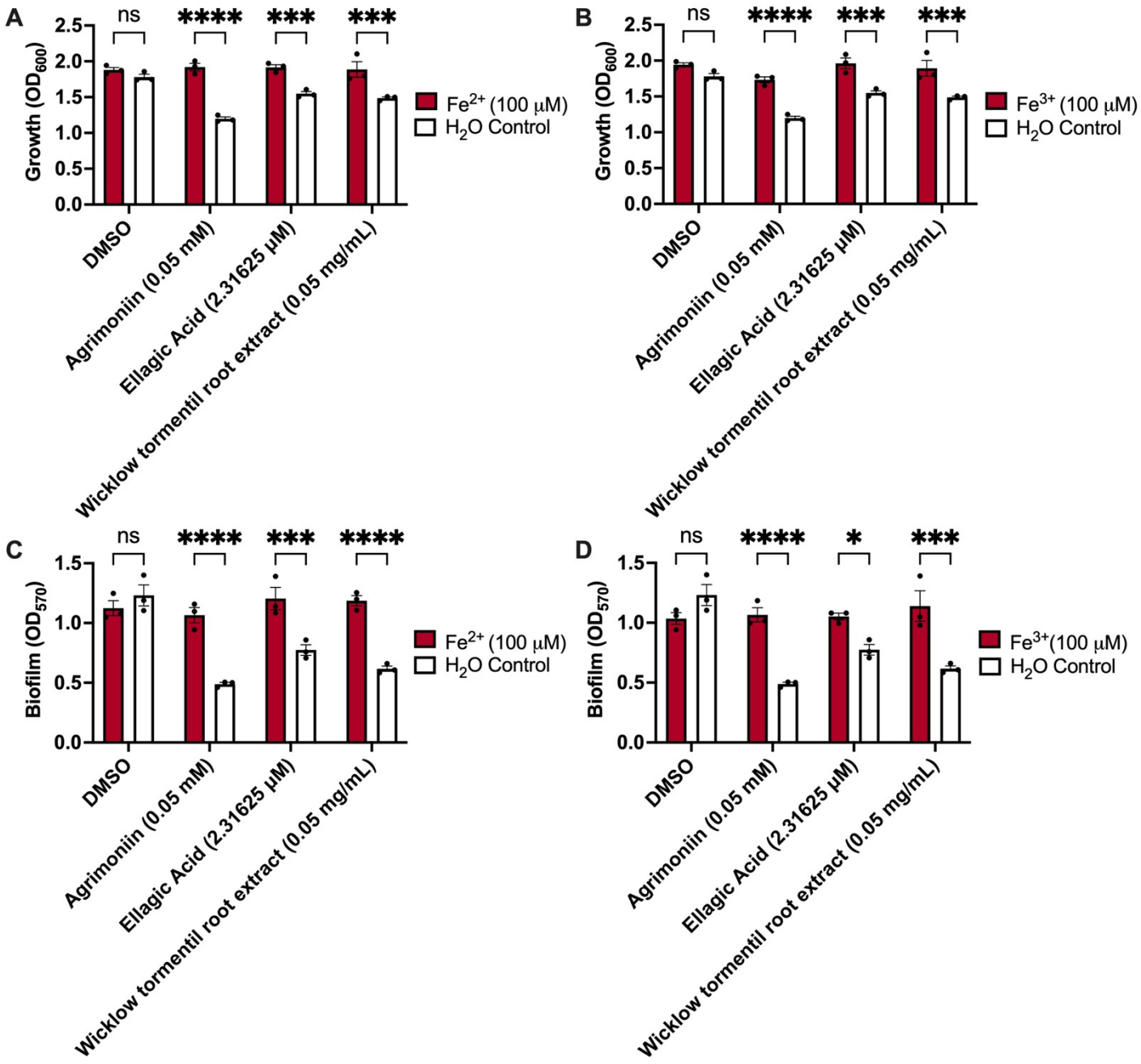

Figure 3.7: Agrimoniin, ellagic acid and Wicklow tormentil root extract affect iron levels in *A. baumannii*. **(A-B)** Growth inhibition of *A. baumannii* in the presence of 50 μM agrimoniin, 2.3 μM ellagic acid, 0.05 mg/mL Wicklow tormentil root extract is rescued by Fe^{2+} **(A)**, and Fe^{3+} **(B)** supplementation, in LB media. **(C-D)** Biofilm inhibition of *A. baumannii* in the presence of 50 μM agrimoniin, 2.3 μM ellagic acid, 0.05 mg/mL Wicklow tormentil root extract is rescued by Fe^{2+} **(C)**, and Fe^{3+} **(D)** supplementation. For all panels, assays were carried out in biological triplicate, with three technical repeats. Analysis consists of two-way ANOVA between the treated samples and the treated samples that were supplemented with Fe^{2+} or Fe^{3+}.

Each comparison includes controls with increasing amounts of H_2O as the second variable factor. Average values ± SD are represented as error bars. Significance is indicated as ns = non-significant, * = p ≤0.05, ** = p ≤0.01, *** = p ≤0.001, **** = p ≤0.0001.

3.3.8 Agrimoniin, ellagic acid and Wicklow tormentil root extract potentiates colistin treatment

In our previous work in chapter 2, we demonstrated that disrupting iron homeostasis can potentiate the activity of the last resort antibiotic, colistin (Gadar *et al*., 2023). Thus, we sought to explore if the iron chelating abilities of agrimoniin and ellagic acid (Shendge *et al*., 2018; Fedotcheva *et al*., 2021) could similarly potentiate colistin. Moreover, our curiosity extended to the colistin-potentiating properties of Wicklow tormentil root extract as it contains high amounts of both agrimoniin and ellagic acid and thus would allow us to explore any combination effects of agrimoniin and ellagic acid (Figure 3.4A).

Our investigation uncovered that agrimoniin, ellagic acid or Wicklow tormentil root extract, at a concentration of 50 µM, 2.3 µM and 0.05 mg/mL respectively, combined with the sub-MIC of colistin (1.22 µg/mL) (Gadar *et al*., 2023), exhibited a capability to impede the growth of *A. baumannii* (Figure 3.8). This synergistic effect surpassed the individual impacts of these components when used singularly, further highlighting their potential in combating *A. baumannii* infections.

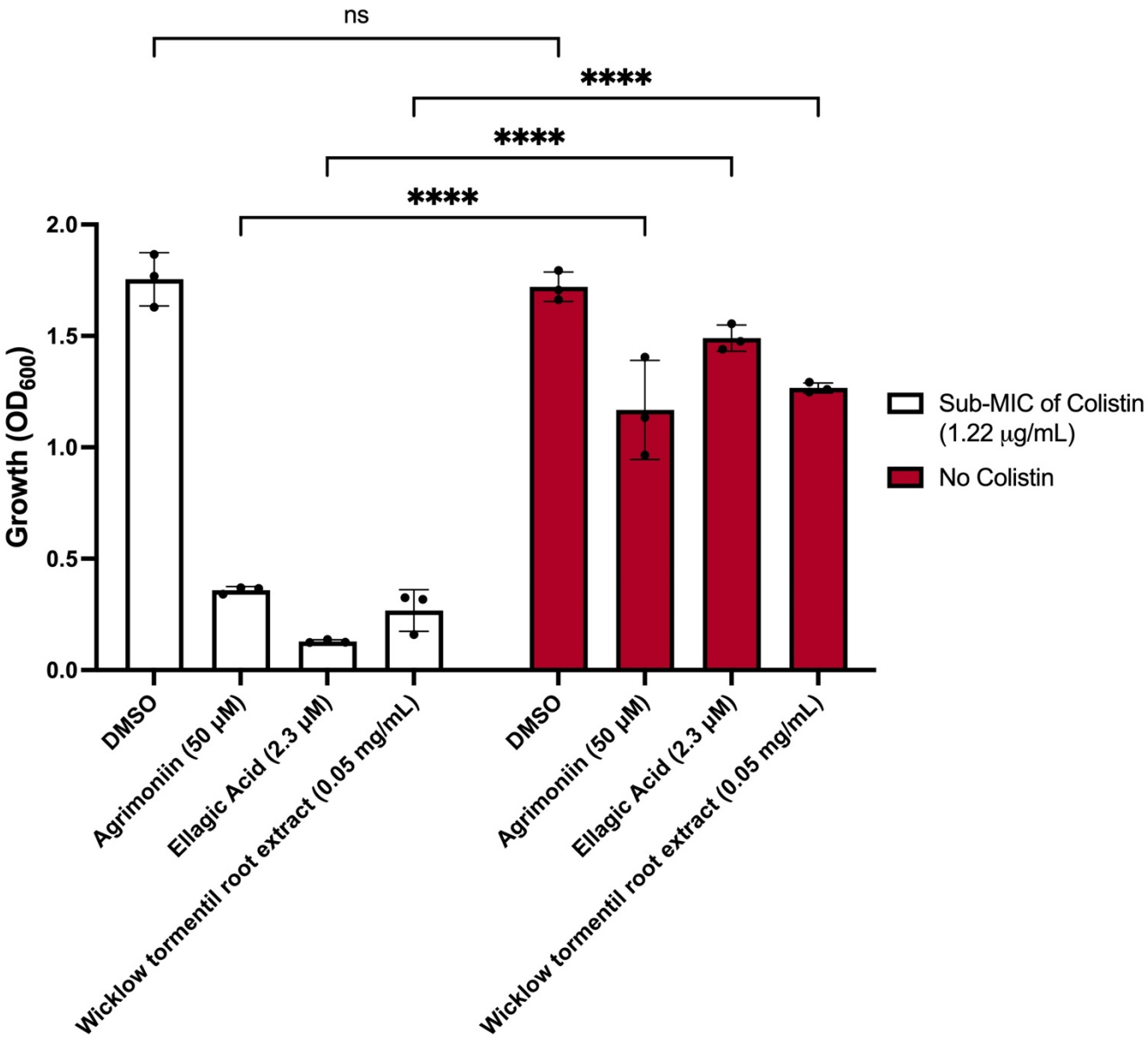

Figure 3.8: Agrimoniin, ellagic acid and Wicklow tormentil root extract potentiates the activity of colistin. Impact of agrimoniin, ellagic acid and Wicklow tormentil root extract at a concentration of 50 µM, 2.3 µM and 0.05 mg/mL respectively, on the growth of *A. baumannii*, when combined with the sub-MIC of colistin (1.22 µg/mL), after 12 hours. Assays were carried out in biological triplicate, with three technical repeats. Statistical analysis consisted of two-way ANOVA between the treated sample and the treated sample combined with the sub-MIC of colistin. Each comparison includes controls with increasing amounts of H_2O as the second variable factor. Average values ± SD are represented as error bars. Significance is indicated as * = $p < 0.05$, ** = $p < 0.01$, *** = $p < 0.001$, and **** = $p < 0.0001$.

3.4 Discussion

The initial screening revealed many potential antibacterial and antibiofilm candidates derived from the Irish bogland species. Among these candidates, *P. erecta* L. stood out as it was one of the potent antimicrobials against *A. baumannii* and displayed antibiofilm effects (Figure 3.1). This extract was able to be studied further due to its large availability. The Potentilla genus has been used in herbal medicine since ancient times by the Greek physician Dioscorides and tormentil is a prominent plant in European herbal texts through the centuries and in other traditional medicine systems such as traditional Chinese medicine (Barua and Yasmin, 2018; Kumari *et al*., 2021). Recent studies have unveiled tormentil's antimicrobial effects against biofilm-forming strains of *Staphylococcus aureus*, including antibiotic-resistant variants (Kryvtsova *et al*., 2022). Additionally, tormentil has demonstrated antimicrobial activity against *Bacillus subtilis* ATCC 6633, as well as certain yeast strains such as *Candida lipolitica* KKP 322 *and Hansenula anomala* R 26 (Synowiec *et al*., 2014).

In this study, we demonstrate the diverse antimicrobial effects displayed by both aerial and root MeOH segments extracted from tormentil plants across various regions of Ireland (Figure 3.2). Notably, these antimicrobial properties are consistently observed irrespective of segment type or geographical origin. However, this antimicrobial effect is not uniformly retained across all ESKAPE pathogens. Despite this, Wicklow tormentil aerial, Wicklow tormentil root, and Tipperary tormentil root extracts exhibit significant effects on the growth of both Gram-negative and Gram-positive pathogens (Figure 3.3). This suggests a potential broad-spectrum application of these extracts in combating a range of bacterial infections. Further exploration of the specific mechanisms underlying these antimicrobial properties and their potential therapeutic applications is required.

Wicklow tormentil root (H_20) extract and Tipperary tormentil root (H_20) extract exhibit non dose dependent antibiofilm formation effects against *A. baumannii* (Figure 3.2C) but the constituents of these extracts, agrimoniin and ellagic acid, display a dose dependent antibiofilm effect against *A. baumannii* (Figure 3.5C and D). This suggests the Wicklow tormentil root (H_20) extract and Tipperary tormentil root (H_20) extracts may contain other components that may interact with the antibiofilm effects of agrimoniin and ellagic acid when their

concentration is also increased. Although the Wicklow tormentil root extract and Kerry tormentil root extract also display antibiofilm effects, their potent antimicrobial effect may impede their classification as true antibiofilm agents. This is due to the possibility that the extract's ability to prevent biofilm formation (Figure 3.2C) could be attributed to their strong antimicrobial properties (Figure 3.2B), leading to the eradication of bacterial cells rather than specifically targeting biofilm formation processes.

The bioactivity of extracts is indicative of their ability to elicit biological effects or responses when they are consumed or applied. It provides a measure of the biological or pharmacological activity exhibited by the constituents present within tormentil derivative extracts. A comprehensive analysis utilising HPLC-PDA to quantify the level of constituents present in each segment derivative was conducted. The data revealed several compounds of interest, some of which could have been responsible for the observed antimicrobial activity (Figure 3.4). Previous studies have demonstrated the antimicrobial properties of these extracts against *Helicobacter pylori*, a Gram-negative bacterium. Ellagic acid, exhibited remarkable efficacy in eradicating 55 different strains of *H. pylori,* as demonstrated *in vitro* with a minimum inhibitory concentration (MIC) range of 5 to 30 mg/L. Furthermore, its effectiveness was also observed *in vivo* through an *H. pylori* SS1-infected mouse model (De *et al*., 2018). Likewise, agrimoniin displayed effectiveness against 32 strains of *H. pylori*, with an MIC range of 12.5 to 50 µg/mL (Funatogawa *et al*., 2004). In correlation to these findings, our data indicates that both agrimoniin and ellagic acid exhibit antibacterial properties against *A. baumannii* (Figure 3.5A and 2B). However, only ellagic acid elicits a dose-dependent inhibition effect on bacterial growth. These findings, in conjunction with the aforementioned studies, indicate the potential of these compounds as candidates for the development of novel antibacterial agents against Gram-negative bacteria, such as *A. baumannii*.

Both agrimoniin and ellagic acid also exhibited antibiofilm effects against *A. baumannii* in a dose-dependent manner, within the concentration range tested (Figure 3.5D and 2E). A downregulation in the *csu* cluster (ABUW_1487-1488), a set of genes essential for biofilm formation, was observed solely in the agrimoniin dataset (Figure 3.6A, B and Table B.1). Additionally, a downregulation in the response regulator *bfmR* (ABUW_3181) of the two-

component system BfmRS, was only observed in the ellagic acid dataset (Figure 3.6C, and D).

This system is involved in regulating genes related to biofilm formation, such as the *csu* operon (Tomaras *et al.,* 2008) and is a known potential drug target for *A. baumannii* (Russo *et al*., 2016). The transcriptional data, alongside the NGA activity of agrimoniin implies that the demonstrated antibiofilm activity attributed to agrimoniin is indeed true antibiofilm activity caused by a downregulation of the *csu* cluster and dysregulation of genes affecting iron availability (Cook-Libin *et al.*, 2022). Contrastingly, the observed antibiofilm activity associated with ellagic acid (Figure 3.5D) could arise from its antimicrobial activity, as well as the dysregulation of genes impacting iron availability (Cook-Libin *et al.*, 2022).

dRNA-Seq analysis also revealed the upregulation of bacterioferritin orthologues, *bfr* (ABUW 0306) and *bfrA* (ABUW 3125), responsible for iron storage, upon exposure to all three treatments (Figure 3.6 and Table B.1). Conversely, the expression of genes involved in the biosynthesis, export, and transport of the siderophores acinetobactin (*bar-bas-bau* cluster) was downregulated by all three extracts (Figure 3.6). Collectively, our transcriptomics data indicates that the tested treatments affect iron levels within *A. baumannii* by impeding the acquisition and increasing the storage of this vital nutrient. Coherently, previous studies have demonstrated that both agrimoniin and ellagic acid possess the ability to chelate iron ions, ultimately leading to their depletion (Shendge *et al*., 2018; Fedotcheva *et al*., 2021). To further challenge our hypothesis that iron depletion was responsible for the antimicrobial activity of tormentil and its constituents, we supplemented the media with free iron. This resulted in the rescuing of the cells from the lethal effects of tormentil and its extract and further confirmed the role of iron sequestration in their antimicrobial activity (Figure 3.7).

Our previous study, which focused on the significance of iron homeostasis in colistin susceptibility, highlighted the potency of various compounds in augmenting colistin's activity. Kaempferol, along with non-specific iron chelators such as EDTA and specific iron chelators like ExJade and 8-Hydroxyquinoline, exhibited promising colistin potentiating effects (Gadar *et al*., 2023). Similarly, a study conducted by Chusri *et al*. (2009) found that ellagic acid can enhance the activity of novobiocin, coumermycin, chlorobiocin, rifampicin and fusidic acid against *A. baumannii* at a concentration of 40 µM. Thus, the iron-chelating abilities of

agrimoniin and ellagic acid, coupled with the demonstrated potentiating effects of ellagic acid (Shendge *et al*., 2018; Fedotcheva *et al*., 2021; Chusri *et al*., 2009), incited us to investigate the colistin-potentiating properties of agrimoniin, ellagic acid, and Wicklow tormentil root extract. These findings indicate that when combined with sub-inhibitory concentration (sub-MIC) of colistin, each tested treatment, at a concentration of 50 μM, 2.3 μM and 0.05 mg/mL respectively, significantly reduced the growth and biofilm formation of *A. baumannii*. This highlights the use of tormentil and its constituents as a promising strategy to increase the efficacy of colistin (Figure 3.8).

Tormentil has a long history of use in traditional medicine including being used to treat microbial infection. In this chapter, we uncover the fundamental mechanisms underpinning the antimicrobial and antibiofilm activity associated with this plant (Figure 3.6, Table A1 and Figure 3.9). We identify and characterise the active components and demonstrate that they limit bacterial cell growth by affecting iron homeostasis (Figures 3.5, 3.6, 3.7). Additionally, we demonstrate the ability of Wicklow tormentil root extract and its bioactive constituents to enhance the efficacy of colistin (Figure 3.8). In the current climate, where we are in urgent need of novel compounds with antimicrobial activity against MDR pathogens, this work highlights the potential of plants as a source of novel antimicrobials and identifies compounds with therapeutic potential as standalone antimicrobials or as potentiators of the last resort antibiotic colistin against MDR *A. baumannii*.

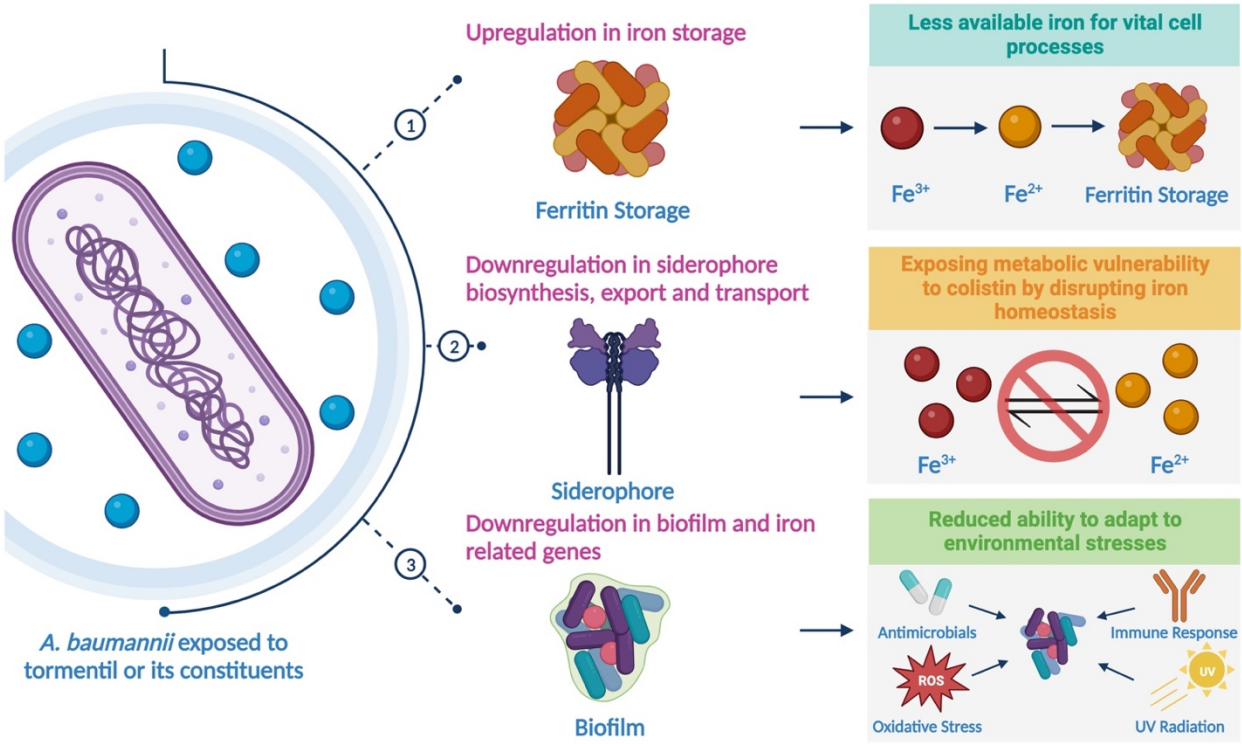

Figure 3.9: Summary figure for the mechanism of action of Tormentil and its constituents against *A. baumannii.* Tormentil and its constituents are able to impact the growth and biofilm formation of *A. baumanii* by acting upon iron homeostasis. They are able to do this by upregulating genes involved in iron storage and simultaneously downregulates genes involved in siderophore biosynthesis, export and transport. This also exposes the cell's metabolic vulnerability to the sub-MIC of colistin. Additionally, they are able to reduce biofilm formation by downregulating biofilm formation related genes resulting in the bacteria having a reduced ability to adapt to environmental stress.

The next step would be to develop the formulation of the DMSO soluble extracts so that they are suitable for *in vivo* clinical testing. This could be done by testing other solvents that are suitable for human use, such as ethyl alcohol or glycerol or potentially converting the DMSO soluble extracts into PBS/water soluble form through chemical modification. This would be preferred for clinical testing as there would be increased bioavailability, ease of dosing and less cytotoxic effects with water soluble formulations.

Following formulation development, a comprehensive safety and toxicity evaluation of the extracts and formulations would then need to be conducted. This assessment is imperative to evaluate the potential adverse effects associated with the treatment in clinical studies. These

assessments would include pharmacokinetics analysis (examining absorption, distribution, metabolism and excretion of the extracts and formulations) and pharmacodynamics (analyzing their effects on the body) to determine their safety for use in clinical settings.

Future work may then include assessing the cytotoxicity and efficacy of tormentil and its constituents *in vivo* in animal models. While *in vivo* assays in *G. mellonella* were initially planned within the scope of our study, unforeseen challenges, such as a decrease in viable *G. mellonella*, prevented us from conducting these experiments. *In vivo,* work in mice would be beneficial as cytotoxicity assays could determine the safety of the treatment against eukaryotic cells. Additionally, efficacy testing against mice injected with a lethal dose of *A. baumannii* would provide insights into the antimicrobial activity of tormentil and its constituents within a more complex environment. Together, this data could be used to design and conduct clinical trials to evaluate the efficacy and safety of the treatment, with the potential for therapeutic use in humans against MDR *A. baumannii* infections.

Findings in this chapter are represented by a single extraction of a single plant from each location thus the observed variation in the antimicrobial/antibiofilm effects of these extracts could be influenced by variations in seasonal changes and differences in the flowering a non-flowering states of the plants. Exploring these aspects in future studies could inform more robust methodologies for antimicrobial/antibiofilm agent screening.

Key Findings:

1. Identification of antimicrobial and antibiofilm activity of tormentil extracts:

- Our study reveals that extracts from tormentil plants exhibit significant antimicrobial and antibiofilm effects against various pathogens, including both Gram-negative and Gram-positive bacteria.
- These effects are consistent across different segments of the plant and regardless of geographical origin, suggesting a broad-spectrum application in combating bacterial infections.

2. Identification of bioactive components:

- Our study identifies two known components, agrimoniin and ellagic acid, present in all tormentil extracts. These components demonstrate antimicrobial and antibiofilm properties against *A. baumannii.*

3. Identifying the mechanism of action of tormentil and its constituents:

- We identify the mechanisms underlying the activity of tormentil, agrimoniin and ellagic acid, particularly their impact on iron homeostasis within bacterial cells.

4. Enhancement of colistin efficacy:

- Our study shows that tormentil extracts, along with its active constituents agrimoniin and ellagic acid, enhance the efficacy of the last resort antibiotic colistin against MDR *A. baumannii.*

5. Contributions:

- Tormentil and its constituents show promise as standalone antimicrobials or as potentiators of colistin, against MDR pathogens like *A. baumannii.* Potentially reducing the therapeutic dose of colistin, improving patient outcomes.

3.5 Materials and Methods

3.5.1 Bacterial strain

A. baumannii was used throughout this study and was routinely grown in Luria-Bertani (LB) media (Miller) at 37^{o}C, under aerobic shaking conditions (180 rpm). The *A. baumannii* strain AB5075 used was sourced from the Manoil Lab (University of Washington, Seattle, USA).

3.5.2 Reagents and chemicals

Agrimoniin was purchased from Wuhan ChemNorm Biotech (Product no. TBW01481) and ellagic acid was purchased from Merck (Product no. 14668).

3.5.3 Plant material acquisition and extraction

P. erecta plant material was collected from three locations in Ireland in the summer (Table 3.1). The collected samples were cleaned, allowed to dry at room temperature (RT) and separated into aerial (leaf, stem and flower) and underground (rhizome and root) parts. Voucher samples were prepared for collection NTP127 from Wicklow and lodged at the National Botanic Gardens of Ireland in Glasnevin, Dublin. Accession code DBN0007669 was obtained for the aerial plant parts and DBN0007670 was obtained for the underground plant parts. Methanol extractions of the dried, separated and milled plant material were carried out using a Buchi Soxhlet extraction system B-811 in 'Soxhlet Standard' mode. The methanol solvent was removed under vacuum to yield the six extracts, three from aerial plant parts and three from underground plant parts.

3.5.4 Plant extracts screen for antibacterial activity and determine their Minimum Inhibitory Concentration (MIC)

Overnight cultures were diluted in cation-adjusted Mueller-Hinton (CAMH) media to OD_{600} 0.1. The bacterial suspension (199 µl) was added to each well on a 96-well plate followed by the addition of 1 µl of each plant extract from a stock concentration of 10 mg/mL. DMSO (1 µl) was added as a carrier control, it is worth noting that the volume of DMSO added is relative to the treatment concentration. OD_{600} readings were taken every 10 min over 12 h with a Clariostar Plus plate reader (BMG LabTech), at 37 °C, 200 rpm. Endpoint OD_{600} was measured after 12 hours using a Clariostar Plus plate reader (BMG LabTech).

For MIC testing 200 µl of the bacterial suspension was added to a 96-well plate. To the first well, 0.5 µl of the treatment, from a 10 mg/mL stock was added. The following wells had an increased volume of the extract added by 0.5 µl each time. As a control, 200 µl of the bacterial solution and 200 µl of sterile LB was plated in separate wells and tested. A control assay was performed in parallel using equivalent volumes of DMSO as a carrier control. The 96-well plate was then incubated at 37 °C, 200 rpm. Endpoint OD_{600} was measured after 16 hours using a Clariostar Plus plate reader (BMG LabTech). The exact same assay was used for testing agrimoniin and ellagic acid however the stock concentration for agrimoniin was 10 mM and due to the low solubility of ellagic acid, the stock concentration was 463.25 µM. The results represent the average of three biological replicates ± SD. For MBIC testing, the same 96-well plate was used as the MIC assessment. The biofilms were stained using the crystal violet protocol as explained above. MBIC was determined as the lowest extract concentration that completely inhibited biofilm formation. The results represent the average of three biological replicates ± S.D.

3.5.5 Plant extracts screen for antibiofilm formation activity

For screening antibiofilm activity, we used the same 96-well plate as the antibacterial screening. Following incubation, the biofilm was stained using the crystal violet method (O'Toole *et al*., 2011), with few modifications (washes were performed by pipetting and the staining was performed with 1% crystal violet). The absorbance of ethanol solubilised crystal violet was then read at 600 nm using a Clariostar Plus plate reader (BMG LabTech). The results represent the average of three biological replicates ± S.D.

3.5.6 Colistin Potentiating Assay

To test the ability of agrimoniin, ellagic acid and Wicklow tormentil root extract to potentiate the sub-MIC of colistin we screened the extract against *A. baumannii* in LB media that was supplemented with the sub-MIC of colistin (1.22 μg/mL). *A. baumannii* overnight cultures were diluted in supplemented LB media to OD_{600} 0.1. 199 μl of the suspension was added to each well on a 96-well plate followed by the addition of 1 μl of each plant extract from a stock concentration of 10 mM for agrimoniin, 463.25 μM for ellagic acid and 10 mg/mL for Wicklow tormentil root extract. 1 μl of DMSO was added as a carrier control, it is worth noting that the volume of DMSO added is relative to the treatment concentration. OD_{600} readings were taken every 10 min over 12 h with a Clariostar Plus plate reader (BMG LabTech), at 37 °C, 200 rpm. The results represent the average of three biological replicates ± SD.

3.5.7 HPLC determination of agrimoniin and ellagic acid in the tormentil methanol extracts

HPLC-PDA analysis of the tormentil methanol extracts was performed based on a reported method for the quantification of tannins and related polyphenols in commercial products of tormentil with some modifications (Fecka *et al*., 2015). A Waters HPLC system consisting of a Waters 600 Controller featuring a quaternary pump and a Waters 717 Plus Autosampler coupled with a Waters 2996 Photo Diode Array (PDA) detector under the control of carried out using a Phenomenex C18 column, 5 μm particle size, 250 mm × 4.6 mm. Gradient elution

Empower® 3 software was used for measurements (Milford, MA, USA). Separations were at a flow rate of 1.2 mL/min was used and the composition of mobile phase A was acetonitrile + 1.5% v/v formic acid and mobile phase B was H_2O + 1.5% v/v formic acid. The elution program was 0 – 30% A in B from 0 min to 30 min, 30 – 70% A in B from 30 min to 33 min and a holding step of 70% A in B from 33 min to 40 min before equilibration to 0% A in B from 40 min to 45 min. All samples were filtered through a 0.45 μm filter prior to analysis and the injection volume was 10 μL. The chromatographic profiles were extracted at the optimised wavelength of 280 nm. Agrimoniin and ellagic acid peaks were identified by comparison with commercially purchased standards and quantification was performed based on standard curves. Agrimoniin was purchased from Wuhan ChemNorm Biotech (Product no. TBW01481) and ellagic acid was purchased from Merck (Product no. 14668).

3.5.8 RNA-seq and gene set enrichment analysis (GSEA)

Triplicate *A. baumannii* AB5075 cells were grown in 20 ml LB to mid-exponential phase (OD_{600} 0.6) in either the presence of 50 μM of agrimoniin, 2.3 μM of ellagic acid, 0.05 mg/mL of Wicklow tormentil root extract or DMSO. The RNA was then isolated using the RNAeasy Kit with in-column DNAase digestion (Qiagen). The RNA integrity of each sample was determined using a Bioanalyzer (Agilent 2100 Bioanalyzer and Agilent RNA 6000 Nano Kit), according to the amplitude and sharpness of the peaks corresponding to the 23S and 16S rRNAs. Sequencing and downstream analyses were performed at the Microbial Genome Sequencing Centre (Pittsburgh, Pennsylvania, U.S.A), using an Illumina MiSeq, with 12 million reads per sample. Quality control and adapter trimming was performed with bclfastq. Read mapping was performed with HISAT. Differential expression analysis was performed using edgeR's exact test for differences between two groups of negative-binomial counts with an estimated dispersion value of 0.1, using the *A. baumannii* AB5075-UW genome annotation as a reference (Gallagher *et al*., 2015). The volcano plot was generated using R, by plotting the log fold change on the x axis and p-value on the y-axis. 414, 636 and 517 genes were differentially expressed in agrimoniin, ellagic acid and Wicklow tormentil root extract respectively, based on a log fold

change ≥ 1 and p-value <0.05 (adjusted p-value). Peak profiles were used in order to determine RNA integrity. A Gene Set Enrichment Analysis (GSEA) was performed using FUNAGE-Pro with the default parameters (de Jong *et al*., 2022).

3.5.9 Iron supplementation assay

A. baumannii AB5075 overnight cultures were diluted in LB to an OD_{600} of 0.1. Treatments were set up in a 96-well plate and consisted of 50 µM of agrimoniin, 2.3 µM of ellagic acid, 0.05 mg/mL of Wicklow tormentil root extract or DMSO. The media was supplemented with FeCl3 or FeCl2 to achieve a final concentration of 100 µM. The plate was then incubated at 37 °C, 200 rpm, in a Clariostar Plus plate reader (BMG LabTech), where an OD_{600} reading was taken every 10 minutes for 12 hours. The results represent the average of three technical replicates and three biological replicates ± SD.

3.5.10 Statistics and Reproducibility

All assays were carried out in biological triplicate (n=3), with three technical repeats, individual data points are included in each graph. Analysis consisted of ANOVA tests comparing the treated samples with the respective carrier control. Average values ± S. D. are represented. Significance is indicated as ns = non-significant, * = p ≤0.05, ** = p ≤0.01, *** = p ≤0.001, **** = p ≤0.0001. Statistical analyses were performed using GraphPad Prism v10.0.3. For normally distributed data, parametric tests (one-way and two-way ANOVA) were applied. Post-hoc analyses included Šídák's multiple comparisons test and Tukey's multiple comparisons test to adjust for multiple comparisons.

Chapter 4

Evolution of Colistin Resistant Mutants

4.1 Introduction

Mutations which mediate colistin resistance have been shown to affect bacterial functions that are associated with the fitness of the pathogen (Da Silva and Domingues, 2017). Understanding the interplay between the evolution of resistance to colistin and the bacteria's fitness cost plays a key role in assessing the spread and virulence of the pathogen. In the context of this study, the fitness of the bacteria is defined by its ability to grow under specific conditions compared to the wild-type (WT) strain. Additionally, we define virulence as the bacteria's ability to infect and cause death within the host.

4.1.1 Fitness Trade-offs associated with *pmrABC* Modifications

Although *A. baumannii* possesses a wide variety of mechanisms that contribute to colistin resistance (Figure 4.1), mutations in membrane components often are accompanied by fitness tradeoffs.

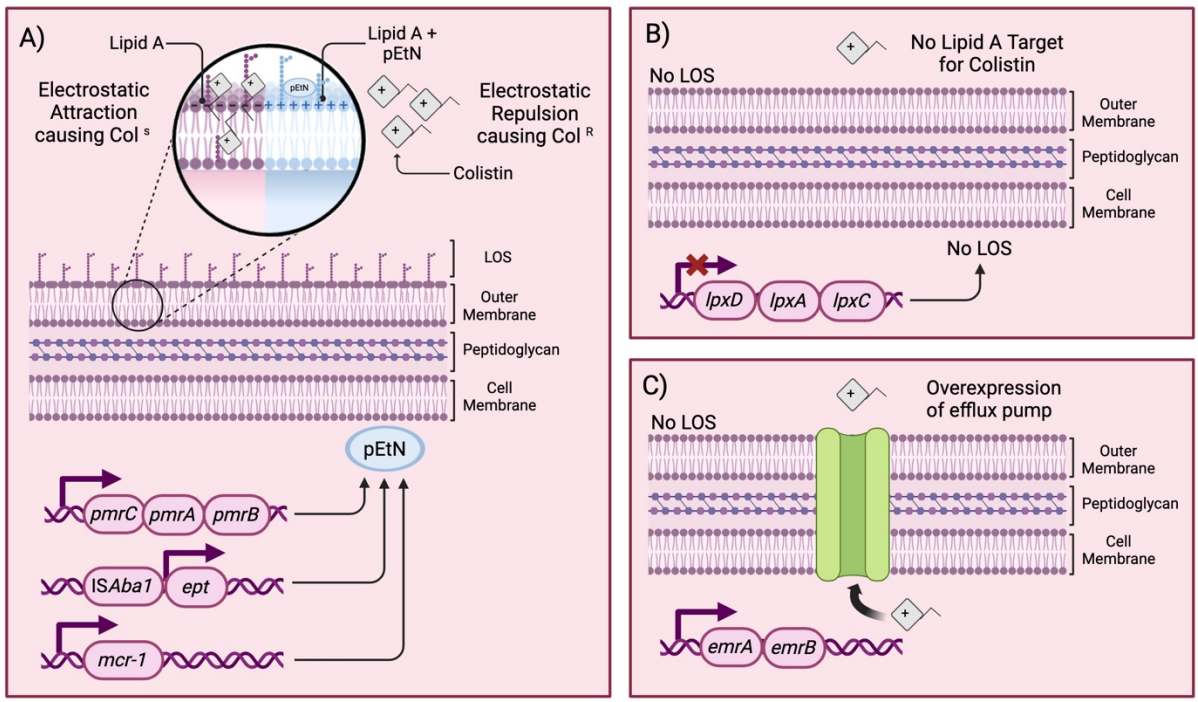

Figure 4.1. Main mechanisms that mediate colistin resistance in *A. baumannii*. A) Addition of phosphoethanolamine to lipid A, changing the overall net charger to positive and thus causing resistance to colistin. B) Complete loss of lipid A on the outer membrane, resulting in the loss of binding targets for colistin. C) Efflux of colistin from the cell due to the upregulation of efflux pump genes.

Mutations in the PmrAB system confer a lower affinity for colistin as they lead to an upregulation of pmrC. This results in the addition of positively charged phosphoethanolamine to lipid A in the outer membrane, thereby altering its net charge to positive and causing resistance against the cationic antibiotic colistin. However, these mutations ultimately prove to be maladaptive. In a clinical setting, the gain of resistance in *A. baumannii* isolates often occurs during the colistin treatment (Rolain *et al*., 2011; Hraiech *et al*., 2013; Snitkin *et al*., 2013; Pournaras *et al*., 2014). In a study conducted by Rolain *et al* (2013), paired clinical isolates recovered from the same patient at different time points of treatment were described as having varied clinical outcomes due to their differences in virulence. The first recovered *A. baumannii* colistin susceptible strain demonstrated a higher virulence than the second recovered colistin resistant strain, designated ABCR, as shown by the loss of clinical symptoms of infection in a rat model (Hraiech *et al*., 2013) and human patient (Rolain *et al*., 2011). In another report, an

A. baumannii resistant strain, designated CR17, demonstrated a decrease in virulence and

fitness compared to the susceptible strain, designated CS01 (López-Rojas *et al*., 2011). Both strains were later found to possess *pmrA* mutations which were associated with their resistance to colistin. The ABCR strain contained a *pmrA* E8D mutation and the *A. baumannii* CR17 strain had a *pmrA* M12L mutation (López-Rojas *et al*., 2013; Rolain *et al*., 2013).

Similarly, clinical isolates Ab249 and Ab347 developed resistance to colistin following treatment with the antibiotic, within the host. Upon analysis, it was determined that the two strains contain *pmrB* P233S and P170L mutations, respectively. A decreased *in vivo* and *in vitro* virulence and a reduced *in vitro* fitness were shown by both strains (Pournaras *et al*., 2014). Another study showed that mutations R134C and A227V in *pmrB* demonstrate a greatly diminished *in vivo* virulence and fitness compared to the wild-type strain (López-Rojas *et al*., 2011). In all aforementioned clinical cases, mutations in *pmrAB* mediating colistin resistance resulted in a decrease in fitness and virulence compared to the susceptible counterpart strains within clinical isolates of colistin resistant *A. baumannii*.

This decrease in fitness and virulence is seen conserved in colistin resistant *A. baumannii* mutants that have evolved resistance in the lab through continuous exposure to colistin in both agar plates and liquid media. These included previously reported mutations in *lpxCAD* and *pmrAB*, along with four novel putative colistin resistance genes (*A1S_1983, hepA, A1S_3026*, and *rsfS*). Of which the A1S 1983 membrane protein has been predicted to influence the integrity of the membrane which may lead to colistin resistance. HepA, A1S 3026 and RsfS are involved in biofilm formation and bacterial adaption, indicating a novel colistin resistance mechanism (Mu *et al*., 2016). The underlying mechanism mediating colistin resistance in these mutants is yet to be uncovered however, it could be related to the impact on biofilm formation influenced by these genes.

Mu *et al*. (2016) found fitness implications in *lpxCAD* mutants, with LOS-deficient mutants exhibiting higher fitness costs than *pmrB* mutants in a nutrient-rich medium. In a separate study, colistin-resistant *A. baumannii* strains with *pmrB* mutations (R134C and A227V) showed lower *in vivo* fitness and decreased virulence compared to colistin-sensitive strains, as demonstrated in a mouse model of peritoneal sepsis (López-Rojas *et al*., 2011). Additionally, mutations in the *pmrAB* gene, such as the A353T substitution in PmrB, were

associated with impaired fitness and virulence in colistin-resistant *A. baumannii* strains (López-Rojas *et al*., 2013). Further investigations revealed that colistin-resistant strains with *pmrB* mutations exhibited a diminished ability to affect the viability of alveolar cells and impaired virulence in animal models. Notably, a number of studies have found that the acquisition of colistin resistance through different mechanisms has been shown to significantly impact virulence and fitness, with LPS loss resulting in a greater biological cost compared to *pmrB* mutation (Moffatt *et al*., 2010; Mu *et al*., 2016). Kamoshida *et al*., 2022 found that this higher biological cost faced by LPS-deficient strains suggests that *pmrAB* mutants are more likely to be isolated in clinical settings.

The conventional belief that the evolution of colistin resistance incurs a fitness and virulence cost to bacteria may not universally hold true. A previous study found that in an immunocompromised patient, an XDR *A. baumannii* strain, which was initially susceptible to colistin and tigecycline, later developed resistance to colistin without any significant reduction in its fitness, growth characteristics, or virulence compared to colistin-sensitive strains. Additionally, the study observed that the mutation conferring colistin resistance in PmrB (P233S), did not translate into an *in vitro* measurable reduction of growth capacity or virulence (Dunrante-Mangoni *et al*., 2015). Similarly, another study found that mutations in *pmrB* (duplication of amino acids Ser17 to Phe26 in strain W1 and T235I in strain UKA8), did not result in a loss of virulence or fitness in *A. baumannii*. These strains with *pmrB* mutations retained similar virulence levels to their respective parental strains, suggesting that the biological fitness cost after acquiring colistin resistance may not always be substantial (Wand *et al*., 2015).

These findings suggest a more intricate and strain-specific relationship between colistin resistance and fitness/virulence, acknowledging varied impacts observed in different bacterial strains. Therefore, the evolution of colistin resistance may not universally entail a fitness and virulence cost to bacteria, as it appears to be influenced by various genetic and environmental factors. Additionally, the scale at which these studies are conducted is limited to a small number of isolates used, as well as the diversity of isolates used between studies. This suggests that a more direct comparison and analysis of resistance-associated fitness costs is required

among a larger pool of genetically related strains. The insights obtained from these studies could significantly contribute to our efforts to control the emergence and evolution of colistin-resistant *A. baumannii* strains.

4.2 Aim of the study

The aim of this study is to explore the effects of evolved colistin resistance on fitness and virulence.

- We will generate a library of colistin-resistant mutants and evaluate the impact on fitness in the presence and absence of colistin.
- Additionally, we will conduct *in vivo* testing for all evolved colistin-resistant mutants to address the discrepancies between *in vitro* and *in vivo* results observed in prior studies.
- We will then explore the genomes of a selection of CRMs, which will all have varying MICs to reveal genetic mutations responsible for colistin resistance, allowing for a direct comparison of the mechanisms/mutations to the MIC and fitness-associated phenotypes of the CRMs.
- Finally, we will characterise the colistin-mediating mutations within these CRMs, allowing for speculation of how resistance is conferred.

4.3 Results

4.3.1 Strategies to develop colistin resistant mutations (CRM) and confirmation

In order to evolve colistin-resistant *A. baumannii* mutants, three different strategies were tested to identify the most efficient one, these strategies are displayed below in Figure 4.2. The first method, colistin agar plates, consisted of AB5075 WT being spread on LB agar, with a consistent concentration of colistin (2.5 μg/mL) present throughout the agar. This concentration was chosen as it is above the MIC of colistin (EUCAST., 2016), indicating that anything growing in the presence of colistin at this concentration is resistant to colistin. Using this method, no mutants were obtained; this could be due to the sudden introduction of colistin to the bacteria. To overcome this issue, a method using liquid cultures was employed (Mu *et al*., 2016). This method allows for a gradual introduction of colistin to the bacteria as the concentration starts low at a sub-MIC level (1 μg/mL) and increases 2-fold every 24 hours. Two mutants were evolved using this method however, the rate of evolving CRMs using this method was slow as only two CRMs were evolved in the time period of one week. Due to the low production rate of CRMs when using liquid cultures, another method was employed comprising aspects from both colistin agar plates and the liquid culture methods. This colistin agar tilt plates method, uses the gradual introduction and increase of colistin concentration, from the liquid culture method, alongside the faster assay time from the colistin agar plate method (Liu *et al*., 2011; Carsenti-Etesse *et al*., 1999). Forty-eight *A. baumannii* CRM's were evolved using this colistin agar tilt plate method. Overall, the most efficient method in evolving CRMs is colistin agar tilt plates.

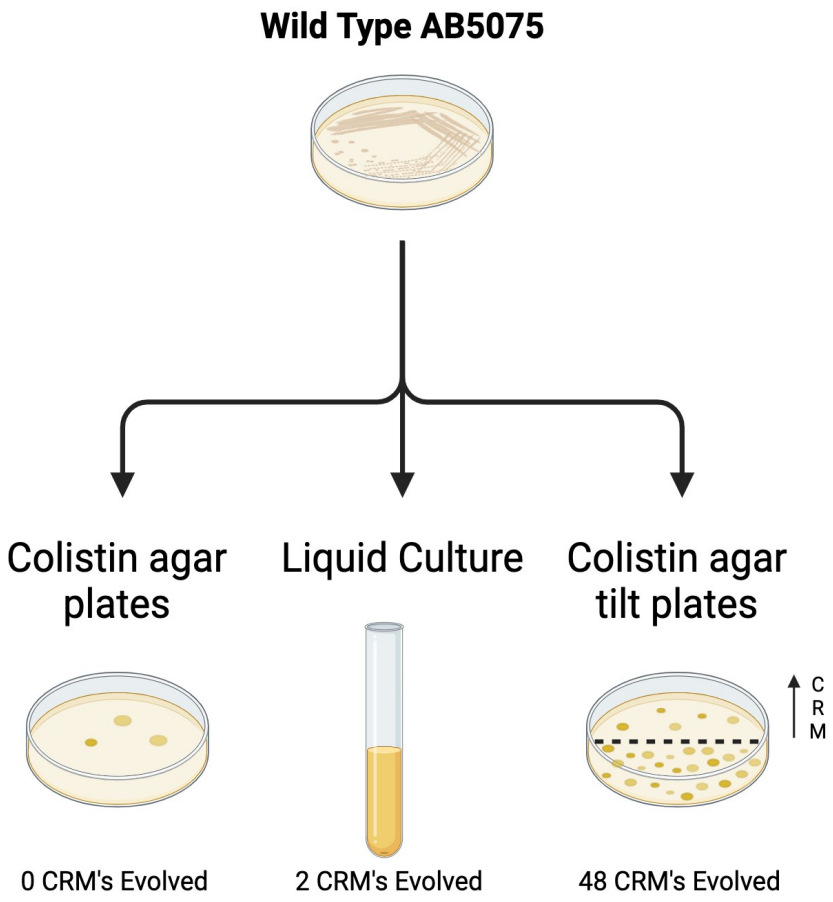

Figure 4.2: A diagram illustrating the number of CRMs produced using three evolution methods. The arrow next to the colistin agar tilt plate indicates that any colony grown above this uniform line was to be considered a CRM in this study. 0 CRMs were evolved using the colistin agar plates method, 2 CRMs were evolved using the liquid cultures method and 48 CRMs were evolved using the colistin agar tilt plates method.

Next, we wanted to verify that each of the evolved mutants was in fact *A. baumannii*, prior to use in further experiments. Primers targeting the gene ABUW 2824, which encodes for a conserved hypothetical protein with 100% homogeneity in *A. baumannii* were used to confirm that the colistin-resistant colonies evolved were derived from *A. baumannii* AB5075. These primers were chosen and designed to minimise the likelihood of amplifying non-target DNA. Figure 4.3 shows the gel electrophoresis assays confirming that all 50 CRMs used within this study were derived from *A. baumannii* and were not contaminants. All 50 CRMS and the parental AB5075 DNA produced a band of the expected size (1250 bp) indicating that the primers successfully amplified the *A. baumannii* ABUW 2824 DNA present in these samples. The negative controls containing *P. aeruginosa* (PA14) and no template controls

(NTC) produced no bands, showing that only the samples containing AB5075 DNA were amplified and that there was no contamination in the PCR master mix.

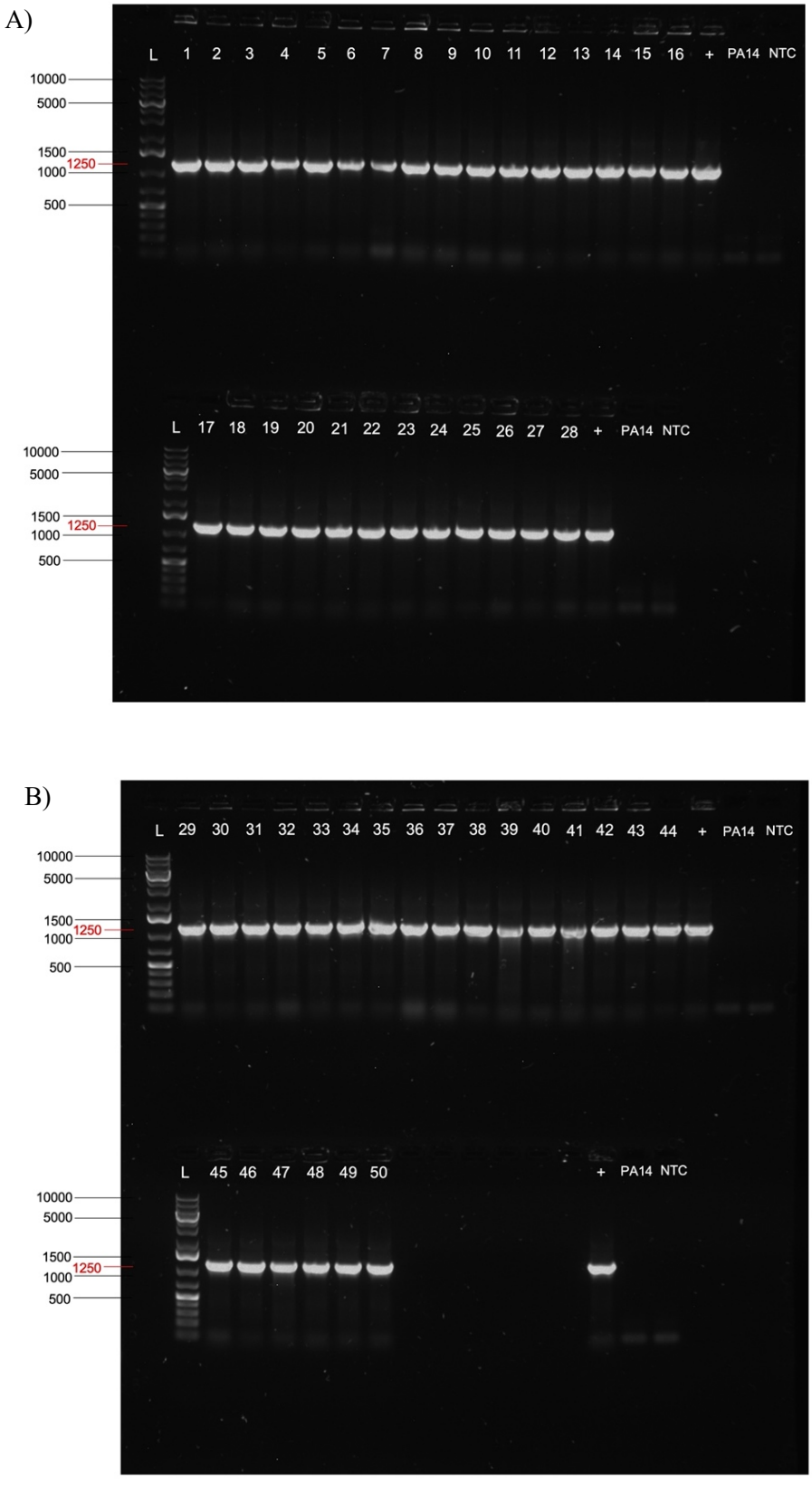

Figure 4.3: Gel electrophoresis images from the colony PCRs confirming the species of all 50 CRMs. (A) and **(B)** show the gel electrophoresis results that contain (from left to right) a DNA hyperladder (L), AB5075 CRMs (CRM X) amplified DNA products, AB5075 (+) amplified DNA products, PA14 (-) amplified DNA products and the no template control (NTC). The image was produced using a BioRad Bio-Imagers Gel-Doc system UV transilluminator (BioRad) and ImageLab software at an exposure time of 0.05 seconds. The positive control showed the expected band size of 1250 bp in length, which was used as a comparator for the other bands. The results also show that all 50 CRMs show the expected band size of 1250 bp, which matches the band seen in the positive control. These bands (labelled with the CRM number) confirm that the samples contain *A. baumannii* DNA. The negative controls containing PA14 and the NTC controls produced no bands, showing that the primers were specific to AB5075 DNA and that there was no contamination in the PCR master mix. All assays were carried out in biological triplicate (n=3).

4.3.2 Colistin Minimum Inhibitory Concentration (MIC) of CRMs and AB5075 parent strain

Minimum Inhibitory Concentration (MIC) is defined as the lowest concentration of an antimicrobial agent that inhibits the growth of an organism. Guidelines for the standard MIC breakpoint of colistin were interpreted according to the European Committee on Antimicrobial Susceptibility Testing (EUCAST). For *A. baumannii* they are described as follows: < 2 μg/mL for colistin susceptible isolates and > 2 μg/mL for colistin resistant isolates (EUCAST, 2017). Using these guidelines, we next evaluated the colistin MIC of AB5075 WT and the CRMs to determine how susceptible the strains are to colistin.

The colistin MIC of the AB5075 WT strain was demonstrated to be 2 μg/ml in this study (Appendix C.1). Any CRM in this study shown to have a higher colistin MIC than 2 μg/ml was therefore considered resistant. All tested CRMs were shown to be resistant to colistin with a MIC breakpoint of 8 μg/ml or higher. From the results (Table 4.1), CRM 9 was identified as the most resistant strain as it has the highest MIC breakpoint of 1024 μg/ml. The CRMs that were evolved in liquid culture did not demonstrate a notable difference from the CRMs evolved in tilt plates; however, a larger pool of liquid culture-derived CRMs would need to be evolved in

order to make a significant comparison.

Table 4.1. Colistin MIC break points for each CRM. The table shows the minimum inhibitory concentration at which the visible growth of each individual CRM is inhibited. The method by which the bacteria was evolved is also listed below. The wild-type was included as a control and comparator strain. All tested CRMs demonstrate a higher MIC than the AB5075 WT strain. All assays were carried out in biological triplicate and the average is shown below.

CRM Isolate Number	MIC Breakpoint (µg/ml)	Media Grown/ Evolved In
A. baumannii AB5075 WT	2.00	Tilt Plate
1	8	Tilt Plate
2	32	Liquid Culture
3	16	Liquid Culture
4	8	Tilt Plate
5	512	Tilt Plate
6	16	Tilt Plate
7	16	Tilt Plate
8	16	Tilt Plate
9	1024	Tilt Plate
10	16	Tilt Plate
11	16	Tilt Plate
12	16	Tilt Plate
13	64	Tilt Plate
14	64	Tilt Plate
15	32	Tilt Plate
16	32	Tilt Plate
17	16	Tilt Plate
18	64	Tilt Plate
19	8	Tilt Plate
20	16	Tilt Plate
21	64	Tilt Plate
22	64	Tilt Plate
23	64	Tilt Plate
24	32	Tilt Plate
25	32	Tilt Plate

CRM Isolate Number	MIC Breakpoint (µg/ml)	Media Grown/ Evolved In
26	32	Tilt Plate
27	32	Tilt Plate
28	64	Tilt Plate
29	32	Tilt Plate
30	32	Tilt Plate
31	32	Tilt Plate
32	32	Tilt Plate
33	32	Tilt Plate
34	256	Tilt Plate
35	32	Tilt Plate
36	512	Tilt Plate
37	64	Tilt Plate
38	256	Tilt Plate
39	256	Tilt Plate
40	64	Tilt Plate
41	256	Tilt Plate
42	64	Tilt Plate
43	256	Tilt Plate
44	32	Tilt Plate
45	16	Tilt Plate
46	8	Tilt Plate
47	256	Tilt Plate
48	256	Tilt Plate
49	256	Tilt Plate
50	128	Tilt Plate

4.3.3 Level of colistin resistance affects how much bacterial fitness is compromised

The fitness of *A. baumannii* has been previously demonstrated to be impacted by the gain of colistin resistance in both laboratory-evolved strains and clinical isolates (López-Rojas *et al*., 2011; Pournaras *et al*., 2014). However, these studies have concluded this using a small pool of resistant bacteria and have not linked the level of resistance to the bacteria's fitness. For these reasons, we set out to determine if the level of resistance in our larger pool of 50 CRMs, correlated with an impact on growth both in the presence and absence of colistin. Testing the impact on growth in the absence of colistin allows for comparison to the colistin-sensitive wild-type strain, facilitating the identification of fitness trade-offs due to evolved resistance when colistin is not present. The results indicate that the CRMs with high MICs (> 120 μg/mL) have a higher growth rate at 24 hrs in the presence of colistin in comparison to the CRMs with lower MICs (< 70 μg/mL). This suggests that the higher the MIC, the less impact on the bacteria's growth (Figure 4.4B and Appendix C.2). In the absence of colistin, all of the CRMs display a similar (16% of the CRMS) or slower (84% of the CRMS) growth rate at 24 hours compared to the wild-type (Figure 4.4A and Appendix C.2). CRMs with a similar growth phenotype were determined by the growth of +/– 0.1 OD_{600} from the AB5075 wild-type growth reading. These findings support previous literature which states that evolving antibiotic resistance in a bacterium affects the rate at which bacteria can grow in the absence of antimicrobials (Martinez, 2016). Additionally, a high level of resistance impacts growth similarly to a low level of resistance in the absence of colistin (Figure 4.4A and Appendix C.2), suggesting that the level of resistance is not the only determining factor on the impact on the bacteria's growth in the absence of colistin.

Throughout this study, we also focused on comparing four CRMs, each characterised by distinct MICs, in order to investigate the relationship between the level of resistance and specific phenotypic traits. Moreover, analysing a range of resistance phenotypes within the CRMs, allows us to gain insights into the genetic diversity and adaptability of *A. baumannii* in response to colistin exposure. The selected CRMs for this comparison were CRM 1, 5, 9, and

38 with MIC's of 8, 512, 1024, and 256 μg/ml, respectively.

Interestingly, in the presence of colistin CRM 5 and 9 have an exponential growth rate up until 11 hours, which is then followed by a plateau in growth, which only CRM 9 overcomes at hour 16 and continues its growth (Figure 4.4B). This suggests that these CRMs reach the stationary phase faster than the other CRMs, indicating that the mechanism mediating colistin resistance in these CRMs may impact the bacteria's fitness in the later stages of growth. In comparison, CRM 1 and 38 appear to have a longer lag phase which is then followed by an exponential growth rate at 11 and 10 hours, respectively. This indicates a negative fitness effect of the bacteria at earlier stages of growth, compared to CRM 5 and 9 (Figure 4.4B). However, this requires further exploration to confirm whether the prolonged lag phase is independent of the growth phase at the time of subculturing.

In the absence of colistin, CRM 1 still possess a decreased growth rate in comparison to the other CRMs. However, the stationary phase is reached at the same time as the AB5075 wild type indicating that there is no delayed growth as a mechanism but rather a stunted growth. This suggests that the ability for CRM 1 to grow in the absence of colistin may be reduced due to the mechanism mediating colistin resistance. The growth of the other CRMs follows the growth of the wild type but CRM 9 and 38 have a slightly reduced initial growth rate. This indicates that in the absence of colistin, these CRMs return to their original wild-type growth phenotype.

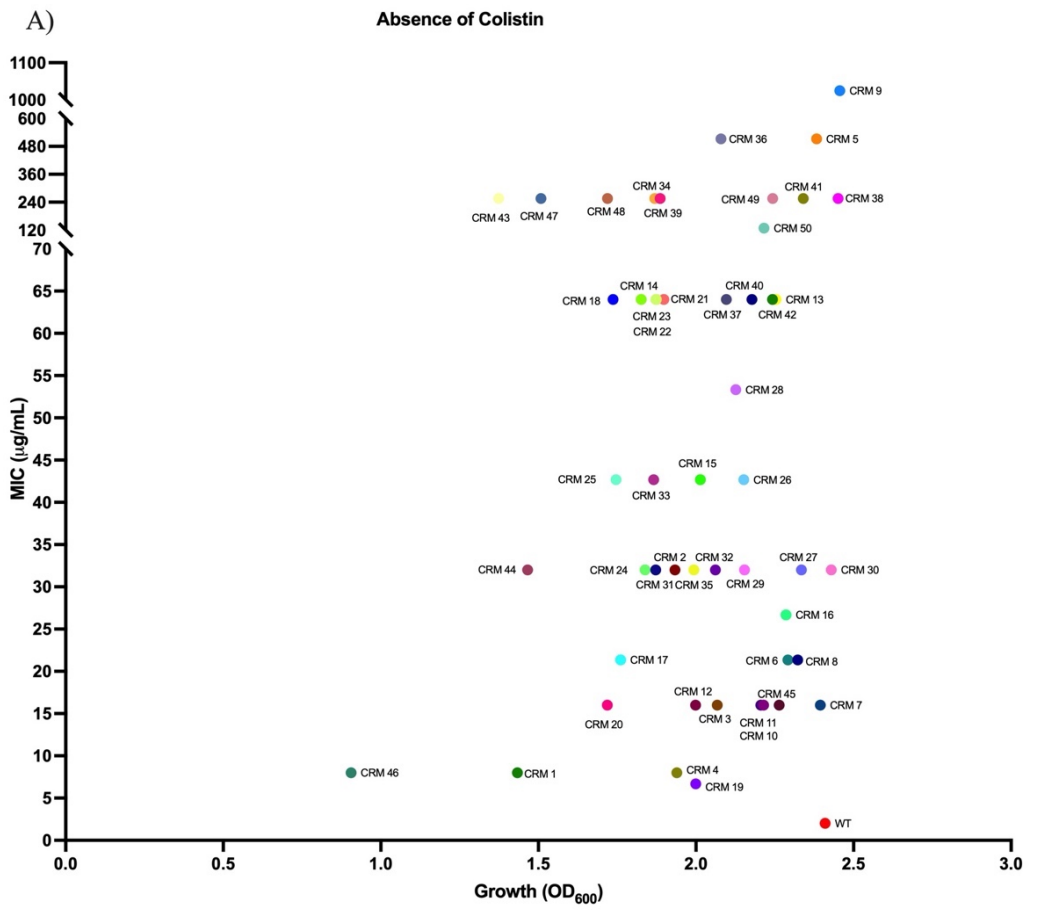
A)
Absence of Colistin
MIC (μg/mL)
Growth (OD600)
CRM 9
CRM 36
CRM 5
CRM 34
CRM 41
CRM 43
CRM 47
CRM 48
CRM 39
CRM 49
CRM 38
CRM 50
CRM 14
CRM 40
CRM 18
CRM 21
CRM 13
CRM 23
CRM 37
CRM 42
CRM 22
CRM 28
CRM 15
CRM 25
CRM 26
CRM 33
CRM 44
CRM 24
CRM 2
CRM 32
CRM 27
CRM 30
CRM 31
CRM 35
CRM 29
CRM 16
CRM 17
CRM 6
CRM 8
CRM 12
CRM 45
CRM 7
CRM 20
CRM 3
CRM 11
CRM 10
CRM 46
CRM 1
CRM 4
CRM 19
WT

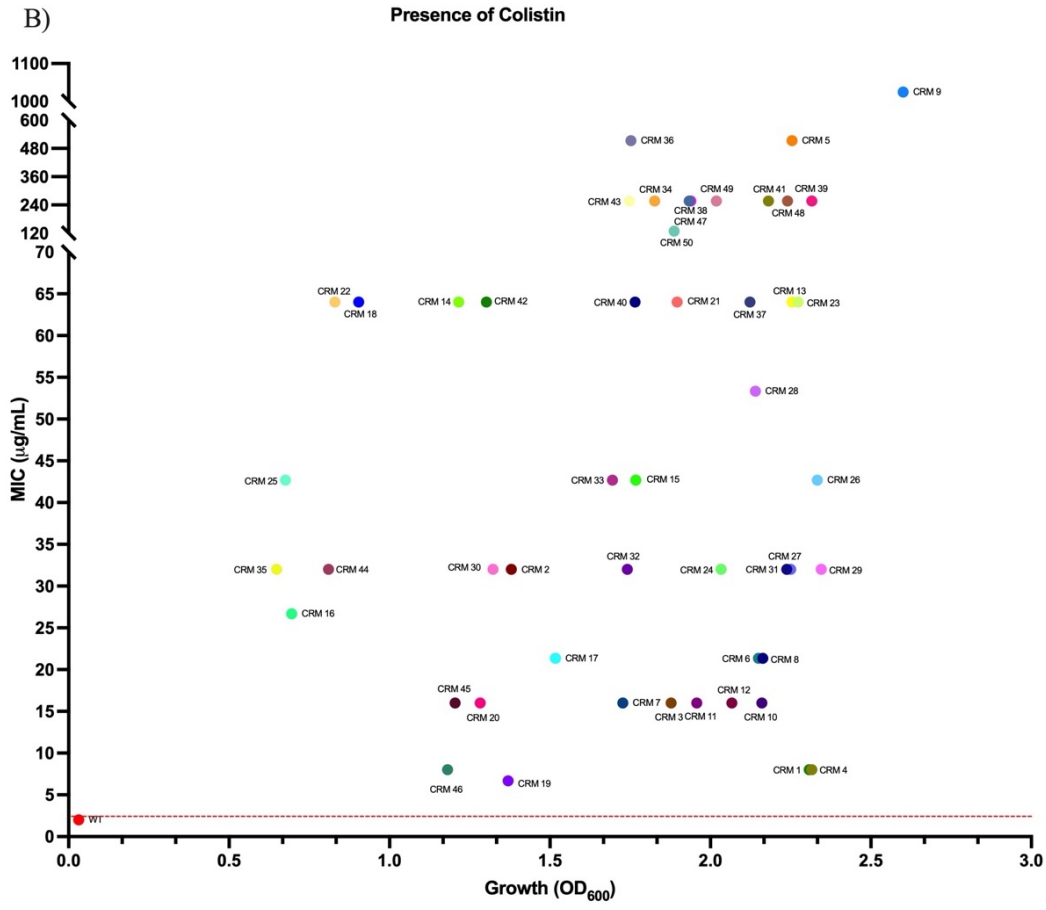
B)
Presence of Colistin
MIC (μg/mL)
Growth (OD600)
CRM 9
CRM 36
CRM 5
CRM 34
CRM 49
CRM 41
CRM 39
CRM 43
CRM 38
CRM 48
CRM 47
CRM 50
CRM 22
CRM 18
CRM 14
CRM 42
CRM 40
CRM 21
CRM 13
CRM 37
CRM 23
CRM 28
CRM 25
CRM 33
CRM 15
CRM 26
CRM 35
CRM 44
CRM 30
CRM 2
CRM 32
CRM 24
CRM 27
CRM 31
CRM 29
CRM 16
CRM 17
CRM 6
CRM 8
CRM 45
CRM 12
CRM 7
CRM 20
CRM 3
CRM 11
CRM 10
CRM 46
CRM 19
CRM 1
CRM 4
WT

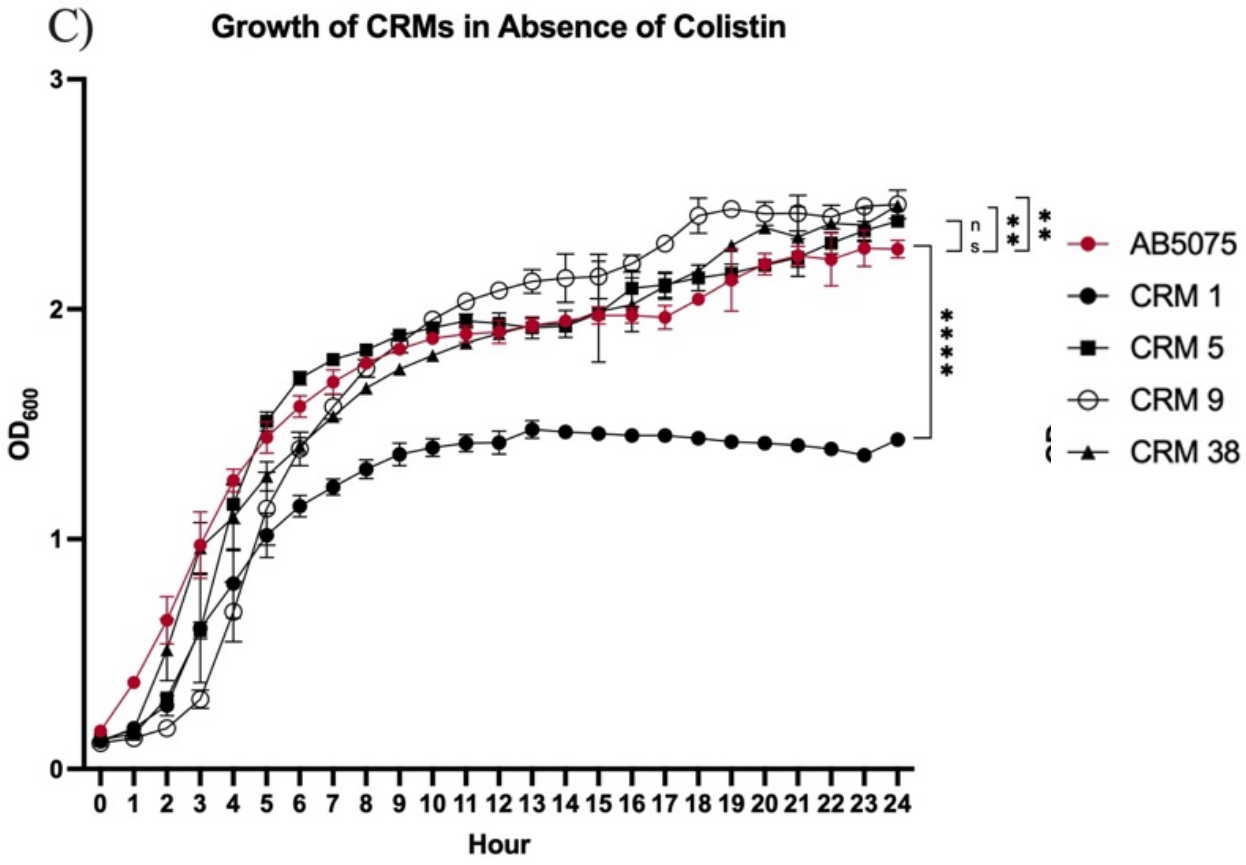
C)
Growth of CRMs in Absence of Colistin
OD600
Hour
AB5075
CRM 1
CRM 5
CRM 9
CRM 38
ns
****

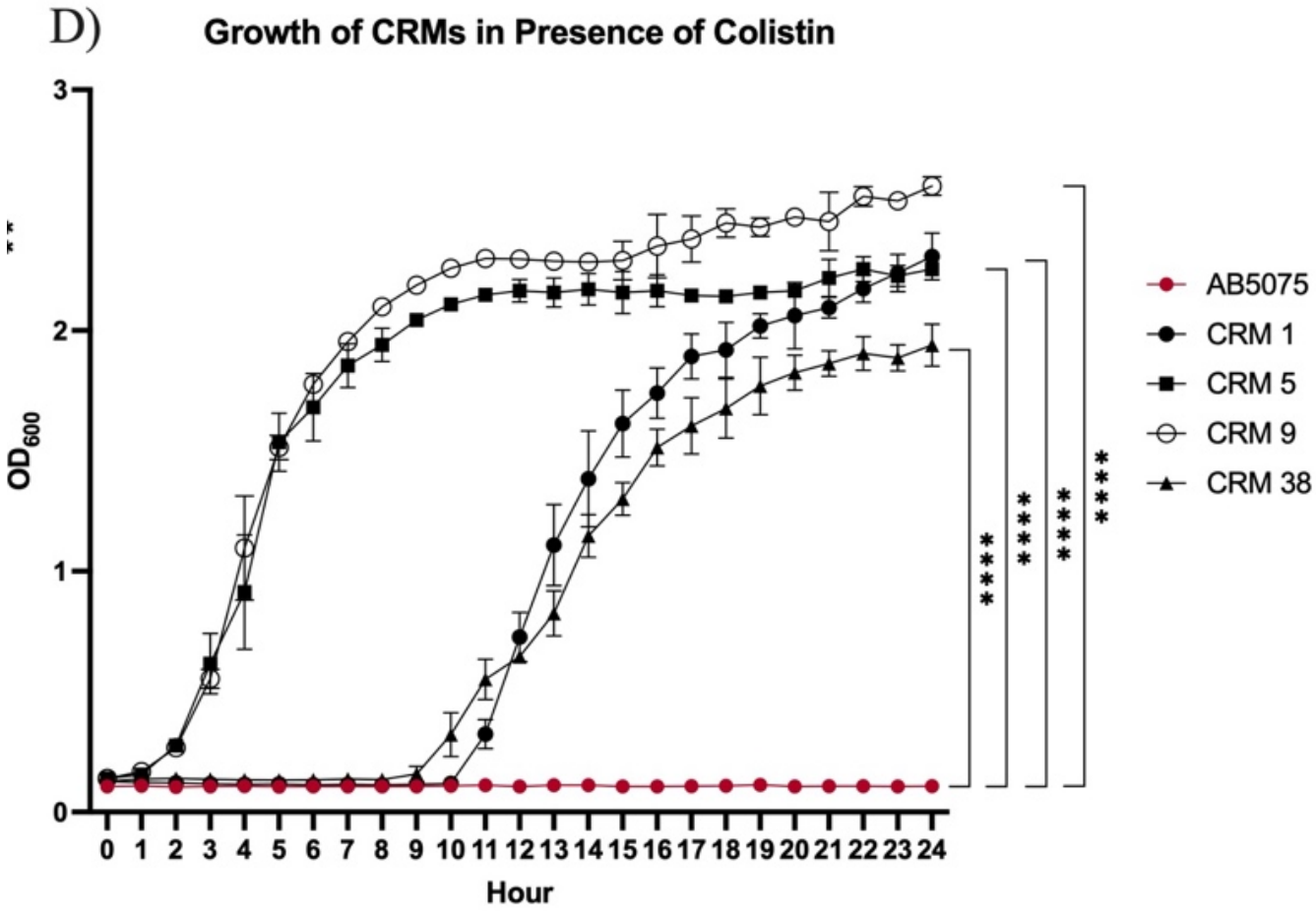
D)
Growth of CRMs in Presence of Colistin
OD600
Hour
AB5075
CRM 1
CRM 5
CRM 9
CRM 38
****

Figure 4.4. Fitness of laboratory-evolved CRMs in the presence and absence of the MIC of colistin. (A) MIC and growth in the absence of colistin comparison. **(B)** MIC and growth in the presence of colistin comparison. The CRM data points above the red dotted line are considered resistant to colistin as they have an MIC of > 2 μg/mL. CRMs with a high MIC impact growth similarly to a low level of resistance in the absence of colistin but gaining resistance does generally impact growth compared to the AB5075 wild-type. CRMs with high MICs (> 120 μg/mL) have less impact on the growth rate of the bacteria in the presence of colistin, in comparison to the CRMs with low MICs (< 70 μg/mL). **(C)** Growth curves of the CRMs in the absence of colistin. **(D)** Growth curves of the CRMs in the presence of colistin (2 μg/mL). All assays were carried out in biological triplicate (n=3), with three technical repeats. Statistical analysis of panel **(C and D)** consisted of two-way ANOVA between the CRMs and AB5075 control. Average values ± S. D. are represented. Significance is indicated as * = p ≤0.05, ** = p ≤0.01, *** = p ≤0.001, **** = p ≤0.0001.

4.3.4 Conservation of biofilm-forming capabilities

In light of the challenges presented by biofilm-associated *A. baumannii* infections, our subsequent step was to explore the potential influence of colistin on the biofilm formation of our CRMs. Colistin has previously been reported to induce resistance through biofilm formation in *E. coli* (Park *et al*., 2021). Thus, understanding this relationship in our CRMs may advance our knowledge of how the development of resistance might alter phenotypes associated with antibiotic tolerance, such as biofilm formation. This investigation aimed to enhance our understanding of how resistant bacteria respond when exposed to antibiotics to which they exhibit resistance. This insight, in turn, could have implications for the treatment strategies employed in addressing bacterial infections of this nature.

Our findings indicate that 64% of the CRMs exhibited an increased biofilm formation in the presence of colistin, in contrast to the 12% that demonstrated higher biofilm formation in

its absence. The general dogma surrounding biofilm formation in resistant bacteria posits that, when exposed to antibiotics, bacteria fortify themselves by increasing their biofilm production, thereby creating a protective shield against the antibiotic's effects (Singh *et al*., 2017). Our results support this consensus, indicating that our CRMs, which are derived from the same parental strain, follow this pattern. This suggests that, upon exposure to antibiotics, these CRMs increase their biofilm production, as a strategy to tolerate the effects of antibiotics. Notably, 24% of these CRMs showed no significant difference in biofilm formation whether colistin was present or absent. This implies that the biofilm-forming capabilities of these CRMs remain unaffected by the presence of an antibiotic to which they have proven resistance. Our findings also show that 90% of CRMs have decreased biofilm formation in the absence of colistin suggesting that in the absence of selective pressure, the CRMs biofilm-forming capabilities are impacted.

Among the selected CRMs chosen for further testing, it was observed CRM 1, 5 and 9 displayed increased biofilm formation in the presence of colistin, while only CRM 38 exhibited lower biofilm production in its absence. Notably, CRM 5 and 9 exhibited the highest MICs at 512 and 1024 µg/mL, respectively, coupled with substantial increases in biofilm formation at 59% and 103.8%, respectively. This suggests a potential link between their mechanism of action against colistin and the notable rise in biofilm formation observed.

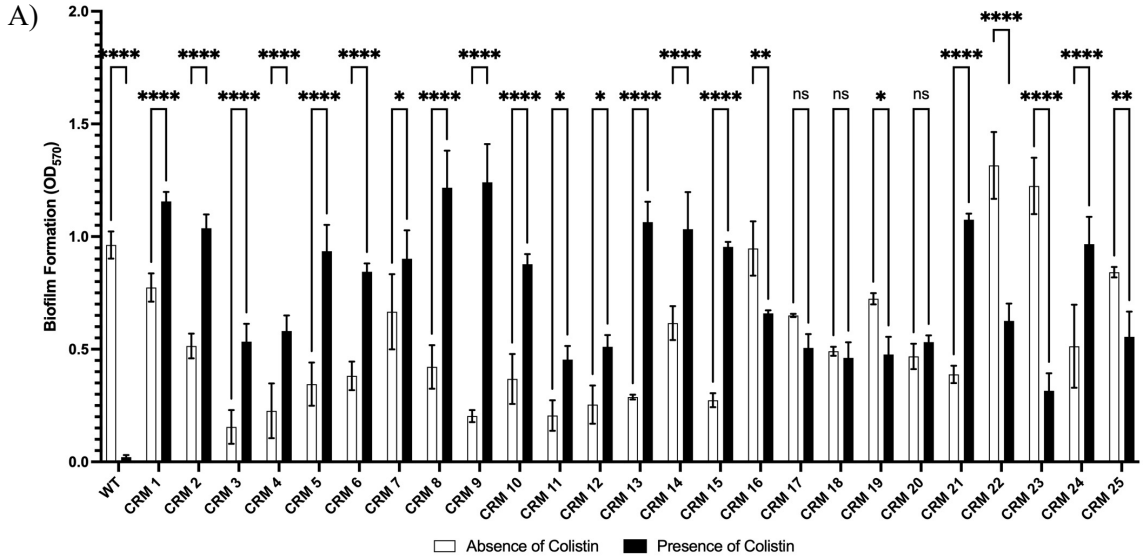
A)
Biofilm Formation (OD_{570})
2.0
1.5
1.0
0.5
0.0
WT
CRM 1
CRM 2
CRM 3
CRM 4
CRM 5
CRM 6
CRM 7
CRM 8
CRM 9
CRM 10
CRM 11
CRM 12
CRM 13
CRM 14
CRM 15
CRM 16
CRM 17
CRM 18
CRM 19
CRM 20
CRM 21
CRM 22
CRM 23
CRM 24
CRM 25
Absence of Colistin
Presence of Colistin

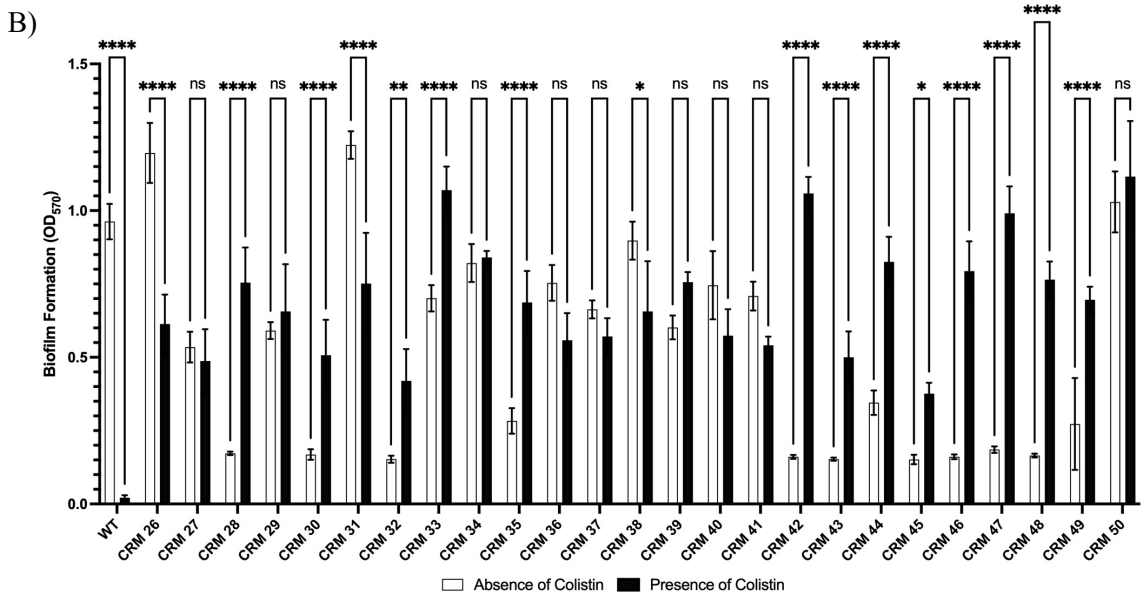
B)
Biofilm Formation (OD_{570})
1.5
1.0
0.5
0.0
WT
CRM 26
CRM 27
CRM 28
CRM 29
CRM 30
CRM 31
CRM 32
CRM 33
CRM 34
CRM 35
CRM 36
CRM 37
CRM 38
CRM 39
CRM 40
CRM 41
CRM 42
CRM 43
CRM 44
CRM 45
CRM 46
CRM 47
CRM 48
CRM 49
CRM 50
Absence of Colistin
Presence of Colistin

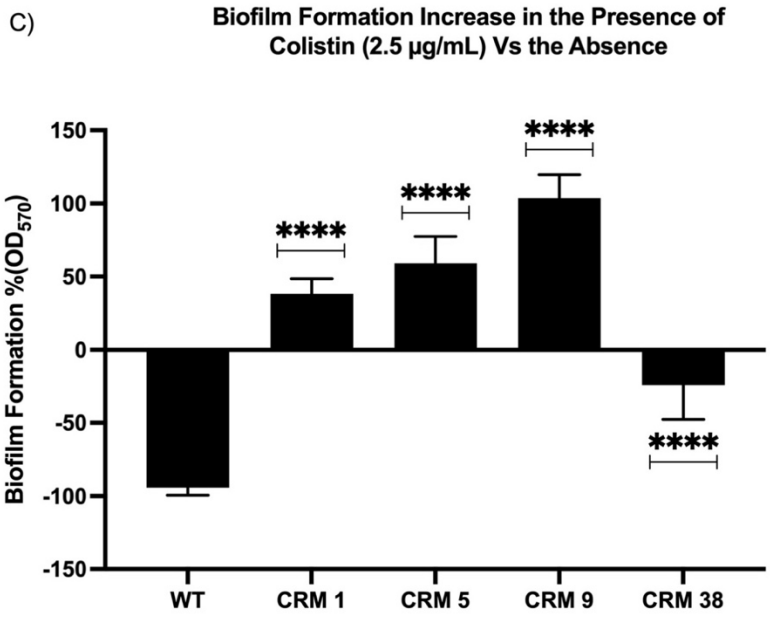
C)
Biofilm Formation Increase in the Presence of Colistin (2.5 µg/mL) Vs the Absence
Biofilm Formation %(OD_{570})
150
100
50
0
-50
-100
-150
WT
CRM 1
CRM 5
CRM 9
CRM 38

Figure 4.5. Biofilm formation of laboratory-evolved CRMs in the absence and presence of the MIC of colistin. (A) Biofilm formation of CRMs 1-25 in the absence and presence of the MIC of colistin (2.5 µg/mL). **(B)** Biofilm formation of CRMs 26-50 in the absence and presence of the MIC of colistin (2.5 µg/mL). 64% of the CRMs exhibited an increased biofilm formation in the presence of colistin. **(C)** Percentage increase of biofilm formation of CRM 1, 5, 9 and 38 in the presence of the MIC of colistin (2.5 µg/mL) from the biofilm formation in the absence of colistin. CRM 5 and 9 exhibited a higher formation of biofilm than CRM 1 and 38. All assays were carried out in biological triplicate (n=3), with three technical repeats. Statistical analysis consisted of two-way ANOVA between the CRMs and AB5075 control, with and without colistin as the second variable. Average values ± S. D. are represented. Significance is indicated as * = $p \leq 0.05$, ** = $p \leq 0.01$, *** = $p \leq 0.001$, **** = $p \leq 0.0001$.

4.3.5 Evaluating virulence as a cost of evolving colistin resistance

It is a well-established paradigm that evolving resistance correlates to a proportional decrease in the bacteria's virulence (López-Rojas *et al*., 2013; Hraiech *et al*., 2013; Rolain *et al*., 2011). To determine if this was the case for our 50 CRMs, we utilised the *Galleria mellonella* model of infection. These experiments were conducted in order to determine the impact that gaining resistance has on the virulence of the CRMs. Figure 4.6A shows that 84% of CRMs have a significantly lower virulence in *G. mellonella* than the AB5075 wild-type strain. This is demonstrated by the CRM-infected *G. mellonella* having a lower survival rate when compared to the AB5075-infected *G. mellonella*. In contrast, Figure 4.6B suggests that 16% of the CRMs have a similar virulence than the wild-type at 32 hours. This is shown by the similar or lower percentage of survival of the CRM-infected *G. mellonella* in comparison to the AB5075-infected *G. mellonella*. PBS was used as a negative control in this assay; a survival percentage of 100% was obtained for each of the three biological repeats. This indicates that there was no contamination in this assay and the method of injection was not a factor in the cause of death of *G. mellonella*.

As 84% of the CRMs displayed a lower virulence than the wild-type strain, it could be speculated that the mutation mediating colistin resistance in these CRMs reduces the bacteria's

virulence. These findings correlate with previous literature that has also demonstrated a decreased virulence in *A. baumannii* colistin-resistant strains (Geisinger and Isberg, 2017; Beceiro *et al*., 2014). In contrast, 16% of the CRMs displayed similar virulence than the wild-type strain but only after 32 hours, this could suggest that the mutation causing resistance to colistin may be increasing the virulence of the bacteria at a later phase of development. This may be attributed to compensatory mutations that occur alongside the resistance mutants, which ameliorated the costs of resistance or enhanced virulence (Mu *et al*., 2016; Andersson, 2003). CRM that have the same level of virulence in comparison to the wild-type strain at 32 hours are indicative of the mutation causing resistance to colistin having no impact on the bacteria's virulence.

CRM 1, 5 and 9 all had a lower virulence than AB5075 wild-type, suggesting that their mechanism of action, which mediates colistin resistance, affects the virulence of the bacteria. It is worth noting that the impact on virulence for CRM 1 could also be due to its slower growth rate in the absence of colistin (Figure 4.4C). In contrast, CRM 38 has the same level of virulence as the AB5075 wild-type strain at 32 hours. This matched the level of virulence to the wild-type strain is not however seen in the early hours, suggesting that compensation mutations may be activated upon later development, which allows for the mutant bacteria to regain its virulence at 32 hours (Figure 4.6C).

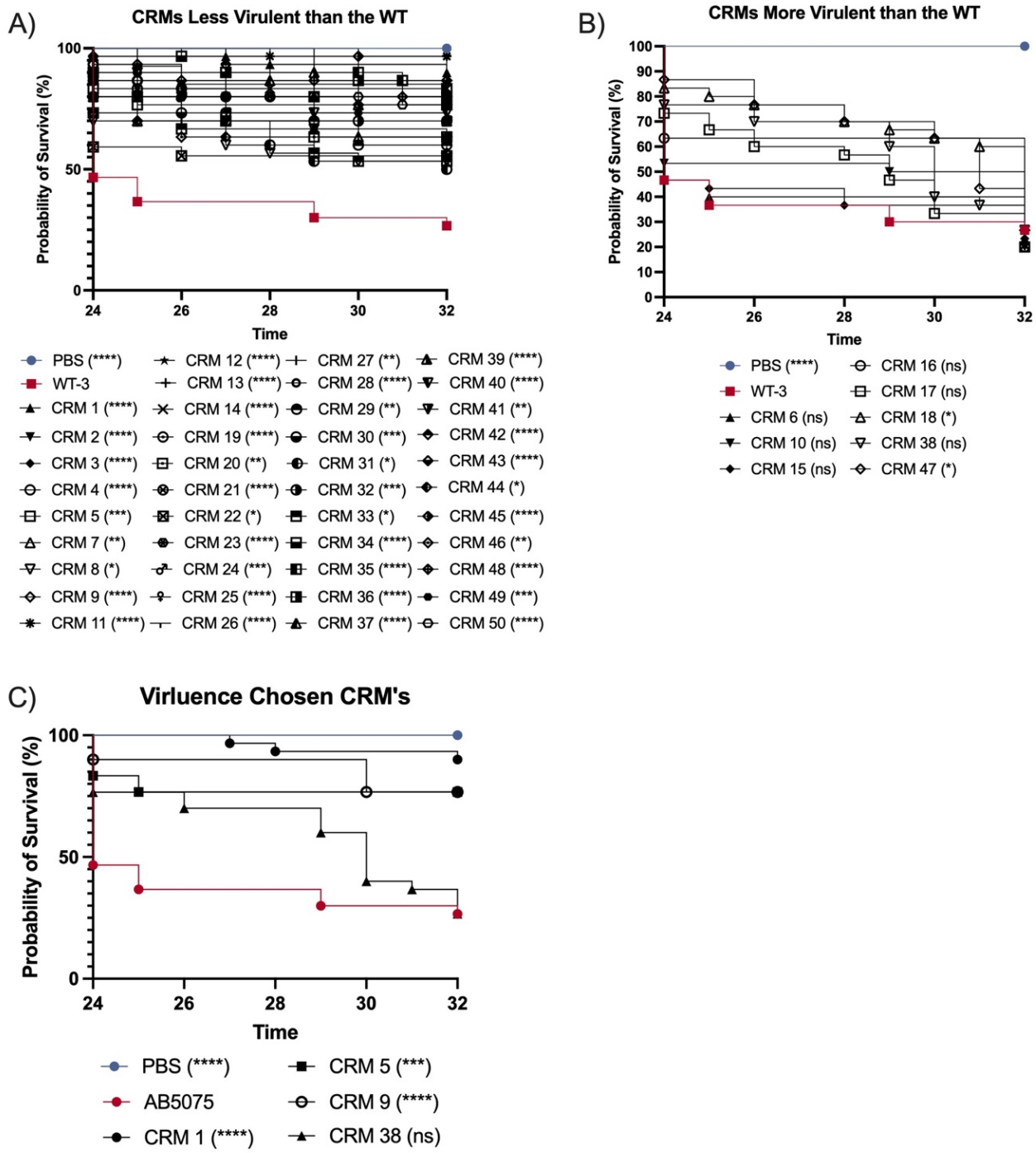

Figure 4.6. Virulence of CRMs compared against AB5075 wild-type strain. (A) CRMs that are less virulent than the wild-type strain. Of the 50 CRMs, 84% were found to have a lower virulence compared to the wild-type strain. **(B)** CRMs that are as virulent as the wild-type strain at 32 hours. Of the 50 CRMs, 16% were found to have a similar virulence compared to the wild-type strain. (C) Virulence of CRMs 1, 5, 9 and 38. Assays were carried out in biological triplicate per treatment group, with 30 *G. mellonella* used per group (N = 30). Analysis consisted of a Log-Rank (Mantel-Cox) test, where *A. baumannii* Vs CRM 6, 10, 15, 16, 17, 18,

38, 47 was not significant and *A. baumannii* Vs CRM 1-5, 7-9 11-14, 19-20, 22, 24-37, 39-46, 48-50 had a Log-Rank of $p < 0.001$.

4.3.6 Identifying novel colistin resistance mediating mutations

The selection of CRMs with diverse MICs was driven by the need to understand the genetic basis underlying variations in resistance levels. By focusing on CRMs with different MICs (such as CRM 1, 5, 9, and 38), we aimed to explore the specific genetic mutations that contribute to varying degrees of resistance. All four CRMs were evolved on different tilt plates to ensure that clonal mutants were not harvested. We hypothesised that different levels of colistin resistance may be due to distinct genetic alterations within the bacterial genomes. Therefore, exploring CRMs with diverse MIC profiles may allow us to pinpoint specific mutations or genetic mechanisms associated with higher or lower resistance levels.

We began by extracting their genomic DNA and sent the samples for sequencing. We then employed BreSeq to map the CRM reads to the reference genome of *A. baumannii* AB5075-UW and analysed the aligned sequences to identify mutations such as single nucleotide polymorphisms, insertions, and deletions. Table 4.2 reveals that CRM 1 and 38, as well as CRM 5 and 9, share mutations that may confer resistance to colistin. This suggests a potential common selective pressure and evolutionary pathway contributing to resistance in these specific mutants.

Specifically examining mutations associated with colistin resistance, CRMs 1, 5, 9 and 38 exhibit mutations in *pmrB*, a component of the PmrAB system. Mutations in *pmrB* are known to reduce *A. baumannii*'s affinity for colistin both within laboratory-evolved and clinical strains. The BreSeq data suggested that CRMs 1 and 38 possess the R263H mutation in the *pmrB* gene, a mutation well-documented in previously published literature for its association with colistin resistance in *A. baumannii* caused by the overexpression of *pmrC* (Lim *et al*., 2015; Choi *et al*., 2017; Cafiso *et al*., 2019). It can thus be inferred that this mutation is the likely cause of colistin resistance in CRM 1 and 38. Notably, the results also predict that CRMs 5 and 9 harbour, to the best of our knowledge, a novel 15 bp duplication mutation within the *pmrB* gene, a colistin resistance hotspot. This novel mutation, whilst not previously reported (Appendix C.6), likely

plays a role in colistin resistance. This discovery prompted further investigation into the potentially novel mechanism by which this mutation confers colistin resistance in these particular CRMs.

Additionally, CRM's 5 and 9 are shown to have different phenotypes (Figure 4.4 C and D, 4.5C, 4.6C) but appear to be similar on the genetic level (Table 4.2). This could be explained by post-transcriptional or post-translational modifications resulting in different phenotypes without causing genetic changes.

Table 4.2: Predicted mutations comparison table. This table is generated from the results of analysing the sequences from CRM 1, 5, 9 and 38. Rows represent specific mutations and columns represent different CRMs. Each column (e.g. 1) displays the frequency of the predicted mutations in that CRM.

Position (bp)	Mutation	Frequency in CRM (%)				Annotation	Gene	Description
		1	5	9	38			
806,640	G→A	100			100	R263H (CG T→CAT)	*pmrB* →	two-component system sensor kinase
806,667	(GGTGA CTCAGC TTTT)$_{1→2}$		100	100		coding (815/ 1335 nt)	*pmrB*→	two-component system sensor kinase
1,584,733	T→G	100			100	F506C (TTT →TGT)	*ABUW_1 591* →	hypothetical protein
1,963,510	IS*Aba1* (–) +9 bp		100	100		coding (40-4 8/633 nt)	*ABUW_1 959* →	hypothetical protein
3,118,303	C→T	100			100	E19E (GAG →GAA)	*hemA* ←	glutamyl-tRNA reductase
308,284	T→G				78.8	T460P (ACC →CCC)	*ABUW_0 289*	penicillin-binding protein 1A

Figure 4.7 illustrates the multiple sequence alignment of PmrB from the CRMs against the wild-type AB5075. Here, the novel duplication mutation present in PmrB of CRM 5 and 9 can be observed at the nucleotide level. The duplication consists of 15 nucleotides

(GGTGACTCAGCTTTT) and is shown to occur at position 816 within the *pmrB* gene sequence. Additionally, the substitution mutation present in PmrB of CRM 1 and 38 is also shown at the nucleotide level. This mutation consists of the nucleotide guanidine (G) being substituted for adenine (A) at position 788 within the *pmrB* gene sequence. Other than the described mutations, the *pmrB* gene sequences are 100% conserved.

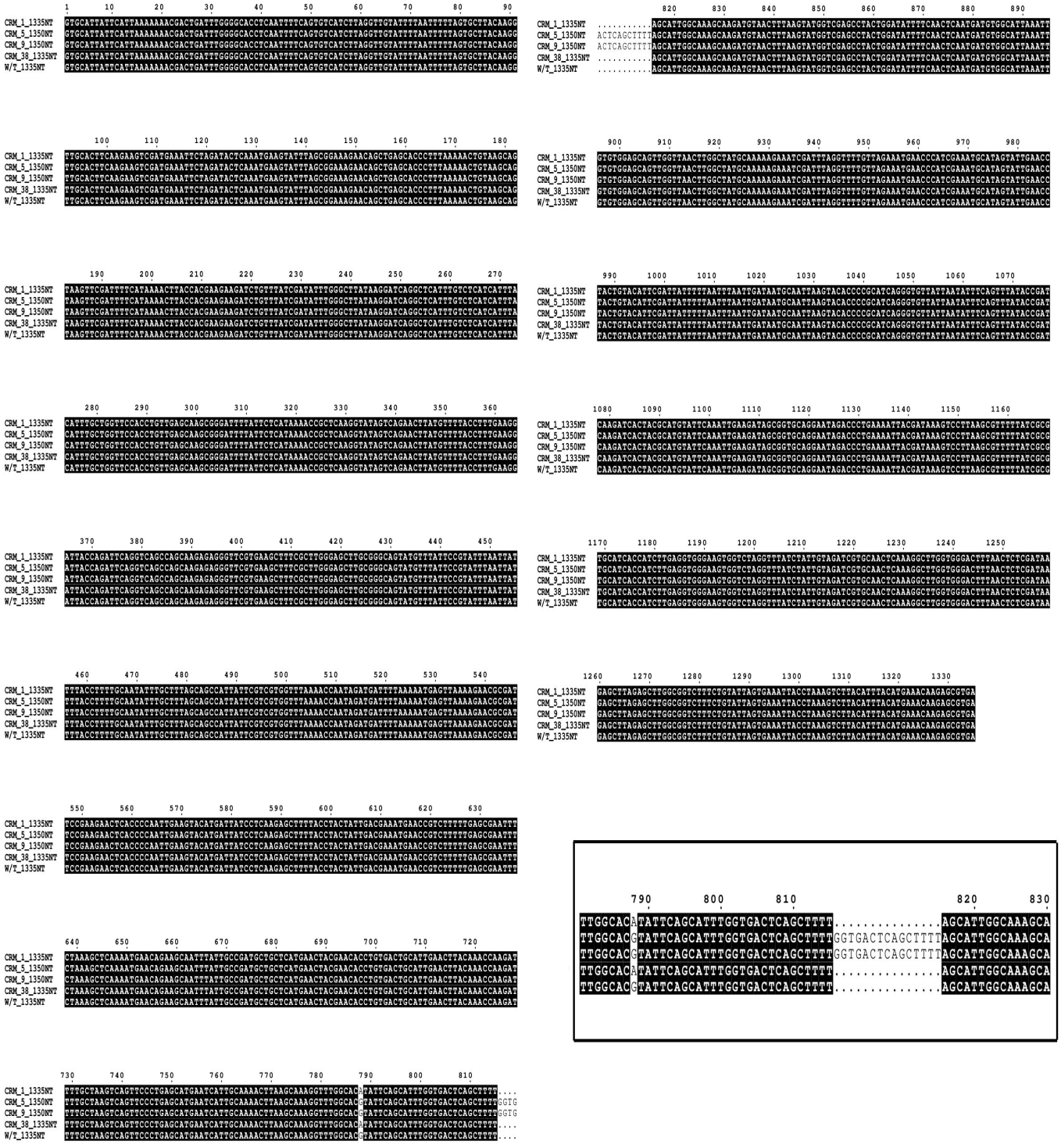

Figure 4.7: Nucleotide multiple sequence alignment (MSA) of the CRMs *pmrB* sequences against the AB5075 wild-type *pmrB* sequence. PmrB gene sequences from the AB5075 wild-type, CRM 1, 5, 9, and 38 were aligned using MUSCLE (within MEGA X) and visualised with ESPript 3.0. The left side of each gene sequence is labelled with its respective identity and the number of nucleotides, e.g. CRM_1_1335NT is CRM 1 which has 1335 nucleotides. Numbering for the position of the nucleotides is annotated above the sequences. Alignment scores are represented as black boxes for conserved residues and white boxes for mutated residues. The mutated region is further highlighted in the black box at the bottom right of the figure.

4.3.7 Characterisation of the colistin resistant mutations

The PmrAB two-component regulatory system plays a major role in regulating the modification of lipid A in the outer membrane of *A. baumannii* (Bartholomew *et al.,* 2019). Under normal circumstances, the PmrAB system is activated in response to environmental stress signals, such as an increased pH or low Mg2+ levels. The histidine kinase component of the system, PmrB, undergoes autophosphorylation in response to the stress signals. Following this, the phosphorylated PmrB acts as a phosphoryl donor and transfers its phosphate group to an aspartate residue on the response regulator component, PmrA. The phosphorylated PmrA then undergoes conformational changes and functions as a transcription factor, binding to the promoter regions and stimulating the transcription of *pmrC,* which is involved in modifying lipid A in the outer membrane. This activation results in the addition of positively charged phosphoethanolamine to lipid A, thereby altering the net charge of the outer membrane to positive and causing resistance against the cationic antibiotic colistin.

To further investigate the impact of these mutations on the PmrB protein and their role in colistin resistance amongst these CRMs, we generated an amino acid multiple sequence alignment and annotated it with the characteristic histidine kinase domains and features, to pinpoint the effect of these mutations on the PmrB protein. Figure 4.8 depicts the novel duplication mutation identified in the PmrB proteins of CRM 5 and 9, characterised by a repeated sequence of 5 amino acids (LVTQL) at residues 272-276 (Figure 4.8A). Notably, this

mutation falls within the C-terminus of PmrB (Figure 4.8D; yellow region), specifically within the 2nd alpha helix (5th alpha helix overall) of the HisKA/DHp domain (Figure 4.8G; green region). It should also be noted that this mutation introduces two additional dimer interface residues at positions 272L and 276L (Figure 4.8A). The C-terminus (Figure 4.8G; lime green to red regions or HisKA/DHp and HATPase C/CA) particularly appears to be affected by the mutation, as differences can be observed in the structures, such as in the distances and angles of the alpha helices. The presence of these additional dimer interface residues, suggests an enhancement in the dimerisation of the PmrB homodimer, potentially leading to an increased stability and function of the HisKA domain. This enhanced stability may impact the function of the domain, potentially improving the efficiency of autophosphorylation (Ma and Phillips-Jones., 2021). This enhancement may be attributed to a more effective binding of the homodimers to each other or, a reduced ability to dissociate causing the PmrB to be stuck in autophosphorylation confirmation. Consequently, this continuous phosphorylation could lead to an increased expression of *pmrC*, ultimately resulting in colistin resistance. The N-terminus, encompassing the TM1, SD, TM2, and HAMP domains (Figure 4.8G; blue to green regions), seems unaffected by the mutation. This is unsurprising, given that the mutation occurs later in the sequence, specifically in the C-terminus and opposite end of the structure.

Figures 4.8C and F illustrate the R263H substitution mutation found in the PmrB protein of CRM 1 and 38. This highlights the substitution of the amino acid residue Arginine (R) for Histidine (H) at position 263 within the sequence, occurring specifically within the 5th alpha helix and in the HisKA domain of the PmrB protein (Figure 4.8A), as previously reported by Cafiso *et al* (2017). This mutation falls in the C-terminus of PmrB (Figure 4.8C; yellow region) specifically within the 2nd alpha helix (5th alpha helix overall) of the HisKA/DHp domain (Figure 4.8F; green region). Additionally, the wild-type, CRM 1 and 38 share a common dimer interface residue at position 260L, which is absent in CRM 5 and 9. Despite these differences, the sequence surrounding the predicted residue in CRM 5 and 9 remains identical to that of the wild-type, CRM 1, and 38. Therefore, it is likely that this predicted dimer interface does not form in CRM 5 and 9.

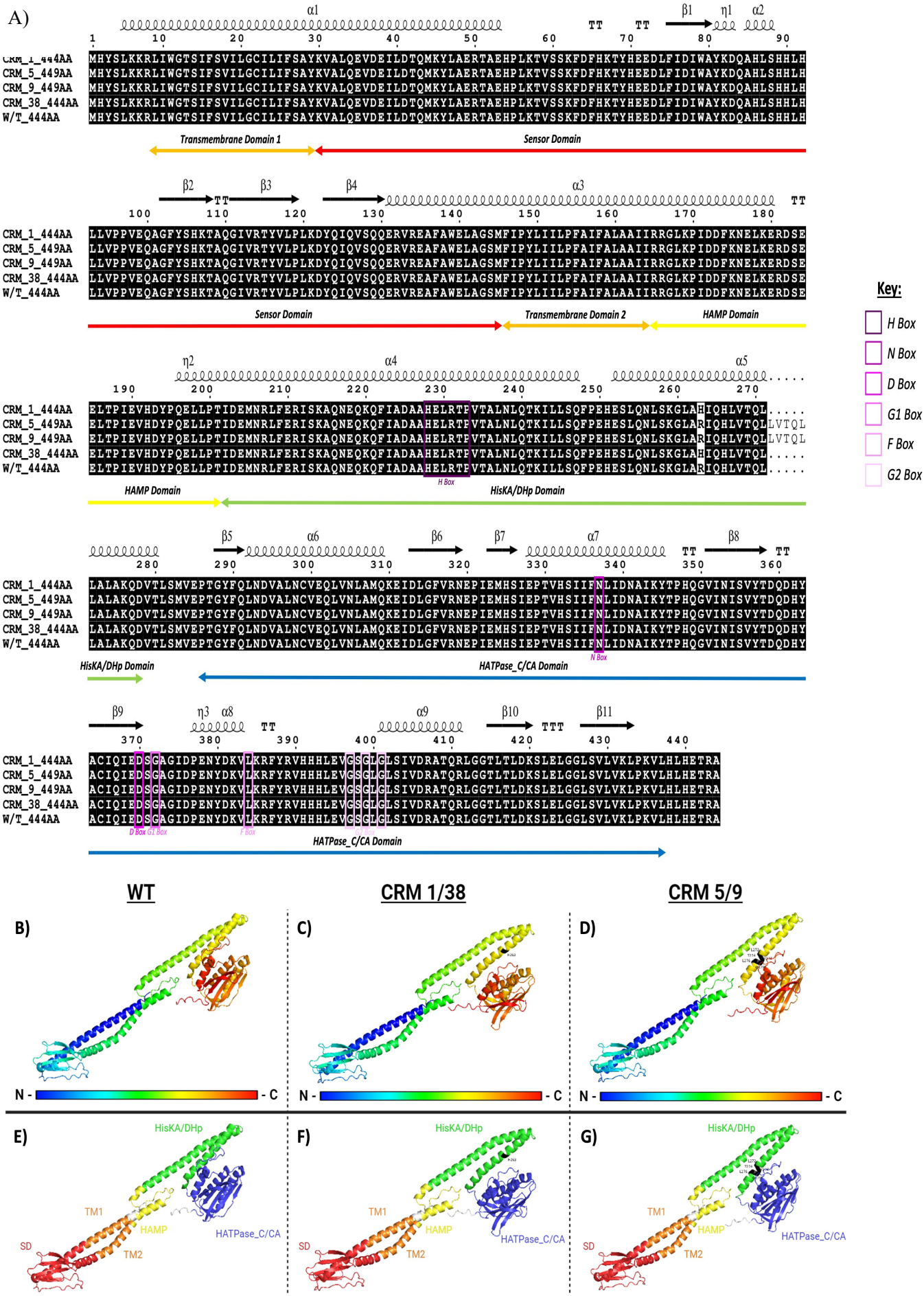
A)
CRM_1_444AA
CRM_5_449AA
CRM_9_449AA
CRM_38_444AA
W/T_444AA
Transmembrane Domain 1
Sensor Domain
Transmembrane Domain 2
HAMP Domain
HisKA/DHp Domain
HATPase_C/CA Domain
H Box
N Box
D Box
G1 Box
F Box
Key:
H Box
N Box
D Box
G1 Box
F Box
G2 Box
WT
CRM 1/38
CRM 5/9
B)
C)
D)
N -
- C
E)
F)
G)
HisKA/DHp
TM1
HAMP
HATPase_C/CA
SD
TM2

Figure 4.8: Amino acid multiple sequence alignments (MSA) and tertiary structures of PmrB from wildtype AB5075 and CRMs. (A) The wild-type, CRM 1, 5, 9 and 38 sequences were translated in MEGA X and aligned with MUSCLE (within MEGA X). The structures were predicted with AlphaFold (ColabFold) and the secondary structures, in addition to the MSA, were then visualised with ESPript 3.0. The domains and features were predicted using InterPro (corroborated by aligning the CRMs' PmrB sequences against the sequences of other histidine kinases with characterised crystal structures [Refer to Appendix C.3 for the MSA]). Note that all domains and features in CRM 5 and 9 after position 271 are +5 residues due to the +5AA duplication (Refer to Appendix C.4 for the exact positions of domains and features [including those not displayed]). The HAMP domain has not been predicted and was assumed to be between Transmembrane domain 2 and HisKA/DHp domain (Cociurovscaia *et al*., 2022). The left side of each amino acid sequence is labelled with its respective identity and the number of amino acids, e.g. CRM _1 _44AA is CRM 1 which has 444 amino acids. Numbering for the position of the nucleotides is annotated above the sequences. Alignment scores are represented as black boxes for conserved residues and white boxes for mutated residues. The domains are annotated at the bottom of the sequences and the colours of the domains match the colours of the tertiary structures. The features are also labelled below the sequences and the colours of the features correspond with the key to the right of the figure. **(B)** and **(E)** Represent the wild-type full-length PmrB structures. **(C)** and **(F)** Represent CRM1/38 full-length PmrB structures.**(D)** and **(G)** Represent CRM5/9 full-length PmrB structures. **(B), (C)**, and **(D)** Represent the PmrB structures as ribbon diagrams with a rainbow colouring (the N-terminus is blue and the C-terminus is red). **(E)**, **(F)**, and **(G)** Represent the PmrB structures as ribbon diagrams with domain-specific colouring (transmembrane domains 1 and 2 are orange, the sensory domain is red, the HAMP domain is yellow, HisKA/DHp domain is green, and HATPase C/CA is blue). Mutations have been coloured black and labelled with the residue initial and position. Sequences were translated in MEGA X, the structures were predicted using AlphaFold (ColabFold), and visualised with PyMol. The structures were positioned using the 1st alpha helix as a reference point).

4.3.8 Structural variation and binding affinity analysis of PmrB through tertiary modelling

In order to assess the structural variation between the predicted CRMs and the wild-type PmrB proteins, we next superimposed the tertiary structure of the affected C-terminus, encompassing the HisKA and HATPase C/CA domains, of the PmrB proteins. From our results in Figure 4.9A and B, structural variation can be observed between the wild-type, CRM 1/38 and CRM5/9, as evidenced by their root mean square deviation (RMSD) values of 0.404, 1.428 and 1.499, respectively. Notably, CRM 5/9 exhibits greater structural variation in contrast to both the wild-type and CRM 1/38. Moreover, we observed significant structural differences between CRM 1/38 and CRM 5/9 themselves, further emphasizing their distinct mutant characteristics, compared to the wild type. These results suggest that the mutations will likely induce conformational changes in PmrB, specifically within the HisKA and ATPase C/CA domains. As structure determines function, these mutations will also likely have functional consequences.

To determine if the presence of the extra dimer interface residues increases the stability and binding of the PmrB homodimer, we delved deeper using *in vivo* analysis and analysed the binding affinity of the predicted homodimer tertiary structures of PmrB from the CRMs and the wild-type. The binding affinity (ΔG) value expressed in kcal mol^{1} is the Gibbs free energy change associated with the binding of a protein to a target protein. Gibbs free energy change is a thermodynamic parameter that describes the spontaneity of a chemical or biochemical reaction. The more negative the ΔG the stronger the binding affinity. Conversely, a positive ΔG indicates an unfavourable or non-spontaneous binding interaction. A ΔG value close to zero suggests a weak or transient binding.

Moreover, the dissociation constant (K_d) quantifies the predicted strength of interactions between a protein and a target protein. Specifically, it denotes the predicted protein concentration at which half of the available binding sites on the protein become occupied. At a given temperature, 25 °C or 298 K, a smaller K_d signifies a heightened binding affinity. This indicates that a lower protein concentration is required to saturate half of the binding sites on the protein based on *in vivo* analysis.

Our findings suggest that the *pmrB* homodimers of the wild-type exhibit the least favourable binding affinity to each other, as shown by the binding affinity (ΔG) and dissociation constant (K_d), -9.4 ΔG kcal mol^{1} and 1.2e- 07 K_d (M), respectively. Subsequently, CRM 1/38

demonstrates improved binding of homodimers, relative to the wild-type, as shown by the binding affinity (ΔG) and dissociation constant (Kd), -10.4 ΔG kcal mol^{1} and 2.2e-08 K_d (M), respectively. While CRM 5/9 shows the highest binding affinity, as shown by the binding affinity (ΔG) and dissociation constant (K_d), -11.3 ΔG kcal mol^{1} and 2.6e-09 K_d (M), respectively. This suggests that there are enhanced effects on binding in CRM 1/38 compared to the wild-type, and CRM 5/9 exhibits even more pronounced effects in binding compared to both the wild-type and CRM 1/38.

Interestingly, a distinction can be observed in the binding residues found within the central channel of the complexes' helical bundle of the HisKA/DHp domain. Specifically, CRM1/38 exhibits more robust binding between the inter-chain residues and cross-links compared to the wild-type suggesting a more rigid binding (Figure 4.9C-G). In contrast, CRM5/9 shows an absence of any discernible inter-chain binding residues and cross-links. Despite this, the scores clearly indicate a greater binding affinity in CRM5/9, relative to the others (Figure 4.9C-H). Consequently, it suggests that CRM5/9 may possess stronger yet less rigid binding, due to the lack of inter-chain cross-links in its predicted homodimeric structure. This absence of inter-chain cross-links could allow more stabilised conformational changes. These structural insights imply that CRM5/9's enhanced binding affinity and flexibility might lead to more efficient and prolonged transmission of signals. Moreover, it could contribute to heightened kinase activity in PmrB, resulting in increased phosphorylation events. In turn, this may increase the activation of PmrA and consequently, result in the upregulation of *pmrC*, ultimately conferring colistin resistance.

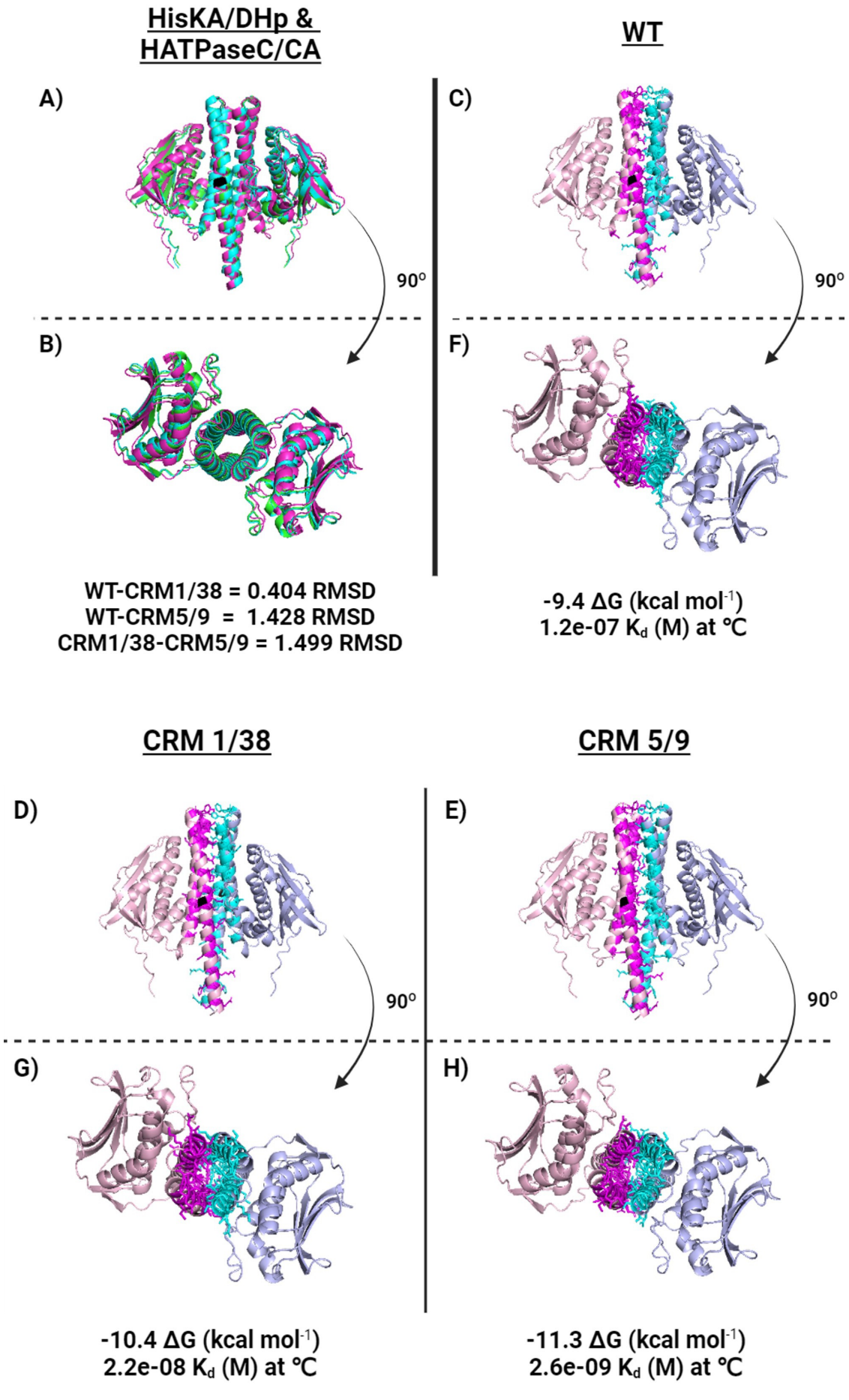
HisKA/DHp &
HATPaseC/CA
WT
A)
C)
90°
90°
B)
F)
WT-CRM1/38 = 0.404 RMSD
WT-CRM5/9 = 1.428 RMSD
CRM1/38-CRM5/9 = 1.499 RMSD
-9.4 ΔG (kcal mol-1)
1.2e-07 Kd (M) at °C
CRM 1/38
CRM 5/9
D)
E)
90°
90°
G)
H)
-10.4 ΔG (kcal mol-1)
2.2e-08 Kd (M) at °C
-11.3 ΔG (kcal mol-1)
2.6e-09 Kd (M) at °C

Figure 4.9: Tertiary structures of the HisKA/DHp and HATPase C/CA domains of PmrB of PmrB from wild-type AB5075 and CRMs. (A-B) Superimposed predicted tertiary structures of the wild type, CRM 1/38, and CRM 5/9 HisKA/DHp and HATPase C/CA domains of PmrB. The wildtype is represented in green, CRM1/38 is cyan, and CRM5/9 is magenta. (C-F) Wild-type HisKA/DHp and HATPase C/CA domains of PmrB structures. (D-G) CRM 1/38 HisKA/DHp and HATPase C/CA domains of PmrB structures. (E-H) CRM 5-9 HisKA/DHp and HATPase C/CA domains of PmrB structures. (A), (C), (D) and (E) represent the PmrB structures as front-view ribbon diagrams. (B), (F), (G), and (H) represent the PmrB structures as top-view ribbon diagrams. (C – H) have a chain- and binding-specific colouring (magenta is chain A [Monomer 1] and cyan is chain B [Monomer 2] of the homodimer. Bright magenta and cyan represent binding residues from chains A and B, respectively, and dull magenta and cyan represent non-binding residues from chains A and B, respectively). The autophosphorylation histidine residues have been coloured black. Alignment scores, provided as RMSD, are noted under (A) and (B). Binding scores have been provided under (C – H) as binding affinity (ΔG) expressed in kcal mol-1 and dissociation constant (Kd) at 25 °C expressed in molar (M). The sequences were translated in MEGA X, the homodimer structures were then predicted using AlphaFold (ColabFold), the structures were superimposed and the RMSD values were calculated using PyMol. The binding affinity and dissociation constant values were calculated using PRODIGY, and the structures were visualised with PyMol (note that the structures were positioned using the autophosphorylation histidine as the reference point).

4.3.9 Validating a novel colistin-resistant mutation

The activation of the PmrAB two-component system tightly regulates the expression of the *pmrC* under normal conditions. Overexpression of *pmrC*, resulting from mutations in *pmrAB,* has been consistently correlated with colistin resistance (Adams *et al*., 2009; Olaitan *et al*., 2014). In Figure 4.10, our findings indicate increased expression of *pmrC* in CRM 1 and 38, both harbouring the colistin-associated *pmrB* mutation R263H and exhibiting colistin resistance, compared to the AB5075 wild-type. These results validate a direct link between mutations in *pmrB* and increased *pmrC* expression. Therefore, by measuring *pmrC* expression,

we can evaluate the downstream effects of *pmrB* mutations, providing supporting evidence that the observed colistin resistance may be mediated or contributed to by these mutations to PmrB. The augmented stability of the HisKA/DHp domain suggests a more effective binding of the homodimers to each other or, a reduced ability to dissociate from each other causing PmrB to be stuck in the autophosphorylation confirmation, possibly resulting in continuous phosphorylation of the PmrA transcription factor and thus an increased expression of *pmrC*. Subsequently, our objective was to ascertain the role of the novel PmrB mutation in CRM 5 and 9 in mediating or contributing to observed colistin resistance by measuring the expression of *pmrC*. To do so we grew the wild-type, CRM 1, 5, 9 and 38 to exponential log phase (OD_{600} of 0.6) in LB containing the sub-MIC of colistin (1 μg/mL). We then extracted and conducted DNase treatment on the RNA from each CRM. Next, we conducted RT-qPCR using the QuantiNova RT-qPCR kit containing a reverse transcriptase step within its protocol. The normalised fold change was calculated relative to the corresponding control sample *proC*. *proC* was chosen as the endogenous control gene as it is considered a housekeeping within AB5075 due to its consistent expression.

Our results indicate a significant increase in *pmrC* expression in both CRM 5 and 9 when compared to the AB5075 wild-type. This suggests that the novel mutation present in these CRMs plays a pivotal role in mediating colistin resistance, as the increased expression of *pmrC* suggests that the number of positively charged phosphoethanolamine to the outer membrane of *A. baumannii* will be increased. Consequently, this process alters the net charge of the outer membrane, rendering it positively charged, and preventing the binding of the cationic peptide colistin (Beceiro *et al*., 2011). These alterations are indicative of the mechanism by which the novel mutation contributes to colistin resistance in *A. baumannii.*

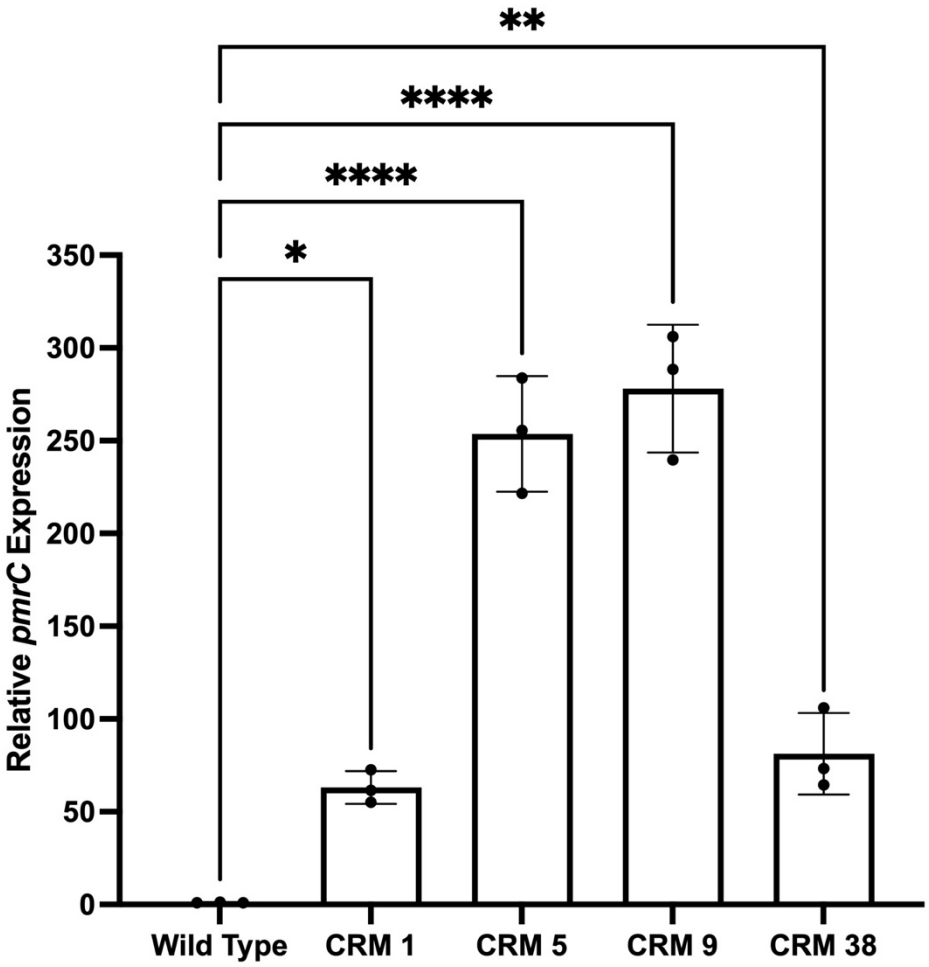

Figure 4.10. *pmrC* expression in CRMs and AB5075 wild type. *pmrC* is upregulated in all CRMs compared to the AB5075 wild-type, with RQ values of 63.08, 81.28, 253.68, and 278.11 for CRM 1, 38, 5, and 9, respectively. The RQ values were calculated using $RQ = 2^{-\Delta\Delta Ct}$. All assays were carried out in biological triplicate (n=3), with three technical repeats. Statistical analysis consisted of one-way ANOVA between the CRMs and AB5075 control. Average values ± S. D. are represented. Significance is indicated as * = p ≤0.05, ** = p ≤0.01, *** = p ≤0.001, **** = p ≤0.0001. Tukeys post hoc test revealed no significant difference between CRM's 5 and 9 and also between CRM's 1 and 38 while there is a p ≤0.0001 difference between CRM 5/9 and 38 and also between CRM 5/9 and CRM 1.

4.4 Discussion

Evolving CRMs in a laboratory setting using a variety of different methods revealed colistin agar tilt plates as the most effective means for generating CRMs that were actually *A. baumannii* and had MICs of 8 ug/mL or higher (Figure 4.3 and Table 4.1). From these methods, we evolved

50 CRMs with varying MICs (Table 4.1). Previous studies have reported that mediating colistin resistance affects the bacterial functions that are associated with the fitness of the pathogen (Da Silva and Domingues, 2017; López-Rojas *et al*., 2011). However, these studies have reported this using a small pool of resistant bacteria derived from varying strains. Thus, in order to advance our knowledge beyond these findings, this study focuses on a pool of 50 CRMs that are derived from a single parental strain of *A. baumannii*. This controlled experimental design allowed for more direct comparison and analysis of resistance-associated fitness costs among a larger pool of genetically related strains. For this reason, we sought to determine if our pool of 50 CRMs, faced any fitness cost due to their evolved resistance. Our results show that in the presence of colistin CRMs that have a high MIC (120 ug/mL or above) all grow to an OD_{600} of 1.7 or higher at 24 hours, whereas CRMs with lower MICs (70 ug/mL or below) have varying growth rates at 24 hours (Figure 4.4B). A high MIC may not have a significant impact on the growth of the CRM as the mutation-conferring resistance may be associated with compensatory mutations. These compensatory mutations, occurring in one or more genes unrelated to resistance, could restore or maintain bacterial growth, offsetting the potential fitness cost of the resistance mutation (Andersson, 2003; Mu *et al*., 2016).

In Mu *et al*.'s (2016) laboratory study of 8 colistin-resistant strains, novel colistin resistance-associated genes were identified. A1S 3026, encoding a T2 family ribonuclease, linked to reduced motility, and RsfS, a putative ribosomal silencing factor, enhance biofilm formation and bacterial adaptation. Mutations in these genes suggest the emergence of novel resistance mechanisms, potentially involving polysaccharide formation. The third gene, A1S 1983, encodes an exported membrane protein influencing bacterial membrane integrity. Despite fitness costs in these lipooligosaccharides (LOS)-deficient mutants, compensatory mutations in A1S 3026 and RsfS facilitated survival and dissemination. This highlights the role of compensatory mutations in the evolution of colistin-resistant *A. baumannii,* potentially explaining the restoration or maintenance of growth in high MIC CRMs with minimal impact on bacterial growth.

We also demonstrate that in the absence of colistin, 84% of all 50 CRMs have a slower growth rate at 24 hours when compared to the wild type and the remaining 16% present have a

similar growth rate as the wild type (Figure 4.4). These findings correlate to previous literature suggesting that in the absence of colistin the resistant bacteria have an impacted growth rate compared to the susceptible wildtype strain. Additionally, the level of resistance was found not to impact the growth of the CRMs in the absence of colistin. This suggests that the CRMs harbour diverse colistin resistance mediating mutations, each with varying fitness costs when in the absence of colistin. This also suggests that the level of resistance may not be the sole determining factor influencing bacterial growth, indicating the presence of additional mediating factors contributing to the observed fitness costs.

Taking a closer look at the growth rates of CRM 1, 5, 9 and 38 over a 24-hour period in the presence of colistin, a distinct pattern is seen. CRMs 5 and 9 exhibit an exponential log phase that plateaus at 11 hours, with only CRM 9 demonstrating the ability to recover from the plateau at 16 hours. In comparison to the wild-type in the absence of colistin, these CRMs reached the stationary phase earlier, suggesting that the resistance mechanisms in CRMs 5 and 9 may impose an additional energy burden on the bacteria. This potential diversion of energy towards maintaining the resistance mechanisms might come at the expense of cellular metabolism and growth, leading to an early entry into the stationary phase for these CRMs. This observation aligns with the well-established knowledge that bacteria in the stationary phase tend to be more resistant to antibiotics compared to exponentially growing cells (Levin and Rozen, 2006). This suggests that the early entry into the stationary phase may be an integral part of the resistance mechanism employed by these CRMs.

The growth curves of CRMs 1 and 38 in the presence of colistin reveal a prolonged lag phase, with the exponential log phase occurring at hours 11 and 10, respectively. This suggests that the fitness cost is more pronounced during the lag phase before the CRMs fully adapt to growing in the presence of colistin. This may be due to the mechanism mediating resistance in these CRMs compromising the metabolic efficiency of the bacteria, leading to a slower adaptation to the growth conditions and consequently lengthening the lag phase. These findings align with previous studies linking an extended lag phase to the development of tolerance and persistence, suggesting that this may be an integral part of the resistance mechanism employed by CRMs 1 and 38 (Li *et al*., 2016).

In the absence of colistin, CRMs 5, 9, and 38 demonstrate a growth rate that reverts to resemble that of the wild-type (Table 4.4). This observation implies that, in the absence of colistin and the associated lack of selection pressure, these CRMs redirect their energy resources toward sustaining energy-efficient growth. This suggests that the energy previously dedicated to sustaining resistance, which may have posed a fitness burden, is no longer necessary for the bacteria in the absence of colistin. This shift in growth rates indicates that the CRMs adapt their resource allocation strategy based on the absence or presence of the antibiotic, emphasising the influence of environmental conditions on bacterial behaviour and resistance (Sahoo *et al*., 2010). However, CRM 1 deviates from this pattern, exhibiting a slow growth rate that plateaus at 10 hours. This suggests that the mechanism mediating resistance in CRM 1 comes with inherent fitness costs. Unlike CRM 5, 9 and 38, CRM 1 may persist in maintaining the resistance mechanism even in the absence of colistin, resulting in a substantial allocation of energy to sustain resistance.

As biofilm formation plays a crucial role in antibiotic resistance, particularly within *A. baumannii*, our subsequent investigation aimed to assess the impact of evolved colistin resistance on biofilm formation. Our findings reveal that 64% of CRMs exhibit increased biofilm formation in the presence of colistin compared to conditions without colistin (Figure 4.5). Conversely, only 12% of CRMs demonstrate higher biofilm formation in the absence of colistin, while 24% show no significant difference in biofilm formation between the presence and absence of colistin. These results suggest that the majority of CRMs enhance biofilm formation in the presence of colistin. This observed increase in biofilm formation in the presence of an antibiotic aligns with a commonly reported bacterial strategy to evade antibiotics. Biofilm formation provides protection to bacteria, enabling survival at higher doses of antimicrobials, even up to 100 times the original MIC (Singh *et al*., 2017; Santos-Lopez *et al*., 2019). More specifically, the effect of colistin has been found to be impaired against biofilm-embedded bacteria, further supporting this consensus (Lora-Tamayo *et al*., 2019). This suggests that the CRMs may be employing biofilm formation in conjunction with other colistin resistance mediating mutations to overcome the challenges posed by colistin treatment.

As for the 12% of CRMs exhibiting a decrease in biofilm formation, it is likely that these

CRMs allocate a substantial amount of energy and resources to uphold the resistance mechanisms. This prioritisation, however, may limit the resources available for biofilm formation, resulting in a notable reduction in biofilm production. This suggests a potential trade-off where the maintenance of resistance mechanisms negatively impacts the capacity for robust biofilm development. Conversely, 24% of CRMs show no significant change in biofilm formation from the wild-type, whether colistin was present or absent. The occurrence of CRMs with a decreased or unchanged biofilm formation suggests the presence of alternative mechanisms of action mediating colistin resistance in these CRMs.

CRM 1, 5, and 9 display higher biofilm formation in the presence of colistin, indicating a potential link between biofilm development and their increased resistance. This observation suggests that biofilm formation may contribute to the increased resistance observed in these CRMs. Conversely, CRM 38 demonstrates reduced biofilm formation in the presence of colistin compared to in the absence of colistin (Table 4.4). This difference suggests that factors other than biofilm formation may be contributing to colistin resistance in CRM 38. Furthermore, the reduced biofilm formation in CRM 38 suggests a potential high fitness cost associated with its resistance mechanisms to colistin. This suggests that CRM 38 may face challenges in maintaining robust biofilm structures due to the energy and resource allocation towards its resistance mechanisms, indicating a complex interplay between resistance and biofilm formation in different CRMs.

In assessing fitness impact, we also used virulence in *G. mellonella* as a key indicator in this study. This allowed us to determine the implications that the evolution of resistance has on each CRM. Our findings reveal that 84% of CRMs exhibit reduced virulence compared to the wildtype, aligning with previous literature indicating a trade-off between resistance gain and reduced virulence (Figure 4.6) (Geisinger and Isberg, 2017; Beceiro *et al*., 2014). This may be due to fitness trade-offs where the resistance bacteria maintain their resistance diverting energy to maintaining the mechanism and in turn negatively impacting the virulence of the bacteria.

Conversely, 16% of the CRMs have a higher or similar virulence to the wildtype after 32 hours. This may be due to the CRM populations adapting over time and accumulating

additional mutations that result in an increased virulence phenotype. It might also be due to some CRMs initially experiencing a fitness cost in growth associated with the resistance mutation. But later in development, compensatory mutations may arise, alleviating the growth fitness cost and allowing the bacteria to maintain or enhance their resistance without the fitness trade-off of decreased virulence (López-Rojas *et al*., 2011, Wand *et al*., 2015, Rolain *et al*., 2011). CRM 1, 5 and 9 are amongst the 84% that exhibit a reduced virulence compared to the wildtype however, CRM 38 demonstrates a similar virulence to the wildtype after 32 hours (Table 4.3). This suggests that additional virulence factors such as biofilm formation or an increase in gene expression of virulence-contributing genes may become more prominent after 32 hours. This may be due to CRM 38 adapting to the environment over time and enhancing its virulence mechanisms to persist and thus, compensating for the fitness costs associated with the evolution of colistin resistance.

Table 4.3: Table comparing the phenotypes of CRM 1, 5, 9 and 38. This table summarises and compares the phenotype results from figures 4.4C - D, 4.5C and 4.6C. Rows represent the phenotype and columns represent different CRMs.

Phenotype	CRM Strain			
	1	5	9	38
Growth at 24 hours	Less than WT	Same as WT	Higher than WT	Higher than WT
Biofilm Formation	Higher in the presence of colistin	Higher in the presence of colistin	Higher in the presence of colistin	Higher in the absence of colistin
Virulence at 32 hours	Less than WT	Less than WT	Less than WT	Same as WT

MIC	8 μg/mL	512 μg/mL	1024 μg/mL	32 μg/mL
Mutation	R263H	$(GGTGACTCAGCTTTT)_{1\rightarrow2}$	$(GGTGACTCAGCTTTT)_{1\rightarrow2}$	R263H

Our genomic analysis of CRMs 1, 5, 9 and 38 revealed that CRMs 1 and 38 were found to carry the well-documented R263H mutation in the *pmrB* gene (Lim *et al*., 2015; Choi *et al*., 2017; Cafiso *et al*., 2018) and CRMs 5 and 9 harbour, to the best of our knowledge, a novel 15 bp duplication mutation within the *pmrB* gene $(GGTGACTCAGCTTTT)_{1\rightarrow2}$ (Table 4.2 and Figure 4.7). Aside from *pmrB* mutations, additional genetic variations were also identified. CRMs 1 and 38 were predicted to harbour an F506C mutation in *ABUW_1591*, a hypothetical protein, and an E19E mutation in *hemA*, a glutamyl-tRNA reductase. On the other hand, CRMs 5 and 9 were both predicted to possess an ISAba1 insertion (+9 bp) in *ABUW_1959*, another hypothetical protein in AB5075_UW (Table 4.2) and a homolog for TetR family transcriptional regulator in AB0057. The ISAba1 mobile genetic element is able to move within the genome and increase the expression or disrupt the coding sequence of its adjacent genes thus altering the function of the affected genes. The concurrent occurrence of these mutations alongside the identified *pmrB* mutations, which potentially mediate colistin resistance, raises the possibility that these additional mutations may act as compensatory mutations, mitigating the fitness trade-offs associated with the evolution of resistance. In order to investigate this, subsequent gene knockout experiments could be conducted. These experiments will delve into the specific involvement of these genes in maintaining the fitness of colistin-resistant *A. baumannii*.

We then characterised the *pmrB* mutations in CRMs 1, 5, 9 and 38 at the amino acid level and visualised the structural changes in the predicted tertiary structures of the mutated PmrB proteins (Figure 4.8). Our analysis pinpointed the localisation of these mutations to the C-terminus region, specifically within the 2nd alpha helix of the HisKA/DHp domain. The PmrB mutation in CRMs 1 and 38 results in the amino acid substitution R263H and the PmrB mutations in CRMs 5 and 9 introduce two additional dimer interface residues at positions 272L and 276L (Figure 4.8A). Figures 4.9A and B suggest that these mutations are likely to induce alterations in the HisKA/ATPase C/CA domains, thereby leading to structural and functional consequences.

These mutations are predicted to result in a greater binding affinity of PmrB homodimers in CRM 1/38 and an even more pronounced binding affinity for CRM 5/9. This enhanced binding affinity, coupled with increased flexibility, suggests a potential for more efficient and

prolonged signal transmission. This augmented binding affinity, particularly evident in CRM 5/9, may contribute to heightened kinase activity in PmrB, leading to an escalation of phosphorylation events. This process occurs through dimerization and conformational changes of PmrB, triggered by environmental signals sensed by the sensory domain. Consequently, the HATPase C/CA domain, responsible for generating the phosphate group, is positioned in close proximity to the HisKA/DHp domain, housing the autophosphorylating histidine residue, allowing for its phosphorylation (Figure 4.11) (Wang *et al*., 2013).

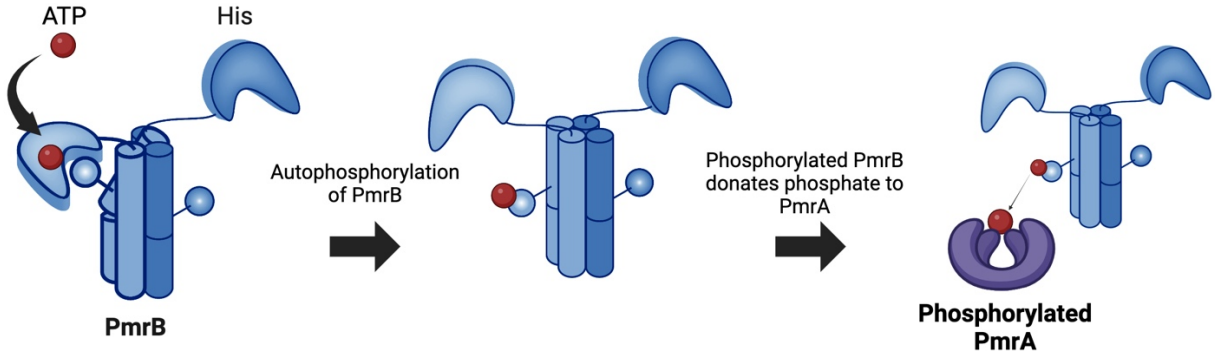

Figure 4.11. Mechanism of PmrAB activation. The blue-coloured proteins represent PmrB and the purple-coloured protein represents PmrA. The histidine kinase component (labelled His) of the system, PmrB, undergoes autophosphorylation and PmrB then acts as a phosphoryl donor and transfers its phosphate group to the response regulator component, PmrA. This figure was made using Biorender.com.

The increased flexibility in this region may facilitate more conformational changes that are required for the process to occur more frequently and efficiently, potentially occurring even in the absence of a signal (Khan and Kumar., 2009). Additionally, these conformational changes have a heightened stability which may be holding the structural conformation in place for greater efficiency or even permanently (Laurance and Middaugh., 2010), thus allowing for continuous autophosphorylation (Figure 4.9C-H) (Ma and Phillip-Jones., 2021). Figure 4.10 further validates these observations by demonstrating an up-regulation of *pmrC* in all tested CRMs. This upregulation is likely attributed to the heightened kinase activity, providing further support that the structural alterations in PmrB contribute to significant functional consequences in the signal transduction pathway.

Furthermore, our findings in Figure 4.10 and Table 4.1 align with previous research

indicating a positive correlation between *pmrC* expression and colistin MIC levels (Nurtop *et al*., 2019). This correlation is consistently observed across the four tested CRMs, where increasing MIC values (8, 32, 512, and 1024 µg/mL for CRM 1, 38, 5, and 9, respectively) correspond to increasing levels of relative *pmrC* expression (63.08, 81.28, 253.68, and 278.11, respectively). Suggesting that the novel PmrB mutation in CRM 5 and 9 confers a higher level of resistance to colistin compared to the R263H PmrB mutation in CRM 1 and 38, as shown by the MIC results in Table 4.1. This difference in resistance may be attributed to the PmrB mutation in CRM 1 and 38 resulting in less stability and a less favorable structural confirmation compared to CRM 5 and 9, as evidenced by the lower binding affinity as shown in Figure 4.9. Consequently, this lower binding affinity may lead to reduced efficiency or less autophosphorylation, ultimately resulting in lower *pmrC* expression and greater susceptibility to colistin, when compared to CRM 5 and 9.

Despite CRM 1 and 38 as well as CRM 5 and 9 potentially harbouring the same colistin mediating mutation, they exhibit varying MICs. This could be attributed to post-translational modifications to the PmrB proteins or other proteins involved in factors that influence MIC values, such as biofilm formation. These post-translational modifications may affect the function, stability or interactions between proteins involved in mediating colistin resistance and ultimately impacting the MICs of the strains.

To conclude, the known R263H mutation present in CRM 1 and 38 is shown to extend the lag phase of the growth of the bacteria in the presence of colistin, with only CRM 1 demonstrating growth impairment even in the absence of colistin. Intriguingly, CRM 1 exhibits lower virulence compared to the wild type, while CRM 38 maintains similar virulence levels after 32 hours (Figure 4.4D and Figure 4.6C). Additionally, CRM 38 shows reduced biofilm formation, whereas CRM 1 displays higher biofilm formation in the presence of colistin (Figure 4.5C). This suggests that even though CRM 1 and 38 have the same PmrB mutation, both CRMs faced different fitness costs. Our potentially novel duplication mutation present in CRMs 5 and 9 enhances kinase activity in PmrB by introducing extra binding residues, thereby increasing the binding affinity and stability of the homodimer (Figure 4.7-4.8). This in turn enhances the signal transduction processes surrounding autophosphorylation, increasing the

expression of *pmrC* resulting in the addition of PeTN mediating colistin resistance (Figure 4.10). However, the evolution of this resistance is accompanied by fitness trade-offs, such as a shorter lag phase in the presence of colistin and reduced virulence (Figure 4.4D and Figure 4.6C). Additionally, it is plausible that biofilm formation plays a role alongside the PmrB mutation in mediating colistin resistance, as biofilm formation in the presence of colistin is increased (Figure 4.5C). This analysis highlights the diverse aspects of the fitness costs associated with different mutations.

The co-occurrence of mutations alongside those in PmrB, observed in both sets of CRMs (1/38 and 5/9), suggest that these additional mutations serve as compensatory mechanisms alleviating the fitness trade-offs encountered in these CRMs. Future investigations using knockout experiments targeting the non-PmrB mutations could assess whether the observed fitness costs, such as the similarity in virulence to the wild-type in CRM 38 and alterations in growth rates across all CRMs, persist in the absence of these mutations. This investigation would offer insights into the essentiality of these compensatory mutations for the survival and pathogenesis of these CRMs. Additionally, gene knockout mutations for the PmrB mutations would allow for the investigation of the specific contributions of other identified mutations in genes, potentially contributing to the maintenance of overall fitness.

Additionally, future work could focus on exploring how CRM 5 and 9 are genetically similar but are phenotypically distinct. This may involve conducting RNA-Seq in order to compare the gene expression profiles of the two CRMs under the same conditions. This would allow for the identification of potential differentially expressed genes that may account for the observed phenotypic differences (Figures 4.4C - D, 4.5C and 4.6C). The novel 15 bp duplication identified in CRMs 5 and 9 can be used to design primers to screen the remaining 46 CRMs to identify the presence of the same duplication. This would allow for rapid screening of the potential colistin resistance mediating mutation in these CRMs and identification of the prevalence of this mutation.

While the *in vivo* analysis provided novel insights into the mechanism od colistin resistance in CRM's 1, 5, 9 and 38, it would be beneficial to experimentally validate the hypothesis. This would consist of expressing, purifying and solving the crystal structure of

recombinant PmrB proteins from the wild-type and CRMs studied herein. The solved structures could then be compared to accurately determine the key structural differences that caused the observed functional differences.

Key Findings:

1. Linking resistance level to the fitness of the CRM:
    - CRMs with high MICs (120 µg/mL or above) grow robustly in the presence of colistin, while those with lower MICs (70 µg/mL or below) showed variable growth rates.
    - In the absence of colistin, 84% of CRMs exhibited slower growth rates compared to the wild type, with 16% growing at similar rates as the wild type. This suggests diverse colistin resistance-mediating mutations with varying fitness costs.
2. CRMs increase biofilm formation to tolerate colistin:
    - 64% of CRMs displayed an increase in biofilm formation in the presence of colistin, a common bacterial strategy to tolerate antibiotics.
3. Evolved colistin resistance affects the virulence of the bacteria:
    - 84% of CRMs exhibited reduced virulence compared to the wild-type strain, suggesting a trade-off between resistance and virulence.
4. Analysis of known and novel colistin mediating mutations:
    - CRMs 1 and 38 harbour the known R263H mutation in the pmrB gene, while CRMs 5 and 9 have a potentially novel 15 bp duplication in pmrB.
    - Structural analysis of both PmrB mutations suggested an increased binding affinity and flexibility, enhancing kinase activity and signal transduction, especially in CRMs 5 and 9.

5. Contributions:

- Evolved colistin resistance in *A. baumannii* results in several trade-offs compared to the sensitive wild-type strain. These include varied growth rates in the presence of colistin, reduced growth rates in its absence, and also decreased virulence. To tolerate colistin, biofilm formation is often increased in resistant CRMs. Additionally, increased binding affinity and flexibility from mutations such as R263H or our novel 15 bp duplication in pmrB may enhance kinase activity and signal transduction, providing an *in vivo*-based prediction into their resistance mechanism to colistin.

4.5 Materials and Methods

4.5.1 Bacterial Strain

A. baumannii strain AB5075 used throughout this study was sourced from the Manoil Lab (University of Washington, Seattle, USA). This strain was used for the evolution of CRMs and as the reference strain for all assays in this study. Stocks of the strain were grown on 20 mL of LB agar and incubated (Pendragon) for 24 hours at 37°c under aerobic conditions. This strain was chosen due to its extensive antibiotic resistance profile and superior virulence in comparison to other strains such as AB4857, AB5256, AB5711 and AB0057 (Jacobs ., 2014). Overnight cultures of AB5075, used in the assays below, were made using 5ml of Luria- Bertani (LB) broth (ThermoFisher), inoculated with a single colony of AB5075 and incubated at 37°C for 24 hours at 200 rpm.

4.5.2 Evolution of Colistin Resistant Mutants (CRM)

Three methods were used to evolve AB5075 isolates into colistin resistant mutants. For the first method, colistin agar plates, 20 mL of LB agar was treated with 20 µl of colistin at a concentration of 2.5 µg/mL and left to solidify in a petri dish. Once solid, 20 µl of AB5075 bacterial solution was made to an OD_{600} of 1, in a volume of 1 mL of LB broth, using AB5075 overnight culture. This was then spread onto the agar using a sterile bacterial cell spreader. The plates were incubated for 24 hours at 37°C. No CRMs were obtained using this method; this may be due to the sudden introduction of colistin to the bacteria.

The second method, liquid cultures, was employed to gradually introduce colistin to the bacteria (Mu *et al*., 2016). Five overnight cultures of AB5075 were treated with 0.5 µl of colistin at a concentration of 0.5 µg/mL and labelled before incubation. Following incubation, 10 µl of each culture was then added to fresh tubes containing 5 mL of LB broth and 1 µl of colistin at a concentration of 0.5 µg/mL and labelled correspondingly. This was then incubated in the same conditions. The concentration of colistin was doubled following each incubation period. Only 2 CRMs were obtained using this method, CRM2 and CRM3.

The third method, colistin agar tilt plates combine the gradual introduction of colistin

from the liquid culture's method with the quickness of the colistin agar plates method (Liu *et al*., 2011; Carsenti-Etesse *et al*., 1999). To begin 10 mL of LB agar was treated with 20 µl of colistin, at a concentration of 2.5 µg/mL; this was left to solidify in a petri dish under sterile conditions at a slant. Once solidified, 10 mL of LB agar was poured on top to level the slant and again left to solidify. Next, 20 µl of the overnight AB5075 culture, made to an OD_{600} of 1 in a volume of 1 mL of LB broth, was spread onto the agar using a sterile bacterial cell spreader. A uniform line was drawn on all tilt plates, and the colonies that grew above the line were considered potential CRMs. This was due to the tilted agar above the line containing colistin (2.5 µg/mL). Thus, colonies growing on this agar were considered resistant as they can grow in the presence of colistin. The plates were then incubated at 37°c for 24 hours. Following PCR species confirmation, these colonies were further validated as resistant using MIC assays.

The colistin treated LB agar slant provided a gradual increase in colistin. The top of the plate had the highest concentration of colistin, and the bottom of the plate had the lowest concentration of colistin. 68 CRMs were obtained using this method. Due to these assays taking place in a communal laboratory, there is a chance for contamination; thus these CRMs would need to be tested to ensure that they are *A. baumannii* bacteria. A colony polymerase chain reaction (PCR) and gel electrophoresis were used to test these CRMs.

4.5.3 PCR amplification of CRM Isolates

A colony PCR was used due to its convenient high-throughput method that removes the need for genomic extractions. KT25 2824 forward (2824-F: AAGGATCCCGTGGCGAATAGGGGAAAT) and reverse (2824-R: TTGAATTCTCAGGCAATTTCAGCGAT) primers, designed and provided by Dr. Ronan McCarthy to specifically target the gene *ABUW_2824* in *A. baumannii* AB5075, were used to identify AB5075 CRMs. The gene *ABUW 2824* is used as it encodes for a conserved protein in AB5075 and can therefore be used as confirmation of that species. For amplification of each suspected AB5075 CRM, the individual colonies were inoculated in 25 µl of PCR master mix containing 12.5 µl of DreamTaq Green PCR Master Mix (ThermoFisher), 1 µl of forward KT25

2824 (final concentration of 1 µm), 1 µl of reverse KT25 2824 (final concentration of 1µm), and 10.5 µl of nuclease-free water. Amplification of the DNA used a GeneAmp PCR System 9700 thermocycler machine (ThermoFisher) in the conditions outlined below.

Table 4.4: Thermocycling conditions.

Step	Temperature (°C)	Time	Number of Cycles
Initial Denaturation	95	10 mins	1
Denaturation	95	30 sec	30
Annealing	55	30 sec	30
Extension	72	1 min	30
Final Extension	72	10 mins	1

4.5.4 Agarose Gel Electrophoresis

To perform the gel electrophoresis, the electrophoresis chamber was filled with 1X TAE buffer and a 1% agarose gel made with 50 mL of 1X TAE buffer and 2.5 µl of Diamond Dye (ThermoFisher) was positioned so the wells are closer to the negative electrode. 3 µl of a 1-kilobase (KB) DNA HyperLadder (ThermoFisher) was added to the first well on both rows, and 10 µl of each PCR sample was then loaded into the remaining wells. A positive control containing AB5075 DNA was produced to check that the PCR was successful and to use as a band length comparator. A negative control containing no DNA was also produced to check for contamination in the PCR master mix. The electric field of the agarose gel electrophoresis tank was then set to 120 v and left to run for 40 minutes before imaging the gel using BadRad Bio-Imagers Gel-Doc system UV transilluminator (BioRad) and ImageLab software at an exposure time of 0.05 seconds.

4.5.5 Minimum Inhibitory Concentration (MIC) Testing

The lowest concentration of colistin required to inhibit the visible growth of the CRMs was determined using MIC assays (Andrews, 2001). This assay validated the CRMs resistance to colistin and determined their level of resistance. A single colony of each CRM was

was dissolved and grown overnight in 5 mL of LB broth, which was treated with 2.5 µg/mL of colistin to prevent the CRM from reverting. Additionally, a culture containing AB5075 wild type was also grown overnight; however, no colistin was added. Following this incubation period, the cultures were diluted in LB broth to get an OD_{600} suspension of 0.2 in a volume of 1 mL. The bacterial solutions were centrifuged at 6,000 rpm for 5 minutes in 1.5 mL Eppendorf tubes; they were then washed in 1 mL of phosphate-buffered saline (PBS). This washing procedure was repeated twice. The bacterial pellet produced was then resuspended in 1.2 mL of cation-adjusted Mueller Hinton broth (CAMHB). The dilution range of antibiotic was prepared in 1. 5 mL Eppendorf tubes, using a colistin stock solution of 50 mg/mL and CAMHB. The starting concentration of colistin in the range of dilution was 2500 µg/mL; this was diluted by ½ for a further 9 dilutions in CAMHB.

In order of highest to lowest dilution, 100 µl of the antibiotic solution was added to each well on a 96 well plate. Next, 100 µl of the washed CRM bacterial solutions were added to each well in rows 1-11. In the growth control, 100 µl of sterile CAMHB and 100 µl of the washed CRM bacterial solutions were added, and in the sterile control, 200 µl of sterile CAMHB was added. The 96 well plate was then incubated in a microplate reader, Clariostar Plus (BMG LabTech), at 37 °C, under aerobic conditions. A reading was taken every ten minutes for 12 hours at OD_{600}.

4.5.6 Testing the Bacteria's Fitness in the Presence and Absence of Colistin

The bacteria's fitness was tested to determine if the mutation causing colistin resistance was affecting the bacteria's ability to grow in the presence and absence of colistin. When tested in the presence of colistin, a concentration of 2 µg/mL was used as this was found to be the colistin MIC for AB5075 (EUCAST, 2017).

A single colony of each CRM was inoculated and grown overnight in 5 mL of LB broth, which was treated with the subMIC (1 µg/mL) of colistin, to maintain selective pressure and prevent the CRM from reverting. Additionally, a culture containing AB5075 wild type (WT) was also grown overnight; however, no colistin was added. Following this incubation period, the cultures were diluted in LB broth to get an OD_{600} suspension of 0.2 in a volume of 1 mL. The

bacterial solutions were centrifuged at 6,000 rpm for 5 minutes in 1.5 mL Eppendorf tubes; they were then washed in 1 mL of phosphate-buffered saline (PBS). This washing procedure was repeated twice. The bacterial pellet produced was then resuspended in 1 mL of cation adjusted Mueller Hinton broth (CAMHB). When testing the growth in the presence of colistin, a concentration of 2 µg/mL of colistin was added to the solution.

On a 96-well plate (Sarstedt), 100 µl of sterile CAMHB was added to the wells. The AB5075 WT and CRM bacterial solutions were then added to three wells each. Three wells were used as sterile controls and only contained 200 µl of CAMHB. The plate was then incubated at 37°C, under aerobic conditions in the microplate reader, Clariostar Plus (BMG LabTech), where a reading was taken every hour for 24 hours at OD_{600}. After 24 hours, the biofilm formation was determined by staining the same 96-well plate using the crystal violet method (O'Toole *et al.,* 2011). The protocol was modified by the washes being performed by pipetting and the staining being performed with 0.1% crystal violet. The absorbance of ethanol solubilised crystal violet was then read at 600 nm using a Clariostar Plus plate reader (BMG LabTech).

4.5.7 Virulence Testing in *Galleria mellonella*

G. mellonella (Live Foods Ltd), wax moths' larvae, was chosen as the model organism to test the virulence of the bacterial strains in this study. This was due to their observable characteristic of melanin production upon infection as a defence mechanism against various pathogens (Durieux ., 2021). The *G. mellonella* were considered dead when they were black in colour and did not respond to stimuli. *G. mellonella* were injected with AB5075 and CRMs to compare and assess the bacteria's virulence in this organism.

AB5075 WT and the CRMs were grown overnight in 5 mL of LB broth in a 37 °C incubator; the CRMs overnight cultures had 2.5 µg/mL of colistin added to the broth to prevent the bacteria from reverting. Following incubation, the cultures were diluted in PBS to an OD_{600} of 1 in a volume of 1 mL. They were then diluted by 1/10 for a further 3 dilutions in PBS, to get a concentration of 2.56 x 10^5 CFU/mL. 10 *G. mellonella* were placed in each petri dish. Ethanol was taken up into a Hamilton 25 µl syringe needle (Sigma-Aldrich) and left for 20

minutes to decontaminate. The ethanol was then removed, and sterile PBS was taken up and expelled twice. 10 µl of the 2.56 x 10^5 CFU/mL bacterial solution was then injected into 10 *G. mellonella*. The needle was washed with ethanol and PBS and cleaned using the nanowire in between every 10 injections. This injection method was repeated for all CRM bacterial solutions, also at a -3 dilution. As a negative control, to test for contamination, 10 µl of sterile PBS was injected into 10 *G. mellonella*. The petri dishes were labelled and placed in the 37 °C incubator for 24 hours before recording the survival rates of the *G. mellonella.*

4.5.8 Comparative Genomic Analysis

Genomic DNA extraction from CRM 1, 5, 9, and 38 was carried out using the Qiagen DNeasy Kit (Qiagen, Germantown, MD). Subsequently, the sample libraries were sent to SeqCenter (Pittsburgh, PA) and prepared with the Illumina DNA Prep kit, incorporating IDT 10 bp UDI indices, and subjected to sequencing on an Illumina NextSeq 2000, generating 2x151bp reads. The data underwent demultiplexing, quality control, and adapter trimming through bcl-convert (v 3.9.3). To identify mutations, the Breseq mapping pipeline was employed, with a set frequency threshold of 100% for variant identification against the complete reference genome of *A. baumannii* AB5075-UW (Genbank accession no. CP008706.1). The Breseq pipeline uses programs bowtie2 (V2.4.1) and R (V3.6.1) in order to identify polymorphism mutations. The parameters are outline in the Read Alignment Evidence table within each CRM HTML file (Appendix C.5).

4.5.9 Multiple Sequence Alignment Analysis

Sequence analysis involved the generation of multiple sequence alignments utilising CRM 5 and CRM 9 sequences against the complete reference genome of *A. baumannii* AB5075-UW (Genbank accession no. CP008706.1). The alignment process involved MUSCLE within the MEGA X software (Kumar., 2018). The sequences were then visualised with ESPript 3.0.

4.5.10 Characterising Mutations

The wildtype, CRM 1, 5, 9 and 38 sequences were translated with MEGA X and aligned with Muscle (within MEGA X). The structures were predicted with ColabFold (AlphaFold) and then visualised with ESPript 3.0. The domains and features were predicted using InterPro (Corroborated by aligning CRMs' PmrB sequences against sequences of other histidine kinases with characterised crystal structures (Refer to Appedix C.3 For MSA)). The HAMP domain was not predicted and was assumed to be between Transmembrane domain 2 and HisKA/DHp domain (Cociurovscaia *et al*., 2022). When predicting the tertiary structures of the CRMs and the wild-type the sequences were translated with MEGA X, the structures were predicted with ColabFold (AlphaFold), and visualised with PyMol. The structures were positioned using the 1st Alpha Helix as a reference point).

4.5.11 Structural Variation and Binding Affinity Analysis

The sequences were translated with MEGA X, the homodimer structures were then predicted with ColabFold (AlphaFold), the structures were superimposed and the RMSD values were calculated with PyMol. The binding affinity and dissociation constant values were calculated using PRODIGY, and the structures were visualised with PyMol. (Note the structures were positioned using the autophosphorylation histidine as a reference point).

4.5.12 RT-qPCR

AB5075, CRM 1, 5, 9 and 38 cells were grown in 20 ml LB to mid-exponential phase (OD_{600} 0.6). To preserve RNA integrity, the bacterial cells were then centrifuged and washed in RNAlater. The RNA was then isolated using the RNAeasy Kit with in-column DNAase treatment steps (Qiagen). After RNA extraction, the amount of RNA was quantified at A260 nm using a NanoDrop 2000/2000c (ThermoFisher). The purity of RNA was assessed using the ratio A260/A280. The primer BLAST software (Basic Local Alignment Search Tool) was used to design primer sequences for *pmrC* and *proC* qRT-PCR assay was performed using the Step One Plus system (Applied Biosciences). Each qPCR reaction was conducted in triplicates,

containing 75 nM of forward and reverse primers, 10 µl SYBR Green RT-PCR Master Mix, 1 µl ROX reference dye, 0.2 µl SYBR Green Reverse Transcriptase Mix (QuantiNova), and 300 ng of RNA. The qPCR samples were run at 50°C for 10 minutes for the reverse transcriptase step, and then at 95°C for 2 minutes for the PCR initial heat activation step. This was then followed by running the amplification template for 40 cycles, each cycle involving 5 s at 95°C for denaturation and 1 second at 60°C for the annealing and extension step. In order to quantify the expression of *pmrC,* we calculated the delta-delta Ct value, where the Ct values of *pmrC* were normalised to the expression of an endogenous control, *proC.* The normalised fold change was then calculated relative to the corresponding control sample. *proC* was chosen as the endogenous control gene as it is considered a housekeeping within AB5075 due to its consistent expression.

4.5.13 Statistics and Reproducibility

All assays were carried out in biological triplicate (n=3), with three technical repeats, individual data points are included in each graph. Analysis consisted of ANOVA tests comparing the treated samples with the respective carrier control. Average values ± S. D. are represented. Significance is indicated as ns = non-significant, * = $p \leq 0.05$, ** = $p \leq 0.01$, *** = $p \leq 0.001$, **** = $p \leq 0.0001$. Statistical analyses were performed using GraphPad Prism v10.0.3. For normally distributed data, parametric tests (one-way and two-way ANOVA) were applied. Post-hoc analyses included Šídák's multiple comparisons test and Tukey's multiple comparisons test to adjust for multiple comparisons. For survival analyses in *G. mellonella* assays, the Log-rank (Mantel-Cox) test and Gehan-Breslow-Wilcoxon test were used.

Chapter 5

Discussion

5.1 General Discussion

Since the discovery of the first antibiotic in 1928 (Smith and Coast, 2013), researchers have engaged in a continuous battle against bacterial infections. The emergence of MDR *A. baumannii* has rendered our once promising arsenal of antibiotics inadequate, highlighting the urgent necessity to advance our understanding of resistance and pursue the development of novel treatments. This thesis aims to expand our understanding of evolved resistance to colistin and the associated fitness costs. We also explore theoretical possibilities for the mechanism of colistin resistance mediated by known and novel mutations. Additionally, we contribute to enhancing our treatment options against colistin resistance *A. baumannii* by investigating the mechanisms of action of kaempferol, tormentil and the constituents of tormentil.

5.1.1 Challenging the mechanism of action of kaempferol

While undertaking this thesis, two highly relevant publications were published, validating our initial findings regarding kaempferol's role as a colistin potentiator and its ability to inhibit the growth of *A. baumannii* (Zhou *et al*., 2022; Zhong *et al*., 2023). However, both studies lacked an in-depth exploration of the underlying mechanism of kaempferol's action. Zhong *et al*. (2023) suggest that flavonoids such as 7,8-dihydroxyflavone, myricetin, and luteolin enhance colistin's activity by targeting iron homeostasis, inducting the reduction of ferric ions to the ferrous form, and deactivating PmrAB in *Salmonella*. Our study complements the findings of Zhou *et al*. (2022), who also demonstrate colistin potentiation. However, their research proposes that this effect is achieved through increased membrane permeability. Through extensive testing, we demonstrate this not to be the case and uncover a novel mechanism involving the disruption of iron homeostasis.

A long-term goal would be to explore the translational potential of the kaempferol and colistin combination *in vivo* using mice studies, considering dosage, safety, and efficacy. These studies could provide valuable insights into the clinical applicability of the kaempferol and colistin combination as a therapeutic strategy. Bacterial reliance on iron homeostasis to counter colistin treatment opens avenues for further research into metabolic vulnerabilities as potential targets for antimicrobial strategies. Previous studies have explored the role of synthetic siderophore-drug conjugates which are derivatives of bacterial iron acquisition siderophores that have been chemically linked to antibiotics. Additionally, other studies have investigated the use of gallium which is a non-functional iron analogue metal (Page., 2013). Gallium elicits its effects by being taken up by the bacteria instead of iron but not being of any use (Kelson *et al*., 2013; Chitambar., 2016; Chitambar 2016b). Additionally, the demonstration of colistin potentiation by iron-chelating compounds serves as a crucial starting point for future investigations aimed at overcoming intrinsic and acquired resistance mechanisms.

Kaempferol combined with colistin is demonstrated to be a potential strategy to combat colistin-resistant *A. baumannii* and *E. coli* clinical strains. Our study provides a potential solution to combat antibiotic resistance and introduces a novel avenue for potentiating colistin. By specifically targeting iron homeostasis and thereby modulating reactive oxygen species (ROS) balance, our research unveils a previously unexplored avenue in antimicrobial strategies. The combination between kaempferol and the sub-MIC of colistin was found to not completely re-sensitise colistin resistant *E. coli* strains WD101 and W3110pDM1 and also colistin resistant *A. baumannii* strains CDC-31 and CDC-35. This may be overcome by increasing the concentration of kaempferol in order to determine the optimal dosage combinations to re-sensitise the strains to colistin. However, this could suggest that there are other factors involved in mediating resistance in these strains that are not targeted by the antibacterial or antibiofilm effects of the combination of kaempferol and colistin. A potential challenge could be the insufficient entry of the treatment into the bacterial cells at the required amounts to induce cell death. This could be addressed by the implementation of a drug-delivery system designed to enhance the bioavailability and intracellular uptake of the treatment within the bacteria. A potential solution could include the use of nanoparticle-based carriers have been shown to facilitate targeted drug delivery, thus enhancing the antimicrobial activity of the treatment (Gao *et al*., 2018).

Our research contributes to the understanding of bacterial vulnerabilities, suggesting broader applications for molecules targeting ROS levels through Fenton's reaction within bacterial cells. Interestingly, conflicting literature reports that pre-treatment with kaempferol can block ROS production induced by arachidonic acid and iron, resulting in reduced hepatocyte death (Cho *et al*., 2019). In line with the findings from this study, it would be interesting to investigate whether the reported antioxidant activity of kaempferol, when used as a pre-treatment in bacteria cells, would affect its antibacterial activity when combined with colistin. This could be assessed by pre-treating the cells with kaempferol at varying time intervals before treating them with colistin, followed by assessing the susceptibility to colistin. Alternatively, we could treat the cells with the sub-MIC of colistin first and then treat them with kaempferol at varying time intervals to assess whether the antioxidant effects of kaempferol are reduced and consequently increase the susceptibility to colistin.

Our research highlights the importance of iron homeostasis in bacterial responses to colistin. Utilising an iron-binding compound, such as kaempferol, in clinical treatment of *A. baumannii* and *E. coli* infections would involve exploiting the difference in iron usage between humans and bacteria. Similarly, to humans, bacteria utilise iron for essential processes, such as growth and metabolism. However, during infection, the immune system alters iron metabolism to minimise iron bioavailability to below the optimal iron concentration for bacteria (Andrews *et al*., 2003). This occurs through increased iron storage, decreased iron release into the circulation, and reduced accessibility of extracellular nonheme iron and heme iron (Parrow *et al*., 2013). The iron-binding capability of kaempferol allows for the binding of free iron from the extracellular environment or from bacterial cells, possibly by targeting their siderophores for iron acquisition (Page., 2019). This allows kaempferol to compete with the bacteria for iron, exerting selective toxicity against the bacteria. This ultimately leads to the deprivation of essential iron from the bacteria, inhibiting bacterial growth and the ability to establish infection.

In this study, a notable strength lies in the strategic utilisation of high-throughput screening methods to evaluate an extensive array of compounds sourced from both the Caithness compound library and the Kew Gardens phytochemical library. This allowed for the broad exploration of potential antimicrobials, potentiators and anti-biofilm agents. The inclusion of known

antimicrobials in our screening assays, which consistently validated their expected effects in our experiments, strengthen the reliability and validity of our results. Additionally, we used a diverse range of techniques such as dRNA-Seq analysis, absorbance spectra, and membrane specific dyes which provided a comprehensive understanding of kaempferol's mechanism. By combining these methodologies, we were able to delve into the intricate details of kaempferol's effects.

In the broader context, our findings have significant implications for clinical practice. The observed reduction in colistin dosage achieved by incorporating kaempferol suggests promising prospects for enhancing patient outcomes. This reduction not only addresses concerns related to neurotoxicity and nephrotoxicity associated with current colistin doses but also underscores the potential for improved tolerability and safety in treatment. This prompts further exploration to extend the life expectancy of colistin as a therapeutic treatment against *A. baumannii* and *E. coli.*

5.1.2 Unveiling the mechanism of action of tormentil

Our understanding of tormentil's antimicrobial effects has been predominantly associated with its historical use in treating diarrhoea in both humans and animals (Koay *et al*., 2020; Kumari *et al*., 2021). Notably, the Committee on Herbal Medicinal Products (HMPC) of the European Medicines Agency (EMA) acknowledges the traditional use of *Potentilla erecta* (tormentil rhizome) in Europe for addressing wound infections, mild diarrhoea or minor oral mucosa inflammations based on extensive historical usage (EMA, 2021). Our research builds upon the historical use of tormentil for microbial infections by unveiling its potent antimicrobial and antibiofilm effects against *A. baumannii*. In doing so, we bridge the gap in our understanding of tormentil's mechanism of action, particularly concerning its unprecedented effects on *A. baumannii*. We also found that these antimicrobial effects were consistent across aerial and root segments from various regions of Ireland. HPLC analysis revealed that the extracts contained agrimoniin and ellagic acid, which both demonstrated antibacterial and antibiofilm properties when used as monotherapies. Delving into the novel mechanism of action, our transcriptomic analysis shed light on tormentil's impact on iron homeostasis in *A. baumannii*. Aside from the

antimicrobial and antibiofilm activity of tormentil and its constituents, we also found these compounds to be able to enhance the efficacy of colistin. This demonstrates the potential of tormentil and its constituents as standalone antimicrobials or colistin potentiators. This emphasises their versatility and promising therapeutic potential in combating MDR *A. baumannii*.

During our project, we encountered unexpected outcomes, specifically with the antibiofilm properties exhibited by certain tormentil extracts. Our data suggests that the potent antimicrobial effects may influence the classification of these extracts as true antibiofilm. The strong antimicrobial properties might inadvertently overshadow their specific antibiofilm effects, creating ambiguity in their categorisation. The antibiofilm effects may be maintained as the extracts may target biofilm-specific pathways that are distinct from those targeted by their antimicrobial properties. These biofilm-specific pathways may include prevention of adhesion to surfaces or quorum sensing. Furthermore, our dRNASeq analysis revealed distinct patterns for agrimoniin and ellagic acid, indicating that these two compounds likely employ different mechanisms of action in their antibiofilm activities. This suggests a more complex mechanism of action for the antibiofilm properties employed by agrimoniin and ellagic acid, as highlighted by the difference in biofilm-associated genes that were differently regulated in both data sets. The previously established link between iron availability and biofilm formation may also play a role in the antibiofilm effects of these compounds (Cook-Libin *et al.*, 2022). While dRNASeq analysis provides valuable insights, experimental validation is important to overcome challenges related to the biofilm assays and the potential influence of antimicrobial properties on these results. These methods can be developed further to allow for a more detailed exploration of mechanistic insights by using microscopy techniques, such as scanning electron microscopy (SEM) or confocal laser scanning microscopy (CLSM) to visualise the structure and thickness of the biofilms in the presence and absence of tormentil or its constituents.

Additionally, testing the impact of potential antibiofilm agents on established biofilms would broaden their potential therapeutic applications. Our study significantly contributes to scientific advancements by identifying the specific constituents of tormentil responsible for its antimicrobial and antibiofilm properties. The analysis of transcriptomics elucidates the

antimicrobial mechanism of action, focusing on iron homeostasis and stress response. This not only provides insights into potential therapeutic strategies but also enhances our understanding of tormentil's role in combating bacterial infections.

Our research addresses knowledge gaps regarding the impact of tormentil plant extract on *A. baumannii* growth, biofilm formation, and iron homeostasis. Our work establishes a connection between the identification of tormentil's antimicrobial properties, characterisation of its active components and exploration of their mechanisms of action. By doing so we highlight the importance of tormentil and its constituents in addressing the challenges posed by MDR *A. baumannii*. We also contribute to findings within the field of new-generation purpose-designed antimicrobial iron chelating compounds.

A long-term goal involves conducting a more detailed analysis of the relationship between the antimicrobial and antibiofilm effects of tormentil and its constituents. One approach could be to knock out genes associated with either antimicrobial or antibiofilm activity and assess whether the other activity still occurs or occurs to the same extent. To do so we could identify the target genes potentially involved in tormentil and its constituent antimicrobial or antibiofilm activity, such as *bfr*, and generate mutant strains using genome editing methods for *A. baumannii* (De Dios *et al*., 2022) or CRISPR/Cas9 to disrupt gene functions. These strains would then be validated using PCR or gene sequencing to confirm the disruption of the target genes in the mutant strains. We could then evaluate the antimicrobial activity of tormentil and its constituents against the mutant strains with the genes associated with antibiofilm activity disrupted. Similarly, we could evaluate the antibiofilm activity against the mutant strains lacking function in the genes associated with antimicrobial activity. Together, these findings would allow us to identify any correlations between the target genes associated with the antimicrobial and antibiofilm effects of tormentil and its constituents. This knowledge could be used to guide further research into tormentil and its constituent's activity and also to identify potential therapeutic targets for combating MDR *A. baumannii* infections. Furthermore, exploring the mechanism of action of tormentil's activity against other ESKAPE pathogens and comparing it to its mechanism of action against *A. baumannii* holds promise. This comparative analysis could unveil its potential as a broad-spectrum antimicrobial, building

upon its already known effects against *S. aureus* and *H. pylori.* This could also identify common targets or pathways that tormentil affects across different bacterial species, allowing for a deeper understanding of the potentially conserved mechanism of tormentils activity. Another route into the exploration of tormentil activity against MDR *A. baumannii* could involve identifying novel components within the extracts that may be contributing to the antimicrobial or antibiofilm effects displayed. This exploration could involve the use of fractionation testing using HPLC, which would allow for each fraction to be tested for its bioactivity. This could provide a systematic way of identifying each component which contributes to the antimicrobial or antibiofilm effects of tormentil (Mani *et al*., 2022). To complement this, nuclear magnetic resonance (NMR) could be used to identify the structure of novel components within the extracts and then a similar pipline used throughout this thesis, of quantification of bioactivity and identification of the mechanism of action using RNASeq, can be followed.

5.1.3 The fitness costs of known and novel colistin resistance mutants

The general dogma associated with the gain of colistin resistance is that there is an impact on bacterial fitness (Da Silva and Domingues, 2017). However, conflicting evidence (Dunrante-Mangoni *et al*., 2015; Wand *et al*., 2015) introduces a more nuanced and strain-specific relationship between colistin resistance, fitness, and virulence. Our study significantly contributes to this discussion by establishing a consistent genetic background for all 50 CRMs with a MIC of 8 µg/mL or higher. In our investigation, we observed fitness trade-offs in the growth rates of CRMs. Those with a high MIC (>120 µg/mL) displayed less impacted growth rates in the presence of colistin compared to the wild type in the absence of the antibiotic. Conversely, CRMs with low MICs (<70 µg/mL) exhibited varying growth rates in the presence of colistin. Furthermore, our findings unveiled that 64% of the CRMs demonstrate increased biofilm formation in the presence of colistin, indicating a potential adaptive strategy to evade antibiotic effects. Assessing virulence, we identified an 84% reduction in virulence among CRMs compared to the wild-type, suggesting a trade-off between resistance gain and virulence.

Further analysis using genomic sequencing revealed both known and potentially novel mutations in *pmrB*, a gene associated with colistin resistance.

Our findings align with existing literature, demonstrating the impact of colistin resistance evolution on bacterial fitness, consistent with studies by López-Rojas *et al*. (2013), Hraiech *et al*. (2013), and Rolain *et al*. (2011). Importantly, our research delves deeper, revealing diverse fitness costs associated with distinct mutations in colistin-resistant *A. baumannii.* Through comprehensive bioinformatic analysis, we contribute valuable insights into both known and novel mutations, enhancing our understanding of colistin resistance mechanisms and their downstream effects. This data underscores the impact of specific mutations on different aspects of bacterial fitness, such as growth, virulence and biofilm formation. This cohesive narrative establishes a clear link between the evolution of colistin resistance and the various fitness costs.

This study provides novelty in assessing the fitness cost of evolved resistance as all the CRMs have the same genetic background ensuring uniformity and consistency in the genetic makeup of the CRMs. This minimises the genetic variations, such as differences in strains, that could introduce cofounding factors, allowing for more reliable and reproducible results. This also offers a more accurate comparison between the CRMs since they share the same baseline genetic information, allowing the direct effects of resistance mechanisms to be assessed without the influence of genetic diversity.

This study demonstrates the successful generation of 50 CRMs that were able to maintain their resistance and the comprehensive evaluation of their fitness. We were also able to evolve CRMs with known colistin resistance mutants, providing validation to the evolution methods used to generate our CRMs. This method was also able to evolve two CRMs with a novel mutation. However, the two CRMs (CRM 1 and 2) may introduce potential biases as they were evolved using liquid cultures, an alternative evolution method from the other forty-eight CRMs which were evolved using tilt plate methods. This is because the liquid culture method involves subjecting the cultures to higher amounts of colistin over time, essentially selecting for certain traits over multiple generations. This may selectively favour certain traits over multiple generations, introducing a potential experimental bias. This emphasises the importance of

cautious interpretation when comparing results from these two subsets of CRMs.

An additional limitation arises from the initial generation of over 100 CRMs during the evolution stages, where a significant portion failed to maintain their resistance, reverting to susceptibility to colistin. This resulted in the final selection of 50 CRMs for further analysis, potentially introducing a selection bias, as the chosen subset may not fully represent the diversity of the initial CRM population. This limitation could potentially be overcome by sequencing the CRMs directly from the tilt plates in order to prevent them from reverting over time.

Our study contributes to the field by shedding light on the diverse fitness costs linked to the well-documented R263H mutation (Lim *et al*., 2015) and a potentially novel duplication mutation associated with colistin resistance. It should be considered that the novel duplication mutation may have emerged in response to the specific environmental conditions within the laboratory or due to the selective pressure of colistin in agar in an *in vitro* assay. Additionally, the fitness cost associated with this mutation may affect the prevalence and persistence within clinical or laboratory settings, causing a lack of previous detection. The identification of a novel resistance mutation highlights the diversity of colistin resistance mechanisms, emphasising the ongoing emergence of the evolution of colistin resistance.

A long-term objective involves a comprehensive exploration of mutations accompanying PmrB mutations in the CRMs. This can be achieved by lowering the frequency threshold for variant identification below 100% and manually confirming the mutations by aligning the affected genes to the wild-type sequence. The effects of these mutations on colistin resistance will be systematically investigated through a series of experiments depending on the type of mutation. For example, if the gene mutation increases the function of the encoded protein, we can knock that gene out and determine its effects on colistin resistance by reassessing the colistin MIC. Similarly, this same method can be used to investigate the specific involvement of identified genes in affecting the fitness of the CRMs. Furthermore, it would be beneficial to investigate the variations in fitness observed between CRMs 1 and 38. Despite both being predicted to harbour the same R263H colistin-resistance mechanism, their distinct fitness costs suggest potential differences arising from the evolution methods employed in their generation.

5.2 Conclusion

Overall, this project addresses the gap in knowledge between evolving colistin resistance and the associated fitness costs and explores potential strategies to disrupt resistance mechanisms using phytochemicals (Figure 5.1). The comprehensive profiling of 50 CRMs with consistent genetic backgrounds provides valuable insights into the intricate relationship between resistance, fitness, and virulence. Our findings reveal strain-specific fitness trade-offs, biofilm formation variations, and reduced virulence, contributing to the understanding of evolved resistance. Our investigation into kaempferol and tormentil unveils promising antimicrobial and antibiofilm properties against multidrug-resistant *A. baumannii*. Kaempferol's role as a colistin potentiator that has a disruptive impact on iron homeostasis, introduces a novel mechanism of action. Tormentil and its constituents emerge as a potent antimicrobial with significant implications for combating *A. baumannii* also by affecting iron homeostasis, introduces a novel mechanism of action. The potential translational impact of kaempferol, tormentil, and insights into fitness costs in CRMs could impact treatment approaches for colistin-resistant bacterial infections. These findings can ultimately contribute to the development of safer, more effective, and targeted therapies to address the challenges posed by antibiotic resistance in clinical settings.

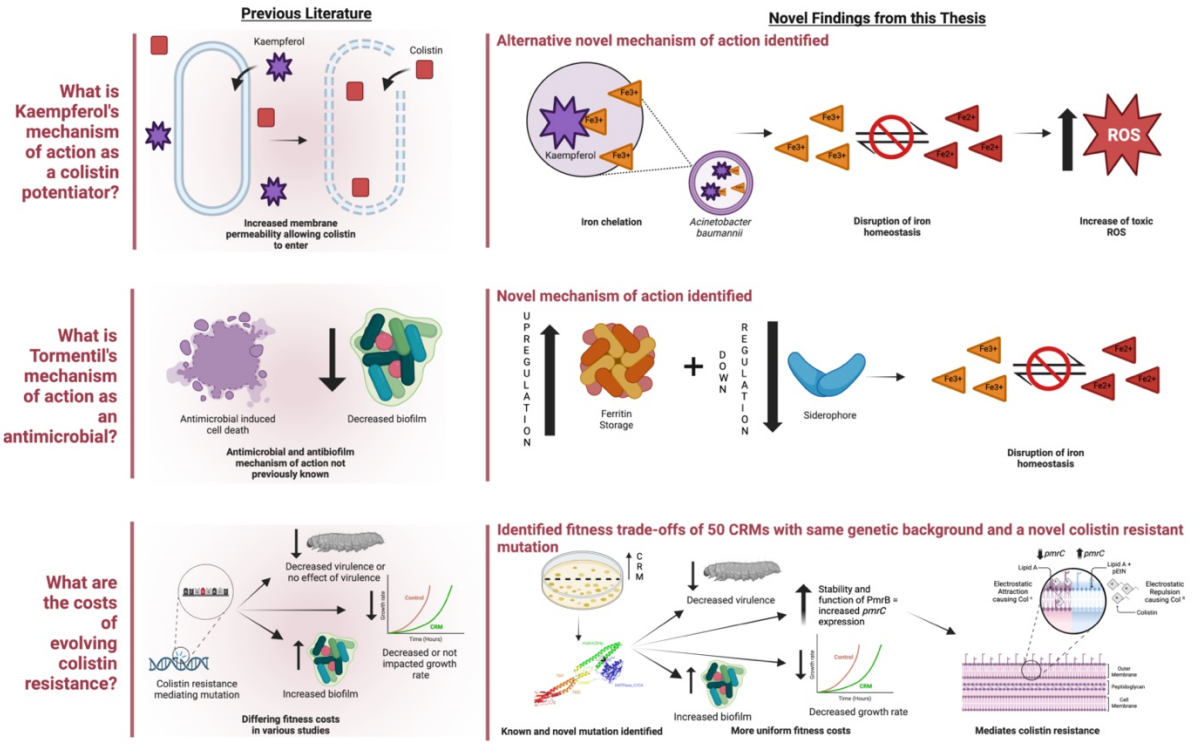

Figure 5.1: Summary of what this work has contributed to the field of evolved colistin resistance and disrupting the colistin resistance mechanisms. Comparison between previous literature (left side of the figure, in red shade) and novel findings (right side of the figure). 1. What is kaempferol's mechanism of action as a colistin potentiator? – previously Zhou *et al* (2022) suggested that increased permeability of the cell wall potentiates colistin. From this work, we suggest that kaempferol disrupts iron homeostasis, exposing a metabolic vulnerability that colistin can exploit. 2. What is tormentil's mechanism of action as an antimicrobial? – the mechanism of action is previously unknown; this work uncovers disruption of iron homeostasis as the mechanism of action. 3. What are the costs of evolving colistin resistance? – Various studies have identified conflicting fitness costs. This work identifies uniform fitness costs of decreased growth rate for CRMs with low MIC (<70 µg/mL) and increased growth rate for CRMs with high MIC (>120 µg /mL) in the presence of colistin, a decreased virulence and increased biofilm formation in the presence of colistin. Additionally, we explore the fitness costs of a known and novel colistin-mediating mutation.

References

Acosta, J. *et al.* (2011) 'Multidrug-Resistant *Acinetobacter baumannii* Harboring OXA-24 Carbapenemase, Spain', *Emerging Infectious Diseases*, 17(6), pp. 1064–1067. Available at: https://doi.org/10.3201/eid1706.091866.

Adams, M.D. *et al.* (2009) 'Resistance to Colistin in *Acinetobacter baumannii* Associated with Mutations in the PmrAB Two-Component System', *Antimicrobial Agents and Chemotherapy*, 53(9), pp. 3628–3634. Available at: https://doi.org/10.1128/AAC.00284-09.

Afzal-Shah, M., Woodford, N. and Livermore, D.M. (2001) 'Characterization of OXA-25, OXA-26, and OXA-27, Molecular Class D β-Lactamases Associated with Carbapenem Resistance in Clinical Isolates of *Acinetobacter baumannii*', *Antimicrobial Agents and Chemotherapy*, 45(2), pp. 583–588. Available at: https://doi.org/10.1128/AAC.45.2.583-588.2001.

Ahmad, T.A. *et al.* (2016) 'Development of immunization trials against *Acinetobacter baumannii*', *Trials in Vaccinology*, 5, pp. 53–60. Available at: https://doi.org/10.1016/j.trivac.2016.03.001.

Ahmed, S.A.K.S. *et al.* (2019) 'Natural quorum sensing inhibitors effectively downregulate gene expression of *Pseudomonas aeruginosa* virulence factors', *Applied Microbiology and Biotechnology*, 103(8), pp. 3521–3535. Available at: https://doi.org/10.1007/s00253-019-09618-0.

Aiello, D. *et al.* (2010) 'Discovery and characterization of inhibitors of *Pseudomonas aeruginosa* type III secretion', *Antimicrobial Agents and Chemotherapy*, 54(5), pp. 1988–1999. Available at: https://doi.org/10.1128/AAC.01598-09.

Ajiboye, T.O., Skiebe, E. and Wilharm, G. (2018) 'Contributions of ferric uptake regulator Fur to the sensitivity and oxidative response of *Acinetobacter baumannii* to antibiotics', *Microbial Pathogenesis*, 119, pp. 35–41. Available at: https://doi.org/10.1016/j.micpath.2018.03.060.

Al-Agamy, M.H. *et al.* (2017) 'First Detection of GES-5 Carbapenemase-Producing *Acinetobacter baumannii* Isolate', *Microbial Drug Resistance (Larchmont, N.Y.)*, 23(5), pp. 556–562. Available at: https://doi.org/10.1089/mdr.2016.0152.

Al-Dahmoshi, H.O.M., Al-Khafaji, N.S.K. and Al-Alaq, F.T. (2020) *Virulence and Antibiotic Resistance of Acinetobacter baumannii among Urinary Tract Infections*, *Urinary Tract Infection and Nephropathy - Insights into Potential Relationship*. IntechOpen. Available at: https://doi.org/10.5772/intechopen.94508.

Alam, W. *et al.* (2020) 'Kaempferol as a Dietary Anti-Inflammatory Agent: Current Therapeutic Standing', *Molecules*, 25(18), p. 4073. Available at: https://doi.org/10.3390/molecules25184073.

Ali, A.M. *et al.* (2000) 'Antiviral, cytotoxic and antimicrobial activities of anthraquinones isolated from the roots of morinda elliptica', *Pharmaceutical Biology*, 38(4), pp. 298–301. Available at: https://doi.org/10.1076/1388-0209(200009)3841-AFT298.

Almasaudi, S.B. (2018) '*Acinetobacter* spp. as nosocomial pathogens: Epidemiology and resistance features', *Saudi Journal of Biological Sciences*, 25(3), pp. 586–596. Available at: https://doi.org/10.1016/j.sjbs.2016.02.009.

Alonso, C.D. and Mahoney, M.V. (2018) 'Bezlotoxumab for the prevention of Clostridium difficile infection: a review of current evidence and safety profile', *Infection and Drug Resistance*, 12, pp. 1–9. Available at: https://doi.org/10.2147/IDR.S159957.

Aly, M.M. *et al.* (2016) 'High prevalence of the PER-1 gene among carbapenem-resistant *Acinetobacter baumannii* in Riyadh, Saudi Arabia', *European Journal of Clinical Microbiology & Infectious Diseases: Official Publication of the European Society of Clinical Microbiology*, 35(11), pp. 1759–1766. Available at: https://doi.org/10.1007/s10096-016-2723-8.

Amanatidou, E. *et al.* (2019) 'Biofilms facilitate cheating and social exploitation of β-lactam resistance in *Escherichia coli*', *npj Biofilms and Microbiomes*, 5(1), pp. 1–10. Available at: https://doi.org/10.1038/s41522-019-0109-2.

Aminov, R. (2010) 'A Brief History of the Antibiotic Era: Lessons Learned and Challenges for the Future', *Frontiers in Microbiology*, 1. Available at: https://www.frontiersin.org/articles/10.3389/fmicb.2010.00134 (Accessed: 5 October 2023).

Amiri, G. *et al.* (2019) 'Determination of imipenem efflux-mediated resistance in Acinetobacter spp., using an efflux pump inhibitor', *Iranian Journal of Microbiology*, 11(5), pp. 368–372.

Anandan, A. *et al.* (2017) 'Structure of a lipid A phosphoethanolamine transferase suggests how conformational changes govern substrate binding', *Proceedings of the National Academy of Sciences of the United States of America*, 114(9), pp. 2218–2223. Available at: https://doi.org/10.1073/pnas.1612927114.

Anantharajah, A. *et al.* (2017) 'Salicylidene Acylhydrazides and Hydroxyquinolines Act as Inhibitors of Type Three Secretion Systems in *Pseudomonas aeruginosa* by Distinct Mechanisms', *Antimicrobial Agents and Chemotherapy*, 61(6), pp. e02566-16. Available at: https://doi.org/10.1128/AAC.02566-16.

Andersen, J.B. *et al.* (2021) 'Identification of small molecules that interfere with c-di-GMP signaling and induce dispersal of *Pseudomonas aeruginosa* biofilms', *npj Biofilms and Microbiomes*, 7(1), pp. 1–13. Available at: https://doi.org/10.1038/s41522-021-00225-4.

Andersson, D.I. (2003) 'Persistence of antibiotic resistant bacteria', *Current Opinion in Microbiology*, 6(5), pp. 452–456. Available at: https://doi.org/10.1016/j.mib.2003.09.001.

Andrade, F.F. *et al.* (2020) 'Colistin Update on Its Mechanism of Action and Resistance, Present and Future Challenges', *Microorganisms*, 8(11), p. 1716. Available at: https://doi.org/10.3390/microorganisms8111716.

Andrews, J.M. (2001) 'Determination of minimum inhibitory concentrations', *Journal of Antimicrobial Chemotherapy*, 48(suppl_1), pp. 5–16. Available at: https://doi.org/10.1093/jac/48.suppl_1.5.

Andrews, S.C., Robinson, A.K. and Rodríguez-Quiñones, F. (2003) 'Bacterial iron homeostasis', *FEMS microbiology reviews*, 27(2–3), pp. 215–237. Available at: https://doi.org/10.1016/S0168-6445(03)00055-X.

Antoniani, D. *et al.* (2013) 'The immunosuppressive drug azathioprine inhibits biosynthesis of the bacterial signal molecule cyclic-di-GMP by interfering with intracellular nucleotide pool availability', *Applied Microbiology and Biotechnology*, 97(16), pp. 7325–7336. Available at:

https://doi.org/10.1007/s00253-013-4875-0.

Armstrong, G.L., Conn, L.A. and Pinner, R.W. (1999) 'Trends in Infectious Disease Mortality in the United States During the 20th Century', *JAMA*, 281(1), pp. 61–66. Available at: https://doi.org/10.1001/jama.281.1.61.

Arroyo, L.A. *et al.* (2011) 'The pmrCAB Operon Mediates Polymyxin Resistance in *Acinetobacter baumannii* ATCC 17978 and Clinical Isolates through Phosphoethanolamine Modification of Lipid A', *Antimicrobial Agents and Chemotherapy*, 55(8), pp. 3743–3751. Available at: https://doi.org/10.1128/aac.00256-11.

Asif, M., Alvi, I.A. and Rehman, S.U. (2018) 'Insight into *Acinetobacter baumannii*: pathogenesis, global resistance, mechanisms of resistance, treatment options, and alternative modalities', *Infection and Drug Resistance*, 11, pp. 1249–1260. Available at: https://doi.org/10.2147/IDR.S166750.

Asokan, G.V. *et al.* (2019) 'WHO Global Priority Pathogens List: A Bibliometric Analysis of Medline-PubMed for Knowledge Mobilization to Infection Prevention and Control Practices in Bahrain', *Oman Medical Journal*, 34(3), pp. 184–193. Available at: https://doi.org/10.5001/omj.2019.37.

Atanasov, A.G. *et al.* (2015) 'Discovery and resupply of pharmacologically active plant-derived natural products: A review', *Biotechnology Advances*, 33(8), pp. 1582–1614. Available at: https://doi.org/10.1016/j.biotechadv.2015.08.001.

Atkinson, S. *et al.* (2011) 'Biofilm Development on Caenorhabditis elegans by Yersinia Is Facilitated by Quorum Sensing-Dependent Repression of Type III Secretion', *PLOS Pathogens*, 7(1), p. e1001250. Available at: https://doi.org/10.1371/journal.ppat.1001250.

Ayukekbong, J.A., Ntemgwa, M. and Atabe, A.N. (2017) 'The threat of antimicrobial resistance in developing countries: causes and control strategies', *Antimicrobial Resistance & Infection Control*, 6(1), p. 47. Available at: https://doi.org/10.1186/s13756-017-0208-x.

Azarnia Tehran, D. *et al.* (2015) 'A Novel Inhibitor Prevents the Peripheral Neuroparalysis of Botulinum Neurotoxins', *Scientific Reports*, 5(1), p. 17513. Available at: https://doi.org/10.1038/srep17513.

Babinski, K.J., Kanjilal, S.J. and Raetz, C.R.H. (2002) 'Accumulation of the Lipid A Precursor UDP-2,3-diacylglucosamine in an *Escherichia coli* Mutant Lacking the lpxH Gene *', *Journal of Biological Chemistry*, 277(29), pp. 25947–25956. Available at: https://doi.org/10.1074/jbc.M204068200.

Bailey, L. *et al.* (2007) 'Small molecule inhibitors of type III secretion in Yersinia block the Chlamydia pneumoniae infection cycle', *FEBS letters*, 581(4), pp. 587–595. Available at: https://doi.org/10.1016/j.febslet.2007.01.013.

Bakour, S. *et al.* (2014) 'Characterization of *Acinetobacter baumannii* clinical isolates carrying bla(OXA-23) carbapenemase and 16S rRNA methylase armA genes in Yemen', *Microbial Drug Resistance (Larchmont, N.Y.)*, 20(6), pp. 604–609. Available at: https://doi.org/10.1089/mdr.2014.0018.

Balaban, N.Q. *et al.* (2004) 'Bacterial Persistence as a Phenotypic Switch', *Science*, 305(5690), pp. 1622–1625. Available at: https://doi.org/10.1126/science.1099390.

Bales, P.M. *et al.* (2013) 'Purification and Characterization of Biofilm-Associated EPS Exopolysaccharides from ESKAPE Organisms and Other Pathogens', *PLOS ONE*, 8(6), p. e67950. Available at: https://doi.org/10.1371/journal.pone.0067950.

Banar, M. *et al.* (2016) 'Evaluation of Mannosidase and Trypsin Enzymes Effects on Biofilm Production of *Pseudomonas aeruginosa* Isolated from Burn Wound Infections', *PLoS ONE*, 11(10), p. e0164622. Available at: https://doi.org/10.1371/journal.pone.0164622.

Bandeira Junior, G. *et al.* (2018) 'Antibacterial potential of phytochemicals alone or in combination with antimicrobials against fish pathogenic bacteria', *Journal of Applied Microbiology*, 125(3), pp. 655–665. Available at: https://doi.org/10.1111/jam.13906.

Baquero, F. and Levin, B.R. (2021) 'Proximate and ultimate causes of the bactericidal action of antibiotics', *Nature Reviews Microbiology*, 19(2), pp. 123–132. Available at: https://doi.org/10.1038/s41579-020-00443-1.

Barbieri, R. *et al.* (2017) 'Phytochemicals for human disease: An update on plant-derived compounds antibacterial activity', *Microbiological Research*, 196, pp. 44–68. Available at: https://doi.org/10.1016/j.micres.2016.12.003.

Barraud, N. *et al.* (2009) 'Nitric oxide-mediated dispersal in single- and multi-species biofilms of clinically and industrially relevant microorganisms', *Microbial Biotechnology*, 2(3), pp. 370–378. Available at: https://doi.org/10.1111/j.1751-7915.2009.00098.x.

Barraud, N. *et al.* (2015) 'Nitric oxide: a key mediator of biofilm dispersal with applications in infectious diseases', *Current Pharmaceutical Design*, 21(1), pp. 31–42. Available at: https://doi.org/10.2174/1381612820666140905112822.

Bartholomew, T.L. *et al.* (2019) '2-Hydroxylation of *Acinetobacter baumannii* Lipid A Contributes to Virulence', *Infection and Immunity*, 87(4). Available at: https://doi.org/10.1128/IAI.00066-19.

Bartlett, J.G., Gilbert, D.N. and Spellberg, B. (2013) 'Seven ways to preserve the miracle of antibiotics', *Clinical Infectious Diseases: An Official Publication of the Infectious Diseases Society of America*, 56(10), pp. 1445–1450. Available at: https://doi.org/10.1093/cid/cit070.

Bartling, C.M. and Raetz, C.R.H. (2009) 'Crystal structure and acyl chain selectivity of *Escherichia coli* LpxD, the N-acyltransferase of lipid A biosynthesis', *Biochemistry*, 48(36), pp. 8672–8683. Available at: https://doi.org/10.1021/bi901025v.

Barua, C.C. and Yasmin, N. (2018) '*Potentilla fulgens*: A Systematic Review on Traditional Uses, Pharmacology and Phytochemical Study with Reference to Anticancer Activity', *Journal of Natural Products and Resources*, pp. 162–170. Available at: https://doi.org/10.30799/jnpr.058.18040103.

Beceiro, A. *et al.* (2011) 'Phosphoethanolamine modification of lipid A in colistin-resistant variants of *Acinetobacter baumannii* mediated by the pmrAB two-component regulatory system', *Antimicrobial Agents and Chemotherapy*, 55(7), pp. 3370–3379. Available at: https://doi.org/10.1128/AAC.00079-11.

Beceiro, A. *et al.* (2014) 'Biological Cost of Different Mechanisms of Colistin Resistance and Their Impact on Virulence in *Acinetobacter baumannii*', *Antimicrobial Agents and Chemotherapy*, 58(1), p. 518. Available at: https://doi.org/10.1128/AAC.01597-13.

Behera, P. *et al.* (2013) 'Anti-Inflammatory and Anti-Microbial Activity of Chalcone from Dalbergia Sissoo Roxb. leaves', *American Journal of Phytomedicine and Clinical Therapeutics*, 1, pp. 186–194.

Beheshti, M. *et al.* (2020) 'Tetracycline resistance mediated by tet efflux pumps in clinical isolates of *Acinetobacter baumannii*', *Revista do Instituto de Medicina Tropical de São Paulo*, 62, p. e88. Available at: https://doi.org/10.1590/S1678-9946202062088.

Bergogne-Bérézin, E. and Towner, K.J. (1996) 'Acinetobacter spp. as nosocomial pathogens: microbiological, clinical, and epidemiological features', *Clinical Microbiology Reviews*, 9(2), pp. 148–165. Available at: https://doi.org/10.1128/CMR.9.2.148.

Bernards, A.T. *et al.* (2004) 'Persistent *Acinetobacter baumannii*? Look inside your medical equipment', *Infection Control and Hospital Epidemiology*, 25(11), pp. 1002–1004. Available at: https://doi.org/10.1086/502335.

Bhargava, N. *et al.* (2015) 'Attenuation of quorum sensing-mediated virulence of *Acinetobacter baumannii* by Glycyrrhiza glabra flavonoids', *Future Microbiology*, 10(12), pp. 1953–1968. Available at: https://doi.org/10.2217/fmb.15.107.

Biglari, S. *et al.* (2017) 'Antimicrobial Resistance Mechanisms and Genetic Diversity of Multidrug-Resistant *Acinetobacter baumannii* Isolated from a Teaching Hospital in Malaysia', *Microbial Drug Resistance (Larchmont, N.Y.)*, 23(5), pp. 545–555. Available at: https://doi.org/10.1089/mdr.2016.0130.

Bogaerts, P. *et al.* (2010) 'GES Extended-Spectrum β-Lactamases in *Acinetobacter baumannii* Isolates in Belgium', *Antimicrobial Agents and Chemotherapy*, 54(11), pp. 4872–4878. Available at: https://doi.org/10.1128/AAC.00871-10.

Boinett, C.J. *et al.* (2019) 'Clinical and laboratory-induced colistin-resistance mechanisms in *Acinetobacter baumannii*', *Microbial Genomics*, 5(2), p. e000246. Available at: https://doi.org/10.1099/mgen.0.000246.

Boll, J.M. *et al.* (2015) 'Reinforcing Lipid A Acylation on the Cell Surface of *Acinetobacter baumannii* Promotes Cationic Antimicrobial Peptide Resistance and Desiccation Survival', *mBio*, 6(3), pp. e00478-15. Available at: https://doi.org/10.1128/mBio.00478-15.

Boll, J.M. *et al.* (2016) 'A penicillin-binding protein inhibits selection of colistin-resistant, lipooligosaccharide-deficient *Acinetobacter baumannii*', *Proceedings of the National Academy of Sciences*, 113(41), pp. E6228–E6237. Available at: https://doi.org/10.1073/pnas.1611594113.

Bonnin, R.A. *et al.* (2011) 'PER-7, an Extended-Spectrum β-Lactamase with Increased Activity toward Broad-Spectrum Cephalosporins in *Acinetobacter baumannii* ▿ ', *Antimicrobial Agents and Chemotherapy*, 55(5), pp. 2424–2427. Available at: https://doi.org/10.1128/AAC.01795-10.

Borges, A. *et al.* (2016) 'New Perspectives on the Use of Phytochemicals as an Emergent Strategy to Control Bacterial Infections Including Biofilms', *Molecules*, 21(7), p. 877. Available at: https://doi.org/10.3390/molecules21070877.

Bou, G. *et al.* (2000) 'Characterization of a Nosocomial Outbreak Caused by a Multiresistant *Acinetobacter baumannii* Strain with a Carbapenem-Hydrolyzing Enzyme: High-Level Carbapenem

Resistance in *A. baumannii* Is Not Due Solely to the Presence of β-Lactamases', *Journal of Clinical Microbiology*, 38(9), pp. 3299–3305.

Boucher, H.W. *et al.* (2009) 'Bad Bugs, No Drugs: No ESKAPE! An Update from the Infectious Diseases Society of America', *Clinical Infectious Diseases*, 48(1), pp. 1–12. Available at: https://doi.org/10.1086/595011.

Bové, M. *et al.* (2021) 'The Quorum-Sensing Inhibitor Furanone C-30 Rapidly Loses Its Tobramycin-Potentiating Activity against *Pseudomonas aeruginosa* Biofilms during Experimental Evolution', *Antimicrobial Agents and Chemotherapy*, 65(7), pp. e00413-21. Available at: https://doi.org/10.1128/AAC.00413-21.

Bowler, P., Murphy, C. and Wolcott, R. (2020) 'Biofilm exacerbates antibiotic resistance: Is this a current oversight in antimicrobial stewardship?', *Antimicrobial Resistance & Infection Control*, 9(1), p. 162. Available at: https://doi.org/10.1186/s13756-020-00830-6.

Bowlin, N.O. *et al.* (2014) 'Mutations in the *Pseudomonas aeruginosa* needle protein gene pscF confer resistance to phenoxyacetamide inhibitors of the type III secretion system', *Antimicrobial Agents and Chemotherapy*, 58(4), pp. 2211–2220. Available at: https://doi.org/10.1128/AAC.02795-13.

Brackman, G. and Coenye, T. (2015) 'Quorum sensing inhibitors as anti-biofilm agents', *Current Pharmaceutical Design*, 21(1), pp. 5–11. Available at: https://doi.org/10.2174/1381612820666140905114627.

Brackman, G. *et al.* (2011) 'Structure-Activity Relationship of Cinnamaldehyde Analogs as Inhibitors of AI-2 Based Quorum Sensing and Their Effect on Virulence of Vibrio spp', *PLOS ONE*, 6(1), p. e16084. Available at: https://doi.org/10.1371/journal.pone.0016084.

Bradley, J.M. *et al.* (2020) 'Bacterial iron detoxification at the molecular level', *Journal of Biological Chemistry*, 295(51), pp. 17602–17623. Available at: https://doi.org/10.1074/jbc.REV120.007746.

Brannon, J.R. and Hadjifrangiskou, M. (2016) 'The arsenal of pathogens and antivirulence therapeutic strategies for disarming them', *Drug Design, Development and Therapy*, 10, pp. 1795–1806. Available at: https://doi.org/10.2147/DDDT.S98939.

Breines, D.M. and Burnham, J.C. (1994) 'Modulation of *Escherichia coli* type 1 fimbrial expression and adherence to uroepithelial cells following exposure of logarithmic phase cells to quinolones at subinhibitory concentrations', *The Journal of Antimicrobial Chemotherapy*, 34(2), pp. 205–221. Available at: https://doi.org/10.1093/jac/34.2.205.

Brossard, K.A. and Campagnari, A.A. (2012) 'The *Acinetobacter baumannii* Biofilm-Associated Protein Plays a Role in Adherence to Human Epithelial Cells', *Infection and Immunity*, 80(1), pp. 228–233. Available at: https://doi.org/10.1128/iai.05913-11.

Brotfain, E. *et al.* (2017) 'Multidrug Resistance Acinetobacter Bacteremia Secondary to Ventilator-Associated Pneumonia: Risk Factors and Outcome', *Journal of Intensive Care Medicine*, 32(9), pp. 528–534. Available at: https://doi.org/10.1177/0885066616632193.

Cafiso, V. *et al.* (2019) 'Colistin Resistant *A. baumannii*: Genomic and Transcriptomic Traits Acquired Under Colistin Therapy', *Frontiers in Microbiology*, 9. Available at: https://www.frontiersin.org/articles/10.3389/fmicb.2018.03195 (Accessed: 2 November 2023).

Cai, Y. and Webb, J.S. (2020) ‘Optimization of nitric oxide donors for investigating biofilm dispersal response in *Pseudomonas aeruginosa* clinical isolates’, *Applied Microbiology and Biotechnology*, 104(20), pp. 8859–8869. Available at: https://doi.org/10.1007/s00253-020-10859-7.

Cai, Y. *et al.* (2012) ‘Colistin resistance of *Acinetobacter baumannii*: clinical reports, mechanisms and antimicrobial strategies’, *The Journal of Antimicrobial Chemotherapy*, 67(7), pp. 1607–1615. Available at: https://doi.org/10.1093/jac/dks084.

Cappellini, M.D. (2007) ‘Exjade® (deferasirox, ICL670) in the treatment of chronic iron overload associated with blood transfusion’, *Therapeutics and Clinical Risk Management*, 3(2), pp. 291–299.

Carretero-Ledesma, M. *et al.* (2018) ‘Phenotypic changes associated with Colistin resistance due to Lipopolysaccharide loss in *Acinetobacter baumannii*’, *Virulence*, 9(1), pp. 930–942. Available at: https://doi.org/10.1080/21505594.2018.1460187.

Carsenti-Etesse, H. *et al.* (1999) ‘Gradient plate method to induce Streptococcus pyogenes resistance’, *Journal of Antimicrobial Chemotherapy*, 44(4), pp. 439–443. Available at: https://doi.org/10.1093/jac/44.4.439.

Catel-Ferreira, M. *et al.* (2016) ‘The outer membrane porin OmpW of *Acinetobacter baumannii* is involved in iron uptake and colistin binding’, *FEBS Letters*, 590(2), pp. 224–231. Available at: https://doi.org/10.1002/1873-3468.12050.

Cavallazzi, R. and Ramirez, J.A. (2022) ‘How and when to manage respiratory infections out of hospital’, *European Respiratory Review*, 31(166). Available at: https://doi.org/10.1183/16000617.0092-2022.

Cavallo, I. et al. (2023) ‘*Acinetobacter baumannii* in the critically ill: complex infections get complicated’, *Frontiers in Microbiology*, 14. Available at: https://doi.org/10.3389/fmicb.2023.1196774.

Cayô, R. *et al.* (2011) ‘Analysis of genes encoding penicillin-binding proteins in clinical isolates of *Acinetobacter baumannii*’, *Antimicrobial Agents and Chemotherapy*, 55(12), pp. 5907–5913. Available at: https://doi.org/10.1128/AAC.00459-11.

Caza, M. and Kronstad, J.W. (2013) ‘Shared and distinct mechanisms of iron acquisition by bacterial and fungal pathogens of humans’, *Frontiers in Cellular and Infection Microbiology*, 3, p. 80. Available at: https://doi.org/10.3389/fcimb.2013.00080.

CDC (1999) *Achievements in Public Health, 1900-1999: Control of Infectious Diseases*. Available at: https://www.cdc.gov/mmwr/preview/mmwrhtml/mm4829a1.htm (Accessed: 7 March 2023).

Centers for Disease Control and Prevention (CDC) (2004) ‘*Acinetobacter baumannii* infections among patients at military medical facilities treating injured U.S. service members, 2002-2004’, *MMWR. Morbidity and mortality weekly report*, 53(45), pp. 1063–1066.

Cerqueira, G.M. *et al.* (2014) ‘A global virulence regulator in *Acinetobacter baumannii* and its control of the phenylacetic acid catabolic pathway’, *The Journal of Infectious Diseases*, 210(1), pp. 46–55. Available at: https://doi.org/10.1093/infdis/jiu024.

Chaignon, P. *et al.* (2007) 'Susceptibility of staphylococcal biofilms to enzymatic treatments depends on their chemical composition', *Applied Microbiology and Biotechnology*, 75(1), pp. 125–132. Available at: https://doi.org/10.1007/s00253-006-0790-y.

Chen, H. *et al.* (2022) 'Recent Advances in Histidine Kinase-Targeted Antimicrobial Agents', *Frontiers in Chemistry*, 10, p. 866392. Available at: https://doi.org/10.3389/fchem.2022.866392.

Chen, S.L. *et al.* (2006) 'Identification of genes subject to positive selection in uropathogenic strains of *Escherichia coli*: a comparative genomics approach', *Proceedings of the National Academy of Sciences of the United States of America*, 103(15), pp. 5977–5982. Available at: https://doi.org/10.1073/pnas.0600938103.

Chen, Y., Azad, M.B. and Gibson, S.B. (2009) 'Superoxide is the major reactive oxygen species regulating autophagy', *Cell Death & Differentiation*, 16(7), pp. 1040–1052. Available at: https://doi.org/10.1038/cdd.2009.49.

Chin, C.Y. *et al.* (2018) 'A high-frequency phenotypic switch links bacterial virulence and environmental survival in Acinetobacter baumannii', *Nature microbiology*, 3(5), pp. 563–569. Available at: https://doi.org/10.1038/s41564-018-0151-5.

Chin, C.-Y. *et al.* (2015) 'A PmrB-Regulated Deacetylase Required for Lipid A Modification and Polymyxin Resistance in *Acinetobacter baumannii*', *Antimicrobial Agents and Chemotherapy*, 59(12), pp. 7911–7914. Available at: https://doi.org/10.1128/aac.00515-15.

Chitambar, C.R. (2016) 'Gallium and its competing roles with iron in biological systems', *Biochimica Et Biophysica Acta*, 1863(8), pp. 2044–2053. Available at: https://doi.org/10.1016/j.bbamcr.2016.04.027.

Chitambar, C.R. (2017) 'The therapeutic potential of iron-targeting gallium compounds in human disease: From basic research to clinical application', *Pharmacological Research*, 115, pp. 56–64. Available at: https://doi.org/10.1016/j.phrs.2016.11.009.

Cho, Y.J. *et al.* (2009) 'Genetic basis of resistance to aminoglycosides in Acinetobacter spp. and spread of armA in *Acinetobacter baumannii* sequence group 1 in Korean hospitals', *Diagnostic Microbiology and Infectious Disease*, 64(2), pp. 185–190. Available at: https://doi.org/10.1016/j.diagmicrobio.2009.02.010.

Choi, C.H. *et al.* (2005) 'Outer membrane protein 38 of *Acinetobacter baumannii* localizes to the mitochondria and induces apoptosis of epithelial cells', *Cellular Microbiology*, 7(8), pp. 1127–1138. Available at: https://doi.org/10.1111/j.1462-5822.2005.00538.x.

Choi, C.H. *et al.* (2008) '*Acinetobacter baumannii* outer membrane protein A targets the nucleus and induces cytotoxicity', *Cellular Microbiology*, 10(2), pp. 309–319. Available at: https://doi.org/10.1111/j.1462-5822.2007.01041.x.

Choi, H.J. *et al.* (2017) 'Characterisation of successive *Acinetobacter baumannii* isolates from a deceased haemophagocytic lymphohistiocytosis patient', *International Journal of Antimicrobial Agents*, 49(1), pp. 102–106. Available at: https://doi.org/10.1016/j.ijantimicag.2016.09.024.

Choi, K.-H. and Schweizer, H.P. (2006) 'mini-Tn7 insertion in bacteria with single attTn7 sites: example *Pseudomonas aeruginosa*', *Nature Protocols*, 1(1), pp. 153–161. Available at:

https://doi.org/10.1038/nprot.2006.24.

Choi, M.-K. *et al.* (2007) 'Transfection of primary human nasal epithelial cells using a biodegradable poly (ester amine) based on polycaprolactone and polyethylenimine as a gene carrier', *Journal of Drug Targeting*, 15(10), pp. 684–690. Available at: https://doi.org/10.1080/10611860701603331.
Chouhdari, A. *et al.* (2018) 'Is a Low Incidence Rate of Ventilation Associated Pneumonia Associated with Lower Mortality? a Descriptive Longitudinal Study in Iran', *Tanaffos*, 17(2), pp. 110–116.

Chu, Y.-W. *et al.* (2001) 'IMP-4, a Novel Metallo-β-Lactamase from Nosocomial Acinetobacter spp. Collected in Hong Kong between 1994 and 1998', *Antimicrobial Agents and Chemotherapy*, 45(3), pp. 710–714. Available at: https://doi.org/10.1128/AAC.45.3.710-714.2001.

Chusri, S. *et al.* (2009) 'Enhancing antibiotic activity: a strategy to control Acinetobacter infections', *Journal of Antimicrobial Chemotherapy*, 64(6), pp. 1203–1211. Available at: https://doi.org/10.1093/jac/dkp381.

Clardy, J., Fischbach, M.A. and Currie, C.R. (2009) 'The natural history of antibiotics', *Current biology: CB*, 19(11), pp. R437-441. Available at: https://doi.org/10.1016/j.cub.2009.04.001.

Clemmer, K.M., Bonomo, R.A. and Rather, P.N. (2011) 'Genetic analysis of surface motility in *Acinetobacter baumannii*', *Microbiology (Reading, England)*, 157(Pt 9), pp. 2534–2544. Available at: https://doi.org/10.1099/mic.0.049791-0.

Cocco, L. *et al.* (2015) 'Phosphoinositide-specific phospholipase C in health and disease', *Journal of Lipid Research*, 56(10), pp. 1853–1860. Available at: https://doi.org/10.1194/jlr.R057984.

Cociurovscaia, A., Bujacz, G. and Pietrzyk-Brzezinska, A.J. (2022) 'Crystal structure of the *Escherichia coli* CusS kinase core', *Journal of Structural Biology*, 214(3), p. 107883. Available at: https://doi.org/10.1016/j.jsb.2022.107883.

Conde-Pérez, K. *et al.* (2021) 'In-Depth Analysis of the Role of the Acinetobactin Cluster in the Virulence of *Acinetobacter baumannii*', *Frontiers in Microbiology*, 12, p. 752070. Available at: https://doi.org/10.3389/fmicb.2021.752070.

Constabel, C.P., Yoshida, K. and Walker, V. (2014) 'Diverse Ecological Roles of Plant Tannins: Plant Defense and Beyond', in *Recent advances in polyphenol research*, p. 464. Available at: https://doi.org/10.1002/9781118329634.ch5.

Cook-Libin, S. *et al.* (2022) 'Iron Acquisition Mechanisms and Their Role in the Virulence of *Acinetobacter baumannii*', *Infection and Immunity*, 90(10), pp. e00223-22. Available at: https://doi.org/10.1128/iai.00223-22.

Coque, T.M. *et al.* (2023) 'Antimicrobial Resistance in the Global Health Network: Known Unknowns and Challenges for Efficient Responses in the 21st Century', *Microorganisms*, 11(4), p. 1050. Available at: https://doi.org/10.3390/microorganisms11041050.

Costa, K.C. *et al.* (2017) 'Pyocyanin degradation by a tautomerizing demethylase inhibits *Pseudomonas aeruginosa* biofilms', *Science (New York, N.Y.)*, 355(6321), pp. 170–173. Available at: https://doi.org/10.1126/science.aag3180.
Coyne, S., Courvalin, P. and Périchon, B. (2011) 'Efflux-mediated antibiotic resistance in Acinetobacter spp', *Antimicrobial Agents and Chemotherapy*, 55(3), pp. 947–953. Available at:

https://doi.org/10.1128/AAC.01388-10.

Craigen, B., Dashiff, A. and Kadouri, D.E. (2011) 'The Use of Commercially Available Alpha-Amylase Compounds to Inhibit and Remove Staphylococcus aureus Biofilms', *The Open Microbiology Journal*, 5, pp. 21–31. Available at: https://doi.org/10.2174/1874285801105010021.

Crichton, R. (2016) *Iron Metabolism: From Molecular Mechanisms to Clinical Consequences: Fourth Edition*, p. 556. Available at: https://doi.org/10.1002/9781118925645.

Cui, H., Ma, C. and Lin, L. (2016) 'Co-loaded proteinase K/thyme oil liposomes for inactivation of *Escherichia coli* O157:H7 biofilms on cucumber', *Food & Function*, 7(9), pp. 4030–4040. Available at: https://doi.org/10.1039/c6fo01201a.

Curtis, M.M. *et al.* (2014) 'QseC Inhibitors as an Antivirulence Approach for Gram-Negative Pathogens', *mBio*, 5(6), pp. e02165-14. Available at: https://doi.org/10.1128/mBio.02165-14.

Cushnie, T.P.T. and Lamb, A.J. (2005) 'Antimicrobial activity of flavonoids', *International Journal of Antimicrobial Agents*, 26(5), pp. 343–356. Available at: https://doi.org/10.1016/j.ijantimicag.2005.09.002.

Cutruzzolà, F. and Frankenberg-Dinkel, N. (2015) 'Origin and Impact of Nitric Oxide in *Pseudomonas aeruginosa* Biofilms', *Journal of Bacteriology*, 198(1), pp. 55–65. Available at: https://doi.org/10.1128/JB.00371-15.

Da Silva, G.J. and Domingues, S. (2017) 'Interplay between Colistin Resistance, Virulence and Fitness in *Acinetobacter baumannii*', *Antibiotics*, 6(4), p. 28. Available at: https://doi.org/10.3390/antibiotics6040028.

Dadgostar, P. (2019) 'Antimicrobial Resistance: Implications and Costs', *Infection and Drug Resistance*, 12, pp. 3903–3910. Available at: https://doi.org/10.2147/IDR.S234610.

Dal, S.M. *et al.* (2002) 'The combination of the SH metabolite of erdosteine (a mucoactive drug) and ciprofloxacin increases the inhibition of bacterial adhesiveness achieved by ciprofloxacin alone', *Drugs Under Experimental and Clinical Research*, 28(2–3), pp. 75–82.

Damier-Piolle, L. *et al.* (2008) 'AdeIJK, a Resistance-Nodulation-Cell Division Pump Effluxing Multiple Antibiotics in *Acinetobacter baumannii*', *Antimicrobial Agents and Chemotherapy*, 52(2), pp. 557–562. Available at: https://doi.org/10.1128/AAC.00732-07.

Dar, D. *et al.* (2021) 'Spatial transcriptomics of planktonic and sessile bacterial populations at single-cell resolution', *Science (New York, N.Y.)*, 373(6556), p. eabi4882. Available at: https://doi.org/10.1126/science.abi4882.
Darby, E.M. *et al.* (2023) 'Molecular mechanisms of antibiotic resistance revisited', *Nature Reviews Microbiology*, 21(5), pp. 280–295. Available at: https://doi.org/10.1038/s41579-022-00820-y.

Das, T.K., Wati, M.R. and Fatima-Shad, K. (2015) 'Oxidative Stress Gated by Fenton and Haber Weiss Reactions and Its Association With Alzheimer's Disease', *Archives of Neuroscience*, 2(2). Available at: https://doi.org/10.5812/archneurosci.20078.

de Breij, A. *et al.* (2009) 'CsuA/BABCDE-dependent pili are not involved in the adherence of *Acinetobacter baumannii* ATCC19606(T) to human airway epithelial cells and their inflammatory

response', *Research in Microbiology*, 160(3), pp. 213–218. Available at: https://doi.org/10.1016/j.resmic.2009.01.002.

de Dios, R. *et al.* (2022) 'Artificial sweeteners inhibit multidrug-resistant pathogen growth and potentiate antibiotic activity', *EMBO Molecular Medicine*, 15(1), p. e16397. Available at: https://doi.org/10.15252/emmm.202216397.

de Jong, A., Kuipers, O.P. and Kok, J. (2022) 'FUNAGE-Pro: comprehensive web server for gene set enrichment analysis of prokaryotes', *Nucleic Acids Research*, 50(W1), pp. W330–W336. Available at: https://doi.org/10.1093/nar/gkac441.

De Rosa, M. *et al.* (2021) 'The Odd Couple(s): An Overview of Beta-Lactam Antibiotics Bearing More Than One Pharmacophoric Group', *International Journal of Molecular Sciences*, 22(2), p. 617. Available at: https://doi.org/10.3390/ijms22020617.

de Sá Cavalcanti, F.L. *et al.* (2016) 'High Frequency of OXA-253-Producing *Acinetobacter baumannii* in Different Hospitals in Recife, Brazil', *Antimicrobial Agents and Chemotherapy*, 61(1), pp. e01309-16. Available at: https://doi.org/10.1128/AAC.01309-16.

De, R. *et al.* (2018) 'Antimicrobial activity of ellagic acid against Helicobacter pylori isolates from India and during infections in mice', *The Journal of Antimicrobial Chemotherapy*, 73(6), pp. 1595–1603. Available at: https://doi.org/10.1093/jac/dky079.

Dean, S.N. and van Hoek, M.L. (2015) 'Screen of FDA-approved drug library identifies maprotiline, an antibiofilm and antivirulence compound with QseC sensor-kinase dependent activity in Francisella novicida', *Virulence*, 6(5), pp. 487–503. Available at: https://doi.org/10.1080/21505594.2015.1046029.

del Valle, P. *et al.* (2016) 'Antimicrobial activity of kaempferol and resveratrol in binary combinations with parabens or propyl gallate against Enterococcus faecalis', *Food Control*, 61, pp. 213–220. Available at: https://doi.org/10.1016/j.foodcont.2015.10.001.

Deng, S.-P. *et al.* (2019) 'Synthesis, Spectroscopic Study and Radical Scavenging Activity of Kaempferol Derivatives: Enhanced Water Solubility and Antioxidant Activity', *International Journal of Molecular Sciences*, 20(4), p. 975. Available at: https://doi.org/10.3390/ijms20040975.

Deris, Z.Z. *et al.* (2014) 'A secondary mode of action of polymyxins against Gram-negative bacteria involves the inhibition of NADH-quinone oxidoreductase activity', *The Journal of Antibiotics*, 67(2), pp. 147–151. Available at: https://doi.org/10.1038/ja.2013.111.

Deveson Lucas, D. *et al.* (2018) 'Emergence of High-Level Colistin Resistance in an *Acinetobacter baumannii* Clinical Isolate Mediated by Inactivation of the Global Regulator H-NS', *Antimicrobial Agents and Chemotherapy*, 62(7), pp. e02442-17. Available at: https://doi.org/10.1128/AAC.02442-17.

Dexter, C. *et al.* (2015) 'Community-acquired *Acinetobacter baumannii*: clinical characteristics, epidemiology and pathogenesis', *Expert Review of Anti-Infective Therapy*, 13(5), pp. 567–573. Available at: https://doi.org/10.1586/14787210.2015.1025055.

DiGiandomenico, A. *et al.* (2014) 'A multifunctional bispecific antibody protects against *Pseudomonas aeruginosa*', *Science Translational Medicine*, 6(262), p. 262ra155. Available at: https://doi.org/10.1126/scitranslmed.3009655.

Djordjevic, J. (2010) ‘Role of Phospholipases in Fungal Fitness, Pathogenicity, and Drug Development – Lessons from Cryptococcus Neoformans’, *Frontiers in Microbiology*, 1. Available at: https://www.frontiersin.org/articles/10.3389/fmicb.2010.00125 (Accessed: 4 November 2023).

Donlan, R.M. (2002) ‘Biofilms: Microbial Life on Surfaces’, *Emerging Infectious Diseases*, 8(9), pp. 881–890. Available at: https://doi.org/10.3201/eid0809.020063.

Dortet, L. *et al.* (2018) ‘Rapid detection and discrimination of chromosome- and MCR-plasmid-mediated resistance to polymyxins by MALDI-TOF MS in *Escherichia coli*: the MALDIxin test’, *The Journal of Antimicrobial Chemotherapy*, 73(12), pp. 3359–3367. Available at: https://doi.org/10.1093/jac/dky330.

Dotto, C. *et al.* (2021) ‘Salicylic acid stabilizes Staphylococcus aureus biofilm by impairing the agr quorum-sensing system’, *Scientific Reports*, 11(1), p. 2953. Available at: https://doi.org/10.1038/s41598-021-82308-y.

Dubrovskaya, Y. *et al.* (2015) ‘Risk factors for nephrotoxicity onset associated with polymyxin B therapy’, *The Journal of Antimicrobial Chemotherapy*, 70(6), pp. 1903–1907. Available at: https://doi.org/10.1093/jac/dkv014.

Duda-Madej, A. *et al.* (2020) ‘Antimicrobial O-Alkyl Derivatives of Naringenin and Their Oximes Against Multidrug-Resistant Bacteria’, *Molecules*, 25(16), p. 3642. Available at: https://doi.org/10.3390/molecules25163642.

Duguid, J.P. and Gillies, R.R. (1957) ‘Fimbrias and Adhesive Properties in Dysentery Bacilli.’, *Journal of Pathology and Bacteriology*, 74(2), pp. 397–411.

Dupont, M. *et al.* (2005) ‘Identification of an OprD homologue in *Acinetobacter baumannii*’, *Journal of Proteome Research*, 4(6), pp. 2386–2390. Available at: https://doi.org/10.1021/pr050143q.

Durante-Mangoni, E. *et al.* (2015) ‘Emergence of colistin resistance without loss of fitness and virulence after prolonged colistin administration in a patient with extensively drug-resistant *Acinetobacter baumannii*’, *Diagnostic Microbiology and Infectious Disease*, 82(3), pp. 222–226. Available at: https://doi.org/10.1016/j.diagmicrobio.2015.03.013.

Durieux, M.-F. *et al.* (2021) ‘Galleria mellonella as a screening tool to study virulence factors of Aspergillus fumigatus’, *Virulence*, 12(1), pp. 818–834. Available at: https://doi.org/10.1080/21505594.2021.1893945.

Eckhart, L. *et al.* (2007) ‘DNase1L2 suppresses biofilm formation by *Pseudomonas aeruginosa* and Staphylococcus aureus’, *British Journal of Dermatology*, 156(6), pp. 1342–1345. Available at: https://doi.org/10.1111/j.1365-2133.2007.07886.x.

Eijkelkamp, B.A. *et al.* (2011) ‘Adherence and motility characteristics of clinical *Acinetobacter baumannii* isolates’, *FEMS Microbiology Letters*, 323(1), pp. 44–51. Available at: https://doi.org/10.1111/j.1574-6968.2011.02362.x.

El-Sayed Ahmed, M.A.E.-G. *et al.* (2020) ‘Colistin and its role in the Era of antibiotic resistance: an extended review (2000–2019)’, *Emerging Microbes & Infections*, 9(1), pp. 868–885. Available at: https://doi.org/10.1080/22221751.2020.1754133.

Elham, B. and Fawzia, A. (2019) 'Colistin resistance in *Acinetobacter baumannii* isolated from critically ill patients: clinical characteristics, antimicrobial susceptibility and outcome', *African Health Sciences*, 19(3), pp. 2400–2406. Available at: https://doi.org/10.4314/ahs.v19i3.13.

EMA (2018) *European Union monographs and list entries*, *European Medicines Agency*. Available at: https://www.ema.europa.eu/en/human-regulatory/herbal-products/european-union-monographs-list-entries (Accessed: 5 October 2023).

EMA (2021) *Tormentillae rhizoma*, *European Medicines Agency*. Available at: https://www.ema.europa.eu/en/medicines/herbal/tormentillae-rhizoma

Endimiani, A. *et al.* (2007) 'Spread in an Italian Hospital of a Clonal *Acinetobacter baumannii* Strain Producing the TEM-92 Extended-Spectrum β-Lactamase', *Antimicrobial Agents and Chemotherapy*, 51(6), pp. 2211–2214. Available at: https://doi.org/10.1128/AAC.01139-06.

Erdönmez, D., Rad, A.Y. and Aksöz, N. (2017) 'Quorum sensing molecules production by nosocomial and soil isolates *Acinetobacter baumannii*', *Archives of Microbiology*, 199(10), pp. 1325–1334. Available at: https://doi.org/10.1007/s00203-017-1408-8.

Espinal, P. *et al.* (2011) 'Dissemination of an NDM-2-Producing *Acinetobacter baumannii* Clone in an Israeli Rehabilitation Center ▿', *Antimicrobial Agents and Chemotherapy*, 55(11), pp. 5396–5398. Available at: https://doi.org/10.1128/AAC.00679-11.

European Centre for Disease Prevention and Control. and World Health Organization. (2022) *Antimicrobial resistance surveillance in Europe 2022: 2020 data.* LU: Publications Office. Available at: https://data.europa.eu/doi/10.2900/112339 (Accessed: 5 March 2024).

European Committee on Antimicrobial Susceptibility Testing, 2016. Recommendations for MIC determination of colistin (polymyxin E) as recommended by the joint CLSI-EUCAST Polymyxin Breakpoints Working Group. *EUCAST: Växjö, Sweden*.

Evans, B.A. *et al.* (2007) 'Eleven novel OXA-51-like enzymes from clinical isolates of *Acinetobacter baumannii*', *Clinical Microbiology and Infection*, 13(11), pp. 1137–1138. Available at: https://doi.org/10.1111/j.1469-0691.2007.01828.x.

Eveillard, M. *et al.* (2013) 'Reservoirs of *Acinetobacter baumannii* outside the hospital and potential involvement in emerging human community-acquired infections', *International journal of infectious diseases: IJID: official publication of the International Society for Infectious Diseases*, 17(10), pp. e802-805. Available at: https://doi.org/10.1016/j.ijid.2013.03.021.

Fadini, G.P. *et al.* (2016) 'NETosis Delays Diabetic Wound Healing in Mice and Humans', *Diabetes*, 65(4), pp. 1061–1071. Available at: https://doi.org/10.2337/db15-0863.

Falagas, M.E. and Kasiakou, S.K. (2005) 'Colistin: the revival of polymyxins for the management of multidrug-resistant gram-negative bacterial infections', *Clinical Infectious Diseases: An Official Publication of the Infectious Diseases Society of America*, 40(9), pp. 1333–1341. Available at: https://doi.org/10.1086/429323.

Falagas, M.E. *et al.* (2006) 'Effectiveness and nephrotoxicity of intravenous colistin for treatment of patients with infections due to polymyxin-only-susceptible (POS) gram-negative bacteria', *European Journal of Clinical Microbiology & Infectious Diseases: Official Publication of the European Society*

of Clinical Microbiology, 25(9), pp. 596–599. Available at: https://doi.org/10.1007/s10096-006-0191-2.

Falagas, M.E., Rafailidis, P.I. and Matthaiou, D.K. (2010) 'Resistance to polymyxins: Mechanisms, frequency and treatment options', *Drug Resistance Updates: Reviews and Commentaries in Antimicrobial and Anticancer Chemotherapy*, 13(4–5), pp. 132–138. Available at: https://doi.org/10.1016/j.drup.2010.05.002.

Fang, F. *et al.* (2016) 'Molecular characterization of carbapenemase genes in *Acinetobacter baumannii* in China', *Genetics and molecular research: GMR*, 15(1). Available at: https://doi.org/10.4238/gmr.15017432.

Farshadzadeh, Z. *et al.* (2018) 'Growth Rate and Biofilm Formation Ability of Clinical and Laboratory-Evolved Colistin-Resistant Strains of *Acinetobacter baumannii*', *Frontiers in Microbiology*, 9, p. 153. Available at: https://doi.org/10.3389/fmicb.2018.00153.

Fedotcheva, T.A., Sheichenko, O.P. and Fedotcheva, N.I. (2021) 'New Properties and Mitochondrial Targets of Polyphenol Agrimoniin as a Natural Anticancer and Preventive Agent', *Pharmaceutics*, 13(12), p. 2089. Available at: https://doi.org/10.3390/pharmaceutics13122089.

Feltner, J.B. *et al.* (2016) 'LasR Variant Cystic Fibrosis Isolates Reveal an Adaptable Quorum-Sensing Hierarchy in *Pseudomonas aeruginosa*', *mBio*, 7(5), pp. e01513-16. Available at: https://doi.org/10.1128/mBio.01513-16.

Feng, C. *et al.* (2019) 'Tanshinones: First-in-Class Inhibitors of the Biogenesis of the Type 3 Secretion System Needle of *Pseudomonas aeruginosa* for Antibiotic Therapy', *ACS Central Science*, 5(7), pp. 1278–1288. Available at: https://doi.org/10.1021/acscentsci.9b00452.

Fernicola, S. *et al.* (2015) 'Synthesis of Triazole-Linked Analogues of c-di-GMP and Their Interactions with Diguanylate Cyclase', *Journal of Medicinal Chemistry*, 58(20), pp. 8269–8284. Available at: https://doi.org/10.1021/acs.jmedchem.5b01184.

Fernicola, S. *et al.* (2016) 'In Silico Discovery and In Vitro Validation of Catechol-Containing Sulfonohydrazide Compounds as Potent Inhibitors of the Diguanylate Cyclase PleD', *Journal of Bacteriology*, 198(1), pp. 147–156. Available at: https://doi.org/10.1128/JB.00742-15.

Ferrali, M. *et al.* (1997) 'Protection against oxidative damage of erythrocyte membrane by the flavonoid quercetin and its relation to iron chelating activity', *FEBS letters*, 416(2), pp. 123–129. Available at: https://doi.org/10.1016/s0014-5793(97)01182-4.

Fiester, S.E. *et al.* (2016) 'Iron-Regulated Phospholipase C Activity Contributes to the Cytolytic Activity and Virulence of *Acinetobacter baumannii*', *PloS One*, 11(11), p. e0167068. Available at: https://doi.org/10.1371/journal.pone.0167068.

Figurski, D.H. and Helinski, D.R. (1979) 'Replication of an origin-containing derivative of plasmid RK2 dependent on a plasmid function provided in trans', *Proceedings of the National Academy of Sciences*, 76(4), pp. 1648–1652. Available at: https://doi.org/10.1073/pnas.76.4.1648.

Fleming, D., Chahin, L. and Rumbaugh, K. (2017) 'Glycoside Hydrolases Degrade Polymicrobial Bacterial Biofilms in Wounds', *Antimicrobial Agents and Chemotherapy*, 61(2), pp. e01998-16. Available at: https://doi.org/10.1128/AAC.01998-16.

Foulkes, D.M. *et al.* (2021) 'A pipeline to evaluate inhibitors of the *Pseudomonas aeruginosa* exotoxin U', *Biochemical Journal*, 478(3), pp. 647–668. Available at: https://doi.org/10.1042/BCJ20200780.

François, B. *et al.* (2021) 'Efficacy and safety of suvratoxumab for prevention of Staphylococcus aureus ventilator-associated pneumonia (SAATELLITE): a multicentre, randomised, double-blind, placebo-controlled, parallel-group, phase 2 pilot trial', *The Lancet. Infectious Diseases*, 21(9), pp. 1313–1323. Available at: https://doi.org/10.1016/S1473-3099(20)30995-6.

Fredheim, E.G.A. *et al.* (2009) 'Biofilm formation by Staphylococcus haemolyticus', *Journal of Clinical Microbiology*, 47(4), pp. 1172–1180. Available at: https://doi.org/10.1128/JCM.01891-08.

Freire, A.T. *et al.* (2010) 'Comparison of tigecycline with imipenem/cilastatin for the treatment of hospital-acquired pneumonia', *Diagnostic Microbiology and Infectious Disease*, 68(2), pp. 140–151. Available at: https://doi.org/10.1016/j.diagmicrobio.2010.05.012.

Frost, I. *et al.* (2018) 'Cooperation, competition and antibiotic resistance in bacterial colonies', *The ISME Journal*, 12(6), pp. 1582–1593. Available at: https://doi.org/10.1038/s41396-018-0090-4.

Funatogawa, K. *et al.* (2004) 'Antibacterial activity of hydrolyzable tannins derived from medicinal plants against Helicobacter pylori', *Microbiology and Immunology*, 48(4), pp. 251–261. Available at: https://doi.org/10.1111/j.1348-0421.2004.tb03521.x.

Furniss, R.C.D. *et al.* (2020) 'The clue is in the lipid A: Rapid detection of colistin resistance', *PLOS Pathogens*, 16(4), p. e1008331. Available at: https://doi.org/10.1371/journal.ppat.1008331.

Gadar, K. and McCarthy, R.R. (2023) 'Using next generation antimicrobials to target the mechanisms of infection', *npj Antimicrobials and Resistance*, 1(1), pp. 1–14. Available at: https://doi.org/10.1038/s44259-023-00011-6.

Gadar, K. *et al.* (2023) 'Disrupting iron homeostasis can potentiate colistin activity and overcome colistin resistance mechanisms in Gram-Negative Bacteria', *Communications Biology*, 6(1), pp. 1–16. Available at: https://doi.org/10.1038/s42003-023-05302-2.

Gaddy, J.A. and Actis, L.A. (2009) 'Regulation of *Acinetobacter baumannii* biofilm formation', *Future microbiology*, 4, pp. 273–278. Available at: https://doi.org/10.2217/fmb.09.5.

Gaddy, J.A. *et al.* (2012) 'Role of acinetobactin-mediated iron acquisition functions in the interaction of *Acinetobacter baumannii* strain ATCC 19606T with human lung epithelial cells, Galleria mellonella caterpillars, and mice', *Infection and Immunity*, 80(3), pp. 1015–1024. Available at: https://doi.org/10.1128/IAI.06279-11.

Gales, A.C. *et al.* (2003) 'Emergence of an IMP-like metallo-enzyme in an *Acinetobacter baumannii* clinical strain from a Brazilian teaching hospital', *Diagnostic Microbiology and Infectious Disease*, 45(1), pp. 77–79. Available at: https://doi.org/10.1016/s0732-8893(02)00500-x.

Gallagher, L.A. *et al.* (2015) 'Resources for Genetic and Genomic Analysis of Emerging Pathogen *Acinetobacter baumannii*', *Journal of Bacteriology*, 197(12), pp. 2027–2035. Available at: https://doi.org/10.1128/JB.00131-15.

Gallego, L. and Towner, K.J. (2001) 'Carriage of class 1 integrons and antibiotic resistance in clinical

isolates of *Acinetobacter baumannii* from northern Spain', *Journal of Medical Microbiology*, 50(1), pp. 71–77. Available at: https://doi.org/10.1099/0022-1317-50-1-71.

Gao, R. *et al.* (2016) 'Dissemination and Mechanism for the MCR-1 Colistin Resistance', *PLoS pathogens*, 12(11), p. e1005957. Available at: https://doi.org/10.1371/journal.ppat.1005957.

Gao, W. *et al.* (2018) 'Nanoparticle-Based Local Antimicrobial Drug Delivery', *Advanced drug delivery reviews*, 127, pp. 46–57. Available at: https://doi.org/10.1016/j.addr.2017.09.015.

Garrett, T.A., Que, N.L. and Raetz, C.R. (1998) 'Accumulation of a lipid A precursor lacking the 4'-phosphate following inactivation of the *Escherichia coli* lpxK gene', *The Journal of Biological Chemistry*, 273(20), pp. 12457–12465. Available at: https://doi.org/10.1074/jbc.273.20.12457.

Gaur, R. *et al.* (2016) 'Drug Resistance Reversal Potential of Isoliquiritigenin and Liquiritigenin Isolated from Glycyrrhiza glabra Against Methicillin-Resistant Staphylococcus aureus (MRSA)', *Phytotherapy Research*, 30(10), pp. 1708–1715. Available at: https://doi.org/10.1002/ptr.5677.

Gawande, P.V. *et al.* (2014) 'Antibiofilm Efficacy of DispersinB® Wound Spray Used in Combination with a Silver Wound Dressing', *Microbiology Insights*, 7, pp. 9–13. Available at: https://doi.org/10.4137/MBI.S13914.

Gedefie, A. *et al.* (2021) '*Acinetobacter baumannii* Biofilm Formation and Its Role in Disease Pathogenesis: A Review', *Infection and Drug Resistance*, 14, pp. 3711–3719. Available at: https://doi.org/10.2147/IDR.S332051.

Gehrlein, M. *et al.* (1991) 'Imipenem resistance in Acinetobacter baumanii is due to altered penicillin-binding proteins', *Chemotherapy*, 37(6), pp. 405–412. Available at: https://doi.org/10.1159/000238887.

Geisinger, E. and Isberg, R.R. (2017) 'Interplay Between Antibiotic Resistance and Virulence During Disease Promoted by Multidrug-Resistant Bacteria', *The Journal of Infectious Diseases*, 215(suppl_1), pp. S9–S17. Available at: https://doi.org/10.1093/infdis/jiw402.

Geisinger, E. *et al.* (2020) 'Antibiotic susceptibility signatures identify potential antimicrobial targets in the *Acinetobacter baumannii* cell envelope', *Nature Communications*, 11, p. 4522. Available at: https://doi.org/10.1038/s41467-020-18301-2.

George, T. and Brady, M.F. (2023) 'Ethylenediaminetetraacetic Acid (EDTA)', in *StatPearls*. Treasure Island (FL): StatPearls Publishing. Available at: http://www.ncbi.nlm.nih.gov/books/NBK565883/ (Accessed: 12 May 2023).

Gerson, S. *et al.* (2019) 'Investigation of Novel pmrB and eptA Mutations in Isogenic *Acinetobacter baumannii* Isolates Associated with Colistin Resistance and Increased Virulence In Vivo', *Antimicrobial Agents and Chemotherapy*, 63(3), pp. e01586-18. Available at: https://doi.org/10.1128/AAC.01586-18.

Giammanco, A. *et al.* (2017) 'Global Assessment of the Activity of Tigecycline against Multidrug-Resistant Gram-Negative Pathogens between 2004 and 2014 as Part of the Tigecycline Evaluation and Surveillance Trial', *mSphere*, 2(1), pp. e00310-16. Available at: https://doi.org/10.1128/mSphere.00310-16.

Giannouli, M. *et al.* (2009) 'Molecular epidemiology of carbapenem-resistant *Acinetobacter baumannii* strains in intensive care units of multiple Mediterranean hospitals', *Journal of Antimicrobial Chemotherapy*, 63(4), pp. 828–830. Available at: https://doi.org/10.1093/jac/dkp032.

Gogry, F.A. *et al.* (2021) 'Current Update on Intrinsic and Acquired Colistin Resistance Mechanisms in Bacteria', *Frontiers in Medicine*, 8, p. 677720. Available at: https://doi.org/10.3389/fmed.2021.677720.

Golkar, Z., Bagasra, O. and Pace, D.G. (2014) 'Bacteriophage therapy: a potential solution for the antibiotic resistance crisis', *Journal of Infection in Developing Countries*, 8(2), pp. 129–136. Available at: https://doi.org/10.3855/jidc.3573.

González-Bello, C. (2019) 'The Inhibition of Lipid A Biosynthesis—The Antidote Against Superbugs?', *Advanced Therapeutics*, 2(3), p. 1800117. Available at: https://doi.org/10.1002/adtp.201800117.

Gonzalez-Villoria, A.M. *et al.* (2016) 'A Multicenter Study in Mexico Finds *Acinetobacter baumannii* Clinical Isolates Belonging to Clonal Complexes 636B (113B) and 92B Harboring OXA-72, OXA-239, and OXA-469', *Antimicrobial Agents and Chemotherapy*, 60(4), pp. 2587–2588. Available at: https://doi.org/10.1128/AAC.02042-15.

Goodman, S.D. *et al.* (2011) 'Biofilms can be dispersed by focusing the immune system on a common family of bacterial nucleoid-associated proteins', *Mucosal Immunology*, 4(6), pp. 625–637. Available at: https://doi.org/10.1038/mi.2011.27.

Gordon, N.C. and Wareham, D.W. (2009) 'A review of clinical and microbiological outcomes following treatment of infections involving multidrug-resistant *Acinetobacter baumannii* with tigecycline', *The Journal of Antimicrobial Chemotherapy*, 63(4), pp. 775–780. Available at: https://doi.org/10.1093/jac/dkn555.

Gould, I.M. and Bal, A.M. (2013) 'New antibiotic agents in the pipeline and how they can help overcome microbial resistance', *Virulence*, 4(2), pp. 185–191. Available at: https://doi.org/10.4161/viru.22507.

Granata, G., Schiavone, F. and Pipitone, G. (2022) 'Bezlotoxumab in Patients with a Primary Clostridioides difficile Infection: A Literature Review', *Antibiotics*, 11(11), p. 1495. Available at: https://doi.org/10.3390/antibiotics11111495.

Greene, C. *et al.* (2016) 'The influence of biofilm formation and multidrug resistance on environmental survival of clinical and environmental isolates of *Acinetobacter baumannii*', *American Journal of Infection Control*, 44(5), pp. e65–e71. Available at: https://doi.org/10.1016/j.ajic.2015.12.012.

Greig, S.L. (2016) 'Obiltoxaximab: First Global Approval', *Drugs*, 76(7), pp. 823–830. Available at: https://doi.org/10.1007/s40265-016-0577-0.

Grochowski, D.M. *et al.* (2017) 'A comprehensive review of agrimoniin', *Annals of the New York Academy of Sciences*, 1401(1), pp. 166–180. Available at: https://doi.org/10.1111/nyas.13421.

Guan, L. *et al.* (2013) 'Development of a Fur-dependent and tightly regulated expression system in *Escherichia coli* for toxic protein synthesis', *BMC Biotechnology*, 13, p. 25. Available at:

https://doi.org/10.1186/1472-6750-13-25.

Gupta, P., Chhibber, S. and Harjai, K. (2015) 'Efficacy of purified lactonase and ciprofloxacin in preventing systemic spread of *Pseudomonas aeruginosa* in murine burn wound model', *Burns: Journal of the International Society for Burn Injuries*, 41(1), pp. 153–162. Available at: https://doi.org/10.1016/j.burns.2014.06.009.

Gurjar, M. (2015) 'Colistin for lung infection: an update', *Journal of Intensive Care*, 3(1), p. 3. Available at: https://doi.org/10.1186/s40560-015-0072-9.

Gustave, J.E. *et al.* (2013) 'Targeting bacterial integration host factor to disrupt biofilms associated with cystic fibrosis', *Journal of Cystic Fibrosis*, 12(4), pp. 384–389. Available at: https://doi.org/10.1016/j.jcf.2012.10.011.

Gutiérrez-Barranquero, J.A. *et al.* (2015) 'Deciphering the role of coumarin as a novel quorum sensing inhibitor suppressing virulence phenotypes in bacterial pathogens', *Applied Microbiology and Biotechnology*, 99(7), pp. 3303–3316. Available at: https://doi.org/10.1007/s00253-015-6436-1.

Gutiérrez-Barranquero, J.A., Cazorla, F.M. and de Vicente, A. (2019) 'Pseudomonas syringae pv. syringae Associated With Mango Trees, a Particular Pathogen Within the "Hodgepodge" of the Pseudomonas syringae Complex', *Frontiers in Plant Science*, 10. Available at: https://www.frontiersin.org/articles/10.3389/fpls.2019.00570 (Accessed: 7 March 2023).

Habboush, Y. and Guzman, N. (2023) 'Antibiotic Resistance', in *StatPearls*. Treasure Island (FL): StatPearls Publishing. Available at: http://www.ncbi.nlm.nih.gov/books/NBK513277/ (Accessed: 5 October 2023).

Hall-Stoodley, L. *et al.* (2008) 'Characterization of biofilm matrix, degradation by DNase treatment and evidence of capsule downregulation in Streptococcus pneumoniae clinical isolates', *BMC Microbiology*, 8, p. 173. Available at: https://doi.org/10.1186/1471-2180-8-173.

Hameed, F. *et al.* (2019) 'Plasmid-mediated mcr-1 gene in *Acinetobacter baumannii* and *Pseudomonas aeruginosa*: first report from Pakistan', *Revista Da Sociedade Brasileira De Medicina Tropical*, 52, p. e20190237. Available at: https://doi.org/10.1590/0037-8682-0237-2019.

Handel, A., Regoes, R.R. and Antia, R. (2006) 'The Role of Compensatory Mutations in the Emergence of Drug Resistance', *PLOS Computational Biology*, 2(10), p. e137. Available at: https://doi.org/10.1371/journal.pcbi.0020137.

He, X. *et al.* (2015) 'Biofilm Formation Caused by Clinical *Acinetobacter baumannii* Isolates Is Associated with Overexpression of the AdeFGH Efflux Pump', *Antimicrobial Agents and Chemotherapy*, 59(8), pp. 4817–4825. Available at: https://doi.org/10.1128/AAC.00877-15.

Heindorf, M. *et al.* (2014) 'Impact of *Acinetobacter baumannii* Superoxide Dismutase on Motility, Virulence, Oxidative Stress Resistance and Susceptibility to Antibiotics', *PLoS ONE*, 9(7), p. e101033. Available at: https://doi.org/10.1371/journal.pone.0101033.

Helander, I.M. and Mattila-Sandholm, T. (2000) 'Fluorometric assessment of gram-negative bacterial permeabilization', *Journal of Applied Microbiology*, 88(2), pp. 213–219. Available at: https://doi.org/10.1046/j.1365-2672.2000.00971.x.

Henry, R. *et al.* (2012) 'Colistin-resistant, lipopolysaccharide-deficient *Acinetobacter baumannii* responds to lipopolysaccharide loss through increased expression of genes involved in the synthesis and transport of lipoproteins, phospholipids, and poly-β-1,6-N-acetylglucosamine', *Antimicrobial Agents and Chemotherapy*, 56(1), pp. 59–69. Available at: https://doi.org/10.1128/AAC.05191-11.

Héritier, C. *et al.* (2005) 'Characterization of the naturally occurring oxacillinase of *Acinetobacter baumannii*', *Antimicrobial Agents and Chemotherapy*, 49(10), pp. 4174–4179. Available at: https://doi.org/10.1128/AAC.49.10.4174-4179.2005.

Hernandez, L.D. *et al.* (2015) 'Broad Coverage of Genetically Diverse Strains of Clostridium difficile by Actoxumab and Bezlotoxumab Predicted by In Vitro Neutralization and Epitope Modeling', *Antimicrobial Agents and Chemotherapy*, 59(2), pp. 1052–1060. Available at: https://doi.org/10.1128/AAC.04433-14.

Higgins, P.G. *et al.* (2004) 'Selection of topoisomerase mutations and overexpression of adeB mRNA transcripts during an outbreak of *Acinetobacter baumannii*', *The Journal of Antimicrobial Chemotherapy*, 54(4), pp. 821–823. Available at: https://doi.org/10.1093/jac/dkh427.

Higgins, P.G. *et al.* (2009) 'OXA-143, a Novel Carbapenem-Hydrolyzing Class D β-Lactamase in *Acinetobacter baumannii*', *Antimicrobial Agents and Chemotherapy*, 53(12), pp. 5035–5038. Available at: https://doi.org/10.1128/AAC.00856-09.

Higgins, P.G. *et al.* (2013) 'OXA-235, a Novel Class D β-Lactamase Involved in Resistance to Carbapenems in *Acinetobacter baumannii*', *Antimicrobial Agents and Chemotherapy*, 57(5), pp. 2121–2126. Available at: https://doi.org/10.1128/AAC.02413-12.

Hobley, L. *et al.* (2015) 'Giving structure to the biofilm matrix: an overview of individual strategies and emerging common themes', *FEMS microbiology reviews*, 39(5), pp. 649–669. Available at: https://doi.org/10.1093/femsre/fuv015.

Hoffmann, J. *et al.* (2016) 'Anti-Inflammatory Effects of Agrimoniin-Enriched Fractions of Potentilla erecta', *Molecules*, 21(6), p. 792. Available at: https://doi.org/10.3390/molecules21060792.

Holden, D. *et al.* (2021) 'Identification and Whole Genome Sequencing Analysis of an Oxacillinase (OXA)-48-like-producing Acinetobacter baumannii Outbreak in California, January-May 2021', *Open Forum Infectious Diseases*, 8(Supplement_1), pp. S109–S110. Available at: https://doi.org/10.1093/ofid/ofab466.179.

Hood, M.I. *et al.* (2010) '*Acinetobacter baumannii* increases tolerance to antibiotics in response to monovalent cations', *Antimicrobial Agents and Chemotherapy*, 54(3), pp. 1029–1041. Available at: https://doi.org/10.1128/AAC.00963-09.

Hood, M.I. *et al.* (2013) 'Genetic Determinants of Intrinsic Colistin Tolerance in *Acinetobacter baumannii*', *Infection and Immunity*, 81(2), pp. 542–551. Available at: https://doi.org/10.1128/IAI.00704-12.

Hou, C. and Yang, F. (2015) 'Drug-resistant gene of blaOXA-23, blaOXA-24, blaOXA-51 and blaOXA-58 in *Acinetobacter baumannii*', *International Journal of Clinical and Experimental Medicine*, 8(8), pp. 13859–13863.

Hou, P.F. *et al.* (2012) 'Study of the correlation of imipenem resistance with efflux pumps AdeABC,

AdeIJK, AdeDE and AbeM in clinical isolates of *Acinetobacter baumannii*', *Chemotherapy*, 58(2), pp. 152–158. Available at: https://doi.org/10.1159/000335599.

Howlin, R.P. *et al.* (2017) 'Low-Dose Nitric Oxide as Targeted Anti-biofilm Adjunctive Therapy to Treat Chronic *Pseudomonas aeruginosa* Infection in Cystic Fibrosis', *Molecular Therapy*, 25(9), pp. 2104–2116. Available at: https://doi.org/10.1016/j.ymthe.2017.06.021.

Hraiech, S. *et al.* (2013) 'Impaired Virulence and Fitness of a Colistin-Resistant Clinical Isolate of *Acinetobacter baumannii* in a Rat Model of Pneumonia', *Antimicrobial Agents and Chemotherapy*, 57(10), pp. 5120–5121. Available at: https://doi.org/10.1128/AAC.00700-13.

Hraiech, S. *et al.* (2014) 'Inhaled Lactonase Reduces *Pseudomonas aeruginosa* Quorum Sensing and Mortality in Rat Pneumonia', *PLOS ONE*, 9(10), p. e107125. Available at: https://doi.org/10.1371/journal.pone.0107125.

Hu, K.-X. *et al.* (2021) 'Antibacterial mechanism of Biochanin A and its efficacy for the control of Xanthomonas axonopodis pv. glycines in soybean', *Pest Management Science*, 77(4), pp. 1668–1673. Available at: https://doi.org/10.1002/ps.6186.

Huang, Y.-H. *et al.* (2015) 'Inhibition of Staphylococcus aureus PriA Helicase by Flavonol Kaempferol', *The Protein Journal*, 34(3), pp. 169–172. Available at: https://doi.org/10.1007/s10930-015-9609-y.

Hudson, D.L. *et al.* (2007) 'Inhibition of type III secretion in Salmonella enterica serovar Typhimurium by small-molecule inhibitors', *Antimicrobial Agents and Chemotherapy*, 51(7), pp. 2631–2635. Available at: https://doi.org/10.1128/AAC.01492-06.

Huemer, M. *et al.* (2020) 'Antibiotic resistance and persistence—Implications for human health and treatment perspectives', *EMBO Reports*, 21(12), p. e51034. Available at: https://doi.org/10.15252/embr.202051034.

Hung, D.T. *et al.* (2005) 'Small-molecule inhibitor of Vibrio cholerae virulence and intestinal colonization', *Science (New York, N.Y.)*, 310(5748), pp. 670–674. Available at: https://doi.org/10.1126/science.1116739.

Husain, F.M. *et al.* (2013) 'Influence of clove oil on certain quorum-sensing-regulated functions and biofilm of *Pseudomonas aeruginosa* and Aeromonas hydrophila', *Journal of Biosciences*, 38(5), pp. 835–844. Available at: https://doi.org/10.1007/s12038-013-9385-9.

Hutchings, M.I., Truman, A.W. and Wilkinson, B. (2019) 'Antibiotics: past, present and future', *Current Opinion in Microbiology*, 51, pp. 72–80. Available at: https://doi.org/10.1016/j.mib.2019.10.008.

Ibberson, C.B. *et al.* (2016) 'Hyaluronan Modulation Impacts Staphylococcus aureus Biofilm Infection', *Infection and Immunity*, 84(6), pp. 1917–1929. Available at: https://doi.org/10.1128/IAI.01418-15.

Islam, A., Actis, L.A. and Wilson, T.J. (2023) 'Natural Antibodies Mediate Protection Against Acinetobacter baumannii Respiratory Infections', *The Journal of Infectious Diseases*, 228(3), pp. 353–363. Available at: https://doi.org/10.1093/infdis/jiad069.

Jackman, J.E., Raetz, C.R. and Fierke, C.A. (1999) 'UDP-3-O-(R-3-hydroxymyristoyl)-N-acetylglucosamine deacetylase of *Escherichia coli* is a zinc metalloenzyme', *Biochemistry*, 38(6), pp. 1902–1911. Available at: https://doi.org/10.1021/bi982339s.

Jahangiri, A. *et al.* (2017) 'In silico design of an immunogen against *Acinetobacter baumannii* based on a novel model for native structure of Outer membrane protein A', *Microbial Pathogenesis*, 105, pp. 201–210. Available at: https://doi.org/10.1016/j.micpath.2017.02.028.

Jahangiri, A. *et al.* (2018) 'Highly conserved exposed immunogenic peptides of Omp34 against *Acinetobacter baumannii*: An innovative approach', *Journal of Microbiological Methods*, 144, pp. 79–85. Available at: https://doi.org/10.1016/j.mimet.2017.11.008.

Jain, M. *et al.* (2004) 'Type III Secretion Phenotypes of *Pseudomonas aeruginosa* Strains Change during Infection of Individuals with Cystic Fibrosis', *Journal of Clinical Microbiology*, 42(11), pp. 5229–5237. Available at: https://doi.org/10.1128/JCM.42.11.5229-5237.2004.

Jakubovics, N.S. and Jenkinson, H.F. (2001) 'Out of the iron age: new insights into the critical role of manganese homeostasis in bacteria', *Microbiology (Reading, England)*, 147(Pt 7), pp. 1709–1718. Available at: https://doi.org/10.1099/00221287-147-7-1709.

Jenal, U., Reinders, A. and Lori, C. (2017) 'Cyclic di-GMP: second messenger extraordinaire', *Nature Reviews Microbiology*, 15(5), pp. 271–284. Available at: https://doi.org/10.1038/nrmicro.2016.190.

Jennings, L.K. *et al.* (2021) '*Pseudomonas aeruginosa* aggregates in cystic fibrosis sputum produce exopolysaccharides that likely impede current therapies', *Cell Reports*, 34(8), p. 108782. Available at: https://doi.org/10.1016/j.celrep.2021.108782.

Jeon, J.H. *et al.* (2015) 'Structural basis for carbapenem-hydrolyzing mechanisms of carbapenemases conferring antibiotic resistance', *International Journal of Molecular Sciences*, 16(5), pp. 9654–9692. Available at: https://doi.org/10.3390/ijms16059654.

Jiao, Y. *et al.* (2010) 'Characterization of extracellular polymeric substances from acidophilic microbial biofilms', *Applied and Environmental Microbiology*, 76(9), pp. 2916–2922. Available at: https://doi.org/10.1128/AEM.02289-09.

Jin, J.S. *et al.* (2011) '*Acinetobacter baumannii* Secretes Cytotoxic Outer Membrane Protein A via Outer Membrane Vesicles', *PLoS ONE*, 6(2), p. e17027. Available at: https://doi.org/10.1371/journal.pone.0017027.

Jouybari, M.A. *et al.* (2021) 'Role of aminoglycoside-modifying enzymes and 16S rRNA methylase (ArmA) in resistance of *Acinetobacter baumannii* clinical isolates against aminoglycosides', *Revista da Sociedade Brasileira de Medicina Tropical*, 54, p. e05992020. Available at: https://doi.org/10.1590/0037-8682-0599-2020.

Jurcisek, J.A. *et al.* (2022) 'Monoclonal antibodies that target extracellular DNABII proteins or the type IV pilus of nontypeable Haemophilus influenzae (NTHI) worked additively to disrupt 2-genera biofilms', *Biofilm*, 4, p. 100096. Available at: https://doi.org/10.1016/j.bioflm.2022.100096.

Kabic, J. *et al.* (2023) 'Comparative genomics and molecular epidemiology of colistin-resistant *Acinetobacter baumannii*', *Computational and Structural Biotechnology Journal*, 21, pp. 574–585. Available at: https://doi.org/10.1016/j.csbj.2022.12.045.

Kalpana, B.J., Aarthy, S. and Pandian, S.K. (2012) 'Antibiofilm activity of α-amylase from Bacillus subtilis S8-18 against biofilm forming human bacterial pathogens', *Applied Biochemistry and Biotechnology*, 167(6), pp. 1778–1794. Available at: https://doi.org/10.1007/s12010-011-9526-2.

Kamoshida, G. *et al.* (2022) 'Preferential Selection of Low-Frequency, Lipopolysaccharide-Modified, Colistin-Resistant Mutants with a Combination of Antimicrobials in *Acinetobacter baumannii*', *Microbiology Spectrum*, 10(5), p. e0192822. Available at: https://doi.org/10.1128/spectrum.01928-22.

Kantha, S.S. (1991) 'A centennial review; the 1890 tetanus antitoxin paper of von Behring and Kitasato and the related developments.', *The Keio Journal of Medicine*, 40(1), pp. 35–39. Available at: https://doi.org/10.2302/kjm.40.35.

Kany, A.M. *et al.* (2018) 'Tackling *Pseudomonas aeruginosa* Virulence by a Hydroxamic Acid-Based LasB Inhibitor', *ACS chemical biology*, 13(9), pp. 2449–2455. Available at: https://doi.org/10.1021/acschembio.8b00257.

Kaplan, J.B. *et al.* (2012) 'Recombinant human DNase I decreases biofilm and increases antimicrobial susceptibility in staphylococci', *The Journal of antibiotics*, 65(2), pp. 73–77. Available at: https://doi.org/10.1038/ja.2011.113.

Kaplan, J.B. *et al.* (2018) 'Extracellular polymeric substance (EPS)-degrading enzymes reduce staphylococcal surface attachment and biocide resistance on pig skin in vivo', *PLOS ONE*, 13(10), p. e0205526. Available at: https://doi.org/10.1371/journal.pone.0205526.

Karash, S. *et al.* (2021) 'Genome Sequences of Two *Pseudomonas aeruginosa* Isolates with Defects in Type III Secretion System Gene Expression from a Chronic Ankle Wound Infection', *Microbiology Spectrum*, 9(1), pp. e00340-21. Available at: https://doi.org/10.1128/Spectrum.00340-21.

Kauppi, A.M. *et al.* (2003) 'Targeting Bacterial Virulence: Inhibitors of Type III Secretion in Yersinia', *Chemistry & Biology*, 10(3), pp. 241–249. Available at: https://doi.org/10.1016/S1074-5521(03)00046-2.

Kaur, A., Capalash, N. and Sharma, P. (2018) 'Quorum sensing in thermophiles: prevalence of autoinducer-2 system', *BMC microbiology*, 18(1), p. 62. Available at: https://doi.org/10.1186/s12866-018-1204-x.

Kaye, K.S. *et al.* (2016) 'Agents of Last Resort: Polymyxin Resistance', *Infectious Disease Clinics of North America*, 30(2), pp. 391–414. Available at: https://doi.org/10.1016/j.idc.2016.02.005.

Keen, E.F. *et al.* (2010) 'Prevalence of multidrug-resistant organisms recovered at a military burn center', *Burns: Journal of the International Society for Burn Injuries*, 36(6), pp. 819–825. Available at: https://doi.org/10.1016/j.burns.2009.10.013.

Kelly, C.P. *et al.* (2020) 'Effect of Endogenous Clostridioides difficile Toxin Antibodies on Recurrence of C. difficile Infection', *Clinical Infectious Diseases: An Official Publication of the Infectious Diseases Society of America*, 71(1), pp. 81–86. Available at: https://doi.org/10.1093/cid/ciz809.

Kelson, A.B., Carnevali, M. and Truong-Le, V. (2013) 'Gallium-based anti-infectives: targeting microbial iron-uptake mechanisms', *Current Opinion in Pharmacology*, 13(5), pp. 707–716. Available at: https://doi.org/10.1016/j.coph.2013.07.001.

Khan, S.H. and Kumar, R. (2009) 'An Overview of the Importance of Conformational Flexibility in Gene Regulation by the Transcription Factors', *Journal of Biophysics*, 2009, p. 210485. Available at: https://doi.org/10.1155/2009/210485.

Khasheii, B., Mahmoodi, P. and Mohammadzadeh, A. (2021) 'Siderophores: Importance in bacterial pathogenesis and applications in medicine and industry', *Microbiological Research*, 250, p. 126790. Available at: https://doi.org/10.1016/j.micres.2021.126790.

Khatoon, Z. *et al.* (2018) 'Bacterial biofilm formation on implantable devices and approaches to its treatment and prevention', *Heliyon*, 4(12), p. e01067. Available at: https://doi.org/10.1016/j.heliyon.2018.e01067.

Kim, C.-K. *et al.* (2010) 'Prevalence and diversity of carbapenemases among imipenem-nonsusceptible Acinetobacter isolates in Korea: emergence of a novel OXA-182', *Diagnostic Microbiology and Infectious Disease*, 68(4), pp. 432–438. Available at: https://doi.org/10.1016/j.diagmicrobio.2010.07.014.

Kim, M. *et al.* (2021) 'Distinctive Roles of Two Acinetobactin Isomers in Challenging Host Nutritional Immunity', *mBio*, 12(5), p. e0224821. Available at: https://doi.org/10.1128/mBio.02248-21.

Kim, S.W. *et al.* (2009) 'Serum resistance of *Acinetobacter baumannii* through the binding of factor H to outer membrane proteins', *FEMS microbiology letters*, 301(2), pp. 224–231. Available at: https://doi.org/10.1111/j.1574-6968.2009.01820.x.

Kiran, M.D. *et al.* (2008) 'Discovery of a quorum-sensing inhibitor of drug-resistant staphylococcal infections by structure-based virtual screening', *Molecular Pharmacology*, 73(5), pp. 1578–1586. Available at: https://doi.org/10.1124/mol.107.044164.

Kleeb, S. *et al.* (2015) 'FimH antagonists: bioisosteres to improve the in vitro and in vivo PK/PD profile', *Journal of Medicinal Chemistry*, 58(5), pp. 2221–2239. Available at: https://doi.org/10.1021/jm501524q.

Klobucar, K. and Brown, E.D. (2022) 'New potentiators of ineffective antibiotics: Targeting the Gram-negative outer membrane to overcome intrinsic resistance', *Current Opinion in Chemical Biology*, 66, p. 102099. Available at: https://doi.org/10.1016/j.cbpa.2021.102099.

Koay, A. *et al.* (2020) 'Exploring the Irish National Folklore Ethnography Database (Dúchas) for Open Data Research on Traditional Medicine Use in Post-Famine Ireland: An Early Example of Citizen Science', *Frontiers in Pharmacology*, 11, p. 584595. Available at: https://doi.org/10.3389/fphar.2020.584595.

Koh, T.H. *et al.* (2007) 'IMP-4 and OXA beta-lactamases in *Acinetobacter baumannii* from Singapore', *The Journal of Antimicrobial Chemotherapy*, 59(4), pp. 627–632. Available at: https://doi.org/10.1093/jac/dkl544.

Kong, X. *et al.* (2022) 'Hinokiflavone Attenuates the Virulence of Methicillin-Resistant Staphylococcus aureus by Targeting Caseinolytic Protease P', *Antimicrobial Agents and Chemotherapy*, 66(8), pp. e00240-22. Available at: https://doi.org/10.1128/aac.00240-22.

Krause, K.M. *et al.* (2016) 'Aminoglycosides: An Overview', *Cold Spring Harbor Perspectives in*

Medicine, 6(6), p. a027029. Available at: https://doi.org/10.1101/cshperspect.a027029.

Krizova, L. *et al.* (2013) 'TEM-1 β-lactamase as a source of resistance to sulbactam in clinical strains of *Acinetobacter baumannii*', *The Journal of Antimicrobial Chemotherapy*, 68(12), pp. 2786–2791. Available at: https://doi.org/10.1093/jac/dkt275.

Kryvtsova, M. *et al.* (2019) 'Antimicrobial, antibiofilm-forming and some biochemical properties of Potentilla erecta rhizome extract.', *Biotechnologia Acta*, 12(5), pp. 72–81.

Kubo, A., Lunde, C.S. and Kubo, I. (1996) 'Indole and (E)-2-hexenal, phytochemical potentiators of polymyxins against *Pseudomonas aeruginosa* and *Escherichia coli*', *Antimicrobial Agents and Chemotherapy*, 40(6), pp. 1438–1441. Available at: https://doi.org/10.1128/aac.40.6.1438.

Kügler, S. *et al.* (2020) 'Rhizobactin B is the preferred siderophore by a novel Pseudomonas isolate to obtain iron from dissolved organic matter in peatlands', *Biometals*, 33(6), pp. 415–433. Available at: https://doi.org/10.1007/s10534-020-00258-w.

Kumar, A. *et al.* (2010) 'Mini-Tn7 vectors as genetic tools for single copy gene cloning in *Acinetobacter baumannii*', *Journal of Microbiological Methods*, 82(3), pp. 296–300. Available at: https://doi.org/10.1016/j.mimet.2010.07.002.

Kumar, D. *et al.* (2023) 'Colistin potentiation in multidrug-resistant *Acinetobacter baumannii* by a non-cytotoxic guanidine derivative of silver', *Frontiers in Microbiology*, 13, p. 1006604. Available at: https://doi.org/10.3389/fmicb.2022.1006604.

Kumar, S. *et al.* (2018) 'MEGA X: Molecular Evolutionary Genetics Analysis across Computing Platforms', *Molecular Biology and Evolution*, 35(6), pp. 1547–1549. Available at: https://doi.org/10.1093/molbev/msy096.

Kumari, S. *et al.* (2021) 'A holistic overview of different species of Potentilla a medicinally important plant along with their pharmaceutical significance: A review', *Journal of Herbal Medicine*, 29, p. 100460. Available at: https://doi.org/10.1016/j.hermed.2021.100460.

Kuo, H.-Y. *et al.* (2016) 'Clonal spread of blaOXA-72-carrying *Acinetobacter baumannii* sequence type 512 in Taiwan', *International Journal of Antimicrobial Agents*, 48(1), pp. 111–113. Available at: https://doi.org/10.1016/j.ijantimicag.2016.04.020.

Kuo, S.-C. *et al.* (2012) 'Emergence of extensively drug-resistant *Acinetobacter baumannii* complex over 10 years: Nationwide data from the Taiwan Surveillance of Antimicrobial Resistance (TSAR) program', *BMC Infectious Diseases*, 12(1), p. 200. Available at: https://doi.org/10.1186/1471-2334-12-200.

Kurbatfinski, N., Goodman, S.D. and Bakaletz, L.O. (2022) 'A Humanized Monoclonal Antibody Potentiates Killing of Diverse Biofilm-Forming Respiratory Tract Pathogens by Antibiotics', *Antimicrobial Agents and Chemotherapy*, 66(3), p. e0187721. Available at: https://doi.org/10.1128/AAC.01877-21.

Laurence, J.S. and Middaugh, C.R. (2010) 'Fundamental Structures and Behaviors of Proteins', in W. Wang and C.J. Roberts (eds) *Aggregation of Therapeutic Proteins*. 1st edn. Wiley, pp. 1–61. Available at: https://doi.org/10.1002/9780470769829.ch1.

Lee, C.-R. *et al.* (2017) 'Biology of *Acinetobacter baumannii*: Pathogenesis, Antibiotic Resistance

Mechanisms, and Prospective Treatment Options', *Frontiers in Cellular and Infection Microbiology*, 7, p. 55. Available at: https://doi.org/10.3389/fcimb.2017.00055.

Lee, K. *et al.* (2005) 'Novel Acquired Metallo-β-Lactamase Gene, blaSIM-1, in a Class 1 Integron from *Acinetobacter baumannii* Clinical Isolates from Korea', *Antimicrobial Agents and Chemotherapy*, 49(11), pp. 4485–4491. Available at: https://doi.org/10.1128/AAC.49.11.4485-4491.2005.

Lee, K.-M. *et al.* (2011) 'Inhibitory effects of broccoli extract on *Escherichia coli* O157:H7 quorum sensing and in vivo virulence', *FEMS Microbiology Letters*, 321(1), pp. 67–74. Available at: https://doi.org/10.1111/j.1574-6968.2011.02311.x.

Lee, M.-F. *et al.* (2008) 'Molecular characterisation of the metallo-beta-lactamase genes in imipenem-resistant Gram-negative bacteria from a university hospital in southern Taiwan', *International Journal of Antimicrobial Agents*, 32(6), pp. 475–480. Available at: https://doi.org/10.1016/j.ijantimicag.2008.07.009.

Leggett, A. *et al.* (2022) 'Differential metabolism between biofilm and suspended *Pseudomonas aeruginosa* cultures in bovine synovial fluid by 2D NMR-based metabolomics', *Scientific Reports*, 12(1), p. 17317. Available at: https://doi.org/10.1038/s41598-022-22127-x.

Leung, W.-S. *et al.* (2006) 'Fulminant Community-Acquired *Acinetobacter baumannii* Pneumonia as a Distinct Clinical Syndrome', *CHEST*, 129(1), pp. 102–109. Available at: https://doi.org/10.1378/chest.129.1.102.

Levin, B. and Rozen, D. (2006) 'Non-inherited antibiotic resistance', *Nature reviews. Microbiology*, 4(7). Available at: https://doi.org/10.1038/nrmicro1445.

Li, B. *et al.* (2016) 'The importance of lag time extension in determining bacterial resistance to antibiotics', *Analyst*, 141(10), pp. 3059–3067. Available at: https://doi.org/10.1039/C5AN02649K.

Li, D., Selyunin, A. and Mukhopadhyay, S. (2020) 'Targeting the Early Endosome-to-Golgi Transport of Shiga Toxins as a Therapeutic Strategy', *Toxins*, 12(5), p. 342. Available at: https://doi.org/10.3390/toxins12050342.

Li, J. *et al.* (2005) 'Evaluation of colistin as an agent against multi-resistant Gram-negative bacteria', *International Journal of Antimicrobial Agents*, 25(1), pp. 11–25. Available at: https://doi.org/10.1016/j.ijantimicag.2004.10.001.

Li, J. *et al.* (2006) 'Heteroresistance to colistin in multidrug-resistant *Acinetobacter baumannii*', *Antimicrobial Agents and Chemotherapy*, 50(9), pp. 2946–2950. Available at: https://doi.org/10.1128/AAC.00103-06.

Li, W. *et al.* (2023) 'Association between antibiotic resistance and increasing ambient temperature in China: an ecological study with nationwide panel data', *The Lancet Regional Health – Western Pacific*, 30. Available at: https://doi.org/10.1016/j.lanwpc.2022.100628.

Li, Y. *et al.* (2015) 'Clonal dissemination of extensively drug-resistant *Acinetobacter baumannii* producing an OXA-23 β-lactamase at a teaching hospital in Shanghai, China', *Journal of Microbiology, Immunology, and Infection = Wei Mian Yu Gan Ran Za Zhi*, 48(1), pp. 101–108. Available at: https://doi.org/10.1016/j.jmii.2014.04.005.

Lim, T.P. *et al.* (2015) 'Multiple Genetic Mutations Associated with Polymyxin Resistance in *Acinetobacter baumannii*', *Antimicrobial Agents and Chemotherapy*, 59(12), pp. 7899–7902. Available at: https://doi.org/10.1128/AAC.01884-15.

Limoli, D.H., Jones, C.J. and Wozniak, D.J. (2015) 'Bacterial Extracellular Polysaccharides in Biofilm Formation and Function', *Microbiology spectrum*, 3(3), p. 10.1128/microbiolspec.MB-0011–2014. Available at: https://doi.org/10.1128/microbiolspec.MB-0011-2014.

Lin, M.-F. and Lan, C.-Y. (2014) 'Antimicrobial resistance in *Acinetobacter baumannii*: From bench to bedside', *World Journal of Clinical Cases : WJCC*, 2(12), pp. 787–814. Available at: https://doi.org/10.12998/wjcc.v2.i12.787.

Lin, M.-F. *et al.* (2013) 'Molecular Epidemiology of Integron-Associated Antimicrobial Gene Cassettes in the Clinical Isolates of *Acinetobacter baumannii* from Northern Taiwan', *Annals of Laboratory Medicine*, 33(4), pp. 242–247. Available at: https://doi.org/10.3343/alm.2013.33.4.242.

Lin, M.-F., Lin, Y.-Y. and Lan, C.-Y. (2017) 'Contribution of EmrAB efflux pumps to colistin resistance in *Acinetobacter baumannii*', *Journal of Microbiology (Seoul, Korea)*, 55(2), pp. 130–136. Available at: https://doi.org/10.1007/s12275-017-6408-5.

Liou, M.-L. *et al.* (2014) 'The sensor kinase BfmS mediates virulence in *Acinetobacter baumannii*', *Journal of Microbiology, Immunology, and Infection = Wei Mian Yu Gan Ran Za Zhi*, 47(4), pp. 275–281. Available at: https://doi.org/10.1016/j.jmii.2012.12.004.

Lipinski, C.A. (2000) 'Drug-like properties and the causes of poor solubility and poor permeability', *Journal of Pharmacological and Toxicological Methods*, 44(1), pp. 235–249. Available at: https://doi.org/10.1016/s1056-8719(00)00107-6.

Lipinski, C.A. *et al.* (2001) 'Experimental and computational approaches to estimate solubility and permeability in drug discovery and development settings', *Advanced Drug Delivery Reviews*, 46(1–3), pp. 3–26. Available at: https://doi.org/10.1016/s0169-409x(00)00129-0.

Liu, G. *et al.* (2011) 'In Vitro Synergy of Biochanin A and Ciprofloxacin against Clinical Isolates of Staphylococcus aureus', *Molecules*, 16(8), pp. 6656–6666. Available at: https://doi.org/10.3390/molecules16086656.

Liu, Q. *et al.* (2014) 'Efficacy and Safety of Polymyxins for the Treatment of Acinectobacter baumannii Infection: A Systematic Review and Meta-Analysis', *PLoS ONE*, 9(6), p. e98091. Available at: https://doi.org/10.1371/journal.pone.0098091.

Liu, X. *et al.* (2023) 'Antibacterial mechanism of inosine against Alicyclobacillus acidoterrestris'. bioRxiv, p. 2023.07.05.547889. Available at: https://doi.org/10.1101/2023.07.05.547889.

LIU, Y. and LIU, X. (2015) 'Detection of AmpC β-lactamases in *Acinetobacter baumannii* in the Xuzhou region and analysis of drug resistance', *Experimental and Therapeutic Medicine*, 10(3), pp. 933–936. Available at: https://doi.org/10.3892/etm.2015.2612.

Liu, Y. *et al.* (2011) 'Accurate assessment of antibiotic susceptibility and screening resistant strains of a bacterial population by linear gradient plate', *Science China Life Sciences*, 54(10), pp. 953–960. Available at: https://doi.org/10.1007/s11427-011-4230-6.

Liu, Y.-H. *et al.* (2012) 'Amino acid substitutions of quinolone resistance determining regions in GyrA

and ParC associated with quinolone resistance in *Acinetobacter baumannii* and *Acinetobacter* genomic species 13TU', *Journal of Microbiology, Immunology and Infection*, 45(2), pp. 108–112. Available at: https://doi.org/10.1016/j.jmii.2011.09.001.

Liu, Y.-Y. *et al.* (2016) 'Emergence of plasmid-mediated colistin resistance mechanism MCR-1 in animals and human beings in China: a microbiological and molecular biological study', *The Lancet Infectious Diseases*, 16(2), pp. 161–168. Available at: https://doi.org/10.1016/S1473-3099(15)00424-7.

Lob, S.H. *et al.* (2016) 'Regional differences and trends in antimicrobial susceptibility of *Acinetobacter baumannii*', *International Journal of Antimicrobial Agents*, 47(4), pp. 317–323. Available at: https://doi.org/10.1016/j.ijantimicag.2016.01.015.

Loehfelm, T.W., Luke, N.R. and Campagnari, A.A. (2008) 'Identification and characterization of an *Acinetobacter baumannii* biofilm-associated protein', *Journal of Bacteriology*, 190(3), pp. 1036–1044. Available at: https://doi.org/10.1128/JB.01416-07.

Lopalco, P. *et al.* (2017) 'Identification of unique cardiolipin and monolysocardiolipin species in *Acinetobacter baumannii*', *Scientific Reports*, 7(1), p. 2972. Available at: https://doi.org/10.1038/s41598-017-03214-w.

López-Rojas, R. *et al.* (2013) 'Colistin Resistance in a Clinical *Acinetobacter baumannii* Strain Appearing after Colistin Treatment: Effect on Virulence and Bacterial Fitness', *Antimicrobial Agents and Chemotherapy*, 57(9), pp. 4587–4589. Available at: https://doi.org/10.1128/AAC.00543-13.

López-Rojas, R., Domínguez-Herrera, J., *et al.* (2011) 'Impaired Virulence and In Vivo Fitness of Colistin-Resistant *Acinetobacter baumannii*', *The Journal of Infectious Diseases*, 203(4), pp. 545–548. Available at: https://doi.org/10.1093/infdis/jiq086.

López-Rojas, R., Jiménez-Mejías, M.E., *et al.* (2011) '*Acinetobacter baumannii* Resistant to Colistin Alters Its Antibiotic Resistance Profile: A Case Report From Spain', *The Journal of Infectious Diseases*, 204(7), pp. 1147–1148. Available at: https://doi.org/10.1093/infdis/jir476.
López-Rojas, R., Smani, Y. and Pachón, J. (2013) 'Treating multidrug-resistant *Acinetobacter baumannii* infection by blocking its virulence factors', *Expert Review of Anti-infective Therapy*, 11(3), pp. 231–233. Available at: https://doi.org/10.1586/eri.13.11.

Lora-Tamayo, J., Murillo, O. and Ariza, J. (2019) 'Clinical Use of Colistin in Biofilm-Associated Infections', *Advances in Experimental Medicine and Biology*, 1145, pp. 181–195. Available at: https://doi.org/10.1007/978-3-030-16373-0_13.

Loughran, A.J. *et al.* (2014) 'Impact of individual extracellular proteases on Staphylococcus aureus biofilm formation in diverse clinical isolates and their isogenic sarA mutants', *MicrobiologyOpen*, 3(6), pp. 897–909. Available at: https://doi.org/10.1002/mbo3.214.

Lowe, M. *et al.* (2022) 'Molecular characterisation of Acinetobacter baumannii isolates from bloodstream infections in a tertiary-level hospital in South Africa', *Frontiers in Microbiology*, 13. Available at: https://doi.org/10.3389/fmicb.2022.863129.

Lowy, I. *et al.* (2010) 'Treatment with Monoclonal Antibodies against Clostridium difficile Toxins', *New England Journal of Medicine*, 362(3), pp. 197–205. Available at: https://doi.org/10.1056/NEJMoa0907635.

Lushniak, B.D. (2014) 'Antibiotic resistance: a public health crisis', *Public Health Reports (Washington, D.C.: 1974)*, 129(4), pp. 314–316. Available at: https://doi.org/10.1177/003335491412900402.

Ma, P. and Phillips-Jones, M.K. (2021) 'Membrane Sensor Histidine Kinases: Insights from Structural, Ligand and Inhibitor Studies of Full-Length Proteins and Signalling Domains for Antibiotic Discovery', *Molecules*, 26(16). Available at: https://doi.org/10.3390/molecules26165110.

MacFadden, D.R. *et al.* (2018) *Antibiotic resistance increases with local temperature | Nature Climate Change*. Available at: https://www.nature.com/articles/s41558-%20018-0161-6 (Accessed: 7 March 2023).

MacLean, R.C. and San Millan, A. (2019) 'The evolution of antibiotic resistance', *Science (New York, N.Y.)*, 365(6458), pp. 1082–1083. Available at: https://doi.org/10.1126/science.aax3879.

MacNair, C.R. and Brown, E.D. (2020) 'Outer Membrane Disruption Overcomes Intrinsic, Acquired, and Spontaneous Antibiotic Resistance', *mBio*, 11(5), pp. e01615-20. Available at: https://doi.org/10.1128/mBio.01615-20.

Mahase, E. (2023) 'Antibiotic resistant infections and deaths rose in England after pandemic controls ended', *BMJ*, 383, p. p2672. Available at: https://doi.org/10.1136/bmj.p2672.

Mak, J.K. *et al.* (2009) 'Antibiotic resistance determinants in nosocomial strains of multidrug-resistant *Acinetobacter baumannii*', *The Journal of Antimicrobial Chemotherapy*, 63(1), pp. 47–54. Available at: https://doi.org/10.1093/jac/dkn454.

Malinverni, J.C. and Silhavy, T.J. (2009) 'An ABC transport system that maintains lipid asymmetry in the gram-negative outer membrane', *Proceedings of the National Academy of Sciences of the United States of America*, 106(19), pp. 8009–8014. Available at: https://doi.org/10.1073/pnas.0903229106.

Mani, J. *et al.* (2022) 'Bioassay Guided Fractionation Protocol for Determining Novel Active Compounds in Selected Australian Flora', *Plants*, 11(21), p. 2886. Available at: https://doi.org/10.3390/plants11212886.

Manioglu, S. *et al.* (2022) 'Antibiotic polymyxin arranges lipopolysaccharide into crystalline structures to solidify the bacterial membrane', *Nature Communications*, 13(1), p. 6195. Available at: https://doi.org/10.1038/s41467-022-33838-0.

Maragakis, L.L. and Perl, T.M. (2008) '*Acinetobacter baumannii*: epidemiology, antimicrobial resistance, and treatment options', *Clinical Infectious Diseases: An Official Publication of the Infectious Diseases Society of America*, 46(8), pp. 1254–1263. Available at: https://doi.org/10.1086/529198.

Marina, A., Waldburger, C.D. and Hendrickson, W.A. (2005) 'Structure of the entire cytoplasmic portion of a sensor histidine-kinase protein', *The EMBO Journal*, 24(24), pp. 4247–4259. Available at: https://doi.org/10.1038/sj.emboj.7600886.

Marković, J.M. *et al.* (2014) 'Oxidation of kaempferol and its iron(III) complex by DPPH radicals: spectroscopic and theoretical study', *Monatshefte für Chemie - Chemical Monthly*, 145(4), pp. 557–563. Available at: https://doi.org/10.1007/s00706-013-1135-z.

Martinez, T. *et al.* (2016) 'Genetic environment of the KPC gene in *Acinetobacter baumannii* ST2

clone from Puerto Rico and genomic insights into its drug resistance', *Journal of Medical Microbiology*, 65(8), pp. 784–792. Available at: https://doi.org/10.1099/jmm.0.000289.

Martinez, T. *et al.* (2016) 'Genetic environment of the KPC gene in *Acinetobacter baumannii* ST2 clone from Puerto Rico and genomic insights into its drug resistance', *Journal of Medical Microbiology*, 65(8), pp. 784–792. Available at: https://doi.org/10.1099/jmm.0.000289.

Maslova, E. *et al.* (2021) 'Burns and biofilms: priority pathogens and in vivo models', *npj Biofilms and Microbiomes*, 7(1), pp. 1–9. Available at: https://doi.org/10.1038/s41522-021-00243-2.

Maure, A., Robino, E. and Henst, C.V. der (2023) 'The intracellular life of Acinetobacter baumannii', *Trends in Microbiology*, 31(12), pp. 1238–1250. Available at: https://doi.org/10.1016/j.tim.2023.06.007.

McCarthy, R.R. *et al.* (2017) 'Cyclic-di-GMP regulates lipopolysaccharide modification and contributes to *Pseudomonas aeruginosa* immune evasion', *Nature Microbiology*, 2(6), pp. 1–10. Available at: https://doi.org/10.1038/nmicrobiol.2017.27.

McCarthy, R.R. *et al.* (2021) 'Antibiotic Resistance Mechanisms and Their Transmission in *Acinetobacter baumannii*', *Advances in Experimental Medicine and Biology*, 1313, pp. 135–153. Available at: https://doi.org/10.1007/978-3-030-67452-6_7.

McCarthy, R.R., Valentini, M. and Filloux, A. (2017) 'Contribution of Cyclic di-GMP in the Control of Type III and Type VI Secretion in *Pseudomonas aeruginosa*', *Methods in Molecular Biology (Clifton, N.J.)*, 1657, pp. 213–224. Available at: https://doi.org/10.1007/978-1-4939-7240-1_17.

McCready, A.R. *et al.* (2019) 'An autoinducer-independent RhlR quorum-sensing receptor enables analysis of RhlR regulation', *PLOS Pathogens*, 15(6), p. e1007820. Available at: https://doi.org/10.1371/journal.ppat.1007820.

McQueary, C.N. *et al.* (2012) 'Extracellular stress and lipopolysaccharide modulate *Acinetobacter baumannii* surface-associated motility', *Journal of Microbiology*, 50(3), pp. 434–443. Available at: https://doi.org/10.1007/s12275-012-1555-1.

Ménard, G. *et al.* (2021) 'Galleria mellonella as a Suitable Model of Bacterial Infection: Past, Present and Future', *Frontiers in Cellular and Infection Microbiology*, 11, p. 782733. Available at: https://doi.org/10.3389/fcimb.2021.782733.

Mendes, R.E. *et al.* (2009) 'Emergence and widespread dissemination of OXA-23, -24/40 and -58 carbapenemases among Acinetobacter spp. in Asia-Pacific nations: report from the SENTRY Surveillance Program', *The Journal of Antimicrobial Chemotherapy*, 63(1), pp. 55–59. Available at: https://doi.org/10.1093/jac/dkn434.

Mihara, K. *et al.* (2004) 'Identification and transcriptional organization of a gene cluster involved in biosynthesis and transport of acinetobactin, a siderophore produced by *Acinetobacter baumannii* ATCC 19606T', *Microbiology (Reading, England)*, 150(Pt 8), pp. 2587–2597. Available at: https://doi.org/10.1099/mic.0.27141-0.

Mikheyeva, I.V. *et al.* (2023) 'Mechanism of outer membrane destabilization by global reduction of protein content', *bioRxiv*, p. 2023.02.19.529137. Available at: https://doi.org/10.1101/2023.02.19.529137.

Miller, S.J. and Morgan, B.W. (2014) 'Deferoxamine', in P. Wexler (ed.) *Encyclopedia of Toxicology (Third Edition)*. Oxford: Academic Press, pp. 1154–1156. Available at: https://doi.org/10.1016/B978-0-12-386454-3.00721-1.

Milliken, W. (2023) 'Ethnoveterinary data in Britain and Ireland: can native herbal medicine promote animal health?', *Ethnobotany Research and Applications*, 26, pp. 1–32.

Ming, D. *et al.* (2017) 'Kaempferol Inhibits the Primary Attachment Phase of Biofilm Formation in Staphylococcus aureus', *Frontiers in Microbiology*, 8. Available at: https://www.frontiersin.org/article/10.3389/fmicb.2017.02263 (Accessed: 13 May 2022).

Mizar, P. *et al.* (2018) 'Total Synthesis of Xanthoangelol B and Its Various Fragments: Toward Inhibition of Virulence Factor Production of Staphylococcus aureus', *Journal of Medicinal Chemistry*, 61(23), pp. 10473–10487. Available at: https://doi.org/10.1021/acs.jmedchem.8b01012.

Moffatt, J.H. *et al.* (2010) 'Colistin resistance in *Acinetobacter baumannii* is mediated by complete loss of lipopolysaccharide production', *Antimicrobial Agents and Chemotherapy*, 54(12), pp. 4971–4977. Available at: https://doi.org/10.1128/AAC.00834-10.

Montaner, M. *et al.* (2023) 'PBP Target Profiling by β-Lactam and β-Lactamase Inhibitors in Intact *Pseudomonas aeruginosa*: Effects of the Intrinsic and Acquired Resistance Determinants on the Periplasmic Drug Availability', *Microbiology Spectrum*, 11(1), pp. e03038-22. Available at: https://doi.org/10.1128/spectrum.03038-22.

Moon, K.H., Weber, B.S. and Feldman, M.F. (2017) 'Subinhibitory Concentrations of Trimethoprim and Sulfamethoxazole Prevent Biofilm Formation by *Acinetobacter baumannii* through Inhibition of Csu Pilus Expression', *Antimicrobial Agents and Chemotherapy*, 61(9), pp. e00778-17. Available at: https://doi.org/10.1128/AAC.00778-17.

Mootz, J.M. *et al.* (2013) 'Staphopains Modulate Staphylococcus aureus Biofilm Integrity', *Infection and Immunity*, 81(9), pp. 3227–3238. Available at: https://doi.org/10.1128/IAI.00377-13.

Morris, F.C. *et al.* (2019) 'The Mechanisms of Disease Caused by *Acinetobacter baumannii*', *Frontiers in Microbiology*, 10, p. 1601. Available at: https://doi.org/10.3389/fmicb.2019.01601.

Mouton, J.W. *et al.* (2018) 'MIC-based dose adjustment: facts and fables', *The Journal of Antimicrobial Chemotherapy*, 73(3), pp. 564–568. Available at: https://doi.org/10.1093/jac/dkx427.

Mu, X. *et al.* (2016) 'The Effect of Colistin Resistance-Associated Mutations on the Fitness of *Acinetobacter baumannii*', *Frontiers in Microbiology*, 7, p. 1715. Available at: https://doi.org/10.3389/fmicb.2016.01715.

Mu, Y., Zeng, H. and Chen, W. (2020) 'Okanin in Coreopsis tinctoria Nutt is a major quorum-sensing inhibitor against Chromobacterium violaceum', *Journal of Ethnopharmacology*, 260, p. 113017. Available at: https://doi.org/10.1016/j.jep.2020.113017.

Mulani, M.S. *et al.* (2019) 'Emerging Strategies to Combat ESKAPE Pathogens in the Era of Antimicrobial Resistance: A Review', *Frontiers in Microbiology*, 10. Available at: https://www.frontiersin.org/articles/10.3389/fmicb.2019.00539 (Accessed: 1 November 2023).

Murray, C.J. *et al.* (2022) 'Global burden of bacterial antimicrobial resistance in 2019: a systematic analysis', *The Lancet*, 399(10325), pp. 629–655. Available at: https://doi.org/10.1016/S0140-

6736(21)02724-0.

Muschiol, S. *et al.* (2006) 'A small-molecule inhibitor of type III secretion inhibits different stages of the infectious cycle of Chlamydia trachomatis', *Proceedings of the National Academy of Sciences of the United States of America*, 103(39), pp. 14566–14571. Available at: https://doi.org/10.1073/pnas.0606412103.

Naas, T. *et al.* (2007) 'Panresistant extended-spectrum β-lactamase SHV-5-producing *Acinetobacter baumannii* from New York City', *Journal of Antimicrobial Chemotherapy*, 60(5), pp. 1174–1176. Available at: https://doi.org/10.1093/jac/dkm366.

Nagano, N. *et al.* (2004) 'Nosocomial Transmission of CTX-M-2 β-Lactamase-Producing *Acinetobacter baumannii* in a Neurosurgery Ward', *Journal of Clinical Microbiology*, 42(9), pp. 3978–3984. Available at: https://doi.org/10.1128/JCM.42.9.3978-3984.2004.

Navia, M.M., Ruiz, J. and Vila, J. (2002) 'Characterization of an integron carrying a new class D beta-lactamase (OXA-37) in *Acinetobacter baumannii*', *Microbial Drug Resistance (Larchmont, N.Y.)*, 8(4), pp. 261–265. Available at: https://doi.org/10.1089/10766290260469516.

Nazaré, A.C. *et al.* (2014) 'Ethyl Ferulate, a Component with Anti-Inflammatory Properties for Emulsion-Based Creams', *Molecules*, 19(6), pp. 8124–8139. Available at: https://doi.org/10.3390/molecules19068124.

Neely, A.N. *et al.* (2005) 'Passive anti-PcrV treatment protects burned mice against *Pseudomonas aeruginosa* challenge', *Burns: Journal of the International Society for Burn Injuries*, 31(2), pp. 153–158. Available at: https://doi.org/10.1016/j.burns.2004.09.002.

Nemec, A. *et al.* (2004) 'Diversity of aminoglycoside-resistance genes and their association with class 1 integrons among strains of pan-European *Acinetobacter baumannii* clones', *Journal of Medical Microbiology*, 53(Pt 12), pp. 1233–1240. Available at: https://doi.org/10.1099/jmm.0.45716-0.

Nemoto, K. *et al.* (2003) 'Effect of Varidase (streptodornase) on biofilm formed by *Pseudomonas aeruginosa*', *Chemotherapy*, 49(3), pp. 121–125. Available at: https://doi.org/10.1159/000070617.

Nguyen, M. and Joshi, S. g. (2021) 'Carbapenem resistance in *Acinetobacter baumannii*, and their importance in hospital-acquired infections: a scientific review', *Journal of Applied Microbiology*, 131(6), pp. 2715–2738. Available at: https://doi.org/10.1111/jam.15130.

Nguyen, T. *et al.* (2021) 'The structural basis of Salmonella A2B5 toxin neutralization by antibodies targeting the glycan-receptor binding subunits', *Cell Reports*, 36(10), p. 109654. Available at: https://doi.org/10.1016/j.celrep.2021.109654.

Nguyen, U.T. and Burrows, L.L. (2014) 'DNase I and proteinase K impair Listeria monocytogenes biofilm formation and induce dispersal of pre-existing biofilms', *International Journal of Food Microbiology*, 187, pp. 26–32. Available at: https://doi.org/10.1016/j.ijfoodmicro.2014.06.025.

Ni, W. *et al.* (2016) 'Effects of Efflux Pump Inhibitors on Colistin Resistance in Multidrug-Resistant Gram-Negative Bacteria', *Antimicrobial Agents and Chemotherapy*, 60(5), pp. 3215–3218. Available at: https://doi.org/10.1128/AAC.00248-16.

Niu, C. *et al.* (2008) 'Isolation and characterization of an autoinducer synthase from *Acinetobacter baumannii*', *Journal of Bacteriology*, 190(9), pp. 3386–3392. Available at: https://doi.org/10.1128/JB.01929-07.

Nielsen, T.B. *et al.* (2017) 'Monoclonal Antibody Protects Against Acinetobacter baumannii Infection by Enhancing Bacterial Clearance and Evading Sepsis', *The Journal of Infectious Diseases*, 216(4), pp. 489–501. Available at: https://doi.org/10.1093/infdis/jix315.

Novotny, L.A. *et al.* (2013) 'Structural Stability of Burkholderia cenocepacia Biofilms Is Reliant on eDNA Structure and Presence of a Bacterial Nucleic Acid Binding Protein', *PLOS ONE*, 8(6), p. e67629. Available at: https://doi.org/10.1371/journal.pone.0067629.

Novotny, L.A. *et al.* (2016) 'Monoclonal antibodies against DNA-binding tips of DNABII proteins disrupt biofilms in vitro and induce bacterial clearance in vivo', *EBioMedicine*, 10, pp. 33–44. Available at: https://doi.org/10.1016/j.ebiom.2016.06.022.

Nowak, J., Seifert, H. and Higgins, P.G. (2015) 'Prevalence of eight resistance-nodulation-division efflux pump genes in epidemiologically characterized *Acinetobacter baumannii* of worldwide origin', *Journal of Medical Microbiology*, 64(6), pp. 630–635. Available at: https://doi.org/10.1099/jmm.0.000069.

Nuccio, S.-P. and Bäumler, A.J. (2007) 'Evolution of the Chaperone/Usher Assembly Pathway: Fimbrial Classification Goes Greek', *Microbiology and Molecular Biology Reviews*, 71(4), pp. 551–575. Available at: https://doi.org/10.1128/MMBR.00014-07.

Nurtop, E. *et al.* (2019) 'Promoters of Colistin Resistance in *Acinetobacter baumannii* Infections', *Microbial Drug Resistance (Larchmont, N.Y.)*, 25(7), pp. 997–1002. Available at: https://doi.org/10.1089/mdr.2018.0396.

Nwugo, C.C. *et al.* (2011) 'Deciphering the iron response in *Acinetobacter baumannii*: A proteomics approach', *Journal of Proteomics*, 74(1), pp. 44–58. Available at: https://doi.org/10.1016/j.jprot.2010.07.010.

O'Connor, K. *et al.* (2022) 'Frequency of quorum-sensing mutations in *Pseudomonas aeruginosa* strains isolated from different environments', *Microbiology*, 168(12), p. 001265. Available at: https://doi.org/10.1099/mic.0.001265.

O'Neill, J (2024) 'Antimicrobial Resistance: Tackling a crisis for the health and wealth of nations'. Available at: https://amr-review.org/sites/default/files/AMR%20Review%20Paper%20-%20Tackling%20a%20crisis%20for%20the%20health%20and%20wealth%20of%20nations_1.pdf.

O'Toole, G.A. (2011) 'Microtiter Dish Biofilm Formation Assay', Journal of Visualized Experiments : JoVE, (47), p. 2437. Available at: https://doi.org/10.3791/2437.

Okshevsky, M. and Meyer, R.L. (2015) 'The role of extracellular DNA in the establishment, maintenance and perpetuation of bacterial biofilms', *Critical Reviews in Microbiology*, 41(3), pp. 341–352. Available at: https://doi.org/10.3109/1040841X.2013.841639.

Olaitan, A.O., Morand, S. and Rolain, J.-M. (2014) 'Mechanisms of polymyxin resistance: acquired and intrinsic resistance in bacteria', *Frontiers in Microbiology*, 5, p. 643. Available at:

https://doi.org/10.3389/fmicb.2014.00643.

ONS (2021) *Causes of death over 100 years - Office for National Statistics*. Available at: https://www.ons.gov.uk/peoplepopulationandcommunity/birthsdeathsandmarriages/deaths/articles/causesofdeathover100years/2017-09-18 (Accessed: 10 March 2023).

Page, M.G.P. (2013) 'Siderophore conjugates', *Annals of the New York Academy of Sciences*, 1277, pp. 115–126. Available at: https://doi.org/10.1111/nyas.12024.

Page, M.G.P. (2019) 'The Role of Iron and Siderophores in Infection, and the Development of Siderophore Antibiotics', *Clinical Infectious Diseases: An Official Publication of the Infectious Diseases Society of America*, 69(Suppl 7), pp. S529–S537. Available at: https://doi.org/10.1093/cid/ciz825.

Pakharukova, N. *et al.* (2018) 'Structural basis for *Acinetobacter baumannii* biofilm formation', *Proceedings of the National Academy of Sciences of the United States of America*, 115(21), pp. 5558–5563. Available at: https://doi.org/10.1073/pnas.1800961115.

Palmieri, M. *et al.* (2020) 'Abundance of Colistin-Resistant, OXA-23- and ArmA-Producing *Acinetobacter baumannii* Belonging to International Clone 2 in Greece', *Frontiers in Microbiology*, 11. Available at: https://www.frontiersin.org/articles/10.3389/fmicb.2020.00668 (Accessed: 29 July 2022).

Pant, N. *et al.* (2022) 'Effect of savirin in the prevention of biofilm-related Staphylococcus aureus prosthetic joint infection', *Frontiers in Pharmacology*, 13. Available at: https://doi.org/10.3389/fphar.2022.989417.

Papa, A., Koulourida, V. and Souliou, E. (2009) 'Molecular epidemiology of carbapenem-resistant *Acinetobacter baumannii* in a newly established Greek hospital', *Microbial Drug Resistance (Larchmont, N.Y.)*, 15(4), pp. 257–260. Available at: https://doi.org/10.1089/mdr.2009.0060.

Park, G.E. *et al.* (2017) 'Bloodstream infections caused by Acinetobacter species with reduced susceptibility to tigecycline: clinical features and risk factors', *International Journal of Infectious Diseases*, 62, pp. 26–31. Available at: https://doi.org/10.1016/j.ijid.2017.06.023.

Pasterán, F. *et al.* (2006) 'Emergence of PER-2 and VEB-1a in *Acinetobacter baumannii* Strains in the Americas', *Antimicrobial Agents and Chemotherapy*, 50(9), pp. 3222–3224. Available at: https://doi.org/10.1128/AAC.00284-06.

Patamatamkul, S. *et al.* (2017) 'A case-control study of community-acquired *Acinetobacter baumannii* pneumonia and melioidosis pneumonia in northeast Thailand: an emerging fatal disease with unique clinical features', *Diagnostic Microbiology and Infectious Disease*, 87(1), pp. 79–86. Available at: https://doi.org/10.1016/j.diagmicrobio.2016.10.014.

Patel, K.K. *et al.* (2019) 'Antibiofilm Potential of Silver Sulfadiazine-Loaded Nanoparticle Formulations: A Study on the Effect of DNase-I on Microbial Biofilm and Wound Healing Activity', *Molecular Pharmaceutics*, 16(9), pp. 3916–3925. Available at: https://doi.org/10.1021/acs.molpharmaceut.9b00527.

Paul, M. *et al.* (2018) 'Colistin alone versus colistin plus meropenem for treatment of severe infections caused by carbapenem-resistant Gram-negative bacteria: an open-label, randomised controlled trial', *The Lancet Infectious Diseases*, 18(4), pp. 391–400. Available at: https://doi.org/10.1016/S1473-

3099(18)30099-9.

Pecharki, D., Petersen, F.C. and Scheie, A.A. (2008) 'Role of hyaluronidase in Streptococcus intermedius biofilm', *Microbiology (Reading, England)*, 154(Pt 3), pp. 932–938. Available at: https://doi.org/10.1099/mic.0.2007/012393-0.

Peleg, A.Y., Seifert, H. and Paterson, D.L. (2008) '*Acinetobacter baumannii*: emergence of a successful pathogen', *Clinical Microbiology Reviews*, 21(3), pp. 538–582. Available at: https://doi.org/10.1128/CMR.00058-07.

Pelletier, M.R. *et al.* (2013) 'Unique Structural Modifications Are Present in the Lipopolysaccharide from Colistin-Resistant Strains of *Acinetobacter baumannii*', *Antimicrobial Agents and Chemotherapy*, 57(10), pp. 4831–4840. Available at: https://doi.org/10.1128/aac.00865-13.

Pelletier, M.R. *et al.* (2013) 'Unique Structural Modifications Are Present in the Lipopolysaccharide from Colistin-Resistant Strains of *Acinetobacter baumannii*', *Antimicrobial Agents and Chemotherapy*, 57(10), pp. 4831–4840. Available at: https://doi.org/10.1128/aac.00865-13.

Penwell, W.F. *et al.* (2015) 'Molecular Mechanisms of Sulbactam Antibacterial Activity and Resistance Determinants in *Acinetobacter baumannii*', *Antimicrobial Agents and Chemotherapy*, 59(3), pp. 1680–1689. Available at: https://doi.org/10.1128/AAC.04808-14.

Perez, F. *et al.* (2007) 'Global Challenge of Multidrug-Resistant *Acinetobacter baumannii*', *Antimicrobial Agents and Chemotherapy*, 51(10), pp. 3471–3484. Available at: https://doi.org/10.1128/aac.01464-06.

Pierre, J.-L., Baret, P. and Serratrice, G. (2003) 'Hydroxyquinolines as iron chelators', *Current Medicinal Chemistry*, 10(12), pp. 1077–1084. Available at: https://doi.org/10.2174/0929867033457584.

Pisithkul, T. *et al.* (2019) 'Metabolic Remodeling during Biofilm Development of Bacillus subtilis', *mBio*, 10(3), pp. e00623-19. Available at: https://doi.org/10.1128/mBio.00623-19.

Poirel, L. *et al.* (2007) 'Identification of the Novel Narrow-Spectrum β-Lactamase SCO-1 in Acinetobacter spp. from Argentina', *Antimicrobial Agents and Chemotherapy*, 51(6), pp. 2179–2184. Available at: https://doi.org/10.1128/AAC.01600-06.

Poirel, L. *et al.* (2004) 'Emergence of oxacillinase-mediated resistance to imipenem in Klebsiella pneumoniae', *Antimicrobial Agents and Chemotherapy*, 48(1), pp. 15–22. Available at: https://doi.org/10.1128/AAC.48.1.15-22.2004.

Poirel, L. *et al.* (2008) 'Carbapenem-Resistant *Acinetobacter baumannii* Isolates from Tunisia Producing the OXA-58-Like Carbapenem-Hydrolyzing Oxacillinase OXA-97', *Antimicrobial Agents and Chemotherapy*, 52(5), pp. 1613–1617. Available at: https://doi.org/10.1128/AAC.00978-07.

Poirel, L. *et al.* (2009) 'ISCR2, Another Vehicle for blaVEB Gene Acquisition', *Antimicrobial Agents and Chemotherapy*, 53(11), pp. 4940–4943. Available at: https://doi.org/10.1128/AAC.00414-09.

Potron, A. *et al.* (2009) 'Genetic and Biochemical Characterization of the First Extended-Spectrum CARB-Type ß-Lactamase, RTG-4, from *Acinetobacter baumannii*', *Antimicrobial Agents and Chemotherapy*, 53(7), pp. 3010–3016. Available at: https://doi.org/10.1128/AAC.01164-08.

Potron, A. *et al.* (2011) 'Genetic Features of CTX-M-15-Producing *Acinetobacter baumannii* from Haiti ▿ ', *Antimicrobial Agents and Chemotherapy*, 55(12), pp. 5946–5948. Available at: https://doi.org/10.1128/AAC.05124-11.

Pournaras, S. *et al.* (2014) 'Growth retardation, reduced invasiveness, and impaired colistin-mediated cell death associated with colistin resistance development in *Acinetobacter baumannii*', *Antimicrobial agents and chemotherapy*, 58(2), pp. 828–832. Available at: https://doi.org/10.1128/aac.01439-13.

Price, R. (2016) 'O'Neill report on antimicrobial resistance: funding for antimicrobial specialists should be improved', *European Journal of Hospital Pharmacy*, 23(4), pp. 245–247. Available at: https://doi.org/10.1136/ejhpharm-2016-001013.

Proctor, C.R., McCarron, P.A. and Ternan, N.G. (2020) 'Furanone quorum-sensing inhibitors with potential as novel therapeutics against *Pseudomonas aeruginosa*', *Journal of Medical Microbiology*, 69(2), pp. 195–206. Available at: https://doi.org/10.1099/jmm.0.001144.

Qais, F.A. *et al.* (2021) 'Coumarin Exhibits Broad-Spectrum Antibiofilm and Antiquorum Sensing Activity against Gram-Negative Bacteria: In Vitro and In Silico Investigation', *ACS Omega*, 6(29), pp. 18823–18835. Available at: https://doi.org/10.1021/acsomega.1c02046.

Quale, J. *et al.* (2003) 'Molecular epidemiology and mechanisms of carbapenem resistance in *Acinetobacter baumannii* endemic in New York City', *Clinical Infectious Diseases: An Official Publication of the Infectious Diseases Society of America*, 37(2), pp. 214–220. Available at: https://doi.org/10.1086/375821.

Quinteira, S. *et al.* (2007) 'Molecular Epidemiology of Imipenem-Resistant Acinetobacter haemolyticus and *Acinetobacter baumannii* Isolates Carrying Plasmid-Mediated OXA-40 from a Portuguese Hospital', *Antimicrobial Agents and Chemotherapy*, 51(9), pp. 3465–3466. Available at: https://doi.org/10.1128/AAC.00267-07.

Raetz, C.R.H. and Whitfield, C. (2002) 'Lipopolysaccharide endotoxins', *Annual Review of Biochemistry*, 71, pp. 635–700. Available at: https://doi.org/10.1146/annurev.biochem.71.110601.135414.

Rajamohan, G., Srinivasan, V.B. and Gebreyes, W.A. (2010) 'Molecular and functional characterization of a novel efflux pump, AmvA, mediating antimicrobial and disinfectant resistance in *Acinetobacter baumannii*', *The Journal of Antimicrobial Chemotherapy*, 65(9), pp. 1919–1925. Available at: https://doi.org/10.1093/jac/dkq195.

Rajkumari, J. *et al.* (2018) 'Cinnamic acid attenuates quorum sensing associated virulence factors and biofilm formation in *Pseudomonas aeruginosa* PAO1', *Biotechnology Letters*, 40(7), pp. 1087–1100. Available at: https://doi.org/10.1007/s10529-018-2557-9.

Ramírez, M.S., Piñeiro, S. and Centrón, D. (2010) 'Novel Insights about Class 2 Integrons from Experimental and Genomic Epidemiology', *Antimicrobial Agents and Chemotherapy*, 54(2), pp. 699–706. Available at: https://doi.org/10.1128/aac.01392-08.

Rangel, K. *et al.* (2020) 'Pan-Drug Resistant *Acinetobacter baumannii*, but Not Other Strains, Are Resistant to the Bee Venom Peptide Melittin', *Antibiotics*, 9(4), p. 178. Available at: https://doi.org/10.3390/antibiotics9040178.

Raorane, C.J. *et al.* (2019) 'Antibiofilm and Antivirulence Efficacies of Flavonoids and Curcumin

Against *Acinetobacter baumannii*', *Frontiers in Microbiology*, 10. Available at: https://www.frontiersin.org/articles/10.3389/fmicb.2019.00990 (Accessed: 16 August 2022).

Rasko, D.A. *et al.* (2008) 'Targeting QseC Signaling and Virulence for Antibiotic Development', *Science (New York, N.Y.)*, 321(5892), pp. 1078–1080. Available at: https://doi.org/10.1126/science.1160354.

Recalcati, S. *et al.* (2017) 'Molecular regulation of cellular iron balance', *IUBMB Life*, 69(6), pp. 389–398. Available at: https://doi.org/10.1002/iub.1628.

Reen, F.J. *et al.* (2018) 'Coumarin: a novel player in microbial quorum sensing and biofilm formation inhibition', *Applied Microbiology and Biotechnology*, 102(5), pp. 2063–2073. Available at: https://doi.org/10.1007/s00253-018-8787-x.

Rémy, B. *et al.* (2018) 'Interference in Bacterial Quorum Sensing: A Biopharmaceutical Perspective', *Frontiers in Pharmacology*, 9, p. 203. Available at: https://doi.org/10.3389/fphar.2018.00203.

Rhouma, M. *et al.* (2016) 'Colistin in Pig Production: Chemistry, Mechanism of Antibacterial Action, Microbial Resistance Emergence, and One Health Perspectives', *Frontiers in Microbiology*, 7, p. 1789. Available at: https://doi.org/10.3389/fmicb.2016.01789.

Ribera, A. *et al.* (2003) 'Partial characterization of a transposon containing the tet(A) determinant in a clinical isolate of *Acinetobacter baumannii*', *The Journal of Antimicrobial Chemotherapy*, 52(3), pp. 477–480. Available at: https://doi.org/10.1093/jac/dkg344.

Ribera, A., Ruiz, J. and Vila, J. (2003) 'Presence of the Tet M Determinant in a Clinical Isolate of *Acinetobacter baumannii*', *Antimicrobial Agents and Chemotherapy*, 47(7), pp. 2310–2312. Available at: https://doi.org/10.1128/AAC.47.7.2310-2312.2003.

Riccio, M.L. *et al.* (2000) 'Characterization of the Metallo-β-Lactamase Determinant of *Acinetobacter baumannii* AC-54/97 Reveals the Existence of blaIMP Allelic Variants Carried by Gene Cassettes of Different Phylogeny', *Antimicrobial Agents and Chemotherapy*, 44(5), pp. 1229–1235.

Rice, K.C. *et al.* (2007) 'The cidA murein hydrolase regulator contributes to DNA release and biofilm development in Staphylococcus aureus', *Proceedings of the National Academy of Sciences of the United States of America*, 104(19), pp. 8113–8118. Available at: https://doi.org/10.1073/pnas.0610226104.

Richards, A.M., Abu Kwaik, Y. and Lamont, R.J. (2015) 'Code blue: *Acinetobacter baumannii*, a nosocomial pathogen with a role in the oral cavity', *Molecular Oral Microbiology*, 30(1), pp. 2–15. Available at: https://doi.org/10.1111/omi.12072.

Richmond, G.E. *et al.* (2016) 'The *Acinetobacter baumannii* Two-Component System AdeRS Regulates Genes Required for Multidrug Efflux, Biofilm Formation, and Virulence in a Strain-Specific Manner', *mBio*. Edited by G.D. Wright, 7(2), pp. e00430-16. Available at: https://doi.org/10.1128/mBio.00430-16.

Robledo, I.E. *et al.* (2010) 'Detection of KPC in Acinetobacter spp. in Puerto Rico', *Antimicrobial Agents and Chemotherapy*, 54(3), pp. 1354–1357. Available at: https://doi.org/10.1128/AAC.00899-09.

Roca, I. *et al.* (2009) 'CraA, a major facilitator superfamily efflux pump associated with

chloramphenicol resistance in *Acinetobacter baumannii*', *Antimicrobial Agents and Chemotherapy*, 53(9), pp. 4013–4014. Available at: https://doi.org/10.1128/AAC.00584-09.

Rolain, J.-M. *et al.* (2011) '*Acinetobacter baumannii* resistant to colistin with impaired virulence: a case report from France', *The Journal of Infectious Diseases*, 204(7), pp. 1146–1147. Available at: https://doi.org/10.1093/infdis/jir475.

Rolain, J.-M. *et al.* (2013) 'Real-time sequencing to decipher the molecular mechanism of resistance of a clinical pan-drug-resistant *Acinetobacter baumannii* isolate from Marseille, France', *Antimicrobial Agents and Chemotherapy*, 57(1), pp. 592–596. Available at: https://doi.org/10.1128/AAC.01314-12.

Rollauer, S.E. *et al.* (2015) 'Outer membrane protein biogenesis in Gram-negative bacteria', *Philosophical Transactions of the Royal Society B: Biological Sciences*, 370(1679), p. 20150023. Available at: https://doi.org/10.1098/rstb.2015.0023.

Rossolini, G.M. *et al.* (2014) 'Update on the antibiotic resistance crisis', *Current Opinion in Pharmacology*, 18, pp. 56–60. Available at: https://doi.org/10.1016/j.coph.2014.09.006.

Roy, S. *et al.* (2021) 'Overexpression of Efflux Pumps, Mutations in the Pumps' Regulators, Chromosomal Mutations, and AAC(6′)-Ib-cr Are Associated With Fluoroquinolone Resistance in Diverse Sequence Types of Neonatal Septicaemic *Acinetobacter baumannii*: A 7-Year Single Center Study', *Frontiers in Microbiology*, 12. Available at: https://doi.org/10.3389/fmicb.2021.602724.

Roychoudhury, S. *et al.* (1998) 'Use of combinatorial library screening to identify inhibitors of a bacterial two-component signal transduction kinase', *Molecular Diversity*, 4(3), pp. 173–182. Available at: https://doi.org/10.1023/A:1009695718427.

Rumbaugh, K.P. and Sauer, K. (2020) 'Biofilm dispersion', *Nature Reviews Microbiology*, 18(10), pp. 571–586. Available at: https://doi.org/10.1038/s41579-020-0385-0.

Rumbo, C. *et al.* (2014) 'The *Acinetobacter baumannii* Omp33-36 porin is a virulence factor that induces apoptosis and modulates autophagy in human cells', *Infection and Immunity*, 82(11), pp. 4666–4680. Available at: https://doi.org/10.1128/IAI.02034-14.

Runci, F. *et al.* (2019) 'Contribution of Active Iron Uptake to *Acinetobacter baumannii* Pathogenicity', *Infection and Immunity*, 87(4), pp. e00755-18. Available at: https://doi.org/10.1128/IAI.00755-18.

Russo, T.A. *et al.* (2016) 'The Response Regulator BfmR Is a Potential Drug Target for *Acinetobacter baumannii*', *mSphere*, 1(3), pp. e00082-16. Available at: https://doi.org/10.1128/mSphere.00082-16.

Ryu, S.Y., Baek, W.-K. and Kim, H.A. (2017) 'Association of biofilm production with colonization among clinical isolates of *Acinetobacter baumannii*', *The Korean Journal of Internal Medicine*, 32(2), pp. 345–351. Available at: https://doi.org/10.3904/kjim.2015.287.

Sabnis, A. *et al.* (2021) 'Colistin kills bacteria by targeting lipopolysaccharide in the cytoplasmic membrane', *eLife*. Edited by P.A. Cole, L. Gao, and W. van Schaik, 10, p. e65836. Available at: https://doi.org/10.7554/eLife.65836.

Sahoo, K.C. *et al.* (2010) 'Antibiotic use, resistance development and environmental factors: a qualitative study among healthcare professionals in Orissa, India', *BMC Public Health*, 10(1), p. 629. Available at: https://doi.org/10.1186/1471-2458-10-629.

Sahu, P.K. *et al.* (2012) 'Characterization of eDNA from the Clinical Strain *Acinetobacter baumannii* AIIMS 7 and Its Role in Biofilm Formation', *The Scientific World Journal*, 2012, p. 973436. Available at: https://doi.org/10.1100/2012/973436.

Sakr, M.M. *et al.* (2021) 'In vivo evaluation of a recombinant N-acylhomoserine lactonase formulated in a hydrogel using a murine model infected with MDR *Pseudomonas aeruginosa* clinical isolate, CCASUP2', *AMB Express*, 11(1), p. 109. Available at: https://doi.org/10.1186/s13568-021-01269-7.

Saleh, N.M. *et al.* (2020) 'Acquisition of Colistin Resistance Links Cell Membrane Thickness Alteration with a Point Mutation in the lpxD Gene in *Acinetobacter baumannii*', *Antibiotics*, 9(4), p. 164. Available at: https://doi.org/10.3390/antibiotics9040164.

Saleh, N.M. *et al.* (2023) 'Contribution of different mechanisms to aminoglycoside resistance in clinical isolates of *Acinetobacter baumannii*', *Microbial Pathogenesis*, 182, p. 106255. Available at: https://doi.org/10.1016/j.micpath.2023.106255.

Salgado, P. *et al.* (2013) 'Fenton Reaction Driven by Iron Ligands', *Journal of the Chilean Chemical Society*, 58(4), pp. 2096–2101. Available at: https://doi.org/10.4067/S0717-97072013000400043.

Sambanthamoorthy, K. *et al.* (2012) 'Identification of Small Molecules That Antagonize Diguanylate Cyclase Enzymes To Inhibit Biofilm Formation', *Antimicrobial Agents and Chemotherapy*, 56(10), pp. 5202–5211. Available at: https://doi.org/10.1128/AAC.01396-12.

Sampson, T.R. *et al.* (2012) 'Rapid Killing of *Acinetobacter baumannii* by Polymyxins Is Mediated by a Hydroxyl Radical Death Pathway', *Antimicrobial Agents and Chemotherapy*, 56(11), pp. 5642–5649. Available at: https://doi.org/10.1128/AAC.00756-12.

Sandri, A.M. *et al.* (2013) 'Population pharmacokinetics of intravenous polymyxin B in critically ill patients: implications for selection of dosage regimens', *Clinical Infectious Diseases: An Official Publication of the Infectious Diseases Society of America*, 57(4), pp. 524–531. Available at: https://doi.org/10.1093/cid/cit334.

Santos-Lopez, A. *et al.* (no date) 'Evolutionary pathways to antibiotic resistance are dependent upon environmental structure and bacterial lifestyle', *eLife*, 8, p. e47612. Available at: https://doi.org/10.7554/eLife.47612.

Satlin, M.J. *et al.* (2020) 'Clinical and Laboratory Standards Institute and European Committee on Antimicrobial Susceptibility Testing Position Statements on Polymyxin B and Colistin Clinical Breakpoints', *Clinical Infectious Diseases: An Official Publication of the Infectious Diseases Society of America*, 71(9), pp. e523–e529. Available at: https://doi.org/10.1093/cid/ciaa121.

Sauer, K. *et al.* (2022) 'The biofilm life cycle: expanding the conceptual model of biofilm formation', *Nature Reviews Microbiology*, 20(10), pp. 608–620. Available at: https://doi.org/10.1038/s41579-022-00767-0.

Savinova, T. *et al.* (2022) 'The Phenomenon of T3SS Inactivation for *Pseudomonas aeruginosa* Strains from a Chronic Infection Locus: Do Mutations in T3SS-Regulators Matter?', *Microbiology Spectrum*, 10(3), pp. e00494-22. Available at: https://doi.org/10.1128/spectrum.00494-22.

Schweppe, D.K. *et al.* (2015) 'Host-Microbe Protein Interactions during Bacterial Infection', *Chemistry & Biology*, 22(11), pp. 1521–1530. Available at: https://doi.org/10.1016/j.chembiol.2015.09.015.

Scott, P. *et al.* (2007) 'An outbreak of multidrug-resistant *Acinetobacter baumannii*-calcoaceticus complex infection in the US military health care system associated with military operations in Iraq', *Clinical Infectious Diseases: An Official Publication of the Infectious Diseases Society of America*, 44(12), pp. 1577–1584. Available at: https://doi.org/10.1086/518170.

Sedlmayer, F. *et al.* (2021) '5-Fluorouracil blocks quorum-sensing of biofilm-embedded methicillin-resistant Staphylococcus aureus in mice', *Nucleic Acids Research*, 49(13), p. e73. Available at: https://doi.org/10.1093/nar/gkab251.

Selyunin, A.S. *et al.* (2019) 'Tamoxifen blocks retrograde trafficking of Shiga toxin 1 and 2 and protects against lethal toxicosis', *Life Science Alliance*, 2(3), p. e201900439. Available at: https://doi.org/10.26508/lsa.201900439.

Shadan, A. *et al.* (2023) 'Deciphering the virulence factors, regulation, and immune response to *Acinetobacter baumannii* infection', *Frontiers in Cellular and Infection Microbiology*, 13. Available at: https://doi.org/10.3389/fcimb.2023.1053968.

Shafiee, F. *et al.* (2021) '*In vitro* synergistic effect of colistin and ampicillin/sulbactam with several antibiotics against clinical strains of multi-drug resistant *Acinetobacter baumannii*', *Indian Journal of Medical Microbiology*, 39(3), pp. 358–362. Available at: https://doi.org/10.1016/j.ijmmb.2021.04.006.

Shakhnovich, E.A., Sturtevant, D. and Mekalanos, J.J. (2007) 'Molecular mechanisms of virstatin resistance by non-O1/non-O139 strains of Vibrio cholerae', *Molecular Microbiology*, 66(6), pp. 1331–1341. Available at: https://doi.org/10.1111/j.1365-2958.2007.05984.x.

Shamprasad, B.R. *et al.* (2022) 'Metal nanoparticles functionalized with nutraceutical Kaempferitrin from edible Crotalaria juncea, exert potent antimicrobial and antibiofilm effects against Methicillin-resistant *Staphylococcus aureus'*, *Scientific Reports*, 12(1), p. 7061. Available at: https://doi.org/10.1038/s41598-022-11004-2.

Shapiro, J.A. and Wencewicz, T.A. (2016) 'Acinetobactin Isomerization Enables Adaptive Iron Acquisition in *Acinetobacter baumannii* through pH-Triggered Siderophore Swapping', *ACS infectious diseases*, 2(2), pp. 157–168. Available at: https://doi.org/10.1021/acsinfecdis.5b00145.

Sharma, A. *et al.* (2017) 'Fosfomycin resistance in *Acinetobacter baumannii* is mediated by efflux through a major facilitator superfamily (MFS) transporter-AbaF', *The Journal of Antimicrobial Chemotherapy*, 72(1), pp. 68–74. Available at: https://doi.org/10.1093/jac/dkw382.

Sharma, A.K. *et al.* (2017) 'Bacterial Virulence Factors: Secreted for Survival', *Indian Journal of Microbiology*, 57(1), pp. 1–10. Available at: https://doi.org/10.1007/s12088-016-0625-1.

Sharma, D., Misba, L. and Khan, A.U. (2019) 'Antibiotics versus biofilm: an emerging battleground in microbial communities', *Antimicrobial Resistance & Infection Control*, 8(1), p. 76. Available at: https://doi.org/10.1186/s13756-019-0533-3.

Sharma, K. and Singh, A.P. (2018) 'Antibiofilm Effect of DNase against Single and Mixed Species Biofilm', *Foods*, 7(3), p. 42. Available at: https://doi.org/10.3390/foods7030042.

Sharma, S. *et al.* (2023) 'Different Efflux Pump Systems in *Acinetobacter baumannii* and Their Role in Multidrug Resistance', *Advances in Experimental Medicine and Biology*, 1370, pp. 155–168. Available at: https://doi.org/10.1007/5584_2023_771.

Shaw-Taylor, L. (2020) ‘An introduction to the history of infectious diseases, epidemics and the early phases of the long-run decline in mortality’, *The Economic History Review*, 73(3), pp. E1–E19. Available at: https://doi.org/10.1111/ehr.13019.

Sheldon, J.R. and Skaar, E.P. (2020) ‘*Acinetobacter baumannii* can use multiple siderophores for iron acquisition, but only acinetobactin is required for virulence’, *PLOS Pathogens*, 16(10), p. e1008995. Available at: https://doi.org/10.1371/journal.ppat.1008995.

Shendge, A.K. *et al.* (2018) ‘An ellagic acid isolated from Clerodendrum viscosum leaves ameliorates iron-overload induced hepatotoxicity in Swiss albino mice through inhibition of oxidative stress and the apoptotic pathway’, *Biomedicine & Pharmacotherapy*, 106, pp. 454–465. Available at: https://doi.org/10.1016/j.biopha.2018.06.133.

Sheremet, A.B. *et al.* (2018) ‘Small Molecule Inhibitor of Type Three Secretion System Belonging to a Class 2,4-disubstituted-4H-[1,3,4]-thiadiazine-5-ones Improves Survival and Decreases Bacterial Loads in an Airway *Pseudomonas aeruginosa* Infection in Mice’, *BioMed Research International*, 2018, p. 5810767. Available at: https://doi.org/10.1155/2018/5810767.

Sherman, E.X., Wozniak, J.E. and Weiss, D.S. (2019) ‘Methods to Evaluate Colistin Heteroresistance in *Acinetobacter baumannii*’, *Methods in molecular biology (Clifton, N.J.)*, 1946, pp. 39–50. Available at: https://doi.org/10.1007/978-1-4939-9118-1_4.

Shukla, S.K. and Rao, T.S. (2013) ‘Dispersal of Bap-mediated Staphylococcus aureus biofilm by proteinase K’, *The Journal of Antibiotics*, 66(2), pp. 55–60. Available at: https://doi.org/10.1038/ja.2012.98.

Shushunov, S. *et al.* (2009) ‘Determination of Acute Toxicity of the Aqueous Extract of Potentilla erecta (Tormentil) Rhizomes in Rats and Mice’, *Journal of Medicinal Food*, 12(5), pp. 1173–1176. Available at: https://doi.org/10.1089/jmf.2008.0281.

Siala, W. *et al.* (2016) ‘The antifungal caspofungin increases fluoroquinolone activity against Staphylococcus aureus biofilms by inhibiting N-acetylglucosamine transferase’, *Nature Communications*, 7(1), p. 13286. Available at: https://doi.org/10.1038/ncomms13286.

Siasat, P.A. and Blair, J.M.A. (2023) ‘Microbial Primer: Multidrug efflux pumps’, *Microbiology*, 169(10), p. 001370. Available at: https://doi.org/10.1099/mic.0.001370.

Singh, S. *et al.* (2017) ‘Understanding the Mechanism of Bacterial Biofilms Resistance to Antimicrobial Agents’, *The Open Microbiology Journal*, 11, pp. 53–62. Available at: https://doi.org/10.2174/1874285801711010053.

Smith, E.E. *et al.* (2006) ‘Genetic adaptation by *Pseudomonas aeruginosa* to the airways of cystic fibrosis patients’, *Proceedings of the National Academy of Sciences of the United States of America*, 103(22), pp. 8487–8492. Available at: https://doi.org/10.1073/pnas.0602138103.

Smith, P.W. *et al.* (2018) ‘Pharmacokinetics of β-Lactam Antibiotics: Clues from the Past To Help Discover Long-Acting Oral Drugs in the Future’, *ACS Infectious Diseases*, 4(10), pp. 1439–1447. Available at: https://doi.org/10.1021/acsinfecdis.8b00160.

Smith, R. and Coast, J. (2013) *The economic burden of antimicrobial resistance: Why it is more*

serious than current studies suggest. London School of Hygiene & Tropical Medicine. Available at: https://doi.org/10.17037/PUBS.00639028.

Smyth, A.R. *et al.* (2010) 'Garlic as an inhibitor of *Pseudomonas aeruginosa* quorum sensing in cystic fibrosis—a pilot randomized controlled trial', *Pediatric Pulmonology*, 45(4), pp. 356–362. Available at: https://doi.org/10.1002/ppul.21193.

Snitkin, E.S. *et al.* (2013) 'Genomic insights into the fate of colistin resistance and *Acinetobacter baumannii* during patient treatment', *Genome Research*, 23(7), pp. 1155–1162. Available at: https://doi.org/10.1101/gr.154328.112.

Snyman, Y. *et al.* (2020) 'Clonal expansion of colistin-resistant *Acinetobacter baumannii* isolates in Cape Town, South Africa', *International journal of infectious diseases: IJID: official publication of the International Society for Infectious Diseases*, 91, pp. 94–100. Available at: https://doi.org/10.1016/j.ijid.2019.11.021.

Song, M. *et al.* (2020) 'A broad-spectrum antibiotic adjuvant reverses multidrug-resistant Gram-negative pathogens', *Nature Microbiology*, 5(8), pp. 1040–1050. Available at: https://doi.org/10.1038/s41564-020-0723-z.

Soon, R.L. *et al.* (2011) 'Different surface charge of colistin-susceptible and -resistant *Acinetobacter baumannii* cells measured with zeta potential as a function of growth phase and colistin treatment', *Journal of Antimicrobial Chemotherapy*, 66(1), pp. 126–133. Available at: https://doi.org/10.1093/jac/dkq422.

Soren, O. *et al.* (2020) 'Cephalosporin nitric oxide-donor prodrug DEA-C3D disperses biofilms formed by clinical cystic fibrosis isolates of *Pseudomonas aeruginosa*', *Journal of Antimicrobial Chemotherapy*, 75(1), pp. 117–125. Available at: https://doi.org/10.1093/jac/dkz378.

Soukarieh, F. *et al.* (2018) '*Pseudomonas aeruginosa* Quorum Sensing Systems as Drug Discovery Targets: Current Position and Future Perspectives', *Journal of Medicinal Chemistry* [Preprint]. Available at: https://doi.org/10.1021/acs.jmedchem.8b00540.

Spaulding, C.N. *et al.* (2018) 'Functional role of the type 1 pilus rod structure in mediating host-pathogen interactions', *eLife*. Edited by M.S. Gilmore, 7, p. e31662. Available at: https://doi.org/10.7554/eLife.31662.

Srinivasan, V.B., Rajamohan, G. and Gebreyes, W.A. (2009) 'Role of AbeS, a novel efflux pump of the SMR family of transporters, in resistance to antimicrobial agents in *Acinetobacter baumannii*', *Antimicrobial Agents and Chemotherapy*, 53(12), pp. 5312–5316. Available at: https://doi.org/10.1128/AAC.00748-09.

Stahl, J. *et al.* (2015) '*Acinetobacter baumannii* Virulence Is Mediated by the Concerted Action of Three Phospholipases D', *PLOS ONE*, 10(9), p. e0138360. Available at: https://doi.org/10.1371/journal.pone.0138360.

Stewart, R.C. (2010) 'Protein Histidine Kinases: Assembly of Active Sites and Their Regulation in Signaling Pathways', *Current opinion in microbiology*, 13(2), pp. 133–141. Available at: https://doi.org/10.1016/j.mib.2009.12.013.

Stothard (2018) *The Sequence Manipulation Suite: JavaScript Programs for Analyzing and Formatting Protein and DNA Sequences | BioTechniques*. Available at: https://www.future-

science.com/doi/abs/10.2144/00286ir01?url_ver=Z39.88-2003&rfr_id=ori%3Arid%3Acrossref.org&rfr_dat=cr_pub++0pubmed (Accessed: 27 February 2024).

Su, C.-H. *et al.* (2012) 'Increase of carbapenem-resistant *Acinetobacter baumannii* infection in acute care hospitals in Taiwan: association with hospital antimicrobial usage', *PloS One*, 7(5), p. e37788. Available at: https://doi.org/10.1371/journal.pone.0037788.

Su, X.-Z. *et al.* (2005) 'AbeM, an H+-coupled *Acinetobacter baumannii* multidrug efflux pump belonging to the MATE family of transporters', *Antimicrobial Agents and Chemotherapy*, 49(10), pp. 4362–4364. Available at: https://doi.org/10.1128/AAC.49.10.4362-4364.2005.

Subhadra, B. *et al.* (2018) 'Control of Biofilm Formation in Healthcare: Recent Advances Exploiting Quorum-Sensing Interference Strategies and Multidrug Efflux Pump Inhibitors', *Materials*, 11(9), p. 1676. Available at: https://doi.org/10.3390/ma11091676.

Sue, K. *et al.* (2024) 'Antimicrobial Indole-3-Carboxamido-Polyamine Conjugates Target Bacterial Membranes and Are Antibiotic Potentiators', *Biomolecules*, 14(3), p. 261. Available at: https://doi.org/10.3390/biom14030261.

Sugawara, E. and Nikaido, H. (2012) 'OmpA Is the Principal Nonspecific Slow Porin of *Acinetobacter baumannii*', *Journal of Bacteriology*, 194(15), pp. 4089–4096. Available at: https://doi.org/10.1128/jb.00435-12.

Sully, E.K. *et al.* (2014) 'Selective chemical inhibition of agr quorum sensing in Staphylococcus aureus promotes host defense with minimal impact on resistance', *PLoS pathogens*, 10(6), p. e1004174. Available at: https://doi.org/10.1371/journal.ppat.1004174.

Sultan, M., Arya, R. and Kim, K.K. (2021) 'Roles of Two-Component Systems in *Pseudomonas aeruginosa* Virulence', *International Journal of Molecular Sciences*, 22(22), p. 12152. Available at: https://doi.org/10.3390/ijms222212152.

Sun, B. *et al.* (2020) 'New Mutations Involved in Colistin Resistance in *Acinetobacter baumannii*', *mSphere*, 5(2), pp. e00895-19. Available at: https://doi.org/10.1128/mSphere.00895-19.

Sun, J.-R. *et al.* (2016) 'Single amino acid substitution Gly186Val in AdeS restores tigecycline susceptibility of *Acinetobacter baumannii*', *The Journal of Antimicrobial Chemotherapy*, 71(6), pp. 1488–1492. Available at: https://doi.org/10.1093/jac/dkw002.

Sun, J., Deng, Z. and Yan, A. (2014) 'Bacterial multidrug efflux pumps: mechanisms, physiology and pharmacological exploitations', *Biochemical and Biophysical Research Communications*, 453(2), pp. 254–267. Available at: https://doi.org/10.1016/j.bbrc.2014.05.090.

Sun, Z. *et al.* (2014) 'Blocking Phosphatidylcholine Utilization in *Pseudomonas aeruginosa*, via Mutagenesis of Fatty Acid, Glycerol and Choline Degradation Pathways, Confirms the Importance of This Nutrient Source In Vivo', *PLOS ONE*, 9(7), p. e103778. Available at: https://doi.org/10.1371/journal.pone.0103778.

Surewaard, B.G.J. *et al.* (2018) 'α-Toxin Induces Platelet Aggregation and Liver Injury during Staphylococcus aureus Sepsis', *Cell Host & Microbe*, 24(2), pp. 271-284.e3. Available at: https://doi.org/10.1016/j.chom.2018.06.017.

Svensson, A. *et al.* (2001) 'Design and Evaluation of Pilicides: Potential Novel Antibacterial Agents

Directed Against Uropathogenic *Escherichia coli*', *ChemBioChem*, 2(12), pp. 915–918. Available at: https://doi.org/10.1002/1439-7633(20011203)2:12<915::AID-CBIC915>3.0.CO;2-M.

Swem, L.R. *et al.* (2009) 'A Quorum-Sensing Antagonist Targets Both Membrane-Bound and Cytoplasmic Receptors and Controls Bacterial Pathogenicity', *Molecular Cell*, 35(2), pp. 143–153. Available at: https://doi.org/10.1016/j.molcel.2009.05.029.

Synowiec, A. *et al.* (2014) 'Antimicrobial effect of an aqueous extract of rhizome', *Herba Polonica*, 60(2), pp. 18–28. Available at: https://doi.org/10.2478/hepo-2014-0007.

Tacconelli, E. *et al.* (2018) 'Discovery, research, and development of new antibiotics: the WHO priority list of antibiotic-resistant bacteria and tuberculosis', *The Lancet. Infectious Diseases*, 18(3), pp. 318–327. Available at: https://doi.org/10.1016/S1473-3099(17)30753-3.

Tam, J. *et al.* (2015) 'Small Molecule Inhibitors of Clostridium difficile Toxin B-Induced Cellular Damage', *Chemistry & Biology*, 22(2), pp. 175–185. Available at: https://doi.org/10.1016/j.chembiol.2014.12.010.

Tedesco, D. and Haragsim, L. (2012) 'Cyclosporine: A Review', *Journal of Transplantation*, 2012, p. 230386. Available at: https://doi.org/10.1155/2012/230386.

Teiber, J.F. *et al.* (2008) 'Dominant Role of Paraoxonases in Inactivation of the *Pseudomonas aeruginosa* Quorum-Sensing Signal N-(3-Oxododecanoyl)-l-Homoserine Lactone', *Infection and Immunity*, 76(6), p. 2512. Available at: https://doi.org/10.1128/IAI.01606-07.

Tetz, G.V., Artemenko, N.K. and Tetz, V.V. (2009) 'Effect of DNase and Antibiotics on Biofilm Characteristics', *Antimicrobial Agents and Chemotherapy*, 53(3), pp. 1204–1209. Available at: https://doi.org/10.1128/AAC.00471-08.

Tetz, V.V. and Tetz, G.V. (2010) 'Effect of Extracellular DNA Destruction by DNase I on Characteristics of Forming Biofilms', *DNA and Cell Biology*, 29(8), pp. 399–405. Available at: https://doi.org/10.1089/dna.2009.1011.

Theodosis-Nobelos, P., Papagiouvannis, G. and Rekka, E.A. (2023) 'Ferulic, Sinapic, 3,4-Dimethoxycinnamic Acid and Indomethacin Derivatives with Antioxidant, Anti-Inflammatory and Hypolipidemic Functionality', *Antioxidants*, 12(7), p. 1436. Available at: https://doi.org/10.3390/antiox12071436.

Thi Khanh Nhu, N. *et al.* (2016) 'The induction and identification of novel Colistin resistance mutations in *Acinetobacter baumannii* and their implications', *Scientific Reports*, 6, p. 28291. Available at: https://doi.org/10.1038/srep28291.

Thomas, V.C. *et al.* (2008) 'Regulation of autolysis-dependent extracellular DNA release by Enterococcus faecalis extracellular proteases influences biofilm development', *Journal of Bacteriology*, 190(16), pp. 5690–5698. Available at: https://doi.org/10.1128/JB.00314-08.

Tipton, K.A., Dimitrova, D. and Rather, P.N. (2015) 'Phase-Variable Control of Multiple Phenotypes in *Acinetobacter baumannii* Strain AB5075', *Journal of Bacteriology*, 197(15), pp. 2593–2599. Available at: https://doi.org/10.1128/JB.00188-15.

Tiwari, S. *et al.* (2017) 'Two-Component Signal Transduction Systems of Pathogenic Bacteria As Targets for Antimicrobial Therapy: An Overview', *Frontiers in Microbiology*, 8. Available at:

https://www.frontiersin.org/articles/10.3389/fmicb.2017.01878 (Accessed: 7 March 2023).

Tkaczyk, C. *et al.* (2016) 'Targeting Alpha Toxin and ClfA with a Multimechanistic Monoclonal-Antibody-Based Approach for Prophylaxis of Serious Staphylococcus aureus Disease', *mBio*, 7(3), pp. e00528-16. Available at: https://doi.org/10.1128/mBio.00528-16.

Tognim, M.C.B. *et al.* (2006) 'Dissemination of IMP-1 metallo- beta -lactamase-producing Acinetobacter species in a Brazilian teaching hospital', *Infection Control and Hospital Epidemiology*, 27(7), pp. 742–747. Available at: https://doi.org/10.1086/504356.

Tomaras, A.P. *et al.* (2008) 'Characterization of a two-component regulatory system from *Acinetobacter baumannii* that controls biofilm formation and cellular morphology', *Microbiology (Reading, England)*, 154(Pt 11), pp. 3398–3409. Available at: https://doi.org/10.1099/mic.0.2008/019471-0.

Tomás, M. del M. *et al.* (2005) 'Cloning and Functional Analysis of the Gene Encoding the 33- to 36-Kilodalton Outer Membrane Protein Associated with Carbapenem Resistance in *Acinetobacter baumannii*', *Antimicrobial Agents and Chemotherapy*, 49(12), pp. 5172–5175. Available at: https://doi.org/10.1128/AAC.49.12.5172-5175.2005.

Tomczyk, M. and Latté, K.P. (2009) 'Potentilla--a review of its phytochemical and pharmacological profile', *Journal of Ethnopharmacology*, 122(2), pp. 184–204. Available at: https://doi.org/10.1016/j.jep.2008.12.022.

Toth, M. *et al.* (2010) 'Mutant APH(2″)-IIa Enzymes with Increased Activity against Amikacin and Isepamicin', *Antimicrobial Agents and Chemotherapy*, 54(4), pp. 1590–1595. Available at: https://doi.org/10.1128/AAC.01444-09.

Tran, T.B. *et al.* (2016) 'Pharmacokinetics/pharmacodynamics of colistin and polymyxin B: are we there yet?', *International Journal of Antimicrobial Agents*, 48(6), pp. 592–597. Available at: https://doi.org/10.1016/j.ijantimicag.2016.09.010.

Tran, T.B. *et al.* (2016) 'Pharmacokinetics/pharmacodynamics of colistin and polymyxin B: are we there yet?', *International Journal of Antimicrobial Agents*, 48(6), pp. 592–597. Available at: https://doi.org/10.1016/j.ijantimicag.2016.09.010.

Trebino, M.A. *et al.* (2021) 'Strategies and Approaches for Discovery of Small Molecule Disruptors of Biofilm Physiology', *Molecules*, 26(15), p. 4582. Available at: https://doi.org/10.3390/molecules26154582.

Trebosc, V. *et al.* (2019) 'Dissecting Colistin Resistance Mechanisms in Extensively Drug-Resistant *Acinetobacter baumannii* Clinical Isolates', *mBio*, 10(4), pp. e01083-19. Available at: https://doi.org/10.1128/mBio.01083-19.

Trebosc, V. *et al.* (2019) 'Dissecting Colistin Resistance Mechanisms in Extensively Drug-Resistant *Acinetobacter baumannii* Clinical Isolates', *mBio*, 10(4), pp. e01083-19. Available at: https://doi.org/10.1128/mBio.01083-19.

Tree, J.J. *et al.* (2009) 'Characterization of the effects of salicylidene acylhydrazide compounds on type III secretion in *Escherichia coli* O157:H7', *Infection and Immunity*, 77(10), pp. 4209–4220. Available at: https://doi.org/10.1128/IAI.00562-09.

Trent, M.S. *et al.* (2001) 'An Inner Membrane Enzyme in Salmonellaand *Escherichia coli* That Transfers 4-Amino-4-deoxy-l-arabinose to Lipid A: induction in polymyxin-resistant mutants and role of a novel lipid-linked donor', *Journal of Biological Chemistry*, 276(46), pp. 43122–43131. Available at: https://doi.org/10.1074/jbc.M106961200.

Trew, S.J. *et al.* (2000) 'Novel streptopyrroles from Streptomyces rimosus with bacterial protein histidine kinase inhibitory and antimicrobial activities', *The Journal of Antibiotics*, 53(1), pp. 1–11. Available at: https://doi.org/10.7164/antibiotics.53.1.

Tripathi, A. *et al.* (2018) 'A Defined and Flexible Pocket Explains Aryl Substrate Promiscuity of the Cahuitamycin Starter Unit-Activating Enzyme CahJ', *Chembiochem: A European Journal of Chemical Biology*, 19(15), pp. 1595–1600. Available at: https://doi.org/10.1002/cbic.201800233.

Tsai, C.-W. and Morris, S. (2015) 'Approval of Raxibacumab for the Treatment of Inhalation Anthrax Under the US Food and Drug Administration "Animal Rule"', *Frontiers in Microbiology*, 6. Available at: https://www.frontiersin.org/articles/10.3389/fmicb.2015.01320

Tsakris, A. *et al.* (2007) 'Identification of a novel blaOXA-51 variant, blaOXA-92, from a clinical isolate of *Acinetobacter baumannii*', *Clinical Microbiology and Infection*, 13(3), pp. 348–349. Available at: https://doi.org/10.1111/j.1469-0691.2006.01598.x.

Turner, P.J. and Greenhalgh, J.M. (2003) *The activity of meropenem and comparators against Acinetobacter strains isolated from European hospitals, 1997–2000 - ScienceDirect*. Available at: https://www.sciencedirect.com/science/article/pii/S1198743X14640118?via%3Dihub

Ulijasz, A.T. and Weisblum, B. (1999) 'Dissecting the VanRS Signal Transduction Pathway with Specific Inhibitors', *Journal of Bacteriology*, 181(2), pp. 627–631.

Uruén, C. *et al.* (2020) 'Biofilms as Promoters of Bacterial Antibiotic Resistance and Tolerance', *Antibiotics*, 10(1), p. 3. Available at: https://doi.org/10.3390/antibiotics10010003.

Ušjak, D. *et al.* (2022) 'In vitro colistin susceptibility of pandrug-resistant Ac. baumannii is restored in the presence of selenium nanoparticles', *Journal of Applied Microbiology*, 133(3), pp. 1197–1206. Available at: https://doi.org/10.1111/jam.15638.

Ušjak, D. *et al.* (2023) 'Targeting outer membrane protein A (OmpA) - inhibitory effect of 2'-hydroxychalcone derivatives on *Acinetobacter baumannii* and Candida albicans dual-species biofilm formation', *Biofouling*, 39(3), pp. 316–326. Available at: https://doi.org/10.1080/08927014.2023.2215693.

Utari, P.D. *et al.* (2018) 'PvdQ Quorum Quenching Acylase Attenuates *Pseudomonas aeruginosa* Virulence in a Mouse Model of Pulmonary Infection', *Frontiers in Cellular and Infection Microbiology*, 8. Available at: https://www.frontiersin.org/articles/10.3389/fcimb.2018.00119 (Accessed: 7 March 2023).

Uusitalo, P. *et al.* (2017) 'The salicylidene acylhydrazide INP0341 attenuates *Pseudomonas aeruginosa* virulence in vitro and in vivo', *The Journal of Antibiotics*, 70(9), pp. 937–943. Available at: https://doi.org/10.1038/ja.2017.64.

Vahaboglu, H. *et al.* (2006) 'High prevalence of OXA-51-type class D beta-lactamases among ceftazidime-resistant clinical isolates of Acinetobacter spp.: co-existence with OXA-58 in multiple centres', *The Journal of Antimicrobial Chemotherapy*, 58(3), pp. 537–542. Available at:

https://doi.org/10.1093/jac/dkl273.

Vaishampayan, A. and Grohmann, E. (2022) 'Antimicrobials Functioning through ROS-Mediated Mechanisms: Current Insights', *Microorganisms*, 10(1), p. 61. Available at: https://doi.org/10.3390/microorganisms10010061.

Valentini, M. and Filloux, A. (2016) 'Biofilms and Cyclic di-GMP (c-di-GMP) Signaling: Lessons from *Pseudomonas aeruginosa* and Other Bacteria', *The Journal of Biological Chemistry*, 291(24), pp. 12547–12555. Available at: https://doi.org/10.1074/jbc.R115.711507.

van Delden, C. *et al.* (2012) 'Azithromycin to prevent *Pseudomonas aeruginosa* ventilator-associated pneumonia by inhibition of quorum sensing: a randomized controlled trial', *Intensive Care Medicine*, 38(7), pp. 1118–1125. Available at: https://doi.org/10.1007/s00134-012-2559-3.

Veenendaal, A.K.J., Sundin, C. and Blocker, A.J. (2009) 'Small-molecule type III secretion system inhibitors block assembly of the Shigella type III secreton', *Journal of Bacteriology*, 191(2), pp. 563–570. Available at: https://doi.org/10.1128/JB.01004-08.

Ventola, C.L. (2015) 'The Antibiotic Resistance Crisis', *Pharmacy and Therapeutics*, 40(4), pp. 277–283.

Vijayakumar, S. *et al.* (2016) 'Biofilm Formation and Motility Depend on the Nature of the *Acinetobacter baumannii* Clinical Isolates', *Frontiers in Public Health*, 4. Available at: https://www.frontiersin.org/articles/10.3389/fpubh.2016.00105 (Accessed: 4 November 2023).

Vila, J. *et al.* (1997) 'Cloning and nucleotide sequence analysis of a gene encoding an OXA-derived beta-lactamase in *Acinetobacter baumannii*.', *Antimicrobial Agents and Chemotherapy*, 41(12), pp. 2757–2759.

Vilacoba, E. *et al.* (2013) 'Emergence and Spread of Plasmid-Borne tet(B)::ISCR2 in Minocycline-Resistant *Acinetobacter baumannii* Isolates', *Antimicrobial Agents and Chemotherapy*, 57(1), pp. 651–654. Available at: https://doi.org/10.1128/AAC.01751-12.

Villegas, M.V. and Hartstein, A.I. (2003) 'Acinetobacter Outbreaks, 1977–2000', *Infection Control & Hospital Epidemiology*, 24(4), pp. 284–295. Available at: https://doi.org/10.1086/502205.

Voulgari, E. *et al.* (2016) 'First report of an NDM-1 metallo-β-lactamase-producing *Acinetobacter baumannii* clinical isolate in Greece', *International Journal of Antimicrobial Agents*, 48(6), pp. 761–762. Available at: https://doi.org/10.1016/j.ijantimicag.2016.09.006.

Walz, J.M. *et al.* (2010) 'Anti-infective external coating of central venous catheters: A randomized, noninferiority trial comparing 5-fluorouracil with chlorhexidine/silver sulfadiazine in preventing catheter colonization*', *Critical Care Medicine*, 38(11), p. 2095. Available at: https://doi.org/10.1097/CCM.0b013e3181f265ba.

Wand, M.E. *et al.* (2015) 'Retention of virulence following adaptation to colistin in *Acinetobacter baumannii* reflects the mechanism of resistance', *The Journal of Antimicrobial Chemotherapy*, 70(8), pp. 2209–2216. Available at: https://doi.org/10.1093/jac/dkv097.

Wang, B.X. *et al.* (2021) 'Mucin Glycans Signal through the Sensor Kinase RetS to Inhibit Virulence-Associated Traits in *Pseudomonas aeruginosa*', *Current Biology*, 31(1), pp. 90-102.e7. Available at: https://doi.org/10.1016/j.cub.2020.09.088.

Wang, C. *et al.* (2013) 'Mechanistic Insights Revealed by the Crystal Structure of a Histidine Kinase with Signal Transducer and Sensor Domains', *PLOS Biology*, 11(2), p. e1001493. Available at: https://doi.org/10.1371/journal.pbio.1001493.

Wang, L. *et al.* (2019) 'Novel Plasmid-Mediated tet(X5) Gene Conferring Resistance to Tigecycline, Eravacycline, and Omadacycline in a Clinical *Acinetobacter baumannii* Isolate', *Antimicrobial Agents and Chemotherapy*, 64(1), pp. e01326-19. Available at: https://doi.org/10.1128/AAC.01326-19.

Waryah, C.B. *et al.* (2017) 'In Vitro Antimicrobial Efficacy of Tobramycin Against Staphylococcus aureus Biofilms in Combination With or Without DNase I and/or Dispersin B: A Preliminary Investigation', *Microbial Drug Resistance (Larchmont, N.Y.)*, 23(3), pp. 384–390. Available at: https://doi.org/10.1089/mdr.2016.0100.

Watters, C. *et al.* (2016) 'Host Responses to Biofilm', *Progress in Molecular Biology and Translational Science*, 142, pp. 193–239. Available at: https://doi.org/10.1016/bs.pmbts.2016.05.007.

Watters, C.M. *et al.* (2016) 'Enzymatic degradation of in vitro Staphylococcus aureus biofilms supplemented with human plasma', *Infection and Drug Resistance*, 9, pp. 71–78. Available at: https://doi.org/10.2147/IDR.S103101.

Weinberg, E.D. (2009) 'Iron availability and infection', *Biochimica Et Biophysica Acta*, 1790(7), pp. 600–605. Available at: https://doi.org/10.1016/j.bbagen.2008.07.002.
Whitchurch, B.C. *et al.* (2002) *Extracellular DNA Required for Bacterial Biofilm Formation | Science*. Available at: https://www.science.org/doi/10.1126/science.295.5559.1487 (Accessed: 7 March 2023).

Whitfield, C. and Trent, M.S. (2014) 'Biosynthesis and export of bacterial lipopolysaccharides', *Annual Review of Biochemistry*, 83, pp. 99–128. Available at: https://doi.org/10.1146/annurev-biochem-060713-035600.

Wiggers, H. *et al.* (2017) 'Identification of Anti-Inflammatory and Anti-Hypertensive Drugs as Inhibitors of Bacterial Diguanylate Cyclases', *Journal of the Brazilian Chemical Society* [Preprint]. Available at: https://doi.org/10.21577/0103-5053.20170141.

Wilcox, M.H. *et al.* (2017) 'Bezlotoxumab for Prevention of Recurrent Clostridium difficile Infection', *New England Journal of Medicine*, 376(4), pp. 305–317. Available at: https://doi.org/10.1056/NEJMoa1602615.

Williams, D.E. and Boon, E.M. (2019) 'Towards Understanding the Molecular Basis of Nitric Oxide-Regulated Group Behaviors in Pathogenic Bacteria', *Journal of Innate Immunity*, 11(3), pp. 205–215. Available at: https://doi.org/10.1159/000494740.

Williams, J.D. *et al.* (2015) 'Synthesis and structure-activity relationships of novel phenoxyacetamide inhibitors of the *Pseudomonas aeruginosa* type III secretion system (T3SS)', *Bioorganic and Medicinal Chemistry*, 23(5), pp. 1027–1043. Available at: https://doi.org/10.1016/j.bmc.2015.01.011.

Williamson, R., Collatz, E. and Gutmann, L. (1986) 'Mechanisms of action of beta-lactam antibiotics and mechanisms of non-enzymatic resistance', *Presse Medicale (Paris, France: 1983)*, 15(46), pp. 2282–2289.

Wisplinghoff, H. *et al.* (2004) 'Nosocomial bloodstream infections in US hospitals: analysis of 24,179 cases from a prospective nationwide surveillance study', *Clinical Infectious Diseases: An Official*

Publication of the Infectious Diseases Society of America, 39(3), pp. 309–317. Available at: https://doi.org/10.1086/421946.

Wojnicz, D. and Jankowski, S. (2007) 'Effects of subinhibitory concentrations of amikacin and ciprofloxacin on the hydrophobicity and adherence to epithelial cells of uropathogenic *Escherichia coli* strains', *International Journal of Antimicrobial Agents*, 29(6), pp. 700–704. Available at: https://doi.org/10.1016/j.ijantimicag.2007.01.007.

Wong, S.L. *et al.* (2015) 'Diabetes primes neutrophils to undergo NETosis, which impairs wound healing', *Nature Medicine*, 21(7), pp. 815–819. Available at: https://doi.org/10.1038/nm.3887.

Wopperer, J. *et al.* (2006) 'A Quorum-Quenching Approach To Investigate the Conservation of Quorum-Sensing-Regulated Functions within the Burkholderia cepacia Complex', *Applied and Environmental Microbiology*, 72(2), pp. 1579–1587. Available at: https://doi.org/10.1128/AEM.72.2.1579-1587.2006.

World Health Organization (2024) *WHO bacterial priority pathogens list, 2024: Bacterial pathogens of public health importance to guide research, development and strategies to prevent and control antimicrobial resistance*. Available at: https://www.who.int/publications-detail-redirect/9789240093461

Wu, X. *et al.* (2016) 'In vivo protein interaction network analysis reveals porin-localized antibiotic inactivation in *Acinetobacter baumannii* strain AB5075', *Nature Communications*, 7, p. 13414. Available at: https://doi.org/10.1038/ncomms13414.

Xu, W. *et al.* (2017) 'A systematic review and meta-analysis of preclinical trials testing anti-toxin therapies for B. anthracis infection: A need for more robust study designs and results', *PLoS ONE*, 12(8), p. e0182879. Available at: https://doi.org/10.1371/journal.pone.0182879.

Yamamoto, M. *et al.* (2011) 'Interspecies dissemination of a novel class 1 integron carrying blaIMP-19 among Acinetobacter species in Japan', *The Journal of Antimicrobial Chemotherapy*, 66(11), pp. 2480–2483. Available at: https://doi.org/10.1093/jac/dkr336.

Yamazaki, A. *et al.* (2012) 'Derivatives of plant phenolic compound affect the type III secretion system of *Pseudomonas aeruginosa* via a GacS-GacA two-component signal transduction system', *Antimicrobial Agents and Chemotherapy*, 56(1), pp. 36–43. Available at: https://doi.org/10.1128/AAC.00732-11.

Yang, F. *et al.* (2014) 'Small-molecule inhibitors suppress the expression of both type III secretion and amylovoran biosynthesis genes in Erwinia amylovora', *Molecular Plant Pathology*, 15(1), pp. 44–57. Available at: https://doi.org/10.1111/mpp.12064.

Yang, Q. *et al.* (2017) 'Balancing mcr-1 expression and bacterial survival is a delicate equilibrium between essential cellular defence mechanisms', *Nature Communications*, 8(1), p. 2054. Available at: https://doi.org/10.1038/s41467-017-02149-0.

Yang, W.-S. *et al.* (2018) 'A potential substrate binding pocket of BdcA plays a critical role in NADPH recognition and biofilm dispersal', *Biochemical and Biophysical Research Communications*, 497(3), pp. 863–868. Available at: https://doi.org/10.1016/j.bbrc.2018.02.143.

Yang, Z. *et al.* (2015) 'Mechanisms of Protection against Clostridium difficile Infection by the Monoclonal Antitoxin Antibodies Actoxumab and Bezlotoxumab', *Infection and Immunity*, 83(2), pp.

822–831. Available at: https://doi.org/10.1128/IAI.02897-14.

Yau, W. *et al.* (2009) 'Colistin hetero-resistance in multidrug-resistant *Acinetobacter baumannii* clinical isolates from the Western Pacific region in the SENTRY antimicrobial surveillance programme', *The Journal of Infection*, 58(2), pp. 138–144. Available at: https://doi.org/10.1016/j.jinf.2008.11.002.

Yoon, E.-J. *et al.* (2021) 'Trajectory of genetic alterations associated with colistin resistance in *Acinetobacter baumannii* during an in-hospital outbreak of infection', *The Journal of Antimicrobial Chemotherapy*, 77(1), pp. 69–73. Available at: https://doi.org/10.1093/jac/dkab363.

Yu, H. *et al.* (2014) 'Elastase LasB of *Pseudomonas aeruginosa* promotes biofilm formation partly through rhamnolipid-mediated regulation', *Canadian Journal of Microbiology*, 60(4), pp. 227–235. Available at: https://doi.org/10.1139/cjm-2013-0667.

Yu, Z. *et al.* (2015) 'Antibacterial Mechanisms of Polymyxin and Bacterial Resistance', *BioMed Research International*, 2015, p. 679109. Available at: https://doi.org/10.1155/2015/679109.

Zahid, M.S.H. *et al.* (2015) 'Suppression of Virulence of Toxigenic Vibrio cholerae by Anethole through the Cyclic AMP (cAMP)-cAMP Receptor Protein Signaling System', *PLOS ONE*, 10(9), p. e0137529. Available at: https://doi.org/10.1371/journal.pone.0137529.

Zeng, X. and Lin, J. (2013) 'Beta-lactamase induction and cell wall metabolism in Gram-negative bacteria', *Frontiers in Microbiology*, 4, p. 128. Available at: https://doi.org/10.3389/fmicb.2013.00128.

Zhang, Y. *et al.* (2018) 'Coumarin Reduces Virulence and Biofilm Formation in *Pseudomonas aeruginosa* by Affecting Quorum Sensing, Type III Secretion and C-di-GMP Levels', *Frontiers in Microbiology*, 9. Available at: https://www.frontiersin.org/articles/10.3389/fmicb.2018.01952 (Accessed: 7 March 2023).

Zhang, Z. *et al.* (2014) 'Translocation domain mutations affecting cellular toxicity identify the Clostridium difficile toxin B pore', *Proceedings of the National Academy of Sciences of the United States of America*, 111(10), pp. 3721–3726. Available at: https://doi.org/10.1073/pnas.1400680111.

Zhang, Z. *et al.* (2015) 'Toxin-Mediated Paracellular Transport of Antitoxin Antibodies Facilitates Protection against Clostridium difficile Infection', *Infection and Immunity*, 83(1), pp. 405–416. Available at: https://doi.org/10.1128/IAI.02550-14.

Zhao, Q. *et al.* (2021) 'Global, regional, and national burden of mortality associated with non-optimal ambient temperatures from 2000 to 2019: a three-stage modelling study', *The Lancet Planetary Health*, 5(7), pp. e415–e425. Available at: https://doi.org/10.1016/S2542-5196(21)00081-4.

Zhao, X. *et al.* (2011) 'Antibacterial Activity of the Flavonoids from Dalbergia odorifera on Ralstonia solanacearum', *Molecules*, 16(12), pp. 9775–9782. Available at: https://doi.org/10.3390/molecules16129775.

Zhou, H. *et al.* (2019) 'Risk factors for acquisition and mortality of multidrug-resistant *Acinetobacter baumannii* bacteremia', *Medicine*, 98(13), p. e14937. Available at: https://doi.org/10.1097/MD.0000000000014937.

Zhou, H. *et al.* (2022) 'The Antibacterial Activity of Kaempferol Combined with Colistin against

Colistin-Resistant Gram-Negative Bacteria', *Microbiology Spectrum*, 10(6), p. e0226522. Available at: https://doi.org/10.1128/spectrum.02265-22.

Zhou, J. *et al.* (2013) 'Potent suppression of c-di-GMP synthesis via I-site allosteric inhibition of diguanylate cyclases with 2'-F-c-di-GMP', *Bioorganic & Medicinal Chemistry*, 21(14), pp. 4396–4404. Available at: https://doi.org/10.1016/j.bmc.2013.04.050.

Zigangirova, N.A. *et al.* (2021) 'Fluorothiazinon, a small-molecular inhibitor of T3SS, suppresses salmonella oral infection in mice', *The Journal of Antibiotics*, 74(4), pp. 244–254. Available at: https://doi.org/10.1038/s41429-020-00396-w.

Appendix A

Chapter 2 Appendices

A.1 Inhibition of growth of *A. baumannii* with 0.05 mM of the compounds

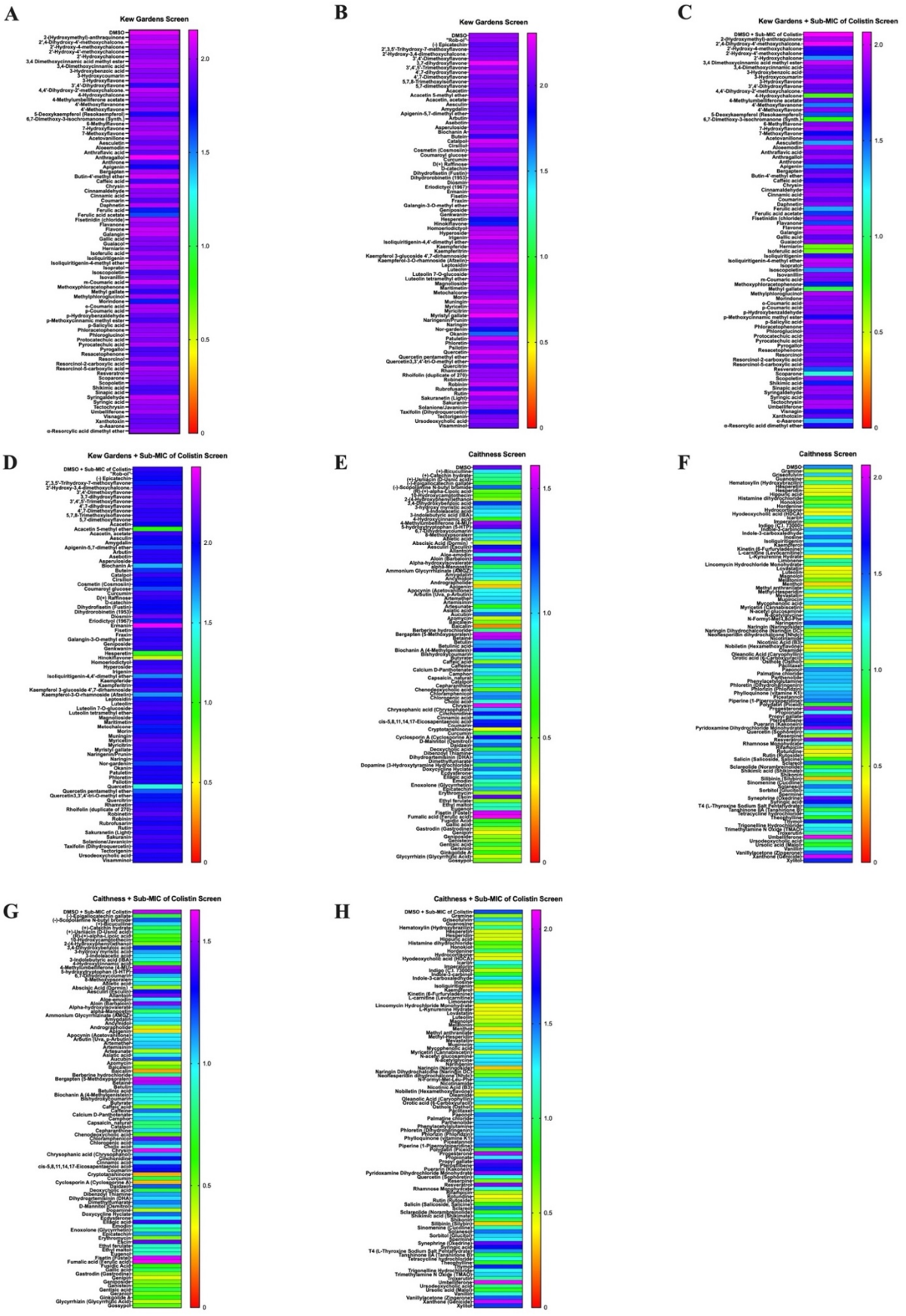
A
Kew Gardens Screen
B
Kew Gardens Screen
C
Kew Gardens + Sub-MIC of Colistin Screen
D
Kew Gardens + Sub-MIC of Colistin Screen
E
Caithness Screen
F
Caithness Screen
G
Caithness + Sub-MIC of Colistin Screen
H
Caithness + Sub-MIC of Colistin Screen

A.2 Inhibition of biofilm formation of *A. baumannii* with 0.05 mM of the compounds

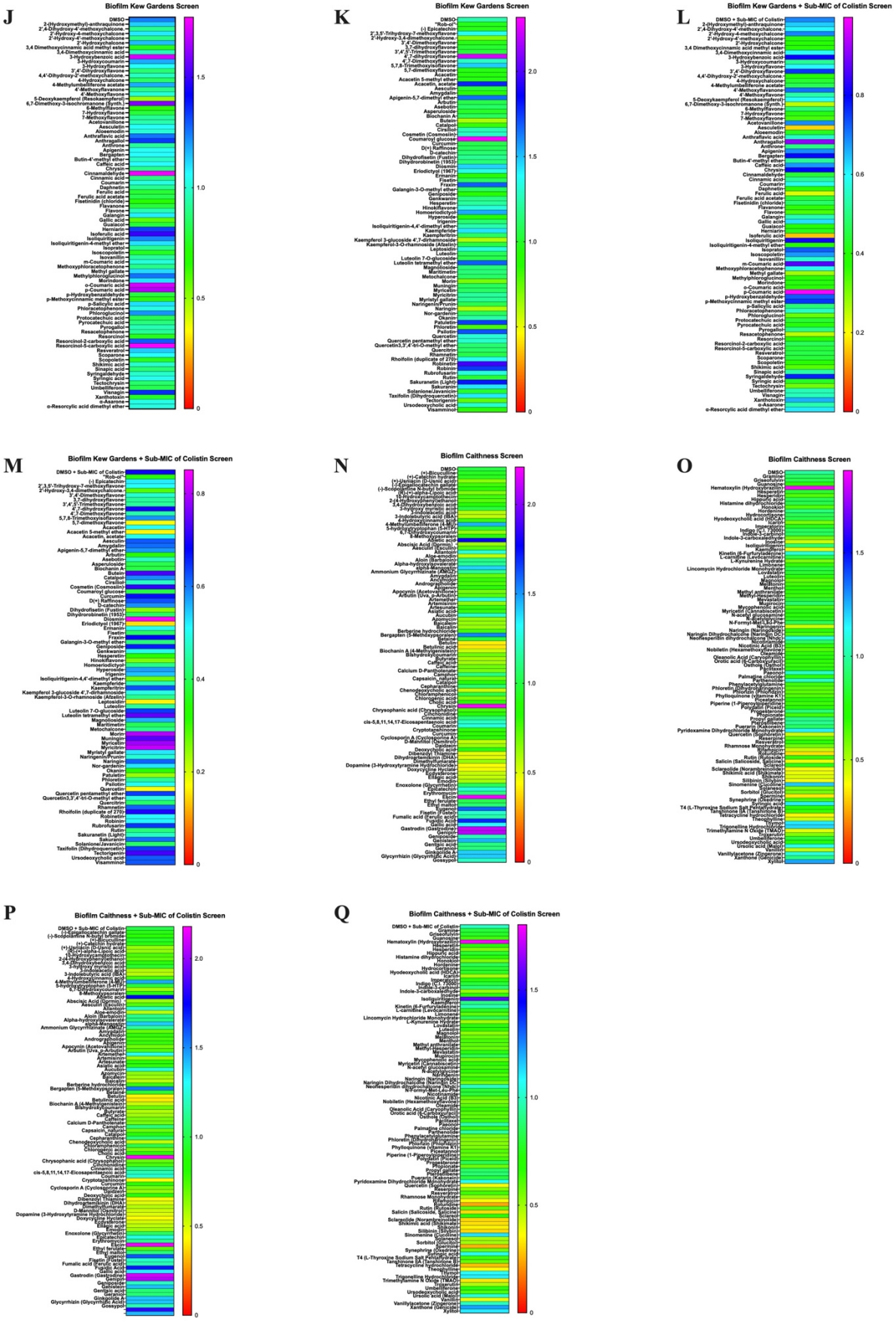

A.3 Kaempferol Gene Set Enrichment Analysis (GSEA)

Gene Set Enrichment Analysis (GSEA) using FUNAGE-Pro (de Jong *et al*., 2022) on genes found to have significantly altered expression during the dRNA-Seq experiment, with upregulated genes and downregulated genes. This analysis indicates an enrichment in genes involved in siderophore biosynthesis and transport, including the acinetobactin (*bar-bas-bau* cluster, ABUW 1168-1188) and bauminoferrin (*bfn* gene cluster, ABUW 2178-2189) biosynthetic pathways. In addition, two bacterioferritin orthologues (*bfr*, ABUW 0306 and *bfrA*, ABUW 3125) that are likely involved in iron storage, are downregulated.

		Upregulated	
ClassID	**Class**	**Description**	**single_list**
Q	COG	METABOLISM; Secondary metabolites biosynthesis, transport, and catabolism	0;6/ 51;0.00024;ABUW_1179,ABUW_1180,ABUW_1181,ABUW_2075,ABUW_2185, ABUW_2186
P	COG	METABOLISM; Inorganic ion transport and metabolism	0;6/124;0.01929;ABUW_0159,ABUW_1175,ABUW_1655,ABUW_2165,ABUW_2187,ABUW_2916
V	COG	CELLULAR PROCESSES AND SIGNALING; Defense mechanisms	0;3/ 20;0.00167;ABUW_0843,ABUW_0844,ABUW_1184
COG1535	eggNOG_COG	isochorismatase	9;2/ 2;0.0e+00;ABUW_1181,ABUW_2075
COG4773	eggNOG_COG	Receptor	9;2/ 2;0.0e+00;ABUW_1655,ABUW_2165
COG4264	eggNOG_COG	IucA IucC family	9;2/ 2;0.0e+00;ABUW_2185,ABUW_2186
COG3433	eggNOG_COG	isochorismatase activity	9;2/ 2;0.0e+00;ABUW_1181,ABUW_2075
COG1020	eggNOG_CO	D-alanine [D-alanyl carrier protein] ligase	2;2/ 4;8.7e-05;ABUW_1170,ABUW_1179

	G	activity	
COG4774	eggNOG_COG	siderophore transport	2;2/ 4;8.7e-05;ABUW_0159,ABUW_1177
GO:0038023	GO	signaling receptor activity	6; 8/ 14;1.1e-11;ABUW_0143,ABUW_0159,ABUW_1177,ABUW_1655,ABUW_2165,ABUW_2182,ABUW_2828,ABUW_2916
GO:0016765	GO	transferase activity, transferring alkyl or aryl (other than methyl) groups	1; 2/ 6;4.9e-04;ABUW_1181,ABUW_2075
GO:0052689	GO	carboxylic ester hydrolase activity	0; 2/ 9;1.7e-03;ABUW_1364,ABUW_2785
GO:0031177	GO	phosphopantetheine binding	4; 5/ 9;3.7e-08;ABUW_1169,ABUW_1170,ABUW_1179,ABUW_1181,ABUW_2075
GO:0042802	GO	identical protein binding	0; 3/ 51;4.8e-02;ABUW_0844,ABUW_1181,ABUW_2075
GO:0019290	GO	siderophore biosynthetic process	4; 3/ 4;9.1e-07;ABUW_2076,ABUW_2185,ABUW_2186
GO:0016874	GO	ligase activity	1; 3/ 10;1.2e-04;ABUW_1169,ABUW_1170,ABUW_1179
GO:0047527	GO	2,3-dihydroxybenzoate-serine ligase activity	9; 3/ 3;0.0e+00;ABUW_1180,ABUW_1181,ABUW_2075
GO:0015675	GO	nickel cation transport	2; 2/ 3;3.8e-05;ABUW_0143,ABUW_2828
GO:0006829	GO	zinc ion transport	1; 2/ 5;2.7e-04;ABUW_0143,ABUW_2828
GO:0055072	GO	iron ion homeostasis	7;11/ 17;2.7e-16;ABUW_0159,ABUW_1173,ABUW_1174,ABUW_1175,ABUW_1176,ABUW_1177,ABUW_1655,ABUW_2165,ABUW_2182,ABUW_2916,ABUW_2987
GO:0019289	GO	rhizobactin 1021 biosynthetic process	9; 3/ 3;0.0e+00;ABUW_1178,ABUW_2188,ABUW_2189

GO:0008908	GO	isochorismatase activity	9; 2/ 2;0.0e+00;ABUW_1181,ABUW_2075
GO:0006811	GO	ion transport	0; 4/ 18;1.1e-04;ABUW_1173,ABUW_1174,ABUW_1175,ABUW_2987
GO:0016021	GO	integral component of membrane	0;18/377;9.7e-04;ABUW_0143,ABUW_0159,ABUW_0843,ABUW_0845,ABUW_1173,ABUW_1174,ABUW_1177,ABUW_1655,ABUW_2054,ABUW_2165,ABUW_2187,ABUW_2494,ABUW_2777,ABUW_2828,ABUW_2916,ABUW_2983,ABUW_2985,ABUW_3425
GO:0009279	GO	cell outer membrane	1;11/ 59;1.5e-08;ABUW_0143,ABUW_0159,ABUW_1177,ABUW_1655,ABUW_2054,ABUW_2165,ABUW_2182,ABUW_2785,ABUW_2828,ABUW_2983,ABUW_2985
GO:0009239	GO	enterobactin biosynthetic process	9; 4/ 4;0.0e+00;ABUW_1180,ABUW_1181,ABUW_1188,ABUW_2075
GO:0016881	GO	acid-amino acid ligase activity	1; 2/ 4;1.2e-04;ABUW_2185,ABUW_2186
GO:0015344	GO	siderophore uptake transmembrane transporter activity	5; 8/ 16;5.1e-11;ABUW_0143,ABUW_0159,ABUW_1177,ABUW_1655,ABUW_2165,ABUW_2182,ABUW_2828,ABUW_2916
IPR029058	IPR	Alpha/Beta hydrolase fold	0;4/37;1.9e-03;ABUW_1170,ABUW_1179,ABUW_1364,ABUW_2785
IPR036736	IPR	ACP-like superfamily	3;5/10;5.7e-08;ABUW_1169,ABUW_1170,ABUW_1179,ABUW_1181,ABUW_2075
IPR007310	IPR	Aerobactin siderophore biosynthesis, IucA/IucC, N-terminal	9;3/ 3;0.0e+00;ABUW_2185,ABUW_2186,ABUW_2189

IPR037455	IPR	Aerobactin siderophore biosynthesis, IucA/IucC-like	9;3/ 3;0.0e+00;ABUW_2185,ABUW_2186,ABUW_2189
IPR020806	IPR	Polyketide synthase, phosphopantetheine-binding domain	2;3/ 7;1.7e-05;ABUW_1169,ABUW_1170,ABUW_1179
IPR001242	IPR	Condensation domain	3;3/ 5;2.8e-06;ABUW_1169,ABUW_1170,ABUW_1179
IPR037294	IPR	ABC transporter, BtuC-like	3;2/ 3;2.2e-05;ABUW_1173,ABUW_1174
IPR039426	IPR	Vitamin B12 transporter BtuB-like	1;3/10;8.0e-05;ABUW_2182,ABUW_2916,ABUW_2985
IPR022770	IPR	Ferric iron reductase FhuF domain	9;3/ 3;0.0e+00;ABUW_2185,ABUW_2186,ABUW_2189
IPR025700	IPR	L-lysine 6-monooxygenase/L-ornithine 5-monooxygenase	9;2/ 2;0.0e+00;ABUW_1178,ABUW_2188
IPR042099	IPR	AMP-dependent synthetase-like superfamily	1;4/14;1.8e-05;ABUW_1169,ABUW_1170,ABUW_1179,ABUW_1180
IPR000531	IPR	TonB-dependent receptor-like, beta-barrel	4;9/20;1.0e-11;ABUW_0143,ABUW_0159,ABUW_1177,ABUW_1655,ABUW_2165,ABUW_2182,ABUW_2828,ABUW_2916,ABUW_2985
IPR010917	IPR	TonB-dependent receptor, conserved site	4;6/11;2.3e-09;ABUW_0159,ABUW_1177,ABUW_1655,ABUW_2165,ABUW_2182,ABUW_2916
IPR010105	IPR	TonB-dependent siderophore receptor	6;8/14;8.4e-12;ABUW_0143,ABUW_0159,ABUW_1177,ABUW_1655,ABUW_2165,ABUW_2182,ABUW_2828,ABUW_2916
IPR009081	IPR	Phosphopantetheine binding ACP domain	3;5/10;5.7e-08;ABUW_1169,ABUW_1170,ABUW_1179,ABUW_1181,ABUW_2075
IPR031043	IPR	Putative histamine N-monooxygenase	9;2/ 2;0.0e+00;ABUW_1178,ABUW_2188

IPR036942	IPR	TonB-dependent receptor-like, beta-barrel domain superfamily	5;9/18;3.8e-12;ABUW_0143,ABUW_0159,ABUW_1177,ABUW_1655,ABUW_2165,ABUW_2182,ABUW_2828,ABUW_2916,ABUW_2985
IPR023213	IPR	Chloramphenicol acetyltransferase-like domain superfamily	1;3/ 8;2.9e-05;ABUW_1169,ABUW_1170,ABUW_1179
IPR000868	IPR	Isochorismatase-like	1;2/ 6;3.2e-04;ABUW_1181,ABUW_2075
IPR006162	IPR	Phosphopantetheine attachment site	1;2/ 6;3.2e-04;ABUW_1169,ABUW_1179
IPR010916	IPR	TonB box, conserved site	4;5/ 9;2.6e-08;ABUW_0159,ABUW_1177,ABUW_1655,ABUW_2165,ABUW_2182
IPR020845	IPR	AMP-binding, conserved site	1;4/13;1.3e-05;ABUW_1169,ABUW_1170,ABUW_1179,ABUW_1180
IPR010071	IPR	Amino acid adenylation domain	3;3/ 5;2.8e-06;ABUW_1169,ABUW_1170,ABUW_1179
IPR036380	IPR	Isochorismatase-like superfamily	1;2/ 6;3.2e-04;ABUW_1181,ABUW_2075
IPR039423	IPR	TonB-dependent receptor-like	5;6/10;9.0e-10;ABUW_0143,ABUW_0159,ABUW_1177,ABUW_1655,ABUW_2165,ABUW_2828
IPR037066	IPR	TonB-dependent receptor, plug domain superfamily	4;9/20;1.0e-11;ABUW_0143,ABUW_0159,ABUW_1177,ABUW_1655,ABUW_2165,ABUW_2182,ABUW_2828,ABUW_2916,ABUW_2985
IPR000873	IPR	AMP-dependent synthetase/ligase	1;4/15;2.5e-05;ABUW_1169,ABUW_1170,ABUW_1179,ABUW_1180
IPR036188	IPR	FAD/NAD(P)-binding domain superfamily	0;3/56;4.9e-02;ABUW_1178,ABUW_2188,ABUW_2487

IPR012910	IPR	TonB-dependent receptor, plug domain	4;9/20;1.0e-11;ABUW_0143,ABUW_0159,ABUW_1177,ABUW_1655,ABUW_2165,ABUW_2182,ABUW_2828,ABUW_2916,ABUW_2985
IPR016291	IPR	Isochorismatase	9;2/ 2;0.0e+00;ABUW_1181,ABUW_2075
IPR025110	IPR	AMP-binding enzyme, C-terminal domain	0;3/12;1.7e-04;ABUW_1169,ABUW_1170,ABUW_1180
IPR000522	IPR	ABC transporter, permease protein, BtuC-like	9;2/ 2;0.0e+00;ABUW_1173,ABUW_1174
01501 beta-Lactam resistance [PATH:ko01501]	KEGG	ko01501	1;2/ 6;3.9e-04;ABUW_0843,ABUW_0844
00362 Benzoate degradation [PATH:ko00362]	KEGG	ko00362	0;3/21;1.5e-03;ABUW_1833,ABUW_2076,ABUW_2487
01053 Biosynthesis of siderophore group nonribosomal peptides [PATH:ko01053]	KEGG	ko01053	6;5/ 7;1.7e-09;ABUW_1170,ABUW_1179,ABUW_1180,ABUW_1181,ABUW_2075
00997	KEGG	ko00997	9;3/ 3;0.0e+00;ABUW_1364,ABUW_2185,ABUW_2186

Biosynthesis of various secondary metabolites - part 3 [PATH:ko00997]			
Ligase	KEYWORDS	keyword	1;2/ 5;6.2e-04;ABUW_1170,ABUW_1179
Cell outer membrane	KEYWORDS	keyword	1;7/32;4.2e-06;ABUW_0143,ABUW_1177,ABUW_2054,ABUW_2182,ABUW_2828,ABUW_2983,ABUW_2985
PF04183	Pfam	IucA / IucC family	9;3/ 3;0.0e+00;ABUW_2185,ABUW_2186,ABUW_2189
PF00668	Pfam	Condensation domain	3;3/ 5;2.0e-06;ABUW_1169,ABUW_1170,ABUW_1179
PF13193	Pfam	AMP-binding enzyme C-terminal domain	0;3/12;1.4e-04;ABUW_1169,ABUW_1170,ABUW_1180
PF07715	Pfam	TonB-dependent Receptor Plug Domain	5;9/20;5.8e-12;ABUW_0143,ABUW_0159,ABUW_1177,ABUW_1655,ABUW_2165,ABUW_2182,ABUW_2828,ABUW_2916,ABUW_2985
PF00501	Pfam	AMP-binding enzyme	1;4/15;2.0e-05;ABUW_1169,ABUW_1170,ABUW_1179,ABUW_1180
PF00593	Pfam	TonB dependent receptor	5;9/20;5.8e-12;ABUW_0143,ABUW_0159,ABUW_1177,ABUW_1655,ABUW_2165,ABUW_2182,ABUW_2828,ABUW_2916,ABUW_2985
PF01032	Pfam	FecCD transport family	9;2/ 2;0.0e+00;ABUW_1173,ABUW_1174
PF13434	Pfam	L-lysine 6-monooxygenase (NADPH-requiring)	9;2/ 2;0.0e+00;ABUW_1178,ABUW_2188

PF00550	Pfam	Phosphopantetheine attachment site	3;5/10;4.1e-08;ABUW_1169,ABUW_1170,ABUW_1179,ABUW_1181,ABUW_2075
PF06276	Pfam	Ferric iron reductase FhuF-like transporter	9;3/ 3;0.0e+00;ABUW_2185,ABUW_2186,ABUW_2189
PF00857	Pfam	Isochorismatase family	1;2/ 6;2.6e-04;ABUW_1181,ABUW_2075
Downregulated			
GO:0004322	GO	ferroxidase activity	9;2/ 2
GO:0006826	GO	iron ion transport	4;2/ 3
GO:0008199	GO	ferric iron binding	2;2/ 5
GO:0006879	GO	cellular iron ion homeostasis	4;2/ 3
IPR009040	IPR	Ferritin-like diiron domain	9;2/2
IPR002024	IPR	Bacterioferritin	9;2/2
IPR008331	IPR	Ferritin/DPS protein domain	9;2/2
IPR012347	IPR	Ferritin-like	2;2/5
IPR009078	IPR	Ferritin-like superfamily	1;2/7
3D-structure	KEYWORDS	keyword	0;5/334
PF00210	Pfam	Ferritin-like domain	9;2/2

A.4 *E. coli* and *A. baumannii* strains, other than wild-type *A. baumannii* AB5075, used in this study.

Name	Description	Source
E. coli strains		
DH5 α	F- ϕ0lacZ Δ M15, ΔlacZYA-argF)U169, recA1, endA1, hsdR17(rK-m K-), supE44, thi-1, gyrA, relA1	McCarthy lab collection, Hanahan, 1983
DH5 $\alpha\lambda pir$	F- ϕ0lacZΔ M15, Δ lacZYA-argF)U169, recA1, endA1, hsdR17(rK-m K-), supE44, thi-1, gyrA, relA1, λpir lysogen	McCarthy lab collection, Mart´ınez-Garc´ıa and de Lorenzo, 2011
E. coli W3110	F– λ - IN (*rrnD-rrnE*)*1* rph-1. MIC 1-2 μg/mL	*E. coli* Genetic Stock Center, Yale University
E. coli WD101	W3110, *pmrA*^{c}, chromosomal colistin^{R}. MIC 16 μg/mL	Trent MS, *et al*. Accumulation of a Polyisoprene-linked Amino Sugar in Polymyxin-resistant *Salmonella typhimurium* and *Escherichia coli*. J. Biol. Chem. 2001; 276: 43132-43144.
A. baumannii AB5075 derivative strains		
AB5075	Wild type strain. MIC 2.44 μg/mL	Manoil Lab at the University of Washington, Seattle, USA. Jacobs *et al*., 2014

AB5075/miniTn7T-Tc-lacI^{q}-Ptac	AB5075 bearing a miniTn7T-Tc-lacIq-Ptac insertion in the *att*Tn7 site	de Dios *et al*. 2022
AB5075/miniTn7T-zeo-gfpmut3	AB5075 bearing a miniTn7T-zeo-gfpmut3 insertion in the *att*Tn7 site	de Dios *et al*. 2022

AB5075/miniTn7T-zeo-PsodB::gfpmut3	AB5075 bearing a miniTn7T-zeo-PsodB::gfpmut3 insertion in the *att*Tn7 site	This work
AB5075/miniTn7T-zeo-PsodC::gfpmut3	AB5075 bearing a miniTn7T-zeo-PsodC::gfpmut3 insertion in the *att*Tn7 site	This work
AB5075/miniTn7T-Tc-lacI^{q}-Ptac::sodB	AB5075 bearing a miniTn7T-Tc-lacIq-Ptac::sodB insertion in the *att*Tn7 site	This work
AB5075/miniTn7T-Tc-lacI^{q}-Ptac::sodC	AB5075 bearing a miniTn7T-Tc-lacIq-Ptac::sodC insertion in the *att*Tn7 site	This work
AB5075*/sodB::Tn26*	IDbarcode tnab1_kr121128p05q196	Manoil AB5075 mutant library; Gallagher *et al*., 2015
AB5075*/sodC::Tn26*	IDbarcode tnab1_kr121203p02q165	Manoil AB5075 mutant library; Gallagher *et al*., 2015
Clinical isolates		

E. coli 1073944 (ST117)	*mcr-1*. MIC 8 μg/mL.	Wise MG, *et al*. Prevalence of *mcr*-type genes among colistin-resistant *Enterobacteriaceae* collected in 2014-2016 as part of the INFORM global surveillance program. *PloS One*. 2018; 13(4): e0195281.

E. coli 1252394	Chromosomal colistin^{R}. MIC 8 μg/mL.	Wise MG, *et al*. Prevalence of *mcr*-type genes among colistin-resistant *Enterobacteriaceae* collected in 2014-2016 as part of the INFORM global surveillance program. *PloS One*. 2018; 13(4): e0195281.
E. coli CNR1728	*pmrB* G160E, chromosomal colistin^{R}. MIC 8-16 μg/mL	Dortet L, *et al*. Rapid detection and discrimination of chromosome- and MCR-plasmid-mediated resistance to polymyxins by MALDI-TOF MS in *Escherichia coli*: the MALDIxin test. *J. Antimicrob. Chemother*. 2018; 73(12): 3359-67.
E. coli ATCC25922	MIC 1-2 μg/mL	ATCC

A. baumannii CDC-22	*aac(3)-IIa, aph(3')-VIa, OXA-23, OXA-65, strA, strB, sul2*, TEM-1B. MIC 1-2 μg/mL	CDC AR Isolate Bank – *Acinetobacter* panel
A. baumannii CDC-26	*ADC-25, aph(3')-Ic, armA, catB8, mph(E), msr(E), OXA-237, OXA-66, strA, strB, sul1, sul2*, TEM-1D. MIC 1-2 μg/mL	CDC AR Isolate Bank – Acinetobacter panel

A. baumannii CDC-31	chromosomal colistin^{R}, *ADC-25, aph(3')-Ic, aph(3')-VIa, armA, catB8, mph(E), msr(E),* OXA-23, OXA-66, *strA, strB, sul1, sul2*. MIC 256 μg/mL	CDC AR Isolate Bank – *Acinetobacter* panel
A. baumannii CDC-35	chromosomal colistin^{R}, *ADC-25, aph(3')-Ic, armA, catB8, mph(E), msr(E)*, OXA-237, OXA-66, *strA, strB, sul1, sul2*. MIC 256 μg/mL	CDC AR Isolate Bank – *Acinetobacter* panel

A.5 Plasmids used in this study.

Name	Description	Source
pDM1	pDM1 vector (GenBank MN128719), p15A ori, Ptac promoter, MCS, Tet^R	Furniss RCD, *et al*. Breaking antimicrobial resistance by disrupting extracytoplasmic protein folding. *Elife*. 2022; 11: e57974.
pDM1-mcr-1	*mcr-1* cloned into pDM1, Tet^R	Furniss RCD, *et al*. Breaking antimicrobial resistance by disrupting extracytoplasmic protein folding. *Elife*. 2022; 11: e57974.
pRK2013	ColE1, tra+. Conjugative helper plasmid. Km^R	McCarthy lab collection, Figurski and Helinski, 1979

pTNS2	R6K replicon-based helper plasmid expressing the Tn7 transposase. Ap^R	McCarthy lab collection, Choi *et al*., 2005
pUC18T-miniTn7T-Tc-lacIq-Ptac	pUC18T derivative vec- tor bearing a miniTn7T backbone including a Tc resistance marker and the *lacI^q-Ptac* expression system. Tc^R, Ap^R	McCarthy lab collection, de Dios *et al*., 2022
pUC18T-miniTn7T-Tc-lacIq-Ptac::*sodB*	pUC18T derivative vec- tor bearing a miniTn7T backbone including a Tc resistance marker and the sodB gene downstream the lacIq-Ptac expression system. Tc^R, Ap^R	This work
pUC18T-miniTn7T-Tc-lacIq-Ptac::sodC	pUC18T derivative vec- tor bearing a miniTn7T backbone including a Tc resistance marker and the *sodC* gene downstream the *lacI^q-Ptac* expression system. Tc^R, Ap^R	This work

pUC18T-miniTn7T-zeo-gfpmut3	pUC18T derivative vector bearing a miniTn7T backbone including a zeocin resistance marker and the *gfpmut3* coding regions to construct transcriptional fusions. Zeo^R, Ap^R	McCarthy lab collection, Choi and Schweizer, 2006
pUC18T-miniTn7T-zeo-PsodB::gfpmut3	pUC18T derivative vector bearing a miniTn7T backbone including a *PsodB::gfpmut3* transcriptional fusion. Zeo^R, Ap^R	This work
pUC18T-miniTn7T-zeo-PsodC::gfpmut3	pUC18T derivative vector bearing a miniTn7T backbone including a *PsodC::gfpmut3* transcriptional fusion. Zeo^R, Ap^R	This work

A.6 Oligonucleotides used in this study.

Name	Description	Source
AB5075-glmS fw	TTTGCTGATGAAAATAGTGG	de Dios *et al*., 2022
Tn7R	CACAGCATAACTGGACTGATTTC	Kumar *et al*., 2010

sodB fw RBS PstI	AAAAACTGCAGGAAAGAGGAGAATAGGAACA-TGACAACCATTAC	This work
sodB rv KpnI	AAAAAGGTACCTTATTTCTCTACACCAGCTGG	This work
sodB trx fw EcoRI	TTTTTGAATTCTGAAATTATTCAGTGGTGCG	This work
sodB trx rv BamHI	TTTTTGGATCCGGTTGTCATGTTCCTATTCC	This work
sodC fw RBS PstI	AAAAACTGCAGGAAAGAGG-AGAAATCTATAATGCCAGTATTTAATAAAATTGG	This work
sodC rv HindIII	AAAAAAAGCTTAAAGCACTTATTTGATTACACC	This work
sodC trx fw EcoRI	TTTTTGAATTCTATTCTACAACATGAAGGCCG	This work
sodC trx rv BamHI	TTTTTGGATCCAAATACTGGCATTATAGATATCC	This work

A.7 Differentially Expressed Genes in Kaempferol Treated and Untreated Samples

Locustag	Gene	Description	Feature Type	Untreated-2	Untreated-3	Treated-1	Treated-2	Untreated Average	Treated Average	logFC
ABUW_5014		hypothetical protein	CDS	1.437	1.586	3.208	2.134	1.512	2.671	0.821
ABUW_4021		hypothetical protein	CDS	2.361	2.141	4.643	4.120	2.251	4.381	0.961
ABUW_3800		transposase, Mutator family	CDS	0.513	1.586	1.351	2.134	1.050	1.742	0.731
ABUW_3633	feoA	iron transporter	CDS	30.793	18.637	55.544	71.511	24.715	63.528	1.362
ABUW_3583	ompW	putative outer membrane protein W	CDS	7897.364	5815.530	4893.593	1277.127	6856.447	3085.360	-1.152
ABUW_3508		hypothetical protein	CDS	399.077	164.642	102.815	47.306	281.859	75.061	-1.909
ABUW_3503		hypothetical protein	CDS	1.232	1.665	3.377	4.635	1.449	4.006	1.467
ABUW_3464		hypothetical protein	CDS	7.801	10.548	23.214	21.924	9.174	22.569	1.299
ABUW_3429	calB	aldehyde dehydrogenase	CDS	421.042	338.087	140.294	110.063	379.565	125.179	-1.600
ABUW_3426		TonB protein	CDS	133.847	144.498	409.150	575.108	139.172	492.129	1.822
ABUW_3425	exbB	MotA/TolQ/ExbB proton channel	CDS	355.145	256.559	685.265	869.026	305.852	777.145	1.345
ABUW_3424	ExbD/TolR	biopolymer transport protein ExbD/TolR	CDS	117.629	102.148	230.110	293.771	109.888	261.940	1.253
ABUW_3217	add2	adenosine deaminase	CDS	82.833	197.951	73.861	41.494	140.392	57.678	-1.283
ABUW_3202		fatty acid desaturase	CDS	4.722	3.172	10.298	6.916	3.947	8.607	1.125
ABUW_3194		transcriptional regulator, TetR family	CDS	0.000	1.110	1.773	1.986	0.555	1.880	1.759
ABUW_3179		hypothetical protein	CDS	259.071	540.083	242.350	182.678	399.577	212.514	-0.911
ABUW_3125	bfr2 / bfrA	bacterioferritin	CDS	435.002	153.460	71.920	57.606	294.231	64.763	-2.184

ABUW_3015		hypothetical protein	CDS	1.129	0.555	1.351	1.766	0.842	1.558	0.888
ABUW_2987	fecI	RNA polymerase sigma factor FecI	CDS	3.285	5.948	6.669	17.951	4.616	12.310	1.415
ABUW_2986		putative transmembrane sensor protein FecR	CDS	3.798	2.459	5.740	10.374	3.128	8.057	1.365
ABUW_2985	bhuA	hypothetical protein	CDS	7.082	8.882	22.623	20.526	7.982	21.575	1.434
ABUW_2984		hypothetical protein	CDS	32.025	24.030	71.329	50.249	28.027	60.789	1.117
ABUW_2983		hypothetical protein	CDS	4.311	4.679	10.720	18.099	4.495	14.410	1.681
ABUW_2982		TonB family protein	CDS	3.695	2.538	4.558	8.166	3.116	6.362	1.030
ABUW_2950	golD	short chain dehydrogenase	CDS	1.334	2.221	6.162	4.709	1.777	5.435	1.613
ABUW_2940		hypothetical protein	CDS	2.053	1.348	3.967	2.575	1.701	3.271	0.944
ABUW_2916	pfeA	TonB dependent outer membrane siderophore receptor protein	CDS	50.398	29.582	249.525	563.116	39.990	406.320	3.345
ABUW_2828	cntO	TonB-dependent siderophore receptor	CDS	276.110	116.503	755.666	833.344	196.306	794.505	2.017
ABUW_2785	hcaG / mhbT	tannase/feruloyl esterase family protein	CDS	17.141	11.500	52.674	89.536	14.320	71.105	2.312
ABUW_2784		hypothetical protein	CDS	0.616	1.745	10.130	16.039	1.180	13.084	3.471
ABUW_2783	yveG	hypothetical protein	CDS	3.798	4.362	23.889	32.666	4.080	28.277	2.793
ABUW_2777	hcaK / mhpT	3-hydroxyphenylpropionic acid transporter	CDS	12.317	12.451	72.342	35.388	12.384	53.865	2.121
ABUW_2761		transcriptional regulator	CDS	18.578	15.782	5.402	8.314	17.180	6.858	-1.325
ABUW_2494	yxlA	permease	CDS	4.619	2.617	5.656	7.504	3.618	6.580	0.863
ABUW_2493		hypothetical protein	CDS	2.258	1.348	4.980	3.605	1.803	4.293	1.251
ABUW_2487	pobA	4-hydroxybenzoate 3-monooxygenase	CDS	3.182	1.586	33.090	11.551	2.384	22.320	3.227
ABUW_2463		hypothetical protein	CDS	2.258	3.648	6.837	5.812	2.953	6.325	1.099
ABUW_2445		hypothetical protein	CDS	2.053	3.965	7.766	5.003	3.009	6.384	1.085

ABUW_2444		hypothetical protein	CDS	7.904	9.913	26.168	16.333	8.908	21.250	1.254
ABUW_2382	tauA	taurine ABC transporter, periplasmic binding protein	CDS	24.121	30.295	13.928	10.447	27.208	12.188	-1.159
ABUW_2189	rhbC	IucA/IucC-family aerobactin siderophore biosynthesis component	CDS	66.718	143.943	813.066	941.052	105.330	877.059	3.058
ABUW_2188	rhbE	hypothetical protein	CDS	58.507	96.200	451.357	538.690	77.353	495.023	2.678
ABUW_2187	yfiu	transporter, major facilitator family	CDS	33.770	58.608	276.453	388.310	46.189	332.381	2.847
ABUW_2186	sbnF	siderophore biosynthesis protein / 2-[(L-alanin-3-ylcarbamoyl)methyl]-3-(2-aminoethylcarbamoyl)-2-hydroxypropanoate synthase	CDS	88.684	121.895	433.123	640.807	105.290	536.965	2.350
ABUW_2185	sbnC	siderophore biosynthesis protein / Staphyloferrin B synthase	CDS	64.152	83.193	253.492	438.633	73.673	346.063	2.232
ABUW_2184		hypothetical protein	CDS	4.619	5.948	15.870	28.914	5.283	22.392	2.083
ABUW_2183		dimethylmenaquinone methyltransferase	CDS	7.801	8.565	14.772	33.034	8.183	23.903	1.546
ABUW_2182	iutA	TonB-dependent receptor	CDS	1387.838	709.325	2103.151	3305.344	1048.582	2704.247	1.367
ABUW_2178		rhizobactin siderophore biosynthesis protein RhbD	CDS	45.881	31.723	162.580	353.511	38.802	258.045	2.733
ABUW_2168		hypothetical protein	CDS	3.079	3.410	10.383	10.594	3.245	10.489	1.693
ABUW_2167		iron-regulated membrane protein	CDS	25.353	11.341	62.803	85.196	18.347	74.000	2.012
ABUW_2166		hypothetical protein	CDS	2.463	1.348	9.876	15.965	1.906	12.921	2.761
ABUW_2165	fhuE	outer-membrane receptor for Fe(III)-coprogen,Fe(III)-ferrioxamine B and Fe(III)-rhodotrulic acid	CDS	104.901	27.520	423.331	539.426	66.210	481.379	2.862

ABUW_2076	dhbA	2,3-dihydro-2,3-dihydroxybenzoate dehydrogenase	CDS	18.168	27.123	69.388	129.339	22.645	99.363	2.133
ABUW_2075	entB	isochorismatase / Enterobactin synthase component B	CDS	13.857	16.655	46.090	69.010	15.256	57.550	1.915
ABUW_2074		transcriptional regulator, fur family	CDS	2.156	8.803	20.090	28.251	5.479	24.171	2.141
ABUW_2054	mrkC	outer membrane fimbrial usher protein	CDS	21.863	43.302	52.505	126.911	32.582	89.708	1.461
ABUW_2053	mrkB	pili assembly chaperone	CDS	3.079	17.527	20.766	72.909	10.303	46.837	2.185
ABUW_2051		hypothetical protein	CDS	113.113	86.762	54.109	37.669	99.938	45.889	-1.123
ABUW_1975	adeB / acrB	multidrug efflux protein AdeB / Multidrug efflux pump subunit Acrb	CDS	6186.405	2807.957	1772.674	1264.252	4497.181	1518.463	-1.566
ABUW_1974	adeA / acrE	multidrug efflux protein AdeA	CDS	2119.684	826.303	481.576	461.072	1472.994	471.324	-1.644
ABUW_1943	ssuA	nicotinamide phosphoribosyltransferase	CDS	195.946	76.770	80.277	57.680	136.358	68.978	-0.983
ABUW_1931		transporter, major facilitator family	CDS	12.215	6.662	26.337	24.279	9.438	25.308	1.423
ABUW_1913		hypothetical protein	CDS	0.924	0.555	1.013	1.619	0.739	1.316	0.831
ABUW_1905	ycaC	isochorismatase hydrolase	CDS	324.866	375.758	192.546	134.489	350.312	163.517	-1.099
ABUW_1904		antibiotic biosynthesis monooxygenase	CDS	74.622	106.986	53.518	34.064	90.804	43.791	-1.052
ABUW_1866	feaR	transcriptional regulator, AraC family	CDS	2.669	2.221	9.454	5.591	2.445	7.523	1.622
ABUW_1850	carC	acyl-CoA dehydrogenase domain protein	CDS	156.428	76.294	61.790	45.835	116.361	53.813	-1.113
ABUW_1840	aroD	3-dehydroquinate dehydratase, type I	CDS	9.033	3.886	16.123	14.346	6.459	15.235	1.238

ABUW_1833	pcaF1 / pcaF	beta-ketoadipyl CoA thiolase	CDS	19.194	21.175	44.570	34.946	20.185	39.758	0.978
ABUW_1722	fumC	fumarate hydratase, class II	CDS	297.562	515.894	979.191	1107.765	406.728	1043.478	1.359
ABUW_1655	fhuE	TonB-dependent siderophore receptor	CDS	32.538	14.275	167.222	372.713	23.407	269.968	3.528
ABUW_1598	fhuA	hypothetical protein	CDS	18.065	20.065	43.810	84.239	19.065	64.025	1.748
ABUW_1538		hypothetical protein	CDS	0.924	1.269	2.279	2.207	1.096	2.243	1.033
ABUW_1516		hypothetical protein	CDS	0.411	0.872	2.195	1.839	0.641	2.017	1.653
ABUW_1510		dehydrogenase	CDS	0.513	1.428	2.026	1.986	0.970	2.006	1.048
ABUW_1488	CsuA	CsuA	CDS	0.205	0.872	1.604	1.913	0.539	1.758	1.706
ABUW_1487	CsuA/B	CsuA/B	CDS	13.446	34.023	86.777	68.127	23.735	77.452	1.706
ABUW_1440		hypothetical protein	CDS	0.513	0.476	1.435	1.030	0.495	1.233	1.317
ABUW_1434		hypothetical protein	CDS	5.543	3.727	1.604	2.501	4.635	2.053	-1.175
ABUW_1420		hypothetical protein	CDS	0.719	1.348	1.604	1.986	1.033	1.795	0.797
ABUW_1403		hypothetical protein	CDS	1.848	1.903	3.292	3.973	1.875	3.632	0.954
ABUW_1396		hypothetical protein	CDS	0.308	0.397	1.857	1.030	0.352	1.444	2.035
ABUW_1364	besA	alpha/beta hydrolase fold protein / Ferri-bacillibactin esterase	CDS	11.085	10.310	35.200	28.693	10.698	31.947	1.578
ABUW_1355		complement control module protein	CDS	222.325	265.918	790.697	641.837	244.121	716.267	1.553
ABUW_1298		hypothetical protein	CDS	0.821	1.428	2.448	2.134	1.124	2.291	1.027
ABUW_1292	wbbL2	hypothetical protein	CDS	2.874	3.569	4.896	4.267	3.221	4.582	0.508
ABUW_1258		hypothetical protein	CDS	0.308	0.793	0.844	1.177	0.551	1.011	0.876
ABUW_1188	basJ / entC	isochorismate synthetase	CDS	26.790	59.005	97.413	132.870	42.897	115.141	1.424
ABUW_1187	basI	phosphopantetheinyl transferase	CDS	1.437	1.031	1.773	2.943	1.234	2.358	0.934
ABUW_1184	metK1	ABC transporter, ATP-binding protein	CDS	15.191	23.158	27.265	50.985	19.174	39.125	1.029

ABUW_1182	basG	histidine decarboxylase	CDS	3.182	9.041	23.382	35.388	6.111	29.385	2.265
ABUW_1181	basF / entB	2,3 dihydro-2,3 dihydroxybenzoate synthase / Enterobactin synthase component b	CDS	3.490	6.583	21.019	45.246	5.036	33.133	2.718
ABUW_1180	basE / entE	2,3-dihydroxybenzoate-AMP ligase / Enterobactin synthase component E	CDS	10.264	12.689	50.563	101.161	11.477	75.862	2.725
ABUW_1179	basD / mbtB	nonribosomal peptide synthetase BasD / Phenyloxazoline synthase MbtB	CDS	17.244	16.337	68.628	105.575	16.791	87.101	2.375
ABUW_1178	basC / rhbE	nonribosomal peptide synthetase BasC	CDS	9.443	11.658	22.876	34.137	10.551	28.507	1.434
ABUW_1177	bauA / fatA	ferric acinetobactin receptor	CDS	67.026	68.918	197.189	448.418	67.972	322.803	2.248
ABUW_1176	bauB / fatB	ferric acinetobactin transport system periplasmic binding protein	CDS	20.221	27.758	79.264	196.583	23.989	137.923	2.523
ABUW_1175	bauE / yclP	ferric acinetobactin transport system ATP-binding protein	CDS	8.109	7.693	22.538	55.399	7.901	38.969	2.302
ABUW_1174	bauC / fatC	ferric acinetobactin transport system permease	CDS	3.593	2.141	6.415	23.396	2.867	14.906	2.378
ABUW_1173	bauD / fatD	ferric acinetobactin transport system permease	CDS	2.977	1.903	5.487	17.731	2.440	11.609	2.250
ABUW_1171		hypothetical protein	CDS	0.103	0.555	1.773	5.003	0.329	3.388	3.365
ABUW_1170	basB / mbtB / dhbF	non-ribosomal peptide synthetase / Dimodular nonribosomal peptide synthase	CDS	26.995	34.499	155.236	382.424	30.747	268.830	3.128
ABUW_1169	basA / bacA	non-ribosomal peptide synthetase	CDS	11.393	26.330	55.122	83.356	18.862	69.239	1.876

ABUW_1168	bauF	siderophore-interacting protein	CDS	9.751	16.179	46.258	55.620	12.965	50.939	1.974
ABUW_1104	hcr	NADH oxidoreductase HCR	CDS	670.876	452.052	336.133	218.949	561.464	277.541	-1.016
ABUW_0845	pgpB	hypothetical protein	CDS	65.178	116.661	229.266	285.163	90.920	257.214	1.500
ABUW_0844	adeI / acrA	multidrug efflux protein AdeI / Multidrug efflux pump subunit AcrA	CDS	458.404	682.202	1037.014	1479.227	570.303	1258.121	1.141
ABUW_0843	adeJ / mexB	multidrug efflux protein AdeJ	CDS	1250.912	1703.205	2625.668	3573.217	1477.059	3099.443	1.069
ABUW_0744		hypothetical protein	CDS	0.205	0.952	1.097	1.030	0.578	1.064	0.879
ABUW_0698	cysJ	flavodoxin/nitric oxide synthase / Sulfite reductase [NADPH] flavoprotein alpha-component	CDS	99.666	80.894	300.257	342.328	90.280	321.293	1.831
ABUW_0436		hypothetical protein	CDS	0.924	0.714	1.266	2.281	0.819	1.773	1.115
ABUW_0307	bfd	hypothetical protein	CDS	7.390	16.179	65.167	47.748	11.785	56.457	2.260
ABUW_0306	bfr1	bacterioferritin	CDS	632.692	248.787	174.482	116.831	440.740	145.657	-1.597
ABUW_0159	fhuA	TonB-dependent receptor protein	CDS	48.448	34.419	109.062	166.345	41.433	137.703	1.733
ABUW_0143	cntO	TonB-dependent receptor protein	CDS	10.880	11.817	35.791	80.193	11.348	57.992	2.353
ABUW_0127	hpxO	monooxygenase, FAD-binding	CDS	2.566	2.617	5.402	5.150	2.592	5.276	1.026

A.8 Absorbance Spectrum of Kaempferol and Iron

Kaempferol binds to Fe^{3+}, absorption spectra in the 300- 500 nm range of kaempferol (peak at 360 nm), compared to the DMSO control (kaempferol carrier) and mixtures of kaempferol with either Fe^{2+} or Fe^{3+}. For each kaempferol:iron proportion, the respective concentrations, in mM units, were: 1:3 -> 0.025:0.075, 1:2 -> 0.033:0.067, 3:4 -> 0.043:0.057, 1:1 -> 0.05:0.05, 3:2 -> 0.06:0.04, 2:1 -> 0.067:0.033, 5:2 -> 0.071:0.029, 3:1 -> 0.075:0.025, 7:2 -> 0.078:0.022, 4:1 -> 0.08:0.02, 5:1 ->0.017:0.083, 6:1 -> 0.086:0.014.

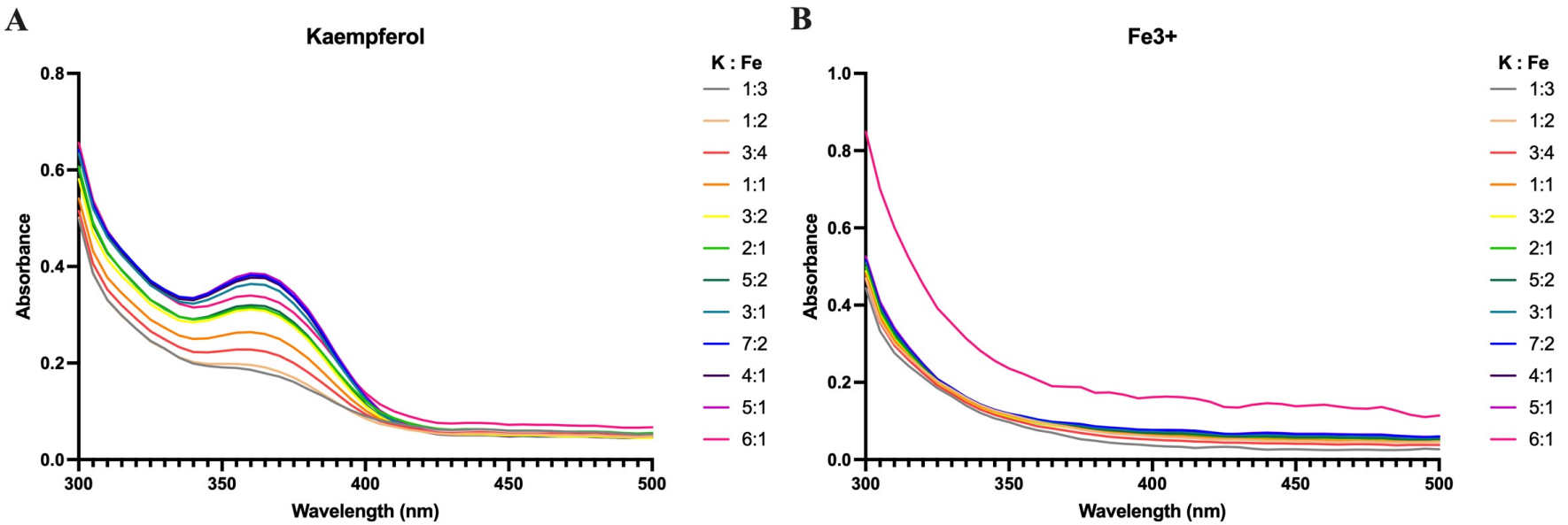

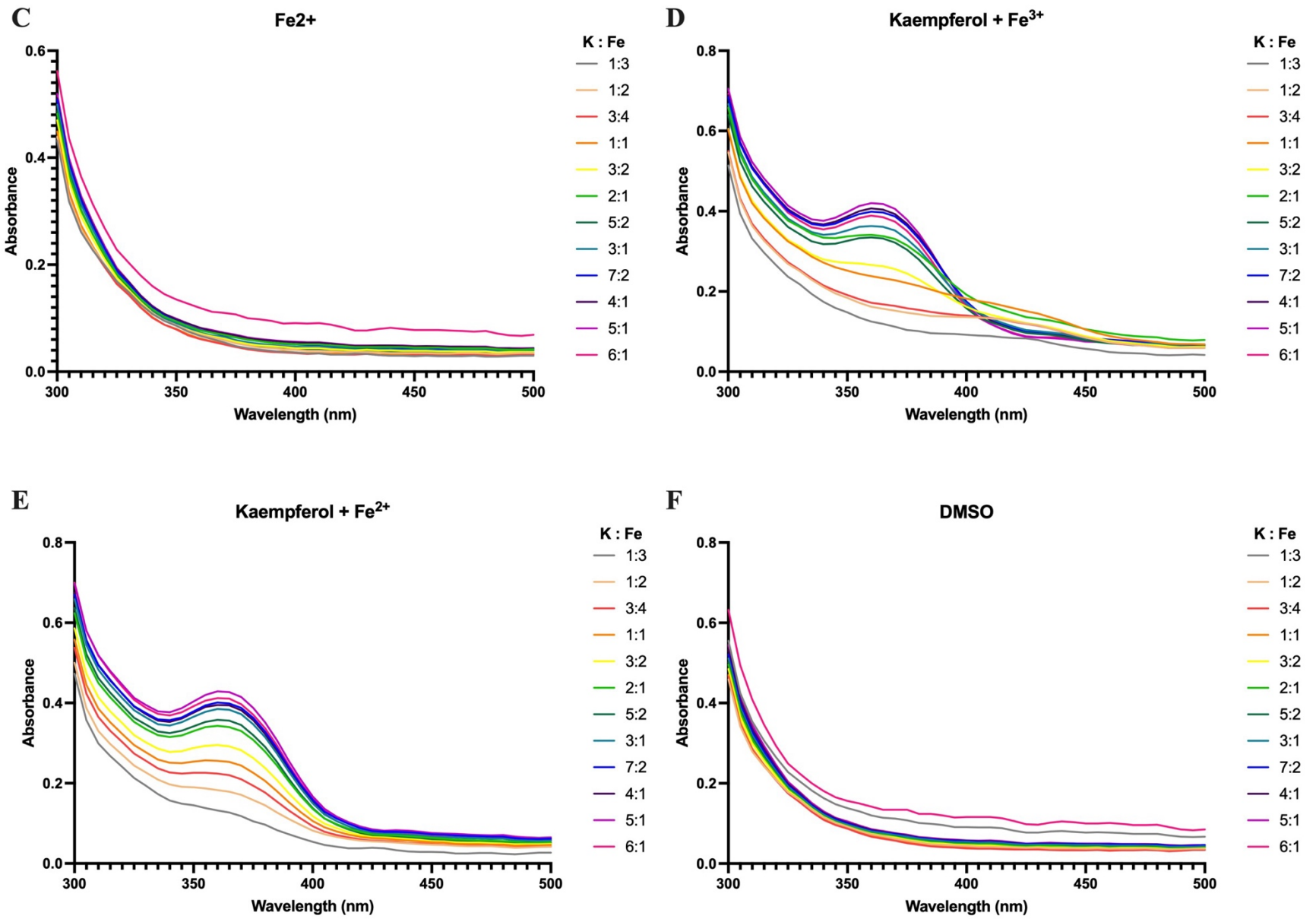
C
Fe2+
D
Kaempferol + Fe3+
E
Kaempferol + Fe2+
F
DMSO
Absorbance
Wavelength (nm)
K : Fe
1:3
1:2
3:4
1:1
3:2
2:1
5:2
3:1
7:2
4:1
5:1
6:1

Appendix B

Chapter 3 Appendices

B.1 Dublin Gene Set Enrichment Analysis (GSEA)

Gene Set Enrichment Analysis (GSEA). GSEA was conducted using FUNAGE-Pro (de Jong *et al*., 2022) on genes found to have significantly altered expression during the dRNA-Seq experiment, with upregulated genes and downregulated genes.

ClassID	Class	Description	Single list
Agrimoniin Downregulated			
IPR037257	IPR	General secretory system II, protein E, N-terminal superfamily	2;2/ 3;2.2e-04;ABUW_RS06590,ABUW_RS17270
Q	COG	METABOLISM; Secondary metabolites biosynthesis, transport, and catabolism	0; 5/ 52;0.0492;ABUW_RS08125,ABUW_RS10105,ABUW_RS10110,ABUW_RS12265,ABUW_RS12280
C	COG	METABOLISM; Energy production and conversion	0;12/137;0.0077;ABUW_RS01250,ABUW_RS06555,ABUW_RS07780,ABUW_RS08735,ABUW_RS08740,ABUW_RS08850,ABUW_RS10115,ABUW_RS12790,ABUW_RS13610,ABUW_RS14045,ABUW_RS16510,ABUW_RS18550

T	COG	CELLULAR PROCESSES AND SIGNALING; Signal transduction mechanisms	0; 8/ 58;0.0027;ABUW_RS03335,ABUW_RS03340,ABUW_RS03355,ABUW_RS05570,ABUW_RS13305,ABUW_RS17655,ABUW_RS17725,ABUW_RS17730
COG1018	eggNOG_COG	Is involved in NO detoxification in an aerobic process, termed nitric oxide dioxygenase (NOD) reaction that utilizes O(2) and NAD(P)H to convert NO to nitrate, which protects the bacterium from various noxious nitrogen compounds. Therefore, plays a central role in the inducible response to nitrosative stress	1;2/ 5;0.0011;ABUW_RS01970,ABUW_RS10115
GO:0007155	GO	cell adhesion	2; 2/ 3;1.9e-04;ABUW_RS01495,ABUW_RS11235
GO:0018618	GO	anthranilate 1,2-dioxygenase (deaminating, decarboxylating) activity	9; 2/ 2;0.0e+00;ABUW_RS10105,ABUW_RS10110
GO:0019646	GO	aerobic electron transport chain	0; 2/ 9;8.0e-03;ABUW_RS08735,ABUW_RS08740
GO:0004109	GO	coproporphyrinogen oxidase activity	2; 2/ 3;1.9e-04;ABUW_RS01850,ABUW_RS03365
GO:0060491	GO	regulation of cell projection assembly	9; 2/ 2;0.0e+00;ABUW_RS17725,ABUW_RS17730
GO:0019556	GO	histidine catabolic process to glutamate and formamide	5; 4/ 5;4.6e-07;ABUW_RS00370,ABUW_RS00385,ABUW_RS00395,ABUW_RS00400
GO:0007165	GO	signal transduction	0; 2/ 6;2.6e-03;ABUW_RS03345,ABUW_RS03350
GO:0044096	GO	type IV pilus	9; 4/ 4;0.0e+00;ABUW_RS01425,ABUW_RS01430,ABUW_RS01435,ABUW_RS14710
GO:0009297	GO	pilus assembly	1; 2/ 5;1.5e-03;ABUW_RS06590,ABUW_RS11245
GO:0070069	GO	cytochrome complex	1; 2/ 4;7.1e-04;ABUW_RS08735,ABUW_RS08740

GO:0006935	GO	chemotaxis	1; 3/ 6;1.6e-04;ABUW_RS03345,ABUW_RS03350,ABUW_RS03355
GO:0006782	GO	protoporphyrinogen IX biosynthetic process	0; 2/ 8;6.1e-03;ABUW_RS01850,ABUW_RS03365
GO:0046872	GO	metal ion binding	0;21/265;9.5e-04;ABUW_RS00800,ABUW_RS01425,ABUW_RS01850,ABUW_RS01970,ABUW_RS02595,ABUW_RS03365,ABUW_RS05555,ABUW_RS05940,ABUW_RS06555,ABUW_RS06590,ABUW_RS07780,ABUW_RS08735,ABUW_RS08740,ABUW_RS08850,ABUW_RS10115,ABUW_RS11945,ABUW_RS12790,ABUW_RS14280,ABUW_RS16510,ABUW_RS17270,ABUW_RS17655
GO:0006119	GO	oxidative phosphorylation	9; 2/ 2;0.0e+00;ABUW_RS08730,ABUW_RS08735
GO:0000160	GO	phosphorelay signal transduction system	1; 4/ 12;1.9e-04;ABUW_RS03335,ABUW_RS03340,ABUW_RS03355,ABUW_RS17730
GO:0019439	GO	aromatic compound catabolic process	0; 4/ 25;5.3e-03;ABUW_RS10105,ABUW_RS10110,ABUW_RS10115,ABUW_RS13510
GO:0043683	GO	type IV pilus biogenesis	6; 5/ 6;2.4e-08;ABUW_RS01425,ABUW_RS01430,ABUW_RS01435,ABUW_RS01445,ABUW_RS17270
GO:0005506	GO	iron ion binding	0; 3/ 30;4.4e-02;ABUW_RS00395,ABUW_RS10105,ABUW_RS14740

GO:0019557	GO	histidine catabolic process to glutamate and formate	5; 4/ 5;4.6e-07;ABUW_RS00370,ABUW_RS00385,ABUW_RS00395,ABUW_RS00400
GO:0009289	GO	pilus	2; 2/ 3;1.9e-04;ABUW_RS01495,ABUW_RS11235
GO:0009055	GO	electron transfer activity	0; 5/ 39;7.2e-03;ABUW_RS00795,ABUW_RS08735,ABUW_RS08740,ABUW_RS10115,ABUW_RS12790
GO:0006879	GO	cellular iron ion homeostasis	2; 2/ 3;1.9e-04;ABUW_RS01505,ABUW_RS15175
GO:0030435	GO	sporulation resulting in formation of a cellular spore	0; 3/ 11;1.5e-03;ABUW_RS11930,ABUW_RS13505,ABUW_RS19650
GO:0043107	GO	type IV pilus-dependent motility	5; 6/ 9;2.6e-08;ABUW_RS01425,ABUW_RS01430,ABUW_RS01435,ABUW_RS14710,ABUW_RS14715,ABUW_RS17270
GO:0051539	GO	4 iron, 4 sulfur cluster binding	0; 6/ 59;1.3e-02;ABUW_RS03365,ABUW_RS06555,ABUW_RS07780,ABUW_RS08850,ABUW_RS12790,ABUW_RS16510
GO:0006826	GO	iron ion transport	2; 2/ 3;1.9e-04;ABUW_RS01505,ABUW_RS15175
GO:0071949	GO	FAD binding	0; 3/ 13;2.8e-03;ABUW_RS01970,ABUW_RS08850,ABUW_RS18550
GO:0008199	GO	ferric iron binding	1; 2/ 5;1.5e-03;ABUW_RS01505,ABUW_RS15175
GO:0005344	GO	oxygen carrier activity	9; 2/ 2;0.0e+00;ABUW_RS01970,ABUW_RS14740

GO:0006457	GO	protein folding	0; 3/ 22;1.7e-02;ABUW_RS04500,ABUW_RS18885,ABUW_RS18890
GO:0004322	GO	ferroxidase activity	9; 2/ 2;0.0e+00;ABUW_RS01505,ABUW_RS15175
GO:0042803	GO	protein homodimerization activity	0; 2/ 9;8.0e-03;ABUW_RS01850,ABUW_RS18885
IPR017900	IPR	4Fe-4S ferredoxin, iron-sulphur binding, conserved site	0;2/ 8;6.9e-03;ABUW_RS06555,ABUW_RS12790
IPR009040	IPR	Ferritin-like diiron domain	9;2/ 2;0.0e+00;ABUW_RS01505,ABUW_RS15175
IPR000595	IPR	Cyclic nucleotide-binding domain	9;2/ 2;0.0e+00;ABUW_RS07790,ABUW_RS13305
IPR008333	IPR	Flavoprotein pyridine nucleotide cytochrome reductase-like, FAD-binding domain	0;2/ 8;6.9e-03;ABUW_RS01970,ABUW_RS10115
IPR023772	IPR	DNA-binding HTH domain, TetR-type, conserved site	0;2/ 8;6.9e-03;ABUW_RS11305,ABUW_RS18085
IPR002024	IPR	Bacterioferritin	9;2/ 2;0.0e+00;ABUW_RS01505,ABUW_RS15175
IPR002545	IPR	CheW-like domain	9;2/ 2;0.0e+00;ABUW_RS03345,ABUW_RS03355
IPR001789	IPR	Signal transduction response regulator, receiver domain	0;4/25;6.7e-03;ABUW_RS03335,ABUW_RS03340,ABUW_RS03355,ABUW_RS17730
IPR006321	IPR	Pilus retraction protein PilT	9;2/ 2;0.0e+00;ABUW_RS14710,ABUW_RS14715
IPR017896	IPR	4Fe-4S ferredoxin-type, iron-sulphur binding domain	0;2/ 9;9.6e-03;ABUW_RS06555,ABUW_RS12790
IPR018490	IPR	Cyclic nucleotide-binding-like	9;2/ 2;0.0e+00;ABUW_RS07790,ABUW_RS13305
IPR010994	IPR	RuvA domain 2-like	0;2/ 7;5.7e-03;ABUW_RS02595,ABUW_RS16025
IPR007831	IPR	General secretory system II, protein E, N-terminal	9;2/ 2;0.0e+00;ABUW_RS06590,ABUW_RS17270
IPR042181	IPR	Type II secretion system, protein E, N-terminal	2;2/ 3;2.2e-04;ABUW_RS06590,ABUW_RS17270

IPR008331	IPR	Ferritin/DPS protein domain	9;2/ 2;0.0e+00;ABUW_RS01505,ABUW_RS15175
IPR013374	IPR	ATPase, type IV, pilus assembly, PilB	9;2/ 2;0.0e+00;ABUW_RS06590,ABUW_RS17270
IPR018488	IPR	Cyclic nucleotide-binding, conserved site	9;2/ 2;0.0e+00;ABUW_RS07790,ABUW_RS13305
IPR011006	IPR	CheY-like superfamily	0;4/25;6.7e-03;ABUW_RS03335,ABUW_RS03340,ABUW_RS03355,ABUW_RS17730
IPR036061	IPR	CheW-like domain superfamily	9;2/ 2;0.0e+00;ABUW_RS03345,ABUW_RS03355
IPR012347	IPR	Ferritin-like	1;2/ 5;2.0e-03;ABUW_RS01505,ABUW_RS15175
IPR009078	IPR	Ferritin-like superfamily	0;2/ 7;5.7e-03;ABUW_RS01505,ABUW_RS15175
IPR001482	IPR	Type II/IV secretion system protein	5;4/ 5;3.7e-07;ABUW_RS06590,ABUW_RS14710,ABUW_RS14715,ABUW_RS17270
00860 Porphyrin and chlorophyll metabolism [PATH:ko00860]	KEGG	ko00860	0;3/17;0.0085;ABUW_RS01505,ABUW_RS01850,ABUW_RS03365
00190 Oxidative phosphorylation [PATH:ko00190]	KEGG	ko00190	0;3/39;0.0496;ABUW_RS08730,ABUW_RS08735,ABUW_RS08740
00627 Aminobenzoate degradation [PATH:ko00627]	KEGG	ko00627	0;3/10;0.0022;ABUW_RS10105,ABUW_RS10110,ABUW_RS10115
00620 Pyruvate metabolism [PATH:ko00620]	KEGG	ko00620	0;3/23;0.0162;ABUW_RS05555,ABUW_RS11945,ABUW_RS18550
00020 Citrate cycle (TCA cycle) [PATH:ko00020]	KEGG	ko00020	0;3/18;0.0085;ABUW_RS01250,ABUW_RS07780,ABUW_RS16510

02020 Two-component system [PATH:ko02020]	KEGG	ko02020	0;5/58;0.0210;ABUW_RS03335,ABUW_RS03340,ABUW_RS03345,ABUW_RS17725,ABUW_RS17730
Phosphoprotein	KEYWORDS	keyword	9;2/2;0.000;ABUW_RS03335,ABUW_RS03340
Electron transport	KEYWORDS	keyword	0;2/6;0.011;ABUW_RS00795,ABUW_RS00800
Iron	KEYWORDS	keyword	0;2/7;0.012;ABUW_RS05940,ABUW_RS14740
operon_0242	operons	NZ_CP008706.1|gene666|ABUW_RS03335	9;8/8;0.0e+00;ABUW_RS03335,ABUW_RS03340,ABUW_RS03345,ABUW_RS03350,ABUW_RS03355,ABUW_RS03360,ABUW_RS03365,ABUW_RS03370
operon_0928	operons	NZ_CP008706.1|gene2941|ABUW_RS14710	9;2/ 2;0.0e+00;ABUW_RS14710,ABUW_RS14715
operon_0058	operons	NZ_CP008706.1|gene112|ABUW_RS00565	2;4/ 8;5.9e-05;ABUW_RS00590,ABUW_RS00595,ABUW_RS00600,ABUW_RS19650
operon_0132	operons	NZ_CP008706.1|gene284|ABUW_RS01425	1;6/16;2.6e-05;ABUW_RS01425,ABUW_RS01430,ABUW_RS01435,ABUW_RS01440,ABUW_RS01445,ABUW_RS01495
operon_1115	operons	NZ_CP008706.1|gene3610|ABUW_RS18050	0;2/ 8;7.4e-03;ABUW_RS18055,ABUW_RS18085
operon_0439	operons	NZ_CP008706.1|gene1350|ABUW_RS06755	0;3/16;9.0e-03;ABUW_RS06780,ABUW_RS06820,ABUW_RS06825
operon_1100	operons	NZ_CP008706.1|gene3561|ABUW_RS17805	1;2/ 5;2.0e-03;ABUW_RS17805,ABUW_RS17810
operon_1096	operons	NZ_CP008706.1|gene3544|ABUW_RS17720|sirA	2;2/ 3;2.7e-04;ABUW_RS17725,ABUW_RS17730

operon_1137	operons	NZ_CP008706.1|gene3686|ABUW_RS18430	2;3/ 5;9.5e-05;ABUW_RS18435,ABUW_RS18440,ABUW_RS18445
operon_0973	operons	NZ_CP008706.1|gene3099|ABUW_RS15495	3;5/ 8;2.7e-06;ABUW_RS15495,ABUW_RS15500,ABUW_RS15505,ABUW_RS15520,ABUW_RS15525
operon_1118	operons	NZ_CP008706.1|gene3623|ABUW_RS18115	2;2/ 3;2.7e-04;ABUW_RS18115,ABUW_RS18120
operon_0419	operons	NZ_CP008706.1|gene1309|ABUW_RS06550	1;2/ 4;8.9e-04;ABUW_RS06555,ABUW_RS06560
operon_0074	operons	NZ_CP008706.1|gene158|ABUW_RS00795	0;2/ 6;3.3e-03;ABUW_RS00795,ABUW_RS00800
operon_0553	operons	NZ_CP008706.1|gene1744|ABUW_RS08725	3;5/ 8;2.7e-06;ABUW_RS08725,ABUW_RS08730,ABUW_RS08735,ABUW_RS08740,ABUW_RS08745
operon_0404	operons	NZ_CP008706.1|gene1206|ABUW_RS06035	0;2/ 6;3.3e-03;ABUW_RS06055,ABUW_RS06060
operon_0844	operons	NZ_CP008706.1|gene2697|ABUW_RS13490	1;3/ 8;7.8e-04;ABUW_RS13505,ABUW_RS13510,ABUW_RS13515
operon_0424	operons	NZ_CP008706.1|gene1317|ABUW_RS06590	1;2/ 4;8.9e-04;ABUW_RS06590,ABUW_RS06595
operon_0050	operons	NZ_CP008706.1|gene73|ABUW_RS00370	2;6/14;1.2e-05;ABUW_RS00370,ABUW_RS00385,ABUW_RS00390,ABUW_RS00395,ABUW_RS00400,ABUW_RS00435
operon_0486	operons	NZ_CP008706.1|gene1552|ABUW_RS07765	1;3/ 6;2.4e-04;ABUW_RS07780,ABUW_RS07785,ABUW_RS07790
operon_1042	operons	NZ_CP008706.1|gene3356|ABUW_RS16780	1;2/ 5;2.0e-03;ABUW_RS16785,ABUW_RS16790

operon_0754	operons	NZ_CP008706.1|gene2385|ABUW_RS11930	4;4/ 5;2.7e-06;ABUW_RS11930,ABUW_RS11935,ABUW_RS11940,ABUW_RS11945
operon_1076	operons	NZ_CP008706.1|gene3454|ABUW_RS17270	3;3/ 4;2.6e-05;ABUW_RS17270,ABUW_RS17275,ABUW_RS17285
operon_1143	operons	NZ_CP008706.1|gene3701|ABUW_RS18505	0;2/ 8;7.4e-03;ABUW_RS18515,ABUW_RS18520
operon_0698	operons	NZ_CP008706.1|gene2246|ABUW_RS11235	2;3/ 5;9.5e-05;ABUW_RS11235,ABUW_RS11245,ABUW_RS11250
operon_1081	operons	NZ_CP008706.1|gene3469|ABUW_RS17345	0;2/ 8;7.4e-03;ABUW_RS17345,ABUW_RS17370
operon_1160	operons	NZ_CP008706.1|gene3776|ABUW_RS18880	1;3/ 6;2.4e-04;ABUW_RS18885,ABUW_RS18890,ABUW_RS18905
operon_0373	operons	NZ_CP008706.1|gene1113|ABUW_RS05570	2;2/ 3;2.7e-04;ABUW_RS05570,ABUW_RS05575
operon_1092	operons	NZ_CP008706.1|gene3528|ABUW_RS17640	0;2/ 6;3.3e-03;ABUW_RS17650,ABUW_RS17655
operon_0134	operons	NZ_CP008706.1|gene306|ABUW_RS01535|ispH	3;7/12;2.6e-07;ABUW_RS01540,ABUW_RS01545,ABUW_RS01550,ABUW_RS01555,ABUW_RS01560,ABUW_RS01565,ABUW_RS01570
operon_0201	operons	NZ_CP008706.1|gene520|ABUW_RS02605	0;2/ 7;5.3e-03;ABUW_RS02625,ABUW_RS02630
operon_0632	operons	NZ_CP008706.1|gene2020|ABUW_RS10105	3;3/ 4;2.6e-05;ABUW_RS10105,ABUW_RS10110,ABUW_RS10115
operon_0849	operons	NZ_CP008706.1|gene2714|ABUW_RS13575	0;2/ 6;3.3e-03;ABUW_RS13580,ABUW_RS13585
operon_0155	operons	NZ_CP008706.1|gene368|ABUW_RS01845	2;2/ 3;2.7e-04;ABUW_RS01845,ABUW_RS01850

operon_1103	operons	NZ_CP008706.1|gene3578|ABUW_RS17890	4;4/ 5;2.7e-06;ABUW_RS17895,ABUW_RS17900,ABUW_RS17905,ABUW_RS17910
PF01584	Pfam	CheW-like domain	9;2/ 2;0.0e+00;ABUW_RS03345,ABUW_RS03355
PF05157	Pfam	Type II secretion system (T2SS), protein E, N-terminal domain	9;2/ 2;0.0e+00;ABUW_RS06590,ABUW_RS17270
PF00970	Pfam	Oxidoreductase FAD-binding domain	0;2/ 8;5.7e-03;ABUW_RS01970,ABUW_RS10115
PF00072	Pfam	Response regulator receiver domain	0;4/25;5.4e-03;ABUW_RS03335,ABUW_RS03340,ABUW_RS03355,ABUW_RS17730
PF00437	Pfam	Type II/IV secretion system protein	5;4/ 5;2.7e-07;ABUW_RS06590,ABUW_RS14710,ABUW_RS14715,ABUW_RS17270
PF00210	Pfam	Ferritin-like domain	9;2/ 2;0.0e+00;ABUW_RS01505,ABUW_RS15175
PF00037	Pfam	4Fe-4S binding domain	2;2/ 3;1.6e-04;ABUW_RS06555,ABUW_RS12790
PF00027	Pfam	Cyclic nucleotide-binding domain	9;2/ 2;0.0e+00;ABUW_RS07790,ABUW_RS13305
Downregulated Wicklow Root			
ClassID	Class	Description	single_list
Q	COG	METABOLISM; Secondary metabolites biosynthesis, transport, and catabolism	0; 6/ 52
V	COG	CELLULAR PROCESSES AND SIGNALING; Defense mechanisms	0; 4/ 20
P	COG	METABOLISM; Inorganic ion transport and metabolism	0;14/122
COG4774	eggNOG_COG	siderophore transport	9;4/ 4

COG4773	eggNOG_COG	Receptor	9;2/ 2
COG1292	eggNOG_COG	Belongs to the BCCT transporter (TC 2.A.15) family	1;2/ 5
COG3433	eggNOG_COG	isochorismatase activity	9;2/ 2
COG4264	eggNOG_COG	IucA IucC family	9;2/ 2
COG1535	eggNOG_COG	isochorismatase	9;2/ 2
COG1020	eggNOG_COG	D-alanine [D-alanyl carrier protein] ligase activity	1;2/ 4
COG1132	eggNOG_COG	(ABC) transporter	1;2/ 4
GO:0018189	GO	pyrroloquinoline quinone biosynthetic process	1; 2/ 4
GO:0008908	GO	isochorismatase activity	9; 2/ 2
GO:0016021	GO	integral component of membrane	0;33/374
GO:0071705	GO	nitrogen compound transport	0; 2/ 6
GO:0015675	GO	nickel cation transport	2; 2/ 3
GO:0047527	GO	2,3-dihydroxybenzoate-serine ligase activity	9; 3/ 3
GO:0030497	GO	fatty acid elongation	0; 2/ 8
GO:0016881	GO	acid-amino acid ligase activity	1; 2/ 4
GO:0015562	GO	efflux transmembrane transporter activity	0; 3/ 15
GO:0016746	GO	transferase activity, transferring acyl groups	0; 2/ 6
GO:0071281	GO	cellular response to iron ion	9; 2/ 2
GO:0038023	GO	signaling receptor activity	8;10/ 14
GO:0019289	GO	rhizobactin 1021 biosynthetic process	9; 3/ 3
GO:0017000	GO	antibiotic biosynthetic process	0; 3/ 13

GO:0009239	GO	enterobactin biosynthetic process	9; 4/ 4
GO:0019290	GO	siderophore biosynthetic process	3; 3/ 4
GO:0006811	GO	ion transport	1; 5/ 18
GO:0008750	GO	NAD(P)+ transhydrogenase (AB-specific) activity	9; 2/ 2
GO:0022857	GO	transmembrane transporter activity	0; 7/ 81
GO:0055072	GO	iron ion homeostasis	9;14/ 17
GO:0009279	GO	cell outer membrane	1;14/ 59
GO:0031177	GO	phosphopantetheine binding	3; 5/ 9
GO:0030288	GO	outer membrane-bounded periplasmic space	0; 3/ 28
GO:0006829	GO	zinc ion transport	1; 2/ 5
GO:0016765	GO	transferase activity, transferring alkyl or aryl (other than methyl) groups	0; 2/ 6
GO:0015344	GO	siderophore uptake transmembrane transporter activity	7;10/ 15
GO:0005886	GO	plasma membrane	0;28/469
GO:0055114	GO	oxidation-reduction process	0; 5/ 31
GO:0016874	GO	ligase activity	0; 3/ 10
GO:0042626	GO	ATPase-coupled transmembrane transporter activity	0; 2/ 10
GO:0016788	GO	hydrolase activity, acting on ester bonds	0; 2/ 6
IPR000873	IPR	AMP-dependent synthetase/ligase	0; 4/15
IPR039426	IPR	Vitamin B12 transporter BtuB-like	1; 3/ 9
IPR036640	IPR	ABC transporter type 1, transmembrane domain superfamily	0; 2/ 6
IPR042099	IPR	AMP-dependent synthetase-like superfamily	1; 4/14

IPR020845	IPR	AMP-binding, conserved site	1; 4/13
IPR029058	IPR	Alpha/Beta hydrolase fold	0; 6/36
IPR011042	IPR	Six-bladed beta-propeller, TolB-like	0; 2/ 8
IPR027463	IPR	Multidrug efflux transporter AcrB TolC docking domain, DN/DC subdomains	0; 2/ 7
IPR039423	IPR	TonB-dependent receptor-like	9; 8/10
IPR000868	IPR	Isochorismatase-like	0; 2/ 6
IPR010916	IPR	TonB box, conserved site	3; 5/ 9
IPR025110	IPR	AMP-binding enzyme, C-terminal domain	0; 3/12
IPR001031	IPR	Thioesterase	1; 2/ 4
IPR036380	IPR	Isochorismatase-like superfamily	0; 2/ 6
IPR031043	IPR	Putative histamine N-monooxygenase	9; 2/ 2
IPR036736	IPR	ACP-like superfamily	2; 5/10
IPR007310	IPR	Aerobactin siderophore biosynthesis, IucA/IucC, N-terminal	9; 3/ 3
IPR010917	IPR	TonB-dependent receptor, conserved site	5; 7/11
IPR025700	IPR	L-lysine 6-monooxygenase/L-ornithine 5-monooxygenase	9; 2/ 2
IPR020806	IPR	Polyketide synthase, phosphopantetheine-binding domain	1; 3/ 7
IPR010105	IPR	TonB-dependent siderophore receptor	8;10/14
IPR018093	IPR	BCCT transporter, conserved site	1; 2/ 5
IPR000531	IPR	TonB-dependent receptor-like, beta-barrel	6;11/19
IPR000060	IPR	BCCT transporter family	0; 2/ 6
IPR037066	IPR	TonB-dependent receptor, plug domain superfamily	6;11/19

IPR011041	IPR	Soluble quinoprotein glucose/sorbosone dehydrogenase	0; 2/ 6
IPR000522	IPR	ABC transporter, permease protein, BtuC-like	9; 2/ 2
IPR037294	IPR	ABC transporter, BtuC-like	2; 2/ 3
IPR009081	IPR	Phosphopantetheine binding ACP domain	2; 5/10
IPR022770	IPR	Ferric iron reductase FhuF domain	9; 3/ 3
IPR001242	IPR	Condensation domain	2; 3/ 5
IPR010071	IPR	Amino acid adenylation domain	2; 3/ 5
IPR016084	IPR	Haem oxygenase-like, multi-helical	1; 2/ 4
IPR023213	IPR	Chloramphenicol acetyltransferase-like domain superfamily	1; 3/ 8
IPR036942	IPR	TonB-dependent receptor-like, beta-barrel domain superfamily	7;11/18
IPR006162	IPR	Phosphopantetheine attachment site	0; 2/ 6
IPR012910	IPR	TonB-dependent receptor, plug domain	6;11/19
IPR016291	IPR	Isochorismatase	9; 2/ 2
IPR012938	IPR	Glucose/Sorbosone dehydrogenase	0; 2/ 6
IPR011527	IPR	ABC transporter type 1, transmembrane domain	1; 2/ 5
IPR037455	IPR	Aerobactin siderophore biosynthesis, IucA/IucC-like	9; 3/ 3
IPR001036	IPR	Acriflavin resistance protein	0; 2/ 7
IPR003439	IPR	ABC transporter-like	0; 3/33
00997 Biosynthesis of various secondary	KEGG	ko00997	9;3/ 3

metabolites - part 3 [PATH:ko00997]			
01053 Biosynthesis of siderophore group nonribosomal peptides [PATH:ko01053]	KEGG	ko01053	5;5/ 7
01501 beta-Lactam resistance [PATH:ko01501]	KEGG	ko01501	1;2/ 5
Cell outer membrane	KEYWORDS	keyword	2;10/31
Ligase	KEYWORDS	keyword	1; 2/ 5
FAD	KEYWORDS	keyword	0; 4/30
Antibiotic biosynthesis	KEYWORDS	keyword	1; 2/ 5
operon_0387	operons	NZ_CP008706.1|gene1149|ABUW_RS05750	9; 2/ 2
operon_1093	operons	NZ_CP008706.1|gene3534|ABUW_RS17670	2; 3/ 5
operon_0386	operons	NZ_CP008706.1|gene1144|ABUW_RS05725	9; 5/ 5
operon_0388	operons	NZ_CP008706.1|gene1151|ABUW_RS05760|entE	9; 8/ 9
operon_0663	operons	NZ_CP008706.1|gene2109|ABUW_RS10550	7;12/20
operon_0893	operons	NZ_CP008706.1|gene2831|ABUW_RS14160	9; 2/ 2
operon_0624	operons	NZ_CP008706.1|gene1990|ABUW_RS09955	3; 4/ 7
operon_0126	operons	NZ_CP008706.1|gene259|ABUW_RS01300	1; 2/ 5
operon_0662	operons	NZ_CP008706.1|gene2103|ABUW_RS10520	4; 4/ 6

operon_0637	operons	NZ_CP008706.1|gene2039|ABUW_RS10200	1; 2/ 4
operon_0631	operons	NZ_CP008706.1|gene2013|ABUW_RS10070	1; 3/ 7
operon_0230	operons	NZ_CP008706.1|gene629|ABUW_RS03150	1; 2/ 6
operon_0629	operons	NZ_CP008706.1|gene2003|ABUW_RS10020	0; 2/ 9
operon_1035	operons	NZ_CP008706.1|gene3329|ABUW_RS16645	2; 3/ 5
operon_1007	operons	NZ_CP008706.1|gene3218|ABUW_RS16090	9; 3/ 3
operon_0917	operons	NZ_CP008706.1|gene2893|ABUW_RS14470	8; 7/ 9
operon_0273	operons	NZ_CP008706.1|gene822|ABUW_RS04115	1; 3/ 9
operon_1151	operons	NZ_CP008706.1|gene3738|ABUW_RS18690	1; 2/ 5
operon_0450	operons	NZ_CP008706.1|gene1429|ABUW_RS07150	1; 2/ 6
operon_0668	operons	NZ_CP008706.1|gene2138|ABUW_RS10695	0; 2/ 8
PF13434	Pfam	L-lysine 6-monooxygenase (NADPH-requiring)	9; 2/ 2
PF06276	Pfam	Ferric iron reductase FhuF-like transporter	9; 3/ 3
PF02028	Pfam	BCCT, betaine/carnitine/choline family transporter	0; 2/ 6
PF00857	Pfam	Isochorismatase family	0; 2/ 6
PF00668	Pfam	Condensation domain	2; 3/ 5
PF01032	Pfam	FecCD transport family	9; 2/ 2
PF04183	Pfam	IucA / IucC family	9; 3/ 3
PF00975	Pfam	Thioesterase domain	1; 2/ 4
PF07715	Pfam	TonB-dependent Receptor Plug Domain	6;11/19
PF07995	Pfam	Glucose / Sorbosone dehydrogenase	0; 2/ 6
PF00593	Pfam	TonB dependent receptor	6;11/19
PF00005	Pfam	ABC transporter	0; 3/33
PF00873	Pfam	AcrB/AcrD/AcrF family	0; 2/ 7
PF13193	Pfam	AMP-binding enzyme C-terminal domain	0; 3/12

PF00501	Pfam	AMP-binding enzyme	0; 4/15
PF00550	Pfam	Phosphopantetheine attachment site	2; 5/10
Downregulated Ellagic Acid			
ClassID	Class	Description	single_list
GO:1990281	GO	efflux pump complex	0; 2/ 6
P	COG	METABOLISM; Inorganic ion transport and metabolism	0;16/122
V	COG	CELLULAR PROCESSES AND SIGNALING; Defense mechanisms	1; 6/ 20
Q	COG	METABOLISM; Secondary metabolites biosynthesis, transport, and catabolism	0; 7/ 52
COG1132	eggNOG_COG	(ABC) transporter	1;2/ 4
COG0715	eggNOG_COG	COG0715 ABC-type nitrate sulfonate bicarbonate transport systems periplasmic components	1;2/ 4
COG1020	eggNOG_COG	D-alanine [D-alanyl carrier protein] ligase activity	1;2/ 4
COG2141	eggNOG_COG	COG2141 Coenzyme F420-dependent N5,N10-methylene tetrahydromethanopterin reductase and related flavin-dependent oxidoreductases	2;2/ 3
COG4264	eggNOG_COG	IucA IucC family	9;2/ 2
COG0845	eggNOG_COG	Belongs to the membrane fusion protein (MFP) (TC 8.A.1) family	0;2/ 6
COG4773	eggNOG_COG	Receptor	9;2/ 2

COG2814	eggNOG_COG	Major facilitator Superfamily	0;4/21
COG0745	eggNOG_COG	RESPONSE REGULATOR receiver	0;2/ 7
COG4774	eggNOG_COG	siderophore transport	3;3/ 4
COG1535	eggNOG_COG	isochorismatase	9;2/ 2
COG3433	eggNOG_COG	isochorismatase activity	9;2/ 2
COG1136	eggNOG_COG	(ABC) transporter	9;2/ 2
GO:0042959	GO	alkanesulfonate transmembrane transporter activity	0; 3/ 9
GO:0019290	GO	siderophore biosynthetic process	3; 3/ 4
GO:0016874	GO	ligase activity	1; 4/ 10
GO:0006829	GO	zinc ion transport	1; 2/ 5
GO:0019289	GO	rhizobactin 1021 biosynthetic process	9; 3/ 3
GO:0016765	GO	transferase activity, transferring alkyl or aryl (other than methyl) groups	0; 2/ 6
GO:0016020	GO	membrane	0; 4/ 32
GO:0008750	GO	NAD(P)+ transhydrogenase (AB-specific) activity	9; 2/ 2
GO:0015562	GO	efflux transmembrane transporter activity	1; 5/ 15
GO:0046677	GO	response to antibiotic	0; 7/ 50
GO:0055114	GO	oxidation-reduction process	0; 5/ 31
GO:0042953	GO	lipoprotein transport	9; 3/ 3
GO:0022857	GO	transmembrane transporter activity	0;10/ 81
GO:0042918	GO	alkanesulfonate transport	0; 3/ 9

GO:0015675	GO	nickel cation transport	2; 2/ 3
GO:0017000	GO	antibiotic biosynthetic process	0; 3/ 13
GO:0006811	GO	ion transport	0; 4/ 18
GO:0046177	GO	D-gluconate catabolic process	2; 2/ 3
GO:0042597	GO	periplasmic space	0; 5/ 31
GO:0015914	GO	phospholipid transport	9; 2/ 2
GO:0016021	GO	integral component of membrane	0;37/374
GO:0016788	GO	hydrolase activity, acting on ester bonds	0; 2/ 6
GO:0015344	GO	siderophore uptake transmembrane transporter activity	6;10/ 15
GO:1990961	GO	xenobiotic detoxification by transmembrane export across the plasma membrane	1; 3/ 7
GO:0055072	GO	iron ion homeostasis	9;14/ 17
GO:0042910	GO	xenobiotic transmembrane transporter activity	0; 3/ 12
GO:0016705	GO	oxidoreductase activity, acting on paired donors, with incorporation or reduction of molecular oxygen	2; 2/ 3
GO:0009239	GO	enterobactin biosynthetic process	3; 3/ 4
GO:0006520	GO	cellular amino acid metabolic process	1; 2/ 4
GO:0047527	GO	2,3-dihydroxybenzoate-serine ligase activity	2; 2/ 3
GO:0031177	GO	phosphopantetheine binding	2; 5/ 9
GO:0006790	GO	sulfur compound metabolic process	1; 3/ 8
GO:0044874	GO	lipoprotein localization to outer membrane	9; 2/ 2
GO:0009279	GO	cell outer membrane	2;17/ 59
GO:0042626	GO	ATPase-coupled transmembrane transporter activity	1; 4/ 10

GO:0016881	GO	acid-amino acid ligase activity	1; 2/ 4
GO:0071281	GO	cellular response to iron ion	9; 2/ 2
GO:0008908	GO	isochorismatase activity	9; 2/ 2
GO:0005886	GO	plasma membrane	0;33/469
GO:0038023	GO	signaling receptor activity	7;10/ 14
GO:0018189	GO	pyrroloquinoline quinone biosynthetic process	1; 2/ 4
IPR025857	IPR	MacB-like periplasmic core domain	9; 2/ 2
IPR006690	IPR	Outer membrane protein, OmpA-like, conserved site	1; 2/ 5
IPR012910	IPR	TonB-dependent receptor, plug domain	6;11/19
IPR036736	IPR	ACP-like superfamily	2; 5/10
IPR042099	IPR	AMP-dependent synthetase-like superfamily	0; 4/14
IPR029046	IPR	Lipoprotein localisation LolA/LolB/LppX	9; 2/ 2
IPR010067	IPR	Aliphatic sulfonates-binding protein	2; 2/ 3
IPR010916	IPR	TonB box, conserved site	2; 5/ 9
IPR039423	IPR	TonB-dependent receptor-like	5; 7/10
IPR010105	IPR	TonB-dependent siderophore receptor	7;10/14
IPR006162	IPR	Phosphopantetheine attachment site	0; 2/ 6
IPR016084	IPR	Haem oxygenase-like, multi-helical	1; 2/ 4
IPR011990	IPR	Tetratricopeptide-like helical domain superfamily	1; 2/ 4
IPR000531	IPR	TonB-dependent receptor-like, beta-barrel	6;11/19
IPR006664	IPR	Outer membrane protein, bacterial	0; 2/ 6
IPR029058	IPR	Alpha/Beta hydrolase fold	0; 5/36
IPR001036	IPR	Acriflavin resistance protein	0; 2/ 7
IPR031043	IPR	Putative histamine N-monooxygenase	9; 2/ 2

IPR015168	IPR	SsuA/THI5-like	2; 2/ 3
IPR037066	IPR	TonB-dependent receptor, plug domain superfamily	6;11/19
IPR025700	IPR	L-lysine 6-monooxygenase/L-ornithine 5-monooxygenase	9; 2/ 2
IPR036661	IPR	Luciferase-like domain superfamily	1; 3/ 6
IPR032317	IPR	RND efflux pump, membrane fusion protein, barrel-sandwich domain	0; 2/ 6
IPR006665	IPR	OmpA-like domain	0; 2/ 6
IPR001638	IPR	Solute-binding protein family 3/N-terminal domain of MltF	0; 3/10
IPR022770	IPR	Ferric iron reductase FhuF domain	9; 3/ 3
IPR007310	IPR	Aerobactin siderophore biosynthesis, IucA/IucC, N-terminal	9; 3/ 3
IPR020845	IPR	AMP-binding, conserved site	0; 3/13
IPR020806	IPR	Polyketide synthase, phosphopantetheine-binding domain	1; 3/ 7
IPR010071	IPR	Amino acid adenylation domain	2; 3/ 5
IPR004764	IPR	Hydrophobe/amphiphile efflux-1 HAE1	1; 2/ 4
IPR016291	IPR	Isochorismatase	9; 2/ 2
IPR003838	IPR	ABC transporter permease protein domain	9; 2/ 2
IPR000868	IPR	Isochorismatase-like	0; 2/ 6
IPR036640	IPR	ABC transporter type 1, transmembrane domain superfamily	0; 2/ 6
IPR036737	IPR	OmpA-like domain superfamily	0; 2/ 6
IPR011251	IPR	Luciferase-like domain	1; 3/ 6

IPR039426	IPR	Vitamin B12 transporter BtuB-like	1; 4/ 9
IPR009081	IPR	Phosphopantetheine binding ACP domain	2; 5/10
IPR000873	IPR	AMP-dependent synthetase/ligase	0; 4/15
IPR017871	IPR	ABC transporter, conserved site	0; 4/31
IPR003439	IPR	ABC transporter-like	0; 5/33
IPR036942	IPR	TonB-dependent receptor-like, beta-barrel domain superfamily	6;11/18
IPR027463	IPR	Multidrug efflux transporter AcrB TolC docking domain, DN/DC subdomains	0; 2/ 7
IPR036380	IPR	Isochorismatase-like superfamily	0; 2/ 6
IPR006143	IPR	RND efflux pump, membrane fusion protein	0; 2/ 7
IPR023213	IPR	Chloramphenicol acetyltransferase-like domain superfamily	1; 3/ 8
IPR001242	IPR	Condensation domain	2; 3/ 5
IPR010917	IPR	TonB-dependent receptor, conserved site	4; 7/11
IPR011527	IPR	ABC transporter type 1, transmembrane domain	1; 2/ 5
IPR000522	IPR	ABC transporter, permease protein, BtuC-like	9; 2/ 2
IPR037455	IPR	Aerobactin siderophore biosynthesis, IucA/IucC-like	9; 3/ 3
IPR016032	IPR	Signal transduction response regulator, C-terminal effector	0; 2/10
IPR037294	IPR	ABC transporter, BtuC-like	2; 2/ 3
IPR001031	IPR	Thioesterase	1; 2/ 4
01501 beta-Lactam resistance	KEGG	ko01501	2;3/ 5

[PATH:ko01501]			
01053 Biosynthesis of siderophore group nonribosomal peptides [PATH:ko01053]	KEGG	ko01053	2;4/ 7
00920 Sulfur metabolism [PATH:ko00920]	KEGG	ko00920	0;6/38
00997 Biosynthesis of various secondary metabolites - part 3 [PATH:ko00997]	KEGG	ko00997	9;3/ 3
02010 ABC transporters [PATH:ko02010]	KEGG	ko02010	0;6/49
Cell outer membrane	KEYWORDS	keyword	2;11/ 31
Flavoprotein	KEYWORDS	keyword	0; 3/ 16
Antibiotic biosynthesis	KEYWORDS	keyword	0; 2/ 5
Cell inner membrane	KEYWORDS	keyword	0;16/188
Carbohydrate metabolism	KEYWORDS	keyword	0; 2/ 9
Ligase	KEYWORDS	keyword	0; 2/ 5

operon_0388	operons	NZ_CP008706.1|gene1151|ABUW_RS05760|entE	7; 7/ 9
operon_0273	operons	NZ_CP008706.1|gene822|ABUW_RS04115	0; 2/ 9
operon_1093	operons	NZ_CP008706.1|gene3534|ABUW_RS17670	2; 3/ 5
operon_0629	operons	NZ_CP008706.1|gene2003|ABUW_RS10020	0; 2/ 9
operon_1048	operons	NZ_CP008706.1|gene3369|ABUW_RS16845	9; 2/ 2
operon_1007	operons	NZ_CP008706.1|gene3218|ABUW_RS16090	9; 3/ 3
operon_1027	operons	NZ_CP008706.1|gene3295|ABUW_RS16475	2; 3/ 5
operon_0156	operons	NZ_CP008706.1|gene371|ABUW_RS01860	1; 4/ 9
operon_1154	operons	NZ_CP008706.1|gene3746|ABUW_RS18730	4; 7/12
operon_0218	operons	NZ_CP008706.1|gene597|ABUW_RS02990	9; 2/ 2
operon_1035	operons	NZ_CP008706.1|gene3329|ABUW_RS16645	2; 3/ 5
operon_0913	operons	NZ_CP008706.1|gene2879|ABUW_RS14400	1; 2/ 4
operon_0438	operons	NZ_CP008706.1|gene1346|ABUW_RS06735	1; 2/ 4
operon_0631	operons	NZ_CP008706.1|gene2013|ABUW_RS10070	1; 3/ 7
operon_0668	operons	NZ_CP008706.1|gene2138|ABUW_RS10695	0; 2/ 8
operon_0386	operons	NZ_CP008706.1|gene1144|ABUW_RS05725	9; 5/ 5
operon_0177	operons	NZ_CP008706.1|gene449|ABUW_RS02250	2; 2/ 3
operon_0914	operons	NZ_CP008706.1|gene2883|ABUW_RS14420	1; 3/ 7
operon_0917	operons	NZ_CP008706.1|gene2893|ABUW_RS14470	9; 8/ 9
operon_0387	operons	NZ_CP008706.1|gene1149|ABUW_RS05750	9; 2/ 2
operon_0322	operons	NZ_CP008706.1|gene952|ABUW_RS04765	1; 2/ 5
operon_0663	operons	NZ_CP008706.1|gene2109|ABUW_RS10550	7;12/20
operon_0662	operons	NZ_CP008706.1|gene2103|ABUW_RS10520	3; 4/ 6
operon_0893	operons	NZ_CP008706.1|gene2831|ABUW_RS14160	9; 2/ 2
operon_0856	operons	NZ_CP008706.1|gene2745|ABUW_RS13730	1; 2/ 4

operon_1020	operons	NZ_CP008706.1|gene3263|ABUW_RS16315	1; 3/ 7
operon_0475	operons	NZ_CP008706.1|gene1523|ABUW_RS07620	2; 2/ 3
PF02687	Pfam	FtsX-like permease family	9; 2/ 2
PF12704	Pfam	MacB-like periplasmic core domain	9; 2/ 2
PF00501	Pfam	AMP-binding enzyme	0; 4/15
PF01032	Pfam	FecCD transport family	9; 2/ 2
PF00873	Pfam	AcrB/AcrD/AcrF family	0; 2/ 7
PF13434	Pfam	L-lysine 6-monooxygenase (NADPH-requiring)	9; 2/ 2
PF06276	Pfam	Ferric iron reductase FhuF-like transporter	9; 3/ 3
PF04183	Pfam	IucA / IucC family	9; 3/ 3
PF00857	Pfam	Isochorismatase family	0; 2/ 6
PF00550	Pfam	Phosphopantetheine attachment site	2; 5/10
PF00691	Pfam	OmpA family	0; 2/ 6
PF00668	Pfam	Condensation domain	2; 3/ 5
PF00975	Pfam	Thioesterase domain	1; 2/ 4
PF09084	Pfam	NMT1/THI5 like	2; 2/ 3
PF16576	Pfam	Barrel-sandwich domain of CusB or HlyD membrane-fusion	0; 2/ 6
PF00296	Pfam	Luciferase-like monooxygenase	1; 3/ 6
PF00005	Pfam	ABC transporter	0; 5/33
PF07715	Pfam	TonB-dependent Receptor Plug Domain	6;11/19
PF00593	Pfam	TonB dependent receptor	6;11/19
Agrimoniin Upregulated			
P	COG	METABOLISM; Inorganic ion transport and metabolism	1;24/122
Q	COG	METABOLISM; Secondary metabolites biosynthesis, transport, and catabolism	0; 6/ 52

COG1020	eggNOG_COG	D-alanine [D-alanyl carrier protein] ligase activity	3;3/ 4
COG4774	eggNOG_COG	siderophore transport	3;3/ 4
COG4773	eggNOG_COG	Receptor	9;2/ 2
COG1132	eggNOG_COG	(ABC) transporter	1;2/ 4
COG4264	eggNOG_COG	IucA IucC family	9;2/ 2
COG3433	eggNOG_COG	isochorismatase activity	9;2/ 2
COG1028	eggNOG_COG	Short-chain dehydrogenase reductase Sdr	0;3/14
COG1535	eggNOG_COG	isochorismatase	9;2/ 2
GO:0008320	GO	protein transmembrane transporter activity	0; 2/ 5
GO:0006865	GO	amino acid transport	0; 5/ 36
GO:0016765	GO	transferase activity, transferring alkyl or aryl (other than methyl) groups	0; 2/ 6
GO:0016874	GO	ligase activity	1; 4/ 10
GO:0015675	GO	nickel cation transport	2; 2/ 3
GO:0006829	GO	zinc ion transport	0; 2/ 5
GO:0009239	GO	enterobactin biosynthetic process	3; 3/ 4
GO:0016021	GO	integral component of membrane	0;36/374
GO:0009279	GO	cell outer membrane	1;15/ 59
GO:0047527	GO	2,3-dihydroxybenzoate-serine ligase activity	2; 2/ 3
GO:0006574	GO	valine catabolic process	2; 2/ 3
GO:0006817	GO	phosphate ion transport	0; 2/ 5
GO:0016788	GO	hydrolase activity, acting on ester bonds	1; 3/ 6
GO:0038023	GO	signaling receptor activity	5; 9/ 14

GO:0071281	GO	cellular response to iron ion	9; 2/ 2
GO:0018189	GO	pyrroloquinoline quinone biosynthetic process	1; 2/ 4
GO:0033281	GO	TAT protein transport complex	2; 2/ 3
GO:0019289	GO	rhizobactin 1021 biosynthetic process	9; 3/ 3
GO:0055114	GO	oxidation-reduction process	0; 5/ 31
GO:0043953	GO	protein transport by the Tat complex	2; 2/ 3
GO:0016757	GO	transferase activity, transferring glycosyl groups	0; 2/ 7
GO:0016881	GO	acid-amino acid ligase activity	1; 2/ 4
GO:0005886	GO	plasma membrane	0;37/469
GO:0008908	GO	isochorismatase activity	9; 2/ 2
GO:0042626	GO	ATPase-coupled transmembrane transporter activity	0; 3/ 10
GO:0016616	GO	oxidoreductase activity, acting on the CH-OH group of donors, NAD or NADP as acceptor	0; 2/ 9
GO:0019290	GO	siderophore biosynthetic process	3; 3/ 4
GO:0015344	GO	siderophore uptake transmembrane transporter activity	5; 9/ 15
GO:0006811	GO	ion transport	0; 5/ 18
GO:0016491	GO	oxidoreductase activity	0; 7/ 67
GO:0055072	GO	iron ion homeostasis	9;13/ 17
GO:0031177	GO	phosphopantetheine binding	4; 6/ 9
GO:0017000	GO	antibiotic biosynthetic process	0; 3/ 13
GO:0005887	GO	integral component of plasma membrane	0; 9/ 93
GO:0008750	GO	NAD(P)+ transhydrogenase (AB-specific) activity	9; 2/ 2
IPR011251	IPR	Luciferase-like domain	0; 2/ 6
IPR012938	IPR	Glucose/Sorbosone dehydrogenase	0; 2/ 6
IPR020806	IPR	Polyketide synthase, phosphopantetheine-binding domain	2; 4/ 7
IPR037066	IPR	TonB-dependent receptor, plug domain	4;10/19

		superfamily	
IPR011041	IPR	Soluble quinoprotein glucose/sorbosone dehydrogenase	0; 2/ 6
IPR006162	IPR	Phosphopantetheine attachment site	0; 2/ 6
IPR010916	IPR	TonB box, conserved site	2; 5/ 9
IPR010071	IPR	Amino acid adenylation domain	4; 4/ 5
IPR036380	IPR	Isochorismatase-like superfamily	0; 2/ 6
IPR010917	IPR	TonB-dependent receptor, conserved site	4; 7/11
IPR025110	IPR	AMP-binding enzyme, C-terminal domain	1; 4/12
IPR023271	IPR	Aquaporin-like	9; 2/ 2
IPR011042	IPR	Six-bladed beta-propeller, TolB-like	0; 2/ 8
IPR035906	IPR	MetI-like superfamily	0; 3/22
IPR022770	IPR	Ferric iron reductase FhuF domain	9; 3/ 3
IPR036661	IPR	Luciferase-like domain superfamily	0; 2/ 6
IPR009081	IPR	Phosphopantetheine binding ACP domain	3; 6/10
IPR001031	IPR	Thioesterase	3; 3/ 4
IPR010105	IPR	TonB-dependent siderophore receptor	5; 9/14
IPR000531	IPR	TonB-dependent receptor-like, beta-barrel	4;10/19
IPR039426	IPR	Vitamin B12 transporter BtuB-like	0; 3/ 9
IPR020845	IPR	AMP-binding, conserved site	1; 5/13
IPR039423	IPR	TonB-dependent receptor-like	5; 7/10
IPR007310	IPR	Aerobactin siderophore biosynthesis, IucA/IucC, N-terminal	9; 3/ 3
IPR000522	IPR	ABC transporter, permease protein, BtuC-like	9; 2/ 2
IPR002898	IPR	MotA/TolQ/ExbB proton channel	1; 2/ 4
IPR011527	IPR	ABC transporter type 1, transmembrane domain	1; 2/ 5
IPR031043	IPR	Putative histamine N-monooxygenase	9; 2/ 2

IPR036942	IPR	TonB-dependent receptor-like, beta-barrel domain superfamily	5;10/18
IPR038404	IPR	TRAP transporter solute receptor DctP superfamily	1; 2/ 4
IPR003369	IPR	Sec-independent protein translocase protein TatA/B/E	9; 2/ 2
IPR012910	IPR	TonB-dependent receptor, plug domain	4;10/19
IPR037294	IPR	ABC transporter, BtuC-like	2; 2/ 3
IPR004872	IPR	Lipoprotein NlpA family	1; 2/ 4
IPR003439	IPR	ABC transporter-like	0; 5/33
IPR016084	IPR	Haem oxygenase-like, multi-helical	1; 2/ 4
IPR036736	IPR	ACP-like superfamily	3; 6/10
IPR001242	IPR	Condensation domain	4; 4/ 5
IPR036640	IPR	ABC transporter type 1, transmembrane domain superfamily	0; 2/ 6
IPR037455	IPR	Aerobactin siderophore biosynthesis, IucA/IucC-like	9; 3/ 3
IPR025700	IPR	L-lysine 6-monooxygenase/L-ornithine 5-monooxygenase	9; 2/ 2
IPR042099	IPR	AMP-dependent synthetase-like superfamily	1; 5/14
IPR016291	IPR	Isochorismatase	9; 2/ 2
IPR023213	IPR	Chloramphenicol acetyltransferase-like domain superfamily	2; 4/ 8
IPR000868	IPR	Isochorismatase-like	0; 2/ 6
IPR020802	IPR	Polyketide synthase, thioesterase domain	9; 2/ 2
IPR000515	IPR	ABC transporter type 1, transmembrane domain MetI-like	0; 3/22
IPR029058	IPR	Alpha/Beta hydrolase fold	0; 7/36
IPR000873	IPR	AMP-dependent synthetase/ligase	1; 5/15
02026 Biofilm formation -	KEGG	ko02026	0;2/10

Escherichia coli [PATH:ko02026]			
02024 Quorum sensing [PATH:ko02024]	KEGG	ko02024	0;3/11
01053 Biosynthesis of siderophore group nonribosomal peptides [PATH:ko01053]	KEGG	ko01053	4;5/ 7
00997 Biosynthesis of various secondary metabolites - part 3 [PATH:ko00997]	KEGG	ko00997	9;3/ 3
00920 Sulfur metabolism [PATH:ko00920]	KEGG	ko00920	0;5/38
02010 ABC transporters [PATH:ko02010]	KEGG	ko02010	0;6/49
Cell outer membrane	KEYWORDS	keyword	1;10/ 31
Amino-acid transport	KEYWORDS	keyword	0; 6/ 50
Cell inner membrane	KEYWORDS	keyword	0;17/188
Ligase	KEYWORDS	keyword	2; 3/ 5
Antibiotic	KEYWORDS	keyword	0; 2/ 5

biosynthesis			
FAD	KEYWORDS	keyword	0; 4/ 30
Glycosyltransferase	KEYWORDS	keyword	0; 2/ 9
Direct protein sequencing	KEYWORDS	keyword	0; 4/ 20
operon_1154	operons	NZ_CP008706.1|gene3746|ABUW_RS18730	0; 3/12
operon_1048	operons	NZ_CP008706.1|gene3369|ABUW_RS16845	9; 2/ 2
operon_0387	operons	NZ_CP008706.1|gene1149|ABUW_RS05750	9; 2/ 2
operon_0351	operons	NZ_CP008706.1|gene1042|ABUW_RS05215	0; 2/ 9
operon_0629	operons	NZ_CP008706.1|gene2003|ABUW_RS10020	0; 2/ 9
operon_0454	operons	NZ_CP008706.1|gene1442|ABUW_RS07215	2; 2/ 3
operon_1007	operons	NZ_CP008706.1|gene3218|ABUW_RS16090	9; 3/ 3
operon_1035	operons	NZ_CP008706.1|gene3329|ABUW_RS16645	2; 3/ 5
operon_0631	operons	NZ_CP008706.1|gene2013|ABUW_RS10070	1; 3/ 7
operon_0893	operons	NZ_CP008706.1|gene2831|ABUW_RS14160	9; 2/ 2
operon_0026	operons	NZ_CP008706.1|gene7|ABUW_RS00040	1; 2/ 4
operon_0230	operons	NZ_CP008706.1|gene629|ABUW_RS03150	1; 3/ 6
operon_1151	operons	NZ_CP008706.1|gene3738|ABUW_RS18690	1; 2/ 5
operon_0637	operons	NZ_CP008706.1|gene2039|ABUW_RS10200	1; 2/ 4
operon_0662	operons	NZ_CP008706.1|gene2103|ABUW_RS10520	3; 4/ 6
operon_0043	operons	NZ_CP008706.1|gene55|ABUW_RS00280	1; 2/ 5
operon_0388	operons	NZ_CP008706.1|gene1151|ABUW_RS05760|entE	7; 7/ 9
operon_0663	operons	NZ_CP008706.1|gene2109|ABUW_RS10550	6;12/20
operon_1135	operons	NZ_CP008706.1|gene3678|ABUW_RS18390	1; 3/ 7
operon_1093	operons	NZ_CP008706.1|gene3534|ABUW_RS17670	2; 3/ 5
operon_0624	operons	NZ_CP008706.1|gene1990|ABUW_RS09955	4; 5/ 7

operon_0450	operons	NZ_CP008706.1|gene1429|ABUW_RS07150	0; 2/ 6
operon_0386	operons	NZ_CP008706.1|gene1144|ABUW_RS05725	9; 5/ 5
operon_0668	operons	NZ_CP008706.1|gene2138|ABUW_RS10695	0; 2/ 8
operon_0368	operons	NZ_CP008706.1|gene1088|ABUW_RS05445	0; 2/ 8
operon_0917	operons	NZ_CP008706.1|gene2893|ABUW_RS14470	9; 8/ 9
operon_0970	operons	NZ_CP008706.1|gene3092|ABUW_RS15460	1; 2/ 4
operon_0458	operons	NZ_CP008706.1|gene1449|ABUW_RS07250	1; 3/ 8
operon_1032	operons	NZ_CP008706.1|gene3316|ABUW_RS16580	1; 2/ 5
operon_0710	operons	NZ_CP008706.1|gene2270|ABUW_RS11355	3; 5/ 8
PF00296	Pfam	Luciferase-like monooxygenase	0; 2/ 6
PF07715	Pfam	TonB-dependent Receptor Plug Domain	4;10/19
PF02416	Pfam	mttA/Hcf106 family	9; 2/ 2
PF00593	Pfam	TonB dependent receptor	4;10/19
PF00975	Pfam	Thioesterase domain	3; 3/ 4
PF00668	Pfam	Condensation domain	4; 4/ 5
PF00528	Pfam	Binding-protein-dependent transport system inner membrane component	0; 3/22
PF03180	Pfam	NLPA lipoprotein	1; 2/ 4
PF00501	Pfam	AMP-binding enzyme	1; 5/15
PF06276	Pfam	Ferric iron reductase FhuF-like transporter	9; 3/ 3
PF13193	Pfam	AMP-binding enzyme C-terminal domain	1; 4/12
PF13434	Pfam	L-lysine 6-monooxygenase (NADPH-requiring)	9; 2/ 2
PF01618	Pfam	MotA/TolQ/ExbB proton channel family	1; 2/ 4
PF00550	Pfam	Phosphopantetheine attachment site	3; 6/10
PF01032	Pfam	FecCD transport family	9; 2/ 2
PF00005	Pfam	ABC transporter	0; 5/33
PF04183	Pfam	IucA / IucC family	9; 3/ 3
PF07995	Pfam	Glucose / Sorbosone dehydrogenase	0; 2/ 6

PF00857	Pfam	Isochorismatase family	0; 2/ 6
Upregulated Wicklow Tormentil Root			
ClassID	Class	Description	single_list
GO:0009073	GO	aromatic amino acid family biosynthetic process	0; 2/ 9
I	COG	METABOLISM; Lipid transport and metabolism	0;13/84
COG1113	eggNOG_COG	amino acid transport	0;3/10
COG1301	eggNOG_COG	dicarboxylic acid transport	0;2/ 5
COG1960	eggNOG_COG	acyl-CoA dehydrogenase activity	0;5/20
COG1024	eggNOG_COG	Enoyl-CoA hydratase	1;4/11
COG1018	eggNOG_COG	Is involved in NO detoxification in an aerobic process, termed nitric oxide dioxygenase (NOD) reaction that utilizes O(2) and NAD(P)H to convert NO to nitrate, which protects the bacterium from various noxious nitrogen compounds. Therefore, plays a central role in the inducible response to nitrosative stress	4;4/ 5
COG5517	eggNOG_COG	Aromatic-ring-hydroxylating dioxygenase beta subunit	9;2/ 2
COG1309	eggNOG_COG	transcriptional regulator	0;4/14
COG1250	eggNOG_COG	3-hydroxyacyl-CoA dehydrogenase	1;2/ 3
GO:0015628	GO	protein secretion by the type II secretion system	0; 4/12
GO:0006935	GO	chemotaxis	5; 5/ 6
GO:0043107	GO	type IV pilus-dependent motility	3; 6/ 9
GO:0015180	GO	L-alanine transmembrane transporter activity	1; 2/ 4

GO:0009297	GO	pilus assembly	0; 2/ 5
GO:0006355	GO	regulation of transcription, DNA-templated	0;10/75
GO:0008199	GO	ferric iron binding	0; 2/ 5
GO:0000160	GO	phosphorelay signal transduction system	0; 4/12
GO:0003995	GO	acyl-CoA dehydrogenase activity	0; 5/16
GO:0019545	GO	arginine catabolic process to succinate	0; 2/ 7
GO:0042944	GO	D-alanine transmembrane transporter activity	1; 2/ 4
GO:0042941	GO	D-alanine transport	1; 2/ 4
GO:0007155	GO	cell adhesion	1; 2/ 3
GO:0006572	GO	tyrosine catabolic process	9; 2/ 2
GO:0009289	GO	pilus	1; 2/ 3
GO:0004322	GO	ferroxidase activity	9; 2/ 2
GO:0015627	GO	type II protein secretion system complex	0; 2/ 8
GO:0006879	GO	cellular iron ion homeostasis	1; 2/ 3
GO:0071949	GO	FAD binding	0; 4/13
GO:0007165	GO	signal transduction	0; 2/ 6
GO:0046274	GO	lignin catabolic process	1; 2/ 4
GO:0001761	GO	beta-alanine transmembrane transporter activity	1; 2/ 4
GO:0018618	GO	anthranilate 1,2-dioxygenase (deaminating, decarboxylating) activity	9; 2/ 2
GO:0016042	GO	lipid catabolic process	0; 3/12
GO:0051537	GO	2 iron, 2 sulfur cluster binding	0; 6/32
GO:0006635	GO	fatty acid beta-oxidation	0; 3/12
GO:0004300	GO	enoyl-CoA hydratase activity	0; 3/10
GO:0015808	GO	L-alanine transport	1; 2/ 4
GO:0043640	GO	benzoate catabolic process via hydroxylation	0; 2/ 5
GO:0006835	GO	dicarboxylic acid transport	0; 2/ 6

GO:0003857	GO	3-hydroxyacyl-CoA dehydrogenase activity	0; 2/ 5
GO:0070069	GO	cytochrome complex	1; 2/ 4
GO:0019646	GO	aerobic electron transport chain	0; 2/ 9
GO:0042945	GO	D-serine transmembrane transporter activity	1; 2/ 4
GO:0019544	GO	arginine catabolic process to glutamate	0; 2/ 7
GO:0001762	GO	beta-alanine transport	1; 2/ 4
GO:0019557	GO	histidine catabolic process to glutamate and formate	9; 5/ 5
GO:0006782	GO	protoporphyrinogen IX biosynthetic process	0; 2/ 8
GO:0030435	GO	sporulation resulting in formation of a cellular spore	0; 4/11
GO:0004364	GO	glutathione transferase activity	1; 2/ 4
GO:0015187	GO	glycine transmembrane transporter activity	1; 2/ 4
GO:0043683	GO	type IV pilus biogenesis	5; 5/ 6
GO:0015816	GO	glycine transport	1; 2/ 4
GO:0019439	GO	aromatic compound catabolic process	0; 6/25
GO:0044096	GO	type IV pilus	9; 4/ 4
GO:0042942	GO	D-serine transport	1; 2/ 4
GO:0006826	GO	iron ion transport	1; 2/ 3
GO:0019556	GO	histidine catabolic process to glutamate and formamide	9; 5/ 5
GO:0004109	GO	coproporphyrinogen oxidase activity	1; 2/ 3
GO:0006631	GO	fatty acid metabolic process	0; 3/12
GO:0008260	GO	3-oxoacid CoA-transferase activity	9; 2/ 2
GO:0005344	GO	oxygen carrier activity	9; 2/ 2
GO:0042803	GO	protein homodimerization activity	0; 2/ 9
GO:0015293	GO	symporter activity	0; 4/14
GO:0010124	GO	phenylacetate catabolic process	2; 7/16

GO:0006119	GO	oxidative phosphorylation	9; 2/ 2
GO:0009055	GO	electron transfer activity	0; 6/39
GO:0006559	GO	L-phenylalanine catabolic process	0; 2/ 5
IPR036061	IPR	CheW-like domain superfamily	9;2/ 2
IPR006176	IPR	3-hydroxyacyl-CoA dehydrogenase, NAD binding	0;2/ 5
IPR029045	IPR	ClpP/crotonase-like domain superfamily	0;5/24
IPR032710	IPR	NTF2-like domain superfamily	1;2/ 3
IPR036282	IPR	Glutathione S-transferase, C-terminal domain superfamily	0;2/ 8
IPR009100	IPR	Acyl-CoA dehydrogenase/oxidase, N-terminal and middle domain superfamily	0;5/24
IPR007831	IPR	General secretory system II, protein E, N-terminal	9;2/ 2
IPR006089	IPR	Acyl-CoA dehydrogenase, conserved site	0;5/15
IPR000391	IPR	Ring-hydroxylating dioxygenase beta subunit	9;2/ 2
IPR013786	IPR	Acyl-CoA dehydrogenase/oxidase, N-terminal	0;5/23
IPR036250	IPR	Acyl-CoA dehydrogenase-like, C-terminal	0;5/24
IPR001482	IPR	Type II/IV secretion system protein	3;4/ 5
IPR001041	IPR	2Fe-2S ferredoxin-type iron-sulfur binding domain	0;3/11
IPR004046	IPR	Glutathione S-transferase, C-terminal	0;2/ 5
IPR013374	IPR	ATPase, type IV, pilus assembly, PilB	9;2/ 2
IPR006321	IPR	Pilus retraction protein PilT	9;2/ 2
IPR037069	IPR	Acyl-CoA dehydrogenase/oxidase, N-terminal domain superfamily	0;5/24
IPR017927	IPR	FAD-binding domain, ferredoxin reductase-type	0;4/11
IPR001991	IPR	Sodium:dicarboxylate symporter	0;2/ 8
IPR006058	IPR	2Fe-2S ferredoxin, iron-sulphur binding site	1;3/ 7
IPR010994	IPR	RuvA domain 2-like	0;2/ 7

IPR012675	IPR	Beta-grasp domain superfamily	0;3/15
IPR011991	IPR	ArsR-like helix-turn-helix domain	0;3/15
IPR018376	IPR	Enoyl-CoA hydratase/isomerase, conserved site	0;3/ 9
IPR035919	IPR	EAL domain superfamily	0;2/ 5
IPR004045	IPR	Glutathione S-transferase, N-terminal	0;2/ 8
IPR004736	IPR	MFS transporter, metabolite:H symporter	0;2/ 6
IPR036922	IPR	Rieske [2Fe-2S] iron-sulphur domain superfamily	0;2/10
IPR005318	IPR	Outer membrane porin, bacterial	1;2/ 3
IPR039261	IPR	Ferredoxin-NADP reductase (FNR), nucleotide-binding domain	0;4/12
IPR012902	IPR	Prokaryotic N-terminal methylation site	1;2/ 4
IPR009057	IPR	Homeobox-like domain superfamily	0;9/43
IPR017938	IPR	Riboflavin synthase-like beta-barrel	0;4/13
IPR018107	IPR	Sodium:dicarboxylate symporter, conserved site	0;2/ 6
IPR037523	IPR	Vicinal oxygen chelate (VOC) domain	1;2/ 4
IPR008333	IPR	Flavoprotein pyridine nucleotide cytochrome reductase-like, FAD-binding domain	0;3/ 8
IPR002024	IPR	Bacterioferritin	9;2/ 2
IPR009078	IPR	Ferritin-like superfamily	0;2/ 7
IPR012347	IPR	Ferritin-like	0;2/ 5
IPR004840	IPR	Amino acid permease, conserved site	0;4/15
IPR023772	IPR	DNA-binding HTH domain, TetR-type, conserved site	2;5/ 8
IPR023614	IPR	Porin domain superfamily	1;2/ 3
IPR014748	IPR	Enoyl-CoA hydratase, C-terminal	0;3/ 9
IPR001647	IPR	DNA-binding HTH domain, TetR-type	0;5/19
IPR004360	IPR	Glyoxalase/fosfomycin resistance/dioxygenase domain	1;2/ 4

IPR006091	IPR	Acyl-CoA oxidase/dehydrogenase, central domain	0;5/20
IPR001633	IPR	EAL domain	0;2/ 5
IPR004746	IPR	Major facilitator superfamily, aromatic acid:H+ symporter family	0;2/ 8
IPR011006	IPR	CheY-like superfamily	0;5/25
IPR036010	IPR	2Fe-2S ferredoxin-like superfamily	0;3/11
IPR037257	IPR	General secretory system II, protein E, N-terminal superfamily	1;2/ 3
IPR016032	IPR	Signal transduction response regulator, C-terminal effector	0;2/10
IPR017941	IPR	Rieske [2Fe-2S] iron-sulphur domain	0;2/ 9
IPR002545	IPR	CheW-like domain	9;2/ 2
IPR009040	IPR	Ferritin-like diiron domain	9;2/ 2
IPR008331	IPR	Ferritin/DPS protein domain	9;2/ 2
IPR009075	IPR	Acyl-CoA dehydrogenase/oxidase C-terminal	0;5/20
IPR015881	IPR	Aromatic-ring-hydroxylating dioxygenase, 2Fe-2S-binding site	0;2/ 7
IPR006108	IPR	3-hydroxyacyl-CoA dehydrogenase, C-terminal	0;2/ 5
IPR042181	IPR	Type II secretion system, protein E, N-terminal	1;2/ 3
IPR010987	IPR	Glutathione S-transferase, C-terminal-like	0;2/ 8
IPR029068	IPR	Glyoxalase/Bleomycin resistance protein/Dihydroxybiphenyl dioxygenase	1;2/ 4
IPR001753	IPR	Enoyl-CoA hydratase/isomerase	0;4/13
IPR038404	IPR	TRAP transporter solute receptor DctP superfamily	1;2/ 4
IPR005829	IPR	Sugar transporter, conserved site	0;4/23
IPR005828	IPR	Major facilitator, sugar transporter-like	0;2/ 8
IPR036458	IPR	Sodium:dicarboxylate symporter superfamily	0;2/ 8
IPR004841	IPR	Amino acid permease/ SLC12A domain	0;4/16

IPR004165	IPR	Coenzyme A transferase family I	0;2/ 8
IPR001433	IPR	Oxidoreductase FAD/NAD(P)-binding	0;4/12
IPR001789	IPR	Signal transduction response regulator, receiver domain	0;5/25
00627 Aminobenzoate degradation [PATH:ko00627]	KEGG	ko00627	2;5/10
00360 Phenylalanine metabolism [PATH:ko00360]	KEGG	ko00360	1;5/15
02020 Two-component system [PATH:ko02020]	KEGG	ko02020	0;7/58
00340 Histidine metabolism [PATH:ko00340]	KEGG	ko00340	0;3/14
00362 Benzoate degradation [PATH:ko00362]	KEGG	ko00362	0;3/21
00640 Propanoate metabolism [PATH:ko00640]	KEGG	ko00640	0;3/18
00860 Porphyrin and chlorophyll metabolism [PATH:ko00860]	KEGG	ko00860	0;3/17
Phosphoprotein	KEYWORDS	keyword	9;2/ 2
Electron	KEYWORDS	keyword	0;2/ 6

transport			
2Fe-2S	KEYWORDS	keyword	0;6/29
Aromatic hydrocarbons catabolism	KEYWORDS	keyword	0;8/29
Lipopolysaccharide biosynthesis	KEYWORDS	keyword	9;2/ 2
operon_0709	operons	NZ_CP008706.1|gene2265|ABUW_RS11330	0;2/ 5
operon_0424	operons	NZ_CP008706.1|gene1317|ABUW_RS06590	1;2/ 4
operon_0569	operons	NZ_CP008706.1|gene1820|ABUW_RS09105	0;2/ 8
operon_1076	operons	NZ_CP008706.1|gene3454|ABUW_RS17270	2;3/ 4
operon_0407	operons	NZ_CP008706.1|gene1221|ABUW_RS06110	0;4/11
operon_0627	operons	NZ_CP008706.1|gene2000|ABUW_RS10005	9;2/ 2
operon_0560	operons	NZ_CP008706.1|gene1769|ABUW_RS08850|fadH	1;2/ 4
operon_0753	operons	NZ_CP008706.1|gene2381|ABUW_RS11910	2;3/ 4
operon_0928	operons	NZ_CP008706.1|gene2941|ABUW_RS14710	9;2/ 2
operon_0582	operons	NZ_CP008706.1|gene1861|ABUW_RS09310	0;3/ 9
operon_0581	operons	NZ_CP008706.1|gene1858|ABUW_RS09295	1;2/ 3
operon_0793	operons	NZ_CP008706.1|gene2544|ABUW_RS12725	9;2/ 2
operon_0050	operons	NZ_CP008706.1|gene73|ABUW_RS00370	4;9/14
operon_1118	operons	NZ_CP008706.1|gene3623|ABUW_RS18115	1;2/ 3
operon_0058	operons	NZ_CP008706.1|gene112|ABUW_RS00565	4;6/ 8
operon_0754	operons	NZ_CP008706.1|gene2385|ABUW_RS11930	9;5/ 5
operon_0650	operons	NZ_CP008706.1|gene2071|ABUW_RS10360	9;2/ 2
operon_0105	operons	NZ_CP008706.1|gene219|ABUW_RS01100	1;2/ 3
operon_0698	operons	NZ_CP008706.1|gene2246|ABUW_RS11235	3;4/ 5
operon_0419	operons	NZ_CP008706.1|gene1309|ABUW_RS06550	1;2/ 4
operon_0773	operons	NZ_CP008706.1|gene2448|ABUW_RS12245	2;8/17

operon_0844	operons	NZ_CP008706.1|gene2697|ABUW_RS13490	2;5/ 8
operon_0203	operons	NZ_CP008706.1|gene529|ABUW_RS02650	0;2/ 9
operon_0957	operons	NZ_CP008706.1|gene3046|ABUW_RS15230	0;2/ 7
operon_0378	operons	NZ_CP008706.1|gene1134|ABUW_RS05675	9;2/ 2
operon_0132	operons	NZ_CP008706.1|gene284|ABUW_RS01425	1;6/16
operon_1017	operons	NZ_CP008706.1|gene3249|ABUW_RS16245	0;2/ 8
operon_1135	operons	NZ_CP008706.1|gene3678|ABUW_RS18390	0;2/ 7
operon_0850	operons	NZ_CP008706.1|gene2720|ABUW_RS13605	0;2/ 9
operon_1042	operons	NZ_CP008706.1|gene3356|ABUW_RS16780	0;2/ 5
operon_0486	operons	NZ_CP008706.1|gene1552|ABUW_RS07765	0;2/ 6
operon_0632	operons	NZ_CP008706.1|gene2020|ABUW_RS10105	9;4/ 4
operon_0987	operons	NZ_CP008706.1|gene3146|ABUW_RS15730	0;2/ 6
operon_0805	operons	NZ_CP008706.1|gene2605|ABUW_RS13030	2;4/ 6
operon_0803	operons	NZ_CP008706.1|gene2597|ABUW_RS12990	1;4/ 7
operon_1100	operons	NZ_CP008706.1|gene3561|ABUW_RS17805	0;2/ 5
operon_0084	operons	NZ_CP008706.1|gene180|ABUW_RS00905	1;2/ 4
operon_0201	operons	NZ_CP008706.1|gene520|ABUW_RS02605	0;2/ 7
operon_0373	operons	NZ_CP008706.1|gene1113|ABUW_RS05570	1;2/ 3
operon_0779	operons	NZ_CP008706.1|gene2479|ABUW_RS12400	1;2/ 4
operon_0155	operons	NZ_CP008706.1|gene368|ABUW_RS01845	1;2/ 3
operon_1137	operons	NZ_CP008706.1|gene3686|ABUW_RS18430	0;2/ 5
operon_0047	operons	NZ_CP008706.1|gene65|ABUW_RS00330	2;3/ 4
operon_0135	operons	NZ_CP008706.1|gene318|ABUW_RS01595	9;2/ 2
operon_0541	operons	NZ_CP008706.1|gene1717|ABUW_RS08590	0;2/ 5
operon_0536	operons	NZ_CP008706.1|gene1705|ABUW_RS08530	1;2/ 3
operon_0801	operons	NZ_CP008706.1|gene2582|ABUW_RS12915	0;3/14
operon_0635	operons	NZ_CP008706.1|gene2030|ABUW_RS10155	1;2/ 4

operon_0309	operons	NZ_CP008706.1|gene915|ABUW_RS04580	1;3/ 5
operon_0134	operons	NZ_CP008706.1|gene306|ABUW_RS01535|ispH	2;7/12
operon_1113	operons	NZ_CP008706.1|gene3603|ABUW_RS18015	1;2/ 4
operon_1143	operons	NZ_CP008706.1|gene3701|ABUW_RS18505	4;6/ 8
operon_0458	operons	NZ_CP008706.1|gene1449|ABUW_RS07250	0;2/ 8
operon_0242	operons	NZ_CP008706.1|gene666|ABUW_RS03335	9;8/ 8
operon_0553	operons	NZ_CP008706.1|gene1744|ABUW_RS08725	2;5/ 8
operon_0326	operons	NZ_CP008706.1|gene962|ABUW_RS04815	1;2/ 4
operon_0636	operons	NZ_CP008706.1|gene2034|ABUW_RS10175	1;3/ 5
operon_0074	operons	NZ_CP008706.1|gene158|ABUW_RS00795	0;2/ 6
operon_0973	operons	NZ_CP008706.1|gene3099|ABUW_RS15495	1;4/ 8
operon_0716	operons	NZ_CP008706.1|gene2292|ABUW_RS11465	0;2/ 8
operon_0799	operons	NZ_CP008706.1|gene2577|ABUW_RS12890	1;2/ 4
operon_0849	operons	NZ_CP008706.1|gene2714|ABUW_RS13575	4;5/ 6
operon_0026	operons	NZ_CP008706.1|gene7|ABUW_RS00040	1;2/ 4
operon_0842	operons	NZ_CP008706.1|gene2692|ABUW_RS13465	9;2/ 2
operon_0841	operons	NZ_CP008706.1|gene2690|ABUW_RS13455	9;2/ 2
PF02771	Pfam	Acyl-CoA dehydrogenase, N-terminal domain	0;5/23
PF02798	Pfam	Glutathione S-transferase, N-terminal domain	0;2/ 6
PF00970	Pfam	Oxidoreductase FAD-binding domain	0;3/ 8
PF00375	Pfam	Sodium:dicarboxylate symporter family	0;2/ 8
PF01144	Pfam	Coenzyme A transferase	0;2/ 8
PF02770	Pfam	Acyl-CoA dehydrogenase, middle domain	0;5/20
PF05157	Pfam	Type II secretion system (T2SS), protein E, N-terminal domain	9;2/ 2
PF00111	Pfam	2Fe-2S iron-sulfur cluster binding domain	0;3/ 9
PF02737	Pfam	3-hydroxyacyl-CoA dehydrogenase, NAD	0;2/ 5

		binding domain	
PF00355	Pfam	Rieske [2Fe-2S] domain	0;2/ 9
PF00866	Pfam	Ring hydroxylating beta subunit	9;2/ 2
PF00083	Pfam	Sugar (and other) transporter	0;2/ 8
PF00378	Pfam	Enoyl-CoA hydratase/isomerase	0;4/13
PF00072	Pfam	Response regulator receiver domain	0;5/25
PF00725	Pfam	3-hydroxyacyl-CoA dehydrogenase, C-terminal domain	0;2/ 5
PF03573	Pfam	outer membrane porin, OprD family	1;2/ 3
PF00440	Pfam	Bacterial regulatory proteins, tetR family	0;5/19
PF00324	Pfam	Amino acid permease	0;4/16
PF00563	Pfam	EAL domain	0;2/ 5
PF00441	Pfam	Acyl-CoA dehydrogenase, C-terminal domain	0;5/20
PF01584	Pfam	CheW-like domain	9;2/ 2
PF00210	Pfam	Ferritin-like domain	9;2/ 2
PF07963	Pfam	Prokaryotic N-terminal methylation motif	1;2/ 4
PF00175	Pfam	Oxidoreductase NAD-binding domain	0;4/12
PF00903	Pfam	Glyoxalase/Bleomycin resistance protein/Dioxygenase superfamily	1;2/ 4
PF00437	Pfam	Type II/IV secretion system protein	4;4/ 5

B.2 Differentially Expressed Genes for Agrimonniin, Ellagic Acid and Wiklow Tormentil Root Treated Samples

Locustag	Gene	Description	Feature Type	logFC	Agri_1	Agri_2	Agri_3	DMSO_1	DMSO_2	DMSO_3

ABUW_RS05760	basE	(2,3-dihydroxybenzoyl)adenylate synthase BasE	CDS	-8.190	2300.477	2215.600	2454.677	7.798	7.080	8.926
ABUW_RS05765	basF	acinetobactin biosynthesis bifunctional isochorismatase/aryl carrier protein BasF	CDS	-7.661	1411.449	1376.038	1520.742	5.757	4.461	10.917
ABUW_RS14490		transferrin-binding protein-like solute binding protein	CDS	-7.651	1839.918	3541.016	3218.877	12.607	10.975	19.072
ABUW_RS05755	basD	acinetobactin non-ribosomal peptide synthetase subunit BasD	CDS	-7.536	3303.750	3510.686	3553.135	12.607	13.736	29.282
ABUW_RS05770	basG	acinetobactin biosynthesis histidine decarboxylase BasG	CDS	-7.529	1747.933	1710.242	1774.712	7.287	7.080	13.806
ABUW_RS14485		porin family protein	CDS	-7.405	220.976	184.490	645.465	2.186	2.407	1.605
ABUW_RS05750	basC	putative histamine N-monooxygenase	CDS	-7.266	2337.903	2491.080	2534.965	13.263	11.753	22.668
ABUW_RS05725	bauD	ferric acinetobactin ABC transporter permease subunit BauD	CDS	-7.242	331.709	325.887	339.627	0.874	2.053	3.532

ABUW_RS05730	bauC	ferric acinetobactin ABC transporter permease subunit BauC	CDS	-7.079	351.511	327.894	318.469	1.530	1.062	4.624
ABUW_RS05800	basJ	acinetobactin biosynthesis isochorismate synthase BasJ	CDS	-7.045	1409.974	1694.038	1937.657	11.004	10.479	16.568
ABUW_RS05780	barA	acinetobactin export ABC transporter permease/ATP-binding subunit BarA	CDS	-6.831	2922.888	3218.643	3851.631	23.247	24.852	39.493
ABUW_RS05710	bauF	acinetobactin utilization protein BauF	CDS	-6.662	433.736	465.850	445.652	3.862	3.823	5.523
ABUW_RS05785	barB	acinetobactin export ABC transporter permease/ATP-binding subunit BarB	CDS	-6.642	2827.392	3252.271	3527.004	24.413	27.826	43.795
ABUW_RS05735	bauE	ferric acinetobactin ABC transporter ATP-binding protein BauE	CDS	-6.496	746.416	779.117	786.858	5.028	6.726	13.678
ABUW_RS20145		hypothetical protein	CDS	-6.492	63.196	57.434	92.051	0.291	0.637	1.349
ABUW_RS05720	basB	acinetobactin non-ribosomal peptide synthetase subunit BasB	CDS	-6.405	1938.504	2130.274	2063.024	15.304	17.701	39.107

ABUW_RS05740	bauB	siderophore-binding periplasmic lipoprotein BauB	CDS	-6.167	2105.552	2322.938	2711.726	22.955	20.816	55.354
ABUW_RS14495		TonB-dependent receptor	CDS	-6.148	713.413	660.521	891.540	10.057	9.488	12.329
ABUW_RS05715	basA	acinetobactin non-ribosomal peptide synthetase subunit BasA	CDS	-5.916	712.922	679.307	793.884	11.733	8.638	15.733
ABUW_RS14480		energy transducer TonB	CDS	-5.770	48.731	57.147	38.999	1.093	0.637	0.899
ABUW_RS05745	bauA	TonB-dependent ferric acinetobactin receptor BauA	CDS	-5.720	4045.461	4464.111	4508.543	65.587	60.820	120.340
ABUW_RS05790	basH	acinetobactin biosynthesis thioesterase BasH	CDS	-5.708	314.997	345.605	368.363	7.943	4.177	7.513
ABUW_RS14470		YbaN family protein	CDS	-5.691	131.518	110.206	172.734	2.769	2.053	3.147
ABUW_RS14475		biliverdin-producing heme oxygenase	CDS	-5.563	347.227	350.839	344.679	7.215	6.443	8.348
ABUW_RS05795	basI	acinetobactin biosynthesis phosphopantetheinyl transferase BasI	CDS	-5.563	77.801	86.114	71.052	1.676	0.779	2.440
ABUW_RS10585		acetyltransferase	CDS	-5.070	577.542	531.529	524.677	12.534	14.727	21.255
ABUW_RS10080		SDR family oxidoreductase	CDS	-5.068	1209.081	1260.024	1419.454	32.283	34.977	48.547

ABUW_RS10075		isochorismatase family protein	CDS	-5.004	556.055	550.745	533.361	13.336	14.515	23.118
ABUW_RS10630		DHA2 family efflux MFS transporter permease subunit	CDS	-4.889	736.164	778.185	986.355	19.312	19.825	45.015
ABUW_RS14160		TonB-dependent siderophore receptor	CDS	-4.885	2056.821	1759.072	1999.630	32.793	49.633	114.047
ABUW_RS10640		siderophore biosynthesis protein	CDS	-4.819	811.016	744.915	914.040	22.227	20.745	44.309
ABUW_RS10635		SidA/IucD/PvdA family monooxygenase	CDS	-4.717	696.280	717.883	885.225	18.947	19.117	49.125
ABUW_RS01510		bacterioferritin-associated ferredoxin	CDS	-4.597	66.988	77.295	64.499	2.623	2.478	3.468
ABUW_RS06610		hemin uptake protein HemP	CDS	-4.587	691.435	949.123	793.410	33.595	26.622	40.970
ABUW_RS00710		TonB-dependent siderophore receptor	CDS	-4.470	460.418	324.453	414.547	11.587	14.090	28.255
ABUW_RS08070		TonB-dependent siderophore receptor	CDS	-4.429	243.094	235.542	303.075	8.818	9.204	18.109
ABUW_RS08385	fumC	class II fumarate hydratase	CDS	-4.419	2043.761	2271.528	2621.174	111.570	90.133	122.395
ABUW_RS10525		hypothetical protein	CDS	-4.381	25.840	23.303	32.842	0.802	0.920	2.119
ABUW_RS10620		IucA/IucC family siderophore biosynthesis protein	CDS	-4.245	966.759	926.465	1071.933	39.498	39.721	76.995

ABUW_RS10520		TonB-dependent siderophore receptor	CDS	-4.216	430.155	333.057	402.310	14.502	18.267	29.796
ABUW_RS10625		siderophore achromobactin biosynthesis protein AcsC	CDS	-4.127	1349.447	1370.445	1525.321	60.777	59.192	122.716
ABUW_RS10615		(2Fe-2S)-binding protein	CDS	-4.121	156.796	132.936	148.656	6.194	5.806	13.036
ABUW_RS06655		alpha/beta hydrolase	CDS	-3.895	274.622	227.655	245.049	12.826	15.648	21.641
ABUW_RS02205		hypothetical protein	CDS	-3.887	4436.925	6132.192	4838.144	399.058	333.980	308.621
ABUW_RS07805		DUF4198 domain-containing protein	CDS	-3.874	192.537	171.584	172.024	10.129	11.258	15.091
ABUW_RS14505		sigma-70 family RNA polymerase sigma factor	CDS	-3.816	28.789	43.810	32.131	1.749	2.266	3.339
ABUW_RS10610		RraA family protein	CDS	-3.708	88.334	85.254	98.762	6.049	5.310	9.375
ABUW_RS14500		FecR domain-containing protein	CDS	-3.468	26.893	26.315	28.736	2.769	1.770	2.825
ABUW_RS16655		energy transducer TonB	CDS	-3.453	944.009	896.708	942.697	72.000	85.885	96.259
ABUW_RS10070		transcriptional repressor	CDS	-3.005	23.804	22.228	18.947	3.206	1.770	3.082
ABUW_RS16845		DUF2061 domain-containing protein	CDS	-2.955	29.913	30.402	20.289	4.664	3.257	2.504
ABUW_RS09965		type 1 fimbrial protein	CDS	-2.919	700.212	1149.244	537.150	138.898	86.309	90.480
ABUW_RS10215		hypothetical protein	CDS	-2.886	3.441	4.589	1.816	0.510	0.354	0.450

ABUW_RS17690		ferrous iron transport protein A	CDS	-2.885	175.194	170.580	173.445	21.279	22.020	26.906
ABUW_RS01160	aqpZ	aquaporin Z	CDS	-2.801	209.741	308.607	354.785	51.522	32.853	40.905
ABUW_RS09975		fimbrial biogenesis outer membrane usher protein	CDS	-2.792	274.130	326.962	179.366	49.117	30.375	33.264
ABUW_RS18705		acyl-CoA desaturase	CDS	-2.772	284.242	300.074	228.549	47.733	33.490	37.759
ABUW_RS18710		ferredoxin reductase	CDS	-2.745	318.368	367.546	213.865	43.579	47.368	43.281
ABUW_RS16645		biopolymer transporter ExbD	CDS	-2.669	959.246	596.348	592.176	91.093	104.860	141.660
ABUW_RS16650		MotA/TolQ/ExbB proton channel family protein	CDS	-2.652	1701.098	1451.110	1495.085	186.776	235.422	316.969
ABUW_RS10530		PepSY domain-containing protein	CDS	-2.648	89.106	77.080	83.130	8.891	10.691	20.035
ABUW_RS09970		molecular chaperone	CDS	-2.632	107.433	143.333	68.762	26.162	11.399	14.063
ABUW_RS19720		Ig-like domain-containing protein	CDS	-2.618	4013.793	5861.588	5447.530	928.197	731.684	835.832
ABUW_RS13590		amino acid permease	CDS	-2.502	48.310	946.685	68.446	69.376	60.325	58.051
ABUW_RS03435		sulfite reductase flavoprotein subunit alpha	CDS	-2.485	472.847	425.696	430.257	68.866	72.998	95.425
ABUW_RS20105		hypothetical protein	CDS	-2.437	36.794	28.824	20.526	7.215	4.956	3.789
ABUW_RS15475		hypothetical protein	CDS	-2.352	34.547	60.158	57.473	11.368	8.780	9.632
ABUW_RS00790		TonB-dependent siderophore receptor	CDS	-2.350	201.244	199.404	225.313	33.303	42.128	47.263

ABUW_RS17685		ferrous iron transporter B	CDS	-2.294	2327.511	2081.373	2287.863	381.642	444.929	538.449
ABUW_RS16100		Re/Si-specific NAD(P)(+) transhydrogenase subunit alpha	CDS	-2.248	422.641	614.775	695.043	94.736	136.368	133.440
ABUW_RS13860		cation diffusion facilitator family transporter	CDS	-2.220	149.213	99.594	135.630	31.263	25.702	25.558
ABUW_RS07215		aldo/keto reductase	CDS	-2.192	54.278	5.019	8.447	5.320	3.257	6.229
ABUW_RS14350	pnuC	nicotinamide riboside transporter PnuC	CDS	-2.184	100.060	7.816	8.447	8.381	9.488	7.770
ABUW_RS20295		hypothetical protein	CDS	-2.183	4.002	9.250	6.631	1.603	1.274	1.477
ABUW_RS15330		mechanosensitive ion channel	CDS	-2.175	944.641	1483.950	1527.768	393.156	191.099	291.925
ABUW_RS20090		hypothetical protein	CDS	-2.106	2.809	3.370	2.526	0.583	0.708	0.706
ABUW_RS09980		type 1 fimbrial protein	CDS	-2.057	61.441	71.129	40.894	15.085	14.161	12.458
ABUW_RS13745		TonB-dependent receptor	CDS	-2.051	258.893	229.806	259.891	53.781	53.669	73.142
ABUW_RS18870		hypothetical protein	CDS	-2.028	62.424	59.871	48.157	13.555	14.090	14.127
ABUW_RS15170		MFS transporter	CDS	-1.991	45.642	131.215	68.446	22.154	21.383	18.173
ABUW_RS16095		proton-translocating transhydrogenase family protein	CDS	-1.980	59.545	83.246	94.420	18.583	22.445	19.072
ABUW_RS10210		hypothetical protein	CDS	-1.956	3.230	4.589	2.053	0.364	0.779	1.349

ABUW_RS04980	carO	ornithine uptake porin CarO type 3	CDS	-1.930	2143.751	3131.883	3113.720	859.185	582.642	759.993
ABUW_RS16090		NAD(P)(+) transhydrogenase (Re/Si-specific) subunit beta	CDS	-1.921	376.227	632.772	644.202	117.473	158.458	160.475
ABUW_RS14395		hypothetical protein	CDS	-1.787	35.249	31.549	26.842	10.421	7.788	8.926
ABUW_RS12640		chloride channel protein	CDS	-1.775	35.530	37.429	40.578	10.640	11.258	11.238
ABUW_RS00285		hypothetical protein	CDS	-1.771	15.799	15.990	11.842	6.267	3.540	3.018
ABUW_RS10590		hypothetical protein	CDS	-1.744	13.763	8.891	9.316	2.696	2.620	4.174
ABUW_RS01140		hypothetical protein	CDS	-1.720	559.355	511.739	467.125	176.210	130.208	160.475
ABUW_RS14370	pgaB	poly-beta-1,6-N-acetyl-D-glucosamine N-deacetylase PgaB	CDS	-1.718	496.861	95.292	84.157	62.745	77.317	65.564
ABUW_RS20200		hypothetical protein	CDS	-1.663	3.370	3.944	3.079	1.749	0.708	0.835
ABUW_RS13220		hypothetical protein	CDS	-1.636	424.748	604.665	542.045	200.914	129.287	175.437
ABUW_RS05700		threo-3-hydroxy-L-aspartate ammonia-lyase	CDS	-1.624	45.852	44.384	40.499	13.044	14.302	15.026
ABUW_RS17680		hypothetical protein	CDS	-1.623	84.613	87.333	77.841	24.194	27.684	29.154
ABUW_RS10595		PepSY domain-containing protein	CDS	-1.597	120.143	110.995	103.420	32.137	29.879	48.483
ABUW_RS10700		Rrf2 family transcriptional regulator	CDS	-1.577	674.653	716.736	609.307	206.525	222.960	241.066
ABUW_RS00260		DUF1328 domain-containing protein	CDS	-1.571	13.692	18.643	15.158	5.466	5.239	5.266

ABUW_RS15080	lysM	peptidoglycan-binding protein LysM	CDS	-1.564	901.738	1138.775	1235.983	408.168	317.129	382.533
ABUW_RS10600		hypothetical protein	CDS	-1.557	15.237	8.819	10.974	2.915	3.328	5.587
ABUW_RS00045		DUF6091 family protein	CDS	-1.543	410.142	891.116	496.335	243.035	189.966	183.978
ABUW_RS18775	ssuC	aliphatic sulfonate ABC transporter permease SsuC	CDS	-1.490	63.898	41.444	33.710	15.741	17.984	15.797
ABUW_RS07500		hypothetical protein	CDS	-1.480	47.467	80.737	58.815	27.109	17.913	22.026
ABUW_RS09185		alpha/beta hydrolase	CDS	-1.478	137.416	167.425	174.077	67.627	49.492	54.776
ABUW_RS01270		bifunctional SulP family inorganic anion transporter/carbonic anhydrase	CDS	-1.453	23.734	42.089	38.447	12.753	10.691	14.577
ABUW_RS09260		sorbosone dehydrogenase family protein	CDS	-1.448	80.329	92.783	87.315	36.510	25.914	33.007
ABUW_RS11960		indolepyruvate ferredoxin oxidoreductase family protein	CDS	-1.448	407.755	1107.800	785.989	328.152	278.470	237.213
ABUW_RS15610		zinc-binding dehydrogenase	CDS	-1.439	22.329	63.743	27.947	13.773	12.391	15.861
ABUW_RS05455		substrate-binding domain-containing protein	CDS	-1.433	38.830	72.993	68.446	16.907	25.843	23.952

ABUW_RS08585		PQQ-dependent sugar dehydrogenase	CDS	-1.420	266.968	322.517	273.707	110.841	97.567	114.111
ABUW_RS11370		MetQ/NlpA family ABC transporter substrate-binding protein	CDS	-1.415	47.537	35.564	20.368	12.316	13.594	12.907
ABUW_RS10310		NAD(P)/FAD-dependent oxidoreductase	CDS	-1.413	27.876	43.953	28.579	15.231	11.470	11.045
ABUW_RS03310		YegP family protein	CDS	-1.412	57.087	118.165	73.025	42.996	22.303	28.062
ABUW_RS20540		hypothetical protein	CDS	-1.411	4.915	5.808	8.605	1.093	2.337	3.725
ABUW_RS04575		non-ribosomal peptide synthetase	CDS	-1.403	55.332	43.595	62.920	19.093	23.011	19.072
ABUW_RS18415	mmsB	3-hydroxyisobutyrate dehydrogenase	CDS	-1.399	22.470	28.681	19.500	11.441	8.780	6.614
ABUW_RS08765		TonB-dependent siderophore receptor	CDS	-1.395	119.019	85.541	101.762	29.805	45.456	41.162
ABUW_RS16585	tatB	Sec-independent protein translocase protein TatB	CDS	-1.367	2.036	3.227	2.447	1.093	0.850	1.027
ABUW_RS16850		LysR family transcriptional regulator	CDS	-1.355	126.322	131.717	118.577	40.809	54.023	52.336
ABUW_RS14460		DUF1275 domain-containing protein	CDS	-1.353	26.332	30.760	31.342	11.514	8.921	14.127
ABUW_RS05995		acyl-CoA dehydrogenase	CDS	-1.342	156.024	195.389	183.708	84.024	54.094	72.949
ABUW_RS08830		YnfA family protein	CDS	-1.329	34.688	32.481	36.000	12.534	14.232	14.256
ABUW_RS15165		trehalose-6-phosphate synthase	CDS	-1.322	29.070	33.485	22.263	11.660	10.054	12.201

ABUW_RS16240		hypothetical protein	CDS	-1.315	93.741	82.601	67.341	33.814	29.737	34.355
ABUW_RS07170		NirD/YgiW/YdeI family stress tolerance protein	CDS	-1.309	1.334	1.649	1.500	0.510	0.496	0.771
ABUW_RS03160		glucose/quinate/shikimate family membrane-bound PQQ-dependent dehydrogenase	CDS	-1.308	3770.558	3490.681	3865.604	1381.037	1497.565	1615.603
ABUW_RS10605		TonB-dependent receptor	CDS	-1.307	1294.396	1155.840	1380.297	387.034	438.840	721.721
ABUW_RS07270	csuD	Csu fimbrial usher CsuD	CDS	-1.303	99.358	123.615	48.315	42.996	27.755	39.236
ABUW_RS13135		heavy metal translocating P-type ATPase	CDS	-1.301	621.428	1183.159	501.151	298.565	303.322	333.601
ABUW_RS15535		LysE family translocator	CDS	-1.300	2.247	1.291	3.158	1.020	0.496	1.156
ABUW_RS16580		Sec-independent protein translocase subunit TatA	CDS	-1.299	3.300	3.083	4.342	1.822	1.982	0.578
ABUW_RS08720		DUF2057 domain-containing protein	CDS	-1.295	7.724	11.186	11.131	2.769	4.531	4.880
ABUW_RS07220		SDR family oxidoreductase	CDS	-1.290	36.303	7.887	9.552	8.672	6.089	7.256
ABUW_RS09985		DUF4882 family protein	CDS	-1.282	52.804	46.750	27.000	19.530	14.798	17.724
ABUW_RS10535		hypothetical protein	CDS	-1.282	6.320	4.876	5.132	1.239	2.195	3.211
ABUW_RS11375		MetQ/NlpA family ABC transporter substrate-binding protein	CDS	-1.282	32.862	25.669	17.368	9.765	10.408	11.045

ABUW_RS01315		CusA/CzcA family heavy metal efflux RND transporter	CDS	-1.264	231.930	198.615	252.075	95.684	96.718	91.764
ABUW_RS18420		CoA-acylating methylmalonate-semialdehyde dehydrogenase	CDS	-1.263	51.751	76.220	55.894	29.805	21.453	25.365
ABUW_RS11860		iron-containing redox enzyme family protein	CDS	-1.262	34.126	34.059	20.368	15.668	9.346	11.944
ABUW_RS14240		galactose mutarotase	CDS	-1.250	115.719	138.600	140.209	64.712	42.624	58.501
ABUW_RS05235		hypothetical protein	CDS	-1.248	37.847	43.165	34.657	19.093	15.435	14.192
ABUW_RS01170		hypothetical protein	CDS	-1.244	8.426	10.469	7.105	3.425	3.682	3.853
ABUW_RS16715		HdeD family acid-resistance protein	CDS	-1.239	40.165	47.108	41.684	20.623	17.276	16.760
ABUW_RS07275	csuE	Csu fimbrial tip adhesin CsuE	CDS	-1.238	34.407	38.146	19.026	16.834	9.983	12.073
ABUW_RS18410		AMP-binding protein	CDS	-1.225	15.729	28.537	25.579	11.878	8.213	9.761
ABUW_RS10045	pqqD	pyrroloquinoline quinone biosynthesis peptide chaperone PqqD	CDS	-1.224	30.966	27.964	21.631	8.745	12.815	12.907
ABUW_RS00050		DUF6091 family protein	CDS	-1.222	26.051	74.427	30.315	18.510	18.480	19.072
ABUW_RS10705		IscS subfamily cysteine desulfurase	CDS	-1.218	1009.662	991.140	786.463	366.629	391.898	439.621
ABUW_RS03180		VOC family protein	CDS	-1.217	41.780	57.147	37.973	24.413	16.285	18.237
ABUW_RS13200		KTSC domain-containing protein	CDS	-1.213	19.099	40.440	23.763	12.534	12.037	11.366

ABUW_RS08645		hypothetical protein	CDS	-1.210	91.213	185.350	137.445	66.534	64.856	47.584
ABUW_RS11385		ABC transporter permease	CDS	-1.208	17.695	16.635	10.026	6.923	6.656	5.651
ABUW_RS20615		stress-induced protein	CDS	-1.207	25.910	34.417	44.052	17.344	12.674	15.155
ABUW_RS07145		DUF2171 domain-containing protein	CDS	-1.205	3.511	4.159	1.895	1.457	1.416	1.284
ABUW_RS01745		hypothetical protein	CDS	-1.204	70.007	85.254	59.762	24.704	34.340	34.227
ABUW_RS14165	nfuA	Fe-S biogenesis protein NfuA	CDS	-1.204	377.983	386.117	407.442	203.392	146.917	158.228
ABUW_RS07155		PIG-L family deacetylase	CDS	-1.196	3.441	8.533	6.237	2.915	1.912	3.082
ABUW_RS07295	proP	glycine betaine/L-proline transporter ProP	CDS	-1.195	145.702	135.517	119.998	59.975	50.271	64.922
ABUW_RS15465		hypothetical protein	CDS	-1.195	32.300	23.877	13.421	7.870	10.833	11.687
ABUW_RS13685		type VI secretion system tip protein VgrG	CDS	-1.191	706.040	731.650	598.808	319.116	246.821	325.959
ABUW_RS10050	pqqC	pyrroloquinoline-quinone synthase PqqC	CDS	-1.186	155.252	128.849	136.972	55.311	62.024	67.683
ABUW_RS15280		hypothetical protein	CDS	-1.180	58.351	87.118	67.104	35.052	26.693	32.044
ABUW_RS10365		transcriptional regulator	CDS	-1.178	32.862	62.166	35.447	20.623	18.409	18.623
ABUW_RS02945		DUF4184 family protein	CDS	-1.174	33.494	28.537	30.079	12.972	14.090	13.742
ABUW_RS11380		ATP-binding cassette domain-containing protein	CDS	-1.163	33.494	25.239	12.316	8.964	9.912	12.843
ABUW_RS01640		hypothetical protein	CDS	-1.161	73.869	81.597	63.868	32.720	32.570	32.814
ABUW_RS20510		hypothetical protein	CDS	-1.159	54.419	127.917	75.946	49.919	33.844	31.915

ABUW_RS11365		LLM class flavin-dependent oxidoreductase	CDS	-1.153	60.879	48.973	36.000	23.611	20.321	21.705
ABUW_RS00920	betT	choline BCCT transporter BetT	CDS	-1.148	1593.594	1649.654	1719.450	766.271	686.865	786.643
ABUW_RS01885	mlaE	lipid asymmetry maintenance ABC transporter permease subunit MlaE	CDS	-1.145	444.830	384.826	412.415	181.967	185.647	193.867
ABUW_RS14720	fur	ferric iron uptake transcriptional regulator	CDS	-1.145	347.578	323.879	371.521	150.485	158.104	163.044
ABUW_RS18540		GntR family transcriptional regulator	CDS	-1.143	50.206	97.300	61.815	34.542	34.198	26.072
ABUW_RS09575		alpha/beta hydrolase	CDS	-1.140	3.441	3.657	2.210	1.457	1.487	1.284
ABUW_RS11850		SDR family oxidoreductase	CDS	-1.140	8.215	11.831	7.658	4.955	3.115	4.495
ABUW_RS15660		cation diffusion facilitator family transporter	CDS	-1.137	20.784	37.213	23.921	14.283	11.683	11.302
ABUW_RS04725		glycosyltransferase family 2 protein	CDS	-1.130	4.424	4.446	5.210	1.895	2.124	2.376
ABUW_RS03155		carbohydrate porin	CDS	-1.126	2225.976	2189.070	2084.576	956.108	988.488	1034.387
ABUW_RS11140		hypothetical protein	CDS	-1.121	26.261	42.878	40.184	20.332	16.780	13.164
ABUW_RS18780		ATP-binding cassette domain-containing protein	CDS	-1.119	43.395	32.123	21.000	13.409	17.134	13.935

ABUW_RS15855		organic hydroperoxide resistance protein	CDS	-1.116	58.702	53.418	58.262	28.202	25.418	24.980
ABUW_RS12795		D-Ala-D-Ala carboxypeptidase family metallohydrolase	CDS	-1.112	188.746	148.782	147.314	67.992	70.379	85.856
ABUW_RS07925		iron-containing alcohol dehydrogenase	CDS	-1.109	157.007	437.742	258.154	148.153	119.870	127.532
ABUW_RS07250	csuAB	Csu fimbrial major subunit CsuAB	CDS	-1.106	151.881	204.495	95.920	77.538	48.500	84.123
ABUW_RS00280		formate/nitrite transporter family protein	CDS	-1.101	23.663	30.545	19.894	12.899	9.700	11.944
ABUW_RS20305		hypothetical protein	CDS	-1.099	7.724	11.114	7.816	3.644	3.753	5.009
ABUW_RS04885	tolQ	protein TolQ	CDS	-1.097	184.673	145.340	159.708	77.538	71.582	79.756
ABUW_RS06520	adeF	multidrug efflux RND transporter periplasmic adaptor subunit AdeF	CDS	-1.097	12.007	2.294	3.553	2.405	3.469	2.504
ABUW_RS04065		phosphatase PAP2 family protein	CDS	-1.092	6.249	3.227	3.789	2.186	1.982	2.055
ABUW_RS15755		hypothetical protein	CDS	-1.085	219.993	514.751	245.523	172.566	158.600	131.129
ABUW_RS18770	ssuD	FMNH2-dependent alkanesulfonate monooxygenase	CDS	-1.068	83.278	59.083	46.736	30.170	27.330	32.686
ABUW_RS03470		patatin-like phospholipase family protein	CDS	-1.066	30.053	35.851	35.447	15.231	16.568	16.568

ABUW_RS18980		GlsB/YeaQ/YmgE family stress response membrane protein	CDS	-1.044	44.378	54.207	44.210	25.943	20.321	22.989
ABUW_RS05460	pstC	phosphate ABC transporter permease subunit PstC	CDS	-1.044	50.557	68.045	72.078	27.255	37.667	27.549
ABUW_RS03150		CoA transferase	CDS	-1.040	21.346	36.066	62.289	21.352	20.037	16.760
ABUW_RS03230	mscL	large conductance mechanosensitive channel protein MscL	CDS	-1.037	279.327	361.594	288.628	165.351	139.554	148.146
ABUW_RS04050		phosphoethanolamine--lipid A transferase	CDS	-1.025	48.099	42.519	44.841	22.810	20.675	23.053
ABUW_RS05225		glycosyltransferase family 2 protein	CDS	-1.016	69.937	75.789	68.131	38.478	33.561	33.713
ABUW_RS18015		DUF2726 domain-containing protein	CDS	-1.006	40.937	80.163	47.762	33.959	25.135	25.044
ABUW_RS14440		hypothetical protein	CDS	-1.003	8.356	6.453	8.289	2.988	4.461	4.046
ABUW_RS20265		hypothetical protein	CDS	1.000	6.460	8.174	7.737	15.231	15.152	14.384
ABUW_RS01375		sulfate ABC transporter substrate-binding protein	CDS	1.004	62.845	61.879	80.762	132.849	146.351	132.734
ABUW_RS13305	crp	cAMP-activated global transcriptional regulator CRP	CDS	1.004	217.394	188.147	235.497	441.398	423.547	420.934
ABUW_RS17725		PAS domain-containing sensor histidine kinase	CDS	1.011	63.336	51.554	54.710	103.335	121.428	117.001

ABUW_RS10510		DUF2797 domain-containing protein	CDS	1.011	69.375	60.660	54.631	120.242	120.083	131.899
ABUW_RS18335		4'-phosphopantetheinyl transferase superfamily protein	CDS	1.015	2.177	1.721	1.500	3.717	3.469	3.789
ABUW_RS17095		LysE family translocator	CDS	1.017	13.271	14.842	15.000	25.433	28.321	33.456
ABUW_RS08605		hypothetical protein	CDS	1.018	3.160	3.227	3.079	6.559	7.010	5.651
ABUW_RS18440		RidA family protein	CDS	1.019	448.903	516.830	619.886	1110.164	1077.700	1024.498
ABUW_RS12280	paaF	phenylacetate--CoA ligase	CDS	1.021	36.654	53.777	44.131	109.821	72.361	90.994
ABUW_RS19800	pqqA	pyrroloquinoline quinone precursor peptide PqqA	CDS	1.023	2.036	1.721	0.632	3.061	1.841	4.110
ABUW_RS11930		isovaleryl-CoA dehydrogenase	CDS	1.027	88.194	141.469	111.472	272.039	196.692	226.617
ABUW_RS12790		ferredoxin family protein	CDS	1.029	26.261	23.160	23.763	42.923	51.828	54.583
ABUW_RS17895		TniQ family protein	CDS	1.029	30.334	43.953	39.947	81.473	71.582	80.013
ABUW_RS06055		AzlC family ABC transporter permease	CDS	1.029	1.966	2.796	1.342	3.279	5.027	4.238
ABUW_RS05110		PaaI family thioesterase	CDS	1.032	23.734	23.447	22.894	55.166	44.111	44.052
ABUW_RS14045		CitMHS family transporter	CDS	1.033	161.571	140.106	150.787	354.241	301.198	270.798
ABUW_RS05555	gloA	lactoylglutathione lyase	CDS	1.035	32.090	28.968	32.131	63.546	66.201	61.198
ABUW_RS06490		hypothetical protein	CDS	1.036	1.334	1.291	0.711	2.405	2.407	2.119
ABUW_RS17370		peptidoglycan hydrolase	CDS	1.039	7.443	6.453	8.053	16.032	14.232	14.834

ABUW_RS18490		SDR family NAD(P)-dependent oxidoreductase	CDS	1.039	9.128	9.465	12.395	24.631	20.391	18.623
ABUW_RS18055		GNAT family N-acetyltransferase	CDS	1.042	5.758	5.306	4.105	11.368	10.479	9.504
ABUW_RS06215		hypothetical protein	CDS	1.044	0.632	0.430	0.474	1.676	0.991	0.578
ABUW_RS01250		acetyl-CoA hydrolase/transferase family protein	CDS	1.045	849.776	924.744	649.254	1784.103	1638.818	1579.514
ABUW_RS00370	hutC	histidine utilization repressor	CDS	1.069	46.906	53.060	45.552	103.117	97.780	104.351
ABUW_RS07175		BLUF domain-containing protein	CDS	1.077	7.935	10.397	8.526	20.259	19.188	17.274
ABUW_RS11475		type II asparaginase	CDS	1.079	133.203	131.860	114.235	282.387	278.187	240.681
ABUW_RS18435		amino acid permease	CDS	1.079	516.452	552.251	475.572	1161.175	1022.615	1078.310
ABUW_RS17810		ATP-binding protein	CDS	1.086	43.886	45.029	48.078	104.647	93.815	92.342
ABUW_RS17900		TniB family NTP-binding protein	CDS	1.094	33.002	45.101	54.947	100.202	91.691	92.021
ABUW_RS03370		alpha/beta fold hydrolase	CDS	1.095	8.847	10.325	11.052	26.672	18.197	19.714
ABUW_RS13690		TetR/AcrR family transcriptional regulator	CDS	1.098	0.492	0.574	0.632	1.020	1.274	1.349
ABUW_RS18445	alr	alanine racemase	CDS	1.101	472.496	690.708	780.463	1488.234	1347.745	1334.210
ABUW_RS15525		DUF1852 domain-containing protein	CDS	1.106	85.174	113.146	110.288	217.602	230.961	215.572
ABUW_RS15175	bfr	bacterioferritin	CDS	1.108	185.937	230.881	220.102	514.782	482.738	375.726

ABUW_RS14280		aldehyde dehydrogenase	CDS	1.114	9.901	11.974	9.789	36.801	15.648	16.247
ABUW_RS06820		hypothetical protein	CDS	1.118	0.421	0.645	0.789	1.968	1.062	1.027
ABUW_RS06845		hypothetical protein	CDS	1.126	0.913	1.434	1.737	2.186	3.682	3.018
ABUW_RS17650		NUDIX domain-containing protein	CDS	1.127	40.726	47.037	38.526	88.688	93.602	93.562
ABUW_RS19835		IS4-like element ISAba1 family transposase	CDS	1.129	0.702	0.717	0.395	1.676	1.558	0.835
ABUW_RS12740		exo-alpha-sialidase	CDS	1.133	16.993	16.850	15.316	34.251	36.818	36.796
ABUW_RS00435		response regulator receiver domain	CDS	1.136	201.244	208.725	235.497	477.981	455.762	484.379
ABUW_RS04500		co-chaperone GroES	CDS	1.136	178.213	184.203	318.153	569.948	427.299	497.993
ABUW_RS08850		NADPH-dependent 2,4-dienoyl-CoA reductase	CDS	1.136	20.433	25.813	18.710	50.866	43.615	48.419
ABUW_RS17905		DDE-type integrase/transposase/recombinase	CDS	1.139	61.581	87.047	104.525	189.691	188.125	179.483
ABUW_RS11290		integrase family protein	CDS	1.139	4.845	4.517	3.710	9.911	10.054	8.926
ABUW_RS20390		hypothetical protein	CDS	1.143	1.123	2.510	2.132	4.008	4.744	3.981
ABUW_RS18630		oligosaccharide flippase family protein	CDS	1.151	80.259	62.453	57.710	144.509	141.890	158.870
ABUW_RS11915		class I SAM-dependent methyltransferase	CDS	1.158	6.600	5.808	5.684	14.065	12.107	14.256
ABUW_RS03365		radical SAM protein	CDS	1.159	12.920	18.427	12.316	42.267	26.551	28.833
ABUW_RS13105		hypothetical protein	CDS	1.163	11.024	15.631	10.895	31.336	25.560	27.292
ABUW_RS13065		N-acetylmuramidase	CDS	1.165	2.036	1.721	3.079	6.267	3.823	5.201

ABUW_RS07450		hypothetical protein	CDS	1.168	33.985	41.157	37.263	102.388	69.387	80.848
ABUW_RS16720		hypothetical protein	CDS	1.175	25.138	21.080	17.684	54.364	47.155	42.960
ABUW_RS02630		hypothetical protein	CDS	1.179	29.702	29.900	23.526	67.117	61.953	59.335
ABUW_RS03295		alkylphosphonate utilization protein	CDS	1.180	2.879	1.936	2.763	6.267	5.877	5.073
ABUW_RS13510		OprD family porin	CDS	1.184	0.983	3.083	1.579	4.154	4.744	3.981
ABUW_RS13750		hypothetical protein	CDS	1.192	0.772	1.219	1.026	2.769	1.982	2.183
ABUW_RS19995		hypothetical protein	CDS	1.216	18.257	20.937	19.658	54.801	40.075	41.933
ABUW_RS06825		hypothetical protein	CDS	1.220	8.286	9.106	10.579	19.020	20.816	25.237
ABUW_RS15520		methionine synthase	CDS	1.223	138.259	177.105	194.445	393.520	420.573	375.983
ABUW_RS00390		amino acid permease	CDS	1.249	80.119	144.122	107.999	318.168	214.747	256.542
ABUW_RS17635		TetR/AcrR family transcriptional regulator	CDS	1.255	1.053	0.502	1.579	2.696	1.982	2.761
ABUW_RS11940		enoyl-CoA hydratase/isomerase family protein	CDS	1.257	47.678	57.218	59.525	150.704	110.595	131.642
ABUW_RS19650		LysM peptidoglycan-binding domain-containing protein	CDS	1.260	99.358	123.543	134.051	318.241	269.195	267.266
ABUW_RS11945		acetyl/propionyl/methylcrotonyl-CoA carboxylase subunit alpha	CDS	1.262	112.700	130.570	111.077	330.338	237.971	281.714
ABUW_RS17345		alpha-ketoglutarate-dependent dioxygenase AlkB	CDS	1.265	10.814	11.544	10.184	15.522	15.364	47.199

ABUW_RS00600		SH3 domain-containing protein	CDS	1.266	6.249	6.095	8.763	18.364	14.019	18.301
ABUW_RS08695		hypothetical protein	CDS	1.270	41.429	44.240	24.947	93.570	82.982	90.480
ABUW_RS01090		carboxymuconolactone decarboxylase family protein	CDS	1.273	1.826	1.362	0.632	2.551	3.469	3.339
ABUW_RS04155		hypothetical protein	CDS	1.277	7.092	4.302	4.026	10.712	13.948	12.843
ABUW_RS02700		hypothetical protein	CDS	1.282	12.007	12.476	8.605	30.388	25.418	24.851
ABUW_RS05940		superoxide dismutase	CDS	1.289	674.442	641.090	601.650	1545.295	1557.182	1582.404
ABUW_RS17655	cpdA	3',5'-cyclic-AMP phosphodiesterase	CDS	1.298	39.673	39.938	43.578	100.639	95.797	106.405
ABUW_RS07780		bifunctional aconitate hydratase 2/2-methylisocitrate dehydratase	CDS	1.301	1424.931	1353.022	1550.821	3532.935	3574.941	3558.579
ABUW_RS18515		hypothetical protein	CDS	1.306	28.368	36.353	36.236	82.348	85.460	81.875
ABUW_RS12935		hypothetical protein	CDS	1.307	67.690	50.407	74.367	187.869	134.810	153.540
ABUW_RS16270		hypothetical protein	CDS	1.308	18.327	19.718	21.552	102.607	23.790	21.320
ABUW_RS17910		heteromeric transposase endonuclease subunit TnsA	CDS	1.312	11.586	12.333	14.447	33.741	31.578	29.925
ABUW_RS13610		gamma-aminobutyraldehyde dehydrogenase	CDS	1.315	14.395	20.292	20.289	52.324	42.270	42.190
ABUW_RS13265		hypothetical protein	CDS	1.316	0.702	1.434	0.553	2.915	1.628	2.248

ABUW_RS14570		hypothetical protein	CDS	1.325	16.010	15.057	16.500	38.915	40.712	39.557
ABUW_RS17805		accessory factor UbiK family protein	CDS	1.336	14.254	19.718	13.973	39.716	41.349	40.071
ABUW_RS18265		DUF3861 domain-containing protein	CDS	1.336	5.758	6.883	6.631	13.700	19.046	15.925
ABUW_RS00635		ion channel protein Tsx	CDS	1.338	39.603	34.991	39.947	93.279	113.144	83.159
ABUW_RS18550	dld	D-lactate dehydrogenase	CDS	1.338	81.031	76.578	88.183	213.084	219.987	188.409
ABUW_RS17285	coaE	dephospho-CoA kinase	CDS	1.353	32.370	34.130	40.657	88.251	87.726	97.608
ABUW_RS00215		hypothetical protein	CDS	1.355	0.281	0.860	0.316	1.530	0.850	1.413
ABUW_RS18890	dnaK	molecular chaperone DnaK	CDS	1.357	2223.869	2172.005	2957.328	7236.541	5367.474	6231.815
ABUW_RS00590		DUF5991 domain-containing protein	CDS	1.363	10.111	11.544	11.447	29.150	28.746	27.292
ABUW_RS18085		TetR/AcrR family transcriptional regulator	CDS	1.364	0.913	2.366	1.026	5.538	3.965	1.734
ABUW_RS18885	grpE	nucleotide exchange factor GrpE	CDS	1.369	180.741	161.545	241.102	518.353	461.356	527.275
ABUW_RS06255		hypothetical protein	CDS	1.370	14.184	16.635	15.789	48.024	35.119	37.374
ABUW_RS18905		hypothetical protein	CDS	1.372	40.937	44.599	21.473	88.906	94.169	94.204
ABUW_RS08395		hypothetical protein	CDS	1.384	8.005	6.453	5.053	16.615	17.630	16.825
ABUW_RS11935		methylcrotonoyl-CoA carboxylase	CDS	1.397	104.554	138.242	132.314	378.362	284.489	325.188
ABUW_RS04590		hypothetical protein	CDS	1.400	1.475	0.860	1.263	3.498	1.841	4.174
ABUW_RS14535		hypothetical protein	CDS	1.400	2.387	1.434	1.658	5.101	5.027	4.431

ABUW_RS00385	hutH	histidine ammonia-lyase	CDS	1.401	194.784	452.370	253.496	970.974	676.315	731.802
ABUW_RS08125		benzoate/H(+) symporter BenE family transporter	CDS	1.417	32.722	34.776	38.842	85.991	107.975	89.902
ABUW_RS06780		hypothetical protein	CDS	1.435	0.070	0.574	0.474	0.510	1.558	0.963
ABUW_RS00925	omp33-36	porin Omp33-36	CDS	1.436	828.220	733.299	718.569	1998.353	2174.943	1994.219
ABUW_RS06595		NirD/YgiW/YdeI family stress tolerance protein	CDS	1.443	10.252	16.635	10.026	33.231	32.924	34.355
ABUW_RS10465		TonB C-terminal domain-containing protein	CDS	1.445	8.707	7.600	7.263	21.644	19.896	22.732
ABUW_RS16025		ComEA family DNA-binding protein	CDS	1.449	11.446	12.333	14.210	32.210	36.251	35.190
ABUW_RS02305		hypothetical protein	CDS	1.489	72.184	72.132	76.736	188.525	221.969	210.114
ABUW_RS12900		DUF4882 family protein	CDS	1.493	9.690	17.280	12.158	42.631	30.375	37.181
ABUW_RS03850		hypothetical protein	CDS	1.502	26.613	24.666	26.921	66.753	67.263	87.462
ABUW_RS01505	bfr	bacterioferritin	CDS	1.504	113.332	147.922	99.946	374.427	356.496	293.980
ABUW_RS00395	hutI	imidazolonepropionase	CDS	1.507	38.269	44.957	44.684	145.311	106.701	111.478
ABUW_RS11245		fimbrial biogenesis outer membrane usher protein	CDS	1.515	3.230	3.872	4.579	12.607	11.541	9.247
ABUW_RS16985	crcB	fluoride efflux transporter CrcB	CDS	1.525	12.850	12.906	12.474	14.721	16.780	78.343
ABUW_RS05575		hypothetical protein	CDS	1.526	58.281	53.777	48.473	158.865	154.777	148.788
ABUW_RS12620		hypothetical protein	CDS	1.550	21.416	20.650	20.526	62.453	57.492	63.381

ABUW_RS09700		hypothetical protein	CDS	1.555	24.576	21.224	15.710	61.797	55.227	63.959
ABUW_RS01100		hypothetical protein	CDS	1.590	2.528	1.936	1.737	6.559	5.735	6.486
ABUW_RS01970		globin domain-containing protein	CDS	1.592	23.523	29.326	25.815	83.076	78.592	75.518
ABUW_RS00830	prfB	peptide chain release factor 2	CDS	1.612	0.281	0.717	0.868	2.623	1.558	1.541
ABUW_RS11305		TetR/AcrR family transcriptional regulator	CDS	1.619	7.092	7.170	4.105	20.478	14.444	21.705
ABUW_RS12265		PaaI family thioesterase	CDS	1.623	0.702	0.717	0.395	2.842	1.274	1.605
ABUW_RS12680		hypothetical protein	CDS	1.635	1.545	2.438	2.842	7.943	6.160	7.064
ABUW_RS14110		SPOR domain-containing protein	CDS	1.653	1.264	1.219	1.026	2.478	5.381	3.275
ABUW_RS17020		DUF4062 domain-containing protein	CDS	1.660	20.574	21.654	17.842	62.817	64.856	62.353
ABUW_RS02265		energy transducer TonB	CDS	1.660	13.271	11.257	11.684	38.550	39.296	36.731
ABUW_RS16785		hypothetical protein	CDS	1.662	29.632	42.018	34.026	114.412	116.472	103.580
ABUW_RS20115		hypothetical protein	CDS	1.683	63.828	38.361	28.184	132.777	146.138	140.183
ABUW_RS13580		DUF4265 domain-containing protein	CDS	1.722	0.843	1.076	0.553	3.498	2.691	2.119
ABUW_RS01120		helix-turn-helix domain-containing protein	CDS	1.730	2.598	2.940	1.342	6.777	9.983	6.293
ABUW_RS04045		DcaP family trimeric outer membrane transporter	CDS	1.738	902.299	943.243	898.724	3357.746	2977.572	2818.685
ABUW_RS13515		DUF3237 domain-containing protein	CDS	1.770	0.070	0.717	0.553	2.186	1.345	1.092

ABUW_RS10965		PilZ domain-containing protein	CDS	1.795	14.605	15.774	14.526	53.198	56.714	46.043
ABUW_RS13585		hypothetical protein	CDS	1.795	1.896	2.581	2.289	9.401	7.364	6.807
ABUW_RS11280		PACE efflux transporter	CDS	1.830	5.617	7.385	5.447	17.636	25.277	22.797
ABUW_RS13505		acyl-CoA dehydrogenase family protein	CDS	1.830	2.598	2.366	2.526	10.275	9.275	7.192
ABUW_RS02445		DUF2147 domain-containing protein	CDS	1.837	28.087	36.855	25.026	117.254	112.153	92.342
ABUW_RS08020		hypothetical protein	CDS	1.843	0.983	0.287	0.000	1.676	1.699	1.413
ABUW_RS09775		hypothetical protein	CDS	1.853	0.772	0.430	0.079	1.457	1.487	1.862
ABUW_RS12685		hypothetical protein	CDS	1.856	2.949	4.302	3.474	15.085	11.045	12.779
ABUW_RS16510		fumarate hydratase	CDS	1.859	207.915	196.177	185.840	690.846	743.508	705.281
ABUW_RS01290		hypothetical protein	CDS	1.867	77.521	58.724	58.104	268.031	230.253	210.756
ABUW_RS07790		ion transporter	CDS	1.884	12.780	12.691	12.079	49.190	40.146	49.382
ABUW_RS02625		LemA family protein	CDS	1.912	50.136	49.976	47.762	192.533	176.230	187.959
ABUW_RS00595		DUF1311 domain-containing protein	CDS	1.928	3.160	2.438	3.789	12.316	8.780	14.577
ABUW_RS02595	radC	DNA repair protein RadC	CDS	2.021	4.564	3.227	5.447	20.186	15.789	17.724
ABUW_RS06060		AzlD domain-containing protein	CDS	2.026	0.281	0.215	0.553	1.603	1.416	1.284
ABUW_RS00400	hutG	formimidoylglutamase	CDS	2.032	8.988	10.325	10.895	51.813	37.313	34.484
ABUW_RS02690		hypothetical protein	CDS	2.080	0.351	0.574	0.395	2.405	1.558	1.734
ABUW_RS15500		hypothetical protein	CDS	2.100	4.283	2.868	2.368	15.376	11.966	13.742
ABUW_RS12885		hypothetical protein	CDS	2.110	30.755	22.873	20.763	122.866	95.018	103.644
ABUW_RS15495		hypothetical protein	CDS	2.123	7.092	4.302	6.947	27.474	25.348	27.099

ABUW_RS15505		hypothetical protein	CDS	2.123	1.896	1.291	1.342	6.559	5.664	7.642
ABUW_RS01845	aroE	shikimate dehydrogenase	CDS	2.126	33.494	30.617	33.394	134.161	151.095	140.504
ABUW_RS10105	antA	anthranilate 1,2-dioxygenase large subunit	CDS	2.169	38.479	46.965	51.236	213.230	205.613	195.922
ABUW_RS05570		EAL domain-containing protein	CDS	2.183	220.273	191.804	212.602	980.011	862.316	994.573
ABUW_RS07410		GNAT family N-acetyltransferase	CDS	2.253	1.053	0.430	0.395	2.696	3.186	3.275
ABUW_RS08735	cydB	cytochrome d ubiquinol oxidase subunit II	CDS	2.253	390.762	302.153	350.916	1859.528	1436.887	1679.434
ABUW_RS11825		LysE family translocator	CDS	2.311	6.109	13.767	19.894	57.571	81.282	57.987
ABUW_RS10115	antC	anthranilate 1,2-dioxygenase electron transfer component AntC	CDS	2.316	18.608	21.367	25.342	112.372	104.294	108.396
ABUW_RS13835		YraN family protein	CDS	2.360	3.932	3.155	3.316	17.636	19.188	16.760
ABUW_RS11250		fimbrial protein	CDS	2.370	3.581	4.230	2.053	21.279	17.488	12.650
ABUW_RS08615		PEGA domain-containing protein	CDS	2.381	15.869	21.224	17.684	99.254	110.454	75.839
ABUW_RS10005		hypothetical protein	CDS	2.408	0.772	1.362	1.342	7.798	3.894	6.807
ABUW_RS10110	antB	anthranilate 1,2-dioxygenase small subunit	CDS	2.416	9.690	13.767	11.131	67.481	56.360	60.941
ABUW_RS18520		hypothetical protein	CDS	2.471	5.407	8.676	3.553	24.850	14.869	58.372

ABUW_RS20675		A24 family peptidase	CDS	2.500	17.133	16.922	20.131	103.554	97.921	104.928
ABUW_RS08725		cyd operon YbgE family protein	CDS	2.518	20.504	13.337	14.447	111.206	78.450	87.333
ABUW_RS16315		DUF4124 domain-containing protein	CDS	2.538	1.404	1.793	1.816	11.004	9.275	8.926
ABUW_RS07785		hypothetical protein	CDS	2.562	4.564	5.664	4.500	34.324	24.286	28.576
ABUW_RS08740		cytochrome ubiquinol oxidase subunit I	CDS	2.569	436.123	363.961	381.153	2549.427	2123.398	2338.544
ABUW_RS13360		hypothetical protein	CDS	2.575	36.162	35.708	39.710	581.681	44.040	39.364
ABUW_RS01570		type IV pilin protein	CDS	2.607	17.625	16.563	15.158	110.841	97.992	92.150
ABUW_RS08730	cydX	cytochrome bd-I oxidase subunit CydX	CDS	2.669	3.932	3.155	3.868	28.057	21.737	20.035
ABUW_RS01850	hemF	oxygen-dependent coproporphyrinogen oxidase	CDS	2.678	109.961	116.229	132.472	828.797	789.601	676.834
ABUW_RS20670		prepilin peptidase	CDS	2.756	18.959	20.005	24.631	142.250	141.253	146.027
ABUW_RS17440		outer membrane beta-barrel protein	CDS	2.808	588.074	534.397	639.386	4039.701	4299.686	4002.694
ABUW_RS01565		prepilin-type N-terminal cleavage/methylation domain-containing protein	CDS	2.810	14.114	11.186	10.105	92.987	80.858	75.004
ABUW_RS03340		response regulator	CDS	3.026	60.247	67.974	87.236	588.385	587.882	578.134
ABUW_RS05525		hypothetical protein	CDS	3.042	4.915	4.087	4.105	35.635	42.199	30.438
ABUW_RS18120	dprA	DNA-processing protein DprA	CDS	3.084	16.010	15.416	14.605	130.226	130.845	129.459

ABUW_RS03335	pilG	twitching motility response regulator PilG	CDS	3.156	59.194	66.038	79.578	590.061	639.851	595.537
ABUW_RS06590	tadA	Flp pilus assembly complex ATPase component TadA	CDS	3.225	17.835	21.941	27.710	219.059	204.693	206.710
ABUW_RS01425		pilus assembly protein PilM	CDS	3.235	78.363	74.068	78.946	759.275	737.560	682.099
ABUW_RS03330		hypothetical protein	CDS	3.279	1.685	1.864	2.289	19.166	20.533	17.081
ABUW_RS06560	yegQ	tRNA 5-hydroxyuridine modification protein YegQ	CDS	3.283	22.399	26.243	37.499	276.411	289.020	272.596
ABUW_RS11235		type 1 fimbrial protein	CDS	3.315	2.809	3.800	3.000	42.631	29.242	24.145
ABUW_RS06555		YfhL family 4Fe-4S dicluster ferredoxin	CDS	3.324	1.404	1.434	1.895	18.219	16.072	13.228
ABUW_RS01560		VWA domain-containing protein	CDS	3.325	86.298	99.021	89.209	1062.868	871.450	817.209
ABUW_RS18115		LysM peptidoglycan-binding domain-containing protein	CDS	3.347	42.201	35.779	42.710	454.078	392.252	381.634
ABUW_RS00800		YkgJ family cysteine cluster protein	CDS	3.403	4.213	4.517	5.053	55.384	44.889	45.657
ABUW_RS13815		hypothetical protein	CDS	3.429	75.484	53.920	72.157	712.053	710.230	748.884
ABUW_RS02525		hypothetical protein	CDS	3.436	52.804	54.924	51.394	593.924	576.624	551.741
ABUW_RS03360		hypothetical protein	CDS	3.511	18.257	17.280	20.526	227.148	208.092	203.821
ABUW_RS14715		PilT/PilU family type 4a pilus ATPase	CDS	3.577	31.738	24.020	33.315	369.690	336.742	356.461

ABUW_RS08010		hypothetical protein	CDS	3.605	0.421	0.287	0.395	4.227	5.806	3.725
ABUW_RS01440		pilus assembly protein PilP	CDS	3.650	22.048	20.363	27.315	316.055	287.179	271.889
ABUW_RS17275		type II secretion system F family protein	CDS	3.671	39.533	34.202	47.605	528.337	518.990	498.186
ABUW_RS14710		type IV pilus twitching motility protein PilT	CDS	3.694	24.857	21.654	32.368	361.383	328.387	330.390
ABUW_RS08745		hypothetical protein	CDS	3.772	2.247	2.151	1.184	25.579	27.967	23.631
ABUW_RS17730		sigma-54 dependent transcriptional regulator	CDS	3.772	45.361	38.289	44.368	569.438	582.784	597.142
ABUW_RS03355		Hpt domain-containing protein	CDS	3.786	192.888	156.454	200.918	2754.494	2383.247	2454.132
ABUW_RS16790		hypothetical protein	CDS	3.828	35.811	40.512	40.026	577.746	559.985	515.395
ABUW_RS03350		methyl-accepting chemotaxis protein	CDS	3.850	207.704	204.853	253.970	3418.231	3030.533	3165.129
ABUW_RS00795		FprA family A-type flavoprotein	CDS	3.954	12.077	11.329	13.658	215.999	181.965	176.401
ABUW_RS09960		hypothetical protein	CDS	3.992	9.620	8.174	8.368	158.137	124.048	134.725
ABUW_RS03345		chemotaxis protein CheW	CDS	4.023	37.005	36.353	47.841	694.271	656.207	620.003
ABUW_RS17270	pilB	type IV-A pilus assembly ATPase PilB	CDS	4.054	38.901	40.082	52.578	728.668	747.119	708.942
ABUW_RS01430		PilN domain-containing protein	CDS	4.099	21.346	16.993	21.315	353.512	338.087	331.032
ABUW_RS01445		type IV pilus secretin PilQ	CDS	4.149	63.968	51.697	64.578	1184.860	1032.669	980.959

ABUW_RS01555		hypothetical protein	CDS	4.209	5.758	5.593	9.868	148.007	129.500	113.983
ABUW_RS01540		GspH/FimT family pseudopilin	CDS	4.320	1.053	0.860	2.210	34.834	24.781	22.347
ABUW_RS01545	pilV	type IV pilus modification protein PilV	CDS	4.362	3.722	2.940	3.868	78.995	73.140	64.794
ABUW_RS01435		type 4a pilus biogenesis protein PilO	CDS	4.379	13.061	10.970	10.974	252.727	247.104	229.314
ABUW_RS14740		bacteriohemerythrin	CDS	4.474	5.969	4.876	5.132	139.408	113.498	103.002
ABUW_RS01550		PilW family protein	CDS	4.721	6.530	5.163	6.395	171.546	157.892	148.274
ABUW_RS20665		hypothetical protein	CDS	5.330	1.475	1.577	0.711	3.352	4.956	145.192
ABUW_RS01495		pilin	CDS	5.631	41.148	28.466	42.315	2122.676	1818.305	1606.613
Ellagic Acid										
ABUW_RS05760	basE	(2,3-dihydroxybenzoyl)adenylate synthase BasE	CDS	-7.661	1730.448	1679.652	1420.077	7.798	7.080	8.926
ABUW_RS05755	basD	acinetobactin non-ribosomal peptide synthetase subunit BasD	CDS	-7.563	3172.103	3793.834	3592.983	12.607	13.736	29.282
ABUW_RS05765	basF	acinetobactin biosynthesis bifunctional isochorismatase/aryl carrier protein BasF	CDS	-7.461	1235.059	1261.473	1255.210	5.757	4.461	10.917

ABUW_RS05750	basC	putative histamine N-monooxygenase	CDS	-7.430	2622.782	2949.053	2677.997	13.263	11.753	22.668
ABUW_RS05770	basG	acinetobactin biosynthesis histidine decarboxylase BasG	CDS	-7.366	1425.793	1656.662	1589.839	7.287	7.080	13.806
ABUW_RS05800	basJ	acinetobactin biosynthesis isochorismate synthase BasJ	CDS	-6.937	1365.996	1849.897	1459.327	11.004	10.479	16.568
ABUW_RS05780	barA	acinetobactin export ABC transporter permease/ATP-binding subunit BarA	CDS	-6.929	3305.636	4062.876	3327.063	23.247	24.852	39.493
ABUW_RS05785	barB	acinetobactin export ABC transporter permease/ATP-binding subunit BarB	CDS	-6.801	3265.932	4068.623	3393.237	24.413	27.826	43.795
ABUW_RS20145		hypothetical protein	CDS	-6.619	89.118	98.797	44.407	0.291	0.637	1.349
ABUW_RS05710	bauF	acinetobactin utilization protein BauF	CDS	-6.469	395.023	421.152	360.679	3.862	3.823	5.523
ABUW_RS14490		transferrin-binding protein-like solute binding protein	CDS	-6.421	1179.204	1549.838	938.239	12.607	10.975	19.072
ABUW_RS02985		hypothetical protein	CDS	-6.324	2753.911	2462.103	2750.989	25.360	34.623	39.364
ABUW_RS14495		TonB-dependent receptor	CDS	-6.180	890.988	898.193	526.333	10.057	9.488	12.329

ABUW_RS05725	bauD	ferric acinetobactin ABC transporter permease subunit BauD	CDS	-5.960	146.031	133.084	131.037	0.874	2.053	3.532
ABUW_RS14485		porin family protein	CDS	-5.894	125.457	135.363	107.872	2.186	2.407	1.605
ABUW_RS05790	basH	acinetobactin biosynthesis thioesterase BasH	CDS	-5.852	338.110	416.693	382.096	7.943	4.177	7.513
ABUW_RS05715	basA	acinetobactin non-ribosomal peptide synthetase subunit BasA	CDS	-5.815	686.026	702.778	649.415	11.733	8.638	15.733
ABUW_RS05730	bauC	ferric acinetobactin ABC transporter permease subunit BauC	CDS	-5.750	130.937	145.173	121.072	1.530	1.062	4.624
ABUW_RS14160		TonB-dependent siderophore receptor	CDS	-5.750	3167.200	4657.245	2765.238	32.793	49.633	114.047
ABUW_RS10630		DHA2 family efflux MFS transporter permease subunit	CDS	-5.748	1341.289	1819.970	1373.397	19.312	19.825	45.015
ABUW_RS10640		siderophore biosynthesis protein	CDS	-5.595	1332.829	1443.015	1452.946	22.227	20.745	44.309
ABUW_RS14470		YbaN family protein	CDS	-5.531	191.022	99.491	80.598	2.769	2.053	3.147
ABUW_RS10525		hypothetical protein	CDS	-5.528	69.122	74.717	37.764	0.802	0.920	2.119
ABUW_RS10635		SidA/IucD/PvdA family monooxygenase	CDS	-5.475	1181.800	1357.694	1349.707	18.947	19.117	49.125

ABUW_RS10520		TonB-dependent siderophore receptor	CDS	-5.389	960.302	833.980	834.213	14.502	18.267	29.796
ABUW_RS05720	basB	acinetobactin non-ribosomal peptide synthetase subunit BasB	CDS	-5.379	823.981	973.802	1213.687	15.304	17.701	39.107
ABUW_RS05735	bauE	ferric acinetobactin ABC transporter ATP-binding protein BauE	CDS	-5.371	301.579	340.984	417.937	5.028	6.726	13.678
ABUW_RS18750		RcnB family protein	CDS	-5.297	3445.033	3628.842	2932.203	73.238	79.796	101.461
ABUW_RS10080		SDR family oxidoreductase	CDS	-5.249	1553.846	1523.975	1330.650	32.283	34.977	48.547
ABUW_RS05740	bauB	siderophore-binding periplasmic lipoprotein BauB	CDS	-5.211	1052.497	1298.634	1330.738	22.955	20.816	55.354
ABUW_RS10075		isochorismatase family protein	CDS	-5.203	657.378	581.487	643.646	13.336	14.515	23.118
ABUW_RS03435		sulfite reductase flavoprotein subunit alpha	CDS	-5.174	2939.261	2881.372	2751.252	68.866	72.998	95.425
ABUW_RS10585		acetyltransferase	CDS	-5.165	603.830	547.695	593.731	12.534	14.727	21.255
ABUW_RS16340		MacB family efflux pump subunit	CDS	-5.082	4637.407	4209.238	3073.206	111.206	119.233	121.496
ABUW_RS08385	fumC	class II fumarate hydratase	CDS	-5.067	3647.976	3889.758	3328.898	111.570	90.133	122.395

ABUW_RS10625		siderophore achromobactin biosynthesis protein AcsC	CDS	-5.067	2337.162	2858.481	2944.791	60.777	59.192	122.716
ABUW_RS10620		IucA/IucC family siderophore biosynthesis protein	CDS	-5.049	1556.057	1850.590	1772.277	39.498	39.721	76.995
ABUW_RS07630		hypothetical protein	CDS	-4.985	1383.589	1467.293	1270.333	42.048	39.579	48.483
ABUW_RS14475		biliverdin-producing heme oxygenase	CDS	-4.978	218.805	259.727	216.792	7.215	6.443	8.348
ABUW_RS05795	basI	acinetobactin biosynthesis phosphopantetheinyl transferase BasI	CDS	-4.932	39.223	49.944	62.590	1.676	0.779	2.440
ABUW_RS04555		transglycosylase SLT domain-containing protein	CDS	-4.926	462.318	339.993	313.387	11.295	12.320	13.036
ABUW_RS20335		hypothetical protein	CDS	-4.872	192.464	212.260	219.677	5.320	9.558	6.422
ABUW_RS02965		RcnB family protein	CDS	-4.845	1399.740	1332.623	1148.300	40.226	39.508	55.161
ABUW_RS14480		energy transducer TonB	CDS	-4.820	25.957	28.837	20.281	1.093	0.637	0.899
ABUW_RS10615		(2Fe-2S)-binding protein	CDS	-4.775	228.707	236.539	224.572	6.194	5.806	13.036
ABUW_RS16345	adeC	AdeC/AdeK/OprM family multidrug efflux complex outer membrane factor	CDS	-4.694	2403.688	2148.270	1762.312	80.817	82.840	80.334

ABUW_RS07640		hypothetical protein	CDS	-4.681	3105.481	3063.607	2033.389	98.453	108.188	112.955
ABUW_RS00710		TonB-dependent siderophore receptor	CDS	-4.629	544.226	385.973	409.545	11.587	14.090	28.255
ABUW_RS05745	bauA	TonB-dependent ferric acinetobactin receptor BauA	CDS	-4.619	1635.177	1959.000	2472.394	65.587	60.820	120.340
ABUW_RS01745		hypothetical protein	CDS	-4.598	719.001	800.882	741.028	24.704	34.340	34.227
ABUW_RS06610		hemin uptake protein HemP	CDS	-4.562	733.229	803.657	855.106	33.595	26.622	40.970
ABUW_RS08070		TonB-dependent siderophore receptor	CDS	-4.540	272.449	299.563	272.039	8.818	9.204	18.109
ABUW_RS10610		RraA family protein	CDS	-4.478	150.645	167.866	145.985	6.049	5.310	9.375
ABUW_RS01510		bacterioferritin-associated ferredoxin	CDS	-4.291	56.143	65.898	46.943	2.623	2.478	3.468
ABUW_RS07805		DUF4198 domain-containing protein	CDS	-4.267	243.897	210.279	250.098	10.129	11.258	15.091
ABUW_RS14500		FecR domain-containing protein	CDS	-4.206	47.299	50.935	38.463	2.769	1.770	2.825
ABUW_RS16335		MacA family efflux pump subunit	CDS	-4.194	2645.662	2476.967	2461.467	125.635	139.129	149.494
ABUW_RS14505		sigma-70 family RNA polymerase sigma factor	CDS	-4.186	43.838	47.466	44.058	1.749	2.266	3.339
ABUW_RS06655		alpha/beta hydrolase	CDS	-4.142	322.921	292.725	271.253	12.826	15.648	21.641
ABUW_RS16655		energy transducer TonB	CDS	-3.611	1114.120	1079.338	913.412	72.000	85.885	96.259

ABUW_RS10530		PepSY domain-containing protein	CDS	-3.606	153.337	176.983	154.290	8.891	10.691	20.035
ABUW_RS17465		hypothetical protein	CDS	-3.602	36.051	24.476	19.581	2.113	2.337	2.119
ABUW_RS05420		SIMPL domain-containing protein	CDS	-3.533	926.751	911.372	1039.467	80.016	82.486	85.985
ABUW_RS06730		hypothetical protein	CDS	-3.513	311.288	322.751	364.963	29.733	27.189	30.567
ABUW_RS18155		hypothetical protein	CDS	-3.471	277.737	249.817	289.348	23.976	24.710	24.980
ABUW_RS04525		multidrug efflux RND transporter permease subunit	CDS	-3.318	512.116	558.001	417.500	49.409	51.687	48.033
ABUW_RS17460		YMGG-like glycine zipper-containing protein	CDS	-3.306	47.972	39.043	34.617	4.008	3.753	4.495
ABUW_RS17690		ferrous iron transport protein A	CDS	-3.240	243.416	216.323	204.117	21.279	22.020	26.906
ABUW_RS04170	lolA	outer membrane lipoprotein chaperone LolA	CDS	-3.195	1312.256	1247.600	1114.557	125.635	134.102	141.339
ABUW_RS00825		putative porin	CDS	-3.122	16802.166	17248.989	16476.303	2093.745	1676.911	2032.235
ABUW_RS18745		RcnB family protein	CDS	-3.119	666.126	611.017	571.178	72.218	66.909	73.655
ABUW_RS16650		MotA/TolQ/ExbB proton channel family protein	CDS	-3.011	2100.667	2005.475	1854.536	186.776	235.422	316.969
ABUW_RS16845		DUF2061 domain-containing protein	CDS	-2.943	27.014	24.179	28.760	4.664	3.257	2.504

ABUW_RS12795		D-Ala-D-Ala carboxypeptidase family metallohydrolase	CDS	-2.783	568.644	530.354	444.949	67.992	70.379	85.856
ABUW_RS00790		TonB-dependent siderophore receptor	CDS	-2.766	280.236	275.582	279.557	33.303	42.128	47.263
ABUW_RS13315		M48 family metallopeptidase	CDS	-2.724	1761.019	2229.528	1551.201	299.585	259.707	279.595
ABUW_RS07625		LLM class flavin-dependent oxidoreductase	CDS	-2.712	67.007	83.140	55.160	9.619	11.329	10.339
ABUW_RS13205		O-methyltransferase	CDS	-2.681	422.710	21.107	25.263	25.069	23.294	24.723
ABUW_RS17685		ferrous iron transporter B	CDS	-2.641	3045.011	2998.105	2469.247	381.642	444.929	538.449
ABUW_RS10535		hypothetical protein	CDS	-2.629	11.632	16.549	13.462	1.239	2.195	3.211
ABUW_RS02995		response regulator	CDS	-2.626	605.080	552.155	469.163	86.429	87.513	89.453
ABUW_RS16645		biopolymer transporter ExbD	CDS	-2.620	737.171	672.455	667.248	91.093	104.860	141.660
ABUW_RS02990	baeS	sensor histidine kinase efflux regulator BaeS	CDS	-2.607	381.852	469.510	414.091	64.858	74.060	68.775
ABUW_RS18865		hypothetical protein	CDS	-2.525	24.034	23.882	34.704	5.684	4.248	4.431
ABUW_RS15005	lolB	lipoprotein insertase outer membrane protein LolB	CDS	-2.483	227.938	208.891	197.736	34.032	40.429	38.979
ABUW_RS02255		DUF3108 domain-containing protein	CDS	-2.467	875.607	940.704	885.964	164.623	153.998	170.236
ABUW_RS06025		OmpW family protein	CDS	-2.414	161.316	142.300	143.800	25.287	24.994	33.585

ABUW_RS01895		ABC transporter substrate-binding protein	CDS	-2.391	2105.859	2213.177	1829.098	372.605	404.359	394.798
ABUW_RS16090		NAD(P)(+) transhydrogenase (Re/Si-specific) subunit beta	CDS	-2.365	1023.464	708.427	516.892	117.473	158.458	160.475
ABUW_RS10070		transcriptional repressor	CDS	-2.344	15.574	11.792	13.724	3.206	1.770	3.082
ABUW_RS14775		OmpA family protein	CDS	-2.288	6096.367	6478.999	6386.457	1359.466	1239.628	1284.571
ABUW_RS10605		TonB-dependent receptor	CDS	-2.239	2139.795	2449.220	2716.198	387.034	438.840	721.721
ABUW_RS13745		TonB-dependent receptor	CDS	-2.226	294.945	271.915	278.159	53.781	53.669	73.142
ABUW_RS16100		Re/Si-specific NAD(P)(+) transhydrogenase subunit alpha	CDS	-2.120	409.251	480.708	694.872	94.736	136.368	133.440
ABUW_RS01140		hypothetical protein	CDS	-2.077	695.063	776.406	499.059	176.210	130.208	160.475
ABUW_RS10600		hypothetical protein	CDS	-1.967	17.785	16.152	12.675	2.915	3.328	5.587
ABUW_RS16095		proton-translocating transhydrogenase family protein	CDS	-1.967	61.335	109.995	63.726	18.583	22.445	19.072
ABUW_RS04980	carO	ornithine uptake porin CarO type 3	CDS	-1.966	2590.192	3146.945	2866.554	859.185	582.642	759.993

ABUW_RS18725		thiol:disulfide interchange protein DsbA/DsbL	CDS	-1.915	2827.744	2103.777	1585.818	611.851	536.549	579.675
ABUW_RS10595		PepSY domain-containing protein	CDS	-1.898	126.227	143.687	142.401	32.137	29.879	48.483
ABUW_RS13935		META and DUF4377 domain-containing protein	CDS	-1.891	2726.032	2327.929	2866.204	714.020	646.649	775.469
ABUW_RS14165	nfuA	Fe-S biogenesis protein NfuA	CDS	-1.876	547.014	649.366	669.958	203.392	146.917	158.228
ABUW_RS17680		hypothetical protein	CDS	-1.874	105.365	100.085	91.787	24.194	27.684	29.154
ABUW_RS18370		fatty acyl-AMP ligase	CDS	-1.832	38.358	3.666	3.584	4.008	4.177	4.559
ABUW_RS10590		hypothetical protein	CDS	-1.826	12.017	10.306	11.539	2.696	2.620	4.174
ABUW_RS01160	aqpZ	aquaporin Z	CDS	-1.818	155.163	168.956	117.837	51.522	32.853	40.905
ABUW_RS13135		heavy metal translocating P-type ATPase	CDS	-1.771	1306.392	1087.166	799.859	298.565	303.322	333.601
ABUW_RS01690		hypothetical protein	CDS	-1.752	125.265	161.524	166.615	47.587	42.482	44.566
ABUW_RS02205		hypothetical protein	CDS	-1.731	1218.043	1337.578	901.786	399.058	333.980	308.621
ABUW_RS18870		hypothetical protein	CDS	-1.708	44.319	52.124	40.124	13.555	14.090	14.127
ABUW_RS05475	sohB	protease SohB	CDS	-1.664	1416.083	2085.643	1850.952	558.580	526.283	603.949
ABUW_RS18755	argA	amino-acid N-acetyltransferase	CDS	-1.661	184.293	223.755	174.133	61.870	60.891	61.262
ABUW_RS20540		hypothetical protein	CDS	-1.613	8.941	9.315	4.021	1.093	2.337	3.725

ABUW_RS14650		DHA2 family efflux MFS transporter permease subunit	CDS	-1.606	84.888	199.378	69.146	34.324	39.721	41.933
ABUW_RS16850		LysR family transcriptional regulator	CDS	-1.582	144.108	161.425	135.408	40.809	54.023	52.336
ABUW_RS15450	bfmR	response regulator transcription factor BfmR	CDS	-1.560	2856.585	2774.052	1927.616	863.558	810.984	889.516
ABUW_RS08035		TonB-dependent receptor	CDS	-1.548	148.049	132.886	139.953	41.684	42.978	59.143
ABUW_RS01900		STAS domain-containing protein	CDS	-1.548	245.627	214.837	266.882	75.862	83.477	89.388
ABUW_RS02945		DUF4184 family protein	CDS	-1.494	44.126	38.746	32.169	12.972	14.090	13.742
ABUW_RS19720		Ig-like domain-containing protein	CDS	-1.481	2302.745	2780.692	1881.810	928.197	731.684	835.832
ABUW_RS10050	pqqC	pyrroloquinoline-quinone synthase PqqC	CDS	-1.456	169.680	181.442	156.563	55.311	62.024	67.683
ABUW_RS05520		hypothetical protein	CDS	-1.428	257.164	250.313	255.693	92.259	88.150	103.130
ABUW_RS05700		threo-3-hydroxy-L-aspartate ammonia-lyase	CDS	-1.389	35.186	43.007	32.956	13.044	14.302	15.026
ABUW_RS08765		TonB-dependent siderophore receptor	CDS	-1.378	123.919	85.816	93.011	29.805	45.456	41.162
ABUW_RS10700		Rrf2 family transcriptional regulator	CDS	-1.378	596.620	630.638	515.144	206.525	222.960	241.066

ABUW_RS16495	edd	phosphogluconate dehydratase	CDS	-1.344	3247.281	3022.383	2176.315	1037.945	1149.283	1140.086
ABUW_RS01890		outer membrane lipid asymmetry maintenance protein MlaD	CDS	-1.327	460.107	445.826	372.655	163.821	172.973	172.676
ABUW_RS14410		choline transporter	CDS	-1.320	569.029	527.579	444.512	158.574	218.146	240.424
ABUW_RS12640		chloride channel protein	CDS	-1.311	29.321	33.494	19.581	10.640	11.258	11.238
ABUW_RS01270		bifunctional SulP family inorganic anion transporter/carbonic anhydrase	CDS	-1.283	29.610	35.179	27.886	12.753	10.691	14.577
ABUW_RS04780	lolD	lipoprotein-releasing ABC transporter ATP-binding protein LolD	CDS	-1.276	207.654	212.756	154.727	78.413	78.663	80.334
ABUW_RS14640		tyrosine-type recombinase/integrase	CDS	-1.263	138.724	39.440	36.103	30.753	30.375	28.126
ABUW_RS16385		4'-phosphopantetheinyl transferase superfamily protein	CDS	-1.258	33.840	8.027	54.285	15.304	11.753	13.228
ABUW_RS15330		mechanosensitive ion channel	CDS	-1.253	685.738	808.909	593.469	393.156	191.099	291.925
ABUW_RS14450		basic amino acid/polyamine antiporter	CDS	-1.244	373.681	253.385	188.469	105.449	118.879	120.019

ABUW_RS16490	eda	bifunctional 4-hydroxy-2-oxoglutarate aldolase/2-dehydro-3-deoxy-phosphogluconate aldolase	CDS	-1.240	856.283	787.306	596.179	282.606	345.450	319.859
ABUW_RS06735		nitroreductase	CDS	-1.239	216.306	256.655	230.429	98.089	96.788	103.130
ABUW_RS08130		Lrp/AsnC family transcriptional regulator	CDS	-1.236	142.666	135.561	74.566	51.449	49.562	48.740
ABUW_RS10705		IscS subfamily cysteine desulfurase	CDS	-1.225	1008.755	935.551	856.854	366.629	391.898	439.621
ABUW_RS07895	eutC	ethanolamine ammonia-lyase subunit EutC	CDS	-1.221	15.382	17.044	8.916	5.466	6.231	5.972
ABUW_RS18765		sulfonate ABC transporter substrate-binding protein	CDS	-1.210	76.332	61.340	44.757	23.393	28.251	27.163
ABUW_RS14405		MarC family protein	CDS	-1.195	116.613	106.923	84.706	37.457	50.908	46.171
ABUW_RS14445		homocysteine S-methyltransferase family protein	CDS	-1.192	286.677	213.450	200.271	83.004	114.419	109.103
ABUW_RS12910		right-handed parallel beta-helix repeat-containing protein	CDS	-1.185	75.851	73.627	101.053	33.085	36.110	40.970
ABUW_RS13185		beta-ketoacyl-ACP synthase III	CDS	-1.173	1075.281	313.436	366.449	237.205	277.833	263.541
ABUW_RS08830		YnfA family protein	CDS	-1.172	31.436	31.611	29.459	12.534	14.232	14.256
ABUW_RS14440		hypothetical protein	CDS	-1.165	11.536	8.324	6.032	2.988	4.461	4.046

ABUW_RS14460		DUF1275 domain-containing protein	CDS	-1.158	25.380	29.530	22.379	11.514	8.921	14.127
ABUW_RS09185		alpha/beta hydrolase	CDS	-1.150	124.112	141.507	115.739	67.627	49.492	54.776
ABUW_RS01050		MFS transporter	CDS	-1.143	27.783	27.945	23.165	11.587	14.444	9.697
ABUW_RS15470		ribonucleotide-diphosphate reductase subunit beta	CDS	-1.137	2511.745	2413.051	2064.772	934.974	1136.751	1106.244
ABUW_RS06740		NAD(P)H-dependent glycerol-3-phosphate dehydrogenase	CDS	-1.131	257.356	289.257	282.180	126.801	122.348	129.266
ABUW_RS04130	adeJ	multidrug efflux RND transporter permease subunit AdeJ	CDS	-1.119	3966.955	4249.372	3672.619	1735.205	1806.481	1930.517
ABUW_RS01640		hypothetical protein	CDS	-1.118	67.199	68.474	77.276	32.720	32.570	32.814
ABUW_RS12115		NAD(P)H-dependent oxidoreductase	CDS	-1.109	57.874	32.503	21.067	15.012	15.010	21.512
ABUW_RS10065		5'-nucleotidase C-terminal domain-containing protein	CDS	-1.109	12.209	13.972	11.364	5.028	6.302	6.036
ABUW_RS20615		stress-induced protein	CDS	-1.105	32.975	39.043	25.263	17.344	12.674	15.155
ABUW_RS07200	gltS	sodium/glutamate symporter	CDS	-1.104	1184.876	1178.135	953.362	506.256	512.618	524.193
ABUW_RS03110		hemolysin III family protein	CDS	-1.104	1122.868	1190.224	796.187	482.281	502.280	462.161
ABUW_RS07795		MFS transporter	CDS	-1.103	115.748	99.986	91.700	41.320	55.439	46.364

ABUW_RS05270		rRNA large subunit pseudouridine synthase E	CDS	-1.100	261.298	233.764	194.851	99.254	111.091	111.414
ABUW_RS03005		acyl-CoA desaturase	CDS	-1.081	1812.452	1828.790	1626.816	781.356	805.036	903.901
ABUW_RS07065		M48 family metalloprotease	CDS	-1.078	103.635	119.805	112.854	56.332	49.208	53.749
ABUW_RS01885	mlaE	lipid asymmetry maintenance ABC transporter permease subunit MlaE	CDS	-1.075	442.226	435.719	304.908	181.967	185.647	193.867
ABUW_RS18775	ssuC	aliphatic sulfonate ABC transporter permease SsuC	CDS	-1.074	47.683	29.530	27.099	15.741	17.984	15.797
ABUW_RS16170		DUF932 domain-containing protein	CDS	-1.066	11.152	13.080	16.522	6.704	6.160	6.614
ABUW_RS04775		lipoprotein-releasing ABC transporter permease subunit	CDS	-1.064	503.945	454.051	401.503	217.019	215.455	217.820
ABUW_RS15065	ribB	3,4-dihydroxy-2-butanone-4-phosphate synthase	CDS	-1.063	166.604	174.605	155.514	77.975	80.220	79.563
ABUW_RS08150	aceI	chlorhexidine efflux PACE transporter AceI	CDS	-1.055	0.961	2.279	1.923	0.656	0.566	1.220
ABUW_RS09260		sorbosone dehydrogenase family protein	CDS	-1.053	63.065	63.222	71.681	36.510	25.914	33.007

ABUW_RS14240		galactose mutarotase	CDS	-1.049	100.943	114.751	127.365	64.712	42.624	58.501
ABUW_RS04135	adeI	multidrug efflux RND transporter periplasmic adaptor subunit AdeI	CDS	-1.044	1366.092	1357.199	1337.643	632.620	641.763	694.943
ABUW_RS12745		DUF2147 domain-containing protein	CDS	-1.037	199.482	167.866	111.718	82.493	65.210	85.664
ABUW_RS10055	pqqB	pyrroloquinoline quinone biosynthesis protein PqqB	CDS	-1.037	165.546	166.479	169.325	69.595	85.177	89.581
ABUW_RS02250		xanthine phosphoribosyltransferase	CDS	-1.022	191.599	176.091	195.463	81.255	102.382	93.691
ABUW_RS18760		sulfonate ABC transporter substrate-binding protein	CDS	-1.018	25.668	20.413	28.585	10.785	14.161	11.944
ABUW_RS18770	ssuD	FMNH2-dependent alkanesulfonate monooxygenase	CDS	-1.013	75.082	61.042	46.068	30.170	27.330	32.686
ABUW_RS00880	sfnG	dimethyl sulfone monooxygenase SfnG	CDS	-1.013	42.300	32.899	28.061	16.324	18.763	16.054
ABUW_RS04865	pal	peptidoglycan-associated lipoprotein Pal	CDS	-1.011	802.062	955.172	834.563	432.508	412.714	440.648
ABUW_RS16485		gluconate:H+ symporter	CDS	-1.011	1393.779	1429.439	982.996	569.001	688.494	631.626
ABUW_RS13735	rnt	ribonuclease T	CDS	-1.007	197.656	207.405	175.444	85.554	103.019	100.241
ABUW_RS05160		hypothetical protein	CDS	1.001	11.344	8.225	13.025	21.425	20.179	23.760

ABUW_RS13625		cache domain-containing protein	CDS	1.002	6.249	6.342	5.420	12.972	10.762	12.329
ABUW_RS18790		5'-nucleosidase	CDS	1.002	6.537	6.441	10.840	15.887	17.064	14.962
ABUW_RS16445		glycosyltransferase family 1 protein	CDS	1.003	4.134	4.955	5.682	9.619	9.134	10.917
ABUW_RS17810		ATP-binding protein	CDS	1.008	51.433	41.719	51.401	104.647	93.815	92.342
ABUW_RS08315		molybdopterin-dependent oxidoreductase	CDS	1.010	9.133	9.612	8.829	20.186	16.780	18.558
ABUW_RS04275		succinate dehydrogenase iron-sulfur subunit	CDS	1.012	537.400	524.210	552.208	991.087	1137.034	1127.371
ABUW_RS04355		metalloprotease	CDS	1.014	17.497	15.756	18.183	39.862	29.454	34.612
ABUW_RS09325		hypothetical protein	CDS	1.014	5.480	4.558	6.294	11.660	10.762	10.660
ABUW_RS04920		multidrug effflux MFS transporter	CDS	1.018	19.804	28.539	22.553	63.765	40.570	39.300
ABUW_RS11340		amino acid ABC transporter permease	CDS	1.021	60.085	54.997	46.156	133.505	89.637	104.094
ABUW_RS18720		TetR/AcrR family transcriptional regulator	CDS	1.024	27.687	28.837	29.722	63.036	59.404	52.978
ABUW_RS12775		Lrp/AsnC family transcriptional regulator	CDS	1.027	1.634	2.081	2.273	3.206	3.611	5.394
ABUW_RS02730		TraR/DksA C4-type zinc finger protein	CDS	1.027	1.057	1.189	1.136	2.186	2.691	2.055
ABUW_RS12360	abaF	fosfomycin efflux MFS transporter AbaF	CDS	1.028	0.769	0.991	1.224	2.113	1.912	2.119

ABUW_RS12000		MFS transporter	CDS	1.031	1.730	1.586	1.836	3.279	4.885	2.440
ABUW_RS04015		MmcQ/YjbR family DNA-binding protein	CDS	1.033	1.057	1.189	2.710	2.259	4.107	3.917
ABUW_RS02365		acyl-CoA dehydrogenase family protein	CDS	1.038	8.075	8.819	8.130	18.656	17.418	15.348
ABUW_RS02520		dihydrolipoyl dehydrogenase	CDS	1.038	64.988	73.627	87.591	157.117	140.687	166.832
ABUW_RS00100		glutathione S-transferase family protein	CDS	1.040	17.208	17.441	19.669	39.279	33.490	38.979
ABUW_RS06065		DUF962 domain-containing protein	CDS	1.045	3.461	4.360	3.322	9.109	6.160	7.706
ABUW_RS07450		hypothetical protein	CDS	1.046	26.918	36.962	58.307	102.388	69.387	80.848
ABUW_RS08285		ANTAR domain-containing protein	CDS	1.048	0.577	1.090	0.524	1.968	1.416	1.156
ABUW_RS00585		hypothetical protein	CDS	1.049	11.056	13.180	13.025	26.162	24.002	26.971
ABUW_RS02160		TRAP transporter large permease subunit	CDS	1.049	52.394	56.286	59.968	138.825	104.081	106.277
ABUW_RS02150		hypothetical protein	CDS	1.051	52.971	56.385	50.090	129.716	97.567	103.002
ABUW_RS17910		heteromeric transposase endonuclease subunit TnsA	CDS	1.051	11.248	14.963	19.669	33.741	31.578	29.925
ABUW_RS11645	madM	malonate transporter subunit MadM	CDS	1.051	2.500	3.171	2.448	6.121	5.310	5.394

ABUW_RS10460		class I SAM-dependent methyltransferase	CDS	1.052	0.769	0.991	1.399	2.259	2.053	2.312
ABUW_RS04600		hypothetical protein	CDS	1.054	1.730	1.784	2.885	4.664	4.177	4.559
ABUW_RS15360		cold shock domain-containing protein	CDS	1.054	16.343	15.756	19.494	53.562	28.605	25.173
ABUW_RS00375		HutD family protein	CDS	1.054	22.015	20.116	18.707	39.643	42.624	44.052
ABUW_RS14330		hypothetical protein	CDS	1.054	0.288	0.694	0.612	1.676	1.133	0.578
ABUW_RS04350		CapA family protein	CDS	1.057	22.015	23.981	23.865	52.761	44.181	48.483
ABUW_RS18405		acyl-CoA dehydrogenase family protein	CDS	1.058	18.074	19.423	20.281	53.417	33.632	33.328
ABUW_RS16880	hcaR	DNA-binding transcriptional regulator HcaR	CDS	1.059	32.398	37.160	48.166	85.336	84.610	75.518
ABUW_RS16210		hypothetical protein	CDS	1.064	30.764	32.206	35.928	68.210	69.529	69.096
ABUW_RS16975		type B 50S ribosomal protein L31	CDS	1.064	1.538	1.784	2.273	4.883	3.186	3.725
ABUW_RS20445		hypothetical protein	CDS	1.067	4.326	4.459	4.983	11.295	10.337	7.321
ABUW_RS18385	abaI	acyl-homoserine-lactone synthase AbaI	CDS	1.068	0.769	1.288	0.262	1.968	1.699	1.156
ABUW_RS17035		electron transfer flavoprotein-ubiquinone oxidoreductase	CDS	1.069	382.044	344.849	358.319	734.716	762.483	779.322
ABUW_RS10670		alkane 1-monooxygenase	CDS	1.072	2.500	2.874	3.584	6.777	5.593	6.550
ABUW_RS05910		hypothetical protein	CDS	1.075	87.580	100.383	100.441	273.424	146.917	187.253

ABUW_RS10355		thiamine pyrophosphate-dependent dehydrogenase E1 component subunit alpha	CDS	1.078	5.287	4.558	3.584	9.765	9.771	8.798
ABUW_RS16160		copper resistance protein CopC	CDS	1.080	0.865	0.793	2.011	3.935	2.620	1.413
ABUW_RS01215		DUF805 domain-containing protein	CDS	1.081	53.644	45.187	59.618	131.829	100.045	103.452
ABUW_RS08420		protein tyrosine phosphatase family protein	CDS	1.082	3.653	5.054	4.021	8.818	10.833	7.321
ABUW_RS15545		AraC family transcriptional regulator	CDS	1.082	7.883	7.135	9.441	20.405	15.152	16.375
ABUW_RS03655		hypothetical protein	CDS	1.088	1.634	1.685	1.311	4.372	3.399	2.119
ABUW_RS12630		hypothetical protein	CDS	1.088	2.596	2.576	1.399	4.372	4.319	5.201
ABUW_RS11835		hypothetical protein	CDS	1.089	3.653	3.270	5.682	10.202	8.001	8.798
ABUW_RS20265		hypothetical protein	CDS	1.090	5.672	6.639	8.654	15.231	15.152	14.384
ABUW_RS04260	sdhC	succinate dehydrogenase, cytochrome b556 subunit	CDS	1.090	437.996	305.608	324.489	671.607	869.397	733.279
ABUW_RS11335		amino acid ABC transporter permease	CDS	1.091	30.860	29.035	26.575	74.259	50.837	59.143
ABUW_RS13470		PDR/VanB family oxidoreductase	CDS	1.095	2.884	3.468	3.759	7.069	7.010	7.577

ABUW_RS03460		hypothetical protein	CDS	1.103	20.573	17.342	29.547	47.150	51.403	46.621
ABUW_RS02675		hypothetical protein	CDS	1.110	1.057	1.586	2.098	2.551	3.045	4.688
ABUW_RS07140		amino acid permease	CDS	1.111	10.287	6.540	6.818	21.425	11.612	18.045
ABUW_RS04895		M20 family metallopeptidase	CDS	1.114	3.845	1.883	2.622	5.976	6.302	5.844
ABUW_RS20685		hypothetical protein	CDS	1.114	0.385	0.297	0.350	0.510	0.779	0.963
ABUW_RS08610		MarR family transcriptional regulator	CDS	1.114	11.248	11.891	18.095	33.814	27.189	28.512
ABUW_RS12285	pcaF	3-oxoadipyl-CoA thiolase	CDS	1.121	59.220	54.007	47.117	140.137	83.265	125.221
ABUW_RS14570		hypothetical protein	CDS	1.126	18.939	16.053	19.581	38.915	40.712	39.557
ABUW_RS03310		YegP family protein	CDS	1.127	9.133	13.080	20.368	42.996	22.303	28.062
ABUW_RS15235		hypothetical protein	CDS	1.129	35.378	36.070	39.425	124.250	60.749	57.666
ABUW_RS11940		enoyl-CoA hydratase/isomerase family protein	CDS	1.132	56.047	70.853	52.450	150.704	110.595	131.642
ABUW_RS15790	raiA	ribosome-associated translation inhibitor RaiA	CDS	1.132	25.188	25.963	43.883	70.323	73.211	65.115
ABUW_RS14045		CitMHS family transporter	CDS	1.133	162.181	144.876	115.215	354.241	301.198	270.798
ABUW_RS11515		chromate transporter	CDS	1.134	1.923	1.090	1.049	2.696	3.399	2.825
ABUW_RS13500		feruloyl-CoA synthase	CDS	1.137	28.649	28.440	26.137	72.801	60.820	49.510
ABUW_RS12505		hypothetical protein	CDS	1.140	7.787	6.738	11.801	22.154	18.905	17.210
ABUW_RS11935		methylcrotonoyl-CoA carboxylase	CDS	1.147	155.260	165.191	125.617	378.362	284.489	325.188

ABUW_RS00410		HAD family hydrolase	CDS	1.153	7.979	9.216	13.987	25.069	22.586	21.898
ABUW_RS07445		dicarboxylate/amino acid:cation symporter	CDS	1.153	28.552	20.513	22.379	69.740	44.465	44.758
ABUW_RS08685		CBS domain-containing protein	CDS	1.154	51.913	56.781	77.101	158.865	117.605	137.293
ABUW_RS00430		ATP-binding protein	CDS	1.158	64.219	64.213	92.661	167.902	162.919	162.915
ABUW_RS16030	mazG	nucleoside triphosphate pyrophosphohydrolase	CDS	1.161	2.884	1.090	4.109	5.830	7.151	5.330
ABUW_RS08395		hypothetical protein	CDS	1.162	7.787	6.243	8.742	16.615	17.630	16.825
ABUW_RS12625		hypothetical protein	CDS	1.163	38.070	26.161	43.358	78.413	79.158	83.609
ABUW_RS04560	greB	transcription elongation factor GreB	CDS	1.164	6.345	5.648	8.654	15.085	17.701	13.678
ABUW_RS15245		hypothetical protein	CDS	1.166	28.745	31.413	32.082	82.931	64.360	59.785
ABUW_RS13225		glutathione binding-like protein	CDS	1.166	91.425	90.771	120.023	242.816	200.728	234.837
ABUW_RS17285	coaE	dephospho-CoA kinase	CDS	1.168	39.993	40.331	41.435	88.251	87.726	97.608
ABUW_RS06820		hypothetical protein	CDS	1.169	0.192	0.595	0.962	1.968	1.062	1.027
ABUW_RS13510		OprD family porin	CDS	1.173	1.346	1.685	2.622	4.154	4.744	3.981
ABUW_RS05480	blp2	Ig-like repeat protein Blp2	CDS	1.173	146.127	139.723	159.797	440.159	261.973	303.227
ABUW_RS02230		helix-turn-helix transcriptional regulator	CDS	1.175	3.172	2.279	5.158	8.526	8.142	7.513
ABUW_RS10945	gspI	type II secretion system minor pseudopilin GspI	CDS	1.176	3.653	2.676	3.409	9.474	7.647	5.009
ABUW_RS11445		LysE family translocator	CDS	1.178	1.442	2.477	1.486	3.571	4.390	4.238
ABUW_RS12965		hypothetical protein	CDS	1.179	0.481	0.198	1.224	1.020	1.558	1.862

ABUW_RS12740		exo-alpha-sialidase	CDS	1.183	17.016	14.567	15.910	34.251	36.818	36.796
ABUW_RS00635		ion channel protein Tsx	CDS	1.183	42.204	36.368	48.866	93.279	113.144	83.159
ABUW_RS05115		GFA family protein	CDS	1.184	2.500	4.856	3.147	8.672	6.797	8.348
ABUW_RS05940		superoxide dismutase	CDS	1.187	640.073	580.793	836.224	1545.295	1557.182	1582.404
ABUW_RS12790		ferredoxin family protein	CDS	1.190	23.938	19.125	22.379	42.923	51.828	54.583
ABUW_RS03910		hypothetical protein	CDS	1.190	34.993	30.917	40.911	73.530	86.947	83.416
ABUW_RS11270		hypothetical protein	CDS	1.195	5.287	4.459	5.857	14.866	9.417	11.559
ABUW_RS15240		hypothetical protein	CDS	1.198	8.748	7.432	7.605	19.166	18.480	16.953
ABUW_RS06160		hypothetical protein	CDS	1.201	0.481	0.793	1.661	3.425	1.770	1.734
ABUW_RS02360		DUF4256 domain-containing protein	CDS	1.213	3.942	3.468	3.759	10.931	7.718	7.321
ABUW_RS09490		hypothetical protein	CDS	1.214	1.730	2.874	2.885	7.215	5.310	4.945
ABUW_RS18625		hypothetical protein	CDS	1.215	167.373	163.605	207.876	420.775	418.166	412.458
ABUW_RS09775		hypothetical protein	CDS	1.216	0.577	0.495	0.962	1.457	1.487	1.862
ABUW_RS13295		GNAT family N-acetyltransferase	CDS	1.218	2.980	2.576	2.885	7.142	5.877	6.678
ABUW_RS16820		hypothetical protein	CDS	1.219	8.460	5.847	9.354	21.425	17.842	15.990
ABUW_RS01345		hypothetical protein	CDS	1.220	13.267	12.882	14.511	31.773	31.437	31.594
ABUW_RS02235		DMT family transporter	CDS	1.220	3.365	4.856	3.934	7.652	9.983	10.660
ABUW_RS06595		NirD/YgiW/YdeI family stress tolerance protein	CDS	1.222	11.729	15.954	15.385	33.231	32.924	34.355
ABUW_RS11540		DUF1427 family protein	CDS	1.222	0.385	0.892	1.049	1.603	1.699	2.183
ABUW_RS18025		esterase-like activity of phytase family protein	CDS	1.224	2.307	2.874	2.185	5.684	5.735	5.779
ABUW_RS05820		DUF3015 family protein	CDS	1.227	773.991	680.779	696.096	2140.093	1490.768	1404.013

ABUW_RS11070		metalloregulator ArsR/SmtB family transcription factor	CDS	1.234	2.211	1.486	3.846	5.174	6.089	6.678
ABUW_RS17640		hypothetical protein	CDS	1.234	7.979	7.432	12.326	23.757	17.064	24.659
ABUW_RS03285		SRPBCC family protein	CDS	1.235	7.114	6.937	8.042	22.227	13.453	16.439
ABUW_RS10365		transcriptional regulator	CDS	1.241	7.595	7.928	8.829	20.623	18.409	18.623
ABUW_RS13845		hypothetical protein	CDS	1.246	1.250	0.198	1.136	2.186	2.478	1.605
ABUW_RS10495		porin	CDS	1.249	2.884	3.964	3.409	7.798	7.788	8.798
ABUW_RS01615		hemerythrin domain-containing protein	CDS	1.250	5.191	7.234	12.763	24.048	15.364	20.806
ABUW_RS10830		TonB-dependent receptor	CDS	1.251	13.267	15.261	17.308	44.890	30.233	34.099
ABUW_RS01790		hypothetical protein	CDS	1.251	17.304	11.990	12.238	27.692	34.269	36.860
ABUW_RS03875		hypothetical protein	CDS	1.253	0.769	0.793	0.262	1.968	1.487	0.899
ABUW_RS11400		Crp/Fnr family transcriptional regulator	CDS	1.256	2.692	1.387	2.710	5.247	6.089	5.009
ABUW_RS00400	hutG	formimidoylglutamase	CDS	1.256	21.054	14.567	16.085	51.813	37.313	34.484
ABUW_RS07245		TetR/AcrR family transcriptional regulator	CDS	1.258	0.865	1.883	1.573	4.227	2.620	3.532
ABUW_RS00420		hypothetical protein	CDS	1.258	0.673	0.297	0.350	1.385	0.920	0.899
ABUW_RS16815		lysozyme inhibitor LprI family protein	CDS	1.259	6.249	6.937	7.168	17.490	14.586	16.696
ABUW_RS12300		enoyl-CoA hydratase-related protein	CDS	1.261	54.028	49.151	56.209	149.756	81.495	150.714
ABUW_RS11875		hypothetical protein	CDS	1.264	0.385	0.297	0.699	1.603	1.204	0.642

ABUW_RS12690		RHS domain-containing protein	CDS	1.267	6.345	7.234	8.392	20.623	15.364	17.017
ABUW_RS16270		hypothetical protein	CDS	1.269	21.534	19.125	20.543	102.607	23.790	21.320
ABUW_RS00395	hutI	imidazolonepropionase	CDS	1.277	57.201	50.835	41.960	145.311	106.701	111.478
ABUW_RS11140		hypothetical protein	CDS	1.278	4.518	6.838	9.266	20.332	16.780	13.164
ABUW_RS07965		fimbria/pilus periplasmic chaperone	CDS	1.280	2.788	2.973	4.546	9.984	6.089	9.119
ABUW_RS16465		alpha/beta hydrolase	CDS	1.281	41.242	42.313	38.900	108.145	91.053	98.314
ABUW_RS11950		hydroxymethylglutaryl-CoA lyase	CDS	1.281	37.108	44.890	38.026	115.214	74.698	101.718
ABUW_RS07180		hypothetical protein	CDS	1.284	4.999	2.180	5.682	9.109	10.337	12.073
ABUW_RS13750		hypothetical protein	CDS	1.286	0.769	1.189	0.874	2.769	1.982	2.183
ABUW_RS12515	tssF	type VI secretion system baseplate subunit TssF	CDS	1.288	19.035	16.945	16.609	45.473	44.181	38.786
ABUW_RS09540		endonuclease/exonuclease/phosphatase family protein	CDS	1.292	4.518	8.225	13.637	23.028	21.099	20.806
ABUW_RS12135		hypothetical protein	CDS	1.294	0.385	0.595	0.524	1.020	1.487	1.220
ABUW_RS09550		GNAT family N-acetyltransferase	CDS	1.301	4.807	3.964	5.332	12.534	10.975	11.366
ABUW_RS15750		C39 family peptidase	CDS	1.303	5.095	3.369	5.070	11.733	11.470	10.339
ABUW_RS18495		IS256-like element ISAba26 family transposase	CDS	1.304	0.385	0.892	2.098	2.405	2.903	3.211

ABUW_RS18145		AraC family transcriptional regulator	CDS	1.307	3.076	3.964	2.885	7.652	9.771	7.128
ABUW_RS12295	paaG	2-(1,2-epoxy-1,2-dihydrophenyl)acetyl-CoA isomerase PaaG	CDS	1.308	43.453	47.962	50.876	134.890	74.769	142.816
ABUW_RS00910		cation acetate symporter	CDS	1.310	261.490	269.240	276.410	783.979	662.296	554.567
ABUW_RS04825	rbtA	rhombotarget A	CDS	1.310	32.879	33.296	32.169	88.323	80.433	75.197
ABUW_RS09140		muconate/chloromuconate family cycloisomerase	CDS	1.312	10.863	8.919	9.091	33.814	23.932	14.063
ABUW_RS13585		hypothetical protein	CDS	1.318	1.827	3.270	4.283	9.401	7.364	6.807
ABUW_RS06435		hypothetical protein	CDS	1.322	28.552	31.215	27.274	74.186	70.166	73.270
ABUW_RS12305	paaK	phenylacetate-CoA oxygenase/reductase subunit PaaK	CDS	1.323	101.039	95.230	120.460	292.735	191.382	308.428
ABUW_RS06060		AzlD domain-containing protein	CDS	1.323	0.865	0.595	0.262	1.603	1.416	1.284
ABUW_RS16520		DUF2846 domain-containing protein	CDS	1.323	13.074	10.603	12.238	33.959	30.091	25.943
ABUW_RS13505		acyl-CoA dehydrogenase family protein	CDS	1.326	2.500	4.657	3.497	10.275	9.275	7.192
ABUW_RS04860		NF038105 family protein	CDS	1.331	3.269	2.775	4.458	10.202	8.709	7.706
ABUW_RS09675		major capsid protein	CDS	1.333	3.461	3.468	6.906	12.243	12.886	10.018
ABUW_RS10230		MFS transporter	CDS	1.333	18.939	16.549	14.686	44.890	43.969	37.566

ABUW_RS18630		oligosaccharide flippase family protein	CDS	1.336	62.777	54.997	58.569	144.509	141.890	158.870
ABUW_RS09205		MerR family transcriptional regulator	CDS	1.348	2.692	4.063	3.497	9.911	8.072	8.155
ABUW_RS11225		hypothetical protein	CDS	1.348	0.288	0.694	0.524	1.385	1.274	1.220
ABUW_RS00045		DUF6091 family protein	CDS	1.349	86.330	79.375	76.402	243.035	189.966	183.978
ABUW_RS12105	pobA	4-hydroxybenzoate 3-monooxygenase	CDS	1.351	2.307	2.279	1.486	5.393	4.602	5.458
ABUW_RS13065		N-acetylmuramidase	CDS	1.352	0.961	2.081	2.885	6.267	3.823	5.201
ABUW_RS00370	hutC	histidine utilization repressor	CDS	1.355	41.435	35.476	42.397	103.117	97.780	104.351
ABUW_RS04495		Ig-like domain-containing protein	CDS	1.355	432.035	435.322	542.942	1400.275	1060.991	1145.930
ABUW_RS09690		zonular occludens toxin	CDS	1.357	14.228	11.891	18.707	35.271	39.792	40.006
ABUW_RS10025		hypothetical protein	CDS	1.364	0.673	0.297	0.262	1.603	0.779	0.835
ABUW_RS07145		DUF2171 domain-containing protein	CDS	1.371	0.288	0.297	0.962	1.457	1.416	1.284
ABUW_RS15945		hypothetical protein	CDS	1.373	5.384	2.576	4.720	10.494	11.045	11.430
ABUW_RS13000		hypothetical protein	CDS	1.375	3.845	5.648	3.671	14.575	9.983	9.568
ABUW_RS09525		DEAD/DEAH box helicase family protein	CDS	1.377	25.284	26.359	45.806	100.129	73.069	80.334
ABUW_RS15195		GntR family transcriptional regulator	CDS	1.377	5.768	4.955	7.168	14.210	15.718	16.696
ABUW_RS13320		hypothetical protein	CDS	1.381	3.269	4.657	4.895	11.223	11.683	10.596
ABUW_RS02155	rrtA	rhombosortase	CDS	1.382	11.632	12.981	11.714	34.324	29.667	30.695
ABUW_RS08540		hypothetical protein	CDS	1.382	8.845	5.847	12.238	27.765	23.507	19.265

ABUW_RS15355		excalibur calcium-binding domain-containing protein	CDS	1.385	4.807	5.549	7.081	15.376	14.444	15.861
ABUW_RS07860	hfq	RNA chaperone Hfq	CDS	1.387	63.065	66.691	99.130	175.627	224.660	198.619
ABUW_RS11425		tautomerase family protein	CDS	1.387	11.536	12.981	17.920	46.056	31.012	34.227
ABUW_RS05415		TetR/AcrR family transcriptional regulator	CDS	1.387	4.518	5.946	5.595	14.575	13.948	13.550
ABUW_RS05675		TetR/AcrR family transcriptional regulator	CDS	1.392	0.961	0.892	1.224	3.134	2.407	2.633
ABUW_RS13030		minor capsid protein	CDS	1.398	1.730	7.531	4.633	12.826	11.612	12.137
ABUW_RS06550	abeS	multidrug efflux SMR transporter AbeS	CDS	1.408	2.596	2.676	3.584	9.911	7.010	6.743
ABUW_RS06780		hypothetical protein	CDS	1.408	0.481	0.198	0.437	0.510	1.558	0.963
ABUW_RS06825		hypothetical protein	CDS	1.415	8.556	6.441	9.354	19.020	20.816	25.237
ABUW_RS02355		GFA family protein	CDS	1.419	1.154	0.694	1.399	3.061	3.186	2.569
ABUW_RS08955	aroD	type I 3-dehydroquinate dehydratase	CDS	1.421	1.538	2.378	1.923	6.850	3.823	5.009
ABUW_RS02700		hypothetical protein	CDS	1.423	9.325	8.423	12.238	30.388	25.418	24.851
ABUW_RS12280	paaF	phenylacetate--CoA ligase	CDS	1.425	37.205	30.026	34.442	109.821	72.361	90.994
ABUW_RS13110		LysE family transporter	CDS	1.426	8.748	7.630	12.326	26.235	24.427	26.714
ABUW_RS06315		hypothetical protein	CDS	1.429	5.480	5.054	8.567	17.854	17.064	16.760
ABUW_RS05165		hypothetical protein	CDS	1.432	2.403	4.063	4.808	9.765	8.567	12.201
ABUW_RS15335		hypothetical protein	CDS	1.436	6.153	9.513	14.861	14.283	58.130	10.596

ABUW_RS00590		DUF5991 domain-containing protein	CDS	1.444	10.575	9.414	11.277	29.150	28.746	27.292
ABUW_RS20660		urease subunit beta	CDS	1.445	0.865	1.486	1.661	3.717	4.107	3.211
ABUW_RS04730		ChbG/HpnK family deacetylase	CDS	1.446	0.769	0.793	0.612	1.530	2.620	1.798
ABUW_RS20630		hypothetical protein	CDS	1.448	1.346	2.576	3.234	7.943	5.523	6.229
ABUW_RS02720		hypothetical protein	CDS	1.451	23.361	23.287	44.233	90.072	75.547	83.352
ABUW_RS01595		triacylglycerol lipase	CDS	1.458	3.076	3.766	2.972	12.170	7.576	7.256
ABUW_RS13010		DUF4142 domain-containing protein	CDS	1.465	2.500	2.477	2.185	7.287	6.160	6.357
ABUW_RS09135	catC	muconolactone Delta-isomerase	CDS	1.471	3.365	1.883	1.573	9.036	6.656	3.275
ABUW_RS08700		hypothetical protein	CDS	1.473	9.998	12.783	23.515	56.040	33.561	39.428
ABUW_RS12885		hypothetical protein	CDS	1.480	27.879	25.071	62.066	122.866	95.018	103.644
ABUW_RS09350		DUF2314 domain-containing protein	CDS	1.482	15.478	13.774	12.675	40.882	36.535	39.685
ABUW_RS09520		HD domain-containing protein	CDS	1.483	2.019	3.171	4.546	9.765	8.142	9.504
ABUW_RS09670		hypothetical protein	CDS	1.487	1.538	2.576	4.283	8.818	8.709	6.293
ABUW_RS13755		RHS repeat-associated core domain-containing protein	CDS	1.488	11.729	16.252	18.095	47.660	39.154	42.639
ABUW_RS18515		hypothetical protein	CDS	1.489	19.612	28.044	41.173	82.348	85.460	81.875
ABUW_RS12880		hypothetical protein	CDS	1.493	0.961	1.586	1.311	3.789	3.186	3.917
ABUW_RS15755		hypothetical protein	CDS	1.496	53.836	59.853	50.264	172.566	158.600	131.129
ABUW_RS09330		DUF2247 family protein	CDS	1.498	3.365	3.865	5.682	12.170	11.470	13.036

ABUW_RS18490		SDR family NAD(P)-dependent oxidoreductase	CDS	1.499	7.210	5.946	9.266	24.631	20.391	18.623
ABUW_RS12290		3-hydroxyacyl-CoA dehydrogenase	CDS	1.503	47.491	49.845	68.534	183.278	100.683	186.482
ABUW_RS10360	lipA	lipoyl synthase	CDS	1.505	3.172	2.576	2.710	9.692	5.239	9.119
ABUW_RS13760		RHS repeat protein	CDS	1.508	60.277	69.366	102.190	260.452	183.381	215.765
ABUW_RS01850	hemF	oxygen-dependent coproporphyrinogen oxidase	CDS	1.515	238.513	251.106	313.562	828.797	789.601	676.834
ABUW_RS01845	aroE	shikimate dehydrogenase	CDS	1.516	52.394	44.097	52.362	134.161	151.095	140.504
ABUW_RS11945		acetyl/propionyl/methylcrotonyl-CoA carboxylase subunit alpha	CDS	1.516	93.156	105.536	98.431	330.338	237.971	281.714
ABUW_RS03370		alpha/beta fold hydrolase	CDS	1.517	6.730	6.937	8.829	26.672	18.197	19.714
ABUW_RS20655		hypothetical protein	CDS	1.518	3.749	1.982	4.283	12.534	7.859	8.541
ABUW_RS13005		hypothetical protein	CDS	1.519	1.730	1.784	2.535	6.413	5.027	6.036
ABUW_RS12510	tssG	type VI secretion system baseplate subunit TssG	CDS	1.520	2.500	2.973	7.168	13.627	11.541	11.495
ABUW_RS16110		RidA family protein	CDS	1.521	1.442	1.189	1.573	3.789	3.469	4.880
ABUW_RS04345		hypothetical protein	CDS	1.523	14.709	13.279	17.221	47.733	39.013	43.410
ABUW_RS04580		hypothetical protein	CDS	1.525	1.538	1.486	0.874	3.789	2.620	4.752

ABUW_RS13265		hypothetical protein	CDS	1.527	0.192	0.793	1.311	2.915	1.628	2.248
ABUW_RS09650		helix-turn-helix domain-containing protein	CDS	1.530	5.095	3.072	3.322	11.077	11.399	10.724
ABUW_RS15490		hypothetical protein	CDS	1.538	3.461	3.567	3.322	13.263	8.709	8.155
ABUW_RS05685		hypothetical protein	CDS	1.538	6.441	6.342	11.277	25.797	21.737	22.668
ABUW_RS18530	prpC	2-methylcitrate synthase	CDS	1.542	119.209	116.436	129.376	377.852	344.601	340.857
ABUW_RS08530		YcgJ family protein	CDS	1.542	4.807	4.063	4.546	14.575	12.461	12.137
ABUW_RS01600		lipase secretion chaperone	CDS	1.550	0.961	0.892	0.437	1.968	3.469	1.284
ABUW_RS10940	gspJ	type II secretion system minor pseudopilin GspJ	CDS	1.552	4.999	5.450	4.720	15.376	13.948	15.155
ABUW_RS11920		AMP-binding protein	CDS	1.552	20.092	19.918	20.106	72.364	49.350	54.712
ABUW_RS08650		heme-binding protein	CDS	1.553	18.939	15.657	27.099	69.522	56.855	55.033
ABUW_RS00285		hypothetical protein	CDS	1.556	1.346	1.586	1.399	6.267	3.540	3.018
ABUW_RS07295	proP	glycine betaine/L-proline transporter ProP	CDS	1.556	21.919	20.810	16.871	59.975	50.271	64.922
ABUW_RS10190		TIGR00366 family protein	CDS	1.558	8.172	7.828	8.654	28.858	25.914	17.980
ABUW_RS20115		hypothetical protein	CDS	1.562	41.627	26.161	73.867	132.777	146.138	140.183
ABUW_RS19650		LysM peptidoglycan-binding domain-containing protein	CDS	1.572	82.677	101.473	103.326	318.241	269.195	267.266
ABUW_RS00715		DUF1737 domain-containing protein	CDS	1.574	4.134	1.982	4.283	9.838	13.665	7.706

ABUW_RS09435		SDR family oxidoreductase	CDS	1.581	0.673	0.991	1.049	3.789	2.124	2.312
ABUW_RS00600		SH3 domain-containing protein	CDS	1.597	5.768	4.558	6.381	18.364	14.019	18.301
ABUW_RS01970		globin domain-containing protein	CDS	1.599	20.285	25.566	32.344	83.076	78.592	75.518
ABUW_RS12540		hypothetical protein	CDS	1.605	12.209	12.684	16.697	42.923	39.508	44.309
ABUW_RS04590		hypothetical protein	CDS	1.614	1.346	0.694	1.049	3.498	1.841	4.174
ABUW_RS02630		hypothetical protein	CDS	1.615	17.304	19.026	25.088	67.117	61.953	59.335
ABUW_RS12895		hypothetical protein	CDS	1.633	0.577	0.396	0.699	1.603	2.761	0.963
ABUW_RS13050		hypothetical protein	CDS	1.633	3.269	2.279	2.797	8.235	7.293	10.403
ABUW_RS16785		hypothetical protein	CDS	1.633	29.418	40.331	38.026	114.412	116.472	103.580
ABUW_RS08050		hypothetical protein	CDS	1.636	0.673	0.991	0.437	2.769	1.699	2.055
ABUW_RS02625		LemA family protein	CDS	1.639	52.202	50.043	76.402	192.533	176.230	187.959
ABUW_RS08735	cydB	cytochrome d ubiquinol oxidase subunit II	CDS	1.641	492.985	454.745	647.929	1859.528	1436.887	1679.434
ABUW_RS02795		phage tail protein I	CDS	1.646	0.481	0.694	0.262	1.385	1.628	1.477
ABUW_RS04045		DcaP family trimeric outer membrane transporter	CDS	1.651	964.340	852.213	1098.385	3357.746	2977.572	2818.685
ABUW_RS17440		outer membrane beta-barrel protein	CDS	1.652	1015.388	972.117	1939.592	4039.701	4299.686	4002.694
ABUW_RS02265		energy transducer TonB	CDS	1.659	11.152	10.900	14.161	38.550	39.296	36.731
ABUW_RS00830	prfB	peptide chain release factor 2	CDS	1.659	0.673	0.495	0.612	2.623	1.558	1.541
ABUW_RS00050		DUF6091 family protein	CDS	1.665	5.480	5.054	7.081	18.510	18.480	19.072

ABUW_RS08740		cytochrome ubiquinol oxidase subunit I	CDS	1.667	633.632	579.901	993.835	2549.427	2123.398	2338.544
ABUW_RS08695		hypothetical protein	CDS	1.669	30.283	18.332	35.229	93.570	82.982	90.480
ABUW_RS19900		glutathione S-transferase	CDS	1.669	0.769	1.586	1.049	3.644	3.540	3.660
ABUW_RS09645		hypothetical protein	CDS	1.672	4.422	2.874	8.217	18.146	15.506	16.247
ABUW_RS09345		hypothetical protein	CDS	1.677	6.441	3.567	5.332	16.470	16.285	16.439
ABUW_RS11345		amino acid ABC transporter substrate-binding protein	CDS	1.689	71.525	76.402	96.682	320.500	227.350	241.066
ABUW_RS01120		helix-turn-helix domain-containing protein	CDS	1.689	1.730	2.576	2.797	6.777	9.983	6.293
ABUW_RS08595		GGDEF domain-containing protein	CDS	1.691	14.132	14.369	13.375	48.899	41.420	44.951
ABUW_RS07285		hypothetical protein	CDS	1.692	1.346	2.973	1.399	7.142	5.947	5.330
ABUW_RS09480		HlyD family secretion protein	CDS	1.697	1.442	1.784	2.011	6.413	5.027	5.651
ABUW_RS03850		hypothetical protein	CDS	1.698	19.035	20.909	28.235	66.753	67.263	87.462
ABUW_RS06275		hypothetical protein	CDS	1.709	1.538	3.567	2.885	10.057	7.010	9.119
ABUW_RS10180		CoA transferase subunit A	CDS	1.712	9.133	9.612	11.189	39.279	35.189	23.824
ABUW_RS13455		OprD family outer membrane porin	CDS	1.717	1.827	1.189	1.748	5.976	6.514	3.339
ABUW_RS08855		nuclear transport factor 2 family protein	CDS	1.721	2.019	1.486	1.573	5.393	5.947	5.458
ABUW_RS13770		hypothetical protein	CDS	1.721	2.211	2.378	3.759	10.129	9.629	8.027

ABUW_RS10105	antA	anthranilate 1,2-dioxygenase large subunit	CDS	1.726	66.142	56.880	62.765	213.230	205.613	195.922
ABUW_RS16720		hypothetical protein	CDS	1.734	15.862	12.387	15.123	54.364	47.155	42.960
ABUW_RS13035		hypothetical protein	CDS	1.740	0.288	0.297	0.175	1.239	1.133	0.257
ABUW_RS13460		MFS transporter	CDS	1.745	6.537	7.432	6.294	24.631	23.011	20.292
ABUW_RS17805		accessory factor UbiK family protein	CDS	1.747	10.383	8.621	16.959	39.716	41.349	40.071
ABUW_RS11300		hypothetical protein	CDS	1.750	3.845	4.558	5.682	16.397	16.285	14.898
ABUW_RS11915		class I SAM-dependent methyltransferase	CDS	1.750	4.326	3.369	4.283	14.065	12.107	14.256
ABUW_RS18905		hypothetical protein	CDS	1.758	17.401	19.918	44.407	88.906	94.169	94.204
ABUW_RS18055		GNAT family N-acetyltransferase	CDS	1.765	1.346	2.874	4.895	11.368	10.479	9.504
ABUW_RS00905		DUF485 domain-containing protein	CDS	1.768	33.263	38.151	38.113	144.509	128.508	100.241
ABUW_RS08535		hypothetical protein	CDS	1.772	1.057	0.396	1.399	4.445	1.912	3.596
ABUW_RS17605		histidine kinase	CDS	1.774	8.460	9.216	10.752	34.980	33.136	29.282
ABUW_RS05605		LysR family transcriptional regulator	CDS	1.774	4.711	4.955	6.207	18.802	17.630	18.045
ABUW_RS13040		hypothetical protein	CDS	1.776	1.250	1.090	2.535	6.704	4.956	5.330
ABUW_RS03920		Arc family DNA-binding protein	CDS	1.781	0.192	0.892	1.136	3.206	2.620	1.991
ABUW_RS12620		hypothetical protein	CDS	1.791	17.401	15.657	19.843	62.453	57.492	63.381
ABUW_RS11250		fimbrial protein	CDS	1.795	3.557	5.252	5.944	21.279	17.488	12.650

ABUW_RS06500		alpha/beta fold hydrolase	CDS	1.795	4.999	4.757	4.983	19.603	17.205	14.449
ABUW_RS06280		hypothetical protein	CDS	1.801	26.918	26.756	41.698	140.574	105.426	86.884
ABUW_RS18085		TetR/AcrR family transcriptional regulator	CDS	1.802	0.961	0.793	1.399	5.538	3.965	1.734
ABUW_RS20510		hypothetical protein	CDS	1.833	10.767	10.009	11.626	49.919	33.844	31.915
ABUW_RS08020		hypothetical protein	CDS	1.835	0.673	0.396	0.262	1.676	1.699	1.413
ABUW_RS10115	antC	anthranilate 1,2-dioxygenase electron transfer component AntC	CDS	1.835	30.283	27.449	33.306	112.372	104.294	108.396
ABUW_RS02595	radC	DNA repair protein RadC	CDS	1.837	5.768	4.162	5.070	20.186	15.789	17.724
ABUW_RS06650		acyl-CoA dehydrogenase family protein	CDS	1.839	7.402	8.621	9.965	35.271	29.029	28.897
ABUW_RS08390		hypothetical protein	CDS	1.852	1.250	1.387	1.399	5.903	3.682	5.073
ABUW_RS06795		hypothetical protein	CDS	1.855	0.673	0.297	0.175	1.312	1.912	0.963
ABUW_RS00390		amino acid permease	CDS	1.855	89.695	69.465	59.093	318.168	214.747	256.542
ABUW_RS08605		hypothetical protein	CDS	1.857	3.172	0.991	1.136	6.559	7.010	5.651
ABUW_RS06425		hypothetical protein	CDS	1.869	22.111	25.170	29.110	91.894	91.124	96.324
ABUW_RS12905		hypothetical protein	CDS	1.872	0.288	0.495	0.000	1.020	1.133	0.706
ABUW_RS14110		SPOR domain-containing protein	CDS	1.876	1.442	0.793	0.787	2.478	5.381	3.275
ABUW_RS05575		hypothetical protein	CDS	1.881	34.128	35.079	56.209	158.865	154.777	148.788

ABUW_RS10465		TonB C-terminal domain-containing protein	CDS	1.885	4.326	5.847	7.168	21.644	19.896	22.732
ABUW_RS11290		integrase family protein	CDS	1.892	2.211	2.279	3.234	9.911	10.054	8.926
ABUW_RS10965		PilZ domain-containing protein	CDS	1.897	11.440	11.594	18.707	53.198	56.714	46.043
ABUW_RS16285		TetR/AcrR family transcriptional regulator	CDS	1.902	5.191	4.162	7.081	22.154	18.975	20.613
ABUW_RS17020		DUF4062 domain-containing protein	CDS	1.910	13.171	14.270	22.990	62.817	64.856	62.353
ABUW_RS04830		CSLREA domain-containing protein	CDS	1.912	17.785	19.522	25.263	90.145	74.131	71.601
ABUW_RS11885		hypothetical protein	CDS	1.916	0.288	0.495	0.787	2.186	1.982	1.926
ABUW_RS10110	antB	anthranilate 1,2-dioxygenase small subunit	CDS	1.918	17.497	15.459	15.910	67.481	56.360	60.941
ABUW_RS05680		hypothetical protein	CDS	1.925	0.385	0.396	0.699	2.696	1.628	1.477
ABUW_RS13105		hypothetical protein	CDS	1.944	5.672	6.045	10.053	31.336	25.560	27.292
ABUW_RS07280		immunity 26 domain-containing protein	CDS	1.967	0.769	1.685	1.136	4.300	4.815	4.945
ABUW_RS13835		YraN family protein	CDS	1.970	5.384	3.072	5.158	17.636	19.188	16.760
ABUW_RS09700		hypothetical protein	CDS	1.975	13.363	12.090	20.455	61.797	55.227	63.959
ABUW_RS12975		hypothetical protein	CDS	1.981	4.711	6.540	6.818	30.753	15.648	25.108
ABUW_RS13275		hypothetical protein	CDS	1.982	1.250	1.189	1.049	6.632	3.257	3.981
ABUW_RS00215		hypothetical protein	CDS	1.983	0.096	0.396	0.437	1.530	0.850	1.413
ABUW_RS01290		hypothetical protein	CDS	1.994	59.220	45.088	73.517	268.031	230.253	210.756

ABUW_RS06255		hypothetical protein	CDS	2.006	6.441	6.838	16.522	48.024	35.119	37.374
ABUW_RS11470		dicarboxylate/amino acid:cation symporter	CDS	2.026	19.035	15.756	18.270	89.416	58.767	68.133
ABUW_RS09640		outer membrane protein transport protein	CDS	2.039	1.923	1.586	2.185	9.547	8.426	5.651
ABUW_RS13580		DUF4265 domain-containing protein	CDS	2.052	0.769	0.595	0.612	3.498	2.691	2.119
ABUW_RS19865		hypothetical protein	CDS	2.058	0.481	0.595	0.437	2.259	1.982	2.119
ABUW_RS03885		hypothetical protein	CDS	2.066	0.288	0.099	0.350	0.947	0.920	1.349
ABUW_RS13690		TetR/AcrR family transcriptional regulator	CDS	2.079	0.096	0.198	0.524	1.020	1.274	1.349
ABUW_RS09545		hypothetical protein	CDS	2.080	2.019	0.991	2.885	9.328	8.142	7.834
ABUW_RS02690		hypothetical protein	CDS	2.083	0.192	0.793	0.350	2.405	1.558	1.734
ABUW_RS12265		PaaI family thioesterase	CDS	2.091	0.192	0.595	0.524	2.842	1.274	1.605
ABUW_RS07790		ion transporter	CDS	2.098	9.998	8.225	14.074	49.190	40.146	49.382
ABUW_RS07800		membrane protein	CDS	2.128	2.500	0.595	1.399	5.830	6.939	7.000
ABUW_RS16025		ComEA family DNA-binding protein	CDS	2.129	4.903	6.144	12.501	32.210	36.251	35.190
ABUW_RS11230		hypothetical protein	CDS	2.133	0.481	0.595	1.573	4.445	3.469	4.046
ABUW_RS15230		hypothetical protein	CDS	2.133	0.865	1.189	1.836	7.069	5.735	4.559
ABUW_RS20155		hypothetical protein	CDS	2.136	0.192	0.198	0.350	1.312	1.204	0.899
ABUW_RS12410	soxR	redox-sensitive transcriptional activator SoxR	CDS	2.139	0.385	0.793	0.524	2.332	2.053	3.147
ABUW_RS10010		hypothetical protein	CDS	2.153	5.480	4.459	5.420	22.445	19.471	26.521

ABUW_RS12725		hypothetical protein	CDS	2.156	8.652	8.919	16.871	65.222	44.465	44.566
ABUW_RS20670		prepilin peptidase	CDS	2.157	30.187	29.233	36.802	142.250	141.253	146.027
ABUW_RS11240		fimbria/pilus periplasmic chaperone	CDS	2.158	2.500	2.180	2.972	12.607	12.815	8.990
ABUW_RS03340		response regulator	CDS	2.169	109.307	118.814	161.895	588.385	587.882	578.134
ABUW_RS11180		hypothetical protein	CDS	2.171	2.980	1.586	4.458	15.668	13.877	11.623
ABUW_RS06560	yegQ	tRNA 5-hydroxyuridine modification protein YegQ	CDS	2.200	47.683	45.980	88.465	276.411	289.020	272.596
ABUW_RS10790		hypothetical protein	CDS	2.205	4.422	2.973	3.846	19.895	15.435	16.696
ABUW_RS13775		hypothetical protein	CDS	2.210	0.865	1.586	1.136	5.247	5.027	6.357
ABUW_RS02445		DUF2147 domain-containing protein	CDS	2.211	19.323	22.197	27.886	117.254	112.153	92.342
ABUW_RS08850		NADPH-dependent 2,4-dienoyl-CoA reductase	CDS	2.212	8.364	9.909	12.501	50.866	43.615	48.419
ABUW_RS15510		TetR/AcrR family transcriptional regulator	CDS	2.229	1.154	0.396	1.311	4.664	4.531	4.495
ABUW_RS06590	tadA	Flp pilus assembly complex ATPase component TadA	CDS	2.229	30.283	37.953	65.999	219.059	204.693	206.710
ABUW_RS09660		replication initiation factor domain-containing protein	CDS	2.242	2.211	2.775	3.234	17.490	10.408	11.238
ABUW_RS07820		hypothetical protein	CDS	2.245	0.577	1.090	3.060	7.360	7.364	8.220
ABUW_RS05570		EAL domain-containing protein	CDS	2.248	166.508	166.182	264.259	980.011	862.316	994.573

ABUW_RS12415		hypothetical protein	CDS	2.253	0.192	0.595	0.437	2.186	1.558	2.183
ABUW_RS16510		fumarate hydratase	CDS	2.269	172.180	138.931	132.698	690.846	743.508	705.281
ABUW_RS20675		A24 family peptidase	CDS	2.287	18.170	17.044	27.449	103.554	97.921	104.928
ABUW_RS03365		radical SAM protein	CDS	2.331	4.807	6.937	7.605	42.267	26.551	28.833
ABUW_RS16280		hypothetical protein	CDS	2.333	8.172	6.243	9.179	59.830	28.959	30.502
ABUW_RS11910		DcaP family trimeric outer membrane transporter	CDS	2.336	4.230	3.567	3.934	25.142	19.188	15.091
ABUW_RS17410		hypothetical protein	CDS	2.337	2.403	4.063	2.098	20.186	13.453	9.568
ABUW_RS12970		hypothetical protein	CDS	2.341	0.577	0.495	0.087	1.968	1.699	2.183
ABUW_RS15495		hypothetical protein	CDS	2.343	6.057	5.054	4.633	27.474	25.348	27.099
ABUW_RS16315		DUF4124 domain-containing protein	CDS	2.345	1.057	2.378	2.273	11.004	9.275	8.926
ABUW_RS12685		hypothetical protein	CDS	2.350	2.019	2.874	2.710	15.085	11.045	12.779
ABUW_RS00595		DUF1311 domain-containing protein	CDS	2.350	2.307	2.775	1.923	12.316	8.780	14.577
ABUW_RS07410		GNAT family N-acetyltransferase	CDS	2.355	0.192	0.297	1.224	2.696	3.186	3.275
ABUW_RS17380		hypothetical protein	CDS	2.356	85.753	74.321	90.651	492.847	429.777	361.791
ABUW_RS13360		hypothetical protein	CDS	2.367	43.838	37.160	47.817	581.681	44.040	39.364
ABUW_RS03335	pilG	twitching motility response regulator PilG	CDS	2.369	86.330	101.374	165.479	590.061	639.851	595.537
ABUW_RS12750		MFS transporter	CDS	2.372	2.596	1.883	3.846	16.470	15.435	11.687
ABUW_RS18540		GntR family transcriptional regulator	CDS	2.407	6.057	6.937	4.895	34.542	34.198	26.072

ABUW_RS05440		Lrp/AsnC family transcriptional regulator	CDS	2.409	2.307	0.892	0.962	7.579	8.355	6.229
ABUW_RS08725		cyd operon YbgE family protein	CDS	2.431	14.228	9.711	27.186	111.206	78.450	87.333
ABUW_RS08730	cydX	cytochrome bd-I oxidase subunit CydX	CDS	2.438	2.884	2.676	7.168	28.057	21.737	20.035
ABUW_RS12900		DUF4882 family protein	CDS	2.443	3.942	6.144	10.053	42.631	30.375	37.181
ABUW_RS13595	astA	arginine N-succinyltransferase	CDS	2.445	11.344	15.459	16.259	87.813	80.999	66.014
ABUW_RS01570		type IV pilin protein	CDS	2.453	16.055	14.666	24.127	110.841	97.992	92.150
ABUW_RS18015		DUF2726 domain-containing protein	CDS	2.475	3.942	4.360	6.731	33.959	25.135	25.044
ABUW_RS13815		hypothetical protein	CDS	2.480	92.483	99.986	196.337	712.053	710.230	748.884
ABUW_RS11245		fimbrial biogenesis outer membrane usher protein	CDS	2.514	1.827	1.883	2.098	12.607	11.541	9.247
ABUW_RS04155		hypothetical protein	CDS	2.596	2.307	1.486	2.360	10.712	13.948	12.843
ABUW_RS13655		hypothetical protein	CDS	2.611	1.442	1.189	0.874	6.996	6.018	8.412
ABUW_RS14535		hypothetical protein	CDS	2.612	0.481	1.189	0.699	5.101	5.027	4.431
ABUW_RS11960		indolepyruvate ferredoxin oxidoreductase family protein	CDS	2.623	45.665	46.079	45.194	328.152	278.470	237.213
ABUW_RS08245		iron-containing redox enzyme family protein	CDS	2.629	23.457	26.855	30.071	223.869	135.376	138.385
ABUW_RS01100		hypothetical protein	CDS	2.717	0.865	1.387	0.612	6.559	5.735	6.486

ABUW_RS06555		YfhL family 4Fe-4S dicluster ferredoxin	CDS	2.731	2.307	2.180	2.622	18.219	16.072	13.228
ABUW_RS20430		hypothetical protein	CDS	2.752	0.000	0.297	0.087	0.947	1.133	0.642
ABUW_RS05525		hypothetical protein	CDS	2.754	3.942	5.946	6.119	35.635	42.199	30.438
ABUW_RS10005		hypothetical protein	CDS	2.756	0.673	0.793	1.224	7.798	3.894	6.807
ABUW_RS08240		TetR/AcrR family transcriptional regulator	CDS	2.763	6.345	3.964	10.053	55.020	42.270	42.061
ABUW_RS15175	bfr	bacterioferritin	CDS	2.777	46.145	47.962	106.036	514.782	482.738	375.726
ABUW_RS10120		AraC family transcriptional regulator	CDS	2.780	1.442	1.288	1.923	12.024	11.399	8.926
ABUW_RS01565		prepilin-type N-terminal cleavage/methylation domain-containing protein	CDS	2.828	10.575	10.207	14.161	92.987	80.858	75.004
ABUW_RS15455		hypothetical protein	CDS	2.838	0.000	0.099	0.350	1.312	1.133	1.092
ABUW_RS00385	hutH	histidine ammonia-lyase	CDS	2.846	147.665	92.653	90.563	970.974	676.315	731.802
ABUW_RS10155		AraC family transcriptional regulator	CDS	2.859	1.057	1.288	2.710	16.397	11.045	9.953
ABUW_RS01505	bfr	bacterioferritin	CDS	2.901	36.628	34.881	65.475	374.427	356.496	293.980
ABUW_RS12680		hypothetical protein	CDS	2.903	0.577	0.793	1.399	7.943	6.160	7.064
ABUW_RS18120	dprA	DNA-processing protein DprA	CDS	2.949	14.805	13.873	21.767	130.226	130.845	129.459
ABUW_RS08745		hypothetical protein	CDS	2.977	1.634	3.171	4.895	25.579	27.967	23.631
ABUW_RS08615		PEGA domain-containing protein	CDS	2.978	11.536	8.027	16.522	99.254	110.454	75.839

ABUW_RS17730		sigma-54 dependent transcriptional regulator	CDS	3.061	52.106	52.223	104.987	569.438	582.784	597.142
ABUW_RS17275		type II secretion system F family protein	CDS	3.067	52.298	42.313	89.602	528.337	518.990	498.186
ABUW_RS13575		hypothetical protein	CDS	3.108	0.096	0.099	0.175	1.239	1.204	1.027
ABUW_RS18115		LysM peptidoglycan-binding domain-containing protein	CDS	3.123	44.703	42.611	53.586	454.078	392.252	381.634
ABUW_RS07785		hypothetical protein	CDS	3.132	2.980	2.973	3.934	34.324	24.286	28.576
ABUW_RS11275		cytosine permease	CDS	3.139	6.153	3.369	4.021	48.753	38.021	32.750
ABUW_RS09960		hypothetical protein	CDS	3.156	10.671	8.720	27.099	158.137	124.048	134.725
ABUW_RS14715		PilT/PilU family type 4a pilus ATPase	CDS	3.195	29.033	30.422	56.383	369.690	336.742	356.461
ABUW_RS14710		type IV pilus twitching motility protein PilT	CDS	3.222	30.571	29.629	48.953	361.383	328.387	330.390
ABUW_RS17270	pilB	type IV-A pilus assembly ATPase PilB	CDS	3.242	60.566	60.547	109.533	728.668	747.119	708.942
ABUW_RS15505		hypothetical protein	CDS	3.249	0.577	0.694	0.787	6.559	5.664	7.642
ABUW_RS01425		pilus assembly protein PilM	CDS	3.255	67.968	59.754	100.354	759.275	737.560	682.099
ABUW_RS16790		hypothetical protein	CDS	3.301	40.762	37.656	88.990	577.746	559.985	515.395
ABUW_RS01560		VWA domain-containing protein	CDS	3.305	68.160	80.564	129.551	1062.868	871.450	817.209
ABUW_RS03350		methyl-accepting chemotaxis protein	CDS	3.316	225.247	246.547	493.028	3418.231	3030.533	3165.129
ABUW_RS03360		hypothetical protein	CDS	3.379	13.074	15.161	32.956	227.148	208.092	203.821

ABUW_RS00350		amino acid permease	CDS	3.396	28.937	23.287	21.679	307.383	265.584	204.912
ABUW_RS00800		YkgJ family cysteine cluster protein	CDS	3.405	3.653	5.747	4.371	55.384	44.889	45.657
ABUW_RS17065		hypothetical protein	CDS	3.406	7.018	9.216	15.822	127.675	112.861	101.076
ABUW_RS03330		hypothetical protein	CDS	3.454	1.057	1.982	2.098	19.166	20.533	17.081
ABUW_RS00345	fahA	fumarylacetoacetase	CDS	3.455	61.527	58.367	53.062	744.554	671.642	480.269
ABUW_RS01440		pilus assembly protein PilP	CDS	3.541	18.170	21.008	35.841	316.055	287.179	271.889
ABUW_RS11305		TetR/AcrR family transcriptional regulator	CDS	3.560	1.154	1.586	2.011	20.478	14.444	21.705
ABUW_RS03355		Hpt domain-containing protein	CDS	3.577	146.223	160.632	329.122	2754.494	2383.247	2454.132
ABUW_RS03345		chemotaxis protein CheW	CDS	3.627	41.531	43.899	73.867	694.271	656.207	620.003
ABUW_RS09300		amidohydrolase	CDS	3.629	2.115	1.784	2.011	30.388	20.675	22.476
ABUW_RS13380		hypothetical protein	CDS	3.631	0.961	1.288	2.535	27.765	20.675	12.073
ABUW_RS00325	hppD	4-hydroxyphenylpyruvate dioxygenase	CDS	3.682	34.801	27.846	38.813	519.155	427.512	357.232
ABUW_RS02525		hypothetical protein	CDS	3.687	34.321	36.863	62.328	593.924	576.624	551.741
ABUW_RS11235		type 1 fimbrial protein	CDS	3.707	2.692	2.081	2.535	42.631	29.242	24.145
ABUW_RS00380	hutU	urocanate hydratase	CDS	3.721	129.976	81.852	107.609	1707.002	1279.137	1226.328
ABUW_RS06270		hypothetical protein	CDS	3.726	0.288	0.099	0.000	1.239	1.628	2.440
ABUW_RS00335		VOC family protein	CDS	3.743	7.595	8.225	8.829	126.072	120.720	83.930
ABUW_RS14740		bacteriohemerythrin	CDS	3.754	7.210	6.243	12.763	139.408	113.498	103.002

ABUW_RS00795		FprA family A-type flavoprotein	CDS	3.757	9.614	9.018	23.602	215.999	181.965	176.401
ABUW_RS15500		hypothetical protein	CDS	3.771	0.577	0.595	1.748	15.376	11.966	13.742
ABUW_RS20665		hypothetical protein	CDS	3.791	2.980	1.685	6.294	3.352	4.956	145.192
ABUW_RS01430		PilN domain-containing protein	CDS	3.913	18.554	17.242	31.907	353.512	338.087	331.032
ABUW_RS01555		hypothetical protein	CDS	3.945	6.730	5.847	12.675	148.007	129.500	113.983
ABUW_RS00340	maiA	maleylacetoacetate isomerase	CDS	4.044	10.479	6.144	7.605	152.088	143.944	104.222
ABUW_RS01445		type IV pilus secretin PilQ	CDS	4.132	45.665	44.394	92.137	1184.860	1032.669	980.959
ABUW_RS08010		hypothetical protein	CDS	4.137	0.673	0.000	0.087	4.227	5.806	3.725
ABUW_RS18520		hypothetical protein	CDS	4.229	1.346	0.991	2.797	24.850	14.869	58.372
ABUW_RS13600		aspartate aminotransferase family protein	CDS	4.366	21.150	21.504	24.914	152.963	1117.421	124.193
ABUW_RS01545	pilV	type IV pilus modification protein PilV	CDS	4.454	2.500	2.477	4.808	78.995	73.140	64.794
ABUW_RS01435		type 4a pilus biogenesis protein PilO	CDS	4.486	7.499	7.234	17.571	252.727	247.104	229.314
ABUW_RS01550		PilW family protein	CDS	4.723	4.134	4.063	9.703	171.546	157.892	148.274
ABUW_RS01540		GspH/FimT family pseudopilin	CDS	5.750	0.096	0.297	1.049	34.834	24.781	22.347
ABUW_RS01495		pilin	CDS	6.211	16.535	9.414	48.516	2122.676	1818.305	1606.613
Wicklow Tormentil Root										

ABUW_RS14485		porin family protein	CDS	-8.176	223.613	243.102	1325.259	2.186	2.407	1.605
ABUW_RS12930		DUF2213 domain-containing protein	CDS	-7.753	5.104	5.211	3188.243	6.559	4.248	4.046
ABUW_RS14490		transferrin-binding protein-like solute binding protein	CDS	-7.583	2731.989	2826.087	2645.754	12.607	10.975	19.072
ABUW_RS05755	basD	acinetobactin non-ribosomal peptide synthetase subunit BasD	CDS	-7.306	3393.390	2609.550	2836.980	12.607	13.736	29.282
ABUW_RS05770	basG	acinetobactin biosynthesis histidine decarboxylase BasG	CDS	-7.240	1644.355	1240.283	1398.876	7.287	7.080	13.806
ABUW_RS05765	basF	acinetobactin biosynthesis bifunctional isochorismatase/aryl carrier protein BasF	CDS	-7.196	1288.808	835.141	998.336	5.757	4.461	10.917
ABUW_RS05750	basC	putative histamine N-monooxygenase	CDS	-7.062	2541.600	1964.209	1887.251	13.263	11.753	22.668
ABUW_RS05760	basE	(2,3-dihydroxybenzoyl)adenylate synthase BasE	CDS	-6.994	1377.117	798.326	865.616	7.798	7.080	8.926

ABUW_RS05780	barA	acinetobactin export ABC transporter permease/ATP-binding subunit BarA	CDS	-6.642	3402.057	2744.170	2616.500	23.247	24.852	39.493
ABUW_RS05785	barB	acinetobactin export ABC transporter permease/ATP-binding subunit BarB	CDS	-6.505	3381.930	2778.935	2575.635	24.413	27.826	43.795
ABUW_RS05730	bauC	ferric acinetobactin ABC transporter permease subunit BauC	CDS	-6.385	245.088	186.384	185.197	1.530	1.062	4.624
ABUW_RS20145		hypothetical protein	CDS	-6.365	68.374	43.905	82.326	0.291	0.637	1.349
ABUW_RS14495		TonB-dependent receptor	CDS	-6.336	832.530	940.805	807.928	10.057	9.488	12.329
ABUW_RS05735	bauE	ferric acinetobactin ABC transporter ATP-binding protein BauE	CDS	-6.313	777.734	685.914	573.157	5.028	6.726	13.678
ABUW_RS05800	basJ	acinetobactin biosynthesis isochorismate synthase BasJ	CDS	-6.297	1188.943	872.384	940.573	11.004	10.479	16.568
ABUW_RS05740	bauB	siderophore-binding periplasmic lipoprotein BauB	CDS	-6.272	2828.002	2755.189	2097.607	22.955	20.816	55.354

ABUW_RS05720	basB	acinetobactin non-ribosomal peptide synthetase subunit BasB	CDS	-6.247	2189.327	1640.044	1665.431	15.304	17.701	39.107
ABUW_RS05725	bauD	ferric acinetobactin ABC transporter permease subunit BauD	CDS	-6.028	181.433	120.526	128.179	0.874	2.053	3.532
ABUW_RS14475		biliverdin-producing heme oxygenase	CDS	-5.984	406.587	480.225	509.887	7.215	6.443	8.348
ABUW_RS05745	bauA	TonB-dependent ferric acinetobactin receptor BauA	CDS	-5.902	5361.512	4914.495	4486.482	65.587	60.820	120.340
ABUW_RS14470		YbaN family protein	CDS	-5.877	152.253	159.306	159.740	2.769	2.053	3.147
ABUW_RS05790	basH	acinetobactin biosynthesis thioesterase BasH	CDS	-5.790	391.467	292.133	405.081	7.943	4.177	7.513
ABUW_RS14480		energy transducer TonB	CDS	-5.652	44.395	41.257	47.862	1.093	0.637	0.899
ABUW_RS05710	bauF	acinetobactin utilization protein BauF	CDS	-5.315	199.634	157.940	171.352	3.862	3.823	5.523
ABUW_RS10630		DHA2 family efflux MFS transporter permease subunit	CDS	-5.007	1060.573	835.825	816.265	19.312	19.825	45.015
ABUW_RS05795	basI	acinetobactin biosynthesis phosphopantetheinyl transferase BasI	CDS	-4.943	50.270	39.036	63.494	1.676	0.779	2.440

ABUW_RS14160		TonB-dependent siderophore receptor	CDS	-4.791	2034.859	1902.964	1509.413	32.793	49.633	114.047
ABUW_RS10635		SidA/IucD/PvdA family monooxygenase	CDS	-4.763	963.789	705.475	705.132	18.947	19.117	49.125
ABUW_RS05715	basA	acinetobactin non-ribosomal peptide synthetase subunit BasA	CDS	-4.742	419.106	272.657	276.976	11.733	8.638	15.733
ABUW_RS10640		siderophore biosynthesis protein	CDS	-4.659	895.222	614.760	700.815	22.227	20.745	44.309
ABUW_RS10075		isochorismatase family protein	CDS	-4.594	503.563	359.528	370.989	13.336	14.515	23.118
ABUW_RS10620		IucA/IucC family siderophore biosynthesis protein	CDS	-4.472	1308.550	979.158	1183.533	39.498	39.721	76.995
ABUW_RS10625		siderophore achromobactin biosynthesis protein AcsC	CDS	-4.433	1981.412	1587.255	1679.500	60.777	59.192	122.716
ABUW_RS08385	fumC	class II fumarate hydratase	CDS	-4.299	2467.640	2160.587	1751.554	111.570	90.133	122.395
ABUW_RS10080		SDR family oxidoreductase	CDS	-4.247	954.159	676.775	570.105	32.283	34.977	48.547
ABUW_RS06610		hemin uptake protein HemP	CDS	-4.200	730.065	534.296	597.126	33.595	26.622	40.970
ABUW_RS10585		acetyltransferase	CDS	-4.139	341.968	213.889	300.870	12.534	14.727	21.255

ABUW_RS08070		TonB-dependent siderophore receptor	CDS	-4.137	266.371	197.830	174.627	8.818	9.204	18.109
ABUW_RS10615		(2Fe-2S)-binding protein	CDS	-4.052	144.260	124.285	149.542	6.194	5.806	13.036
ABUW_RS10525		hypothetical protein	CDS	-4.032	23.883	17.169	23.298	0.802	0.920	2.119
ABUW_RS00710		TonB-dependent siderophore receptor	CDS	-3.996	345.339	259.845	258.367	11.587	14.090	28.255
ABUW_RS10520		TonB-dependent siderophore receptor	CDS	-3.747	353.235	251.644	237.749	14.502	18.267	29.796
ABUW_RS07805		DUF4198 domain-containing protein	CDS	-3.708	198.671	126.847	152.594	10.129	11.258	15.091
ABUW_RS10610		RraA family protein	CDS	-3.491	86.479	69.702	78.232	6.049	5.310	9.375
ABUW_RS02205		hypothetical protein	CDS	-3.426	4291.598	3225.591	3677.809	399.058	333.980	308.621
ABUW_RS14945		hypothetical protein	CDS	-3.382	246.918	6.492	8.486	8.308	8.992	7.706
ABUW_RS06655		alpha/beta hydrolase	CDS	-3.382	190.581	139.831	193.236	12.826	15.648	21.641
ABUW_RS01510		bacterioferritin-associated ferredoxin	CDS	-3.213	28.024	19.817	32.082	2.623	2.478	3.468
ABUW_RS16655		energy transducer TonB	CDS	-3.082	698.478	683.096	770.710	72.000	85.885	96.259
ABUW_RS09965		type 1 fimbrial protein	CDS	-2.853	711.671	632.955	936.405	138.898	86.309	90.480
ABUW_RS09970		molecular chaperone	CDS	-2.822	109.977	94.986	159.442	26.162	11.399	14.063
ABUW_RS16650		MotA/TolQ/ExbB proton channel family protein	CDS	-2.808	1911.015	1652.345	1614.219	186.776	235.422	316.969
ABUW_RS10530		PepSY domain-containing protein	CDS	-2.807	103.332	82.258	92.971	8.891	10.691	20.035

ABUW_RS14505		sigma-70 family RNA polymerase sigma factor	CDS	-2.796	16.853	12.471	22.182	1.749	2.266	3.339
ABUW_RS10215		hypothetical protein	CDS	-2.732	2.215	1.623	4.913	0.510	0.354	0.450
ABUW_RS16845		DUF2061 domain-containing protein	CDS	-2.706	22.727	16.230	28.807	4.664	3.257	2.504
ABUW_RS20105		hypothetical protein	CDS	-2.680	31.876	25.797	44.289	7.215	4.956	3.789
ABUW_RS16645		biopolymer transporter ExbD	CDS	-2.620	766.467	640.386	670.073	91.093	104.860	141.660
ABUW_RS14500		FecR domain-containing protein	CDS	-2.613	16.564	12.898	15.855	2.769	1.770	2.825
ABUW_RS03435		sulfite reductase flavoprotein subunit alpha	CDS	-2.445	450.886	402.323	439.768	68.866	72.998	95.425
ABUW_RS17690		ferrous iron transport protein A	CDS	-2.416	134.245	130.179	110.835	21.279	22.020	26.906
ABUW_RS01160	aqpZ	aquaporin Z	CDS	-2.416	249.711	229.521	189.663	51.522	32.853	40.905
ABUW_RS19720		Ig-like domain-containing protein	CDS	-2.341	4608.817	4278.380	3761.847	928.197	731.684	835.832
ABUW_RS09975		fimbrial biogenesis outer membrane usher protein	CDS	-2.334	180.855	155.975	231.347	49.117	30.375	33.264
ABUW_RS20540		hypothetical protein	CDS	-2.333	22.149	3.758	10.868	1.093	2.337	3.725
ABUW_RS16095		proton-translocating transhydrogenase family protein	CDS	-2.298	118.740	118.391	58.730	18.583	22.445	19.072

ABUW_RS10535		hypothetical protein	CDS	-2.224	9.630	7.688	13.994	1.239	2.195	3.211
ABUW_RS16090		NAD(P)(+) transhydrogenase (Re/Si-specific) subunit beta	CDS	-2.108	810.092	598.445	472.743	117.473	158.458	160.475
ABUW_RS17685		ferrous iron transporter B	CDS	-2.100	2181.142	1910.054	1759.965	381.642	444.929	538.449
ABUW_RS00790		TonB-dependent siderophore receptor	CDS	-2.038	200.404	139.062	164.950	33.303	42.128	47.263
ABUW_RS12640		chloride channel protein	CDS	-1.987	38.328	36.474	56.497	10.640	11.258	11.238
ABUW_RS15330		mechanosensitive ion channel	CDS	-1.979	1224.671	1212.522	1017.019	393.156	191.099	291.925
ABUW_RS04980	carO	ornithine uptake porin CarO type 3	CDS	-1.948	2925.652	3021.354	2549.657	859.185	582.642	759.993
ABUW_RS16100		Re/Si-specific NAD(P)(+) transhydrogenase subunit alpha	CDS	-1.909	600.153	436.833	332.357	94.736	136.368	133.440
ABUW_RS15475		hypothetical protein	CDS	-1.826	39.965	33.484	32.231	11.368	8.780	9.632
ABUW_RS18710		ferredoxin reductase	CDS	-1.727	119.607	123.089	201.349	43.579	47.368	43.281
ABUW_RS00985		AzlC family ABC transporter permease	CDS	-1.692	56.144	63.125	64.387	17.417	22.162	17.274
ABUW_RS10605		TonB-dependent receptor	CDS	-1.685	1868.835	1606.475	1500.853	387.034	438.840	721.721
ABUW_RS13745		TonB-dependent receptor	CDS	-1.681	222.361	181.686	175.371	53.781	53.669	73.142

ABUW_RS17680		hypothetical protein	CDS	-1.640	91.872	83.540	77.339	24.194	27.684	29.154
ABUW_RS14395		hypothetical protein	CDS	-1.593	29.757	24.515	27.616	10.421	7.788	8.926
ABUW_RS10210		hypothetical protein	CDS	-1.582	2.889	1.452	3.275	0.364	0.779	1.349
ABUW_RS03160		glucose/quinate/shikimate family membrane-bound PQQ-dependent dehydrogenase	CDS	-1.563	4575.785	4553.771	4145.565	1381.037	1497.565	1615.603
ABUW_RS10070		transcriptional repressor	CDS	-1.554	10.978	4.356	8.486	3.206	1.770	3.082
ABUW_RS09980		type 1 fimbrial protein	CDS	-1.551	39.869	35.534	46.671	15.085	14.161	12.458
ABUW_RS10590		hypothetical protein	CDS	-1.550	7.704	8.542	11.612	2.696	2.620	4.174
ABUW_RS10595		PepSY domain-containing protein	CDS	-1.492	102.850	95.157	113.068	32.137	29.879	48.483
ABUW_RS20090		hypothetical protein	CDS	-1.474	2.408	1.538	1.712	0.583	0.708	0.706
ABUW_RS07500		hypothetical protein	CDS	-1.456	59.803	62.185	61.931	27.109	17.913	22.026
ABUW_RS05475	sohB	protease SohB	CDS	-1.427	1511.940	1686.939	1343.198	558.580	526.283	603.949
ABUW_RS10600		hypothetical protein	CDS	-1.422	9.149	8.286	14.366	2.915	3.328	5.587
ABUW_RS01315		CusA/CzcA family heavy metal efflux RND transporter	CDS	-1.419	268.105	262.663	229.412	95.684	96.718	91.764
ABUW_RS03940		hypothetical protein	CDS	-1.415	1.348	1.708	1.042	0.510	0.071	0.899
ABUW_RS18870		hypothetical protein	CDS	-1.366	34.765	34.509	38.409	13.555	14.090	14.127
ABUW_RS10855		GNAT family acetyltransferase	CDS	-1.363	0.482	1.367	2.308	0.291	0.496	0.835
ABUW_RS18705		acyl-CoA desaturase	CDS	-1.347	93.317	94.644	114.557	47.733	33.490	37.759

ABUW_RS13135		heavy metal translocating P-type ATPase	CDS	-1.314	811.247	790.723	723.444	298.565	303.322	333.601
ABUW_RS13220		hypothetical protein	CDS	-1.301	479.006	384.044	382.676	200.914	129.287	175.437
ABUW_RS04130	adeJ	multidrug efflux RND transporter permease subunit AdeJ	CDS	-1.272	4715.038	4577.090	3927.318	1735.205	1806.481	1930.517
ABUW_RS00920	betT	choline BCCT transporter BetT	CDS	-1.257	1843.026	1881.182	1630.744	766.271	686.865	786.643
ABUW_RS14460		DUF1275 domain-containing protein	CDS	-1.246	25.038	28.103	28.956	11.514	8.921	14.127
ABUW_RS10700		Rrf2 family transcriptional regulator	CDS	-1.245	540.446	545.400	503.857	206.525	222.960	241.066
ABUW_RS04135	adeI	multidrug efflux RND transporter periplasmic adaptor subunit AdeI	CDS	-1.224	1608.434	1610.831	1380.193	632.620	641.763	694.943
ABUW_RS03155		carbohydrate porin	CDS	-1.222	2324.921	2409.840	2215.365	956.108	988.488	1034.387
ABUW_RS14165	nfuA	Fe-S biogenesis protein NfuA	CDS	-1.218	446.167	401.213	336.079	203.392	146.917	158.228
ABUW_RS07160		class I SAM-dependent methyltransferase	CDS	-1.217	3.948	5.979	2.159	2.332	1.628	1.220
ABUW_RS07155		PIG-L family deacetylase	CDS	-1.211	6.934	6.834	4.689	2.915	1.912	3.082
ABUW_RS14410		choline transporter	CDS	-1.201	573.285	447.168	398.605	158.574	218.146	240.424
ABUW_RS20600		TIGR01244 family phosphatase	CDS	-1.193	10.690	17.425	12.059	5.830	6.089	5.651

ABUW_RS13100		exodeoxyribonuclease VII small subunit	CDS	-1.191	4.526	4.271	6.848	2.186	1.770	2.890
ABUW_RS01140		hypothetical protein	CDS	-1.187	337.057	383.787	342.033	176.210	130.208	160.475
ABUW_RS20200		hypothetical protein	CDS	-1.183	1.830	2.819	2.754	1.749	0.708	0.835
ABUW_RS15065	ribB	3,4-dihydroxy-2-butanone-4-phosphate synthase	CDS	-1.180	162.750	181.088	194.799	77.975	80.220	79.563
ABUW_RS10050	pqqC	pyrroloquinoline-quinone synthase PqqC	CDS	-1.169	137.038	148.629	130.635	55.311	62.024	67.683
ABUW_RS10310		NAD(P)/FAD-dependent oxidoreductase	CDS	-1.166	23.401	36.047	25.159	15.231	11.470	11.045
ABUW_RS09185		alpha/beta hydrolase	CDS	-1.159	134.726	135.304	113.738	67.627	49.492	54.776
ABUW_RS01640		hypothetical protein	CDS	-1.151	73.767	69.531	74.659	32.720	32.570	32.814
ABUW_RS12115		NAD(P)H-dependent oxidoreductase	CDS	-1.144	31.587	31.263	50.989	15.012	15.010	21.512
ABUW_RS10705		IscS subfamily cysteine desulfurase	CDS	-1.138	959.360	822.072	855.940	366.629	391.898	439.621
ABUW_RS08585		PQQ-dependent sugar dehydrogenase	CDS	-1.135	250.481	225.677	232.240	110.841	97.567	114.111
ABUW_RS11190		OXA-51 family carbapenem-hydrolyzing class D beta-lactamase OXA-69	CDS	-1.104	48.825	55.779	51.956	24.850	22.586	25.365
ABUW_RS20305		hypothetical protein	CDS	-1.103	7.897	6.834	11.910	3.644	3.753	5.009

ABUW_RS09260		sorbosone dehydrogenase family protein	CDS	-1.098	69.241	68.164	66.918	36.510	25.914	33.007
ABUW_RS14220		MFS transporter	CDS	-1.089	32.357	8.969	8.783	8.308	7.222	7.834
ABUW_RS03380		entericidin A/B family lipoprotein	CDS	-1.084	7.993	8.200	16.078	5.101	5.452	4.752
ABUW_RS15280		hypothetical protein	CDS	-1.083	92.739	47.493	58.730	35.052	26.693	32.044
ABUW_RS01270		bifunctional SulP family inorganic anion transporter/carbonic anhydrase	CDS	-1.078	25.809	26.224	28.286	12.753	10.691	14.577
ABUW_RS08765		TonB-dependent siderophore receptor	CDS	-1.071	89.561	81.661	73.617	29.805	45.456	41.162
ABUW_RS04125	adeK	multidrug efflux RND transporter outer membrane channel subunit AdeK	CDS	-1.067	1887.710	1887.845	1489.018	799.137	830.879	883.351
ABUW_RS01050		MFS transporter	CDS	-1.066	26.483	26.822	21.512	11.587	14.444	9.697
ABUW_RS01305		TolC family protein	CDS	-1.062	59.803	59.537	57.613	29.441	27.967	27.356
ABUW_RS08635		alpha/beta fold hydrolase	CDS	-1.060	18.394	21.098	19.130	10.275	9.700	8.155
ABUW_RS10055	pqqB	pyrroloquinoline quinone biosynthesis protein PqqB	CDS	-1.050	171.514	165.115	169.267	69.595	85.177	89.581
ABUW_RS08160		3-oxoacyl-ACP reductase	CDS	-1.045	297.862	392.842	255.762	149.392	145.784	163.365

ABUW_RS02945		DUF4184 family protein	CDS	-1.027	25.231	29.470	28.435	12.972	14.090	13.742
ABUW_RS16540		TonB-dependent siderophore receptor	CDS	-1.022	709.456	457.760	453.911	198.946	270.186	328.849
ABUW_RS05995		acyl-CoA dehydrogenase	CDS	-1.018	150.905	151.619	125.127	84.024	54.094	72.949
ABUW_RS01745		hypothetical protein	CDS	-1.014	61.537	61.758	65.206	24.704	34.340	34.227
ABUW_RS07195		alpha/beta fold hydrolase	CDS	-1.003	11.460	17.767	10.570	6.996	5.239	7.577
ABUW_RS18420		CoA-acylating methylmalonate-semialdehyde dehydrogenase	CDS	1.002	14.253	9.994	13.994	29.805	21.453	25.365
ABUW_RS17570		H-NS histone family protein	CDS	1.002	98.613	74.656	105.922	189.837	200.799	168.695
ABUW_RS15245		hypothetical protein	CDS	1.009	29.757	29.726	43.247	82.931	64.360	59.785
ABUW_RS13525		tannase/feruloyl esterase family alpha/beta hydrolase	CDS	1.011	4.622	2.819	3.871	8.745	7.293	6.743
ABUW_RS03695		AAA family ATPase	CDS	1.013	1.637	2.135	1.265	3.498	3.965	2.697
ABUW_RS06435		hypothetical protein	CDS	1.014	32.261	27.676	47.639	74.186	70.166	73.270
ABUW_RS09295		hypothetical protein	CDS	1.014	1.541	1.110	0.521	1.749	2.124	2.376
ABUW_RS10370		iron-containing redox enzyme family protein	CDS	1.020	22.631	22.038	22.554	51.813	43.190	41.419
ABUW_RS06825		hypothetical protein	CDS	1.022	8.860	9.225	13.845	19.020	20.816	25.237
ABUW_RS19890		hypothetical protein	CDS	1.023	0.963	1.196	3.126	4.300	3.257	3.532
ABUW_RS01970		globin domain-containing protein	CDS	1.024	34.476	40.574	41.461	83.076	78.592	75.518

ABUW_RS09345		hypothetical protein	CDS	1.026	9.438	6.321	8.411	16.470	16.285	16.439
ABUW_RS19865		hypothetical protein	CDS	1.028	0.578	1.367	1.117	2.259	1.982	2.119
ABUW_RS12890		hypothetical protein	CDS	1.028	32.454	25.882	32.380	65.514	58.555	61.005
ABUW_RS10465		TonB C-terminal domain-containing protein	CDS	1.030	9.245	8.115	13.994	21.644	19.896	22.732
ABUW_RS19995		hypothetical protein	CDS	1.032	19.742	19.988	27.020	54.801	40.075	41.933
ABUW_RS12725		hypothetical protein	CDS	1.037	21.861	26.651	26.574	65.222	44.465	44.566
ABUW_RS05335	cas1f	type I-F CRISPR-associated endonuclease Cas1f	CDS	1.038	23.787	20.928	22.256	49.992	47.297	40.199
ABUW_RS01375		sulfate ABC transporter substrate-binding protein	CDS	1.040	66.159	80.806	53.445	132.849	146.351	132.734
ABUW_RS09315		hypothetical protein	CDS	1.042	6.645	6.834	6.848	15.304	11.966	14.641
ABUW_RS13030		minor capsid protein	CDS	1.044	4.815	5.211	7.592	12.826	11.612	12.137
ABUW_RS05660	yddG	aromatic amino acid DMT transporter YddG	CDS	1.046	1.059	1.110	1.638	1.603	3.540	2.825
ABUW_RS08740		cytochrome ubiquinol oxidase subunit I	CDS	1.047	874.229	1576.834	942.583	2549.427	2123.398	2338.544
ABUW_RS07445		dicarboxylate/amino acid:cation symporter	CDS	1.050	26.290	24.686	25.755	69.740	44.465	44.758
ABUW_RS02680		hypothetical protein	CDS	1.050	0.674	0.598	0.893	1.312	1.770	1.477
ABUW_RS00420		hypothetical protein	CDS	1.053	0.482	0.598	0.447	1.385	0.920	0.899
ABUW_RS10185		3-oxoacid CoA-transferase subunit B	CDS	1.057	17.334	15.546	15.706	36.364	37.172	27.549

ABUW_RS18630		oligosaccharide flippase family protein	CDS	1.065	57.974	59.879	94.757	144.509	141.890	158.870
ABUW_RS05915		hypothetical protein	CDS	1.074	0.578	0.940	1.861	2.186	2.266	2.890
ABUW_RS13320		hypothetical protein	CDS	1.074	4.334	4.613	6.848	11.223	11.683	10.596
ABUW_RS10165		GntP family permease	CDS	1.078	13.386	13.752	14.515	36.000	29.313	22.797
ABUW_RS17810		ATP-binding protein	CDS	1.081	40.543	53.814	43.098	104.647	93.815	92.342
ABUW_RS08595		GGDEF domain-containing protein	CDS	1.082	18.971	22.124	22.703	48.899	41.420	44.951
ABUW_RS05820		DUF3015 family protein	CDS	1.084	828.678	787.307	759.768	2140.093	1490.768	1404.013
ABUW_RS11400		Crp/Fnr family transcriptional regulator	CDS	1.092	3.178	2.135	2.382	5.247	6.089	5.009
ABUW_RS00215		hypothetical protein	CDS	1.093	0.482	0.513	0.744	1.530	0.850	1.413
ABUW_RS15510		TetR/AcrR family transcriptional regulator	CDS	1.093	1.348	0.940	3.945	4.664	4.531	4.495
ABUW_RS11475		type II asparaginase	CDS	1.097	137.423	112.497	124.606	282.387	278.187	240.681
ABUW_RS18435		amino acid permease	CDS	1.098	525.616	473.819	524.923	1161.175	1022.615	1078.310
ABUW_RS16465		alpha/beta hydrolase	CDS	1.104	49.307	46.895	42.280	108.145	91.053	98.314
ABUW_RS18405		acyl-CoA dehydrogenase family protein	CDS	1.105	15.890	24.772	15.259	53.417	33.632	33.328
ABUW_RS12310	paaJ	phenylacetate-CoA oxygenase subunit PaaJ	CDS	1.110	92.257	108.140	113.515	255.788	167.096	254.744
ABUW_RS05480	blp2	Ig-like repeat protein Blp2	CDS	1.111	170.262	150.167	145.001	440.159	261.973	303.227
ABUW_RS12620		hypothetical protein	CDS	1.113	25.616	23.576	35.432	62.453	57.492	63.381
ABUW_RS13490		p-hydroxycinnamoyl CoA hydratase/lyase	CDS	1.113	140.408	148.714	80.986	309.350	244.839	246.139

ABUW_RS13625		cache domain-containing protein	CDS	1.121	5.200	4.527	6.774	12.972	10.762	12.329
ABUW_RS18535	prpB	methylisocitrate lyase	CDS	1.128	91.583	87.982	64.983	177.230	195.772	161.181
ABUW_RS00575		type VI secretion system tip protein VgrG	CDS	1.132	195.782	170.496	162.717	419.900	386.729	352.673
ABUW_RS02630		hypothetical protein	CDS	1.137	23.979	26.822	34.687	67.117	61.953	59.335
ABUW_RS12730		3-hydroxyacyl-CoA dehydrogenase NAD-binding domain-containing protein	CDS	1.139	9.630	8.713	13.845	29.660	20.321	21.191
ABUW_RS13465		aromatic ring-hydroxylating dioxygenase subunit alpha	CDS	1.142	6.549	9.140	6.625	17.344	17.559	14.384
ABUW_RS18625		hypothetical protein	CDS	1.145	168.239	172.119	225.318	420.775	418.166	412.458
ABUW_RS03875		hypothetical protein	CDS	1.149	0.385	0.769	0.744	1.968	1.487	0.899
ABUW_RS14045		CitMHS family transporter	CDS	1.157	136.941	132.912	145.522	354.241	301.198	270.798
ABUW_RS13060		LysE family translocator	CDS	1.159	5.874	7.090	9.677	17.781	16.780	16.311
ABUW_RS20115		hypothetical protein	CDS	1.161	46.995	62.014	78.232	132.777	146.138	140.183
ABUW_RS10945	gspI	type II secretion system minor pseudopilin GspI	CDS	1.164	2.215	3.502	4.020	9.474	7.647	5.009
ABUW_RS11915		class I SAM-dependent methyltransferase	CDS	1.168	5.200	7.261	5.508	14.065	12.107	14.256
ABUW_RS13000		hypothetical protein	CDS	1.172	3.948	4.271	6.774	14.575	9.983	9.568
ABUW_RS03850		hypothetical protein	CDS	1.173	28.409	17.425	52.105	66.753	67.263	87.462

ABUW_RS09525		DEAD/DEAH box helicase family protein	CDS	1.176	40.158	30.665	41.312	100.129	73.069	80.334
ABUW_RS00715		DUF1737 domain-containing protein	CDS	1.182	4.911	4.442	4.392	9.838	13.665	7.706
ABUW_RS13005		hypothetical protein	CDS	1.185	2.889	1.794	2.977	6.413	5.027	6.036
ABUW_RS12305	paaK	phenylacetate-CoA oxygenase/reductase subunit PaaK	CDS	1.191	90.235	117.451	139.270	292.735	191.382	308.428
ABUW_RS12540		hypothetical protein	CDS	1.199	16.468	15.461	23.150	42.923	39.508	44.309
ABUW_RS11070		metalloregulator ArsR/SmtB family transcription factor	CDS	1.199	2.600	0.940	4.168	5.174	6.089	6.678
ABUW_RS06025		OmpW family protein	CDS	1.201	11.460	12.044	12.952	25.287	24.994	33.585
ABUW_RS16025		ComEA family DNA-binding protein	CDS	1.201	14.349	13.838	16.823	32.210	36.251	35.190
ABUW_RS07180		hypothetical protein	CDS	1.203	4.622	2.733	6.253	9.109	10.337	12.073
ABUW_RS17605		histidine kinase	CDS	1.205	12.327	12.898	16.897	34.980	33.136	29.282
ABUW_RS14330		hypothetical protein	CDS	1.206	0.385	0.598	0.447	1.676	1.133	0.578
ABUW_RS20505		hypothetical protein	CDS	1.214	0.482	0.769	0.595	1.530	1.133	1.670
ABUW_RS11340		amino acid ABC transporter permease	CDS	1.215	46.899	50.483	43.620	133.505	89.637	104.094
ABUW_RS11470		dicarboxylate/amino acid:cation symporter	CDS	1.215	31.780	24.686	36.623	89.416	58.767	68.133
ABUW_RS18025		esterase-like activity of phytase family protein	CDS	1.218	1.541	2.221	3.498	5.684	5.735	5.779
ABUW_RS12630		hypothetical protein	CDS	1.219	1.252	1.452	3.126	4.372	4.319	5.201

ABUW_RS08855		nuclear transport factor 2 family protein	CDS	1.220	1.830	2.477	2.829	5.393	5.947	5.458
ABUW_RS16285		TetR/AcrR family transcriptional regulator	CDS	1.221	8.089	6.663	11.612	22.154	18.975	20.613
ABUW_RS10360	lipA	lipoyl synthase	CDS	1.225	2.985	2.904	4.317	9.692	5.239	9.119
ABUW_RS03975		hypothetical protein	CDS	1.225	19.068	13.752	22.182	42.996	43.332	42.447
ABUW_RS06795		hypothetical protein	CDS	1.227	0.193	0.940	0.595	1.312	1.912	0.963
ABUW_RS02135		acyl-CoA dehydrogenase family protein	CDS	1.229	5.008	4.954	6.699	15.522	11.753	12.008
ABUW_RS03710		hypothetical protein	CDS	1.231	0.385	0.769	0.447	1.093	1.628	1.092
ABUW_RS06130		hypothetical protein	CDS	1.232	0.482	1.196	0.893	2.040	2.195	1.926
ABUW_RS18720		TetR/AcrR family transcriptional regulator	CDS	1.232	25.135	19.732	29.700	63.036	59.404	52.978
ABUW_RS05415		TetR/AcrR family transcriptional regulator	CDS	1.233	4.719	6.150	6.923	14.575	13.948	13.550
ABUW_RS09660		replication initiation factor domain-containing protein	CDS	1.236	5.682	4.783	6.104	17.490	10.408	11.238
ABUW_RS02355		GFA family protein	CDS	1.236	1.059	1.623	1.042	3.061	3.186	2.569
ABUW_RS10365		transcriptional regulator	CDS	1.237	6.549	8.115	9.677	20.623	18.409	18.623
ABUW_RS04590		hypothetical protein	CDS	1.241	1.252	0.940	1.786	3.498	1.841	4.174
ABUW_RS05165		hypothetical protein	CDS	1.244	4.815	3.075	4.987	9.765	8.567	12.201
ABUW_RS18430		amino acid permease	CDS	1.247	82.820	72.777	65.280	187.942	180.407	155.530
ABUW_RS18390		MHS family MFS transporter	CDS	1.252	4.815	4.527	4.913	13.846	9.842	10.339

ABUW_RS15545		AraC family transcriptional regulator	CDS	1.252	7.800	4.698	9.230	20.405	15.152	16.375
ABUW_RS13265		hypothetical protein	CDS	1.253	0.578	0.683	1.489	2.915	1.628	2.248
ABUW_RS02155	rrtA	rhombosortase	CDS	1.254	14.542	12.300	12.877	34.324	29.667	30.695
ABUW_RS17440		outer membrane beta-barrel protein	CDS	1.255	1364.694	2115.230	1692.898	4039.701	4299.686	4002.694
ABUW_RS13055		cold-shock protein	CDS	1.256	39.484	22.721	83.741	117.765	120.508	111.286
ABUW_RS12995		hypothetical protein	CDS	1.258	1.156	1.708	1.414	3.935	4.177	2.248
ABUW_RS08745		hypothetical protein	CDS	1.258	4.719	7.431	19.726	25.579	27.967	23.631
ABUW_RS13575		hypothetical protein	CDS	1.262	0.096	0.769	0.521	1.239	1.204	1.027
ABUW_RS02700		hypothetical protein	CDS	1.263	13.001	8.627	11.984	30.388	25.418	24.851
ABUW_RS13750		hypothetical protein	CDS	1.277	0.674	0.769	1.340	2.769	1.982	2.183
ABUW_RS11930		isovaleryl-CoA dehydrogenase	CDS	1.278	107.377	91.825	87.537	272.039	196.692	226.617
ABUW_RS11445		LysE family translocator	CDS	1.279	1.926	1.708	1.414	3.571	4.390	4.238
ABUW_RS06160		hypothetical protein	CDS	1.283	1.156	1.196	0.521	3.425	1.770	1.734
ABUW_RS13595	astA	arginine N-succinyltransferase	CDS	1.286	27.350	29.384	39.377	87.813	80.999	66.014
ABUW_RS00430		ATP-binding protein	CDS	1.287	68.952	54.070	79.274	167.902	162.919	162.915
ABUW_RS11650	madL	malonate transporter subunit MadL	CDS	1.290	0.963	0.342	0.223	1.457	1.062	1.092
ABUW_RS00370	hutC	histidine utilization repressor	CDS	1.295	41.314	42.026	41.014	103.117	97.780	104.351
ABUW_RS00375		HutD family protein	CDS	1.296	18.297	16.657	16.525	39.643	42.624	44.052
ABUW_RS08390		hypothetical protein	CDS	1.302	1.637	1.538	2.680	5.903	3.682	5.073

ABUW_RS10995		MotA/TolQ/ExbB proton channel family protein	CDS	1.306	36.210	36.218	33.645	80.234	91.478	90.544
ABUW_RS12300		enoyl-CoA hydratase-related protein	CDS	1.307	39.195	54.924	60.070	149.756	81.495	150.714
ABUW_RS13775		hypothetical protein	CDS	1.308	1.541	1.623	3.424	5.247	5.027	6.357
ABUW_RS09585		hypothetical protein	CDS	1.311	0.867	1.025	1.563	4.081	2.266	2.440
ABUW_RS15355		excalibur calcium-binding domain-containing protein	CDS	1.317	4.815	5.808	7.592	15.376	14.444	15.861
ABUW_RS13770		hypothetical protein	CDS	1.320	4.911	2.135	4.094	10.129	9.629	8.027
ABUW_RS07820		hypothetical protein	CDS	1.323	2.408	1.623	4.987	7.360	7.364	8.220
ABUW_RS06245		DUF559 domain-containing protein	CDS	1.323	0.963	0.256	0.447	1.822	1.133	1.156
ABUW_RS12060		acyl-CoA dehydrogenase family protein	CDS	1.327	0.674	0.683	0.298	1.895	1.204	1.027
ABUW_RS05680		hypothetical protein	CDS	1.331	0.867	0.513	0.893	2.696	1.628	1.477
ABUW_RS08650		heme-binding protein	CDS	1.337	21.572	16.828	33.198	69.522	56.855	55.033
ABUW_RS08735	cydB	cytochrome d ubiquinol oxidase subunit II	CDS	1.344	522.438	933.886	504.155	1859.528	1436.887	1679.434
ABUW_RS20335		hypothetical protein	CDS	1.346	3.659	2.648	2.159	5.320	9.558	6.422
ABUW_RS18085		TetR/AcrR family transcriptional regulator	CDS	1.348	0.385	2.819	1.117	5.538	3.965	1.734
ABUW_RS15750		C39 family peptidase	CDS	1.352	3.082	2.392	7.444	11.733	11.470	10.339
ABUW_RS10965		PilZ domain-containing protein	CDS	1.354	17.816	18.792	24.266	53.198	56.714	46.043
ABUW_RS04600		hypothetical protein	CDS	1.362	2.504	1.110	1.638	4.664	4.177	4.559

ABUW_RS07005		acyltransferase	CDS	1.363	0.867	0.171	2.456	2.623	3.399	3.339
ABUW_RS03655		hypothetical protein	CDS	1.364	1.156	1.538	1.117	4.372	3.399	2.119
ABUW_RS05685		hypothetical protein	CDS	1.367	7.800	6.748	12.505	25.797	21.737	22.668
ABUW_RS12740		exo-alpha-sialidase	CDS	1.372	14.542	9.396	17.641	34.251	36.818	36.796
ABUW_RS07285		hypothetical protein	CDS	1.377	2.600	1.538	2.903	7.142	5.947	5.330
ABUW_RS12295	paaG	2-(1,2-epoxy-1,2-dihydrophenyl)acetyl-CoA isomerase PaaG	CDS	1.380	30.239	46.297	58.656	134.890	74.769	142.816
ABUW_RS05115		GFA family protein	CDS	1.382	4.141	2.221	2.829	8.672	6.797	8.348
ABUW_RS13225		glutathione binding-like protein	CDS	1.383	86.864	60.647	112.398	242.816	200.728	234.837
ABUW_RS13610		gamma-aminobutyraldehyde dehydrogenase	CDS	1.386	19.164	15.973	17.195	52.324	42.270	42.190
ABUW_RS00045		DUF6091 family protein	CDS	1.390	80.412	76.108	78.902	243.035	189.966	183.978
ABUW_RS20685		hypothetical protein	CDS	1.391	0.385	0.256	0.223	0.510	0.779	0.963
ABUW_RS13010		DUF4142 domain-containing protein	CDS	1.392	2.985	1.794	2.754	7.287	6.160	6.357
ABUW_RS02265		energy transducer TonB	CDS	1.397	12.134	15.888	15.408	38.550	39.296	36.731
ABUW_RS13510		OprD family porin	CDS	1.399	1.348	1.538	1.935	4.154	4.744	3.981
ABUW_RS11180		hypothetical protein	CDS	1.402	5.104	3.673	6.699	15.668	13.877	11.623
ABUW_RS18530	prpC	2-methylcitrate synthase	CDS	1.402	144.549	138.720	119.023	377.852	344.601	340.857
ABUW_RS13275		hypothetical protein	CDS	1.406	1.445	1.708	2.010	6.632	3.257	3.981
ABUW_RS09350		DUF2314 domain-containing protein	CDS	1.406	13.771	11.532	18.758	40.882	36.535	39.685

ABUW_RS18510		IS5-like element ISAba13 family transposase	CDS	1.407	0.096	1.196	0.447	1.020	2.974	0.771
ABUW_RS04825	rbtA	rhombotarget A	CDS	1.413	30.046	27.761	33.720	88.323	80.433	75.197
ABUW_RS05675		TetR/AcrR family transcriptional regulator	CDS	1.417	1.156	0.769	1.117	3.134	2.407	2.633
ABUW_RS13585		hypothetical protein	CDS	1.420	2.119	3.246	3.350	9.401	7.364	6.807
ABUW_RS08530		YcgJ family protein	CDS	1.424	5.200	3.075	6.253	14.575	12.461	12.137
ABUW_RS18490		SDR family NAD(P)-dependent oxidoreductase	CDS	1.430	7.704	8.371	7.518	24.631	20.391	18.623
ABUW_RS02235		DMT family transporter	CDS	1.434	2.600	2.990	4.764	7.652	9.983	10.660
ABUW_RS11950		hydroxymethylglutaryl-CoA lyase	CDS	1.434	38.906	34.680	34.389	115.214	74.698	101.718
ABUW_RS00910		cation acetate symporter	CDS	1.440	242.103	229.008	266.034	783.979	662.296	554.567
ABUW_RS12885		hypothetical protein	CDS	1.450	36.980	34.936	45.629	122.866	95.018	103.644
ABUW_RS13040		hypothetical protein	CDS	1.453	1.926	1.367	2.829	6.704	4.956	5.330
ABUW_RS12280	paaF	phenylacetate--CoA ligase	CDS	1.454	31.491	34.253	33.943	109.821	72.361	90.994
ABUW_RS11940		enoyl-CoA hydratase/isomerase family protein	CDS	1.462	45.069	50.141	47.416	150.704	110.595	131.642
ABUW_RS12965		hypothetical protein	CDS	1.465	0.482	0.427	0.670	1.020	1.558	1.862
ABUW_RS06425		hypothetical protein	CDS	1.468	28.409	21.013	51.286	91.894	91.124	96.324

ABUW_RS11245		fimbrial biogenesis outer membrane usher protein	CDS	1.468	3.756	3.161	5.062	12.607	11.541	9.247
ABUW_RS16280		hypothetical protein	CDS	1.469	16.660	13.496	12.952	59.830	28.959	30.502
ABUW_RS16985	crcB	fluoride efflux transporter CrcB	CDS	1.471	11.941	12.898	14.813	14.721	16.780	78.343
ABUW_RS11935		methylcrotonoyl-CoA carboxylase	CDS	1.472	121.051	109.934	125.127	378.362	284.489	325.188
ABUW_RS03800		terminase large subunit	CDS	1.473	0.674	0.513	1.191	2.988	1.628	2.183
ABUW_RS11345		amino acid ABC transporter substrate-binding protein	CDS	1.476	91.872	97.036	94.683	320.500	227.350	241.066
ABUW_RS08850		NADPH-dependent 2,4-dienoyl-CoA reductase	CDS	1.476	16.949	20.757	13.696	50.866	43.615	48.419
ABUW_RS08240		TetR/AcrR family transcriptional regulator	CDS	1.478	15.505	12.557	21.810	55.020	42.270	42.061
ABUW_RS13455		OprD family outer membrane porin	CDS	1.478	1.445	2.392	1.786	5.976	6.514	3.339
ABUW_RS12285	pcaF	3-oxoadipyl-CoA thiolase	CDS	1.481	40.928	42.368	41.610	140.137	83.265	125.221
ABUW_RS01845	aroE	shikimate dehydrogenase	CDS	1.481	44.299	60.989	47.192	134.161	151.095	140.504
ABUW_RS14570		hypothetical protein	CDS	1.481	13.675	11.873	17.046	38.915	40.712	39.557
ABUW_RS07620		hypothetical protein	CDS	1.481	1.252	1.281	2.233	6.632	3.115	3.853
ABUW_RS01595		triacylglycerol lipase	CDS	1.487	3.082	3.075	3.424	12.170	7.576	7.256
ABUW_RS16270		hypothetical protein	CDS	1.488	18.201	14.777	19.577	102.607	23.790	21.320

ABUW_RS01850	hemF	oxygen-dependent coproporphyrinogen oxidase	CDS	1.495	222.650	342.018	249.658	828.797	789.601	676.834
ABUW_RS16520		DUF2846 domain-containing protein	CDS	1.496	10.978	8.798	12.059	33.959	30.091	25.943
ABUW_RS00905		DUF485 domain-containing protein	CDS	1.500	40.158	38.780	52.850	144.509	128.508	100.241
ABUW_RS02625		LemA family protein	CDS	1.501	62.211	68.848	65.653	192.533	176.230	187.959
ABUW_RS17285	coaE	dephospho-CoA kinase	CDS	1.502	31.298	35.022	30.295	88.251	87.726	97.608
ABUW_RS07410		GNAT family N-acetyltransferase	CDS	1.504	1.348	0.683	1.191	2.696	3.186	3.275
ABUW_RS13110		LysE family transporter	CDS	1.512	8.378	10.165	8.560	26.235	24.427	26.714
ABUW_RS10025		hypothetical protein	CDS	1.512	0.289	0.598	0.223	1.603	0.779	0.835
ABUW_RS20430		hypothetical protein	CDS	1.513	0.289	0.342	0.298	0.947	1.133	0.642
ABUW_RS16510		fumarate hydratase	CDS	1.516	233.147	288.204	226.583	690.846	743.508	705.281
ABUW_RS10190		TIGR00366 family protein	CDS	1.519	7.608	7.773	9.900	28.858	25.914	17.980
ABUW_RS11250		fimbrial protein	CDS	1.522	5.778	5.894	6.178	21.279	17.488	12.650
ABUW_RS11230		hypothetical protein	CDS	1.526	1.541	1.025	1.563	4.445	3.469	4.046
ABUW_RS11945		acetyl/propionyl/methylcrotonyl-CoA carboxylase subunit alpha	CDS	1.527	101.502	96.951	96.544	330.338	237.971	281.714
ABUW_RS04860		NF038105 family protein	CDS	1.535	3.082	2.392	3.647	10.202	8.709	7.706

ABUW_RS03370		alpha/beta fold hydrolase	CDS	1.537	8.571	5.638	8.039	26.672	18.197	19.714
ABUW_RS20460		hypothetical protein	CDS	1.539	0.867	0.256	0.223	1.166	0.920	1.670
ABUW_RS17065		hypothetical protein	CDS	1.541	27.928	32.032	57.092	127.675	112.861	101.076
ABUW_RS08955	aroD	type I 3-dehydroquinate dehydratase	CDS	1.552	1.637	2.050	1.638	6.850	3.823	5.009
ABUW_RS00830	prfB	peptide chain release factor 2	CDS	1.553	0.385	0.513	0.968	2.623	1.558	1.541
ABUW_RS04730		ChbG/HpnK family deacetylase	CDS	1.555	0.289	0.683	0.968	1.530	2.620	1.798
ABUW_RS06155		hypothetical protein	CDS	1.556	0.193	0.427	0.223	0.437	0.920	1.156
ABUW_RS04345		hypothetical protein	CDS	1.560	12.423	10.592	20.917	47.733	39.013	43.410
ABUW_RS17805		accessory factor UbiK family protein	CDS	1.563	12.038	12.386	16.450	39.716	41.349	40.071
ABUW_RS13500		feruloyl-CoA synthase	CDS	1.563	24.846	18.194	18.981	72.801	60.820	49.510
ABUW_RS18515		hypothetical protein	CDS	1.567	26.290	25.369	32.529	82.348	85.460	81.875
ABUW_RS08100		hypothetical protein	CDS	1.575	0.674	0.342	0.372	1.457	1.841	0.835
ABUW_RS06560	yegQ	tRNA 5-hydroxyuridine modification protein YegQ	CDS	1.576	75.212	135.731	70.193	276.411	289.020	272.596
ABUW_RS12105	pobA	4-hydroxybenzoate 3-monooxygenase	CDS	1.577	1.926	1.538	1.712	5.393	4.602	5.458
ABUW_RS13470		PDR/VanB family oxidoreductase	CDS	1.582	2.119	2.306	2.754	7.069	7.010	7.577
ABUW_RS12230		hypothetical protein	CDS	1.588	0.289	0.171	0.521	0.364	1.345	1.349
ABUW_RS15490		hypothetical protein	CDS	1.599	3.659	2.050	4.168	13.263	8.709	8.155

ABUW_RS02690		hypothetical protein	CDS	1.604	0.482	0.598	0.744	2.405	1.558	1.734
ABUW_RS12975		hypothetical protein	CDS	1.605	7.319	7.261	8.858	30.753	15.648	25.108
ABUW_RS08730	cydX	cytochrome bd-I oxidase subunit CydX	CDS	1.608	4.622	10.421	7.741	28.057	21.737	20.035
ABUW_RS09150		TorF family putative porin	CDS	1.616	2.696	4.271	2.977	12.607	10.054	7.963
ABUW_RS18540		GntR family transcriptional regulator	CDS	1.627	8.186	13.838	8.635	34.542	34.198	26.072
ABUW_RS10230		MFS transporter	CDS	1.630	14.638	12.727	13.473	44.890	43.969	37.566
ABUW_RS04045		DcaP family trimeric outer membrane transporter	CDS	1.630	993.739	1011.702	951.516	3357.746	2977.572	2818.685
ABUW_RS16785		hypothetical protein	CDS	1.630	32.357	39.207	36.399	114.412	116.472	103.580
ABUW_RS12290		3-hydroxyacyl-CoA dehydrogenase	CDS	1.632	36.306	50.226	64.983	183.278	100.683	186.482
ABUW_RS11300		hypothetical protein	CDS	1.635	5.778	4.100	5.434	16.397	16.285	14.898
ABUW_RS12900		DUF4882 family protein	CDS	1.636	12.423	12.557	10.495	42.631	30.375	37.181
ABUW_RS09670		hypothetical protein	CDS	1.640	2.600	2.563	2.456	8.818	8.709	6.293
ABUW_RS17020		DUF4062 domain-containing protein	CDS	1.646	20.127	18.365	22.182	62.817	64.856	62.353
ABUW_RS00050		DUF6091 family protein	CDS	1.650	4.526	6.919	6.327	18.510	18.480	19.072
ABUW_RS08285		ANTAR domain-containing protein	CDS	1.653	0.193	0.256	0.893	1.968	1.416	1.156
ABUW_RS08605		hypothetical protein	CDS	1.653	1.541	1.708	2.754	6.559	7.010	5.651

ABUW_RS10115	antC	anthranilate 1,2-dioxygenase electron transfer component AntC	CDS	1.656	36.980	36.901	29.328	112.372	104.294	108.396
ABUW_RS10010		hypothetical protein	CDS	1.657	6.645	5.040	9.900	22.445	19.471	26.521
ABUW_RS00590		DUF5991 domain-containing protein	CDS	1.660	7.512	7.688	11.612	29.150	28.746	27.292
ABUW_RS01110		helix-turn-helix transcriptional regulator	CDS	1.665	1.059	1.025	2.159	4.737	4.956	4.110
ABUW_RS13155	benB	benzoate 1,2-dioxygenase small subunit	CDS	1.666	0.674	0.256	0.372	1.530	1.770	0.835
ABUW_RS06845		hypothetical protein	CDS	1.668	0.770	1.025	0.968	2.186	3.682	3.018
ABUW_RS08050		hypothetical protein	CDS	1.669	0.674	0.683	0.670	2.769	1.699	2.055
ABUW_RS04830		CSLREA domain-containing protein	CDS	1.672	21.379	20.757	31.710	90.145	74.131	71.601
ABUW_RS20655		hypothetical protein	CDS	1.690	2.311	2.904	3.647	12.534	7.859	8.541
ABUW_RS04580		hypothetical protein	CDS	1.697	1.059	0.683	1.638	3.789	2.620	4.752
ABUW_RS15755		hypothetical protein	CDS	1.701	49.595	47.322	45.257	172.566	158.600	131.129
ABUW_RS13460		MFS transporter	CDS	1.708	8.571	7.261	5.062	24.631	23.011	20.292
ABUW_RS06150		hypothetical protein	CDS	1.712	0.096	0.513	0.372	1.457	0.354	1.541
ABUW_RS10110	antB	anthranilate 1,2-dioxygenase small subunit	CDS	1.713	23.979	15.973	16.525	67.481	56.360	60.941
ABUW_RS07790		ion transporter	CDS	1.713	12.904	12.557	16.748	49.190	40.146	49.382

ABUW_RS12410	soxR	redox-sensitive transcriptional activator SoxR	CDS	1.713	0.867	0.683	0.744	2.332	2.053	3.147
ABUW_RS09140		muconate/chloromuconate family cycloisomerase	CDS	1.715	8.282	7.517	6.104	33.814	23.932	14.063
ABUW_RS13050		hypothetical protein	CDS	1.718	2.022	1.708	4.020	8.235	7.293	10.403
ABUW_RS05575		hypothetical protein	CDS	1.719	44.684	46.980	48.756	158.865	154.777	148.788
ABUW_RS15230		hypothetical protein	CDS	1.727	1.733	1.367	2.084	7.069	5.735	4.559
ABUW_RS08535		hypothetical protein	CDS	1.734	0.482	0.427	1.935	4.445	1.912	3.596
ABUW_RS09135	catC	muconolactone Delta-isomerase	CDS	1.737	2.793	1.452	1.489	9.036	6.656	3.275
ABUW_RS09545		hypothetical protein	CDS	1.740	1.926	1.794	3.722	9.328	8.142	7.834
ABUW_RS20510		hypothetical protein	CDS	1.743	12.038	9.738	12.729	49.919	33.844	31.915
ABUW_RS06280		hypothetical protein	CDS	1.755	30.720	23.576	44.141	140.574	105.426	86.884
ABUW_RS00400	hutG	formimidoylglutamase	CDS	1.766	14.253	12.642	9.528	51.813	37.313	34.484
ABUW_RS02445		DUF2147 domain-containing protein	CDS	1.769	29.372	28.786	36.101	117.254	112.153	92.342
ABUW_RS17380		hypothetical protein	CDS	1.772	139.927	113.693	122.522	492.847	429.777	361.791
ABUW_RS16720		hypothetical protein	CDS	1.777	14.253	10.165	17.641	54.364	47.155	42.960
ABUW_RS13655		hypothetical protein	CDS	1.779	1.541	1.538	3.052	6.996	6.018	8.412
ABUW_RS01600		lipase secretion chaperone	CDS	1.795	0.289	0.171	1.340	1.968	3.469	1.284
ABUW_RS19650		LysM peptidoglycan-binding domain-containing protein	CDS	1.803	91.294	68.848	84.857	318.241	269.195	267.266

ABUW_RS08245		iron-containing redox enzyme family protein	CDS	1.818	47.573	41.941	51.510	223.869	135.376	138.385
ABUW_RS01100		hypothetical protein	CDS	1.822	1.156	1.110	2.903	6.559	5.735	6.486
ABUW_RS12685		hypothetical protein	CDS	1.823	3.371	2.221	5.285	15.085	11.045	12.779
ABUW_RS12750		MFS transporter	CDS	1.826	4.815	4.015	3.498	16.470	15.435	11.687
ABUW_RS06555		YfhL family 4Fe-4S dicluster ferredoxin	CDS	1.829	3.756	5.638	3.945	18.219	16.072	13.228
ABUW_RS10105	antA	anthranilate 1,2-dioxygenase large subunit	CDS	1.830	66.641	58.939	47.490	213.230	205.613	195.922
ABUW_RS06275		hypothetical protein	CDS	1.830	2.022	1.965	3.275	10.057	7.010	9.119
ABUW_RS08725		cyd operon YbgE family protein	CDS	1.838	19.742	35.022	22.629	111.206	78.450	87.333
ABUW_RS03365		radical SAM protein	CDS	1.848	7.415	7.175	12.356	42.267	26.551	28.833
ABUW_RS16315		DUF4124 domain-containing protein	CDS	1.852	2.408	2.648	2.977	11.004	9.275	8.926
ABUW_RS11240		fimbria/pilus periplasmic chaperone	CDS	1.857	3.371	2.904	3.201	12.607	12.815	8.990
ABUW_RS00585		hypothetical protein	CDS	1.876	8.571	4.015	8.411	26.162	24.002	26.971
ABUW_RS15175	bfr	bacterioferritin	CDS	1.882	139.445	124.797	108.379	514.782	482.738	375.726
ABUW_RS02595	radC	DNA repair protein RadC	CDS	1.893	5.682	4.100	4.689	20.186	15.789	17.724
ABUW_RS10120		AraC family transcriptional regulator	CDS	1.914	2.696	2.392	3.424	12.024	11.399	8.926
ABUW_RS13380		hypothetical protein	CDS	1.917	4.237	2.135	9.379	27.765	20.675	12.073

ABUW_RS06595		NirD/YgiW/YdeI family stress tolerance protein	CDS	1.918	9.919	9.140	7.592	33.231	32.924	34.355
ABUW_RS18375	abaR	LuxR family transcriptional regulator AbaR	CDS	1.922	0.289	0.427	1.117	2.769	2.195	2.376
ABUW_RS11920		AMP-binding protein	CDS	1.945	18.105	12.727	15.036	72.364	49.350	54.712
ABUW_RS12970		hypothetical protein	CDS	1.948	0.289	0.085	1.042	1.968	1.699	2.183
ABUW_RS12415		hypothetical protein	CDS	1.952	0.482	0.256	0.744	2.186	1.558	2.183
ABUW_RS06255		hypothetical protein	CDS	1.959	9.149	8.371	13.324	48.024	35.119	37.374
ABUW_RS00395	hutI	imidazolonepropionase	CDS	1.970	33.995	29.555	29.253	145.311	106.701	111.478
ABUW_RS13580		DUF4265 domain-containing protein	CDS	1.972	0.385	0.598	1.042	3.498	2.691	2.119
ABUW_RS05570		EAL domain-containing protein	CDS	1.975	241.814	259.247	220.703	980.011	862.316	994.573
ABUW_RS10180		CoA transferase subunit A	CDS	1.979	7.993	7.944	8.932	39.279	35.189	23.824
ABUW_RS07800		membrane protein	CDS	1.986	1.830	1.196	1.935	5.830	6.939	7.000
ABUW_RS05605		LysR family transcriptional regulator	CDS	1.997	3.563	2.904	6.997	18.802	17.630	18.045
ABUW_RS05440		Lrp/AsnC family transcriptional regulator	CDS	2.001	0.770	1.367	3.201	7.579	8.355	6.229
ABUW_RS06500		alpha/beta fold hydrolase	CDS	2.003	4.141	3.588	4.987	19.603	17.205	14.449
ABUW_RS09775		hypothetical protein	CDS	2.005	0.289	0.427	0.447	1.457	1.487	1.862
ABUW_RS11290		integrase family protein	CDS	2.031	1.830	2.563	2.605	9.911	10.054	8.926
ABUW_RS14535		hypothetical protein	CDS	2.035	1.156	0.854	1.489	5.101	5.027	4.431

ABUW_RS20670		prepilin peptidase	CDS	2.049	32.743	39.891	31.189	142.250	141.253	146.027
ABUW_RS01290		hypothetical protein	CDS	2.061	62.693	47.322	59.921	268.031	230.253	210.756
ABUW_RS12265		PaaI family thioesterase	CDS	2.065	0.193	0.427	0.670	2.842	1.274	1.605
ABUW_RS13835		YraN family protein	CDS	2.068	2.696	3.331	6.550	17.636	19.188	16.760
ABUW_RS17410		hypothetical protein	CDS	2.080	4.430	3.161	2.680	20.186	13.453	9.568
ABUW_RS18015		DUF2726 domain-containing protein	CDS	2.085	6.645	5.211	7.890	33.959	25.135	25.044
ABUW_RS12430		winged helix DNA-binding domain-containing protein	CDS	2.085	67.411	60.647	62.973	72.728	64.714	672.660
ABUW_RS10790		hypothetical protein	CDS	2.087	4.526	3.075	4.615	19.895	15.435	16.696
ABUW_RS00600		SH3 domain-containing protein	CDS	2.091	3.082	3.246	5.434	18.364	14.019	18.301
ABUW_RS12210		TetR/AcrR family transcriptional regulator	CDS	2.107	0.096	0.171	0.298	1.166	0.708	0.771
ABUW_RS01505	bfr	bacterioferritin	CDS	2.121	74.249	70.214	90.961	374.427	356.496	293.980
ABUW_RS09650		helix-turn-helix domain-containing protein	CDS	2.122	2.793	2.135	2.680	11.077	11.399	10.724
ABUW_RS14085		SRPBCC domain-containing protein	CDS	2.152	0.482	0.513	1.191	4.154	2.761	3.211
ABUW_RS20675		A24 family peptidase	CDS	2.155	22.246	25.797	20.768	103.554	97.921	104.928
ABUW_RS11885		hypothetical protein	CDS	2.158	0.289	0.342	0.670	2.186	1.982	1.926
ABUW_RS07280		immunity 26 domain-containing protein	CDS	2.181	0.578	0.854	1.563	4.300	4.815	4.945
ABUW_RS01125		GNAT family N-acetyltransferase	CDS	2.190	0.193	0.171	0.670	2.040	1.628	1.413

ABUW_RS15495		hypothetical protein	CDS	2.193	3.659	5.040	8.560	27.474	25.348	27.099
ABUW_RS01570		type IV pilin protein	CDS	2.208	18.875	24.174	22.033	110.841	97.992	92.150
ABUW_RS03885		hypothetical protein	CDS	2.209	0.289	0.171	0.223	0.947	0.920	1.349
ABUW_RS13505		acyl-CoA dehydrogenase family protein	CDS	2.221	2.119	2.221	1.414	10.275	9.275	7.192
ABUW_RS03960		hypothetical protein	CDS	2.237	0.096	0.000	0.595	0.947	1.274	1.413
ABUW_RS14110		SPOR domain-containing protein	CDS	2.281	0.385	1.025	0.819	2.478	5.381	3.275
ABUW_RS10155		AraC family transcriptional regulator	CDS	2.292	2.985	1.794	2.829	16.397	11.045	9.953
ABUW_RS00595		DUF1311 domain-containing protein	CDS	2.323	1.445	0.769	4.689	12.316	8.780	14.577
ABUW_RS03340		response regulator	CDS	2.350	111.999	138.464	93.715	588.385	587.882	578.134
ABUW_RS13360		hypothetical protein	CDS	2.353	48.632	40.659	40.865	581.681	44.040	39.364
ABUW_RS13815		hypothetical protein	CDS	2.372	133.571	159.819	125.946	712.053	710.230	748.884
ABUW_RS06270		hypothetical protein	CDS	2.373	0.289	0.171	0.521	1.239	1.628	2.440
ABUW_RS08615		PEGA domain-containing protein	CDS	2.394	19.646	17.938	16.748	99.254	110.454	75.839
ABUW_RS03335	pilG	twitching motility response regulator PilG	CDS	2.408	109.014	138.208	96.841	590.061	639.851	595.537
ABUW_RS10005		hypothetical protein	CDS	2.412	1.156	0.940	1.340	7.798	3.894	6.807
ABUW_RS01565		prepilin-type N-terminal cleavage/methylation domain-containing protein	CDS	2.430	12.808	17.938	15.334	92.987	80.858	75.004

ABUW_RS11305		TetR/AcrR family transcriptional regulator	CDS	2.577	2.504	1.367	5.434	20.478	14.444	21.705
ABUW_RS12680		hypothetical protein	CDS	2.646	1.059	0.769	1.489	7.943	6.160	7.064
ABUW_RS06590	tadA	Flp pilus assembly complex ATPase component TadA	CDS	2.693	34.283	39.122	24.192	219.059	204.693	206.710
ABUW_RS00390		amino acid permease	CDS	2.729	45.743	35.363	38.037	318.168	214.747	256.542
ABUW_RS11960		indolepyruvate ferredoxin oxidoreductase family protein	CDS	2.772	45.551	41.343	36.697	328.152	278.470	237.213
ABUW_RS01560		VWA domain-containing protein	CDS	2.844	116.622	152.815	113.813	1062.868	871.450	817.209
ABUW_RS17275		type II secretion system F family protein	CDS	2.869	69.048	88.067	54.562	528.337	518.990	498.186
ABUW_RS18750		RcnB family protein	CDS	2.876	11.653	11.532	11.463	73.238	79.796	101.461
ABUW_RS18520		hypothetical protein	CDS	2.886	3.563	2.306	7.220	24.850	14.869	58.372
ABUW_RS14715		PilT/PilU family type 4a pilus ATPase	CDS	2.908	45.936	59.708	36.027	369.690	336.742	356.461
ABUW_RS15500		hypothetical protein	CDS	2.919	2.119	1.281	2.010	15.376	11.966	13.742
ABUW_RS03350		methyl-accepting chemotaxis protein	CDS	2.936	421.321	513.966	320.968	3418.231	3030.533	3165.129
ABUW_RS15505		hypothetical protein	CDS	2.940	0.482	0.256	1.712	6.559	5.664	7.642
ABUW_RS11910		DcaP family trimeric outer membrane transporter	CDS	2.950	3.467	1.794	2.456	25.142	19.188	15.091

ABUW_RS01425		pilus assembly protein PilM	CDS	2.994	85.227	109.080	79.200	759.275	737.560	682.099
ABUW_RS03360		hypothetical protein	CDS	3.063	20.801	32.288	23.298	227.148	208.092	203.821
ABUW_RS18120	dprA	DNA-processing protein DprA	CDS	3.078	12.519	17.767	15.855	130.226	130.845	129.459
ABUW_RS14710		type IV pilus twitching motility protein PilT	CDS	3.082	41.217	53.899	25.532	361.383	328.387	330.390
ABUW_RS05525		hypothetical protein	CDS	3.127	5.104	3.758	3.573	35.635	42.199	30.438
ABUW_RS03355		Hpt domain-containing protein	CDS	3.136	273.112	360.041	230.305	2754.494	2383.247	2454.132
ABUW_RS07785		hypothetical protein	CDS	3.165	3.178	2.050	4.392	34.324	24.286	28.576
ABUW_RS16790		hypothetical protein	CDS	3.221	57.589	70.471	49.277	577.746	559.985	515.395
ABUW_RS00795		FprA family A-type flavoprotein	CDS	3.228	16.757	23.832	20.619	215.999	181.965	176.401
ABUW_RS17270	pilB	type IV-A pilus assembly ATPase PilB	CDS	3.229	77.619	97.036	58.432	728.668	747.119	708.942
ABUW_RS01440		pilus assembly protein PilP	CDS	3.303	28.216	38.182	22.331	316.055	287.179	271.889
ABUW_RS03345		chemotaxis protein CheW	CDS	3.308	57.396	83.967	57.539	694.271	656.207	620.003
ABUW_RS13600		aspartate aminotransferase family protein	CDS	3.312	41.602	50.653	48.086	152.963	1117.421	124.193
ABUW_RS00800		YkgJ family cysteine cluster protein	CDS	3.319	4.911	5.552	4.168	55.384	44.889	45.657
ABUW_RS14740		bacteriohemerythrin	CDS	3.341	8.089	11.019	15.780	139.408	113.498	103.002

ABUW_RS01555		hypothetical protein	CDS	3.348	12.808	16.315	9.379	148.007	129.500	113.983
ABUW_RS17730		sigma-54 dependent transcriptional regulator	CDS	3.368	45.936	70.129	53.296	569.438	582.784	597.142
ABUW_RS18115		LysM peptidoglycan-binding domain-containing protein	CDS	3.398	37.461	47.408	31.635	454.078	392.252	381.634
ABUW_RS02525		hypothetical protein	CDS	3.482	47.092	56.633	50.319	593.924	576.624	551.741
ABUW_RS11275		cytosine permease	CDS	3.569	2.408	3.758	3.796	48.753	38.021	32.750
ABUW_RS01430		PilN domain-containing protein	CDS	3.577	27.831	33.911	23.968	353.512	338.087	331.032
ABUW_RS01445		type IV pilus secretin PilQ	CDS	3.580	87.827	105.749	73.989	1184.860	1032.669	980.959
ABUW_RS09300		amidohydrolase	CDS	3.621	2.504	1.708	1.786	30.388	20.675	22.476
ABUW_RS09960		hypothetical protein	CDS	3.645	8.956	8.884	15.259	158.137	124.048	134.725
ABUW_RS01435		type 4a pilus biogenesis protein PilO	CDS	3.777	16.275	21.355	15.557	252.727	247.104	229.314
ABUW_RS00350		amino acid permease	CDS	3.780	16.564	21.696	18.311	307.383	265.584	204.912
ABUW_RS00385	hutH	histidine ammonia-lyase	CDS	3.807	64.907	47.408	57.688	970.974	676.315	731.802
ABUW_RS20570		hypothetical protein	CDS	4.003	0.000	0.000	0.074	0.437	0.779	0.578
ABUW_RS01545	pilV	type IV pilus modification protein PilV	CDS	4.065	4.430	6.150	2.456	78.995	73.140	64.794
ABUW_RS00335		VOC family protein	CDS	4.089	6.645	5.979	6.774	126.072	120.720	83.930
ABUW_RS11235		type 1 fimbrial protein	CDS	4.093	2.119	1.794	1.712	42.631	29.242	24.145
ABUW_RS00345	fahA	fumarylacetoacetase	CDS	4.220	34.283	32.032	35.432	744.554	671.642	480.269

ABUW_RS01550		PilW family protein	CDS	4.259	7.993	9.738	7.220	171.546	157.892	148.274
ABUW_RS03330		hypothetical protein	CDS	4.308	0.578	0.769	1.414	19.166	20.533	17.081
ABUW_RS00340	maiA	maleylacetoacetate isomerase	CDS	4.372	5.778	5.296	8.114	152.088	143.944	104.222
ABUW_RS00325	hppD	4-hydroxyphenylpyruvate dioxygenase	CDS	4.492	22.824	16.571	18.609	519.155	427.512	357.232
ABUW_RS01540		GspH/FimT family pseudopilin	CDS	4.664	1.059	0.940	1.191	34.834	24.781	22.347
ABUW_RS08010		hypothetical protein	CDS	4.686	0.193	0.000	0.298	4.227	5.806	3.725
ABUW_RS00380	hutU	urocanate hydratase	CDS	4.728	48.921	57.145	52.850	1707.002	1279.137	1226.328
ABUW_RS01495		pilin	CDS	5.027	50.655	80.806	38.707	2122.676	1818.305	1606.613
ABUW_RS02965		RcnB family protein	CDS	5.499	1.059	0.854	1.042	40.226	39.508	55.161

Appendix C

Chapter 4 Appendices

C.1 *A. baumannii* AB5075 Colistin MIC

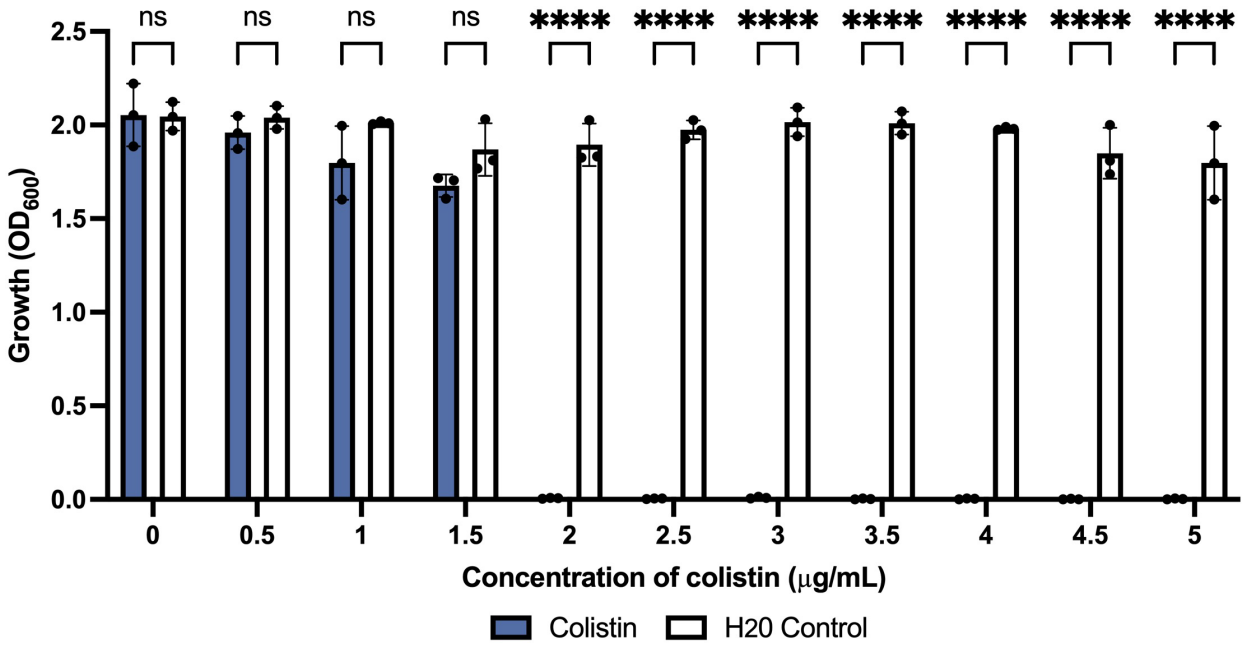

C.2 Colistin MIC Break Points and Final OD_{600} in the Presence and Absence of Colistin, for Each CRM.

CRM Isolate Number	MIC Breakpoint (μg/ml)	Growth in Presence of Colistin		% Growth in Absence of Colistin (OD_{600})	
		%	OD_{600}	%	OD_{600}
AB5075 WT	2.00	100	2.409667	100.0	0.031667
1	8	59.5	1.433	7288.4	2.308
2	32	80.2	1.933	4356.8	1.379667
3	16	100.8	2.067333	5928.4	1.877333
4	8	77.7	1.939	7313.7	2.316

5	512	85.5	2.382667	7118.9	2.254333
6	16	77.4	2.291333	6788.4	2.149667
7	16	77.6	2.394667	5452.6	1.726667
8	16	82.7	2.322667	6831.6	2.163333
9	1024	86.3	2.456	8212.6	2.600667
10	16	87.0	2.205333	6822.1	2.160333
11	16	101.7	2.214667	6181.1	1.957333
12	16	78.3	1.998667	6526.3	2.066667
13	64	90.4	2.254	7120.0	2.254667
14	64	97.1	1.826333	3838.9	1.215667
15	32	93.1	2.014	5582.1	1.767667
16	32	57.0	2.285333	2195.8	0.695333
17	16	60.8	1.761	4790.5	1.517
18	64	94.0	1.737	2854.7	0.904
19	8	37.6	1.999333	4325.3	1.369667
20	16	62.6	1.718333	4049.5	1.282333
21	64	71.3	1.897667	5987.4	1.896
22	64	93.1	1.874667	2621.1	0.83
23	64	91.9	1.872667	7177.9	2.273
24	32	100.8	1.838667	6421.1	2.033333
25	32	77.7	1.746	2134.7	0.676
26	32	85.5	2.151667	7367.4	2.333
27	32	77.4	2.334667	7105.3	2.25
28	64	77.6	2.126	6757.9	2.14
29	32	82.7	2.153667	7407.4	2.345667
30	32	100.8	2.429	4176.8	1.322667
31	32	77.7	1.872333	7066.3	2.237667
32	32	85.5	2.061333	5497.9	1.741

33	32	77.4	1.865333	5351.6	1.694667
34	256	77.6	1.869	5767.4	1.826333
35	32	82.7	1.993	2047.4	0.648333
36	512	86.3	2.079333	5533.7	1.752333
37	64	87.0	2.096	6705.3	2.123333
38	256	101.7	2.451	6122.1	1.938667
39	256	78.3	1.886333	7313.7	2.316
40	64	90.4	2.177333	5573.7	1.765
41	256	97.1	2.340333	6886.3	2.180667
42	64	93.1	2.242667	4111.6	1.302
43	256	57.0	1.374	5517.9	1.747333
44	32	60.8	1.465333	2556.8	0.809667
45	16	94.0	2.264	3803.2	1.204333
46	8	37.6	0.905333	3728.4	1.180667
47	256	62.6	1.507667	6107.4	1.934
48	256	71.3	1.719	7074.7	2.240333
49	256	93.1	2.243333	6374.7	2.018667
50	128	91.9	2.215333	5957.9	1.886667

C.3 Amino Acid MSA of PmrB Against the *Escherichia coli* CusS kinase core

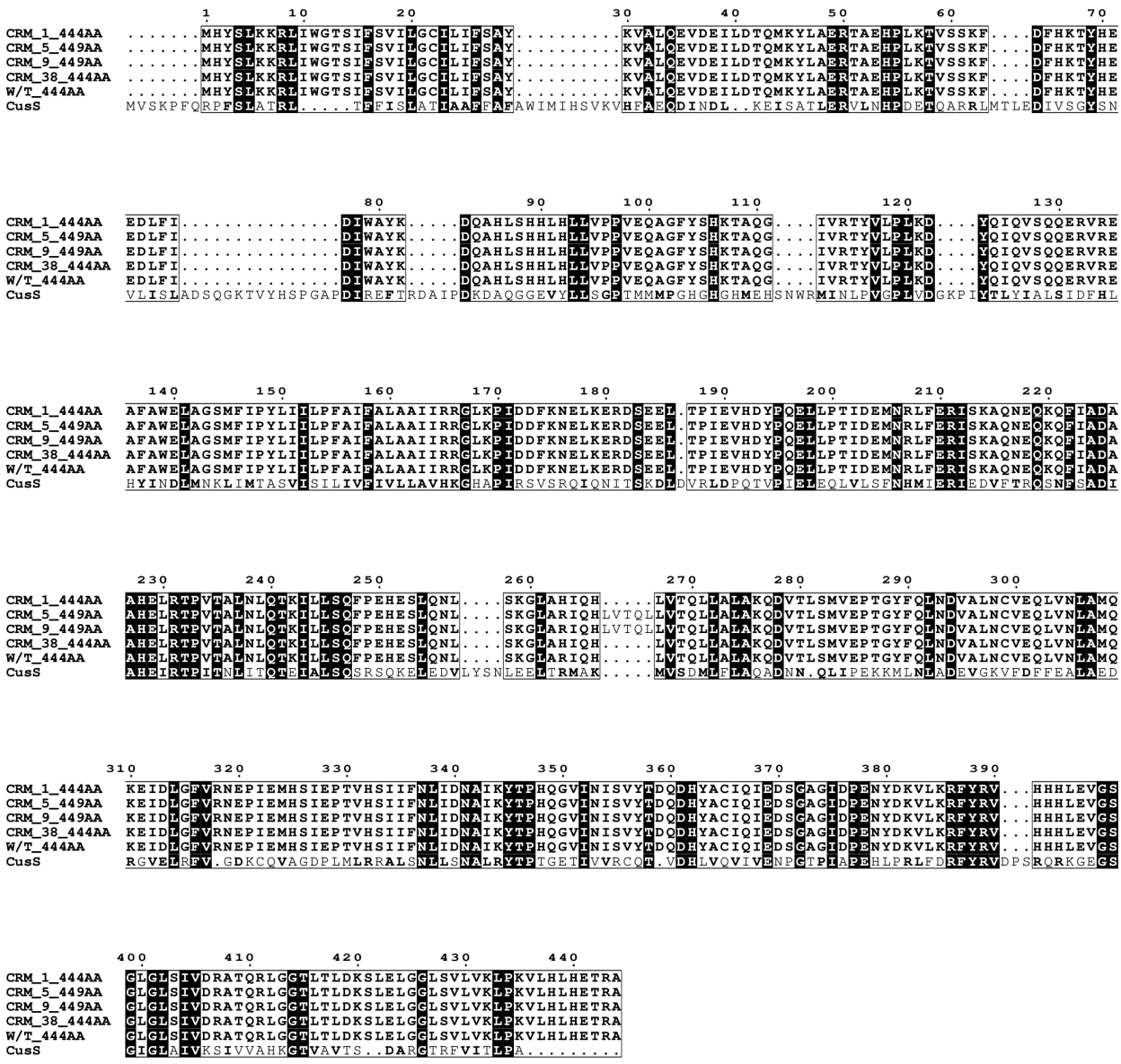

C.4 All domains and features in CRM 5 and 9

All domains and features in CRM 5 and 9 after position 271 are +5 residues due to the +5AA duplication.

WT				CRM1/38				CRM5/9			
TM	9	29	Phobius	TM	9	29	Phobius	TM	9	29	Phobius
select TM1, chain A and resi 9-29				select TM1, chain A and resi 9-29				select TM1, chain A and resi 9-29			
Sensor	30	145	Phobius	Sensor	30	145	Phobius	Sensor	30	145	Phobius
select SD, chain A and resi 30-145				select SD, chain A and resi 30-145				select SD, chain A and resi 30-145			
TM	146	164	Phobius	TM	146	164	Phobius	TM	146	164	Phobius
select TM2, chain A and resi 146-164				select TM2, chain A and resi 146-164				select TM2, chain A and resi 146-164			
HAMP	165	201	Assumed	HAMP	165	201	Assumed	HAMP	165	201	Assumed
select HAMP, chain A and resi 165-201				select HAMP, chain A and resi 165-201				select HAMP, chain A and resi 165-201			
HisKA/DHp	202	278	CDD	HisKA/DHp	202	278	CDD	HisKA/DHp	202	273	CDD
select HKA, chain A and resi 202-282				select HKA, chain A and resi 202-282				select HKA, chain A and resi 202-287			
HATPase/C	286	437	CDD	HATPase/C	286	437	CDD	HATPase/C	291	442	CDD
select HAA, chain A and resi 283-437				select HAA, chain A and resi 283-437				select HAA, chain A and resi 288-442			
Dimerisation Site		222	CDD	Dimerisation Site		222	CDD	Dimerisation Site		222	CDD
		226	CDD			226	CDD			226	CDD
		230	CDD			230	CDD			230	CDD
		233	CDD			233	CDD			233	CDD
		237	CDD			237	CDD			237	CDD
		240	CDD			240	CDD			240	CDD
		257	CDD			257	CDD			257	CDD
		260	CDD			260	CDD				
		264	CDD			264	CDD			264	CDD
		267	CDD			267	CDD			267	CDD
		271	CDD			271	CDD			271	CDD
										272	CDD
										276	CDD
Phosphorylation Site		228	CDD	Phosphorylation Site		228	CDD	Phosphorylation Site		228	CDD
ATP Binding Site		337	CDD	ATP Binding Site		337	CDD			342	CDD
		341	CDD			341	CDD			346	CDD
		344	CDD			344	CDD			349	CDD
		368	CDD			368	CDD			373	CDD
		370	CDD			370	CDD			375	CDD
		372	CDD			372	CDD			377	CDD
		374	CDD			374	CDD			379	CDD
		399	CDD			399	CDD			404	CDD
		400	CDD			400	CDD			405	CDD
		401	CDD			401	CDD			406	CDD
		402	CDD			402	CDD			407	CDD
		418	CDD			418	CDD			423	CDD
		421	CDD			421	CDD			426	CDD
		426	CDD			426	CDD			431	CDD
		427	CDD			427	CDD			432	CDD
		429	CDD			429	CDD			434	CDD
ATP Lid		384	CDD	ATP Lid		384	CDD			389	CDD
		402	CDD			402	CDD			407	CDD
				Mg2+		341	CDD	Mg2+		346	CDD

C.5 CRM Breseq Analysis

CRM	Link to Breseq Analysis File (HTML)
CRM 1	file:///Users/kavitagadar/Desktop/PhD%20Y3/Thesis%20Chapters/CRM%20Chapter/CRM/Genomic%20Analysis/BreSeq/CRM%201/BreSeq%20CRM1/output/summary.html

CRM 5	file:///Users/kavitagadar/Desktop/PhD%20Y3/Thesis%20Chapters/CRM%20Chapter/CRM/Genomic%20Analysis/BreSeq/CRM%205/%20BreSeq%20CRM2/output/summary.html
CRM 9	file:///Users/kavitagadar/Desktop/PhD%20Y3/Thesis%20Chapters/CRM%20Chapter/CRM/Genomic%20Analysis/BreSeq/CRM%209/BreSeq%20CRM3/output/summary.html
CRM 38	file:///Users/kavitagadar/Desktop/PhD%20Y3/Thesis%20Chapters/CRM%20Chapter/CRM/Genomic%20Analysis/BreSeq/CRM%2038/BreSeq%20CRM4/output/summary.html

C.6 Sequences Producing Significant Alignments

A. Nucleotide BLAST search demonstrating that the 15 bp duplication mutation have not been reported previously in other Genbank databases.

Sequences producing significant alignments Download Select columns Show 100

select all *100 sequences selected* GenBank Graphics Distance tree of results MSA Viewer

Description	Scientific Name	Max Score	Total Score	Query Cover	E value	Per. Ident	Acc. Len	Accession
Acinetobacter baumannii strain C20AB12 chromos...	Acinetobacter bauma...	6951	9221	98%	0.0	99.61%	3967213	CP142667.1
Acinetobacter baumannii strain FDAARGOS_1036...	Acinetobacter bauma...	6951	9221	98%	0.0	99.61%	4040084	CP066016.1
Acinetobacter baumannii strain D13 chromosome, ...	Acinetobacter bauma...	6951	9221	98%	0.0	99.61%	4089266	CP156044.1
Acinetobacter baumannii strain 9102 chromosome,...	Acinetobacter bauma...	6951	13979	98%	0.0	99.61%	3971623	CP023029.1
Acinetobacter baumannii strain Nord12-3 chromos...	Acinetobacter bauma...	6951	9221	98%	0.0	99.61%	3860344	CP139831.1
Acinetobacter baumannii strain AB5075-T chromos...	Acinetobacter bauma...	6951	9221	98%	0.0	99.61%	3952981	CP113080.1
Acinetobacter baumannii strain SIMBA089 chromo...	Acinetobacter bauma...	6951	11611	98%	0.0	99.61%	4089412	CP162145.1
Acinetobacter baumannii strain AB6870155 chrom...	Acinetobacter bauma...	6951	9221	98%	0.0	99.61%	3990368	CP114381.1
Acinetobacter baumannii strain XH1047 chromoso...	Acinetobacter bauma...	6951	11600	98%	0.0	99.61%	3942255	CP134552.1
Acinetobacter baumannii strain Ex003 chromosom...	Acinetobacter bauma...	6951	9221	98%	0.0	99.61%	3935232	CP049314.1
Acinetobacter baumannii strain AB5075 chromoso...	Acinetobacter bauma...	6951	9221	98%	0.0	99.61%	4001395	CP144559.1
Acinetobacter baumannii strain UC22850 chromos...	Acinetobacter bauma...	6951	11622	98%	0.0	99.61%	4132446	CP076821.1
Acinetobacter baumannii strain D36, complete gen...	Acinetobacter bauma...	6951	11589	98%	0.0	99.61%	4063596	CP012952.1
Acinetobacter baumannii strain OC064 chromoso...	Acinetobacter bauma...	6951	9221	98%	0.0	99.61%	4058693	CP087317.1
Acinetobacter baumannii strain MRSN 56 chromos...	Acinetobacter bauma...	6951	9221	98%	0.0	99.61%	4153776	CP090606.1
Acinetobacter baumannii strain C20AB05 chromos...	Acinetobacter bauma...	6951	9221	98%	0.0	99.61%	3954338	CP143262.1
Acinetobacter baumannii strain G7 chromosome, c...	Acinetobacter bauma...	6951	9221	98%	0.0	99.61%	4087022	CP175642.1
Acinetobacter baumannii str. AYE, complete genome	Acinetobacter bauma...	6951	9221	98%	0.0	99.61%	3936291	CU459141.1
Acinetobacter baumannii strain MRSN576822 chro...	Acinetobacter bauma...	6951	9221	98%	0.0	99.61%	4058653	CP130628.2
Acinetobacter baumannii strain AB5075-UW, comp...	Acinetobacter bauma...	6951	9221	98%	0.0	99.61%	3972672	CP008706.1
Acinetobacter baumannii strain JRCGR-ACBMN01...	Acinetobacter bauma...	6951	9221	98%	0.0	99.61%	3898738	CP157212.1

B. Sequence query results with the highest percentage coverage results of PmrB with the 15bp duplication mutation. Results show 3830/3845 (99%) nucleotide identity match and 15/3845 gaps in the match, which accounts of the 15 bp duplication.